NUREG/CR-0814
TREE-1228
For U.S. Nuclear Regulatory Commission

EXPERIMENT DATA REPORT FOR SEMISCALE MOD-3 LOWER PLENUM INJECTION TEST S-07-8 (BASELINE TEST SERIES)

KENNETH E. SACKETT ROBERT L. GILLINS
DAVID R. PACK

JUNE 1979

EG&G Idaho, Inc.

IDAHO NATIONAL ENGINEERING LABORATORY

DEPARTMENT OF ENERGY

IDAHO OPERATIONS OFFICE UNDER CONTRACT DE-AC07-76IDO1570

Available from
National Technical Information Service
Springfield, Virginia 22161
Price: Printed Copy A12; Microfiche $3.00

The price of this document for requesters outside the North American continent can be obtained from the National Technical Information Service.

NUREG/CR-0814
TREE-1228
R2

EXPERIMENT DATA REPORT FOR SEMISCALE MOD-3 LOWER PLENUM INJECTION TEST S-07-8 (BASELINE TEST SERIES)

Kenneth E. Sackett
Robert L. Gillins
David R. Pack

EG&G Idaho, Inc.
Idaho Falls, Idaho 83401

Published June 1979

PREPARED FOR THE
U.S. NUCLEAR REGULATORY COMMISSION
AND THE U.S. DEPARTMENT OF ENERGY
IDAHO OPERATIONS OFFICE
UNDER CONTRACT NO. DE-AC07-76IDO1570
NRC FIN NO. A6038

ABSTRACT

Recorded test data are presented for Test S-07-8 of the Semiscale Mod-3 baseline test series. This test is one of several Semiscale Mod-3 experiments conducted to investigate the thermal and hydraulic phenomena accompanying a hypothesized loss-of-coolant accident in a pressurized water reactor (PWR) system. Test S-07-8 was conducted from initial conditions of 15.7 MPa and 556 K to investigate the response of the Semiscale Mod-3 system to a blowdown transient following a simulated double-ended offset shear of the broken loop cold leg piping. The specific objective of this test was to provide reference data to evaluate integral blowdown and reflood behavior during a 200% cold leg break with emergency core coolant (ECC) injection into the vessel lower plenum of the Mod-3 system. The purpose of this report is to make available the uninterpreted data from Test S-07-8 for future data analysis. The data, presented in the form of graphics in engineering units, have been analyzed only to the extent necessary to ensure that they are reasonable and consistent.

SUMMARY

Test S-07-8 was performed as part of the Semiscale Mod-3 portion of the Semiscale Program conducted by EG&G Idaho, Inc., for the United States Government. This test was part of the Mod-3 baseline test series (Test Series 7) performed to investigate the response of the Mod-3 system during a blowdown and reflood transient. Hardware configuration and test parameters were selected to yield a system response that simulates the response of a pressurized water reactor to the blowdown and reflood portions of a hypothesized loss-of-coolant accident (LOCA).

The objective of Test S-07-8 was to provide reference data to evaluate integral blowdown and reflood behavior during a 200% cold leg break with emergency core coolant injection into the vessel lower plenum of the Mod-3 system.

The Mod-3 system was equipped with a pressure vessel with simulated reactor internals and an external downcomer assembly; an intact loop with steam generator, pump, and pressurizer; a broken loop with steam generator, pump, and rupture assembly; high and low pressure coolant injection pumps and coolant injection accumulator for the vessel lower plenum; and a pressure suppression system with header, suppression tank, and steam supply system. The electrically heated core consisted of 25 rods of which 23 were powered.

Test S-07-8 was conducted from initial conditions of 15.7 MPa and 556 K with a simulated full size (200%) double-ended offset shear of the broken loop piping at an initial core power level of 1.99 MW. After initiation of blowdown, power to the heated core was reduced to simulate the predicted heat flux response of nuclear fuel rods during a LOCA.

The test was generally conducted as specified. Conditions which did not conform to the specified test configuration were considered acceptable for analysis purposes within the test objectives. The instrumentation used generally functioned as intended. Of 211 measurements taken, 208 produced usable data.

CONTENTS

ABSTRACT ii

SUMMARY iii

I. INTRODUCTION 1

II. SYSTEM, PROCEDURES, CONDITIONS, AND EVENTS FOR TEST S-07-8 2

1. SYSTEM CONFIGURATION AND TEST PROCEDURES 2

2. INITIAL TEST CONDTIONS AND SEQUENCE OF EVENTS 5

III. DATA PRESENTATION 9

IV. REFERENCES 183

APPENDIX A — DATA ACQUISITION SYSTEM CAPABILITIES 185

APPENDIX B — POSTTEST ADJUSTMENTS TO DATA FROM SEMISCALE MOD-3 TEST S-07-8 189

1. DIFFERENTIAL PRESSURE MEASUREMENTS 191

2. DENSITY MEASUREMENTS 193

APPENDIX C — SELECTED DATA WITH ESTIMATED TOTAL UNCERTAINTY BANDS FROM SEMISCALE MOD-3 TEST S-07-8 197

FIGURES

1. Semiscale Mod-3 system for cold leg break configuration — isometric 3

2. Semiscale Mod-3 system for cold leg break configuration — schematic 4

3. Semiscale Mod-3 system and instrumentation for cold leg break configuration — isometric 10

4. Semiscale Mod-3 system and instrumentation for cold leg break configuration — schematic 11

5. Semiscale Mod-3 pressure vessel and downcomer — cross section showing instrumentation 12

6. Semiscale Mod-3 pressure vessel — isometric showing instrumentation 13

7. Semiscale Mod-3 pressure vessel — penetrations and instrumentation 14

8. Semiscale Mod-3 downcomer — isometric showing instrumentation 15

9. Semiscale Mod-3 downcomer — penetrations and instrumentation 16

10. Semiscale Mod-3 heater core — plan view 17

11. Fluid temperature in intact loop hot leg (RFI-2 and TFI-1), from -20 to 260 s 28

12. Fluid temperature in intact loop hot leg (RFI-2 and TFI-1), from -6 to 42 s 28

13. Fluid temperature in intact loop cold leg (TFI-11), from -20 to 260 s 29

14. Fluid temperature in intact loop cold leg (TFI-11), from -6 to 42 s 29

15. Fluid temperature in intact loop cold leg (RFI-17 and TFI-17), from -20 to 260 s 30

16. Fluid temperature in intact loop cold leg (RFI-17 and TFI-17), from -6 to 42 s 30

17. Fluid temperature in broken loop hot leg (RFB-20 and TFB-20), from -20 to 260 s 31

18. Fluid temperature in broken loop hot leg (RFB-20 and TFB-20), from -6 to 42 s 31

19. Fluid temperature in broken loop cold leg (TFB-37), from -20 to 260 s 32

20. Fluid temperature in broken loop cold leg (TFB-37), from -6 to 42 s 32

21. Fluid temperature in broken loop cold leg (TFB-40), from -20 to 260 s 33

22. Fluid temperature in broken loop cold leg (TFB-40), from -6 to 42 s 33

23. Fluid temperature in broken loop cold leg (RFB-45 and TFB-45), from -20 to 260 s 34

24. Fluid temperature in broken loop cold leg (RFB-45 and TFB-45), from -6 to 42 s 34

25. Fluid temperature in downcomer (TFD-18F, TFD-153, TFD-294, TFD-364, and TFD-435), from -20 to 260 s 35

26. Fluid temperature in downcomer (TFD-18F, TFD-153, TFD-294, TFD-364, and TFD-435), from -6 to 42 s 35

27. Fluid temperature in vessel (TFV + 221Q), from -20 to 260 s 36

28. Fluid temperature in vessel (TFV + 221Q), from -6 to 42 s 36

29. Fluid temperature in vessel (TFV-11 and TFV-63R), from -20 to 260 s 37

30. Fluid temperature in vessel (TVF-11 and TFV-63R), from -6 to 42 s 37

31. Fluid temperature in vessel (TFV-552A, TFV-572W, and TFV-578A), from -20 to 260 s 38

32. Fluid temperature in vessel (TFV-552A, TFV-572W, and TFV-578A), from -6 to 42 s 38

33. Fluid temperature in vessel filler insulator gap (TIFV + 79D), from -20 to 260 s 39

34. Fluid temperature in vessel filler insulator gap (TIFV + 79D), from -6 to 42 s 39

35. Fluid temperature in vessel, core guide tube (TFGV + 330), from -20 to 260 s 40

36. Fluid temperature in vessel, core guide tube (TFGV + 330), from -6 to 42 s 40

37. Fluid temperature in vessel support tube (TFSV + 148D), from -20 to 260 s 41

38. Fluid temperature in vessel support tube (TFSV + 148D), from -6 to 42 s 41

39. Fluid temperature in core, Grid Spacer 1 (TFG-1AB-12), from -20 to 260 s 42

40. Fluid temperature in core, Grid Spacer 1 (TFG-1AB-12), from -6 to 42 s 42

41. Fluid temperature in core, Grid Spacer 3 (TFG-3AB-12), from -20 to 260 s 43

42. Fluid temperature in core, Grid Spacer 3 (TFG-3AB-12), from -6 to 42 s 43

43. Fluid temperature in core, Grid Spacer 5 (TFG-5AB-45), from -20 to 260 s 44

44. Fluid temperature in core, Grid Spacer 5 (TFG-5AB-45), from -6 to 42 s 44

45. Fluid temperature in core, Grid Spacer 6 (TFG-6BC-34), from -20 to 260 s 45

46. Fluid temperature in core, Grid Spacer 6 (TFG-6BC-34), from -6 to 42 s 45

47. Fluid temperature in core, Grid Spacer 8 (TFG-8AB-23), from -20 to 260 s 46

48. Fluid temperature in core, Grid Spacer 8 (TFG-8AB-23), from -6 to 42 s 46

49. Fluid temperature in core, Grid Spacer 10 (TFG-10AB-45), from -20 to 260 s 47

50. Fluid temperature in core, Grid Spacer 10 (TFG-10AB-45), from -6 to 42 s 47

51. Fluid temperature in vessel accumulator, coolant injection line (TFV-ECC-LP), from -20 to 260 s 48

52. Fluid temperature in vessel accumulator, coolant injection line (TFV-ECC-LP), from -6 to 42 s 48

53. Fluid temperature in intact loop steam generator, secondary feedwater line TFI-SGFW), from -20 to 260 s 49

54. Fluid temperature in intact loop steam generator, secondary feedwater line (TFI-SGFW), from -6 to 42 s 49

55. Fluid temperature in intact loop steam generator, secondary side steam dome (TFI-SD), from -20 to 260 s 50

56. Fluid temperature in intact loop steam generator, secondary side steam dome (TFI-SD), from -6 to 42 s 50

57. Fluid temperature in broken loop, pressure suppression system tank (TFB-PS43 and TFB-PS330), from -20 to 260 s 51

58. Fluid temperature in broken loop, pressure suppression system tank (TFB-PS43 and TFB-PS330), from -6 to 42 s 51

59. Material temperat... intact loop (TMI-1T16 and TMI-17S16), from -20 to 260 s 52

60. Material temperature in intact loop (TMI-1T16 and TMI-17S16), from -6 to 42 s 52

61. Material temperature in broken loop (TMB-20B16), from -20 to 260 s 53

62. Material temperature in broken loop (TMB-20B16), from -6 to 42 s 53

63. Mate ial temperature in b oken loop (TMB-40B16 and TMB-45B16), from -20 to 260 s 54

64. Material temperature in broken loop (TMB-40B16 and TMB-45B16), from -6 to 42 s 54

65. Material temperature in downcomer (TMD-18F, TMD-152, and TMD-364), from -20 to 260 s 55

66. Material temperature in downcomer (TMD-18F, TMD-152, and TMD-364), from -6 to 42 s 55

67. Material temperature in downcomer insulator (TIMD-18F, TIMD-152, TIMD-294, and TIMD-364), from -20 to 260 s 56

68. Material temperature in downcomer insulator (TIMD-18F, TIMD-152, TIMD-294, and TIMD-364), from -6 to 42 s 56

69. Material temperature in upper vessel (TMV + 221F and TMV + 79D), from -20 to 260 s 57

70. Material temperature in upper vessel (TMV + 221F and TMV + 79D), from -6 to 42 s 57

71. Material temperature in vessel, core guide tube (TGMV + 280 and TGMV-63), from -20 to 260 s 58

72. Material temperature in vessel, core guide tube (TGMV + 280 and TGMV-63), from -6 to 42 s 58

73. Material temperature in intact loop, steam generator tube (TMI-SGT61), from -20 to 260 s 59

74. Material temperature in intact loop, steam generator tube (TMI-SGT61), from -6 to 42 s 59

75. Material temperature in broken loop, steam generator tube (TMB-SGT734), from -20 to 260 s 60

76. Material temperature in broken loop, steam generator tube TMB-SGT734), from -6 to 42 s 60

77. Core heater temperature, Rod B-3 (TH-B3-180, TH-B3-226, and TH-B3-353), from -20 to 260 s 61

78. Core heater temperature, Rod B-3 (TH-B3-180, TH-B3 '26, and TH-B3-353), from -6 to 42 s 61

79. Core heater temperature, Rod C-2 (TH-C2-8, TH-C2-164, TH-C2-180, TH-C2-277, and TH-C2-321), from -20 to 260 s 62

80. Core heater temperature, Rod C-2 (TH-C2-8, TH-C2-164, TH-C2-180, TH-C2-277, and TH-C2-321), from -6 to 42 s 62

81. Core heater temperature, Rod C-3 (TH-C3-49, TH-C3-115, TH-C3-184, TH-C3-194, and TH-C3-230), from -20 to 260 s 63

82. Core heater temperature, Rod C-3 (TH-C3-49, TH-C3-115, TH-C3-184, TH-C-3-194, and TH-C3-230), from -6 to 42 s 63

83. Core heater temperature, Rod D-2 (TH-D2-10, TH-D2-134, TH-D2-166, TH-D2-179, and TH-D2-254), from -20 to 260 s 64

84. Core heater temperature, Rod D-2 (TH-D2-10, TH-D2-134, TH-D2-166, TH-D2-179, and TH-D2-254), from -6 to 42 s 64

85. Core heater temperature, Rod D-3 (TH-D3-71, TH-D3-132, TH-D3-206, and TH-D3-226), from -20 to 260 s 65

86. Core heater temperature, Rod D-3 (TH-D3-71, TH-D3-132, TH-D3-206, and TH-D3-226), from -6 to 42 s 65

87. Core heater temperature, Rod A-3 (TH-A3-208, TH-A3-229, and TH-A3-291), from -20 to 260 s 66

88. Core heater temperature, Rod A-3 (TH-A3-208, TH-A3-229, and TH-A3-291), from -6 to 42 s 66

89. Core heater temperature, Rod A-4 (TH-A4-40, TH-A4-108, TH-A4-181, and TH-A4-191), from -20 to 260 s 67

90. Core heater temperature, Rod A-4 (TH-A4-40, TH-A4-108, TH-A4-181, and TH-A4-191), from -6 to 42 s 67

91. Core heater temperature, Rod A-5 (TH-A5-164, TH-A5-179, and TH-A5-252), from -20 to 260 s 68

92. Core heater temperature, Rod A-5 (TH-A5-164, TH-A5-179, and TH-A5-252), from -6 to 42 s 68

93. Core heater temperature, Rod B-1 (TH-B1-321), from -20 to 260 s 69

94. Core heater temperature, Rod B-1 (TH-B1-321), from -6 to 42 s 69

95. Core heater temperature, Rod D-1 (TH-D1-178 and TH-D1-251), from -20 to 260 s 70

96. Core heater temperature, Rod D-1 (TH-D1-178 and TH-D1-251), from -6 to 42 s 70

97. Core heater temperature, Rod D-5 (TH-D5-137, TH-D5-179, TH-D5-254, and TH-D5-322), from -20 to 260 s 71

98. Core heater temperature, Rod D-5 (TH-D5-137, TH-D5-179, TH-D5-254, and TH-D5-322), from -6 to 42 s 71

99. Core heater temperature, Rod E-1 (TH-E1-252 and TH-E1-321), from -20 to 260 s 72

100. Core heater temperature, Rod E-1 (TH-E1-252 and TH-E1-321), from -6 to 42 s 72

101. Core heater temperature, Rod E-2 (TH-E2-109, TH-E2-190, and TH-E2-353), from -20 to 260 s 73

102. Core heater temperature, Rod E-2 (TH-E2-109, TH-E2-190, and TH-E2-353), from -6 to 42 s 73

103. Core heater temperature, Rod E-3 (TH-E3-134, TH-E3,207, TH-E3-223, and TH-E3-290), from -20 to 260 s 74

104. Core heater temperature, Rod E-3 (TH-E3-134, TH-E3-207, TH-E3-223, and TH-E3-290), from -6 to 42 s 74

105. Core heater temperature, Rod E-4 (TH-E4-180 and TH-E4-354), from -20 to 260 s 75

106. Core heater temperature, Rod E-4 (TH-E4-180 and TH-E4-354) from -6 to 42 s 75

107. Core heater temperature, Rod E-5 (TH-E5-227), from -20 to 260 s 76

108. Core heater temperature, Rod E-5 (TH-E5-227), from -6 to 42 s 76

109. Pressure in intact loop cold leg (PI-16 and PI-17AL), from -20 to 260 s 77

110. Pressure in intact loop cold leg (PI-16 and PI-17AL), from -6 to 42 s 77

111. Pressure in broken loop hot leg (PB-20B), from -20 to 260 s 78

112. Pressure in broken loop hot leg (PB-20B), from -6 to 42 s 78

113. Pressure in broken loop cold leg, pump side (PB-40B), from -20 to 260 s 79

114. Pressure in broken loop cold leg, pump side (PB-40B), from -6 to 42 s 79

115. Pressure in broken loop blowdown nozzle (PB-44-6A), from -20 to 260 s 80

116. Pressure in broken loop blowdown nozzle (PB-44-6A), from -6 to 42 s 80

117. Pressure in broken loop cold leg, vessel side (PB-45A), from -20 to 260 s 81

118. Pressure in broken loop cold leg, vessel side (PB-45A), from -6 to 42 s 81

119. Pressure in vessel upper and lower plenum (PV-13 and PV-442), from -20 to 260 s 82

120. Pressure in vessel upper and lower plenum (PV-13 and PV-442), from -6 to 42 s 82

121. Pressure in vessel ECC injection accumulator (PV-ACC1), from -20 to 260 s 83

122. Pressure in vessel ECC injection accumulator (PV-ACC1), from -6 to 42 s 83

123. Pressure in system steam generators, secondary side steam dome (PI-SD and PB-SD), from -20 to 260 s 84

124. Pressure in system steam generators, secondary side steam dome (PI-SD and PB-SD), from -6 to 42 s 84

125. Pressure in pressurizer (PI-PRIZE), from -20 to 260 s 85

126. Pressure in pressurizer (PI-PRIZE), from -6 to 42 s 85

127. Pressure in broken loop pressure suppression tank (PB-PSS), from -20 to 260 s 86

128. Pressure in broken loop pressure suppression tank (PB-PSS), from -6 to 42 s 86

129. Differential pressure in intact loop (DI-13V-1A), from -20 to 260 s 87

130. Differential pressure in intact loop (DI-13V-1A), from -6 to 42 s 87

131. Differential pressure in intact loop (DI-1A-6), from -20 to 260 s 88

132. Differential pressure in intact loop (DI-1A-6), from -6 to 42 s 88

133. Differential pressure in intact loop (DI-6-7), from -20 to 260 s 89

134. Differential pressure in intact loop (DI-6-7), from -6 to 42 s 89

135. Differential pressure in intact loop steam generator, inlet plenum to outlet plenum (DI-SGI-SGO), from -20 to 260 s 90

136. Differential pressure in intact loop steam generator, inlet plenum to outlet plenum (DI-SGI-SGO), from -6 to 42 s 90

137. Differential pressure in intact loop (DI-7-13), from -20 to 260 s 91

138. Differential pressure in intact loop (DI-7-13), from -6 to 42 s 91

139. Differential pressure in intact loop (DI-13-15), from -20 to 260 s 92

140. Differential pressure in intact loop (DI-13-15), from -6 to 42 s 92

141. Differential pressure in intact loop (DI-15-17A), from -20 to 260 s 93

142. Differential pressure in intact loop (DI-15-17A), from -6 to 42 s 93

143. Differential pressure in intact loop (DI-17A-DIA), from -20 to 260 s 94

144. Differential pressure in intact loop (DI-17A-DIA), from -6 to 42 s 94

145. Differential pressure in broken loop (DB-13V-20B), from -20 to 260 s 95

146. Differential pressure in broken loop (DB-13V-20B), from -6 to 42 s 95

147. Differential pressure in broken loop (DB-20B-21), from -20 to 260 s 96

544 012

148. Differential pressure in broken loop (DB-2JB-21), from -6 to 42 s 96

149. Differential pressure in broken loop (DB-21-27A), from -20 to 260 s 97

150. Differential pressure in broken loop (DB-21-27A), from -6 to 42 s 97

151. Differential pressure in broken loop steam generator (DB-SGI-SGO), from -20 to 260 s 98

152. Differential pressure in broken loop steam generator (DB-SGI-SGO), from -6 to 42 s 98

153. Differential pressure in broken loop (DB-27A-37A), from -20 to 260 s 99

154. Differential pressure in broken loop (DB-27A-37A), from -6 to 42 s 99

155. Differential pressure in broken loop (DB-37A-40B), from -20 to 260 s 100

156. Differential pressure in broken loop (DB-37A-40B), from -6 to 42 s 100

157. Differential pressure in broken loop (DB-37A-40L), from -20 to 260 s 101

158. Differential pressure in broken loop (DB-37A-40L), from -6 to 42 s 101

159. Differential pressure in broken loop (DB-40B-43A), from -20 to 260 s 102

160. Differential pressure in broken loop (DB-40B-43A), from -6 to 42 s 102

161. Differential pressure in broken loop (DB-40B-45A), from -20 to 260 s 103

162. Differential pressure in broken loop (DB-40B-45A), from -6 to 42 s 103

163. Differential pressure in broken loop (DB-45A-43), from -20 to 260 s 104

164. Differential pressure in broken loop (DB-45A-43), from -6 to 42 s 104

165. Differential pressure in broken loop (DB-45A-DIA), from -20 to 260 s 105

166. Differential pressure in broken loop (DB-45A-DIA), from -6 to 42 s 105

167. Differential pressure in downcomer (DD-DIA-13V), from -20 to 260 s 106

168. Differential pressure in downcomer (DD-DIA-13V), from -6 to 42 s 106

169. Differential pressure in downcomer (DD-DIA-170), from -20 to 260 s 107

170. Differential pressure in downcomer (DD-DIA-170), from -6 to 42 s 107

171. Differential pressure in downcomer (DD-DIA-578), from -20 to 260 s 108

172. Differential pressure in downcomer (DD-DIA-578), from -6 to 42 s 108

173. Differential pressure in downcomer (DD-170-435), from -20 to 260 s 109

174. Differential pressure in downcomer (DD-170-435), from -6 to 42 s 109

175. Differential pressure in downcome. (DD-435-578), from -20 to 260 s 110

176. Differential pressure in downcomer (DD-435-578), from -6 to 42 s 110

177. Differential pressure in vessel (DV-578-501), from -20 to 260 s 111

178. Differential pressure in vessel (DV-578-501), from -6 to 42 s 111

179. Differential pressure in vessel (DV-578-13), from -20 to 260 s 112

180. Differential pressure in vessel (DV-578-13), from -6 to 42 s 112

181. Differential pressure in vessel (DV-501-442), from -20 to 260 s 113

182. Differential pressure in vessel (DV-501-442), from -6 to 42 s 113

183. Differential pressure in vessel (DV-501-105), from -20 to 260 s 114

184. Differential pressure in vessel (DV-501-105), from -6 to 42 s 114

185. Differential pressure in vessel (DV-501-13A), from -20 to 260 s 115

186. Differential pressure in vessel (DV-501-13A), from -6 to 42 s 115

187. Differential pressure in vessel (DV-442-278), from -20 to 260 s 116

188. Differential pressure in vessel (DV-442-278), from -6 to 42 s 116

189. Differential pressure in vessel (DV-278-154), from -20 to 260 s 117

190. Differential pressure in vessel (DV-278-154), from -6 to 42 s 117

191. Differential pressure in vessel (DV-105-13), from -20 to 260 s 118

192. Differential pressure in vessel (DV-105-13), from -6 to 42 s 118

193. Differential pressure in vessel (DV + 421 + 154), from -20 to 260 s 119

194. Differential pressure in vessel (DV + 421 + 154), from -6 to 42 s 119

195. Differential pressure in vessel (DV + 159-105), from -20 to 260 s 120

196. Differential pressure in vessel (DV + 159-105), from -6 to 42 s 120

197. Differential pressure in vessel (DV + 154-105), from -20 to 260 s 121

198. Differential pressure in vessel (DV + 154-105), from -6 to 42 s 121

199. Differential pressure in vessel ECC accumulator (DV-ACC1-LL), from -20 to 260 s 122

200. Differential pressure in vessel ECC accumulator (DV-ACC1-LL), from -6 to 42 s 122

201. Differential pressure in intact loop steam generator, secondary side liquid level (DI-SG-LL), from -20 to 260 s 123

202. Differential pressure in intact loop steam generator, secondary side liquid level (DI-SG-LL), from -6 to 42 s 123

203. Differential pressure in broken loop steam generator, secondary liquid level (DB-SS1-SS4), from -20 to 260 s 124

204. Differential pressure in broken loop steam generator, secondary liquid level (DB-SS1-SS4), from -6 to 42 s 124

205. Volumetric flow in intact loop (FI-1 and FI-11), from -20 to 260 s 125

206. Volumetric flow in intact loop (FI-1 and FI-11), from -6 to 42 s 125

207. Volumetric flow in intact loop (FI-16 and FI-17), from -20 to 260 s 126

208. Volumetric flow in intact loop (FI-16 and FI-17), from -6 to 42 s 126

209. Volumetric flow in broken loop (FB-20 and FB-37), from -20 to 260 s 127

210. Volumetric flow in broken loop (FB-20 and FB-37), from -6 to 42 s 127

211. Volumetric flow in broken loop (FB-40 and FB-45), from -20 to 260 s 128

212. Volumetric flow in broken loop (FB-40 and FB-45), from -6 to 42 s 128

213. Volumetric flow in downcomer (FD-424), from -20 to 260 s 129

214. Volumetric flow in downcomer (FD-424), from -6 to 42 s 129

215. Volumetric flow in vessel upper plenum (FV + 1), from -20 to 260 s 130

216. Volumetric flow in vessel upper plenum (FV + 1), from -6 to 42 s 130

217. Volumetric flow in vessel, high pressure injection system (FV-HPIS), from -20 to 260 s 131

218. Volumetric flow in vessel, high pressure injection system (FV-HPIS), from -6 to 42 s 131

219. Volumetric flow in vessel, low pressure injection system (FV-LPIS), from -20 to 260 s 132

220. Volumetric flow in vessel, low pressure injection system (FV-LPIS), from -6 to 42 s 132

221. Volumetric flow in vessel, ECC accumulator (FV-ACC1), from -20 to 260 s 133

222. Volumetric flow in vessel, ECC accumulator (FV-ACC1), from -6 to 42 s 133

223. Volumetric flow in intact loop, pressurizer surge line (FI-PRIZE), from -20 to 260 s 134

224. Volumetric flow in intact loop, pressurizer surge line (FI-PRIZE), from -6 to 42 s 134

225. Momentum flux in broken loop (NB-20), from -20 to 260 s 135

226. Momentum flux in broken loop (NB-20), from -6 to 42 s 135

227. Momentum flux in broken loop (NB-40), from -20 to 260 s 136

228. Momentum flux in broken loop (NB-40), from -6 to 42 s 136
229. Momentum flux in broken loop (NB-45), from -20 to 260 s 137
230. Momentum flux in broken loop (NB-45), from -6 to 42 s 137
231. Momentum flux in core outlet (NV-9), from -20 to 260 s 138
232. Momentum flux in core outlet (NV-9), from -6 to 42 s 138
233. Momentum flux in core inlet (NV-499), from -20 to 260 s 139
234. Momentum flux in core inlet (NV-499), from -6 to 42 s 139
235. Density in intact loop (GI-1T and GI-1B), from -20 to 260 s 140
236. Density in intact loop (GI-1T and GI-1B), from -6 to 42 s 140
237. Density in intact loop (GI-1C), from -20 to 260 s 141
238. Density in intact loop (GI-1C), from -6 to 42 s 141
239. Density in intact loop (GI-5VR), from -20 to 260 s 142
240. Density in intact loop (GI-5VR), from -6 to 42 s 142
241. Density in intact loop (GI-13T and GI-13B), from -20 to 260 s 143
242. Density in intact loop (GI-13T and GI-13B), from -6 to 42 s 143
243. Density in intact loop (GI-13C), from -20 to 260 s 144
244. Density in intact loop (GI-13C), from -6 to 42 s 144
245. Density in intact loop (GI-17T and GI-17B), from -20 to 260 s 145
246. Density in intact loop (GI-17T and GI-17B), from -6 to 42 s 145
247. Density in intact loop (GI-17C), from -20 to 260 s 146
248. Density in intact loop (GI-17C), from -6 to 42 s 146
249. Density in broken loop (GB-37), from -20 to 260 s 147
250. Density in broken loop (GB-37), from -6 to 42 s 147
251. Density in broken loop (GB-40VR), from -20 to 260 s 148
252. Density in broken loop (GB-40VR), from -6 to 42 s 148
253. Density in broken loop (GB-45VR), from -20 to 260 s 149
254. Density in broken loop (GB-45VR), from -6 to 42 s 149
255. Density in downcomer (GD-72B), from -20 to 260 s 150

256. Density in downcomer (GD-72B), from -6 to 42 s 150
257. Density in downcomer (GD-260B), from -20 to 260 s 151
258. Density in downcomer (GD-260B), from -6 to 42 s 151
259. Density in downcomer (GD-456B), from -20 to 260 s 152
260. Density in downcomer (GD-456B), from -6 to 42 s 152
261. Density in vessel (GV + 339), from -20 to 260 s 153
262. Density in vessel (GV + 339), from -6 to 42 s 153
263. Density in vessel (GV + 174), from -20 to 260 s 154
264. Density in vessel (GV + 174), from -6 to 42 s 154
265. Density in vessel (GV-11), from -20 to 260 s 155
266. Density in vessel (GV-11), from -6 to 42 s 155
267. Density in vessel (GV-154-23 and GV-164-AB), from -20 to 260 s 156
268. Density in vessel (GV-154-23 and GV-164-AB), from -6 to 42 s 156
269. Density in vessel (GV-243-23), from -20 to 260 s 157
270. Density in vessel (GV-243-23), from -6 to 42 s 157
271. Density in vessel (GV-313-23 and GV-323-AB), from -20 to 260 s 158
272. Density in vessel (GV-313-23 and GV-323-AB), from -6 to 42 s 158
273. Density in vessel (GV-383-23), from -20 to 260 s 159
274. Density in vessel (GV-383-23), from -6 to 42 s 159
275. Density in vessel (GV-483-23), from -20 to 260 s 160
276. Density in vessel (GV-483-23), from -6 to 42 s 160
277. Density in vessel (GV-528-588), from -20 to 260 s 161
278. Density in vessel (GV-528-588), from -6 to 42 s 161
279. Density in vessel (GV-546-23), from -20 to 260 s 162
280. Density in vessel (GV-546-23), from -6 to 42 s 162
281. Density in intact loop pressurizer (GI-PRIZE), from -20 to 260 s 163
282. Density in intact loop pressurizer (GI-PRIZE), from -6 to 42 s 163
283. Mass flow in intact loop (FI-1 and GI-1C), from -20 to 260 s 164

544 017

284. Mass flow in intact loop (FI-1 and GI-1C), from -6 to 42 s 164
285. Mass flow in intact loop (FI-16 and GI-17C), from -20 to 260 s 165
286. Mass flow in intact loop (FI-16 and GI-17C), from -6 to 42 s 165
287. Mass flow in intact loop (FI-17 and GI-17C), from -20 to 260 s 166
288. Mass flow in intact loop (FI-17 and GI-17C), from -6 to 42 s 166
289. Mass flow in broken loop (FB-37 and GB-37), from -20 to 260 s 167
290. Mass flow in broken loop (FB-37 and GB-37), from -6 to 42 s 167
291. Mass flow in broken loop (FB-40 and GB-40VR) from -20 to 260 s 168
292. Mass flow in broken loop (FB-40 and GB-40VR), from -6 to 42 s 168
293. Mass flow in broken loop (NB-40 and GB-40VR), from -20 to 260 s 169
294. Mass flow in broken loop (NB-40 and GB-40VR), from -6 to 42 s 169
295. Mass flow in broken loop (FB-45 and GB-45), from -20 to 260 s 170
296. Mass flow in broken loop (FB-45 and GB-45), from -6 to 42 s 170
297. Mass flow in broken loop (NB-45 and GB-45), from -20 to 260 s 171
298. Mass flow in broken loop (NB-45 and GB-45), from -6 to 42 s 171
299. Mass flow in downcomer (FD-424 and GD-456B), from -20 to 260 s 172
300. Mass flow in downcomer (FD-424 and GD-456B), from -6 to 42 s 172
301. Mass flow in vessel (FV + 1 and GV-11), from -20 to 260 s 173
302. Mass flow in vessel (FV + 1 and GV-11), from -6 to 42 s 173
303. Mass flow in vessel (NV-9 and GV-11), from -20 to 260 s 174
304. Mass flow in vessel (NV-9 and GV-11), from -6 to 42 s 174
305. Mass flow in vessel (NV-499 and GV-483-23), from -20 to 260 s 175
306. Mass flow in vessel (NV-499 and GV-483-23), from -6 to 42 s 175
307. Core heater high power bus amperage (AH-HI), from -20 to 260 s 176
308. Core heater high power bus amperage (AH-HI), from -6 to 42 s 176
309. Core heater high power bus voltage (VH-HI), from -20 to 260 s 177
310. Core heater high power bus voltage (VH-HI), from -6 to 42 s 177
311. Core heater low power bus amperage (AH-LO), from -20 to 260 s 178

312. Core heater low power bus amperage (AH-LO), from -6 to 42 s 178

313. Core heater low power bus voltage (VH-LO), from -20 to 260 s 179

314. Core heater low power bus voltage (VH-LO), from -6 to 42 s 179

315. Intact loop pump speed (SI-PUMP), from -20 to 260 s 180

316. Intact loop pump speed (SI-PUMP), from -6 to 42 s 180

317. Broken loop pump speed (SB-PUMP), from -20 to 260 s 181

318. Broken loop pump speed (SB-PUMP), from -6 to 42 s 181

319. Broken loop pump power (WB-PUMP), from -20 to 260 s 182

320. Broken loop pump power (WB-PUMP), from -6 to 42 s 182

B-1. Geometry used for processing of density data obtained from two-beam gamma densitometers 194

C-1. Fluid temperature in intact loop (TFI-1) 206

C-2. Fluid temperature in broken loop (TFB-20) 206

C-3. Fluid temperature in downcomer (TFD-294) 207

C-4. Fluid temperature in vessel (TFV-578A) 207

C-5. Fluid temperature in vessel (TIFV + 79D) 208

C-6. Fluid temperature in core, Grid Spacer 5 (TFG-5AB-45) 208

C-7. Material temperature in intact loop hot leg (TMI-1T16) 209

C-8. Material temperature in broken loop hot leg (TMB-20B16) 209

C-9. Material temperature in downcomer (TMD-364) 210

C-10. Material temperature in vessel (TMV + 79D) 210

C-11. Core heater temperature, Rod C-2 (TH-C2-8) 211

C-12. Core heater temperature, Rod C-2 (TH-C2-180) 211

C-13. Pressure in intact loop cold leg (PI-16) 212

C-14. Pressure in broken loop cold leg (PB-45A) 212

C-15. Pressure in vessel accumulator (PV-ACC1) 213

C-16. Pressure in broken loop steam generator, secondary side steam dome (PB-SD) 213

C-17. Differential pressure in intact loop (DI-6-7) 214

544 019

C-18. Differential pressure in intact loop (DI-7-13) 214

C-19. Differential pressure in broken loop (DB-37A-40L) 215

C-20. Differential pressure in downcomer (DD-DIA-578) 215

C-21 Differential pressure in vessel (DV-501-105) 216

C-22. Differential pressure in intact loop steam generator, secondary side liquid level (DV-501-442) 216

C-23. Volumetric flow in intact loop (FI-1) 217

C-24. Volumetric flow in intact loop (FI-1) 217

C-25. Volumetric flow in broken loop (FB-45) 218

C-26. Volumetric flow in downcomer (FD-424) 218

C-27. Volumetric flow in vessel upper plenum (FV + 1) 219

C-28. Volumetric flow in vessel lower plenum, low pressure injection system (FV-LPIS) 219

C-29. Density in intact loop (GI-1T) 220

C-30. Density in intact loop (GI-1B) 220

C-31. Density in intact loop (GI-1C) 221

C-32. Density in intact loop (GI-17T) 221

C-33. Density in intact loop (GI-17B) 222

C-34. Density in intact loop (GI-17C) 222

C-35. Density in broken loop (GB-45VR) 223

C-36. Density in vessel (GV-11) 223

C-37. Mass flow in intact loop (FI-1 and GI-1C) 224

C-38. Mass flow in intact loop (FI-17 and GI-17C) 224

C-39. Mass flow in broken loop (FB-45 and GB-45VR) 225

C-40. Mass flow in vessel (FV + 1 and GV-11) 225

TABLES

I. Conditions at Blowdown Initiation 6

II. Primary Coolant Temperature Distribution Prior to Rupture 7

III. Sequence of Events During Test S-07-8 8

IV. Data Presentation for Semiscale Mod-3 Test S-07-8 18

B-I. Constants for Differential Pressure Measurement Corrections 192

C-I. Random Uncertainty Standard Deviation 201

C-II. General Measurement Engineering Uncertainty Sources and Uncertainty Values 226

C-III. Time Periods When Flow Regime Uncertainties Were Applied 231

EXPERIMENT DATA REPORT FOR SEMISCALE MOD-3 LOWER PLENUM INJECTION TEST S-07-8 (BASELINE TEST SERIES)

I. INTRODUCTION

The Semiscale Mod-3 experiments represent the current phase of the Semiscale Program conducted by EG&G Idaho, Inc., for the United States Government. The program, which is sponsored by the Nuclear Regulatory Commission through the Department of Energy, is part of the overall program designed to investigate the response of a pressurized water reactor (PWR) system to a hypothesized loss-of-coolant accident (LOCA). The underlying objectives of the Semiscale Program are to quantify the physical processes controlling system behavior during a LOCA and to provide an experimental data base for assessing reactor safety evaluation models. The Semiscale Mod-3 Program has the further objective of providing support to other experimental programs in the form of instrumentation assessment, optimization of test series, selection of test parameters, and evaluation of test results.

Test S-07-8 was conducted March 16, 1979, in the Semiscale Mod-3 system as part of the baseline test series (Test Series 7). This series was designed to obtain thermal-hydraulic response data from blowdown, refill, and reflood transients in a simulated nuclear reactor having an electrically heated core. The specific objective of Test S-07-8 was to provide reference data to evaluate integral blowdown and reflood behavior during a 200% cold leg break with emergency core coolant (ECC) injection into the vessel lower plenum of the Mod-3 system. Hardware configuration and test parameters were selected to yield a system response that simulates the response of a PWR to a hypothesized LOCA blowdown transient.

The purpose of this report is to present the test in an uninterpreted but readily usable form for use by the nuclear community in advance of detailed analysis and interpretation. Section II briefly describes the system configuration, procedures, and initial test conditions, and events that are applicable to Test S-07-8; Section III presents the data graphs and provides comments and supporting information necessary for interpretation of the data. A description of the overall Semiscale Program and test series, a more detailed description of the Semiscale Mod-3 system, and a description of the measurement and data processing techniques and uncertainties can be found in References 1 and 2.

II. SYSTEM, PROCEDURES, CONDITIONS, AND EVENTS FOR TEST S-07-8

The following system configuration, procedures, initial test conditions, and events are specific to Test S-07-8 as indicated.

1. SYSTEM CONFIGURATION AND TEST PROCEDURES

The Semiscale Mod-3 system used for the test consisted of a pressure vessel with simulated reactor internals, including a 25-rod core with 23 electrically heated rods and an external downcomer assembly; an intact loop with steam generator, pump, and pressurizer; a broken loop with steam generator, pump, and rupture assembly; high and low pressure injection pumps and coolant injection accumulator for the vessel lower plenum; and a pressure suppression system with a suppression tank, header, and steam supply system. The Semiscale Mod-3 experimental system configuration is described further in Reference 2. Figures 1 and 2 show the system configuration for the test.

For Test S-07-8, the nine center rods were powered 12.5% higher than the remaining 14 low powered rods, resulting in high and low power rod peak densities of 39.5 kW/m and 35.1 kW/m, respectively. The total core power was 1.99 MW. One rod (Rod E-5) was unpowered and another rod (Rod A-1) was replaced by a liquid level probe.

In preparation for the test, the system was filled with treated demineralized water and vented at strategic points to ensure a liquid-full system. Treated demineralized water in the steam generator feedwater tank was heated to 490 K, and the required levels were established in the steam generator secondary sides. The accumulator for the vessel lower plenum was filled with treated demineralized water, drained to specified initial levels, and pressurized with nitrogen to 4.14 MPa.[a] Prior to warmup, the system was pressurized to check for leakage; system instrumentation was checked; and transducer readings were set to zero. Warmup to initial test conditions was accomplished with the heaters in the vessel core. During warmup, the purification and sampling systems were valved into the primary system to maintain water chemistry requirements and to provide a water sample at system conditions for subsequent analysis. At 50-K temperature intervals during warmup, detector readings were sampled to allow the integrity of the measurement instrumentation and the operability of the data acquisition system to be checked.

Prior to the initial core power level being established, the pressure suppression system was pressurized to 0.24 MPa with saturated steam from the steam supply system. After the core power was increased to 1.99 MW, initial test conditions were held for 915 s to establish equilibrium in the system. At the end of this period all auxiliary systems were isolated to prevent blowdown through those systems.

The system was successfully subjected to a simulated double-ended cold leg break through a rupture assembly and two blowdown nozzels having a total break area of 4.59 cm^2. Pressure to operate the rupture assembly and initiate blowdown was taken from an accumulator system filled with water and pressurized to 15.6 MPa with gaseous nitrogen. Immediately (within 0.02 s) after initiation for blowdown, the lines to the accumulator were again isolated. The effluent was ejected from the primary system into the pressure suppression system which was vented to maintain a constant pressure of 0.243 MPa. At blowdown, power to the primary coolant circulation pump was reduced and the pump was allowed to coast down to a speed of 130 rad/s which was maintained for the duration of the test. During the blowdown transient, power to the electrically heated core was automatically controlled to simulate the thermal response of nuclear heated fuel rods.

For Test S-07-8, the coolant injection systems were arranged to discharge into the vessel lower plenum. The high pressure coolant injection pumps were started at initiation of blowdown with coolant injection

a. All pressures are presented as absolute values.

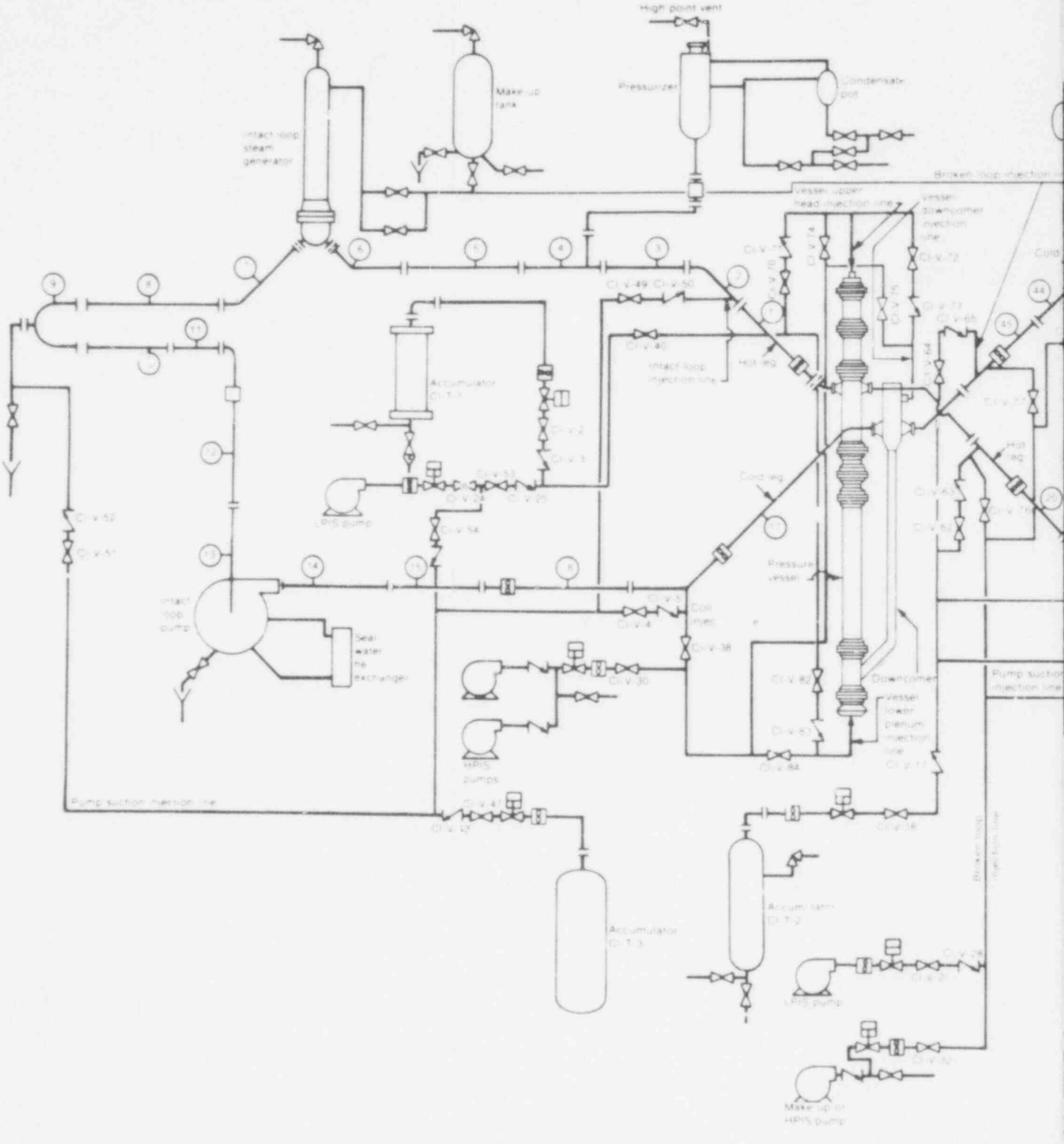

Fig. 2 Semiscale Mod-3 system for cold leg brea

544 024

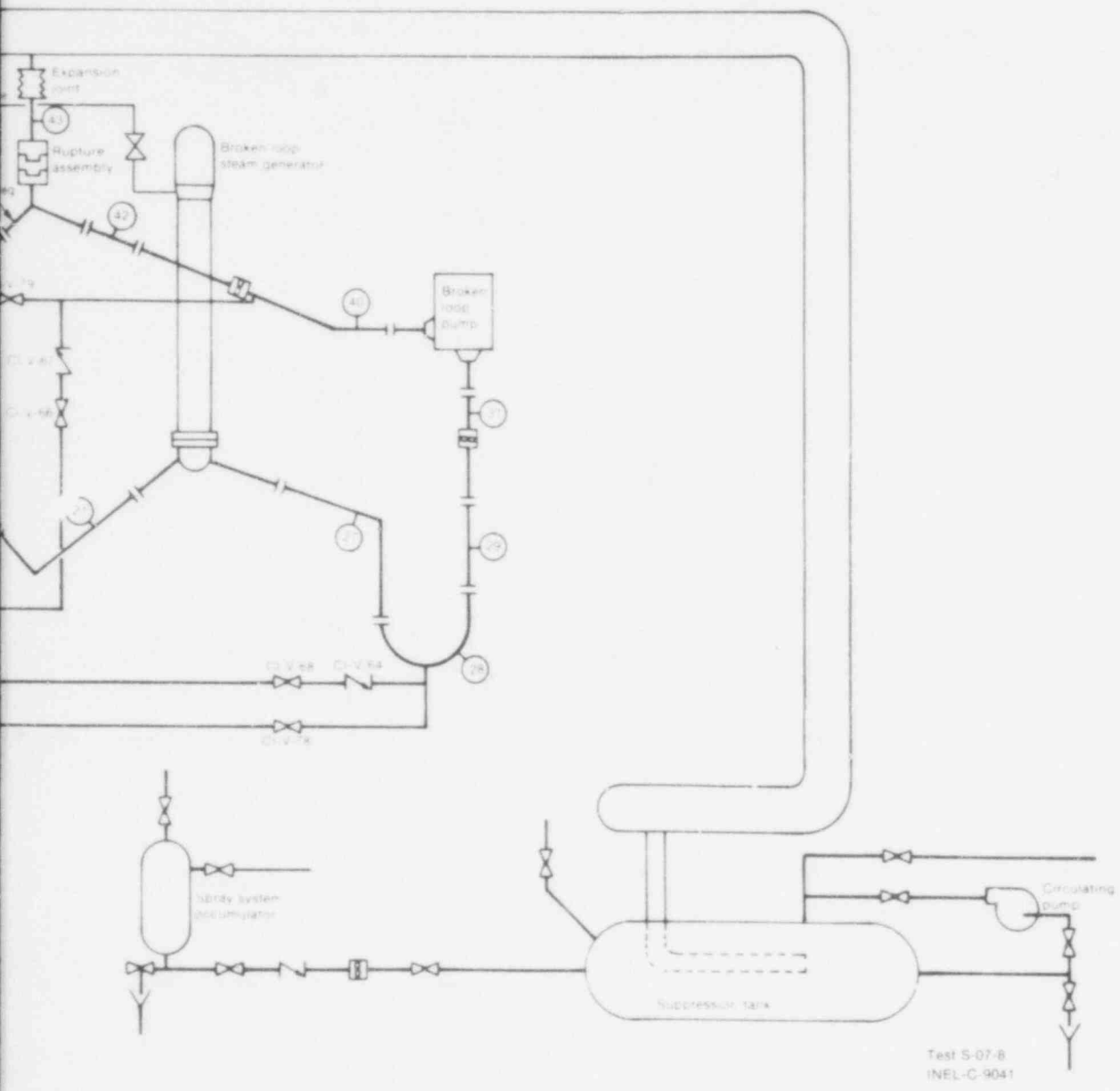

configuration — schematic.

starting at a pressure of 12.4 MPa, and continued running (as pressure descreased) until the end of the test (800 s). Low pressure coolant injection was initiated 29.5 s after blowdown at a system pressure of 1.0 MPa and continued until test termination (800 s). Coolant injection from the vessel accumulator started 19 s and terminated 55 s after blowdown. The total volume of coolant injected into the vessel from the accumulator and injection line was 46.2 l. Nitrogen was not discharged into the system.

2. INITIAL TEST CONDITIONS AND SEQUENCE OF EVENTS

Conditions in the Semiscale Mod-3 system at initiation of blowdown are given in Tables I and II, and the sequence of events relative to rupture is given in Table III.

TABLE I

CONDITIONS AT BLOWDOWN INITIATION

	Test S-07-8	
	Measured[a]	Specified
Core power (MW)	1.99	2.0 ± 0.05
System pressure (MPa)	15.73	15.51 ± 0.12
Intact loop cold leg fluid temperature (K)	556	557 ± 1
Broken loop cold leg fluid temperature (K)	559	557 ± 1
Intact loop hot leg to cold leg temperature differential (K)	38	37 ± 1
Broken loop hot leg to cold leg temperature differential (K)	36	37 ± 1
Intact loop cold leg flow (l/s)	9.14	b
Broken loop cold leg flow (l/s)	2.94	b
Steam generator feedwater temperature[c] (K)	490	497 ± 6
Intact loop steam generator liquid level (cm) (above top of tube sheet)	284	295 ± 5
Broken loop steam generator liquid level (cm) (above top of tube sheet)	984	996 ± 5
Pressure suppression tank pressure (MPa)	244	0.241 ± 0.007
Pressure suppression tank temperature (K)	299	297 ± 1

a. Measured initial conditions are taken from the digital acquisition system read just prior to blowdown initiation. Those measured conditions which did not meet the specified conditions were considered acceptable.

b. Flow is not specified, since it must be adjusted to achieve the required differential temperature across the core.

c. One source of feedwater for both intact and broken loops.

TABLE II

PRIMARY COOLANT TEMPERATURE DISTRIBUTION
PRIOR TO RUPTURE[a]

	Test S-07-8	
	Detector	Temperature (K)
Vessel lower plenum (bottom of lower plenum)	TFV-572W	555
Vessel lower plenum (top of lower plenum)	TFV-552A	555
Intact loop hot leg (near vessel)	RFI-2	594
Broken loop hot leg (near vessel)	RFB-20	595
Intact loop cold leg (near pump inlet)	TFI-11	555
Broken loop cold leg (near pump inlet)	TFB-37	559
Intact loop cold leg (near downcomer)	RFI-17	556
Broken loop cold leg (near downcomer)	RFB-45	559
Vessel upper head (middle)	TFV+221Q	555
Downcomer (top)	TFD-18F	558
Downcomer (middle)	TFD-294	559
Downcomer (bottom)	TFD-435	558

a. Average of data taken from -5 s to -0.5 s prior to blowdown initiation.

TABLE III

SEQUENCE OF EVENTS DURING TEST S-07-8[a]

Event	Time Relative To Rupture (s)
Core power level established	-915
Makeup pump and pressurizer heaters off	-2.5
Intact and broken loop steam generator feedwater and discharge valves closed	-1
Intact and broken loop pump controls initiated	0
Core power decay transient started	0
High pressure injection system flow started	0
ECC accumulator vessel lower plenum flow started[b]	19
Low pressure injection system flow started[b]	29.5
Broken loop pump power terminated	800
Core power terminated	800

a. A time controlled sequencer was used to control critical events during the test.

b. Injection from high and low pressure injection system pumps and ECC accumulators did not start until system pressure dropped below preset pump or accumulator pressure, respectively.

III. DATA PRESENTATION

The data from Semiscale Mod-3 Test S-07-8 are presented with brief comment. Processing analysis has been performed only to the extent necessary to obtain appropriate engineering units and to ensure that the data are reasonable and consistent. In all cases, in converting transducer output to engineering units, a homogeneous fluid was assumed. Further interpretation and analysis should consider that sudden decompression processes such as those occurring during blowdown may have subjected the measurement devices to nonhomogeneous fluid conditions.

The performance of the system during Test S-07-8 was monitored by 211 detectors. The data obtained were recorded on both digital and analog data acquisition systems. The analog system was used to provide redundant data. The long-term data (-20 to 260 s) presented in this report were recorded at an effective sample rate of 3.194 points per second. Short-term data (-6 to 42 s) were recorded at an effective sample rate of 19.16 points per second.

The data are presented in some instances in the form of composite graphs to facilitate comparison of the values of given variables at several locations. The scales selected for the graphs do not reflect the obtainable resolution of the data. (The data processing techniques are described further in Reference 2 and Appendix A.)

Figures 3 through 10 and Table IV provide supporting information for interpretation of the data graphs shown in Figures 11 through 320 and provide relative locations of all detectors used during Test S-07-8. Table IV groups the measurements according to measurement type, identifies the specific measurement location and range of the detector and actual recording range of the data acquisition system, provides brief comments regarding the data, and references the measurements and comments to the corresponding figure. Figures 11 through 320 present all the blowdown data obtained. Time zero on the graphs is the time of rupture initiation. Appendix A provides information explaining the data acquisition system capabilities. Appendix B explains posttest data processing for data conversion into engineering units and data adjustments. Appendix C presents an analysis of selected data which provide a guide to the uncertainty associated with data measurements in the Semiscale Mod-3 system.

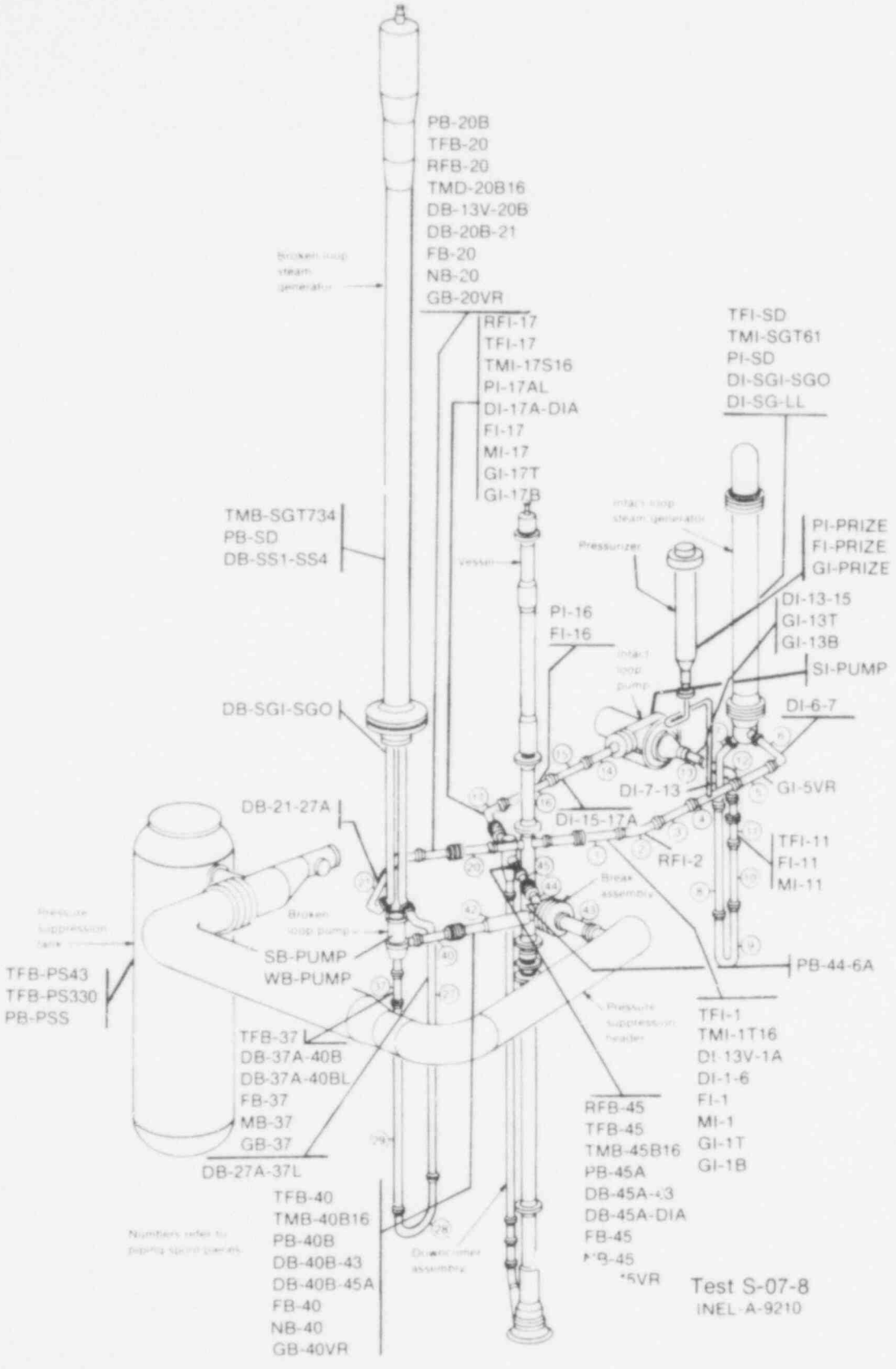

Fig. 3 Semiscale Mod-3 system and instrumentation for cold leg break configuration — isometric.

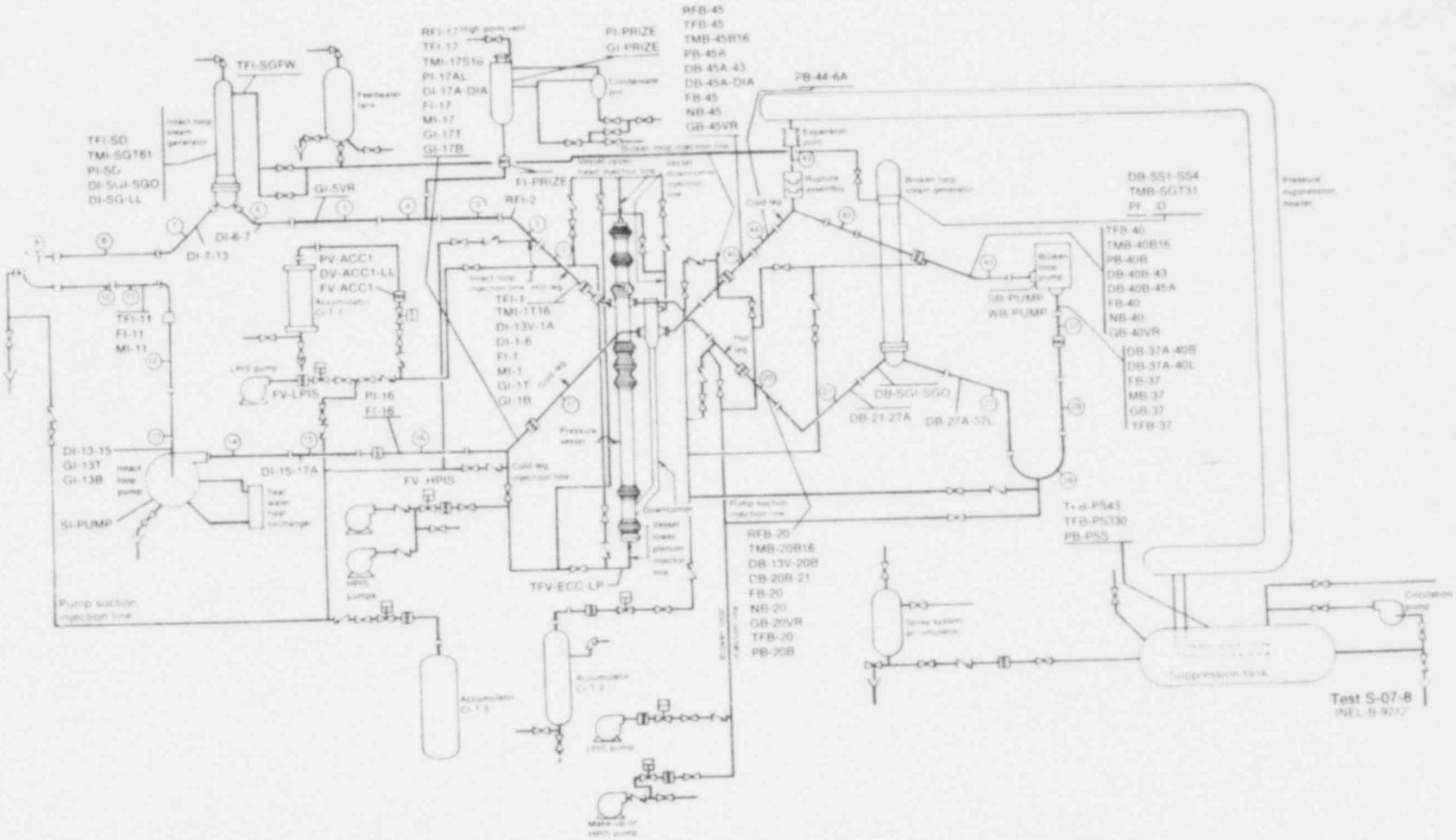

Fig. 4 Semiscale Mod-3 system and instrumentation for cold leg break configuration — schematic.

544 032

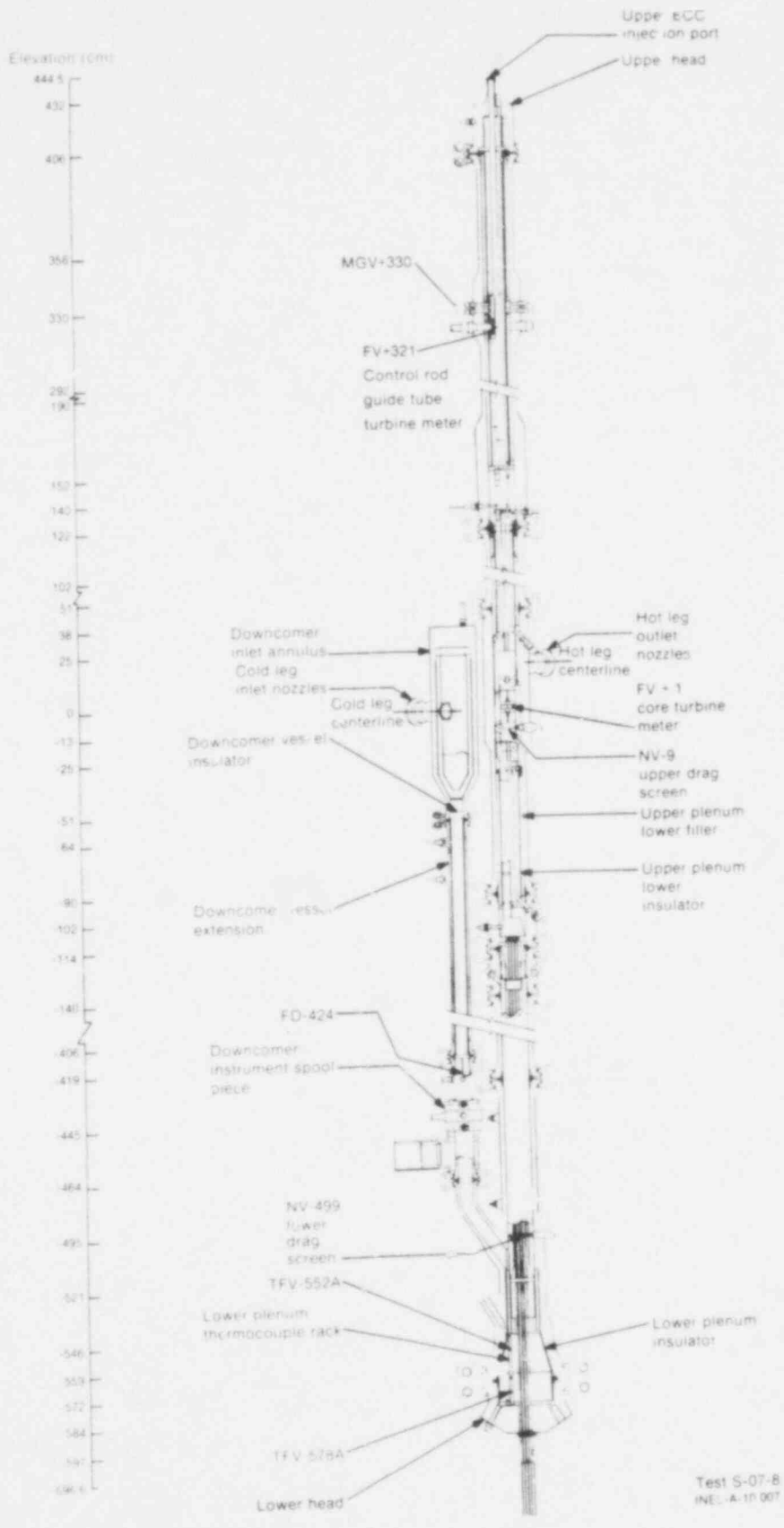

Fig. 5 Semiscale Mod-3 pressure vessel and downcomer — cross section showing instrumentation.

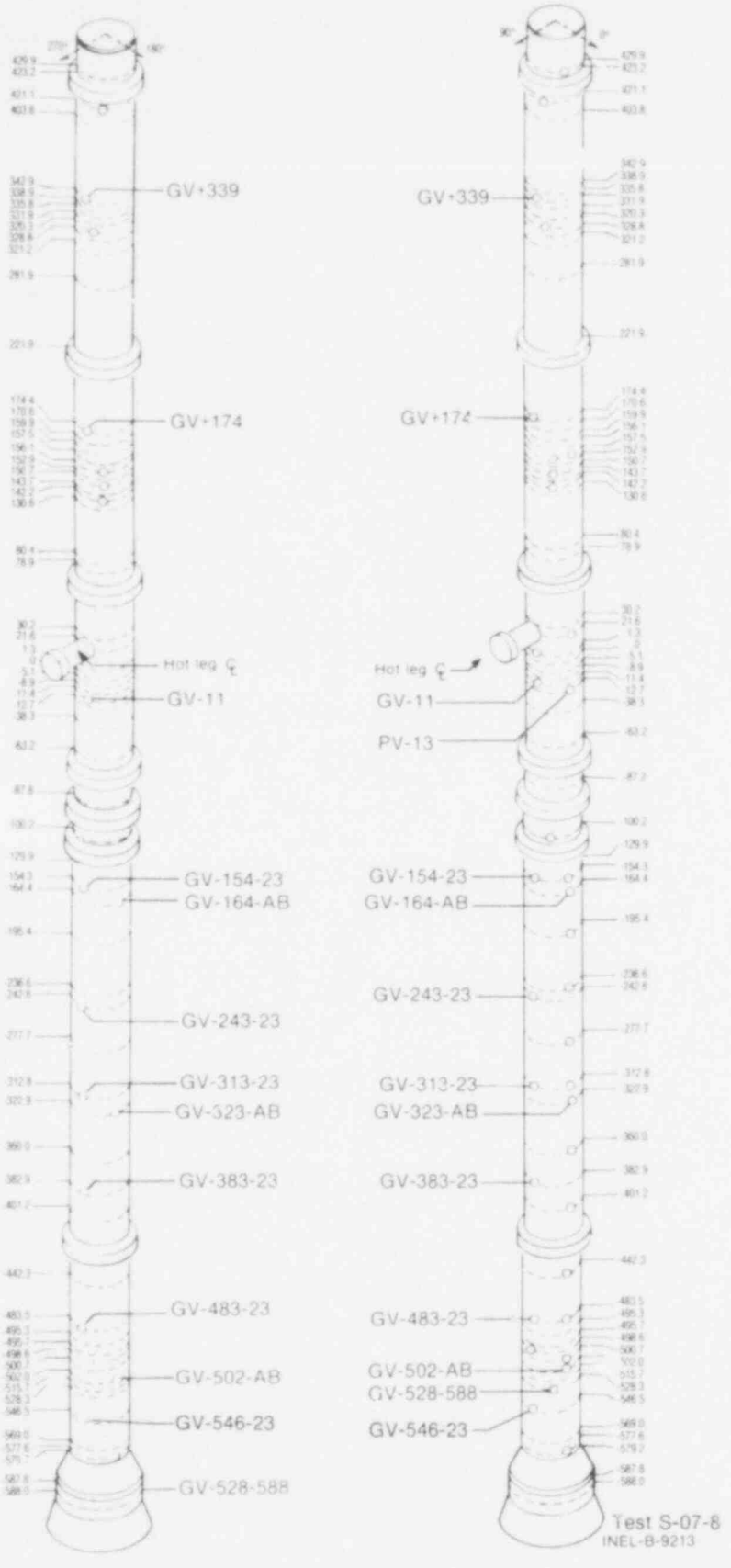

Fig. 6 Semiscale Mod-3 pressure vessel — isometric showing instrumentation.

544 034

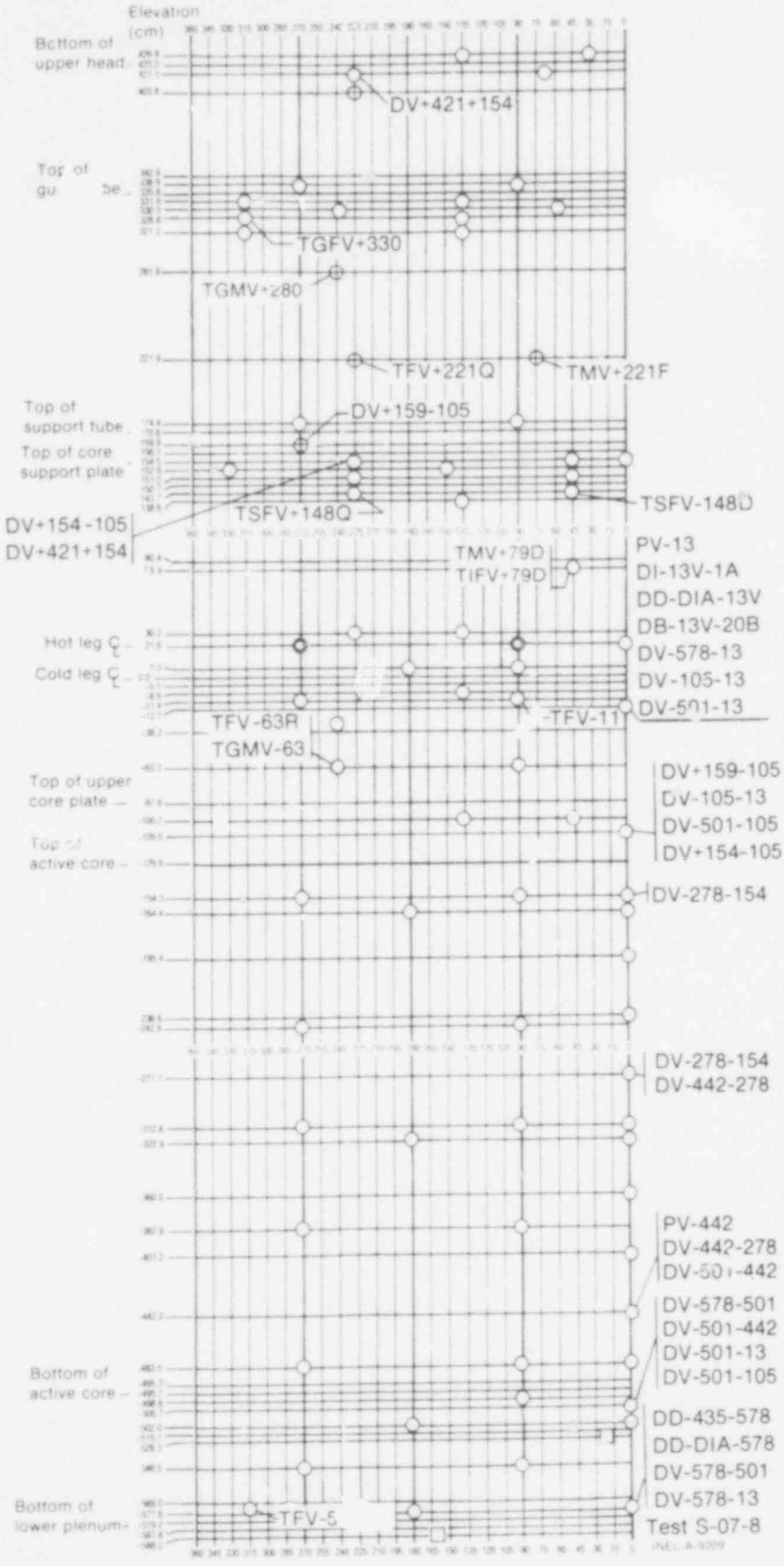

Fig. 7 Semiscale Mod-3 pressure vessel — penetrations and instrumentation.

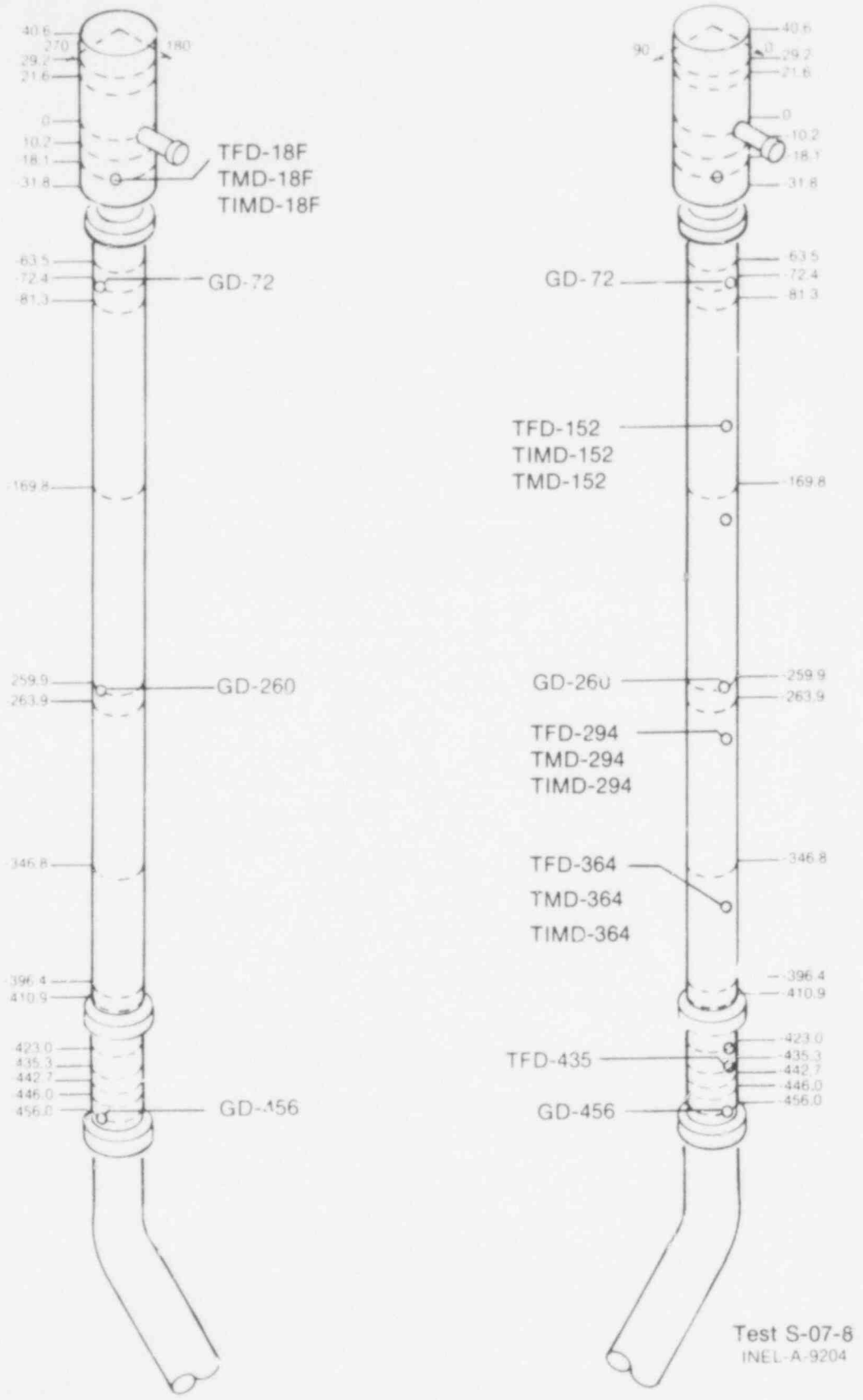

Fig. 8 Semiscale Mod-3 downcomer — isometric showing instrumentation.

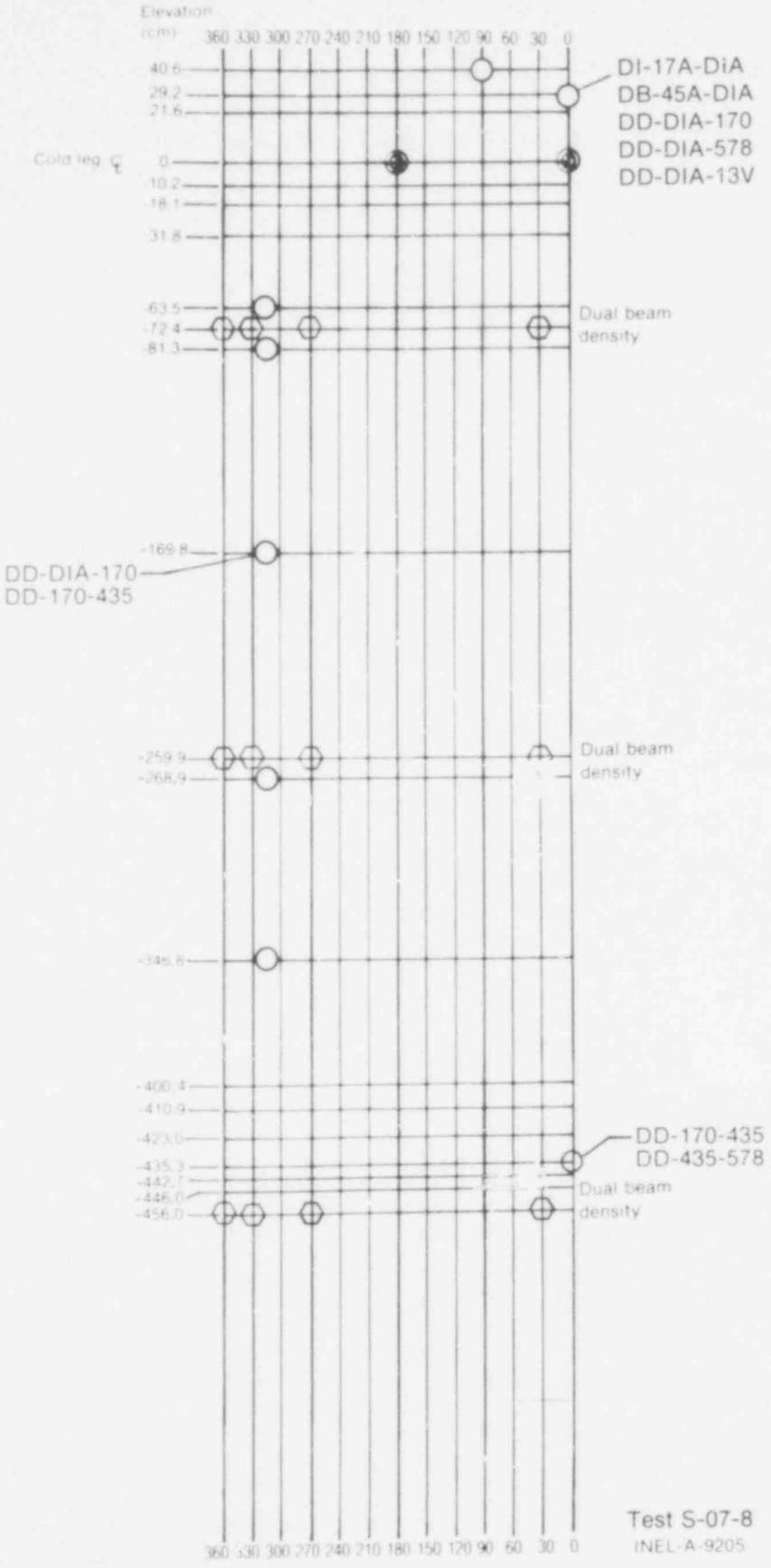

Fig. 9 Semiscale Mod-3 downcomer — penetrations and instrumentation.

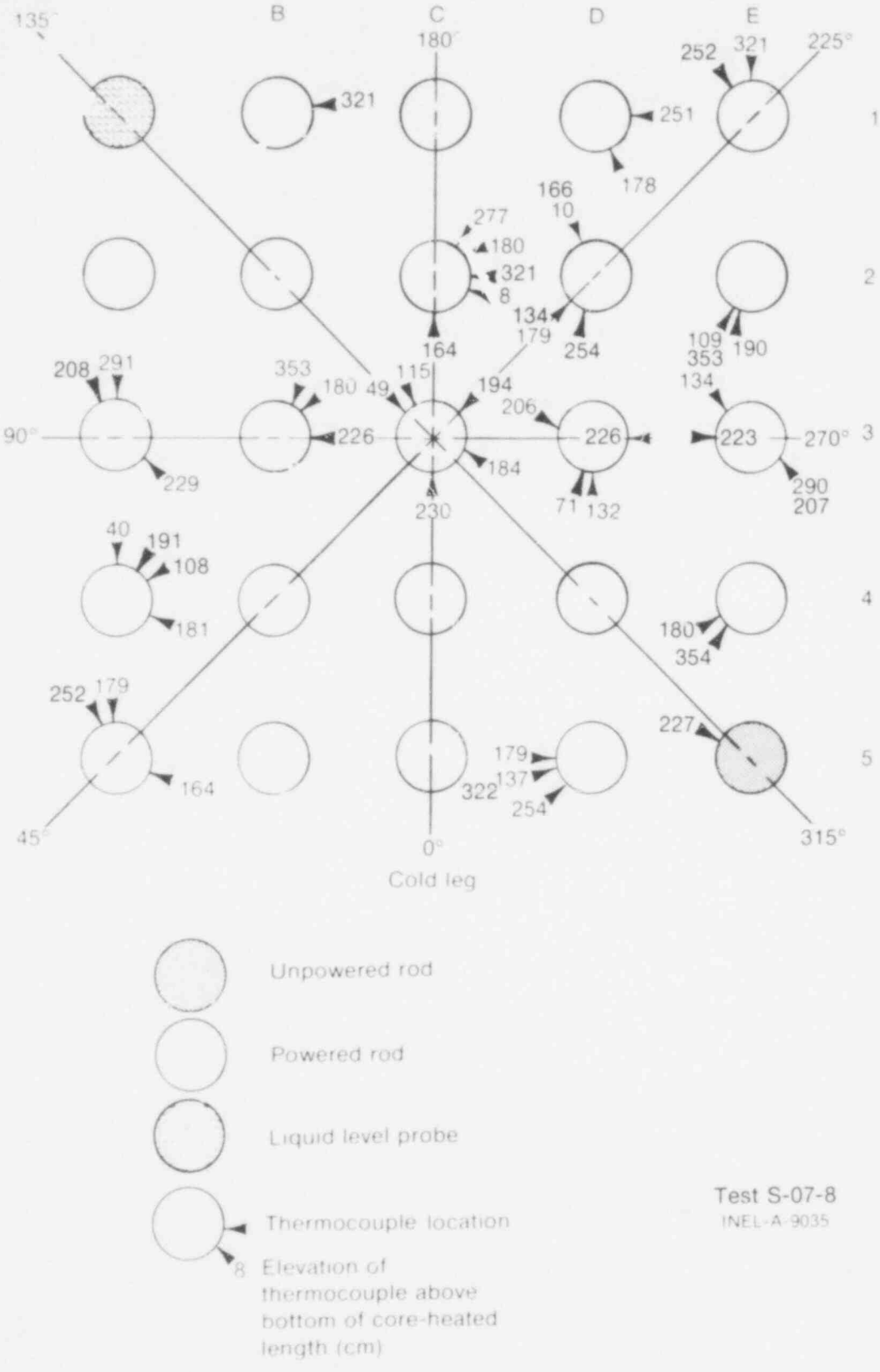

Fig. 10 Semiscale Mod-3 heater core — plan view.

TABLE IV

DATA PRESENTATION FOR SEMISCALE MOD-3 TEST S-07-8

Measurement	Location and Comments[a]	Data Acquisition Range[a] Detector	System	Figure[a]	Measurement Comments[b]
FLUID TEMPERATURE	Chrome-Alumel thermocouples unless specified otherwise.				
Intact Loop		0 to 1533 K	0 to 820 K		
TFI-1	Hot leg, Spool 1, 50 cm from vessel center.			11,12	
RFI-2	Hot leg, Spool 2, 99 cm from vessel center, 10 cm upstream of hot leg injection port (platinum resistance bulb).	0 to 811 K	0 to 811 K	11,12	Temperature data applicable only for initial conditions. Transient temperatures is to be used for trend only.
TFI-11	Cold leg, Spool 11, 438 cm from downcomer center.			13,14	Data acquisition noise caused an uncertainty of 1.5% of full scale.
RFI-17	Cold leg, Spool 17, 97 cm from downcomer center, 7 cm upstream of cold leg injection port (platinum resistance bulb).	0 to 811 K	0 to 811 K	15,16	Temperature applicable only for initial conditions. Transient temperature is to be used for trend only.
TFI-17	Cold leg, Spool 17, 60 cm from downcomer center.			15,16	
Broken Loop		0 to 1533 K	0 to 820 K		
RFB-20	Hot leg, Spool 20, 73 cm from vessel center, 14 cm downstream of hot leg injection port (platinum resistance bulb).	0 to 811 K	0 to 811 K	17,18	Temperature data applicable only for initial conditions. Transient temperatures is to be used for trend only.
TFB-20	Hot leg, Spool 20, 84 cm from vessel center, 25 cm downstream of hot leg injection port.			17,18	
TFB-37	Cold leg, Spool 37, 348 cm from downcomer center.			19,20	Data acquisition noise caused an uncertainty of 1.5% of full scale.
TFB-40	Cold leg, Spool 40, 220 cm from downcomer center, 16 cm downstream of cold leg injection port.			21,22	
RFB-45	Cold leg, Spool 45, 89 cm from downcomer center (platinum resistance bulb).	0 to 811 K	0 to 811 K	23,24	Temperature data applicable only for initial conditions. Transient temperature is to be used for trend only.
TFB-45	Cold leg, Spool 45 78 cm from downcomer center.			23,24	
Downcomer		0 to 1533 K	0 to 820 K		
TFD-18F	In downcomer inlet annulus, 18 cm below cold leg centerline at 75°.			25,26	
TFD-153	In downcomer extension, 152 cm below cold leg centerline.			25,26	
TFD-294	In downcomer extension, 294 cm below cold leg centerline.			25,26	
TFD-364	In downcomer extension, 364 cm below cold leg centerline.			25,26	
TFD-435	In downcomer instrument spool, 435 cm below cold leg centerline.			25,26	
Vessel		0 to 1533 K	0 to 820 K		
Vessel Upper Plenum					
TFV+221Q	In vessel upper head filler, 221 cm above cold leg centerline at 225°.			27,28	
TFV-11	In vessel, 11 cm below cold leg centerline.			29,30	
TFV-63R	In vessel, 63 cm below cold leg center at 240°.			29,30	
Vessel Lower Plenum		0 to 1533 K	0 to 820 K		
TFV-552A	On thermocouple rack in vessel lower plenum 552 cm below cold leg centerline at 0°.			31,32	
TFV-572W	In vessel lower plenum, 572 cm below cold leg centerline at 315°.			31,32	
TFV-578A	On thermocouple rack in vessel lower plenum 578 cm below cold leg centerline at 0°.			31,32	

TABLE IV (continued)

Measurement	Location and Comments[a]	Data Acquisition Range[a] Detector	System	Figure[a]	Measurement Comments[b]
Vessel Filler Insulator Gap		0 to 1533 K	0 to 820 K		
TIFV+79D	In vessel upper filler insulator gap, 79 cm above cold leg centerline at 45°.			33,34	Data acquisition noise caused an uncertainty of 1.5% of full scale.
Vessel Guide Tube		0 to 1533 K	0 to 820 K		
TFGV+330	In vessel guide tube, 330 cm above cold leg centerline.			35,36	Data acquisition noise caused an uncertainty of 1.5% of full scale.
Vessel Support Tube					
TFSV+148D	In a vessel support tube, 148 cm above cold leg centerline at 45°.			37,38	
Core Grid Spacers		0 to [illegible]3 K	0 to 1580 K		
Grid Spacer 1	490 cm below cold leg centerline, 6 cm above bottom of heated length.				
TFG-1AB-12	Thermocouple in space defined by Columns A and B, Rows 1 and 2.			39,40	
Grid Spacer 3	410 cm below cold leg centerline, 86 cm above bottom of heated length.				
TFG-3AB-12	Thermocouple in space defined by Columns A and B, Rows 1 and 2.			41,42	
Grid Spacer 5	330 cm below cold leg centerline, 166 cm above bottom of heated length.				
TFG-5AB-45	Thermocouple in space defined by Columns A and B, Rows 4 and 5.			43,44	
Grid Spacer 6	290 cm below cold leg centerline, 206 cm above bottom of heated length.				
TFG-6BC-34	Thermocouple in space defined by Columns B and C, Rows 3 and 4.			45,46	
Grid Spacer 8	210 cm below cold leg centerline, 286 cm above bottom of heated length.				
TFG-8AB-23	Thermocouple in space defined by Columns A and B, Rows 2 and 3.			47,48	Questionable data. Detector indicates lower temperature than expected. Trend information only.
Grid Spacer 10	130 cm below cold leg centerline, 366 cm above bottom of heated length.				
TFG-10AB-45	Thermocouple in space defined by Columns A and B, Rows 4 and 5.			49,50	Data acquisition noise caused an uncertainty of 1.5% of full scale.
ECC System		0 to 1533 K	0 to 820 K		
TFV-ECC-LP	In ECC line leading to vessel lower plenum, 49 cm from vessel center.			51,52	
Steam Generator		0 to 1533 K	0 to 820 K		
Intact Loop					
TFI-SGFW	In feedwater line leading to steam generator.			53,54	Data acquisition noise caused an uncertainty of 1.5% of full scale.
TFI-SD	In steam generator steam dome, 320 cm above bottom of tube sheet.			55,56	
Pressure Suppression System		0 to 1533K	0 to 820 K		
TFB-PS43	43 cm above bottom of suppression tank.			57,58	
TFB-PS330	330 cm above bottom of suppression tank.			57,58	
MATERIAL TEMPERATURE	Chromel-Alumel thermocouples unless specified otherwise.				
Intact Loop		0 to 1533 K	0 to 820 K		
TMI-1T16	Hot leg, Spool 1, top, 1.6 mm from pipe inside diameter (ID) 68 cm from vessel center.			59,60	
TMI-17S16	Cold leg, Spool 17, side, 1.6 mm from pipe ID, 68 cm from downcomer center.			59,60	

TABLE IV (continued)

Measurement	Location and Comments[a]	Data Acquisition Range[a] Detector	System	Figure[a]	Measurement Comments[b]
Broken loop		0 to 1533 K	0 to 820 K		
TMB-20B16	Hot leg, Spool 20, bottom, 1.6 cm from pipe ID, 91 cm from vessel center.			61,62	
TMB-40B16	Cold leg, Spool 40, bottom, 1.6 cm from pipe ID, 202 cm from downcomer center.			63,64	
TMB-45B16	Cold leg, Spool 45, bottom, 1.6 cm from pipe ID, 98 cm from downcomer center.			65,66	
Downcomer		0 to 1533 K	0 to 820 K		Data acquisition noise caused an uncertainty of 1.5% of full scale.
TMD-18F	On downcomer inlet annulus, 18 cm below cold leg centerline at 75°.			65,66	
TMD-152	On downcomer extension, 152 cm below cold leg centerline.			65,66	
TMD-294	On downcomer extension, 294 cm below cold leg centerline.				Detector failed.
TMD-364	On downcomer extension, 364 cm below cold leg centerline.			65,66	
Downcomer Insulator		0 to 1533 K	0 to 820 K		
TIMD-18F	On downcomer inlet annulus insulator, 18 cm below cold leg centerline at 225°.			67,68	
TIMD-152	On downcomer extension insulator, 152 cm below cold leg centerline.			67,68	
TIMD-294	On downcomer extension insulator, 294 cm below cold leg centerline.			67,68	
TIMD-364	On downcomer extension insulator, 364 cm below cold leg centerline.			67,68	
Vessel		0 to 1533 K	0 to 820 K		
TMV+221F	In vessel on upper head filler, 221 cm above cold leg centerline at 75°.			69,70	
TMV+79D	In vessel on upper plenum upper filler, 79 cm above cold leg centerline at 45°.			69,70	
Guide Tube		0 to 1533 K	0 to 820 K		
TGMV+280	On guide tube, 280 cm above cold leg centerline.			71,72	
TGMV-63	On guide tube, 63 cm below cold leg centerline.			71,72	
Steam Generator		0 to 1533 K	0 to 820 K		
Intact Loop					
TMI-6GT61	On a steam generator tube, 61 cm above bottom of tube sheet on OD of tube.			73,74	Data acquisition noise caused an uncertainty of 1 % of full scale.
Broken Loop		0 to 1533 K	0 to 820 K		
TMB-SGT234	On steam generator tube, 787 cm above bottom of tube sheet on OD of tube.			75,76	Data acquisition noise caused an uncertainty of 1.5% of full scale.
CORE HEATER CLADDING TEMPERATURE	Chromel-Alumel thermocouples.				
High Power Heaters		0 to 1533 K	0 to 1580 K		
TH-B3-180 TH-B3-226 TH-B3-353	Heater at Column B, Row 3. Thermocouples 180 cm (225°), 226 cm (270°), and 353 cm (210°) above bottom of heated length.			77,78	
TH-C2-8 TH-C2-164 TH-C2-130 TH-C2-277 TH-C2-321	Heater at Column C, Row 2. Thermocouples 8 cm (285°), 164 cm (0°), 180 cm (225°), 277 cm (210°), and 321 cm (270°) above bottom of heated length.			79,80	
TH-C3-49 TH-C3-115 TH-C3-184 TH-C3-194 TH-C3-230	Heater at Column C, Row 3. Thermocouples 49 cm (135°), 115 cm (165°), 184 cm (285°), 194 cm (225°), and 230 cm (0°) above bottom of heated length.			81,82	

TABLE IV (continued)

Measurement	Location and Comments[a]	Data Acquisition Range[a] Detector	System	Figure[a]	Measurement Comments[b]
High Power Heaters (continued)					
TH-D2-40 TH-D2-134 TH-D2-166 TH-D2-179 TH-D2-254	Heater at Column D, Row 2. Thermocouples at 10 cm (150°), 134 cm (45°), 166 cm (150°), 179 cm (45°), and 254 cm (15°) above bottom of heated length.			83,84	
TH-D3-71 TH-D3-132 TH-D3-206 TH-D3-226	Heater at Column D, Row 3. Thermocouples 71 cm (15°), 132 cm (0°), 206 cm (120°), and 226 cm (270°) above bottom of heated length.			85,86	
Low Power Heaters		0 to 1533 K	0 to 1580 K		
TH-A3-208 TH-A3-229 TH-A3-291	Heater at Column A, Row 3. Thermocouples 208 cm (165°), 229 cm (315°), and 291 cm (180°) above bottom of heated length.			87,88	
TH-A4-40 TH-A4-108 TH-A4-181 TH-A4-191	Heater at Column A, Row 4. Thermocouples 40 cm (195°), 108 cm (225°), 181 cm (300°), and 191 (210°) above bottom of heated length.			89,90	
TH-A5-164 TH-A5-179 TH-A5-252	Heater at Column A, Row 5. Thermocouples 164 cm (300°), 179 (180°), and, 252 cm (165°), above bottom of heated length.			91,92	TH-A5-179 thermocouple questionable. Detector indicates higher temperature than expected.
TH-B1-321	Heater at Column B, Row 1. Thermocouple 321 cm (270°) above bottom of heated length.			93,94	
TH-D1-178 TH-D1-251	Heater at Column D, Row 1. Thermocouples 178 cm (330°) and 251 (270°) above bottom of heated length.			95,96	
TH-D5-137 TH-D5-179 TH-D5-254 TH-D5-322	Heater at Column D, Row 5. Thermocouples 137 cm (75°), 179 cm (90°), 254 cm (45°), and 322 cm (75°) above bottom of heated length.			97,98	
TH-E1-252 TH-E1-321	Heater at Column E, Row 1. Thermocouples 252 cm (120°), and 321 cm (180°) above bottom of heated length.			99,100	
TH-E2-109 TH-E2-190 TH-E2-353	Heater at Column E, Row 2. Thermocouples 109 cm (30°), 190 cm (15°), and 353 cm (30°) above bottom of heated length.			101,102	
TH-E3-134 TH-E3-207 TH-E3-223 TH-E3-290	Heater at Column E, Row 3. Thermocouples 134 cm (135°), 207 cm (300°), 223 (90°), and 290 cm (300°) above bottom of heated length.			103,104	
TH-E4-180 TH-E4-354	Heater at Column E, Row 4. Thermocouples 180 cm (60°) and 354 cm (45°) above bottom of heated length.			105,106	
TH-E5-227	Heater at Column E, Row 5. Thermocouple 227 cm (120°) above bottom of heated length.			107,108	
PRESSURE					
Intact Loop					
PI-16	Cold leg, Spool 16, 144 cm from downcomer center (tee off DP tap).	0 to 17.237 MPa	0 to 20.29 MPa	109,110	
PI-17AL	Cold leg, Spool 17, 60 cm from downcomer center (low range).	0 to 3.447 MPa	0 to 3.45 MPa	109,110	Data acquisition system saturated to t = 21 s.
Broken Loop		0 to 17.237 MPa			
PB-20B	Hot leg, Spool 20, 84 cm from vessel center.		0 to 21.08 MPa	111,112	
PB-40B	Cold leg, Spool 40, 209 cm from downcomer center.		0 to 21.96 MPa	113,114	
PB-44-6A	Cold leg, Spool 44, downcomer side nozzle throat, 125 cm from downcomer center, 0°.		0 to 20.[illegible] MPa	115,116	
PB-45A	Cold leg, Spool 45, 90 cm from downcomer center, 0°.		0 to 20.77 MPa	117,118	

TABLE IV (continued)

Measurement	Location and Comments[a]	Data Acquisition Range[a] Detector	System	Figure[a]	Measurement Comments[b]
Vessel		0 to 17.237 MPa			
PV-13	In vessel hot leg extension, 13 cm below cold leg centerline (tee off DP tap).		0 to 21.00 MPa	119,120	
PV-442	In vessel, 442 cm below cold leg centerline.		0 to 20.67 MPa	119,120	
ECC System					
PV-ACC1	In accumulator for vessel.	0 to 6.895 MPa	0 to 8.53 MPa	121,122	
Steam Generator		0 to 17.237 MPa			
Intact Loop					
PI-SD	Intact loop steam generator, secondary side steam dome.		0 to 21.02 MPa	123,124	
Broken Loop					
PI-SD	Broken loop steam generator, secondary side steam dome.		0 to 21.54 MPa	123,124	
Pressurizer		0 to 17.237 MPa			
PI-PRIZE	Pressurizer steam dome.		0 to 32.83 MPa	125,126	
Pressure Suppression System		0 to 0.689 MPa			
PB-PSS	Suppression tank top.		0 to 0.856 kPa	127,128	
DIFFERENTIAL PRESSURE	Elevation difference between transducer taps is zero unless specified otherwise.				
Intact Loop					
DI-13V-1A	From vessel lower section of upper plenum, 13 cm below cold leg centerline to hot leg, Spool 1, 60 cm from vessel center. Lower upper plenum tap is 35 cm below Spool 1 tap.	±127 cm water	±16.78 kPa	129, 130	
DI-1A-6	Hot leg, Spool 1, 60 cm from vessel center to hot leg, Spool 6, 271 cm from vessel center.	±254 cm water	±33.76 kPa	131,132	
DI-6-7	Hot leg, Spool 6, 271 cm from vessel center to cold leg, Spool 7, 927 cm from downcomer center. Spool 6 tap is 47 cm above Spool 7 tap.	±345 kPa	±345 kPa	133,134	
DI-SGI-SGO	Intact loop steam generator, inlet plenum to outlet plenum, across primary side tubes.	±254 cm water	±33.49 kPa	135,136	
DI-7-13	Cold leg, Spool 7, 927 cm from downcomer center to primary pump suction, Spool 13, 332 cm from downcomer center.	±254 cm water	±33.42 kPa	137,138	
DI-13-15	Cold leg, Spool 13, 332 cm from downcomer center, across primary pump to cold leg, Spool 15, 175 cm from downcomer center. Spool 13 tap is 25 cm below Spool 15 tap.	±690 kPa	±690 kPa	139,140	
DI-15-17A	Cold leg, Spool 15, 175 cm from downcomer center, across cold leg injection port to cold leg, Spool 17, 50 cm from downcomer center.	±254 cm water	±34.0 kPa	141,142	
DI-17A-DIA	Cold leg, Spool 17, 60 cm from downcomer to downcomer inlet annulus, 30 cm above cold leg centerline. Spool 17 tap is 30 cm below DIA tap.	±254 cm water	±33.6 kPa	143,144	
Broken Loop					
DB-13V-20B	In vessel from lower section of upper plenum, 13 cm below cold leg centerline to hot leg, Spool 20, 22 cm above cold leg centerline, 84 cm from vessel center. 13V tap is 35 cm below Spool 20 tap.	±762 cm water	±105 kPa	145,146	
DB-20B-21	Hot leg, Spool 20, 84 cm from vessel center to hot leg, Spool 21, 220 cm from vessel center.	±762 cm water	±100 kPa	147,148	

TABLE IV (continued)

Measurement	Location and Comments[a]	Data Acquisition Range[a] Detector	System	Figure[a]	Measurement Comments[b]
Vessel (continued)					
DB-21-27A	Hot leg, Spool 21, 220 cm from vessel center to cold leg, Spool 27, 897 cm from downcomer center. Spool 21 tap is 4 cm above Spool 27A tap.	±345 kPa	±344 kPa	,150	Data acquisition system saturated from t = 0 to t = 1 s and t = 8 to t = 15 s.
DB-SGI-SGO	Broken loop steam generator inlet leg, 382 cm from vessel center across primary side tubes to steam generator outlet leg, 953 cm from downcomer center. SGI tap is 72 cm above SGO tap.	±1380 kPa	±1381 kPa	151,152	Questionable data. Differential pressure cell exhibits pressure sensitivities in the order of magnitude of the measurement.
DB-27A-37A	Cold leg, Spool 27, 897 cm from downcomer center across broken loop pump suction to Spool 37, 348 cm from downcomer center. Spool 27 tap is 87 cm above Spool 37 tap.	±1270 cm water	±170 kPa	153,154	
DB-37A-40B	Cold leg, Spool 37, broken loop pump inlet, 348 cm from downcomer center to cold leg, Spool 40 pump discharge, 209 cm from downcomer center. Spool 37 tap is 68 cm below Spool 40 tap.	±6895 kPa	±9223 kPa	155,156	
DB-37A-40L	Cold leg, Spool 37, broken loop pump inlet, 348 cm from downcomer center to cold leg, Spool 40 pump discharge 209 cm from downcomer center. Spool 37 tap is 68 cm below Spool 40 tap (low range).	±690 kPa	±710 kPa	157,158	Data acquisition system saturated from t = 0 to t = 2b s. Differential pressure cell exhibits pressure sensitivities in the order of magnitude of the measurement.
DB-40B-43A	Cold leg, Spool 40 pump discharge, 209 cm from downcomer center across noncommunicative break nozzle and rupture assembly to cold leg, Spool 43, 180 cm from downcomer center.	±10 342 kPa	±13 799 kPa	159,160	
DB-40B-45A	Cold leg, Spool 40 pump discharge, 209 cm from downcomer center across noncommunicative break nozzle to cold leg, Spool 45, 89 cm from downcomer center.	±254 cm water	±33.75 kPa	161,162	
DB-45A-43	Cold leg, Spool 45, 89 cm from downcomer across noncommunicative break nozzle to cold leg, Spool 43, 180 cm from downcomer center.	±10 342 kPa	±13 782 kPa	163,164	
DB-45A-DIA	Cold leg, Spool 45, 89 cm from downcomer center to downcomer inlet annulus, 30 cm above cold leg centerline. Spool 45 tap is 30 cm below DIA tap.	±690 kPa	±690 kPa	165,166	
Downcomer					
DD-DIA-13V	Downcomer inlet annulus, 30 cm above cold leg centerline to vessel lower upper plenum, 13 cm below cold leg centerline. Elevation difference between taps is 43 cm.	±345 kPa	±342 kPa	167,168	
DD-DIA-170	Downcomer inlet annulus, 30 cm above cold leg centerline to downcomer extension, 170 cm below cold leg centerline. Elevation difference between taps is 200 cm.	±762 cm water	±102 kPa	169,170	
DD-DIA-578	Downcomer inlet annulus, 30 cm above cold leg centerline to vessel lower head, 578 cm below cold leg centerline. Elevation difference between taps is 608 cm.	±1270 cm water	±174 kPa	171,172	
DD-170-435	Downcomer extension, 170 cm below cold leg centerline to downcomer instrumented spool piece, 435 cm below cold leg centerline. Elevation difference between taps is 265 cm.	±762 cm water	±104 kPa	173,174	
DD-435-578	Downcomer instrumented spool piece, 435 cm below cold leg centerline to vessel lower head, 578 cm below cold leg centerline. Elevation difference between taps is 143 cm.	±254 cm water	±33.5 kPa	175,176	
DV-578-501	Vessel lower head, 578 cm below cold leg centerline to lower core region, 501 cm below cold leg centerline. Elevation difference between taps is 77 cm.	±127 cm water	±33.8 kPa	177,178	

TABLE IV (continued)

Measurement	Location and Comments[a]	Data Acquisition Range[a] Detector	System	Figure[a]	Measurement Comments[b]
Downcomer (continued)					
DV-578-13	Vessel lower head, 578 cm below cold leg centerline to lower section of upper plenum, 13 cm below cold leg centerline. Elevation difference between taps is 565 cm.	±690 kPa	±687 kPa	179,180	
DV-501-442	Vessel lower core region, 501 cm below cold leg centerline to lower core region, 442 cm below cold leg centerline. Elevation difference between taps is 59 cm.	±254 cm water	±34.2 kPa	181,182	
DV-501-105	Vessel lower core region, 501 cm below cold leg centerline to heater rod ground hub, 105 cm below cold leg centerline. Elevation difference between taps is 396 cm.	±762 cm water	±102 kPa	183,184	
DV-501-13A	Vessel lower plenum extension, 501 cm below cold leg centerline to lower upper plenum, 13 cm below cold leg centerline. Elevation difference between taps is 488 cm.	±345 kPa	±345 kPa	185,186	
DV-442-278	Vessel lower core region, 442 cm below cold leg centerline, to mid-core region, 278 cm below cold leg centerline. Elevation difference between taps is 164 cm.	±1270 cm water	±168.8 kPa	187,188	
DV-278-154	Vessel mid-core region, 278 cm below cold leg centerline to upper core region 154 cm below cold leg centerline. Elevation difference between taps is 124 cm.	±1270 cm water	±172 kPa	189,190	
DV-105-13A	Heater rod ground hub, 105 cm below cold leg centerline to lower section of upper plenum, 13 cm below cold leg centerline elevation difference between taps is 92 cm.	±762 cm water	±10. ...	191,192	
DV+421+154	Vessel top head, 421 cm above cold leg centerline to core support tube, 154 cm above cold leg centerline. Elevation difference between taps is 267 cm.	±762 cm water	± 99.89 kPa	193,194	
DV+159-105	Lower section of vessel upper head extension, 159 cm above cold leg centerline to heater ground rod hub, 105 cm below cold leg centerline. Elevation difference between taps is 264 cm.	±2032 cm water	±266.2 kPa	195,196	
DV+154-105	Core support tube, 154 cm above cold leg centerline to heater ground rod hub, 105 cm below cold leg centerline. Elevation difference between taps is 259 cm.	±762 cm water	±102.8 kPa	197,198	
ECC System					
DV-ACC1-LL	Top to bottom of vessel accumulator. Elevation difference between taps is 284 cm.	±762 cm water	±104 kPa	199,200	
Steam Generator					
DI-SG-LL	Liquid level for intact loop steam generator. Elevator difference between taps is 206 cm.	±1270 cm water	±166 kPa	201,202	
DB-SGI-SGA	Liquid level for broken loop steam generator. Elevation difference between taps is 1067 cm.	±1270 cm water	±168.6 kPa	203,204	
VOLUMETRIC FLOW RATE	Turbine flowmeter, bidirectional.				Data acquisition system range may exceed rated detection range; however, turbine response is linear to flow rates well beyond the rated range.
Intact Loop	3-in. Schedule 160 pipe.				
FI-1	Hot leg, Spool 1, 38 cm from vessel center.	±2.52 to ±25.2 l/s	±80 l/s	205,206	
FI-11	Cold leg, Spool 11, 429 cm from downcomer center.	±2.52 to ±25.2 l/s	±100 l/s	205,206	
FI-16	Cold leg, Spool 16, 145 cm from downcomer center.	±5.05 to ±50.5 l/s	±100 l/s	207,208	
FI-17	Cold leg, Spool 17, 38 cm from downcomer center.	±2.52 to ±25.2 l/s	±100 l/s	207,208	

TABLE IV (continued)

Measurement	Location and Comments[a]	Data Acquisition Range[a] Detector	System	Figure[a]	Measurement Comments[b]
Broken Loop					
FB-20	Hot leg, Spool 20, 100 cm from vessel center.	±2.52 to ±25.2 l/s	±60 l/s	209,210	
FB-37	Cold leg, Spool 37, 316 cm from downcomer center.	±2.52 to ±25.2 l/s	±60 l/s	209,210	
FB-40	Cold leg, Spool 40, 193 cm from downcomer center.	±2.52 to ±25.2 l/s	±80 l/s	211,212	
FB-45	Cold leg, Spool 45, 110 cm from downcomer center.	±2.52 to ±25.2 l/s	±80 l/s	211,212	
Downcomer					
FD-424	In downcomer, upstream of instrumented spool piece, 424 cm below cold leg centerline.	±2.52 to ±25.2 l/s	±40 l/s	213,214	
Vessel					
FV-1	Core exit, 1 cm above cold leg centerline.	±2.52 to ±25.2 l/s	±80 l/s	215,216	
ECC System					
FV-HPIS	In line immediately after HPIS pump for vessel; 1/2-in. line.	±0.0316 to ±0.315 l/s	±0.10 l/s	217,218	
FV-LPIS	In line leading from LPIS pump for vessel, 1/2-in. line.	±0.047 to ±0.473 l/s	±0.20 l/s	219,220	
FV-ACC1	In line leading from vessel accumulator.	±0.315 to ±3.15 l/s	±5.0 l/s	221,222	
Pressurizer					
FI-PRIZE	In pressurizer surge line.	±0.920 to ±8.20 l/s	±9.0 l/s	223,224	
MOMENTUM FLUX	Drag-screen, bidirectional.				
Broken Loop					
MB-20	Hot leg, Spool 20, 79 cm from vessel center.	±0.05 to ±10.7 N	±16.07 N	225,226	
MB-40	Cold leg, Spool 40, 215 cm from downcomer center.	±0.09 to ±17.8 N	±24.08 N	227,228	
MB-45	Cold leg, Spool 45, 84 cm from downcomer center.	±0.22 to ±44.5 N	±61.71 N	229,230	
Vessel					
MV-9	In vessel lower upper plenum region, 9 cm below cold leg centerline. Drag screen target flow area 34% of flow area.	±0.11 to ±22.2 N	±30.95 N	231,232	
MV-499	In vessel at entrance to heated core, 499 cm below cold leg centerline. Drag screen target area 34% of flow area.	±0.08 to ±15.1 N	±23.54 N	233,234	
DENSITY					
Intact Loop		1.6 to 1600 kg/m^3	0 to 1600 kg/m^3		
GI-1T GI-1B GI-1C	Hot leg, Spool 1, 77 cm from vessel center. T (tangential) ranges 270° to 360°. B (body) ranges 30° to 330°. C is a mathematical composite of T and B.			235,236 235,236 237,238	
GI-5VR	Hot leg, Spool 5, 228 cm from vessel center, vertical.			239,240	
GI-13T GI-13B GI-13C	Cold leg, Spool 13, 342 cm from downcomer center. T (tangential) ranges 270° to 360°. B (body) ranges 30° to 330°. C is a mathematical composite of T and B.			241,242 241,242 243,244	
GI-17T GI-17B GI-17C	Cold leg, Spool 17, 73 cm from downcomer center. T (tangential) ranges 270° to 360°. B (body) ranges 30° to 330°. C is a mathematical composite of T and B.			245,246 245,246 247,248	

TABLE IV (continued)

Measurement	Location and Comments[a]	Data Acquisition Range[a] Detector	System	Figure[a]	Measurement Comments[b]
Broken Loop		1.6 to 1600 kg/m^3	0 to 1600 kg/m^3		
GB-20VR	Hot leg, Spool 20, 64 cm from vessel center, vertical.				Detector failed.
GB-37	Cold leg, Spool 37, 360 cm from downcomer center.			249,250	
GB-40VB	Cold leg, Spool 40, 230 cm from downcomer vertical.			251,252	
GB-45VB	Cold leg, Spool 45, 66 cm from downcomer vertical.			253,254	
Downcomer		1.6 to 1600 kg/m^3	0 to 1600 kg/m^3		
GD-72B	Downcomer, 72 cm below cold leg centerline. B (body) ranges 30° to 330°.			255,256	
GD-260B	Downcomer, 260 cm below cold leg centerline. B (body) ranges 30° to 330°.			257,258	
GD-456B	Downcomer, 456 cm below cold leg centerline. B (body) ranges 30° to 330°.			259,260	
Vessel		1.6 to 1600 kg/m^3	0 to 1600 kg/m^3		
GV+339	Vessel at top of control rod guide tube, 339 cm above cold leg centerline.			261,262	
GV+174	Vessel at top of core support tube, 174 cm above cold leg centerline.			263,264	Questionable data. Analysis of beam path indicated possible obstruction by thermocouple or heater rod. Effect is unknown. Data to be used for trend only.
GV-11	Vessel at base of core flow instrument housing, 11 cm below cold leg centerline.			265,266	
GV-154-23	Near top of core heated length, 154 cm below cold leg centerline between heater rod Rows 2 and 3.			267,268	Questionable data. Analysis of beam path indicated possible obstruction by thermocouple or heater rod. Effect is unknown. Data to be used for trend only.
GV-164-AB	Near top of core heated length, 164 cm below cold leg centerline between heater rod Columns A and B.			267,268	Questionable data. Analysis of beam path indicated possible obstruction by thermocouple or heater rod. Effect is unknown. Data to be used for trend only.
GV-263-23	Upper part of core heated length, 313 cm below cold leg centerline between heater rod Rows 2 and 3.			269,270	
GV-313-23	Near center of core heated length, 313 cm below cold leg centerline between heater rod Columns A and B.			271,272	
GV-323-AB	Near center of core heated length, 323 cm below cold leg centerline between heater rod Columns A and B.			271,272	Questionable data. Analysis of beam path indicated possible obstruction by thermocouple or heater rod. Effect is unknown. Data to be used for trend only.
GV-383-23	Lower part of core heated length, 383 cm below cold leg centerline between heater rod Rows 2 and 3.			273,274	
GV-483-23	At bottom of core heated length, 483 cm below cold leg centerline between heater rod Rows 2 and 3.			275,276	Questionable data. Analysis of beam path indicated possible obstruction by thermocouple or heater rod. Effect is unknown. Data to be used for trend only.
GV-502-AB	At bottom of core heated length, 502 cm below cold leg centerline between heater rod Columns A and B.				Detector failed.
GV-528-588	Vessel lower head, 528 cm below cold leg centerline, at 13° to 588 cm below cold leg centerline at 165°.			277,278	
GV-546-23	In upper part of vessel lower plenum 546 cm below cold leg centerline between heater rod Rows 2 and 3.			279,280	
Pressurizer		1.6 to 1600 kg/m^3	0 to 1600 kg/m^3		
CI-PRIZE	Pressurizer surge line.			281,282	

TABLE IV (continued)

Measurement	Location and Comments[a]	Data Acquisition Range[a] Detector	Data Acquisition Range[a] System	Figure[a]	Measurement Comments[b]
MASS FLOW RATE	Mass flow rate obtained by combining density (gamma attenuation technique) with volumetric flow rate (turbine flowmeter) or momentum flux (drag screen).	Range for mass flow is determined from ranges of individual detectors used in calculation.			
Intact Loop					
FI-1, GI-1C	Hot leg, Spool 1.			283,284	
FI-16, GI-17C	Cold leg, Spool 16.			285,286	
FI-17, GI-17C	Cold leg, Spool 17.			287,288	
Broken Loop					
FB-37, GB-37	Cold leg, Spool 37.			289,290	
FB-40, GB-40VR NB-40, GB-40VR	Cold leg, Spool 40.			291,292 293,294	
FB-45, GB-45VR NB-45, GB-45VR	Cold leg, Spool 45.			295,296 297,298	
Downcomer					
FD-424, GD-456B	Instrumented spool piece.			299,300	
Vessel					
FV-1, GV-11	Core outlet.			301,302	
NV-9, GV-11	Core inlet.			303,304	
NV-499, GV-483-23	Core inlet.			305,306	
CORE CHARACTERISTICS					Loose heater rod ground connections resulted in uncertainties, in-core power level of up to 2% of actual power, with a probability of effects being 0.2% of actual power or less.
High Power Bus					
AH-HI	Core amperage.	0 to 10 000 A	0 to 10 030 A	307,308	
VH-HI	Core voltage.	0 to 400 V	0 to 402 V	309,310	
Low Power Bus					
AH-LO	Core amperage.	0 to 10 000 A	0 to 9330 A	311,312	
VH-LO	Core voltage.	0 to 400 V	0 to 402 V	313,314	
PUMP CHARACTERISTICS					
Intact Loop					
SI-PUMP	Pump speed.	377 rads/s	377 rad/s	315,316	
Broken Loop					
SB-PUMP	Pump speed.	3770 rads/s	3770 rad/s	317,318	
WB-PUMP	Pump power.		20 kW	319,320	

a. Statements at the beginning of a measurement category regarding location and comments, range, and figure apply to all subsequent measurements within the given category unless specified otherwise.

b. Detectors which were subjected to overrange conditions during portions of t test were capable of withstanding these conditions without change in operating or measuring characteristics when the physical conditions were again within the detector range.

544 048

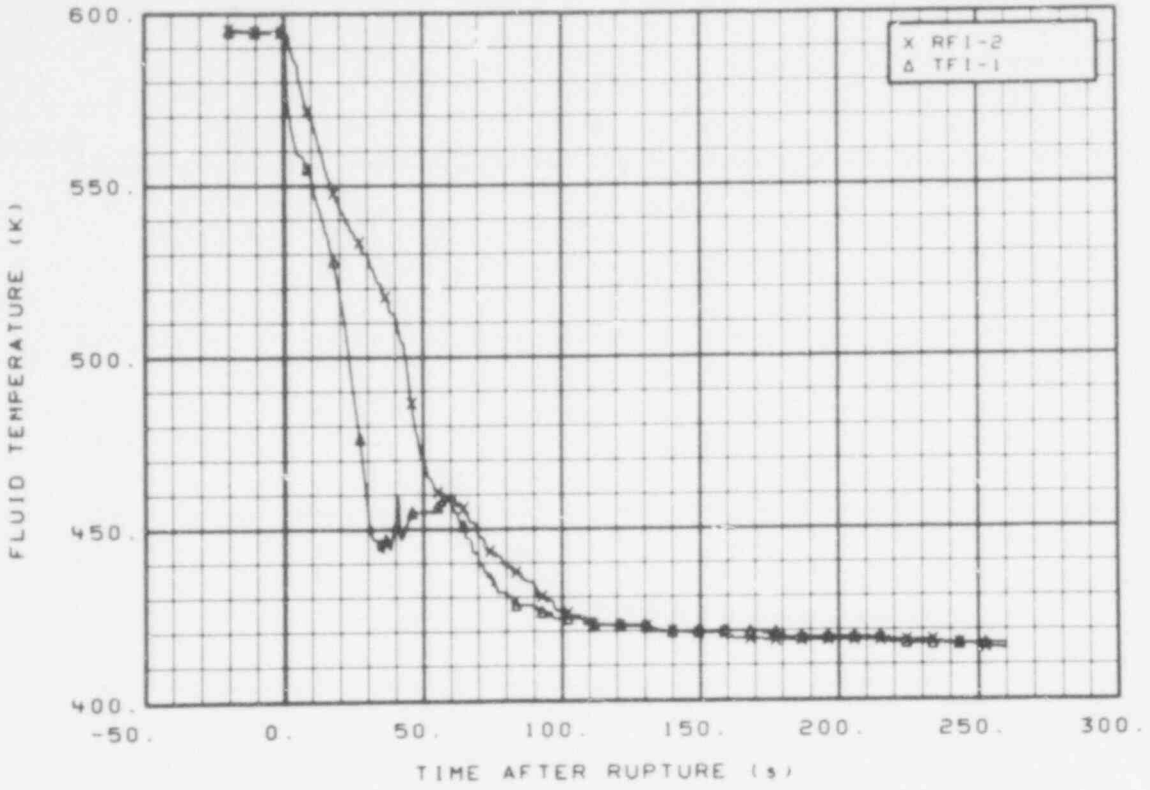

Fig. 11 Fluid temperature in intact loop hot leg (RFI-2 and TFI-1), from -20 to 260 s.

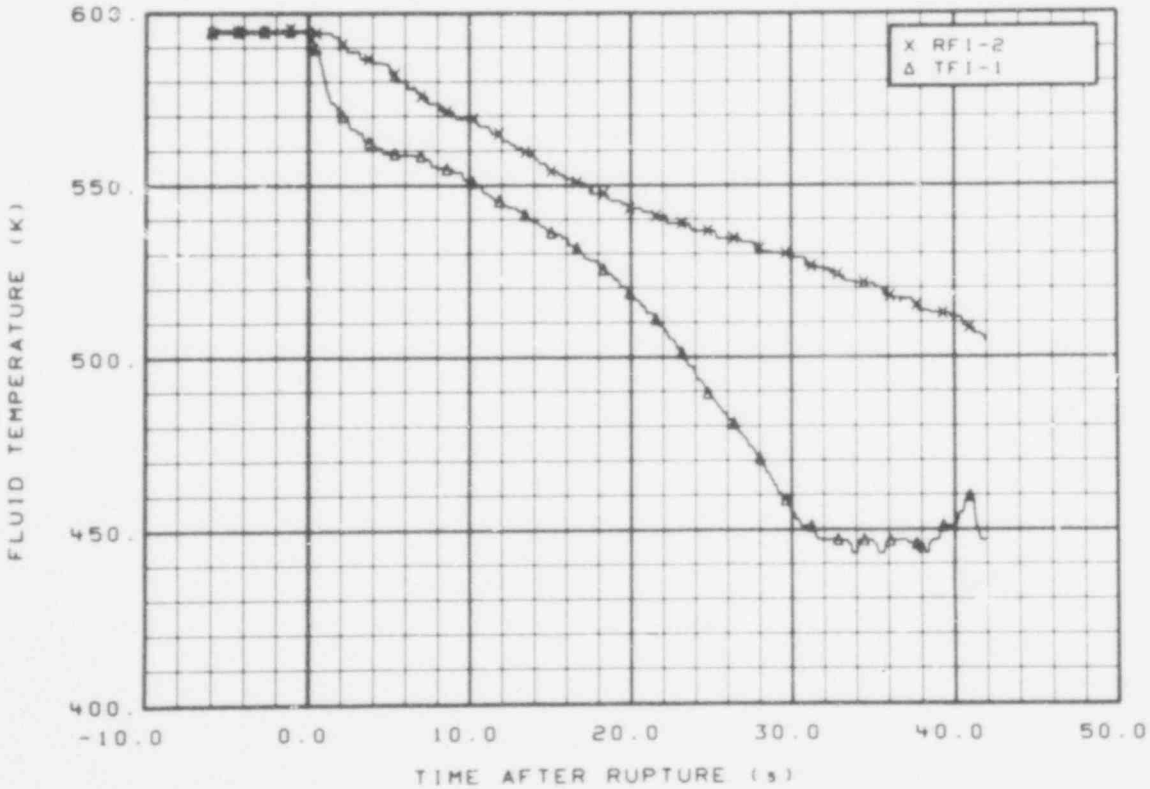

Fig. 12 Fluid temperature in intact loop hot leg (RFI-2 and TFI-1), from -6 to 42 s.

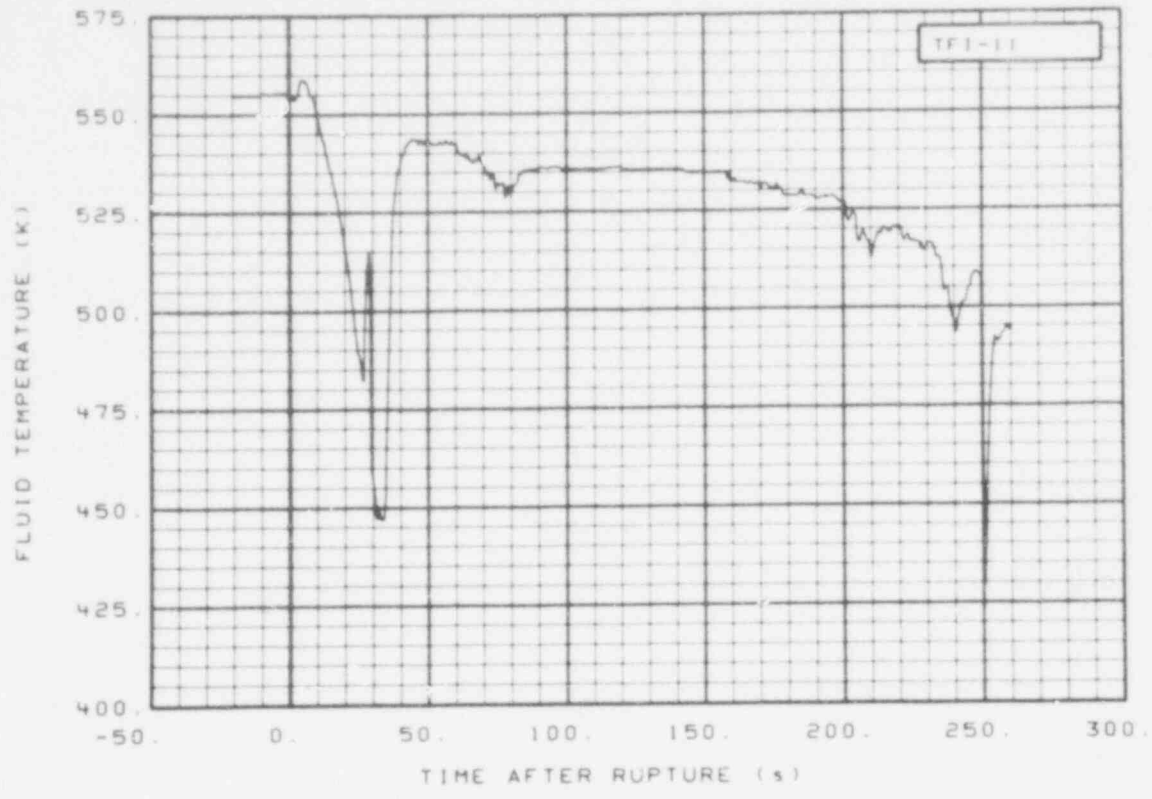

Fig. 13 Fluid temperatare in intact loop cold leg (TFI-11), from -20 to 260 s.

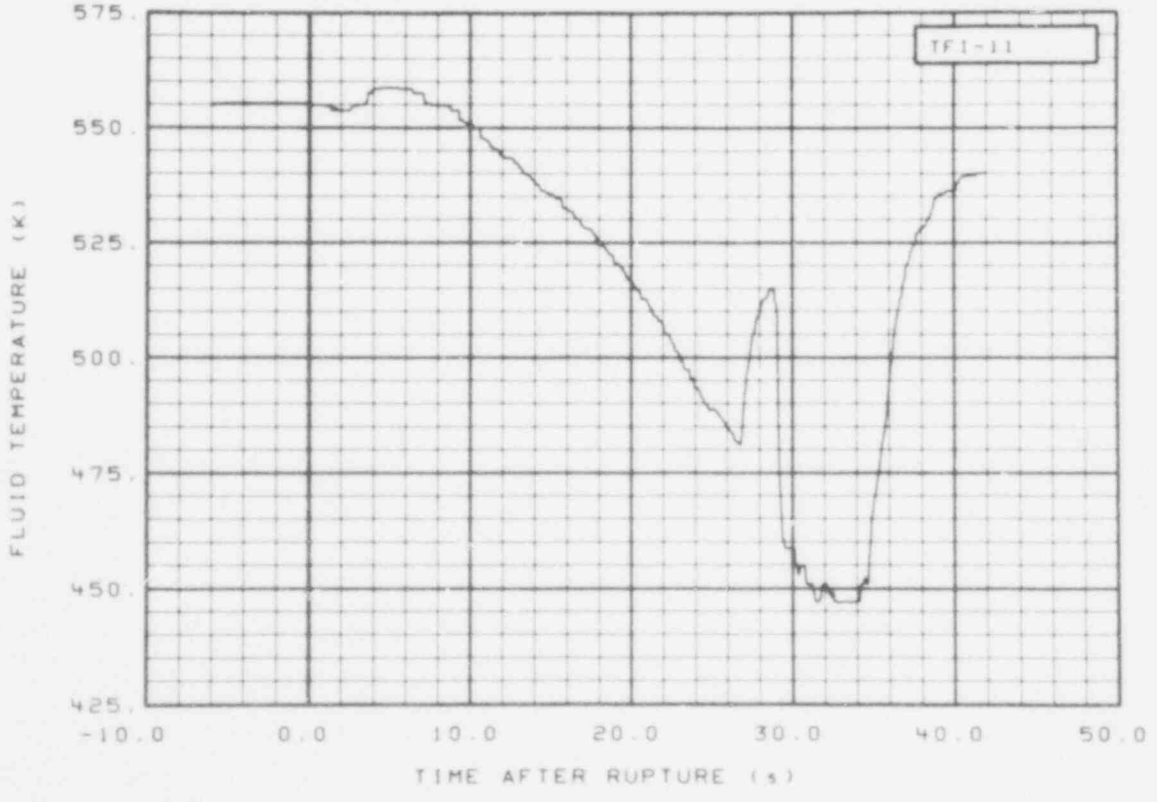

Fig. 14 Fluid temperature in intact loop cold leg (TFI-11), from -6 to 42 s.

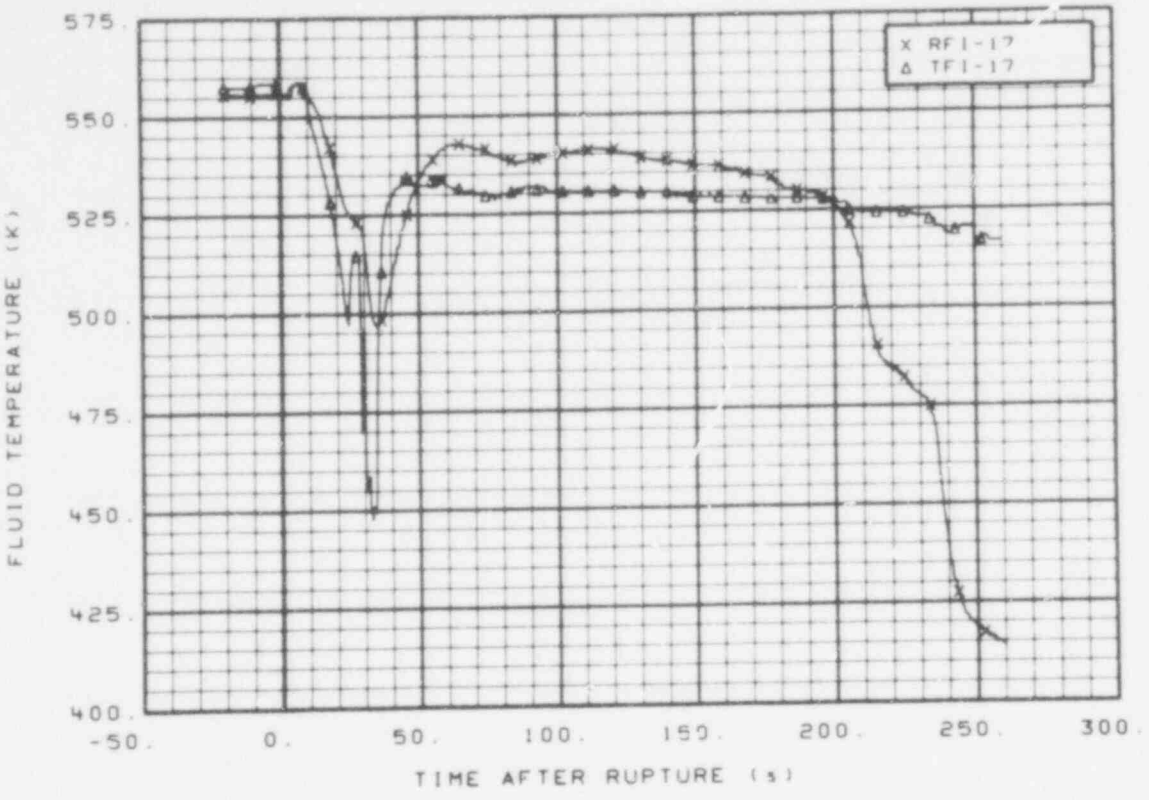

Fig. 15 Fluid temperature in intact loop cold leg (RFI-17 and TFI-17), from -20 to 260 s.

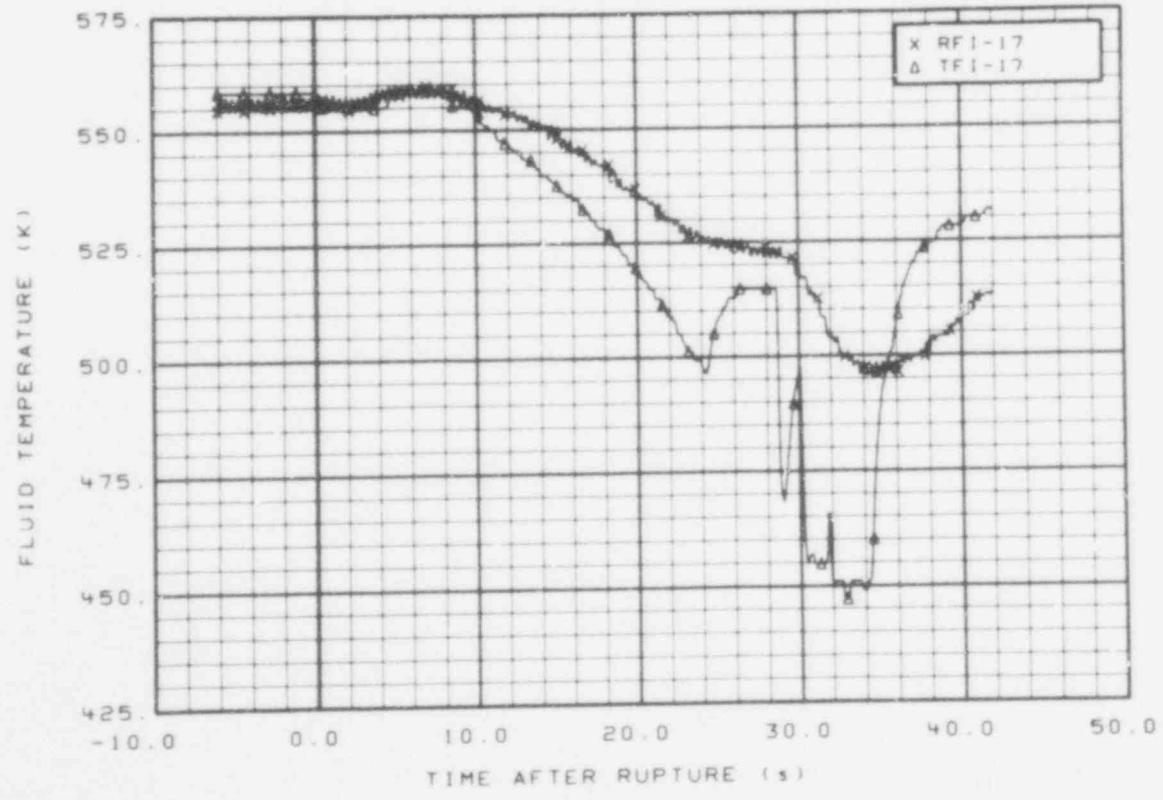

Fig. 16 Fluid temperature in intact loop cold leg (RFI-17 and TFI-17), from -6 to

544 051

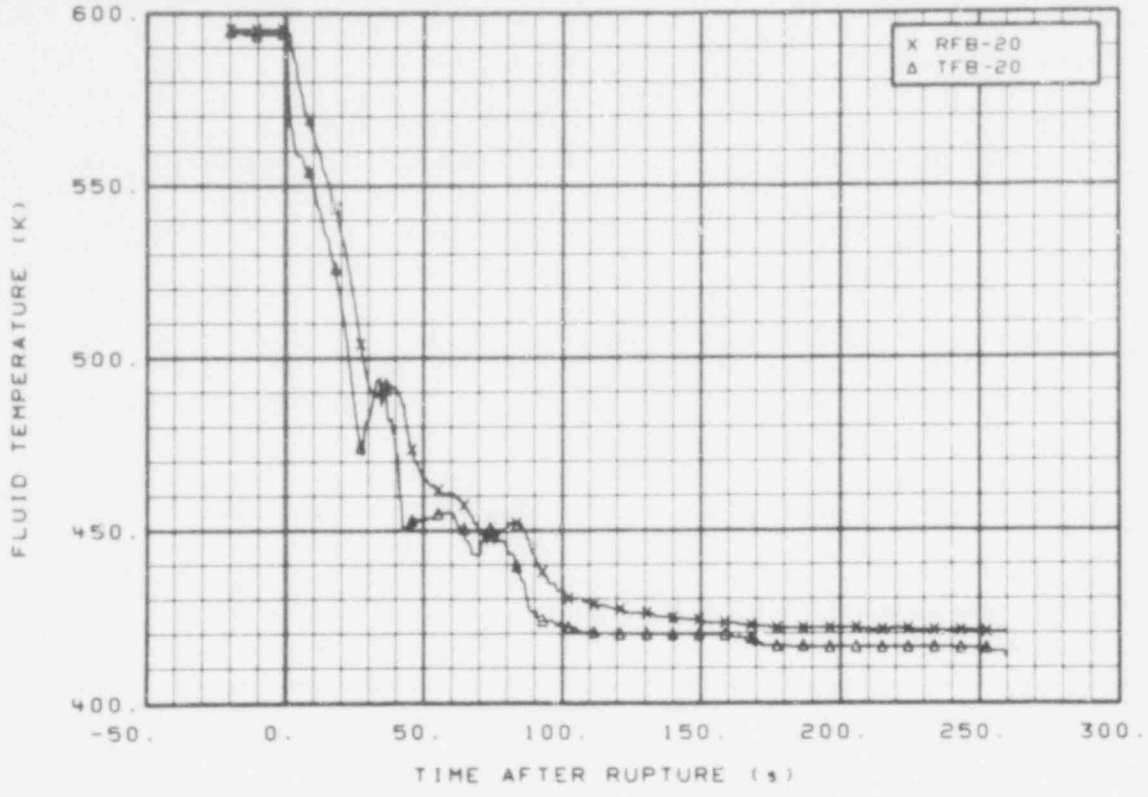

Fig. 17 Fluid temperature in broken loop hot leg (RFB-20 and TFB-20), from -20 to 260 s.

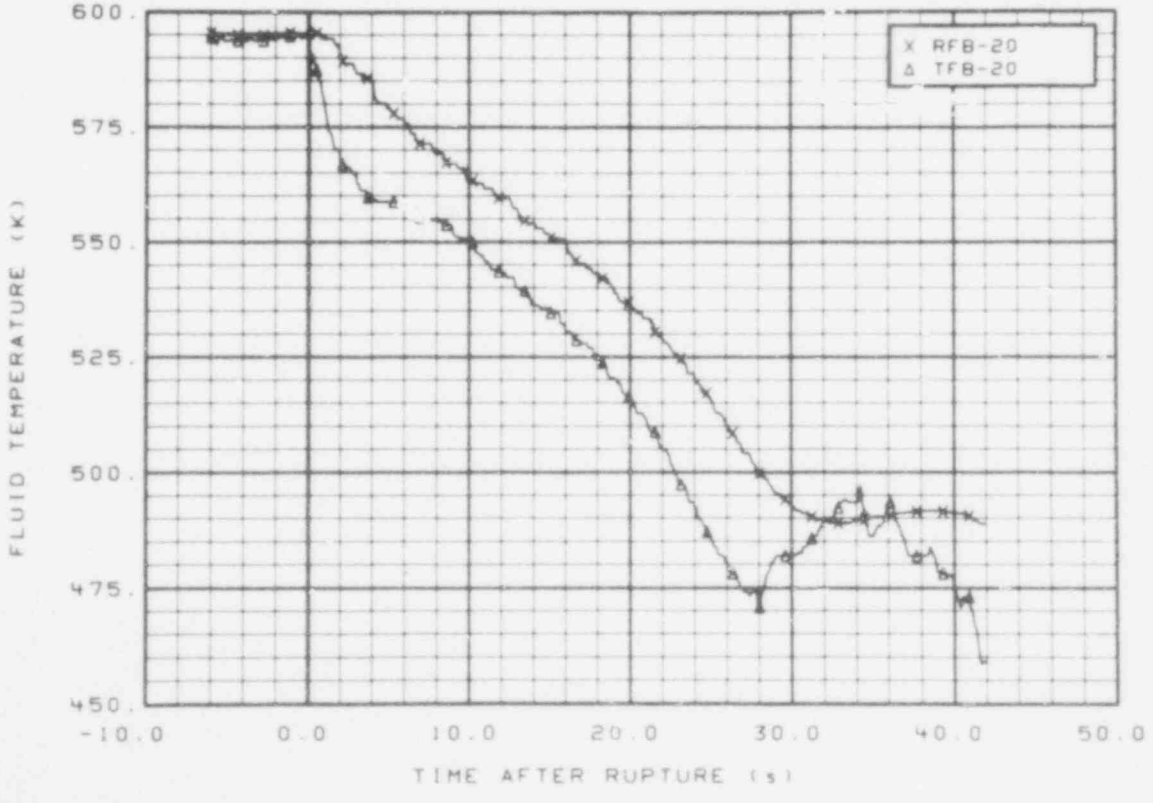

Fig. 18 Fluid temperature in broken loop hot leg (RFB-20 and TFB-20), from -6 to 42 s.

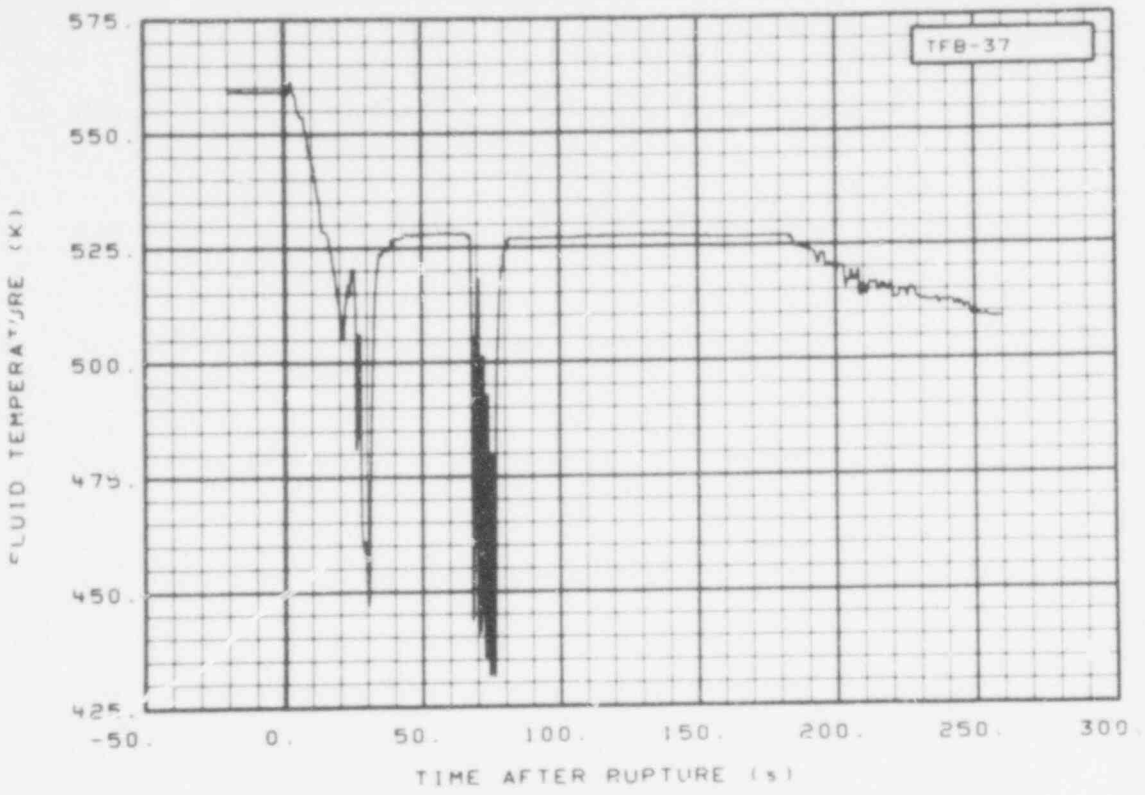

Fig. 19 Fluid temperature in broken loop cold leg (TFB-37), from -20 to 260 s.

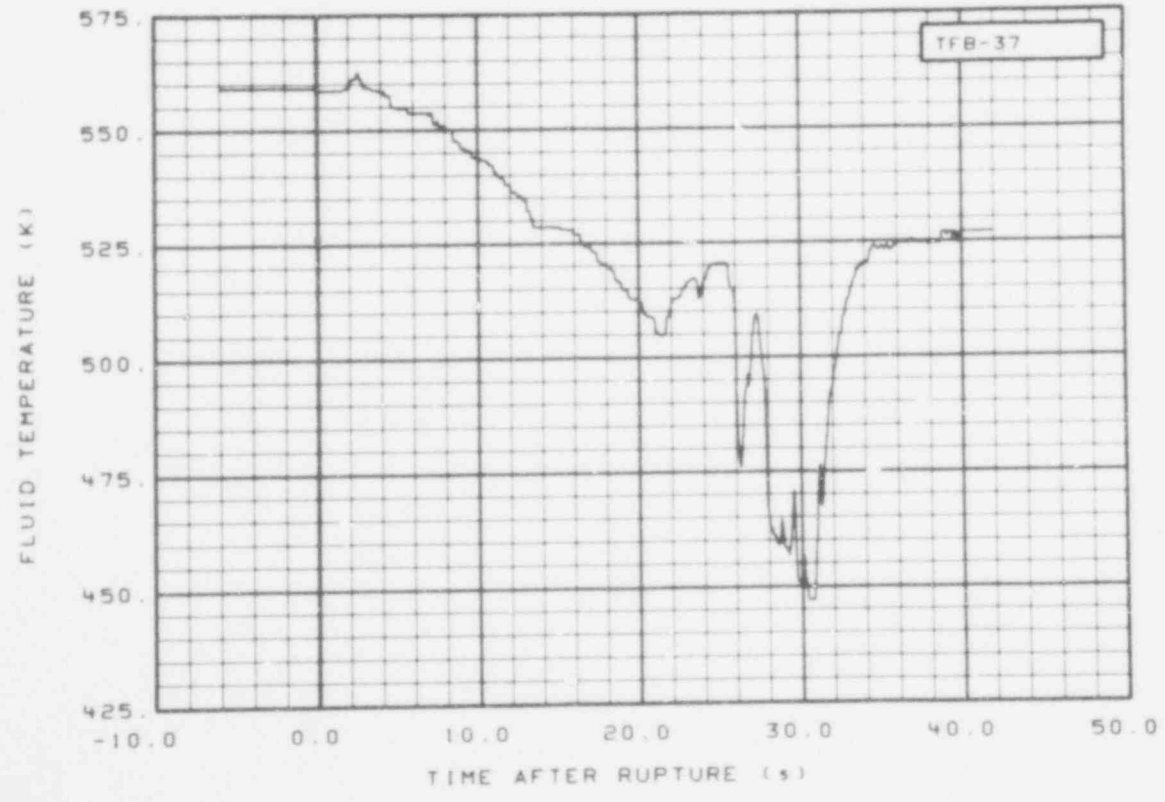

Fig. 20 Fluid temperature in broken loop cold leg (TFB-37), from -6 to 42 s.

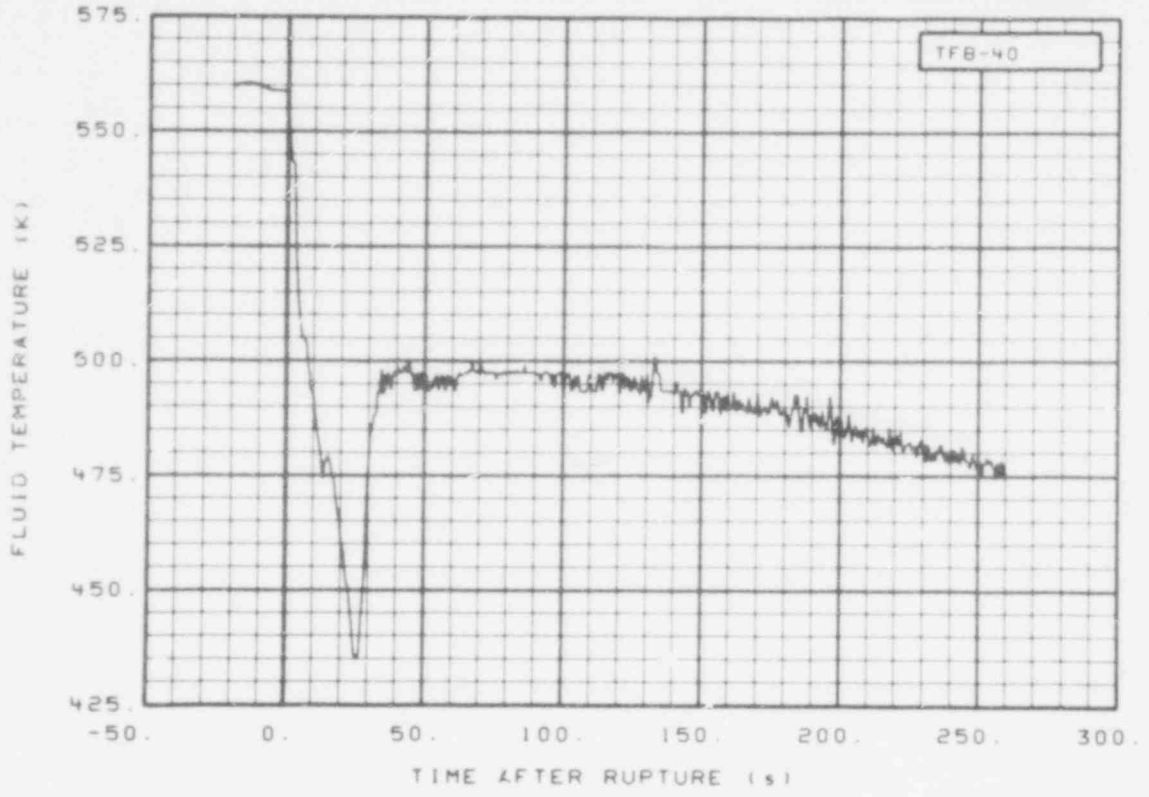

Fig. 21 Fluid temperature in broken loop cold leg (TFB-40), from -20 to 260 s.

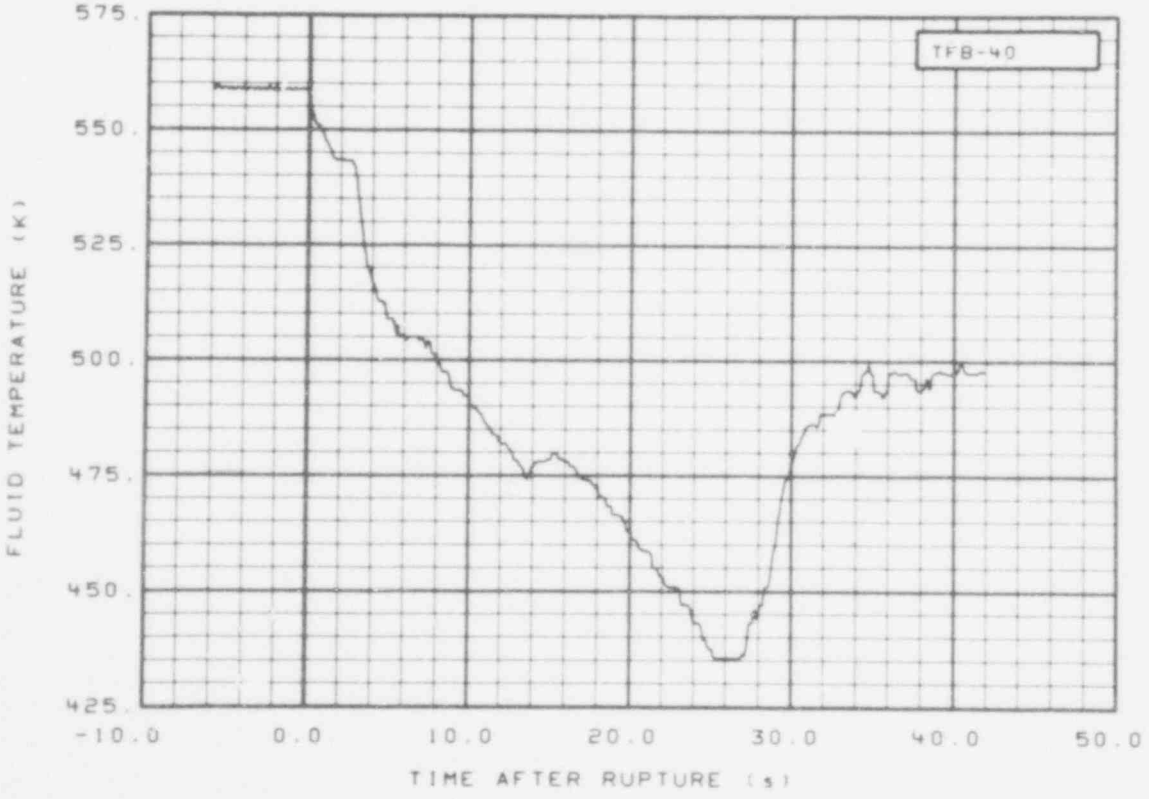

Fig. 22 Fluid temperature in broken loop cold leg (TFB-40), from -6 to 42 s.

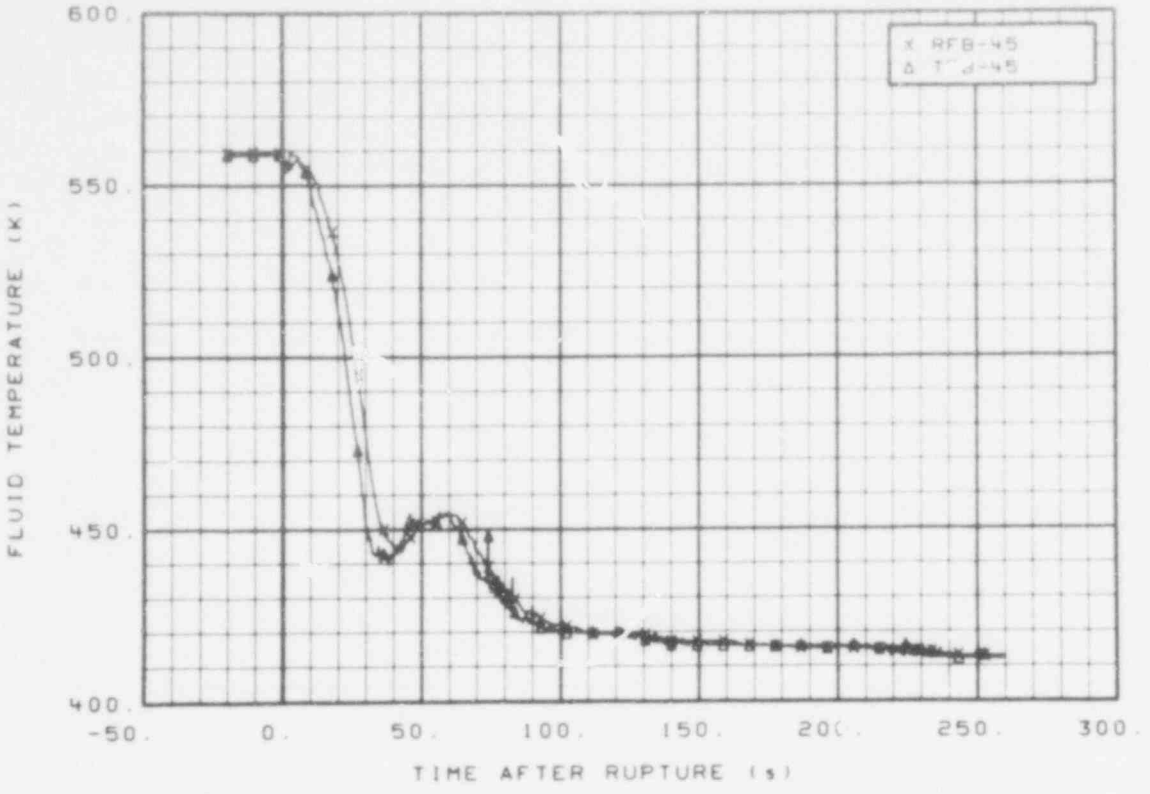

Fig. 23 Fluid temperature in broken loop cold leg (RFB-45 and TFB-45), from -20 to 260 s.

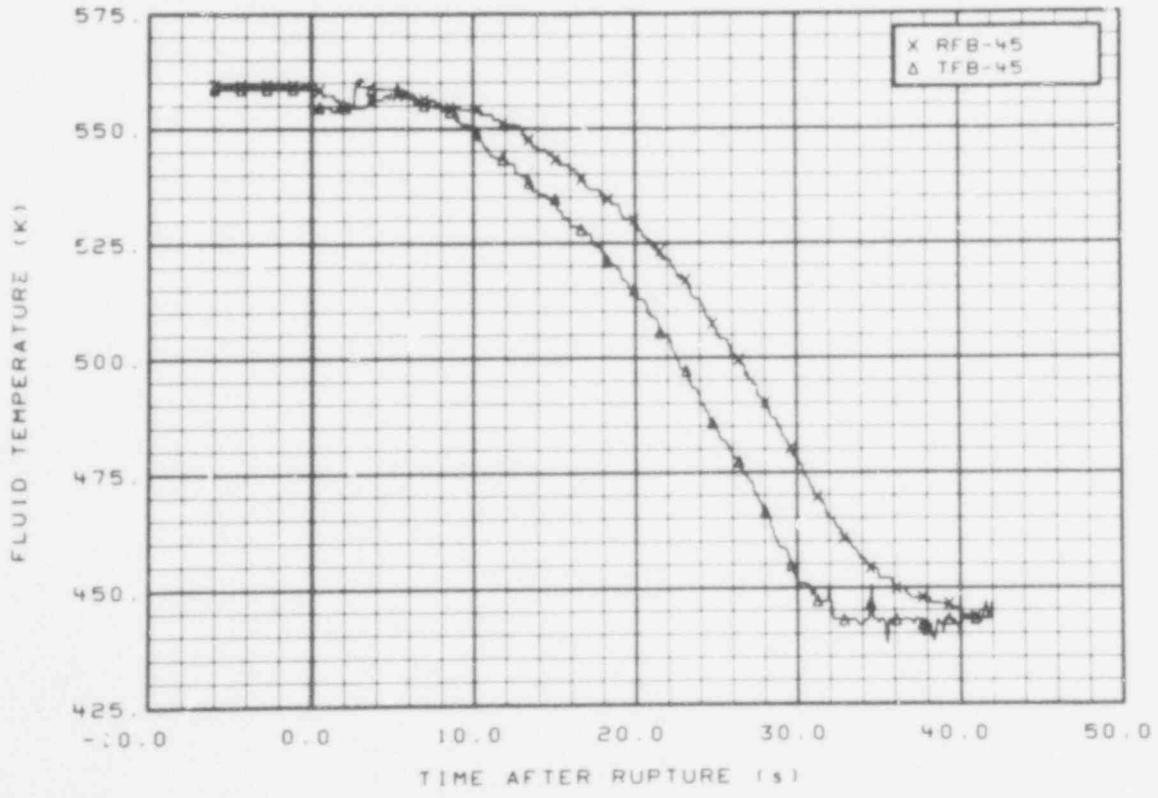

Fig. 24 Fluid temperature in broken loop cold leg (RFB-45 and TFB-45), from -6 to 42 s.

544 055

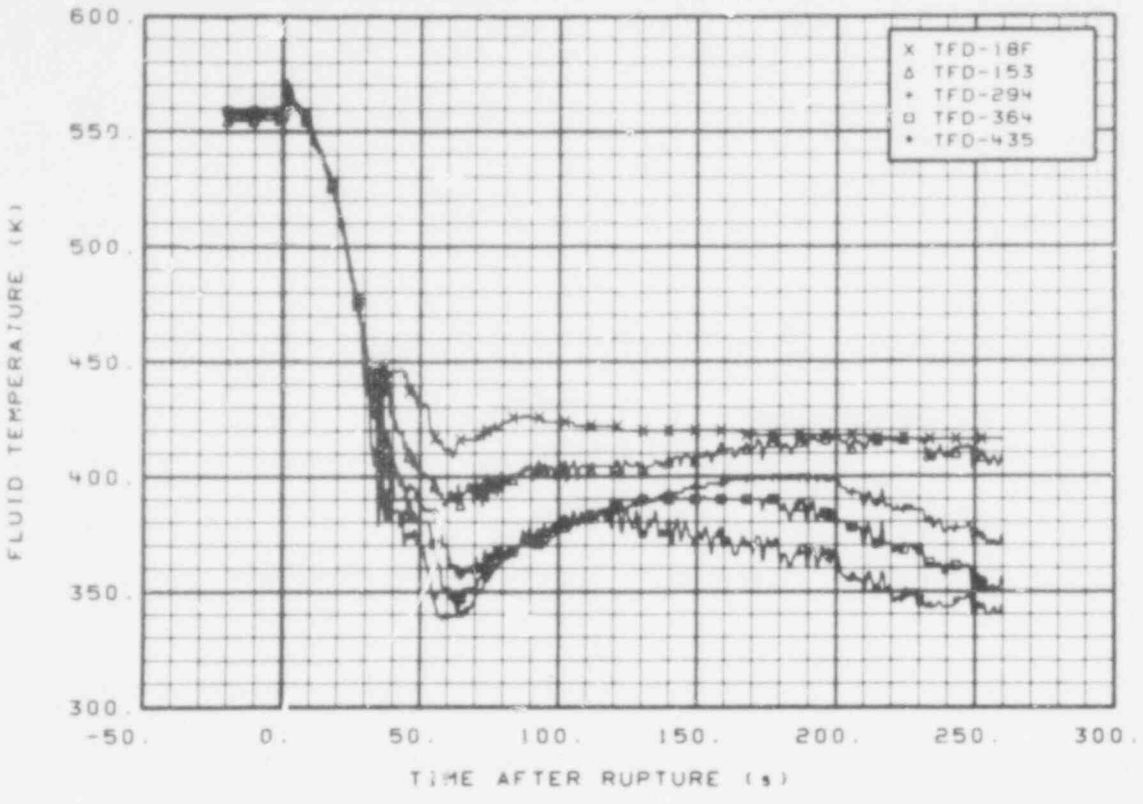

Fig. 25 Fluid temperature in downcomer (TFD-18F, TFD-153, TFD-294, TFD-364, and TFD-435), from -20 to 260 s.

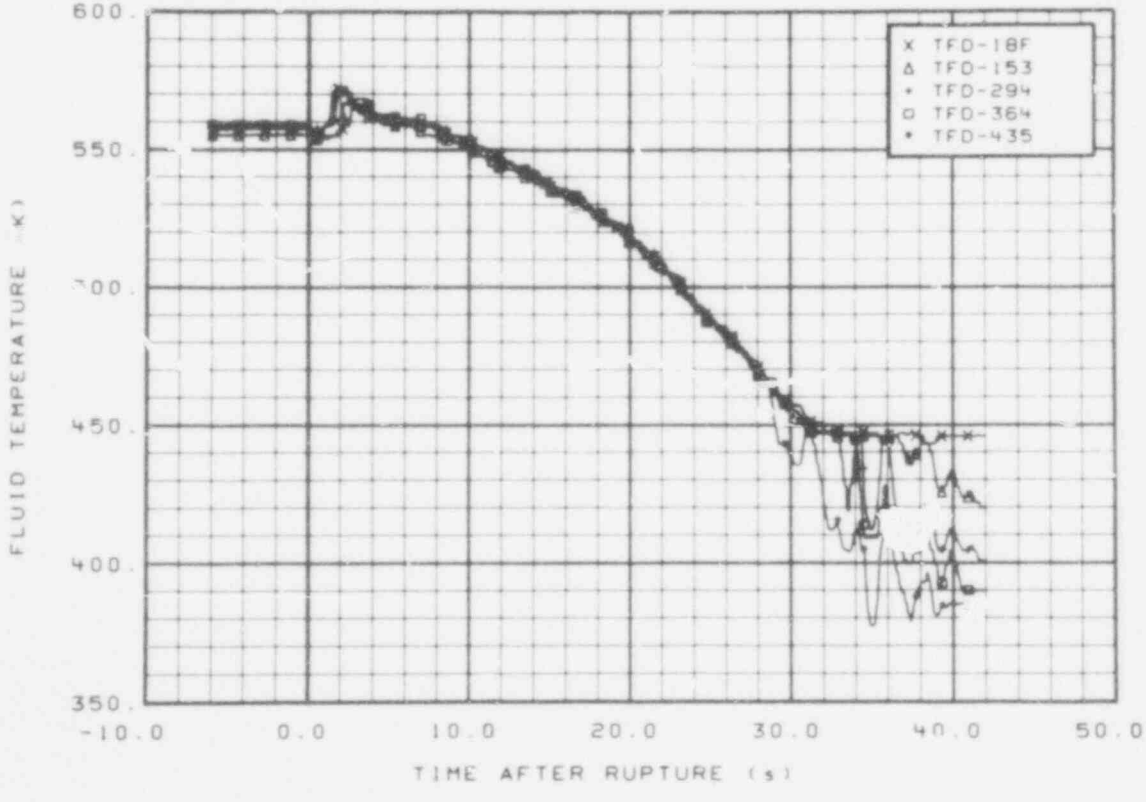

Fig. 26 Fluid temperature in downcomer (TFD-18F, TFD-153, TFD-294, TFD-364, and TFD-435), from -6 to 42 s.

514 056

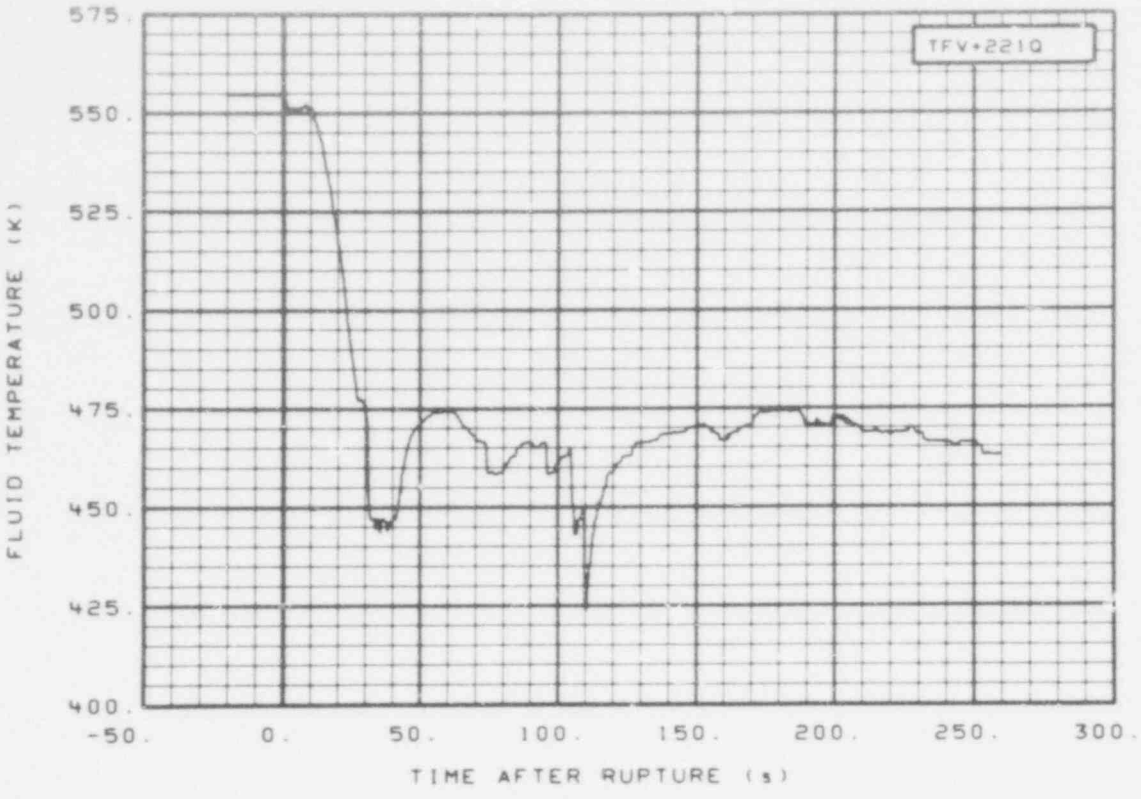

Fig. 27 Fluid temperature in vessel (TFV + 221Q), from -20 to 260 s.

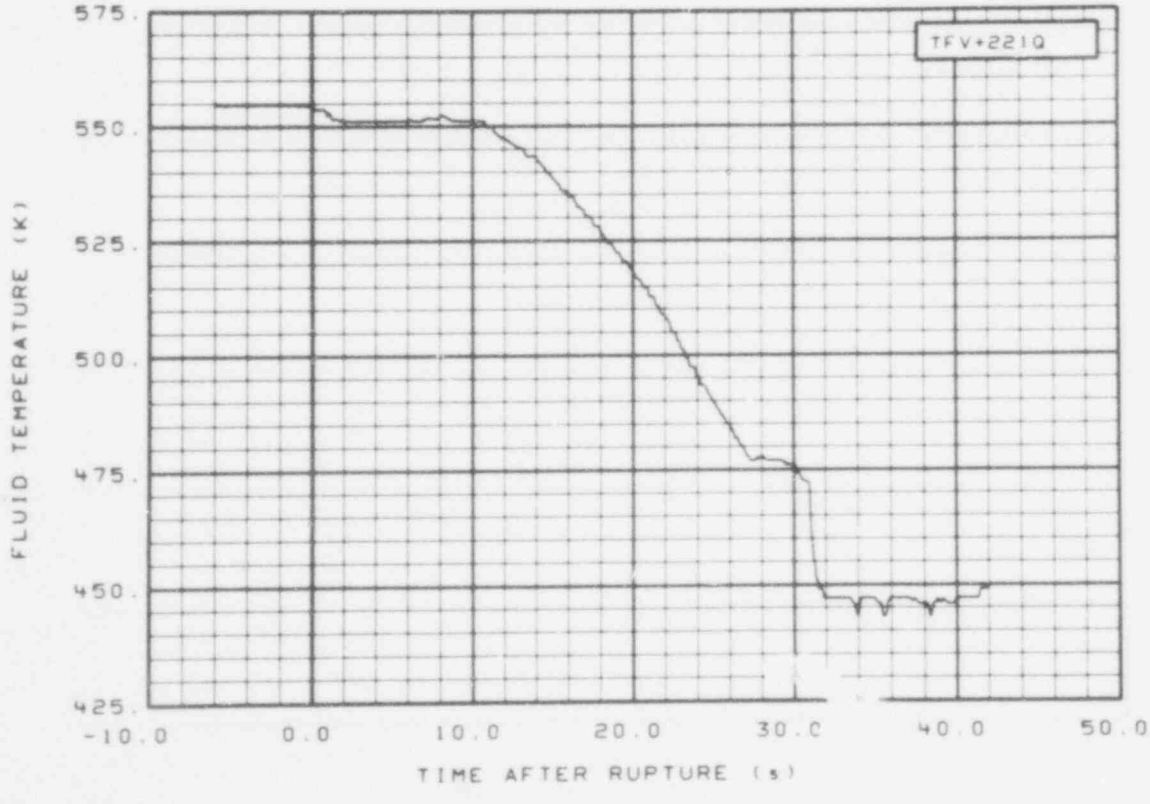

Fig. 28 Fluid temperature in vessel (TFV + 221Q), from -6 to 42 s.

057

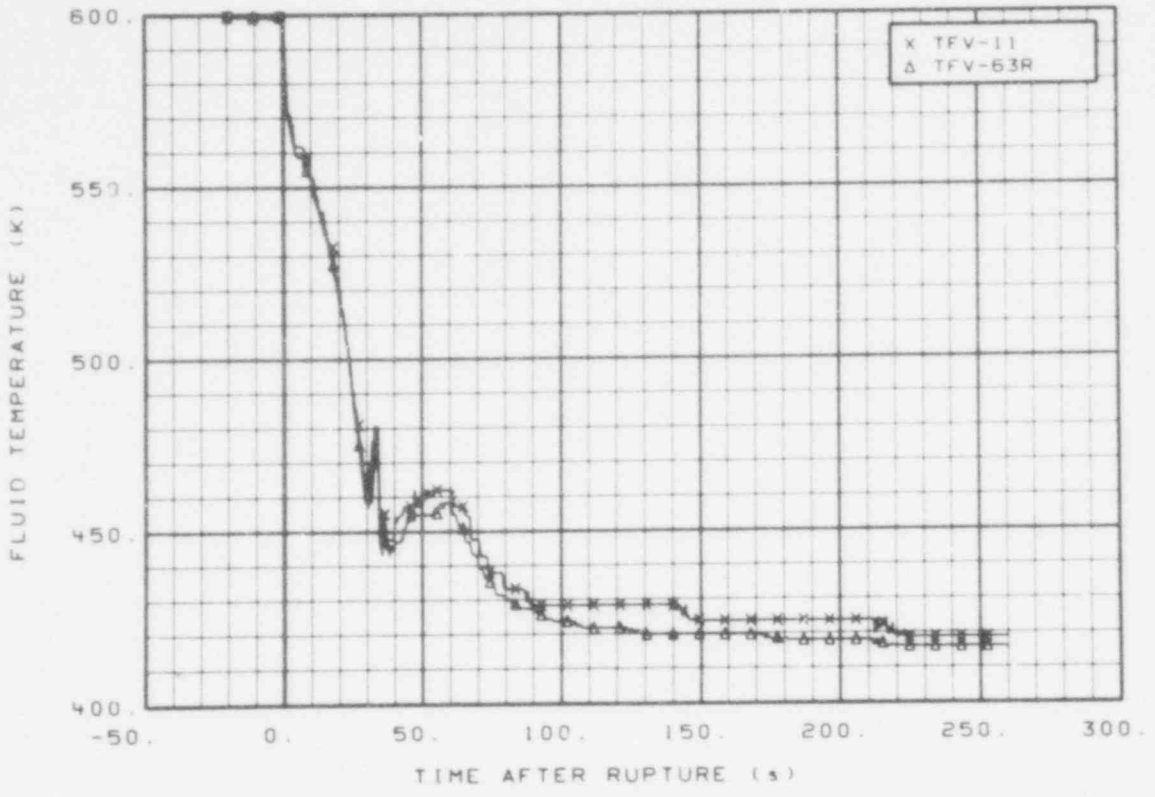

Fig. 29 Fluid temperature in vessel (TFV-11 and TFV-63R), from -20 to 260 s.

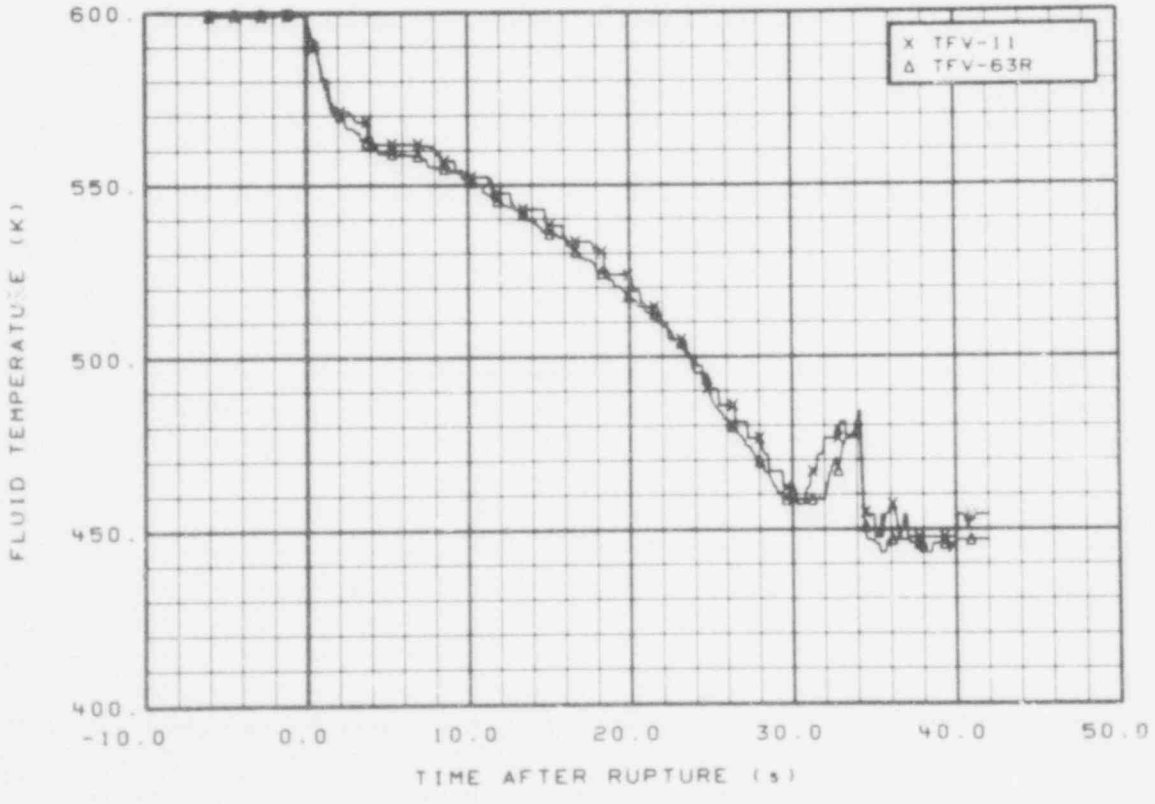

Fig. 30 Fluid temperature in vessel (TVF-11 and TFV-63R), from -6 to 42 s.

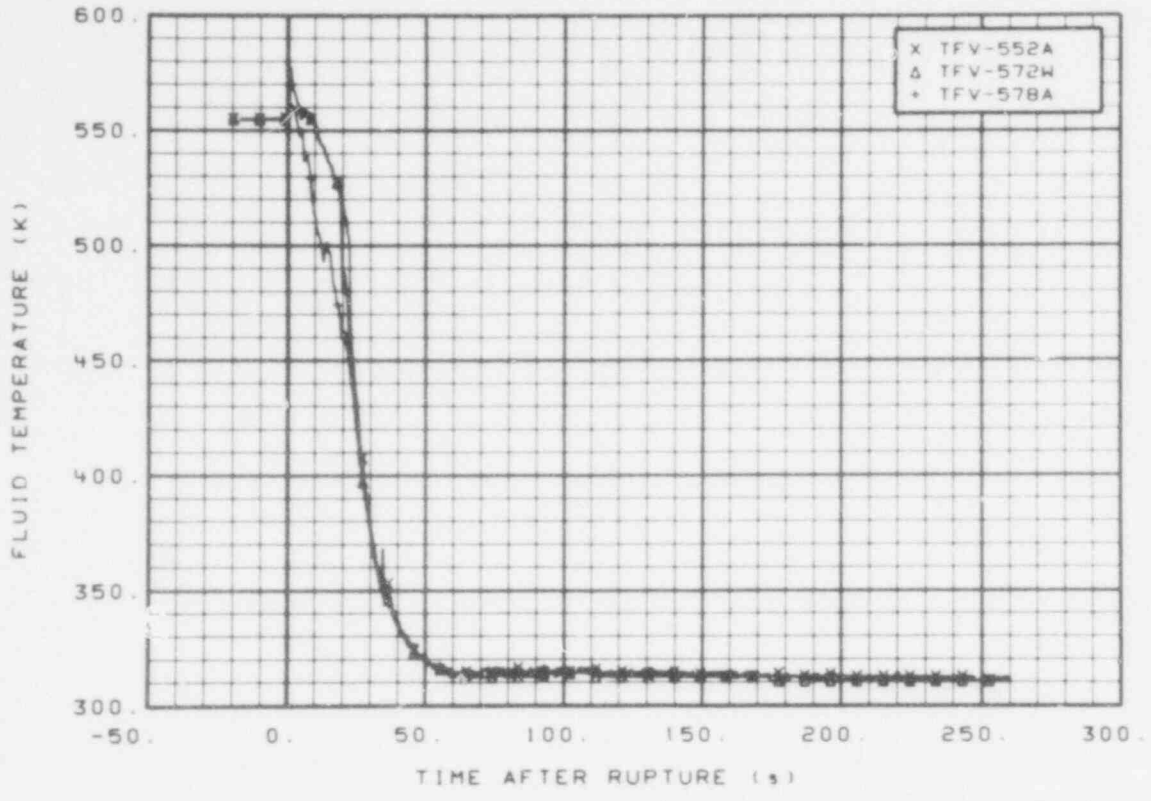

Fig. 31 Fluid temperature in vessel (TFV-552A, TFV-572W, and TFV-578A), from -20 to 260 s.

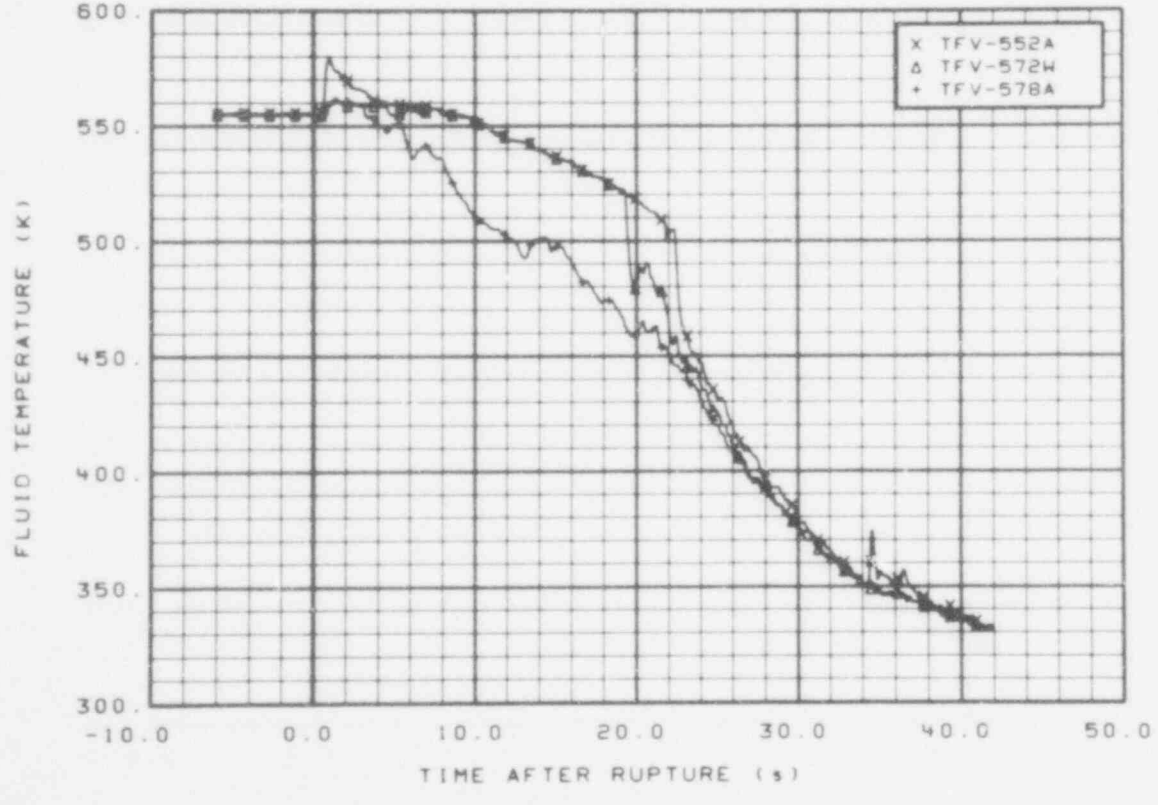

Fig. 32 Fluid temperature in vessel (TFV-552A, TFV-572W, and TFV-578A), from -6 to 42 s.

059

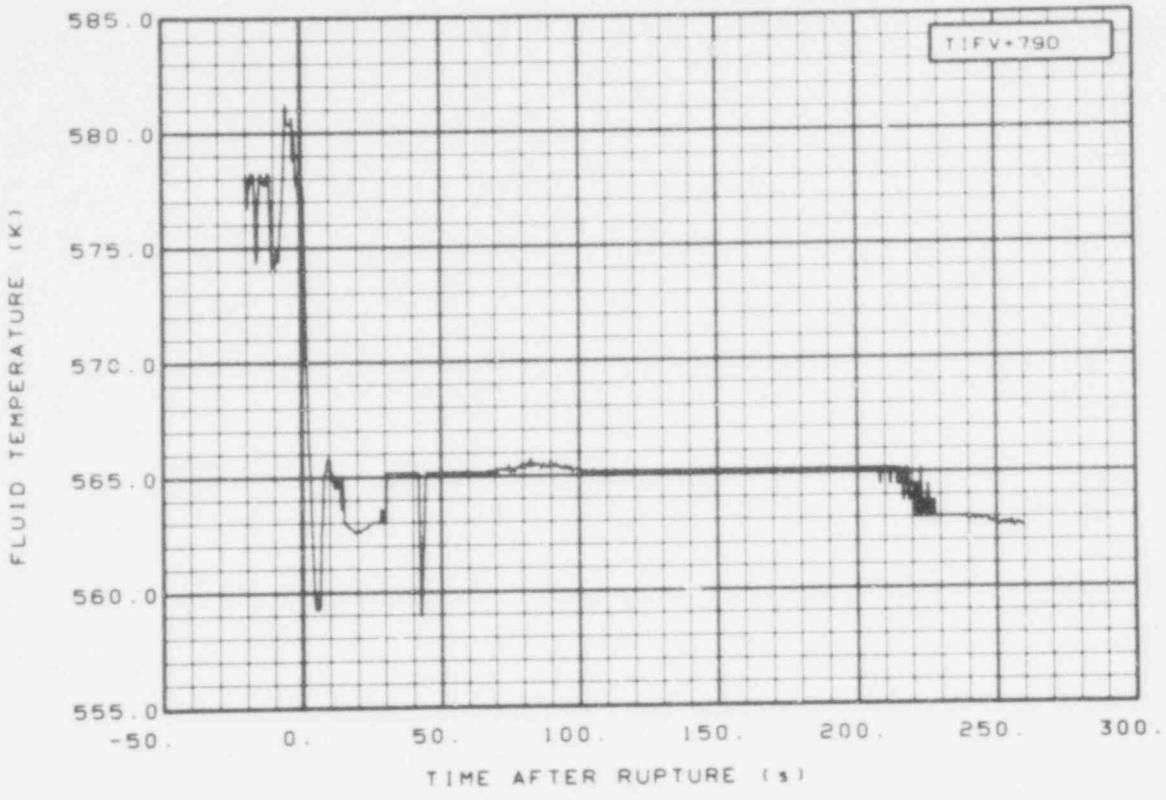

Fig. 33 Fluid temperature in vessel filler insulator gap (TIFV + 79D), from -20 to 260 s.

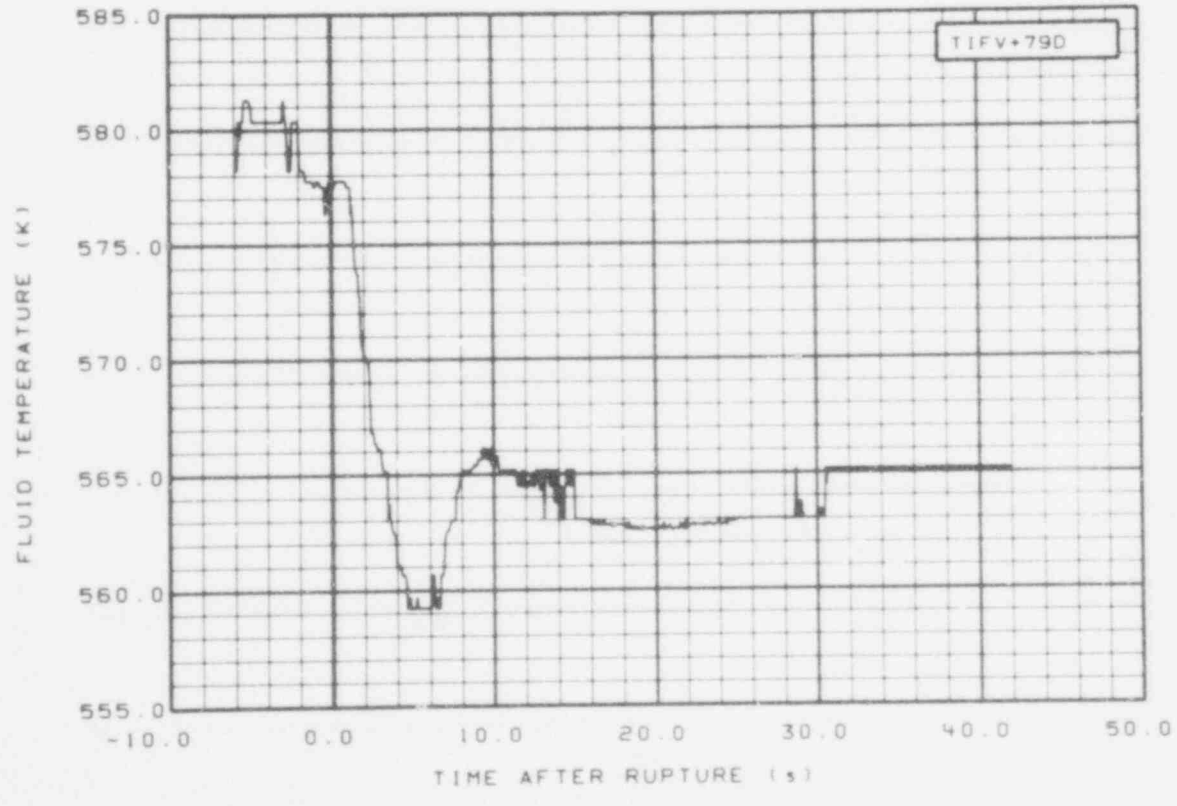

Fig. 34 Fluid temperature in vessel filler insulator gap (TIFV + 79D), from -6 to 42 s.

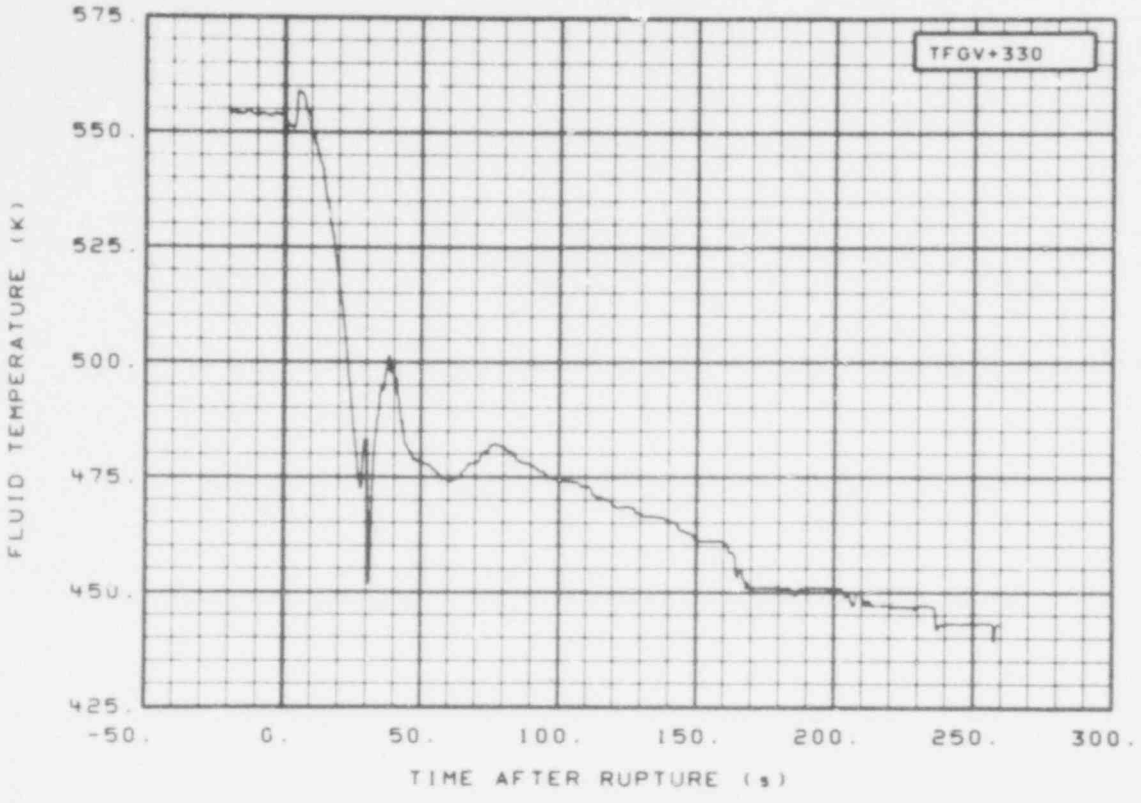

Fig. 35 Fluid temperature in vessel, core guide tube (TFGV + 330), from -20 to 260 s.

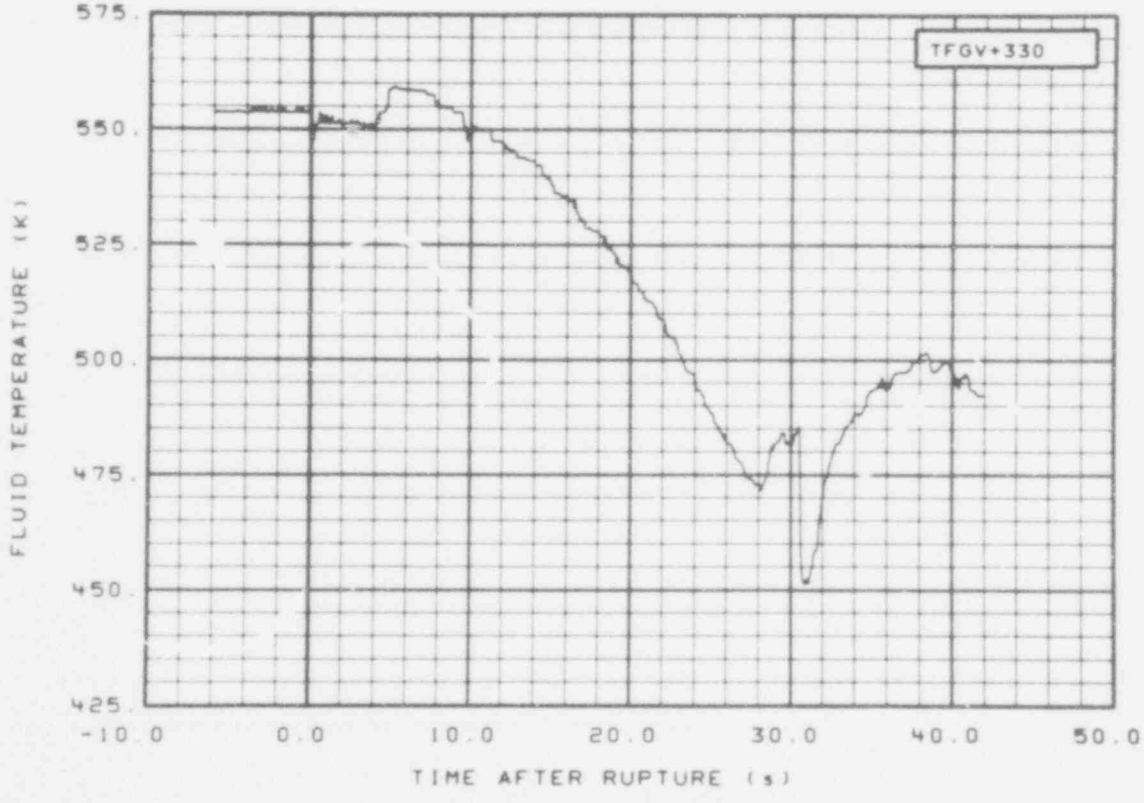

Fig. 36 Fluid temperature in vessel, core guide tube (TFGV + 330), from -6 to 42 s.

544 061

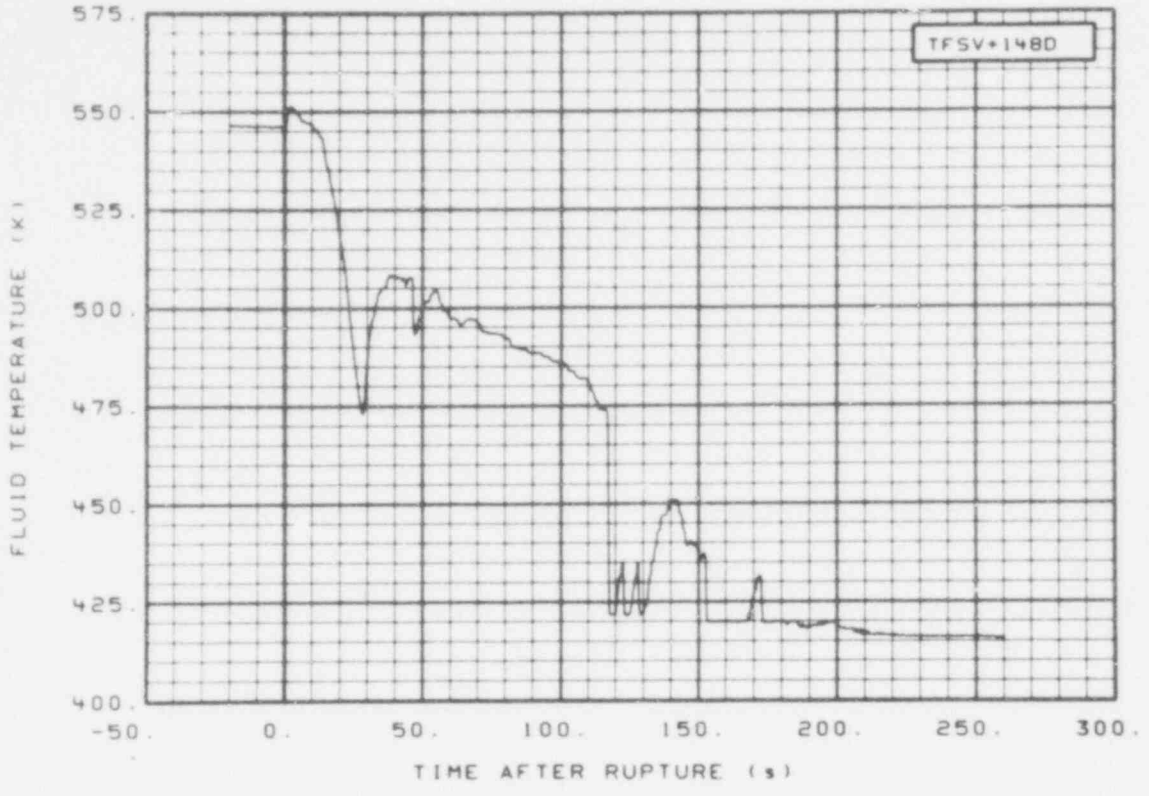

Fig. 37 Fluid temperature in vessel support tube (TFSV + 148D), from -20 to 260 s.

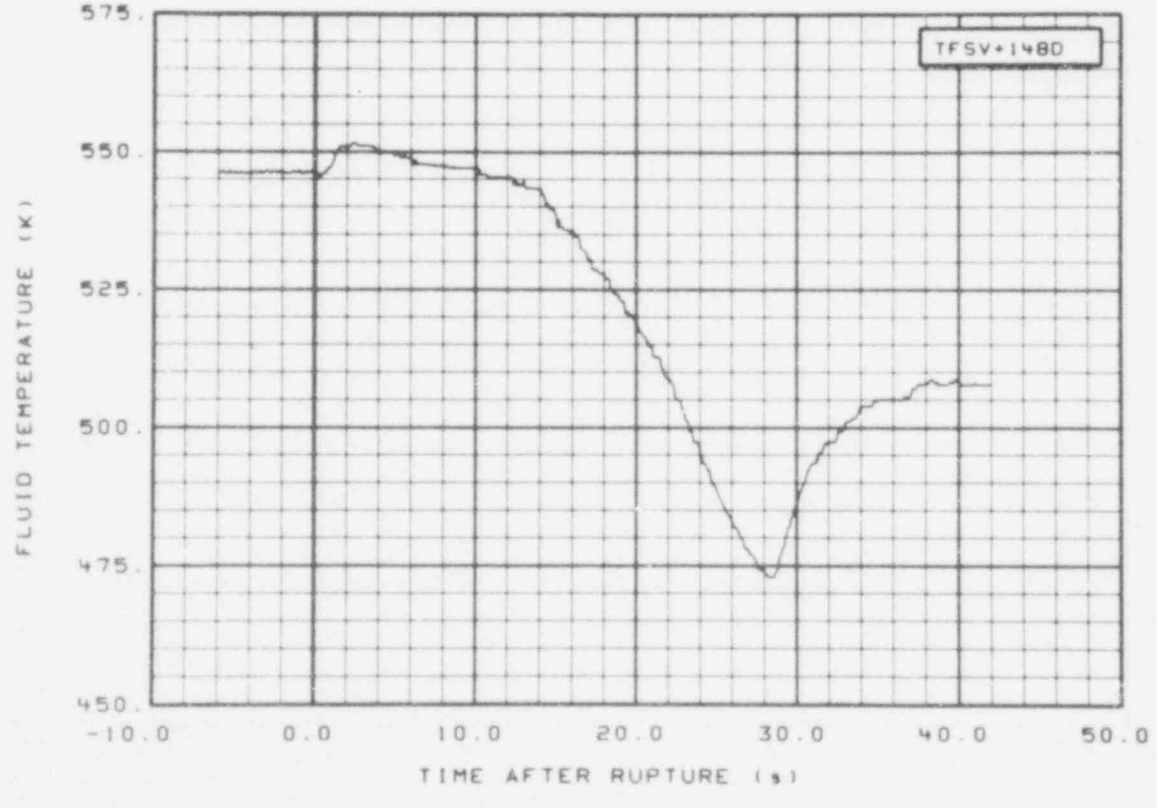

Fig. 38 Fluid temperature in vessel support tube (TFSV + 148D), from -6 to 42 s.

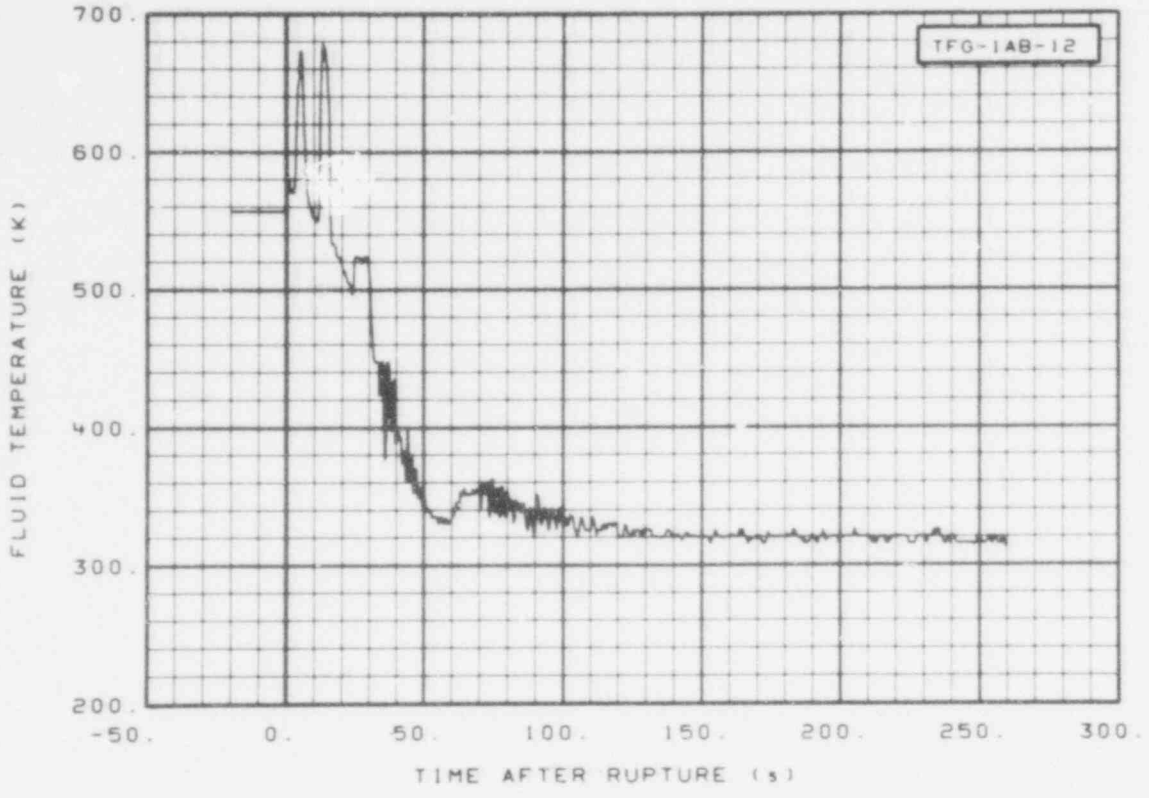

Fig. 39 Fluid temperature in core, Grid Spacer 1 (TFG-1AB-12), from -20 to 260 s.

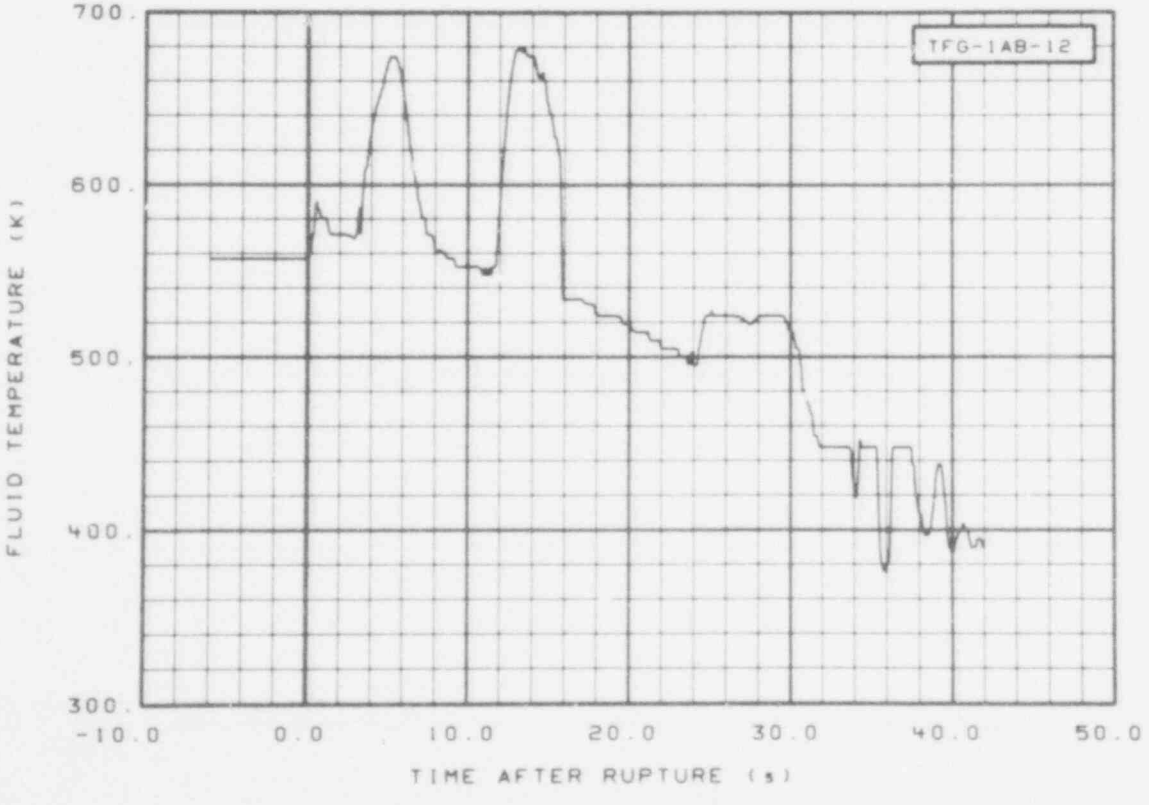

Fig. 40 Fluid temperature in core, Grid Spacer 1 (TFG-1AB-12), from -6 to 42 s.

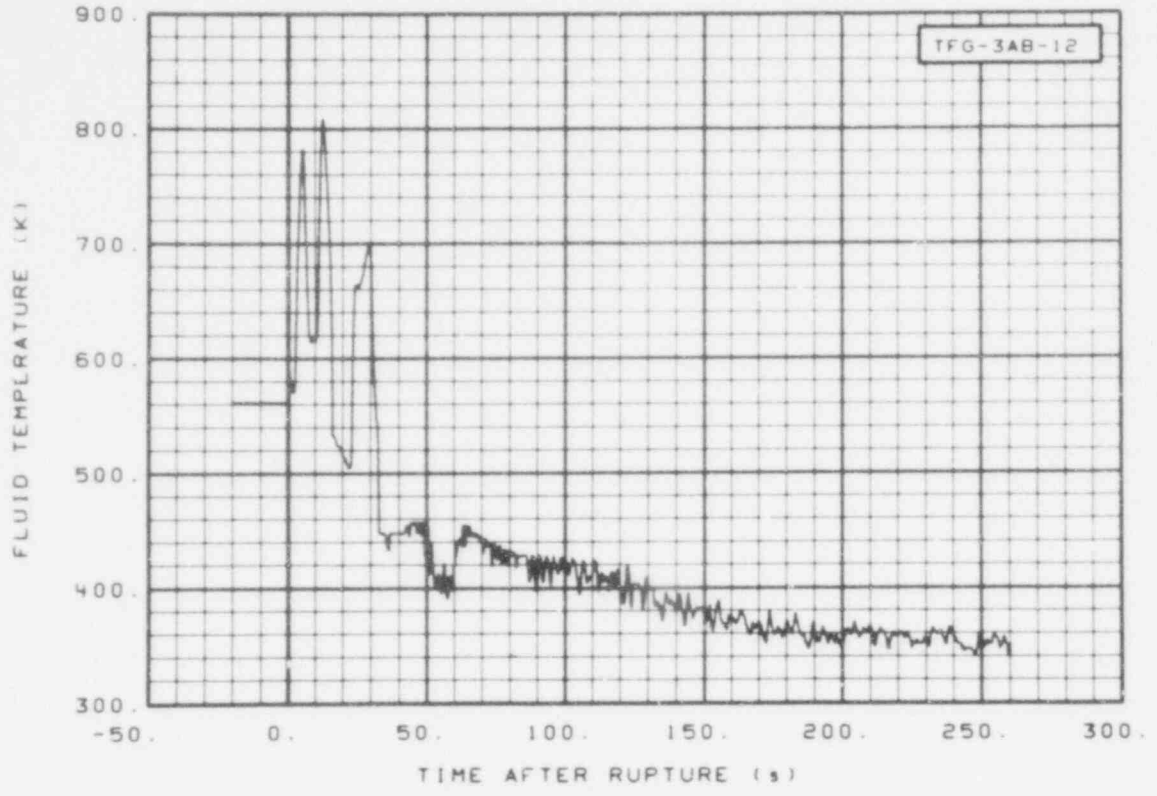

Fig. 41 Fluid temperature in core, Grid Spacer 3 (TFG-3AB-12), from -20 to 260 s.

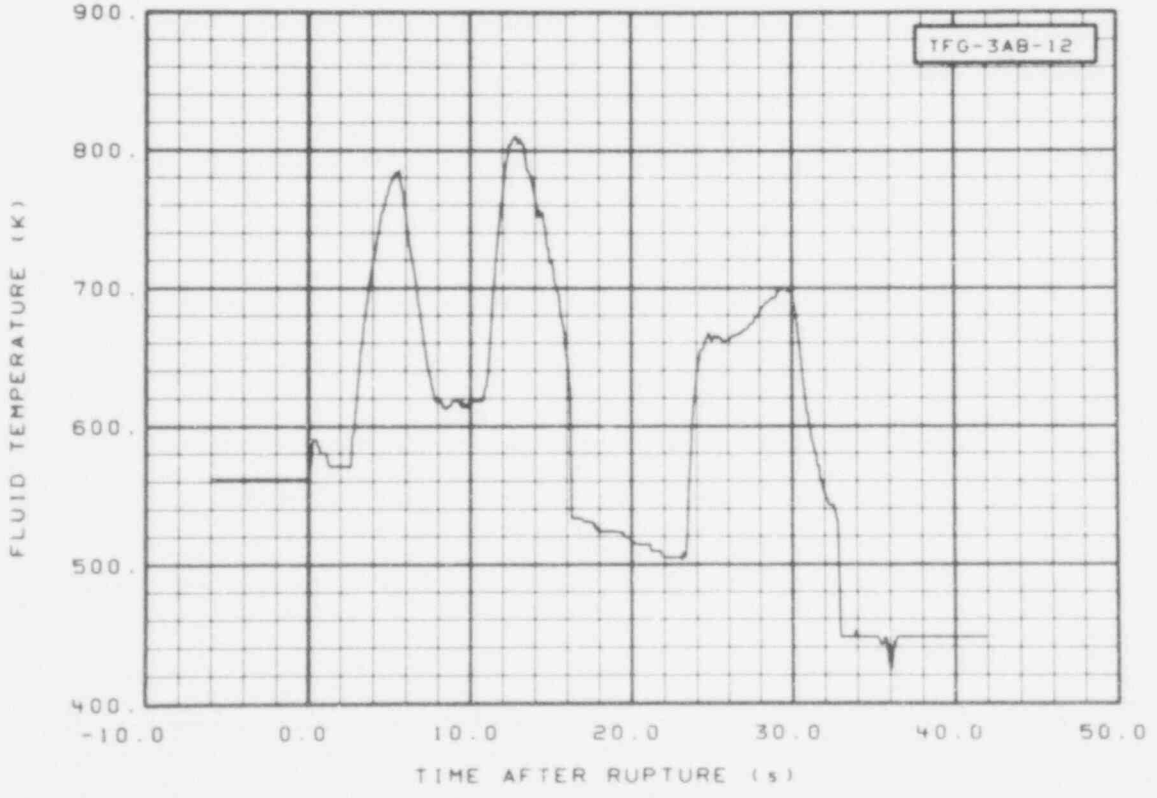

Fig. 42 Fluid temperature in core, Grid Spacer 3 (TFG-3AB-12), from -6 to 42 s.

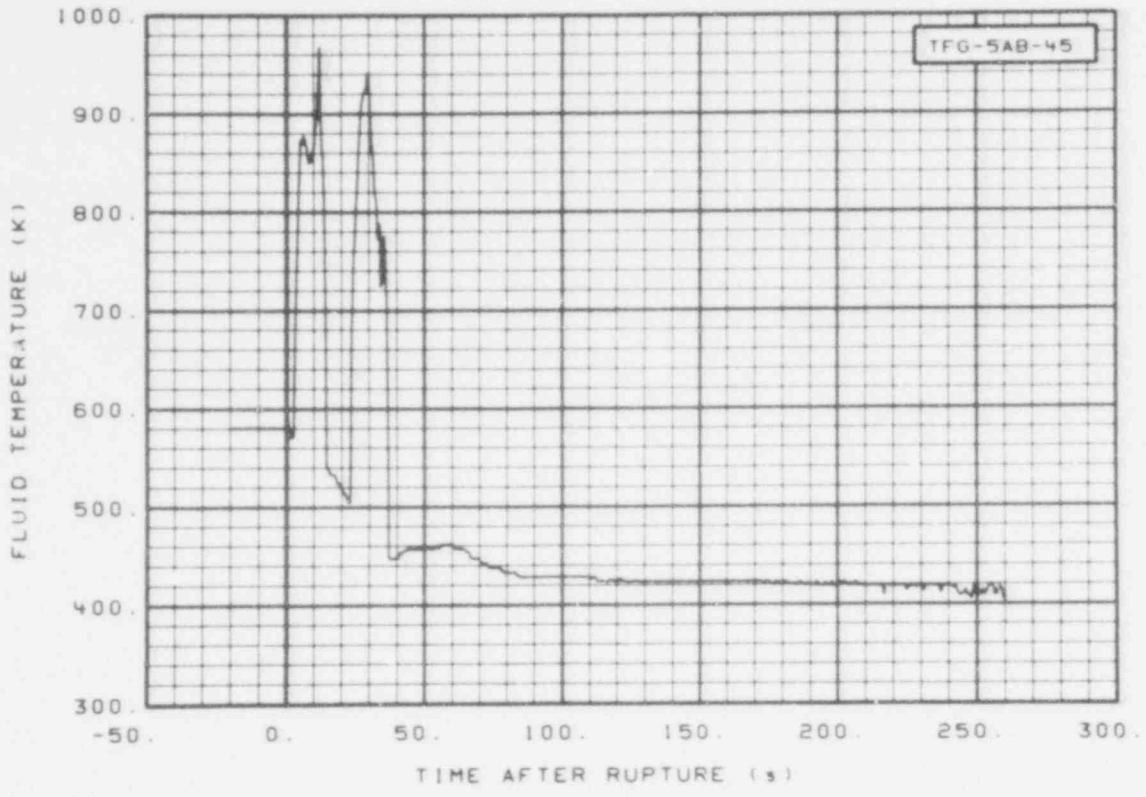

Fig. 43 Fluid temperature in core, Grid Spacer 5 (TFG-5AB-45), from -20 to 260 s.

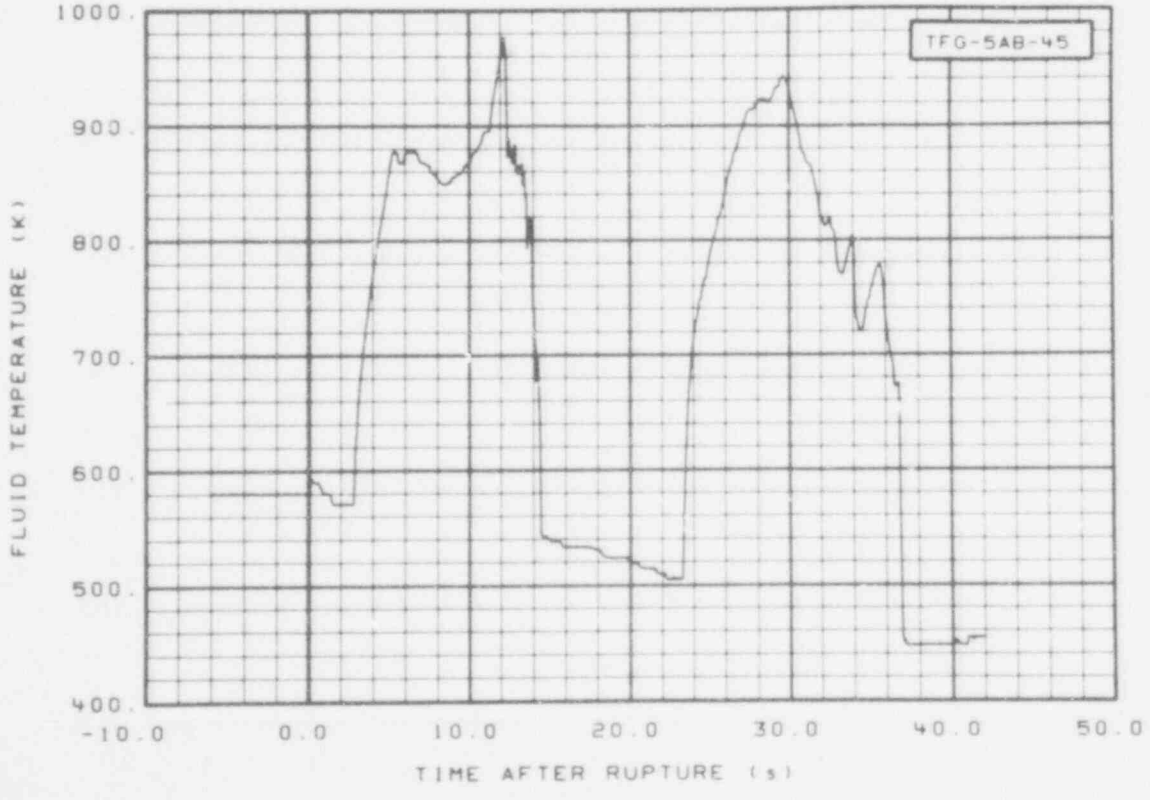

Fig. 44 Fluid temperature in core, Grid Spacer 5 (TFG-5AB-45), from -6 to 42 s.

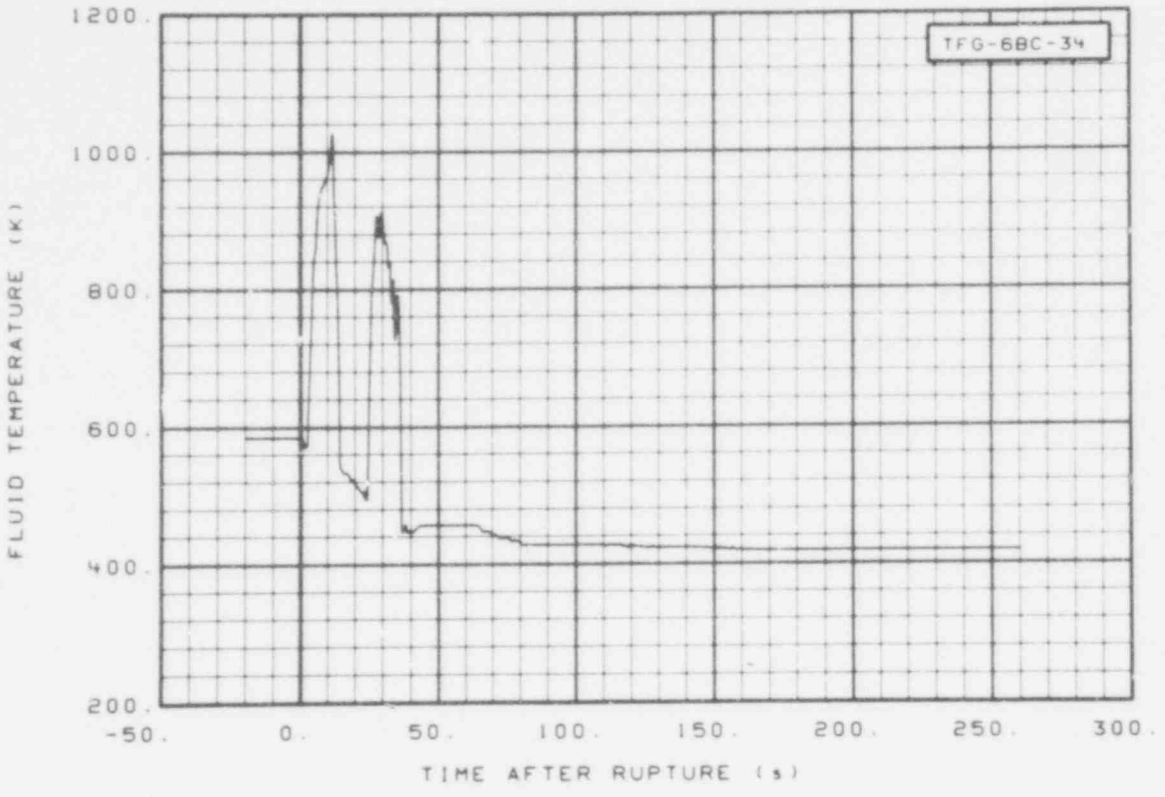

Fig. 45 Fluid temperature in core, Grid Spacer 6 (TFG-6BC-34), from -20 to 260 s.

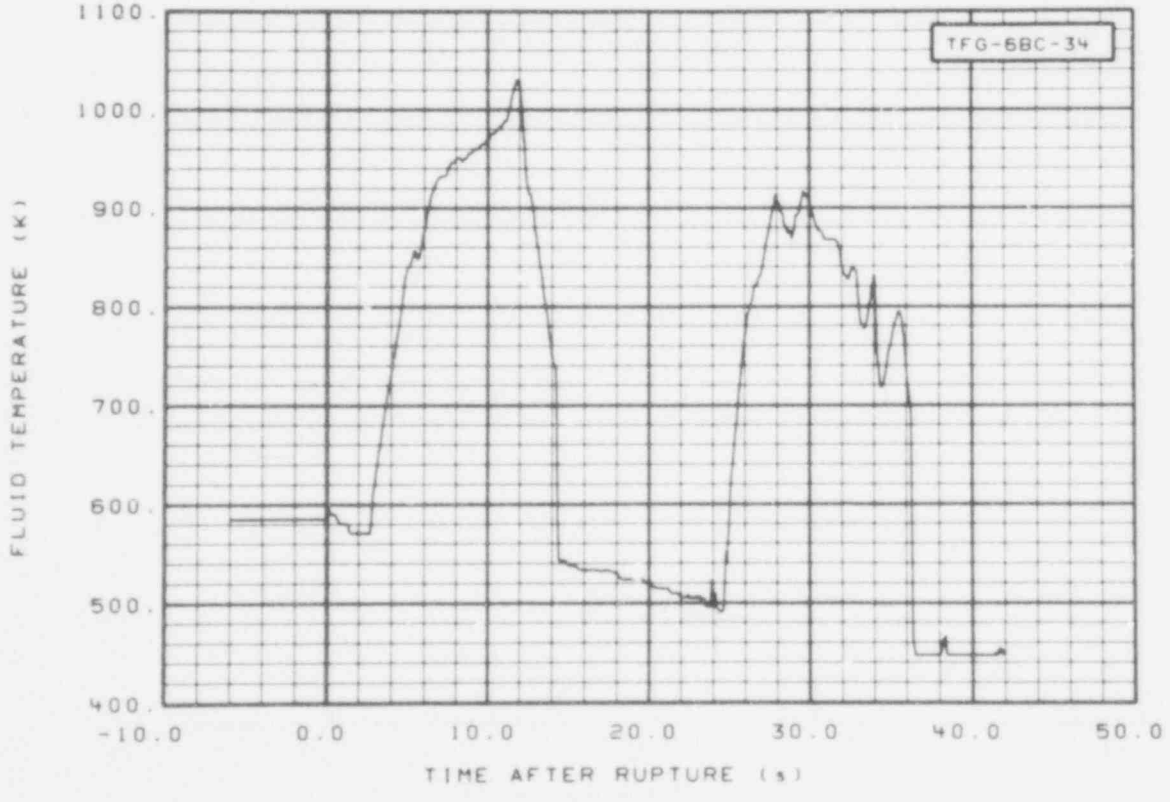

Fig. 46 Fluid temperature in core, Grid Spacer 6 (TFG-6BC-34), from -6 to 42 s.

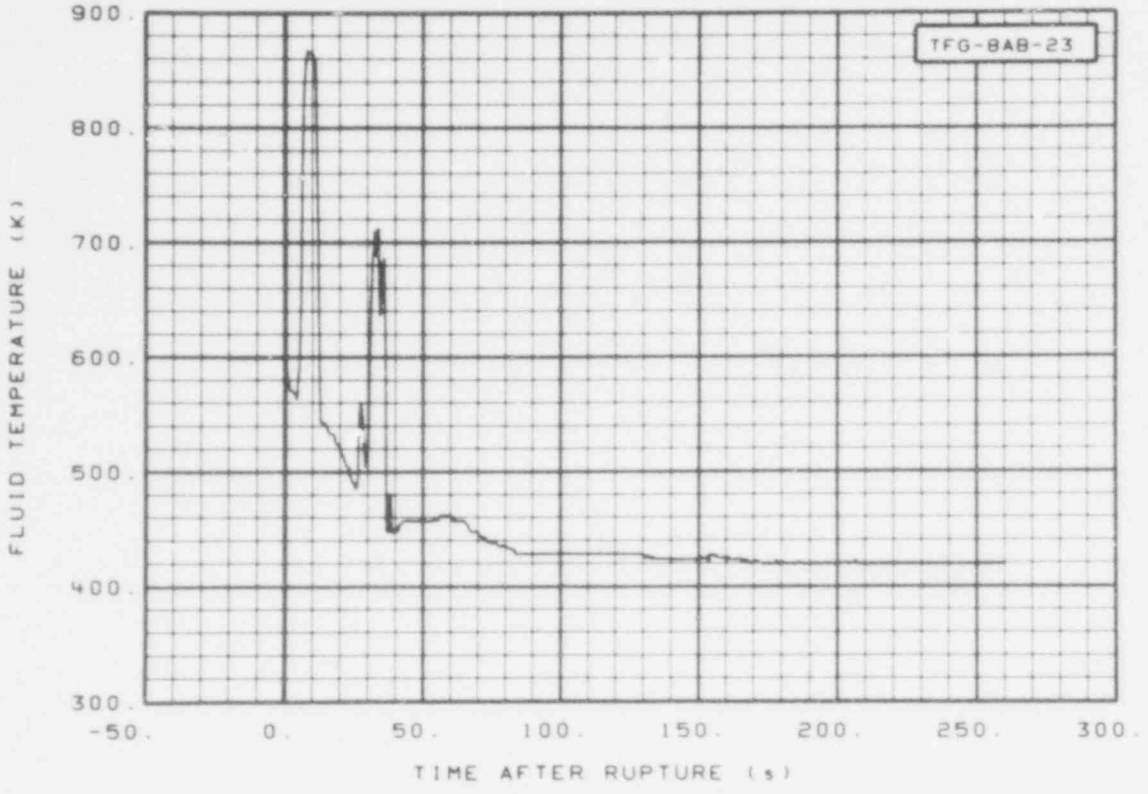

Fig. 47 Fluid temperature in core, Grid Spacer 8 (TFG-8AB-23), from -20 to 260 s.

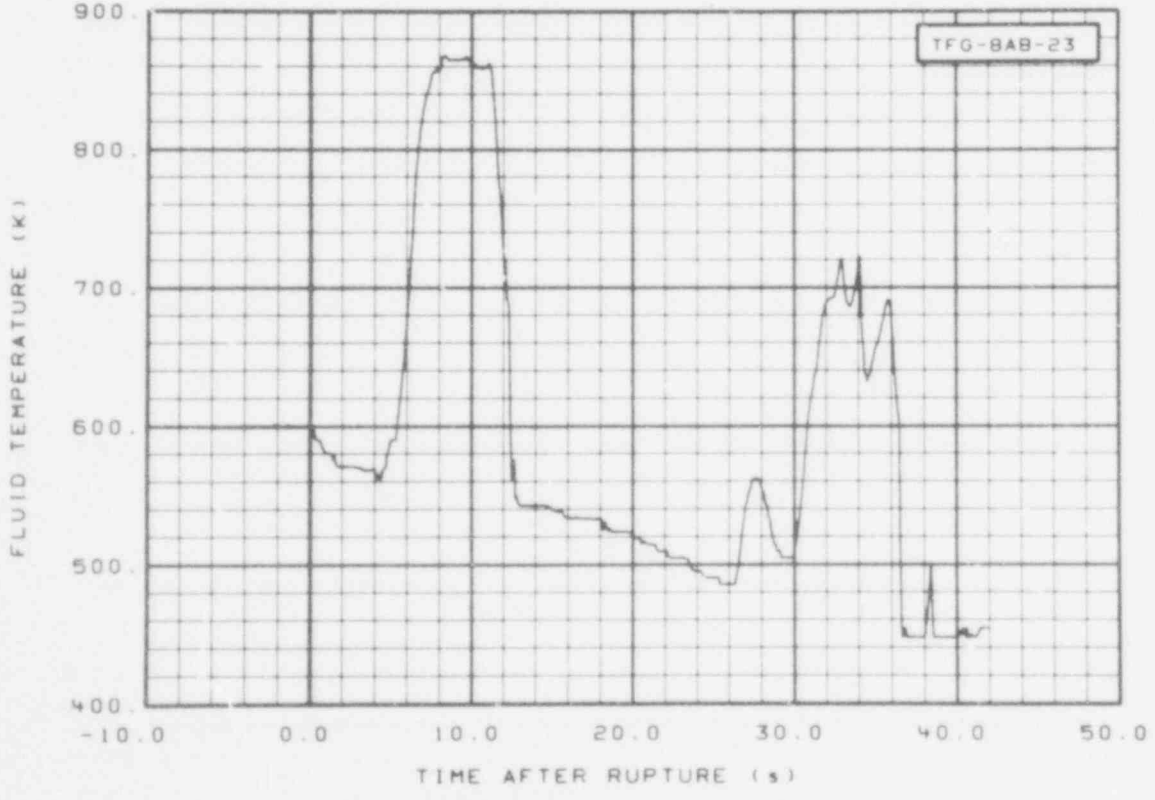

Fig. 48 Fluid temperature in core, Grid Spacer 8 (TFG-8AB-23), from -6 to 42 s.

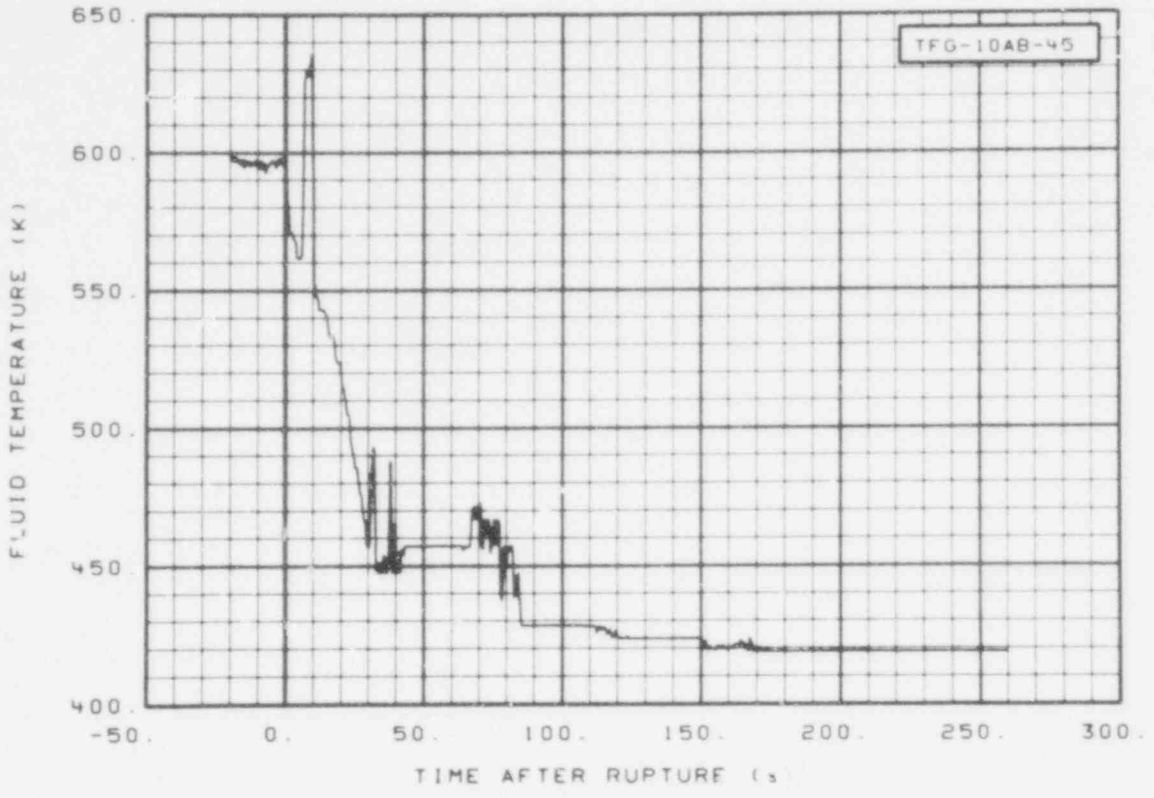

Fig. 49 Fluid temperature in core, Grid Spacer 10 (TFG-10AB-45), from -20 to 260 s.

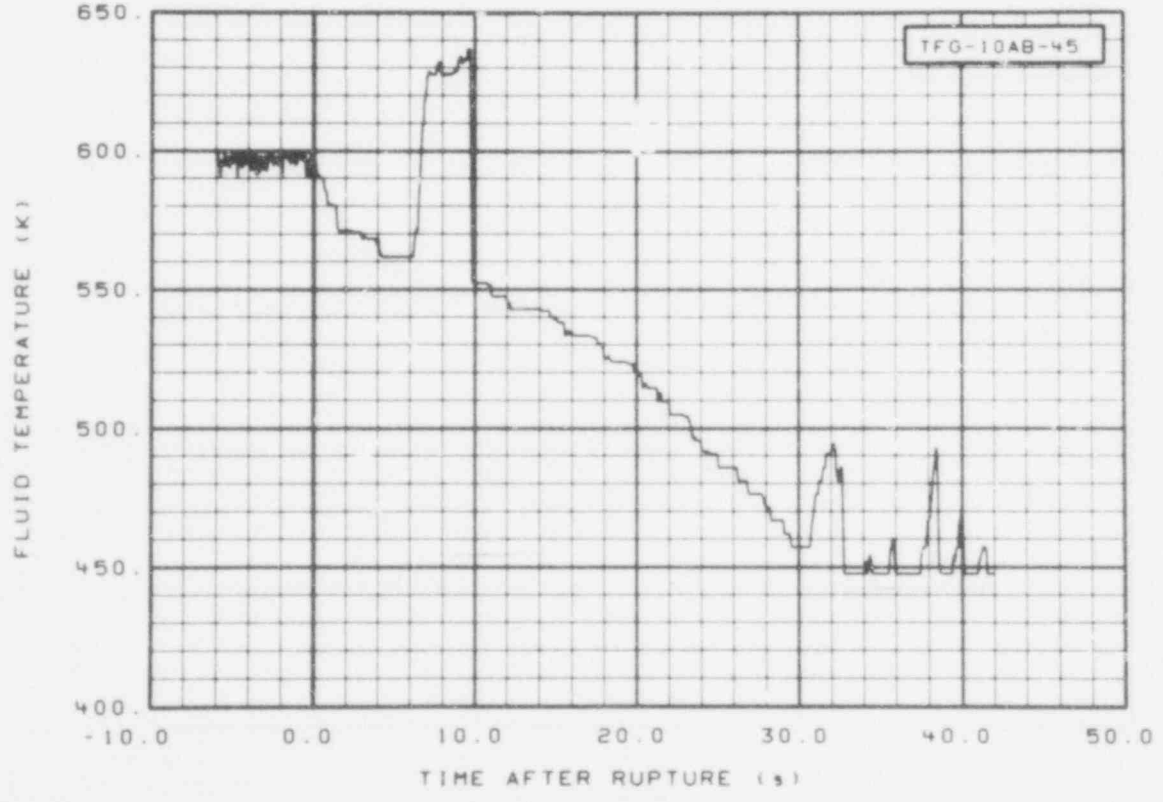

Fig. 50 Fluid temperature in core, Grid Spacer 10 (TFG-10AB-45), from -6 to 42 s.

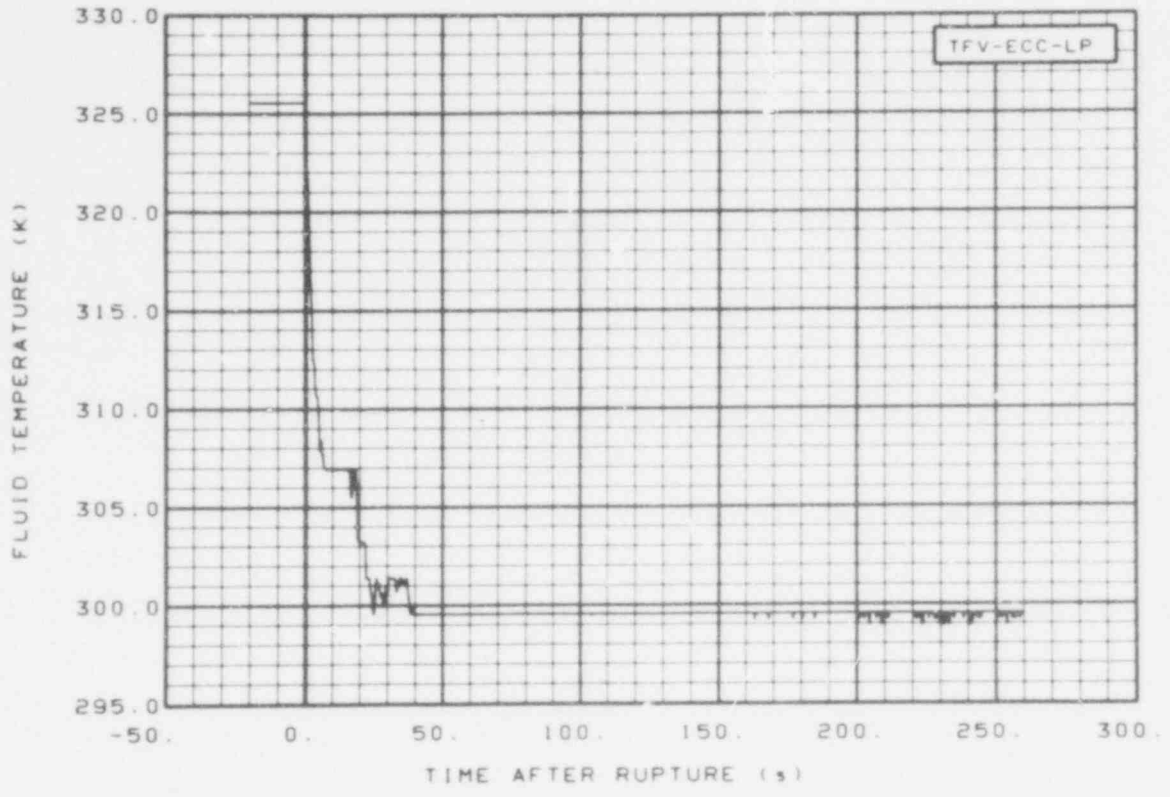

Fig. 51 Fluid temperature in vessel accumulator, coolant injection line (TFV-ECC-LP), from -20 to 260 s.

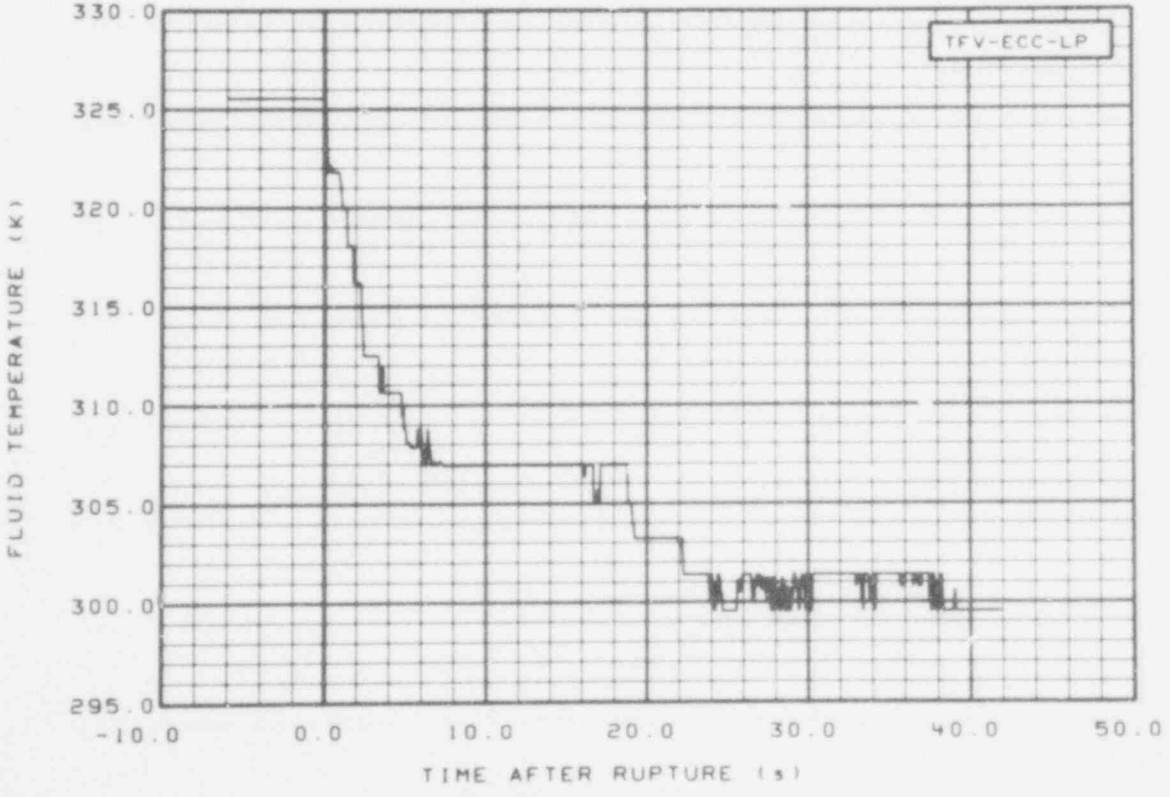

Fig. 52 Fluid temperature in vessel accumulator, coolant injection line (TFV-ECC-LP), from -6 to 42 s.

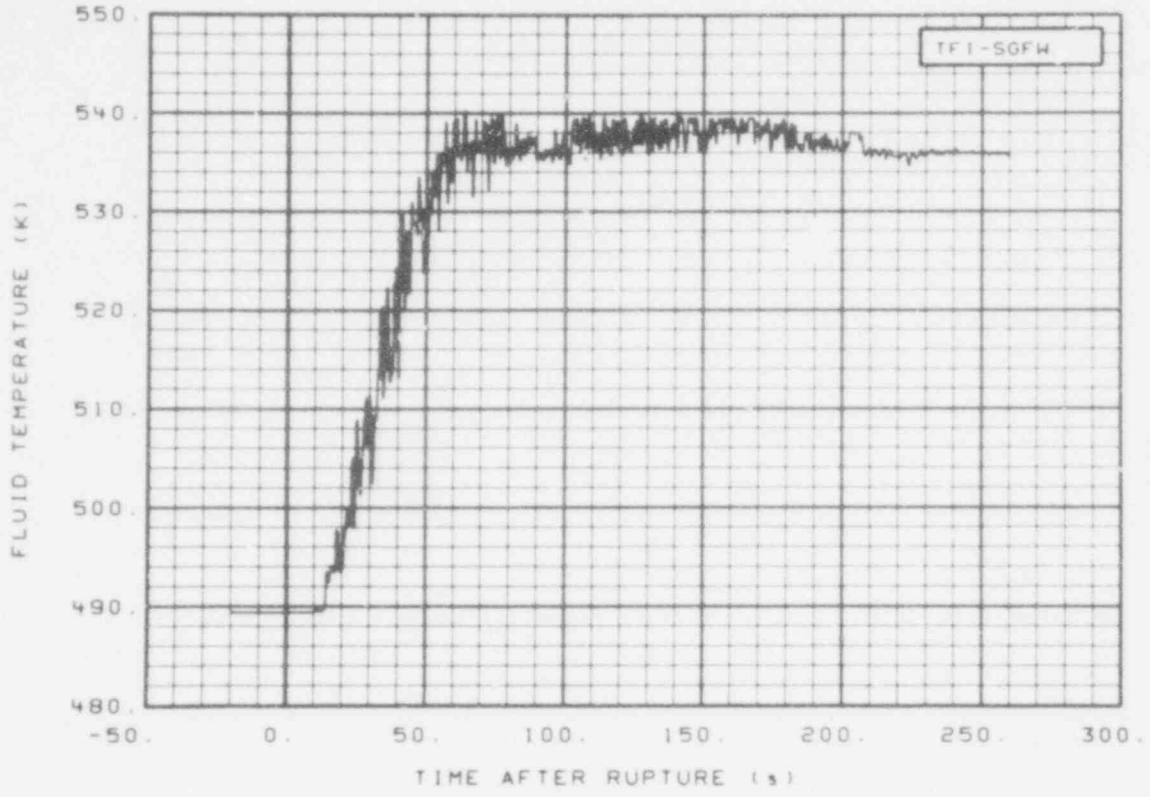

Fig. 53 Fluid temperature in intact loop steam generator, secondary feedwater line (TFI-SGFW), from -20 to 260 s.

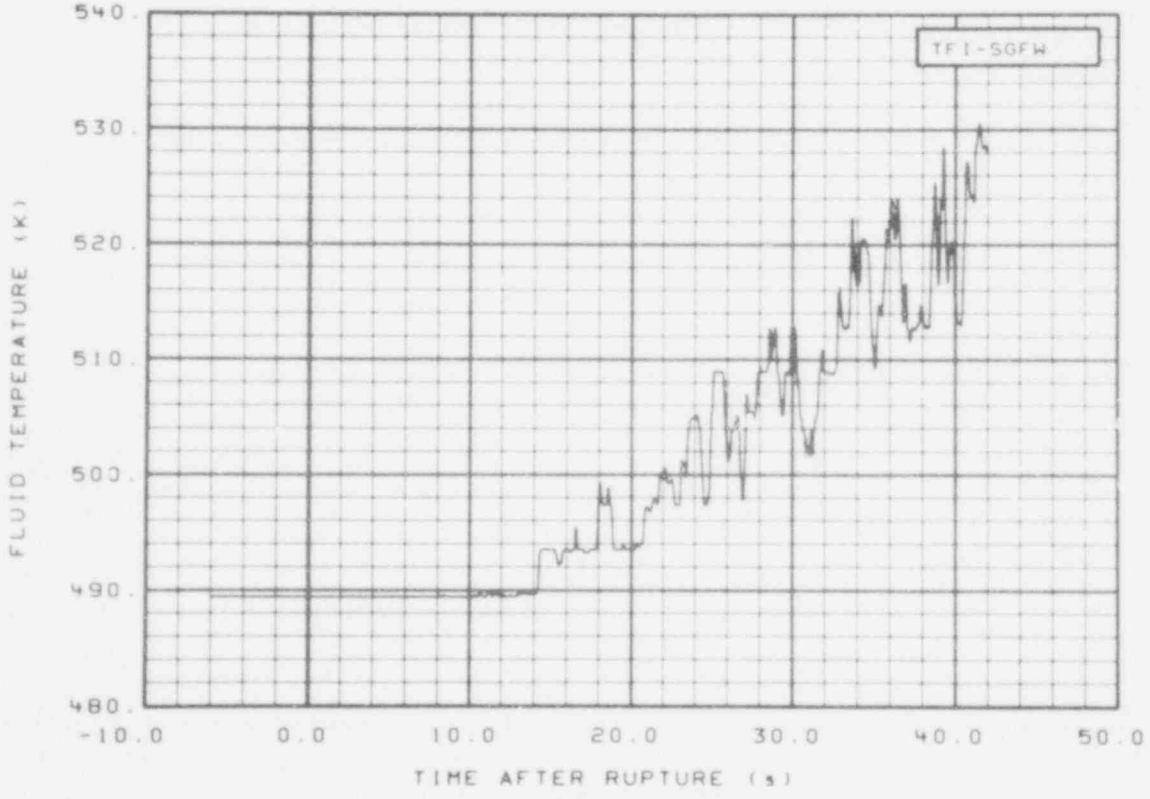

Fig. 54 Fluid temperature in intact loop steam generator, secondary feedwater line (TFI-SGFW), from -6 to 42 s.

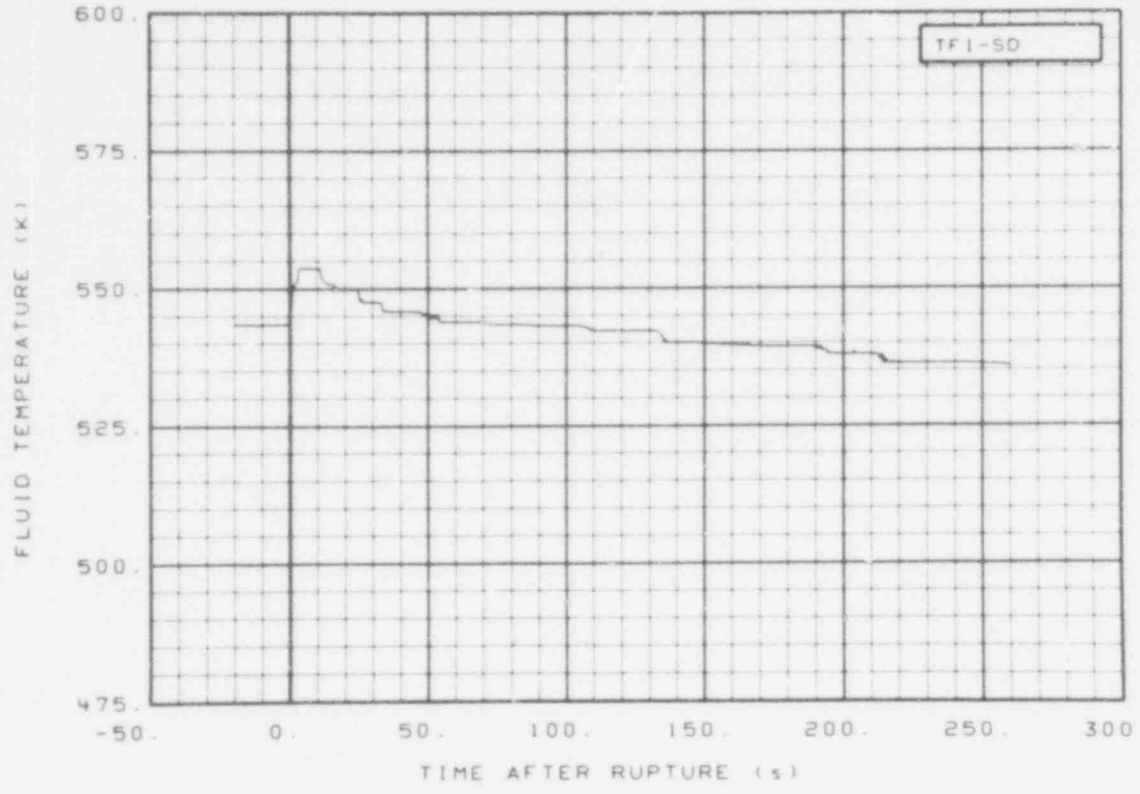

Fig. 55 Fluid temperature in intact loop steam generator, secondary side steam dome (TFI-SD), from -20 to 260 s.

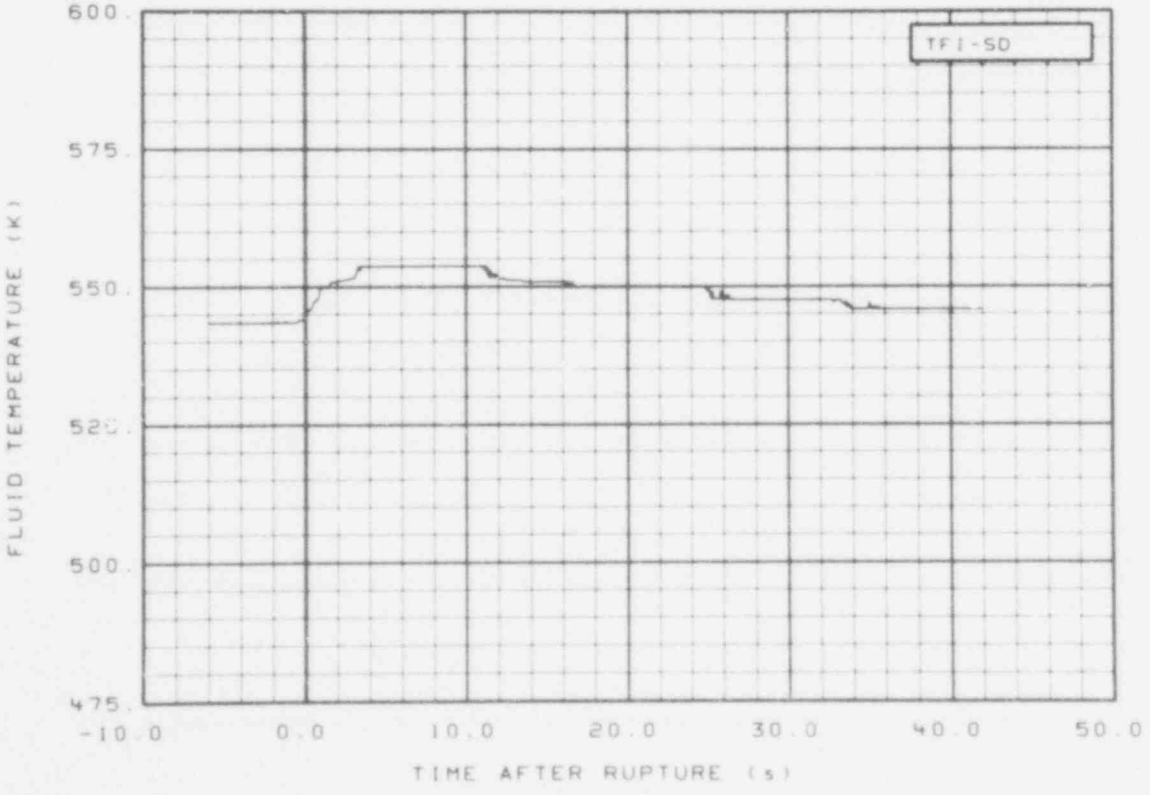

Fig. 56 Fluid temperature in intact loop steam generator, secondary side steam dome (TFI-SD), from -6 to 42 s.

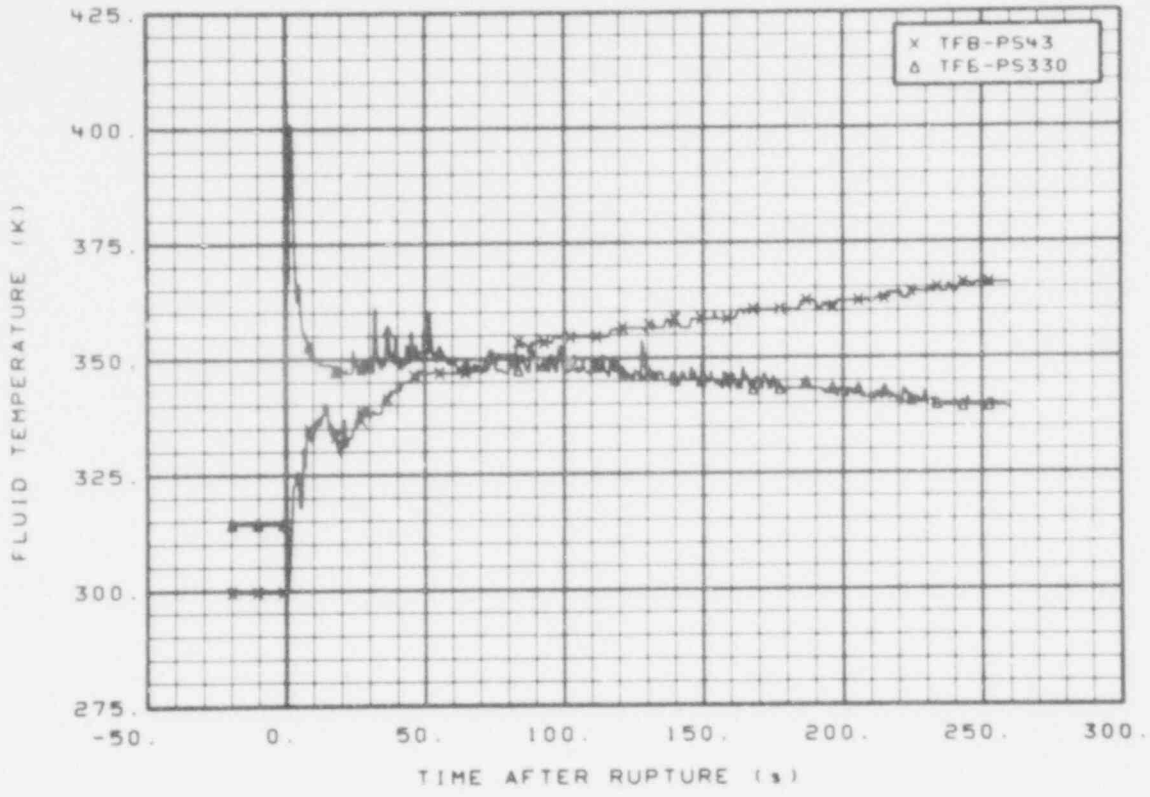

Fig. 57 Fluid temperature in broken loop, pressure suppression system tank (TFB-PS43 and TFB-PS330), from -20 to 260 s.

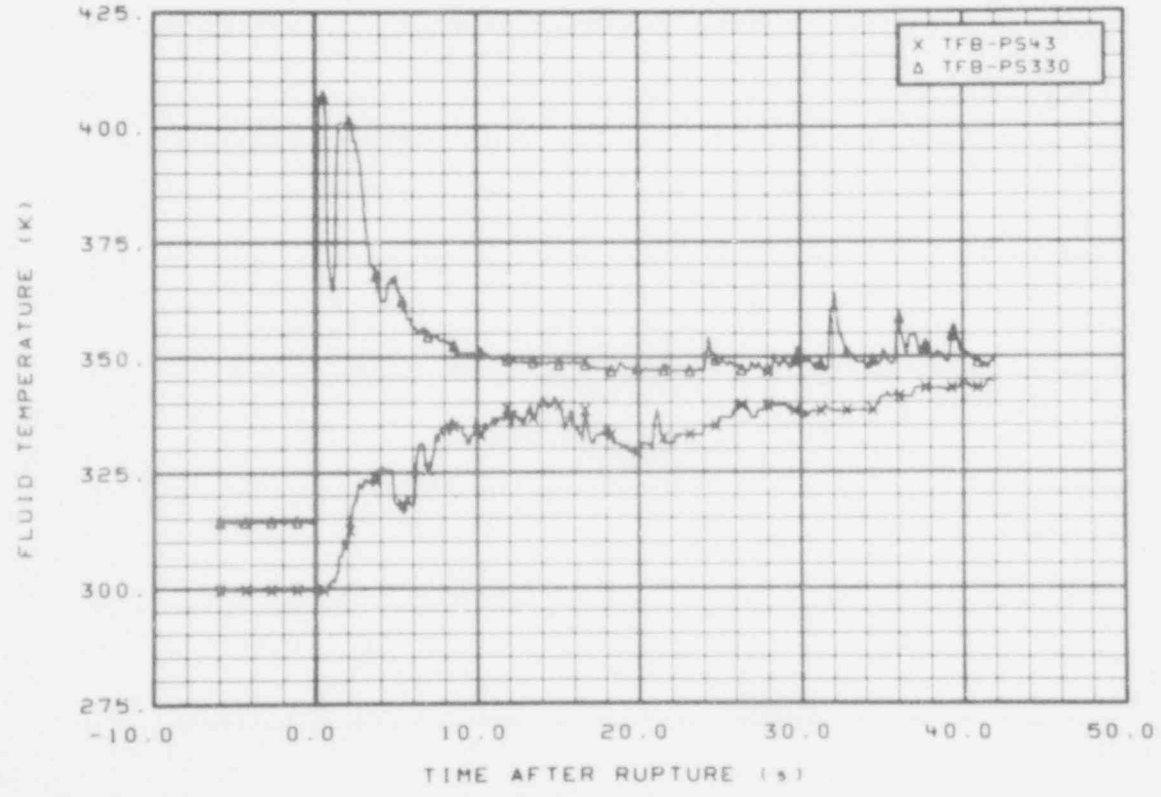

Fig. 58 Fluid temperature in broken loop, pressure suppression system tank (TFB-PS43 and TFB-PS330), from -6 to 42 s.

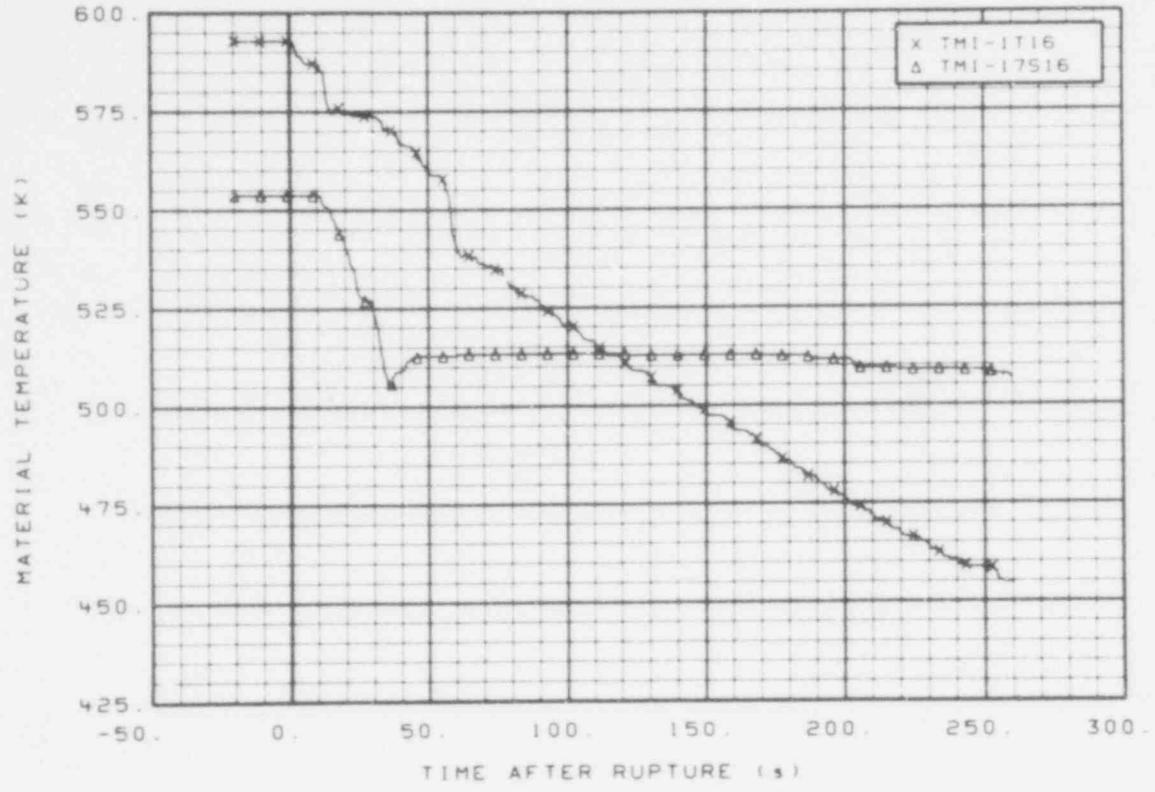

Fig. 59 Material temperature in intact loop (TMI-1T16 and TMI-17S16), from -20 to 260 s.

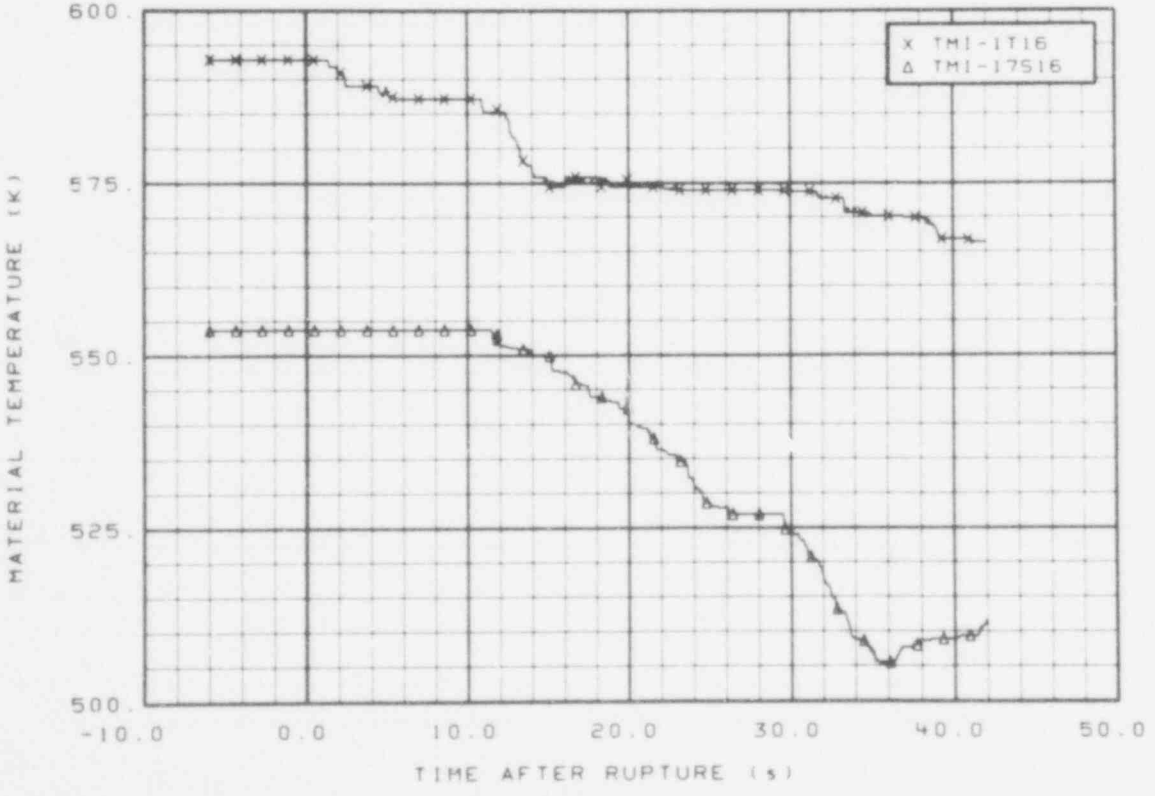

Fig. 60 Material temperature in intact loop (TMI-1T16 and TMI-17S16), from -6 to 42 s.

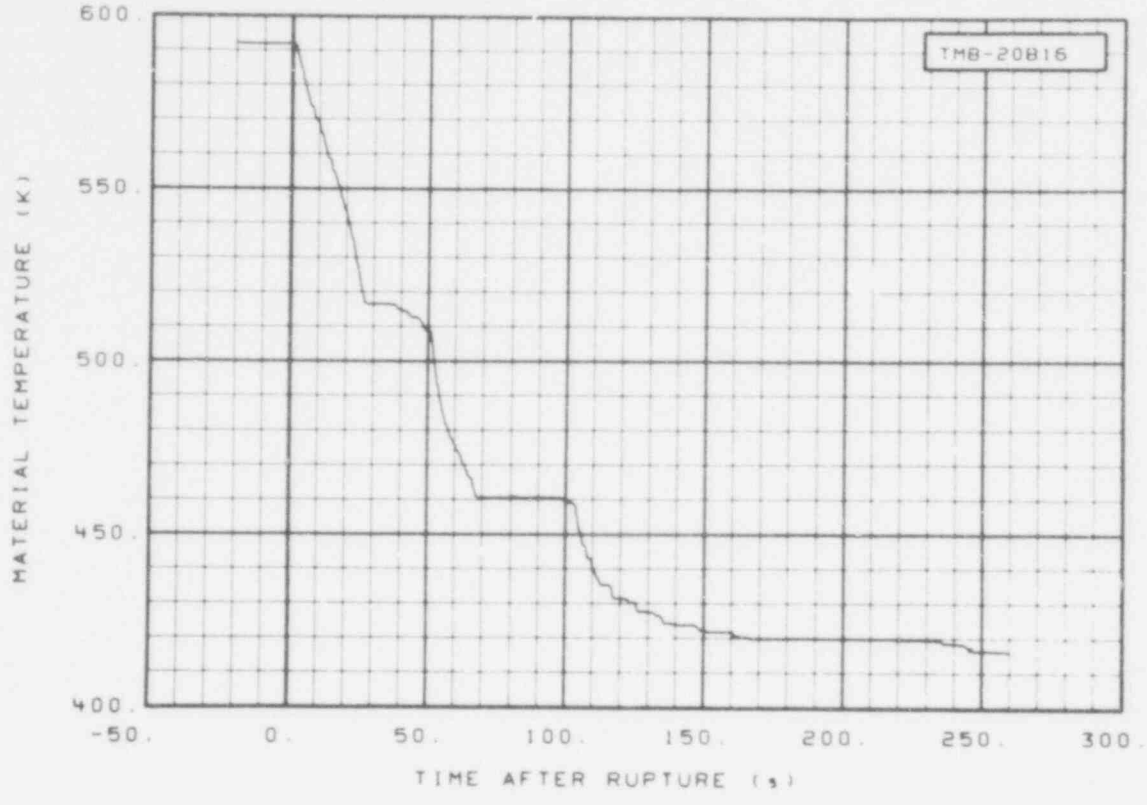

Fig. 61 Material temperature in broken loop (TMB-20B16), from -20 to 260 s.

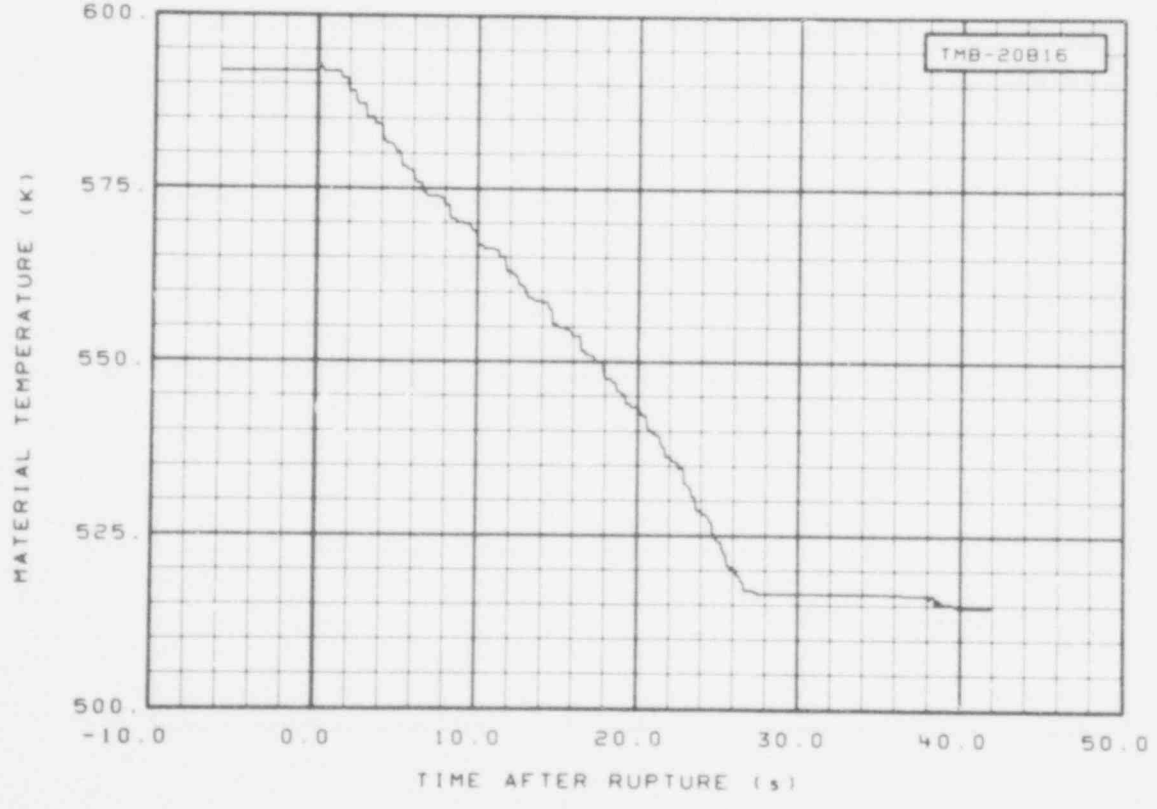

Fig. 62 Material temperature in broken loop (TMB-20B16), from -6 to 42 s.

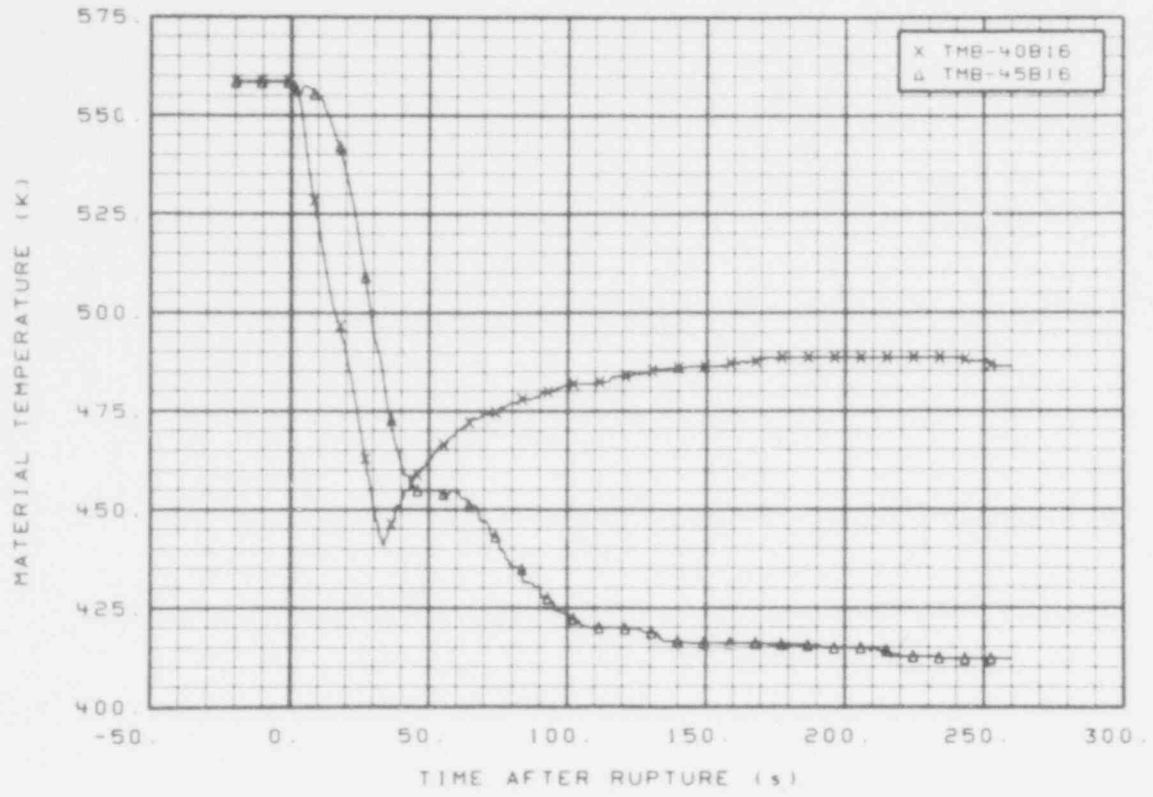

Fig. 63 Material temperature in broken loop (TMB-40B16 and TMB-45B16), from -20 to 260 s.

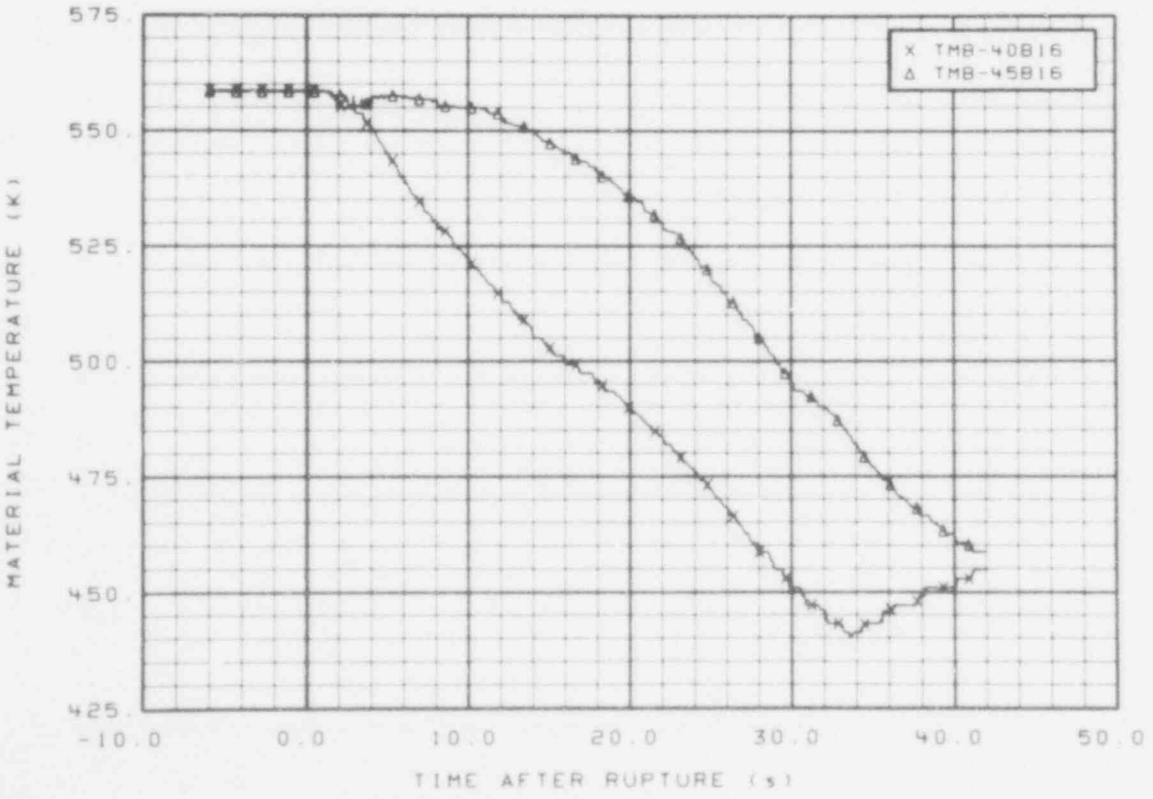

Fig. 64 Material temperature in broken loop (TMB-40B16 and TMB-45B16), from -6 to 42 s.

544 075

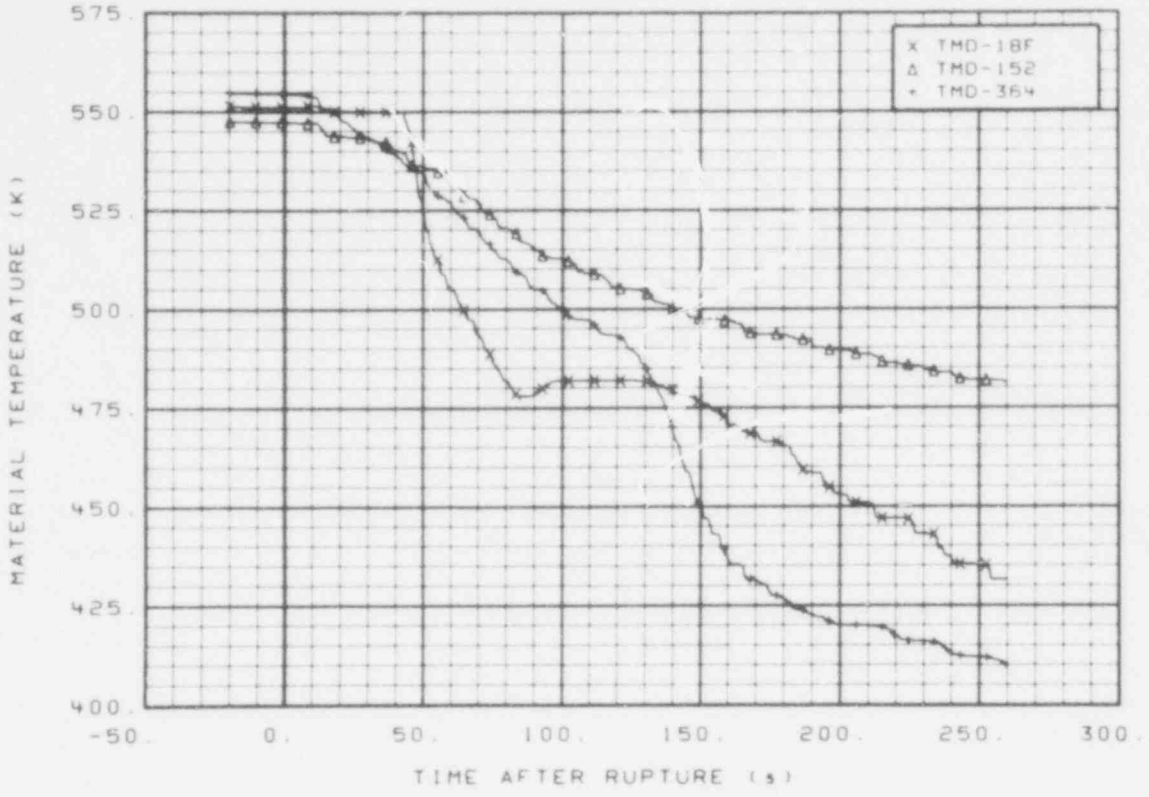

Fig. 65 Material temperature in downcomer (TMD-18F, TMD-152, and TMD-364), from -20 to 260 s.

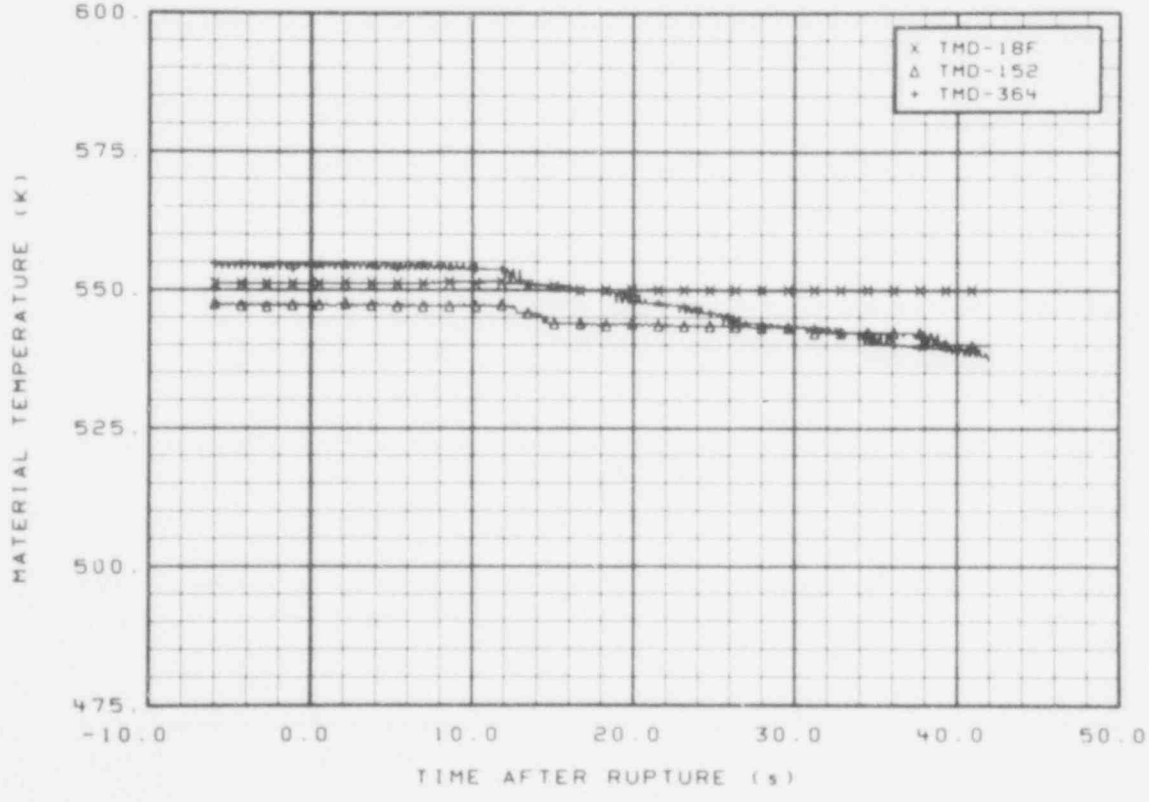

Fig. 66 Material temperature in downcomer (TMD-18F, TMD-152, and TMD-364), from -6 to 42 s.

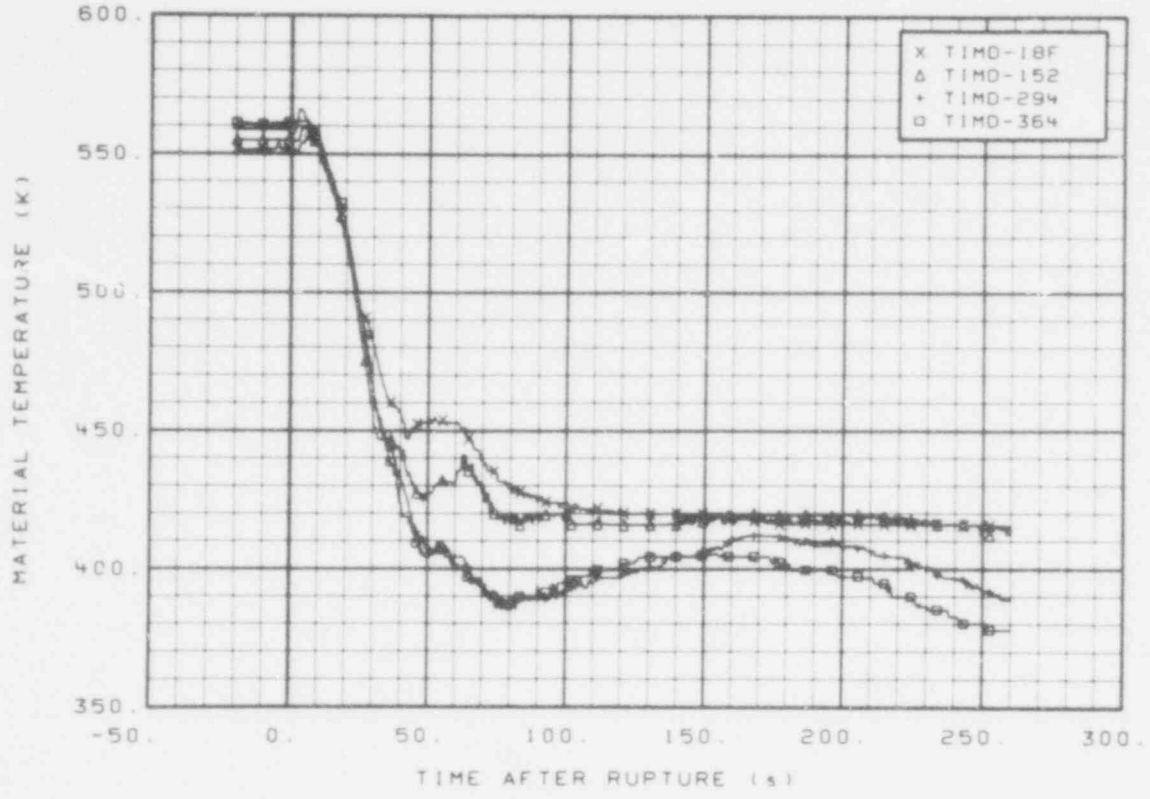

Fig. 67 Material temperature in downcomer insulator (TIMD-18F, TIMD-152, TIMD-294, and TIMD-364), from -20 to 260 s.

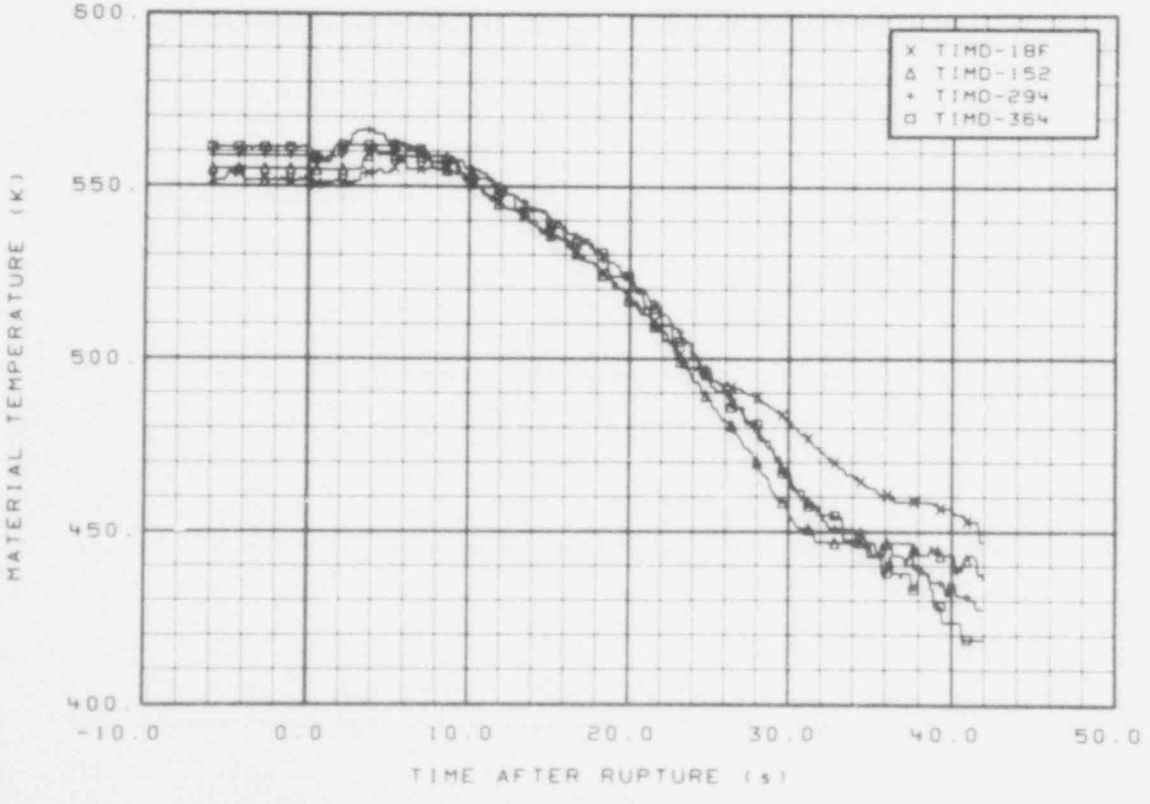

Fig. 68 Material temperature in downcomer insulator (TIMD-18F, TIMD-152, TIMD-294, and TIMD-364), from -6 to 42 s.

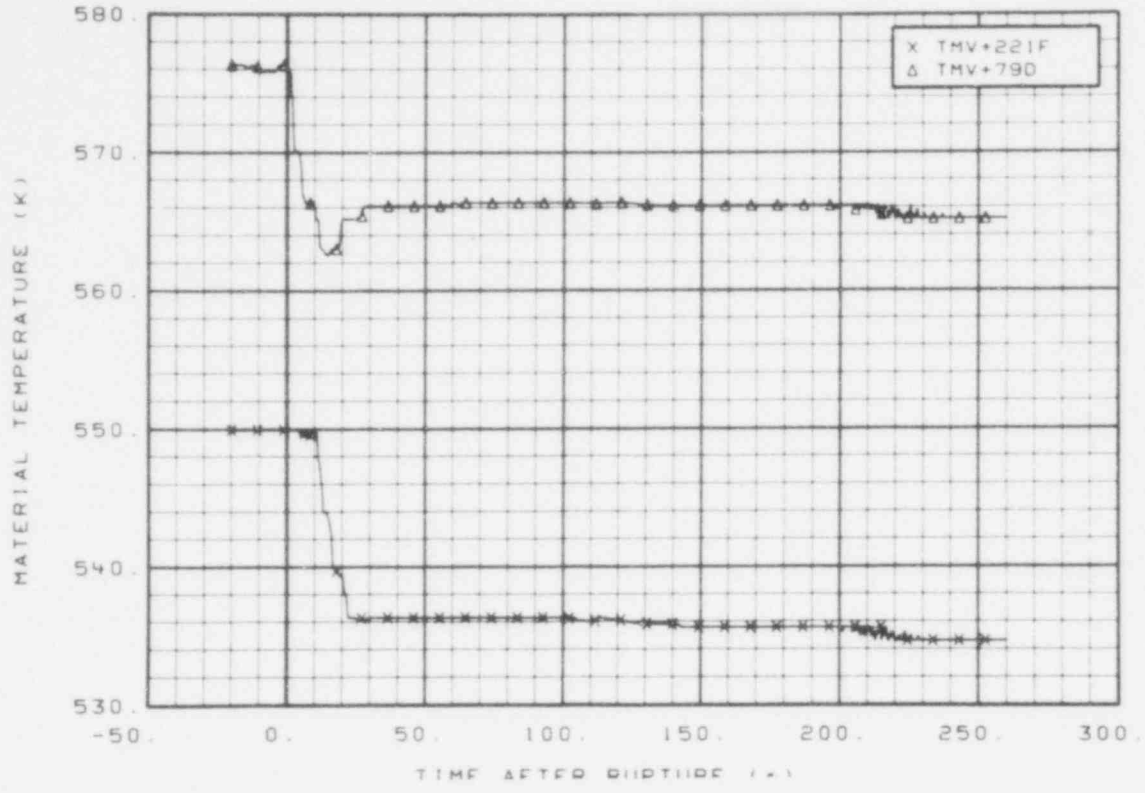

Fig. 69 Material temperature in upper vessel (TMV + 221F and TMV + 79D), from -20 to 260 s.

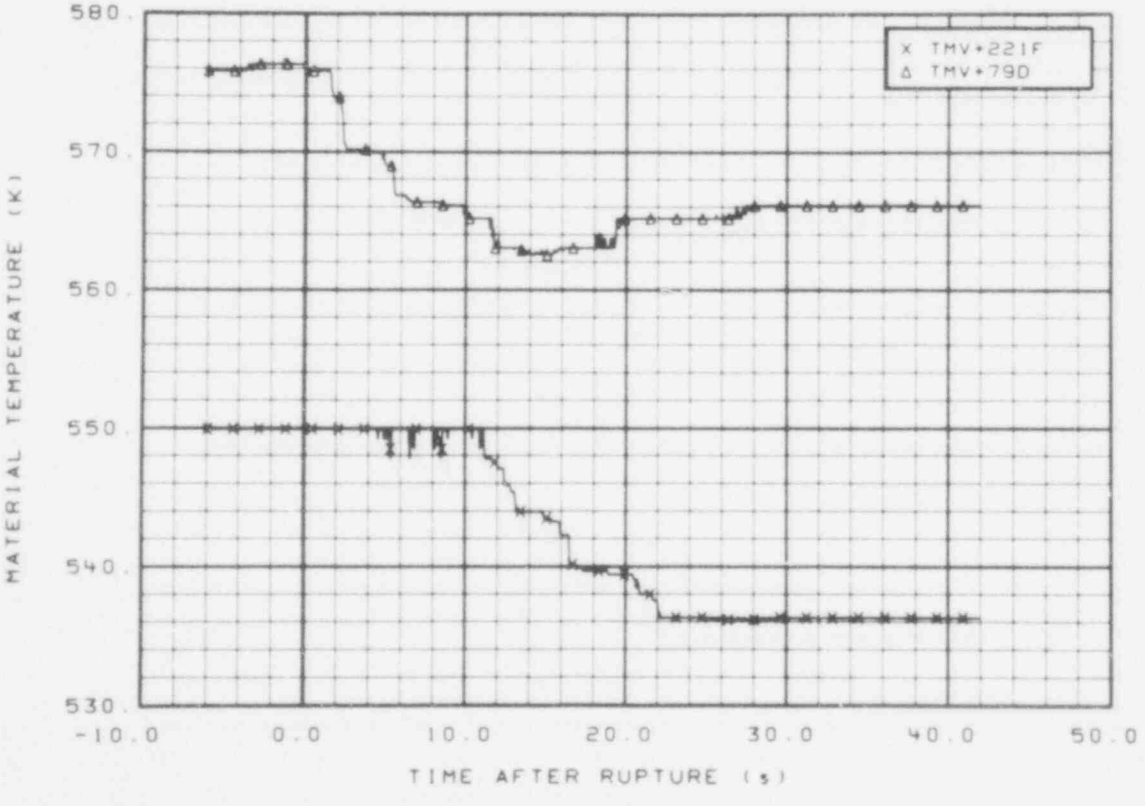

Fig. 70 Material temperature in upper vessel (TMV + 221F and TMV + 79D), from -6 to 42 s.

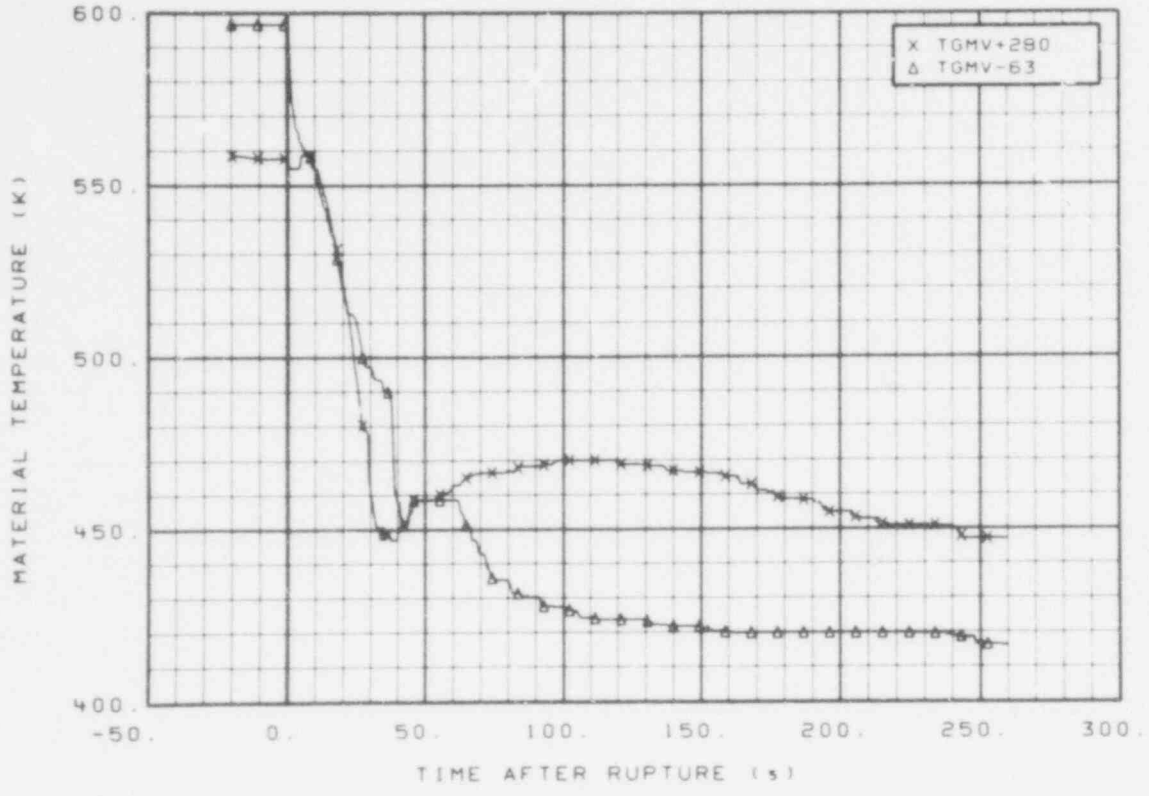

Fig. 71 Material temperature in vessel, core guide tube (TGMV + 280 and TGMV-63), from -20 to 260 s.

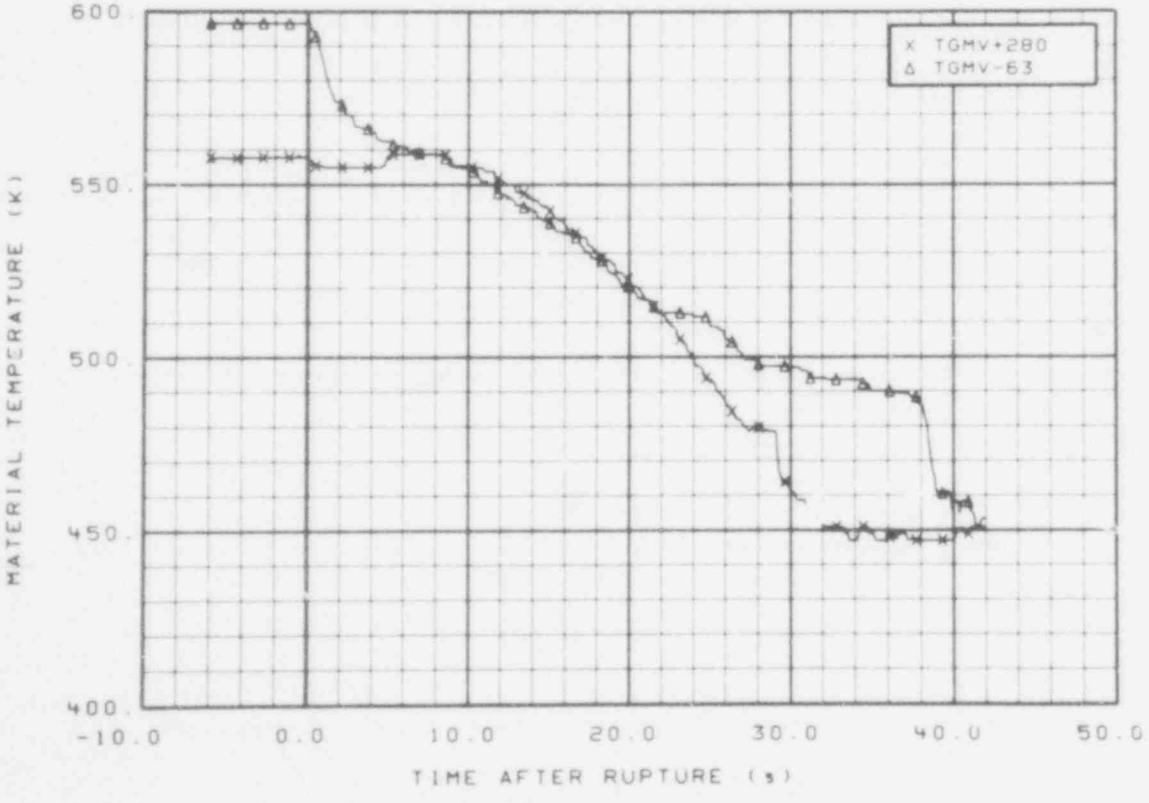

Fig. 72 Material temperature in vessel, core guide tube (TGMV + 280 and TGMV-63), from -6 to 42 s.

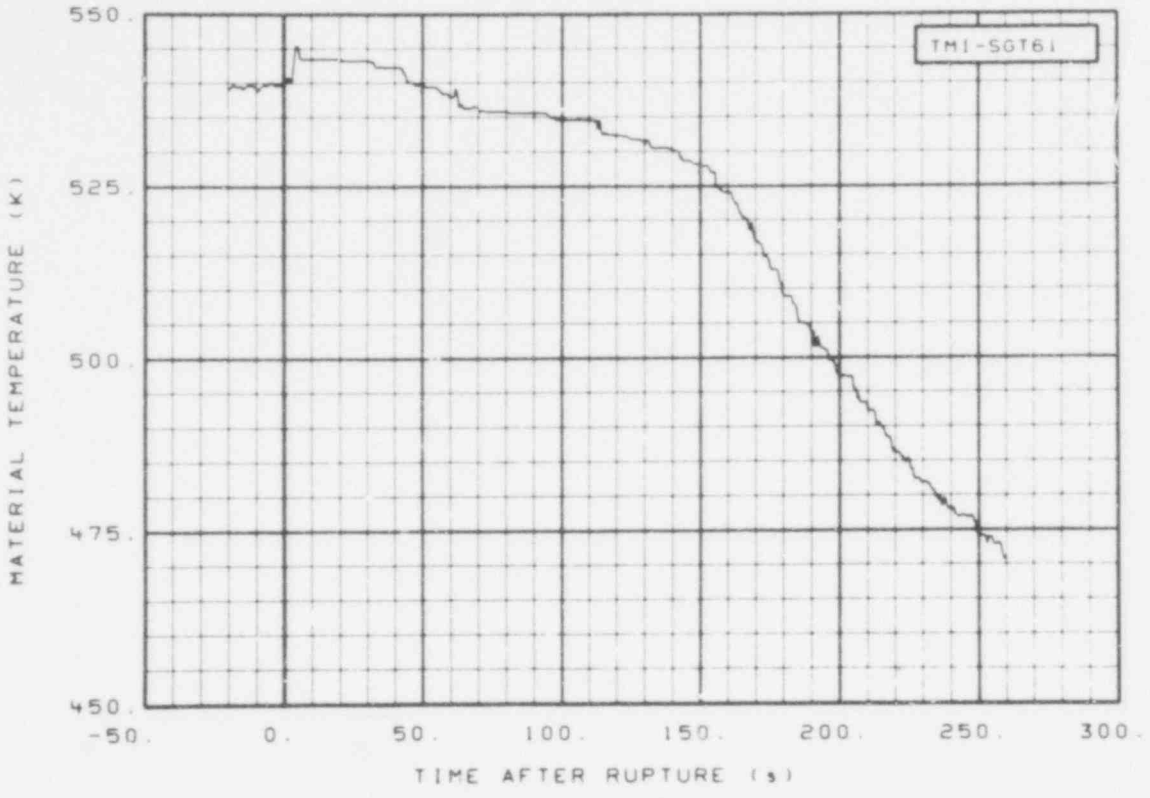

Fig. 73 Material temperature in intact loop, steam generator tube (TMI-SGT61), from -20 to 260 s.

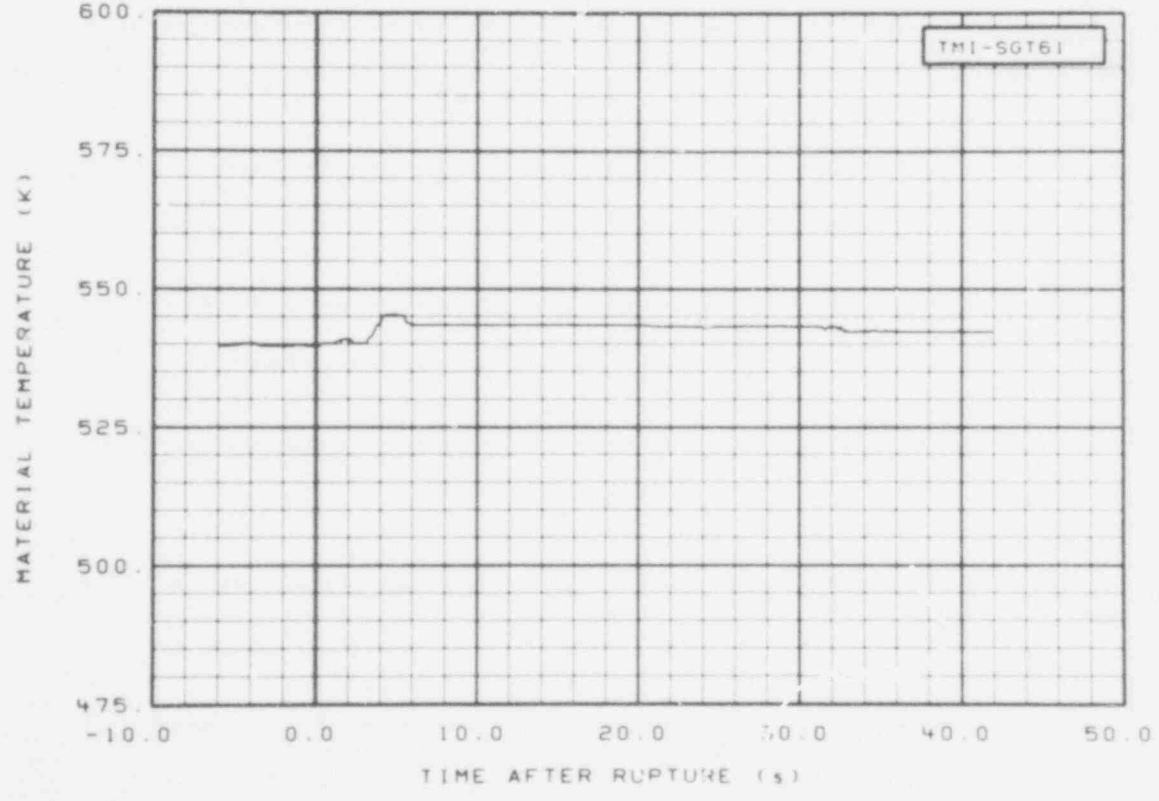

Fig. 74 Material temperature in intact loop, steam generator tube (TMI-SGT61), from -6 to 42 s.

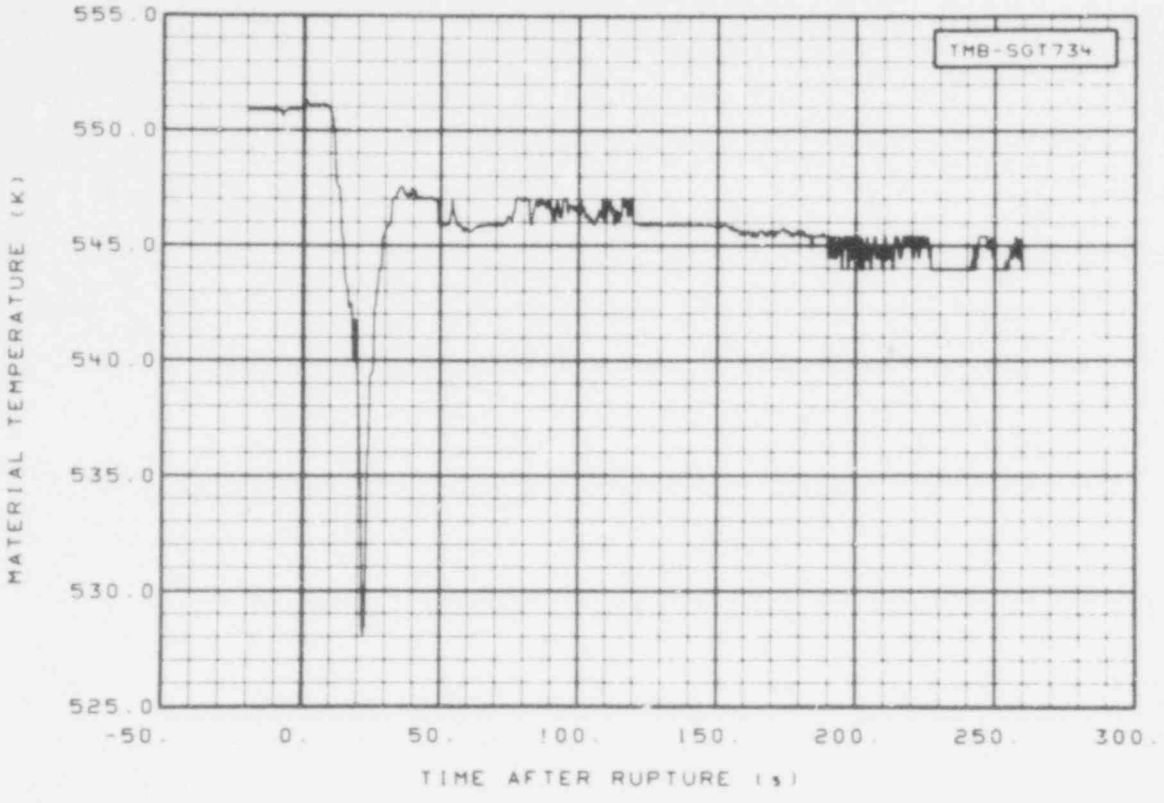

Fig. 75 Material temperature in broken loop, steam generator tube (TMB-SGT734), from -20 to 260 s.

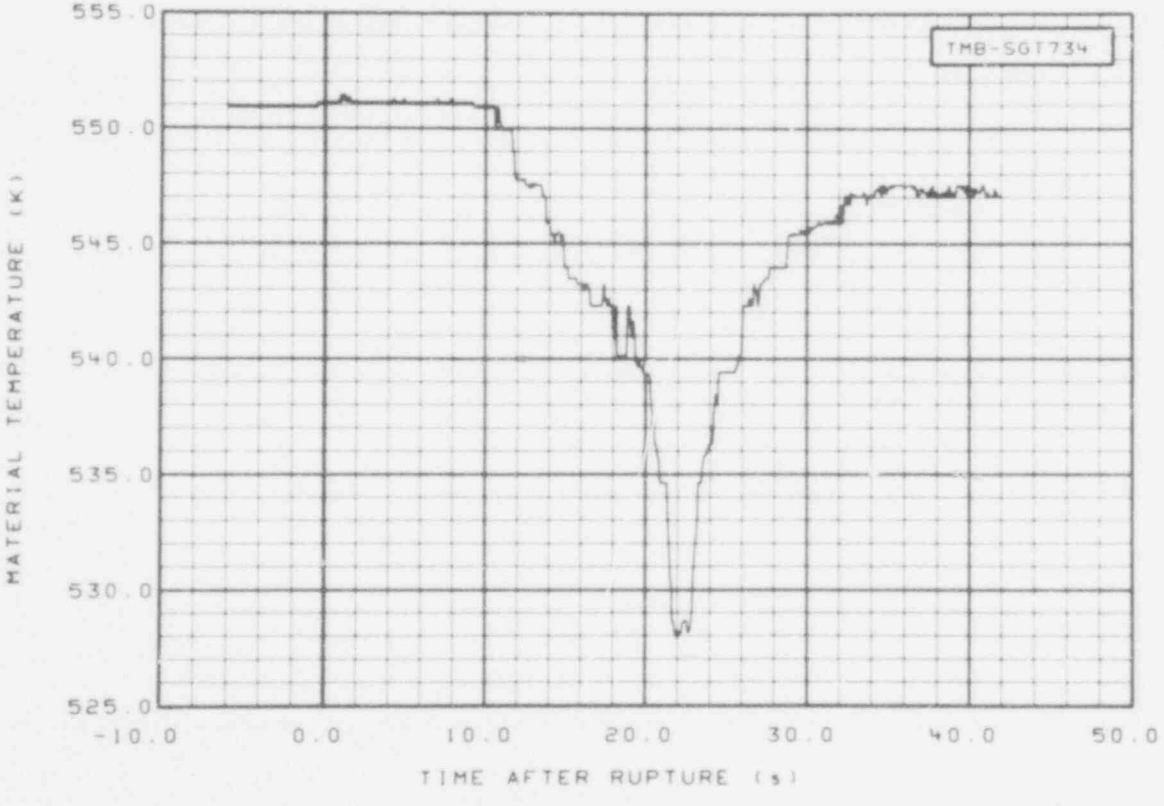

Fig. 76 Material temperature in broken loop, steam generator tube (TMB-SGT734), from -6 to 42 s.

544 081

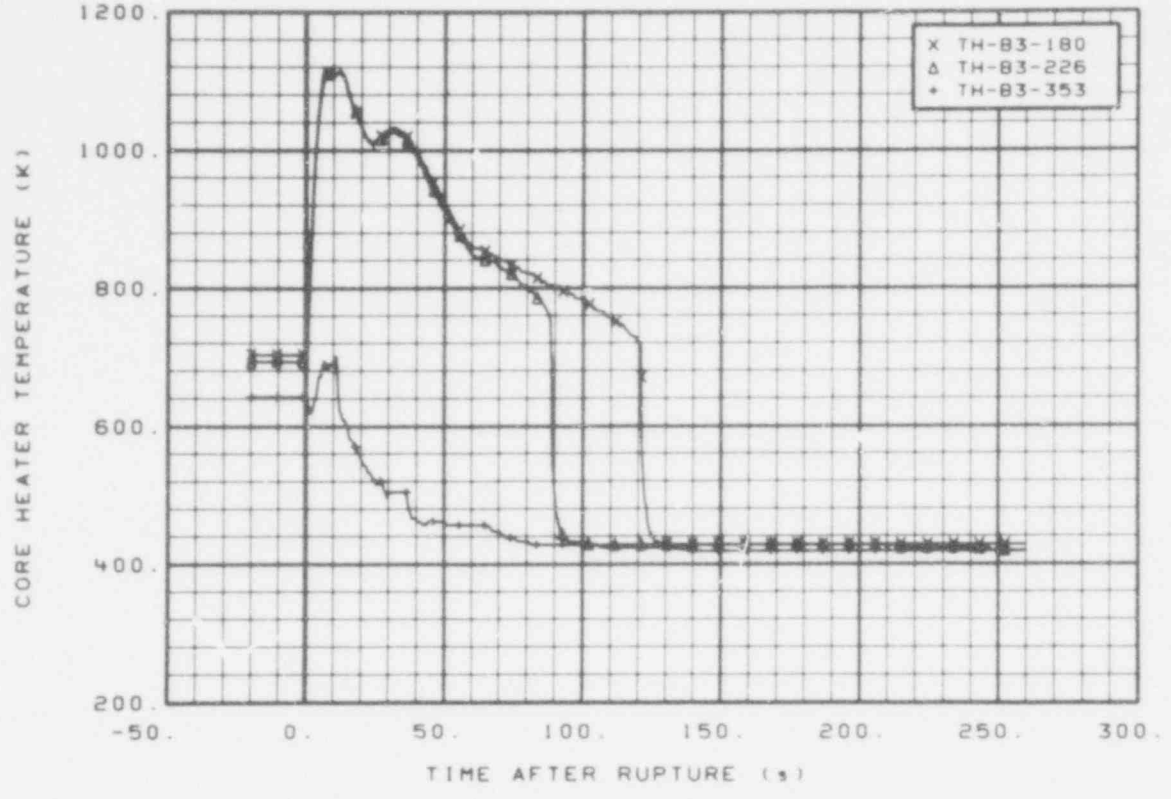

Fig. 77 Core heater temperature, Rod B-3 (TH-B3-180, TH-B3-226, and TH-B3-353), from -20 to 260 s.

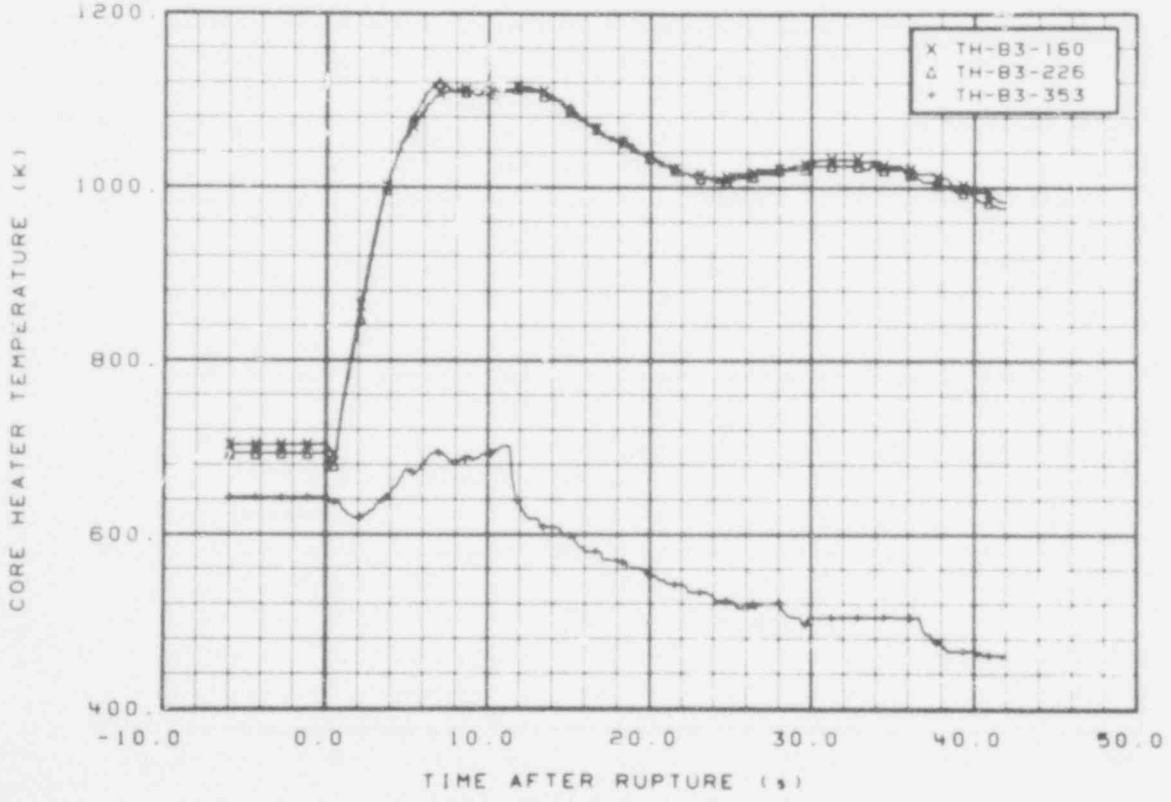

Fig. 78 Core heater temperature, Rod B-3 (TH-B3-180, TH-B3-226, and TH-B3-353), from -6 to 42 s.

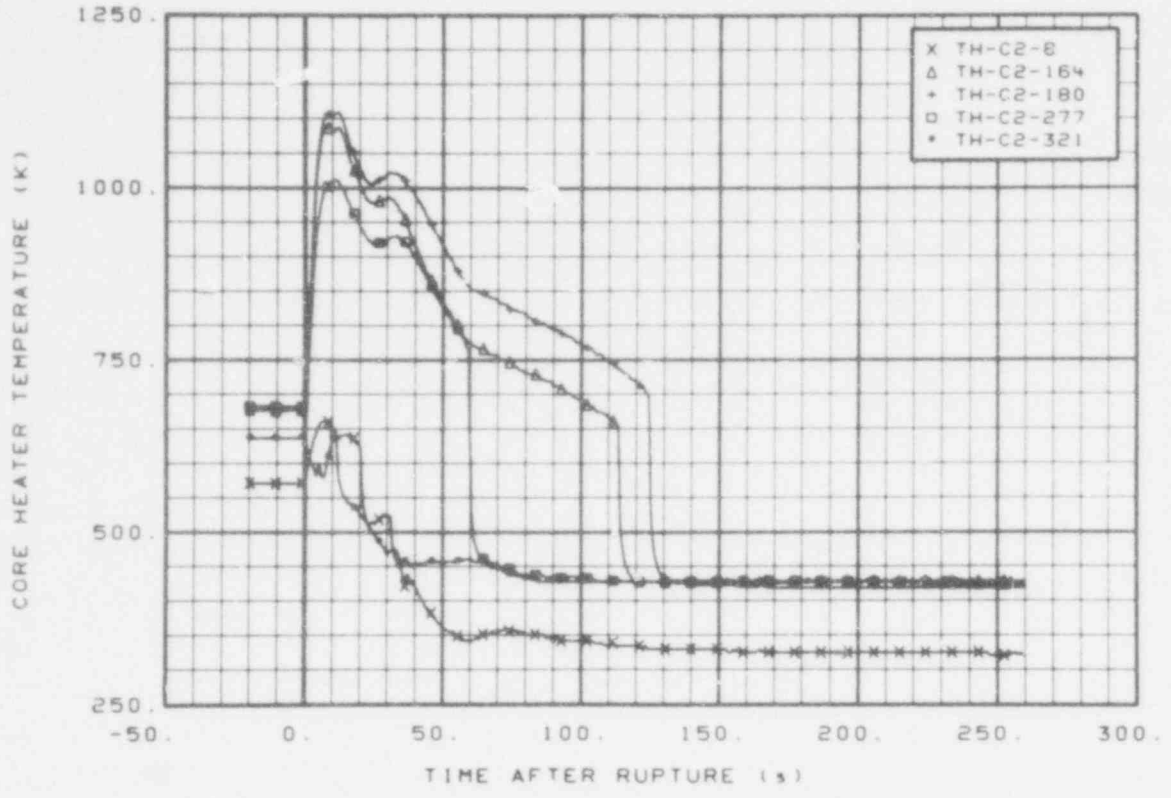

Fig. 79 Core heater temperature, Rod C-2 (TH-C2-8, TH-C2-164, TH-C2-180, TH-C2-277, and TH-C2-321), from -20 to 260 s.

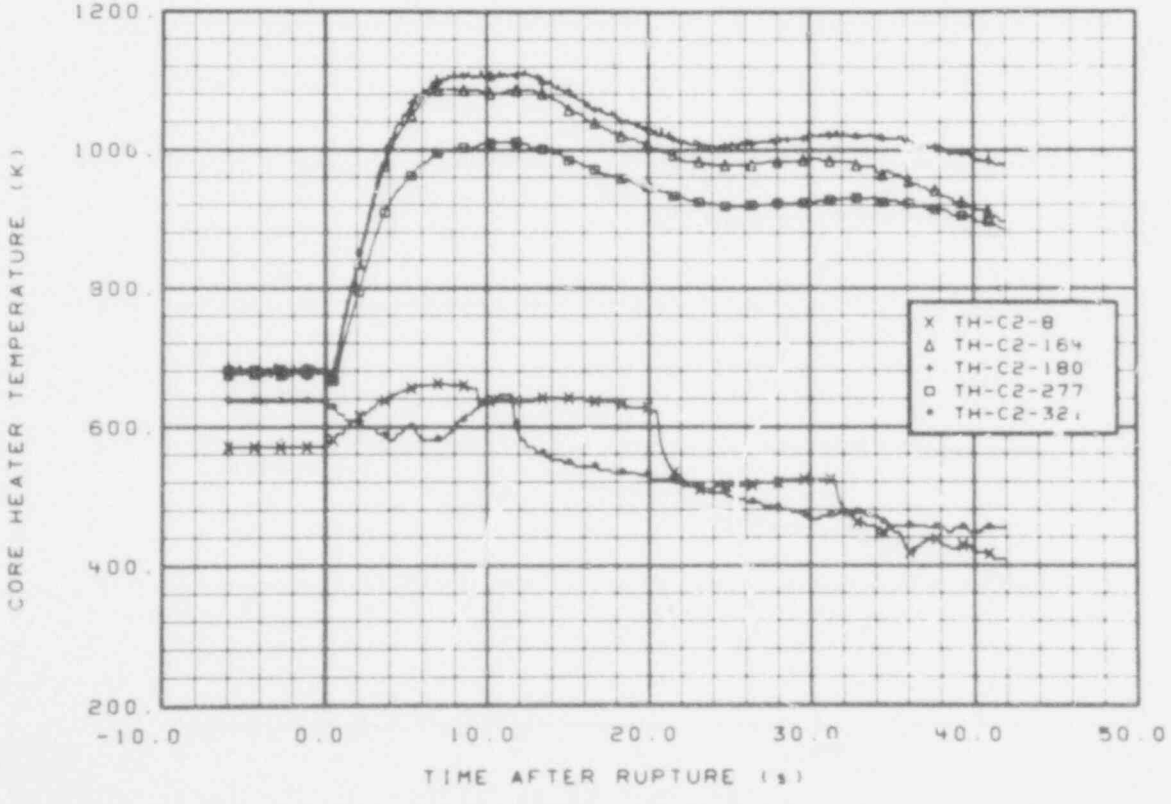

Fig. 80 Core heater temperature, Rod C-2 (TH-C2-8, TH-C2-164, TH-C2-180, TH-C2-277, and TH-C2-321), from -6 to 42 s.

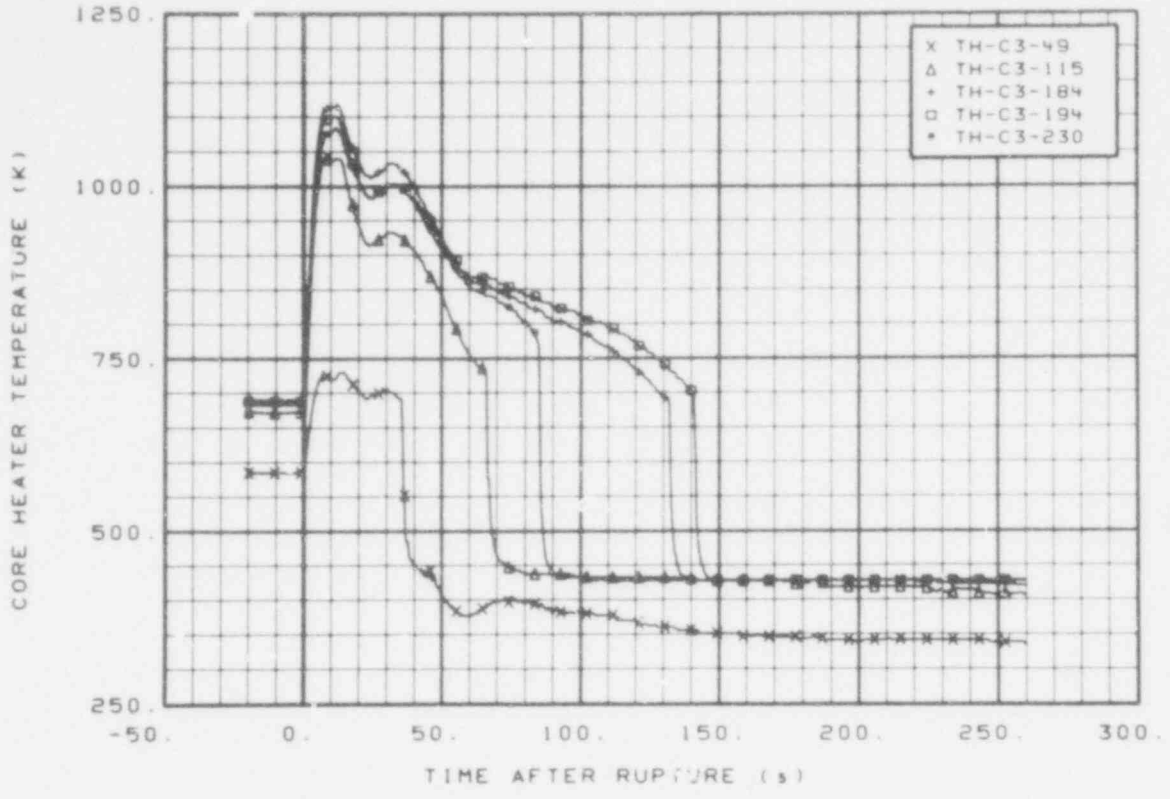

Fig. 81 Core heater temperature, Rod C-3 (TH-C3-49, TH-C3-115, TH-C3-184, TH-C3-194, and TH-C3-230), from -20 to 260 s.

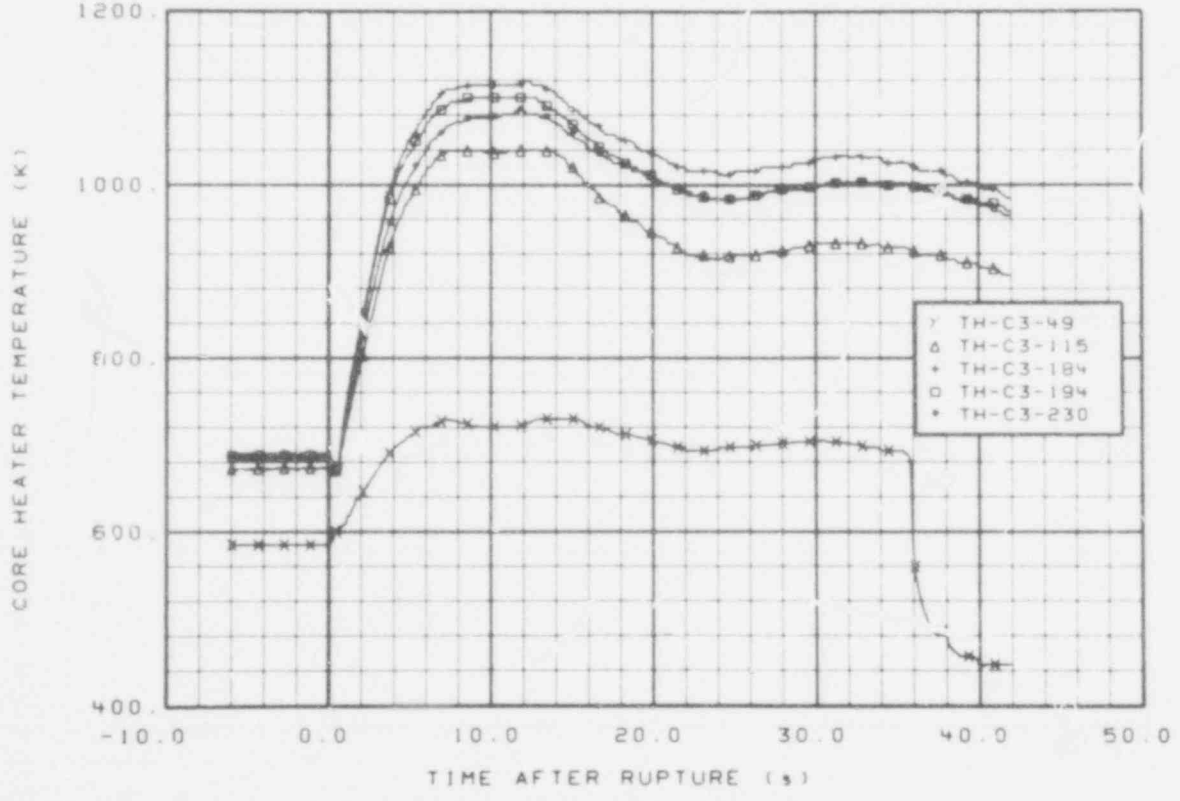

Fig. 82 Core heater temperature, Rod C-3 (TH-C3-49, TH-C3-115, TH-C3-184, TH-C3-194, and TH-C3-230), from -6 to 42 s.

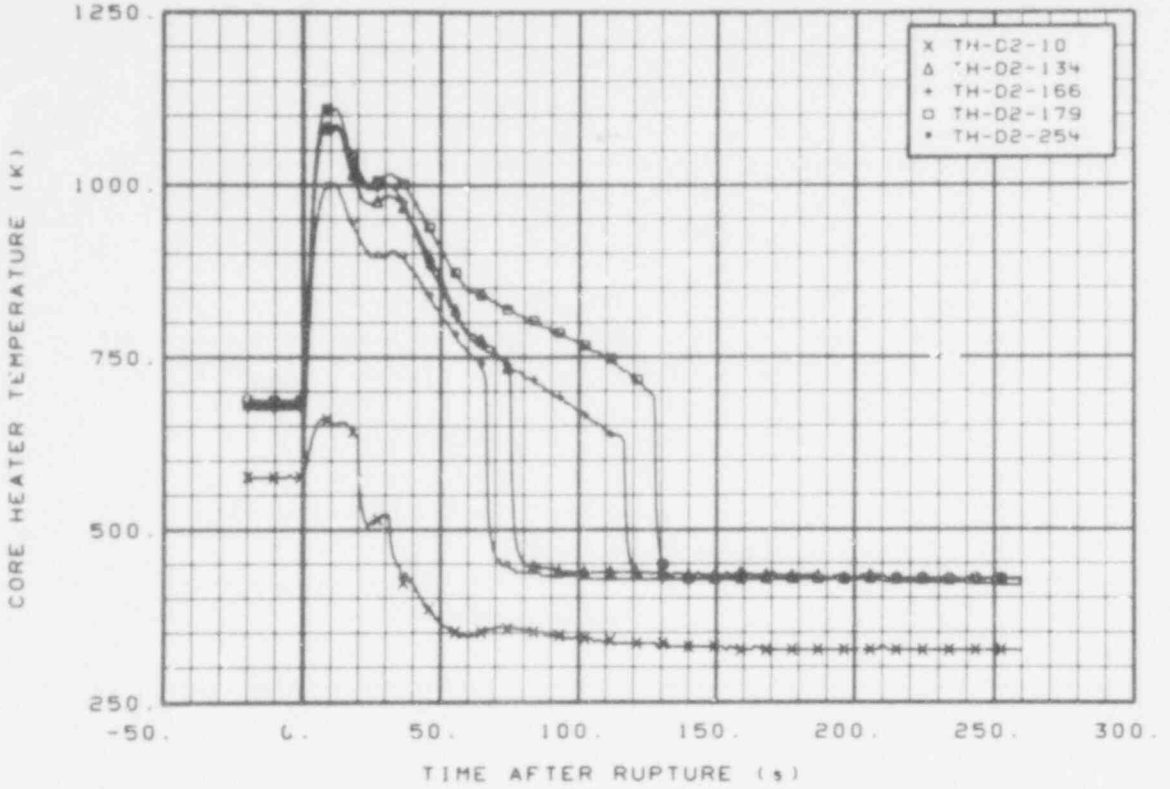

Fig. 83 Core heater temperature, Rod D-2 (TH-D2-10, TH-D2-134, TH-D2-166, TH-D2-179, and TH-D2-254), from -20 to 260 s.

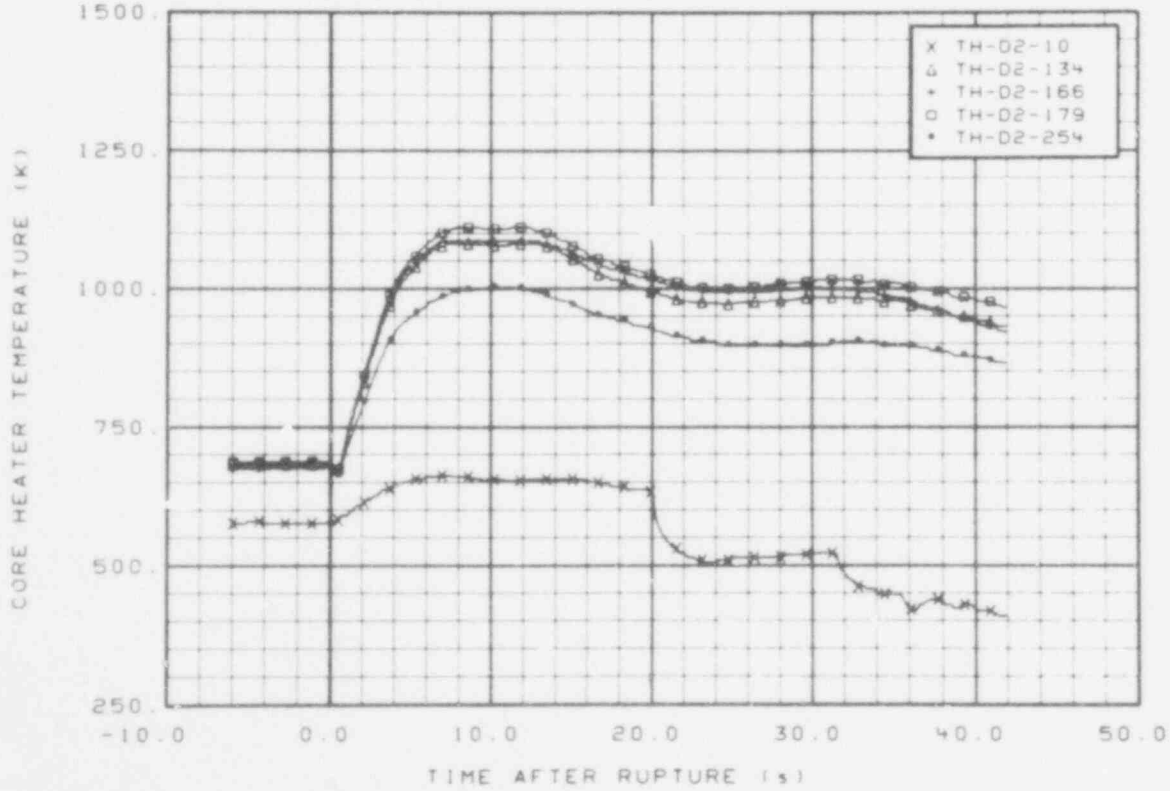

Fig. 84 Core heater temperature, Rod D-2 (TH-D2-10, TH-D2-134, TH-D2-166, TH-D2-179, and TH-D2-254), from -6 to 42 s.

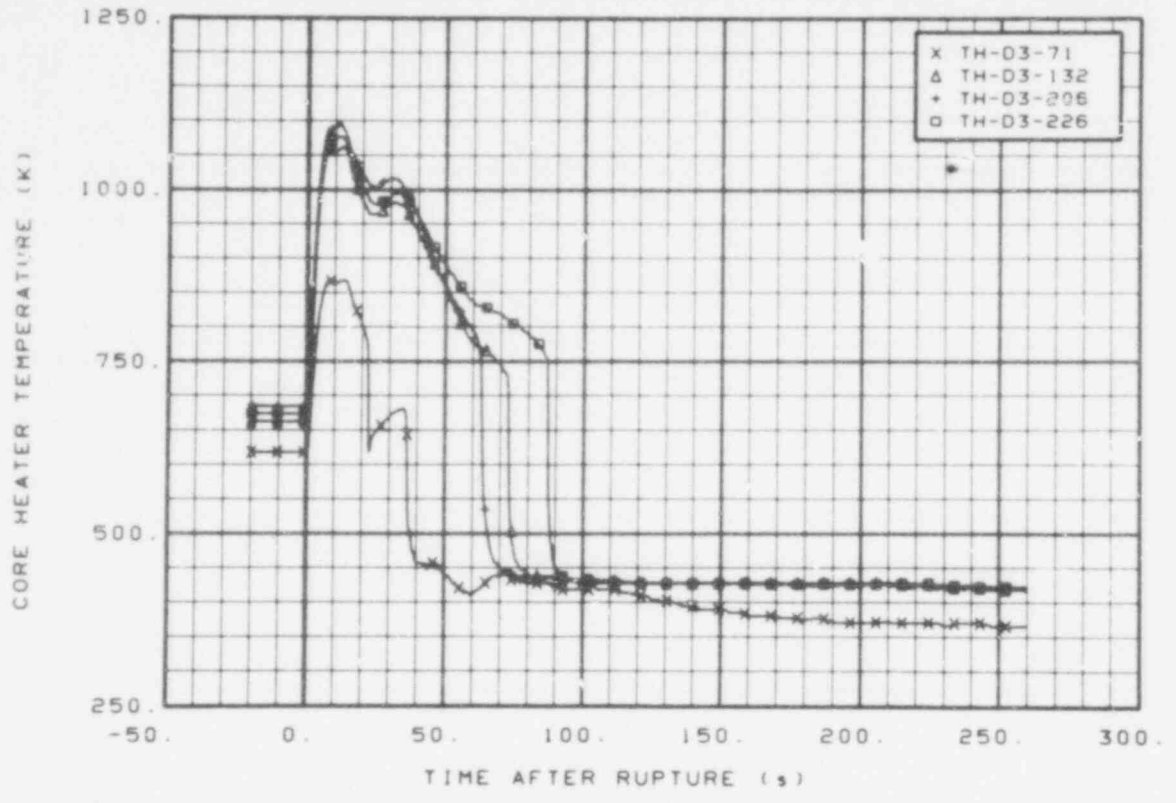

Fig. 85 Core heater temperature, Rod D-3 (TH-D3-71, TH-D3-132, TH-D3-206, and TH-D3-226), from -20 to 260 s.

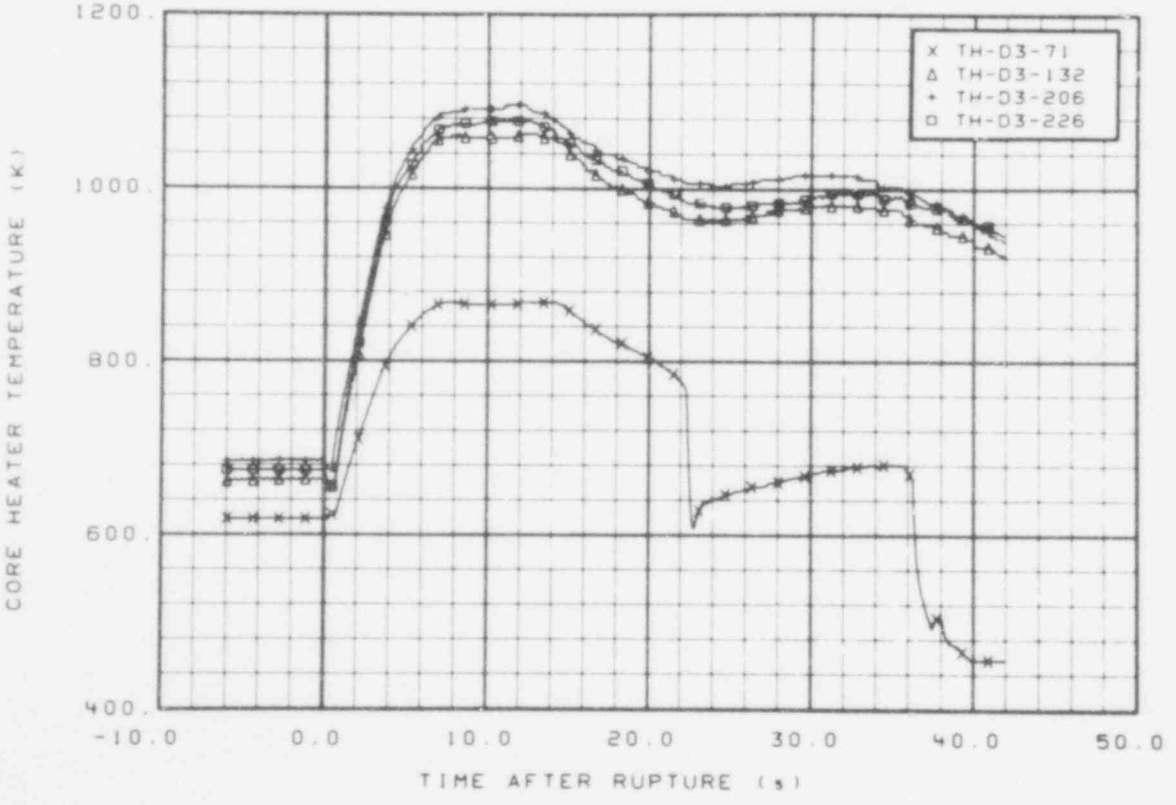

Fig. 86 Core heater temperature, Rod D-3 (TH-D3-71, TH-D3-132, TH-D3-206, and TH-D3-226), from -6 to 42 s.

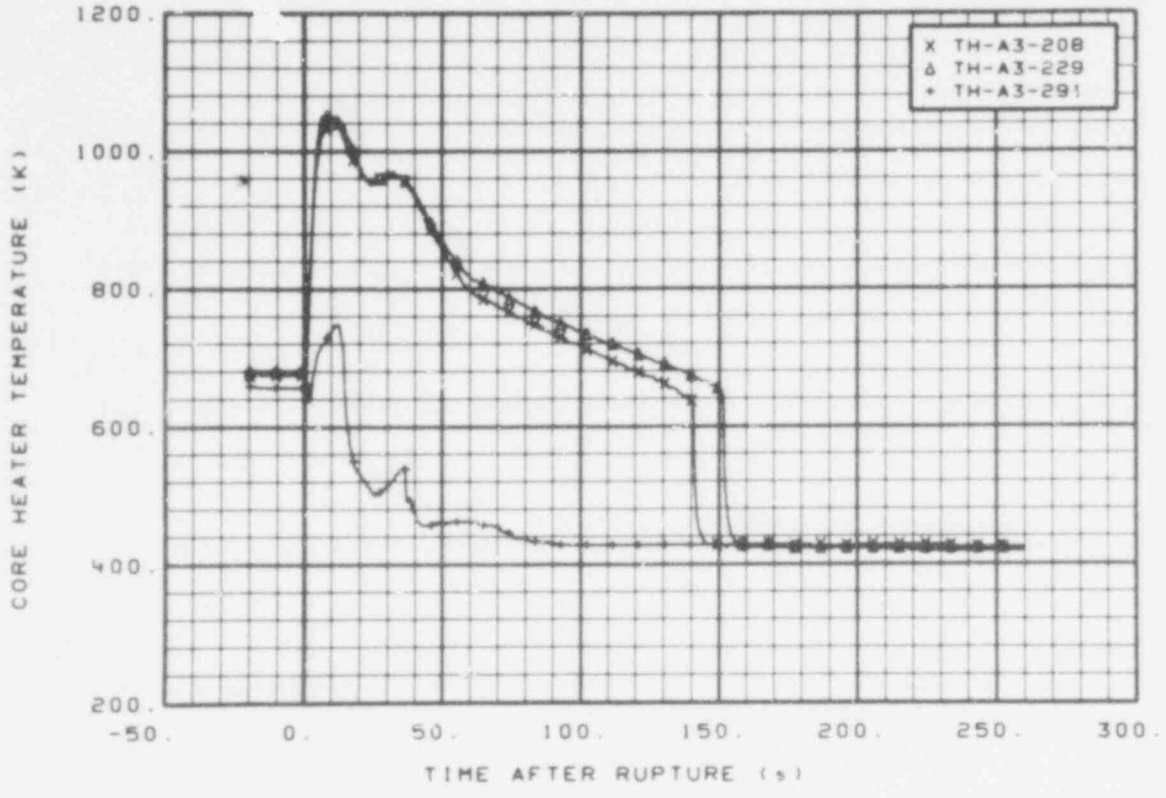

Fig. 87 Core heater temperature, Rod A-3 (TH-A3-208, TH-A3-229, and TH-A3-291), from -20 to 260 s.

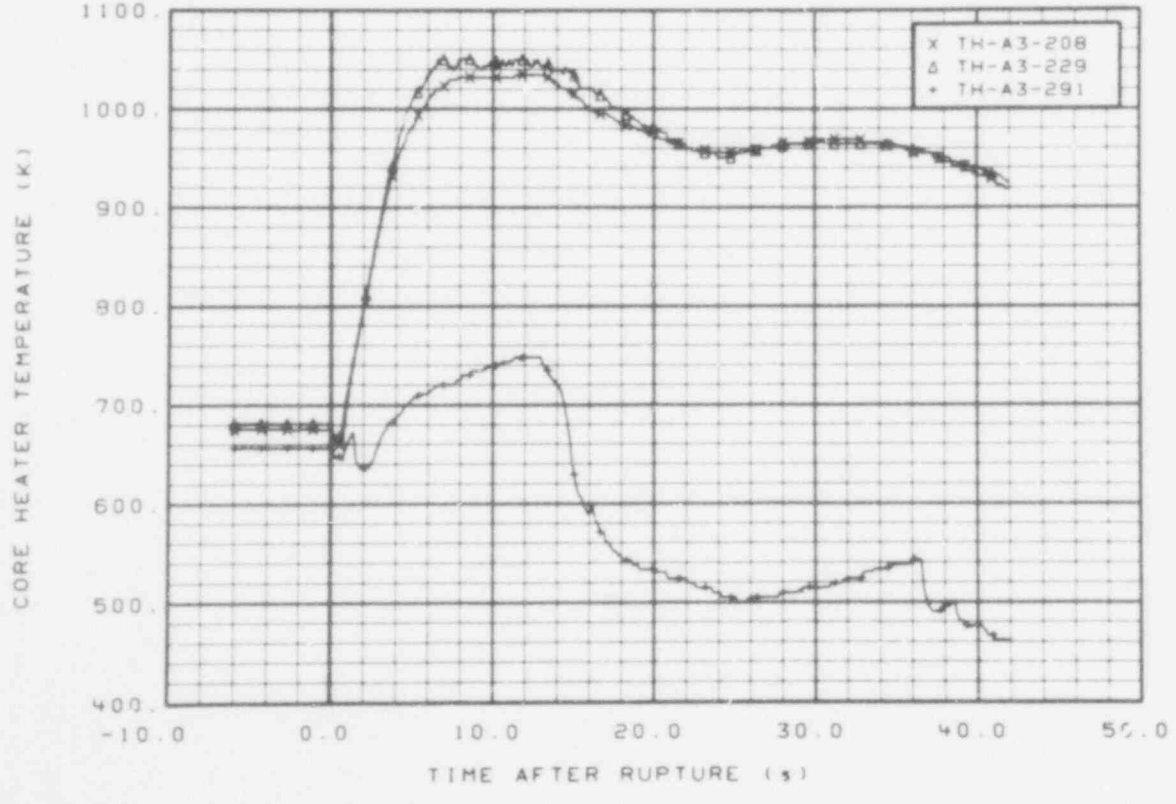

Fig. 88 Core heater temperature, Rod A-3 (TH-A3-208, TH-A3-229, and TH-A3-291), from -6 to 42 s.

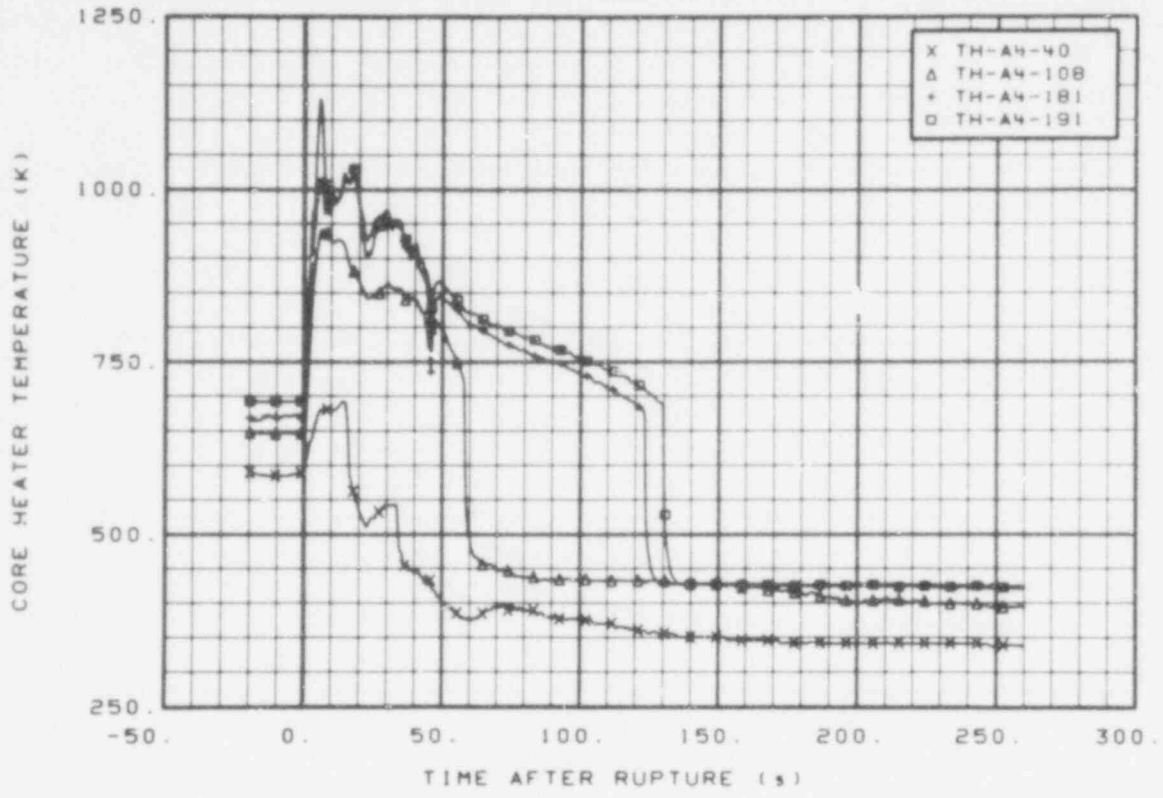

Fig. 89 Core heater temperature, Rod A-4 (TH-A4-40, TH-A4-108, TH-A4-181, and TH-A4-191), from -20 to 260 s.

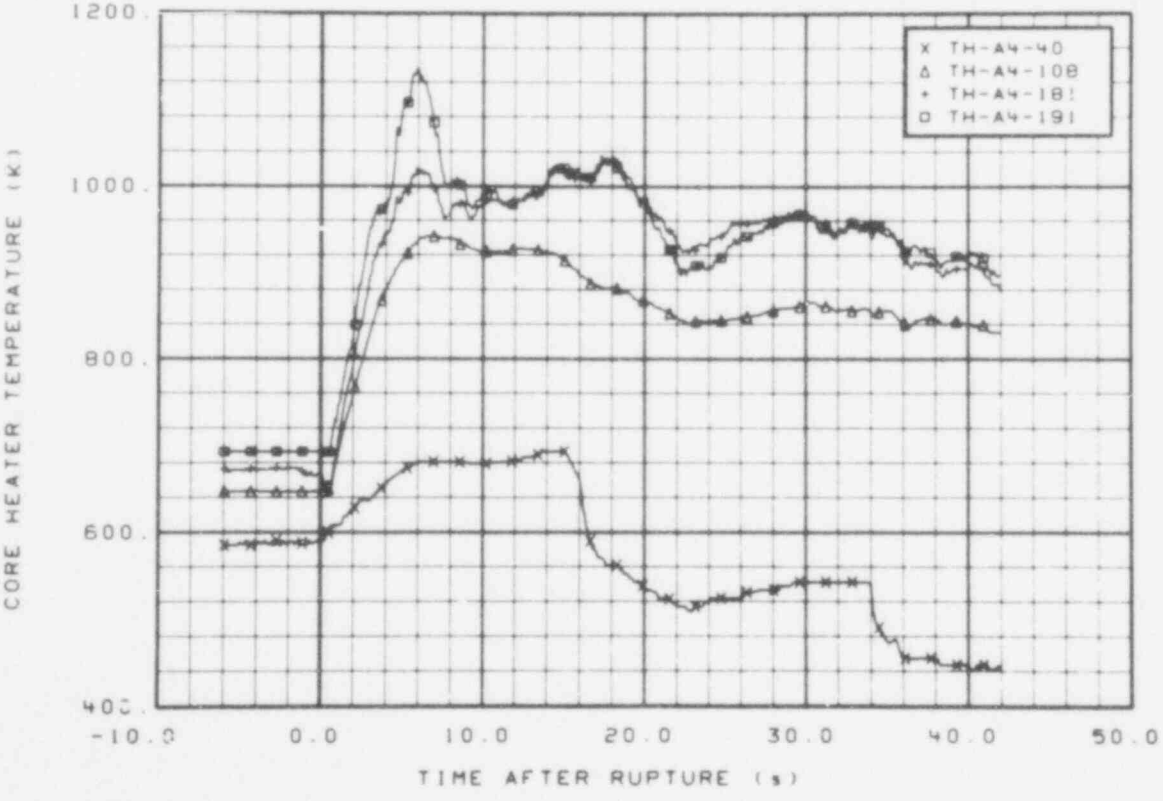

Fig. 90 Core heater temperature, Rod A-4 (TH-A4-40, TH-A4-108, TH-A4-181, and TH-A4-191), from -6 to 42 s.

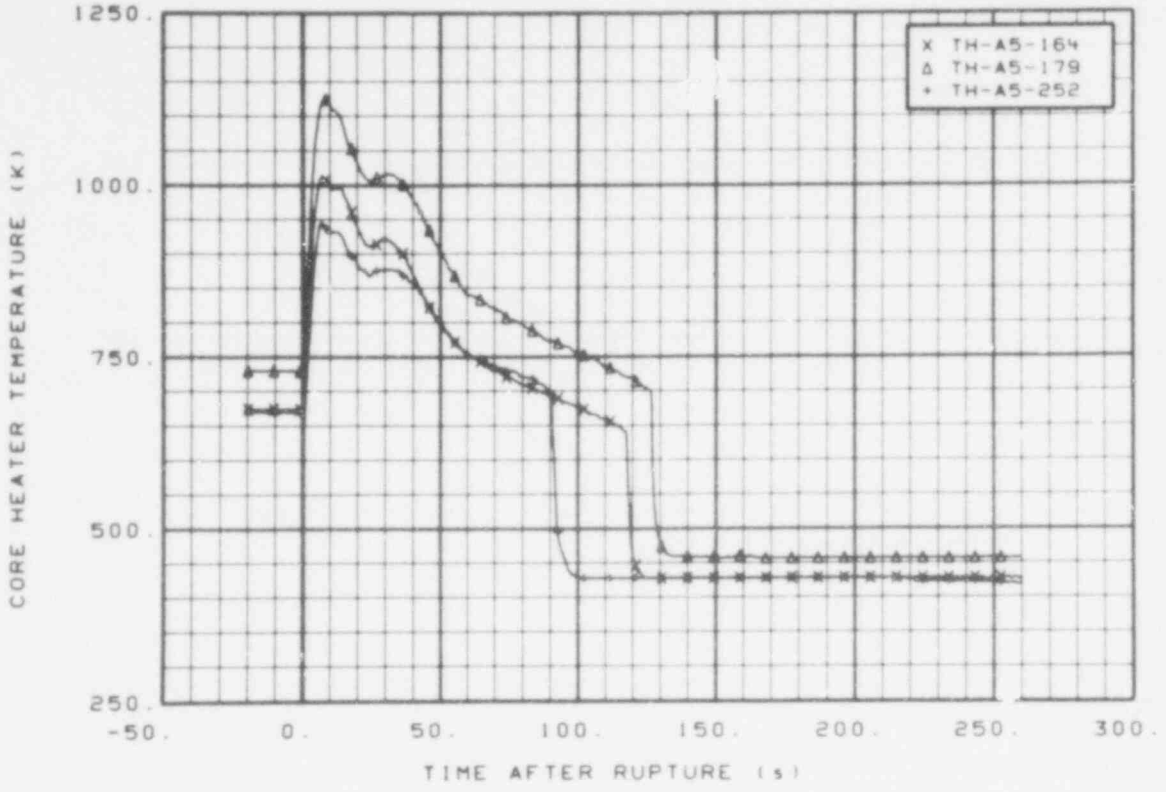

Fig. 91 Core heater temperature, Rod A-5 (TH-A5-164, TH-A5-179, and TH-A5-252), from -20 to 260 s.

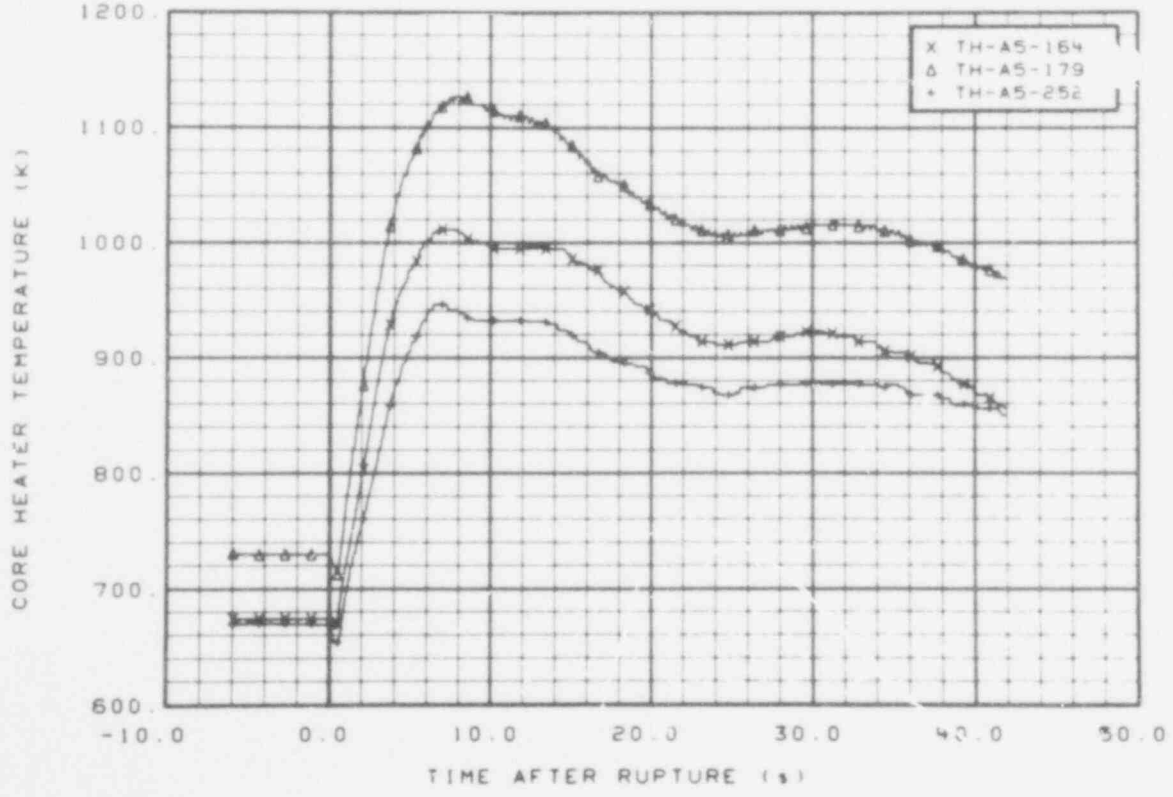

Fig. 92 Core heater temperature, Rod A-5 (TH-A5-164, TH-A5-179, and TH-A5-252), from -6 to 42 s.

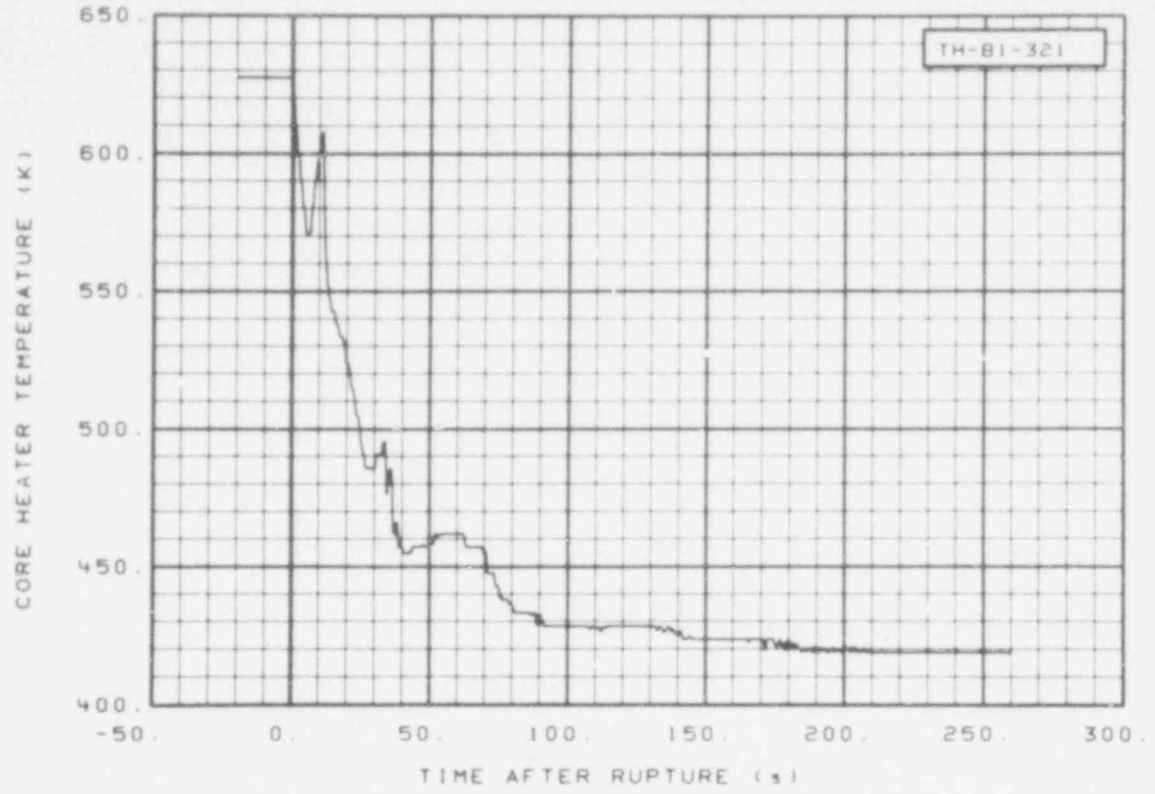

Fig. 93 Core heater temperature, Rod B-1 (TH-B1-321), from -20 to 260 s.

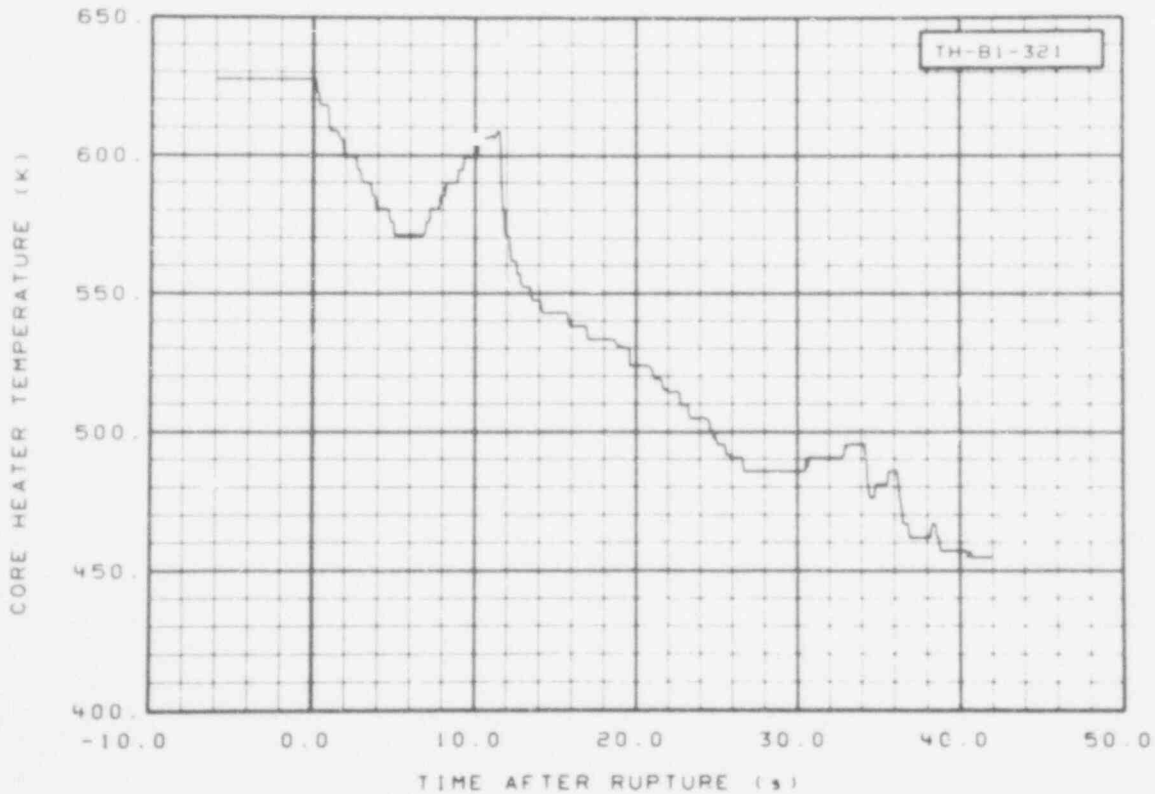

Fig. 94 Core heater temperature, Rod B-1 (TH-B1-321), from -6 to 42 s.

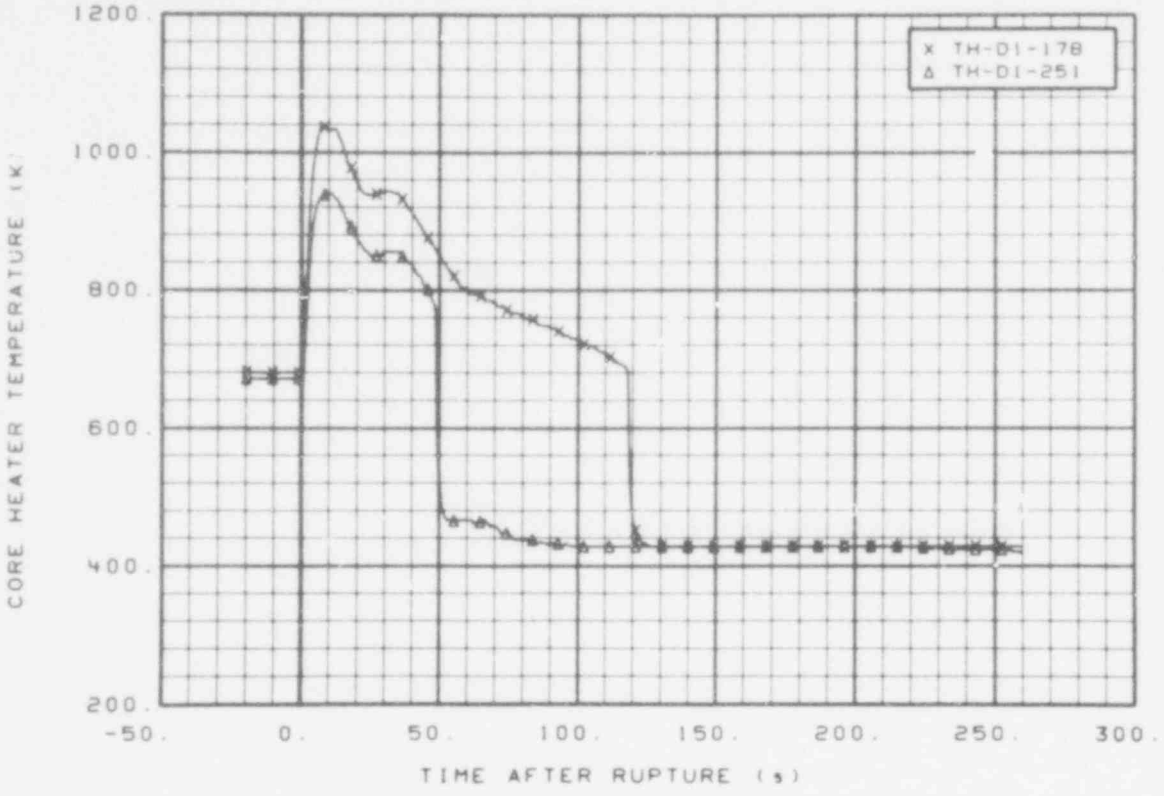

Fig. 95 Core heater temperature, Rod D-1 (TH-D1-178 and TH-D1-251), from -20 to 260 s.

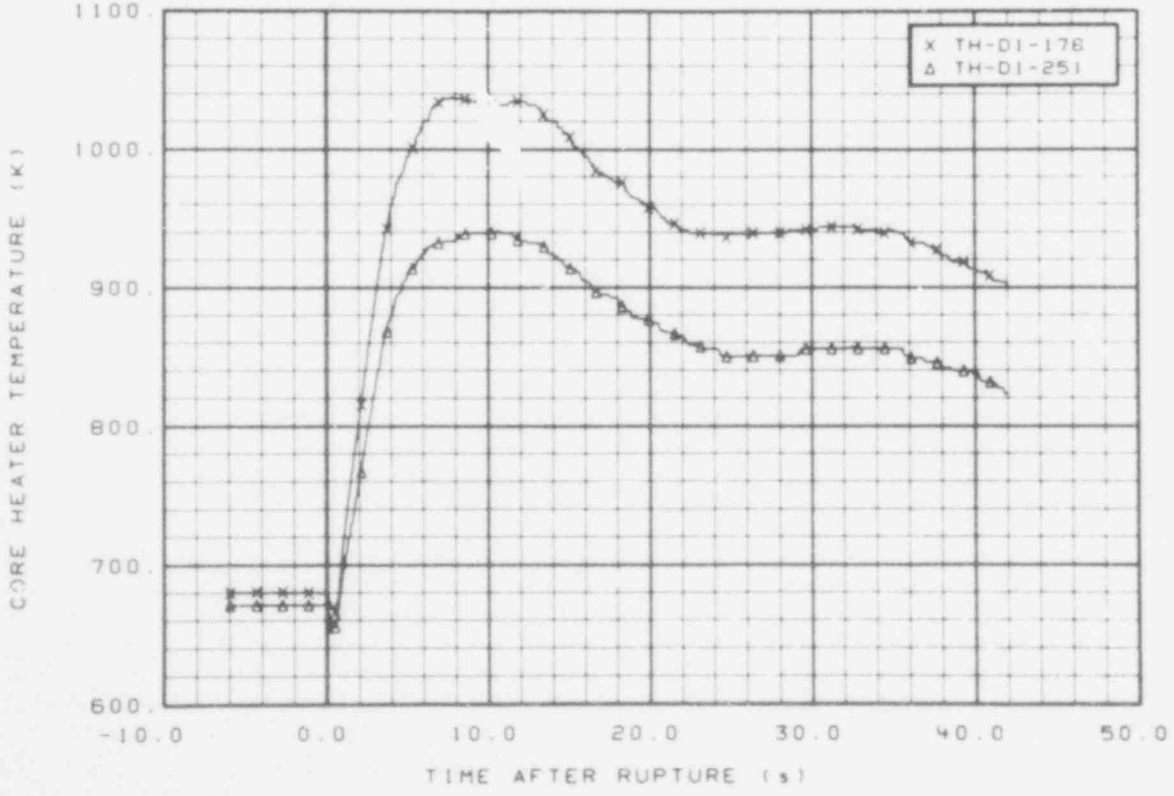

Fig. 96 Core heater temperature, Rod D-1 (TH-D1-178 and TH-D1-251), from -6 to 42 s.

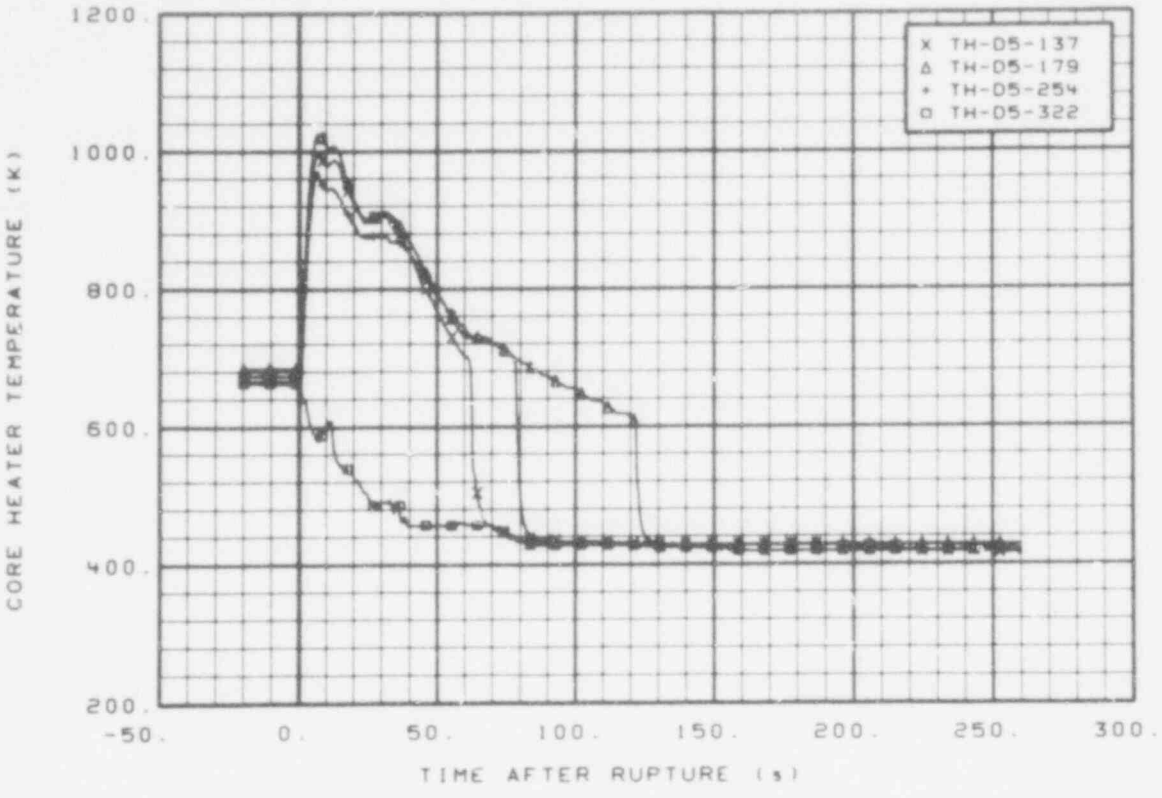

Fig. 97 Core heater temperature, Rod D-5 (TH-D5-137, TH-D5-179, TH-D5-254, and TH-D5-322), from -20 to 260 s.

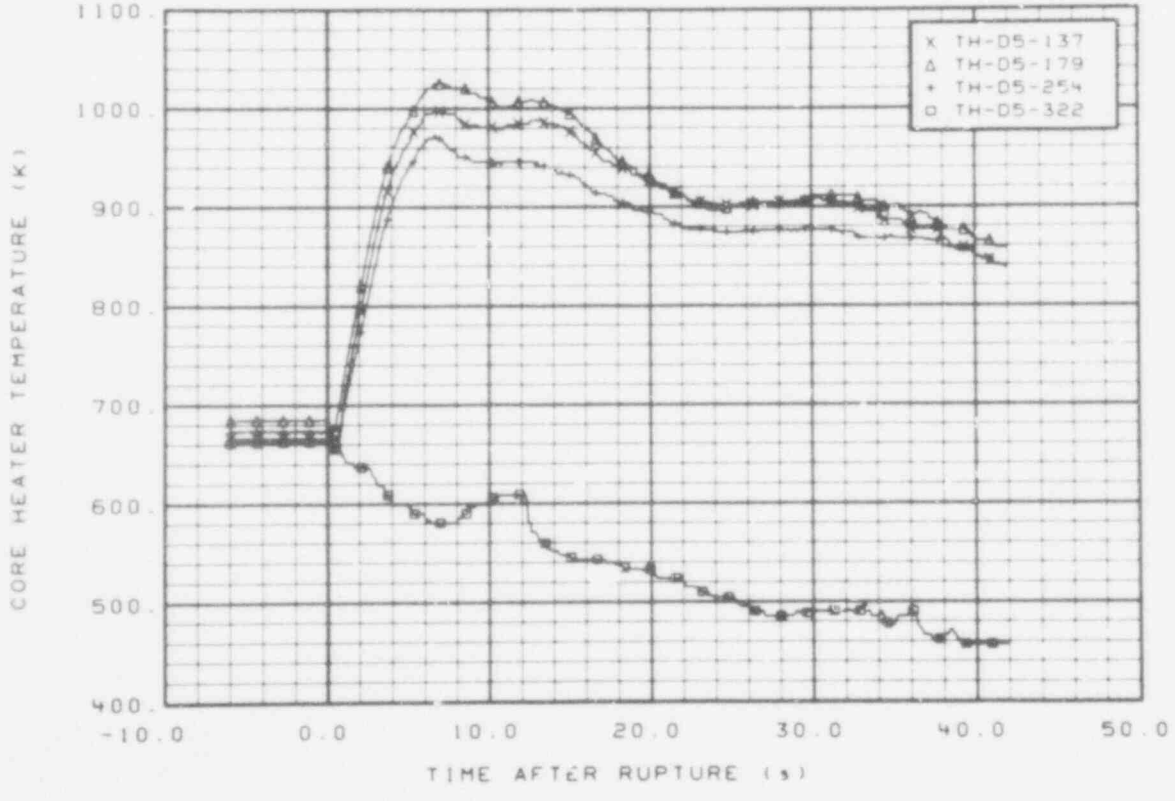

Fig. 98 Core heater temperature, Rod D-5 (TH-D5-137, TH-D5-179, TH-D5-254, and TH-D5-322), from -6 to 42 s.

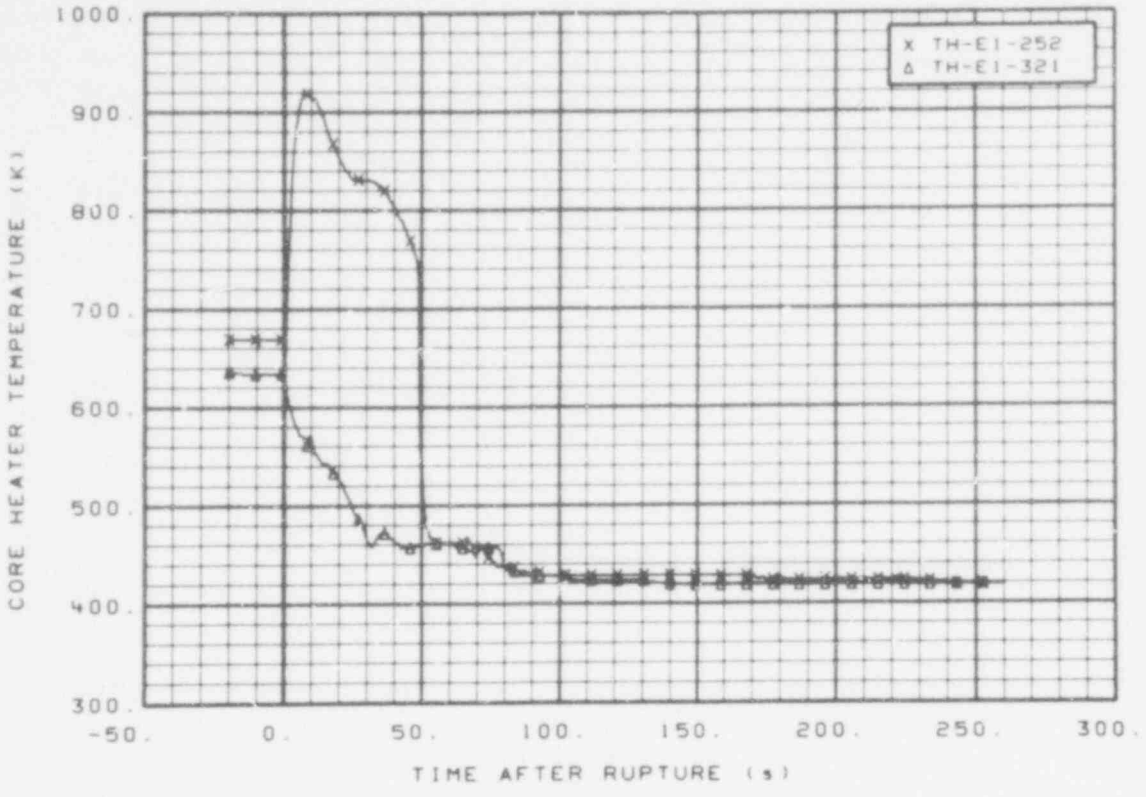

Fig. 99 Core heater temperature, Rod E-1 (TH-E1-252 and TH-E1-321), from -20 to 260 s.

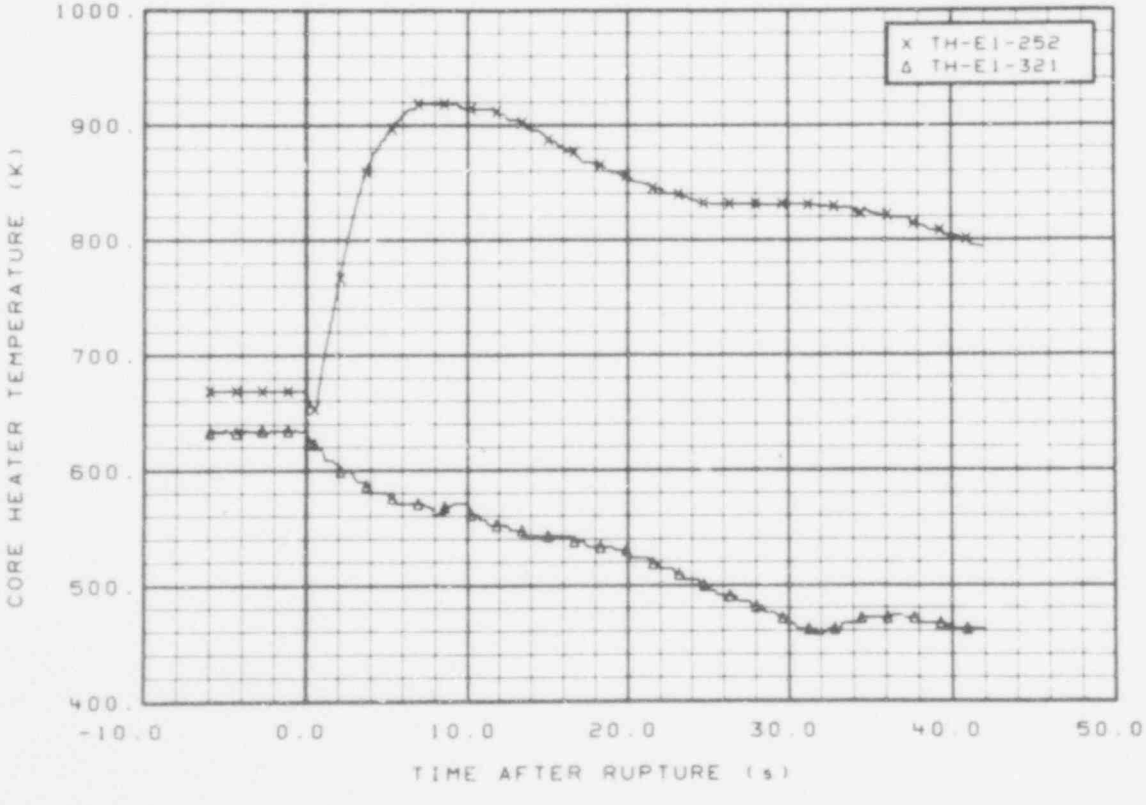

Fig. 100 Core heater temperaiure, Rod E-1 (TH-E1-252 and TH-E1-321), from -6 to 42 s.

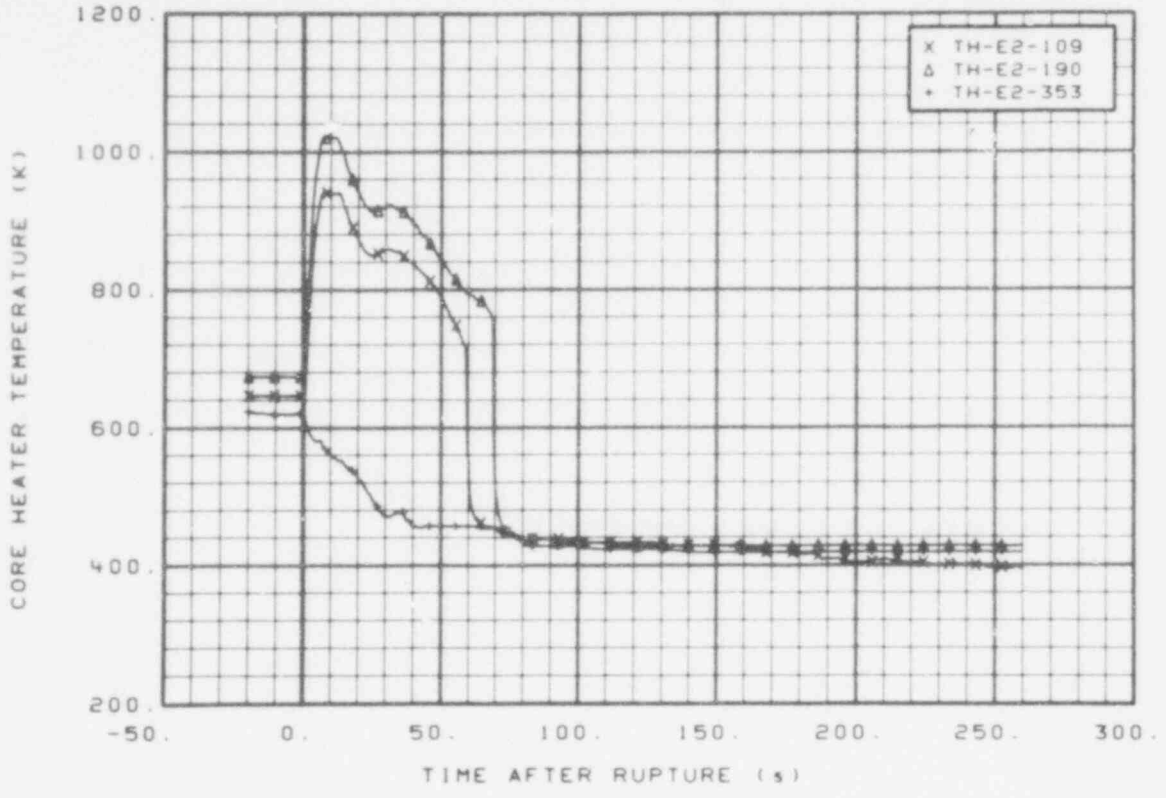

Fig. 101 Core heater temperature, Rod E-2 (TH-E2-109, TH-E2-190, and TH-E2-353), from -20 to 260 s.

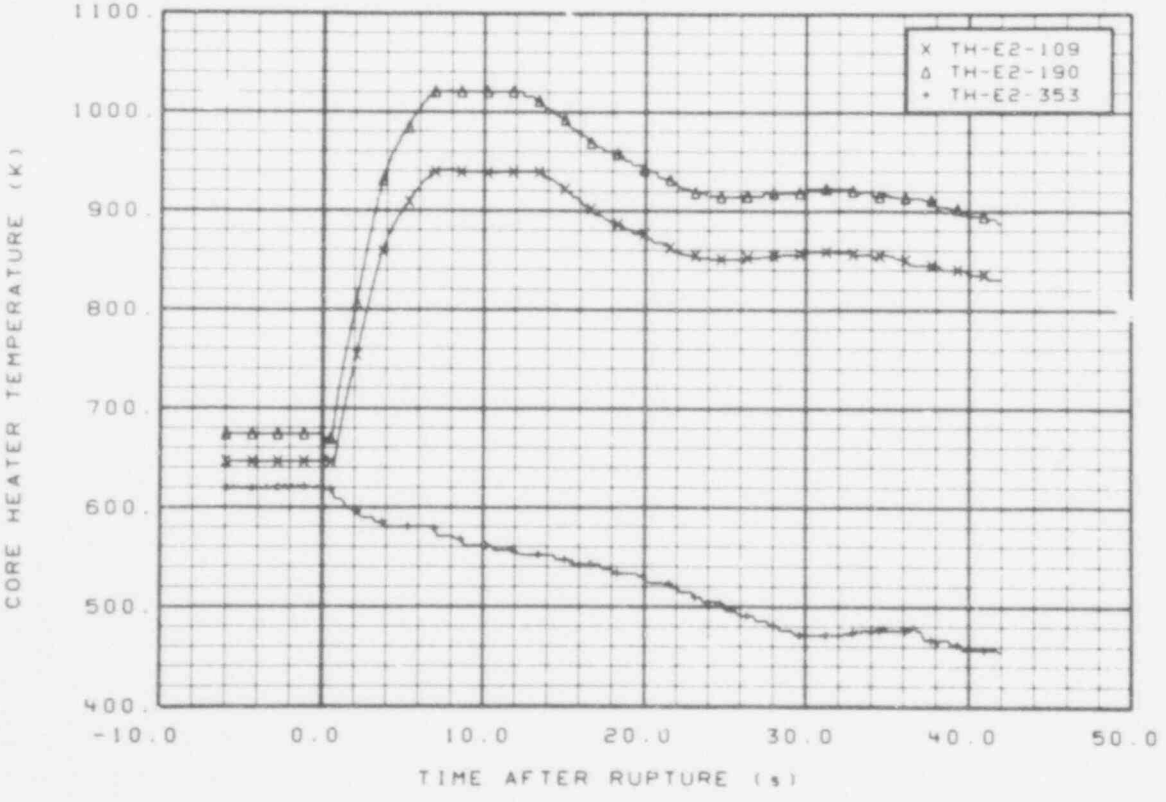

Fig. 102 Core heater temperature, Rod E-2 (TH-E2-109, TH-E2-190, and TH-E2-353), from -6 to 42 s.

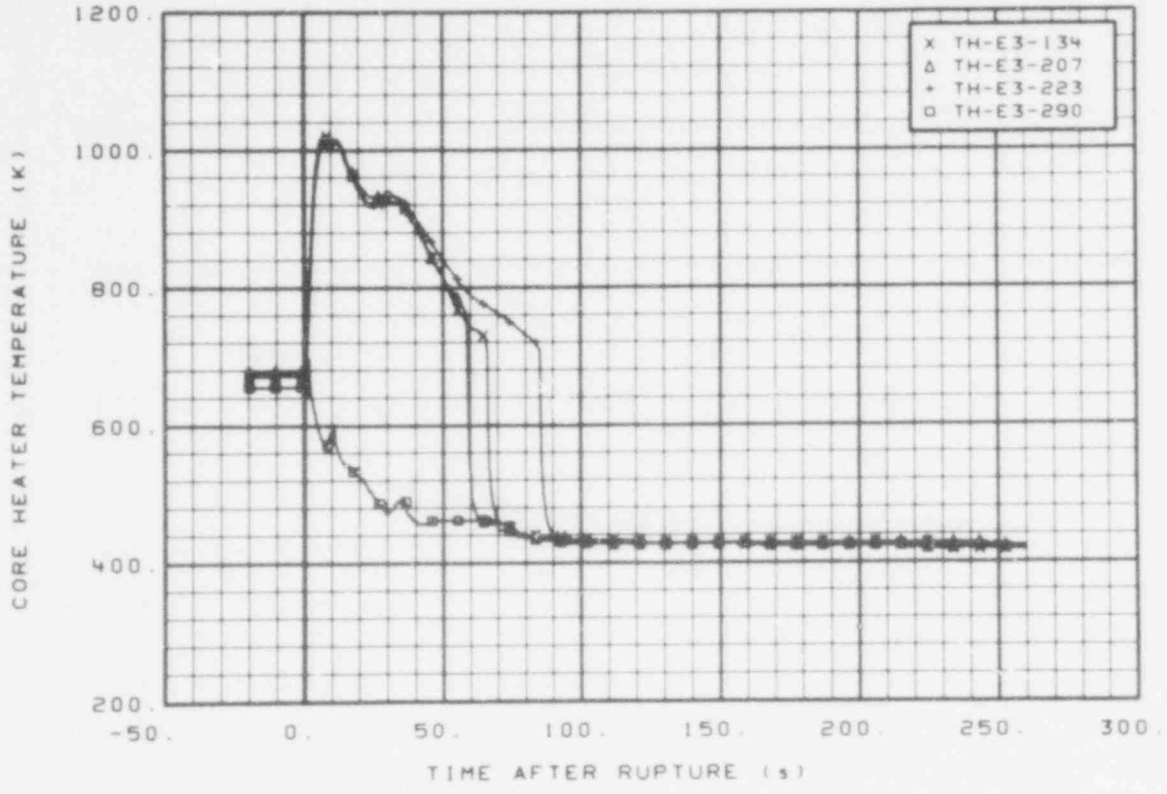

Fig. 103 Core heater temperature, Rod E-3 (TH-E3-134, TH-E3-207, TH-E3-223, and TH-E3-290), from -20 to 260 s.

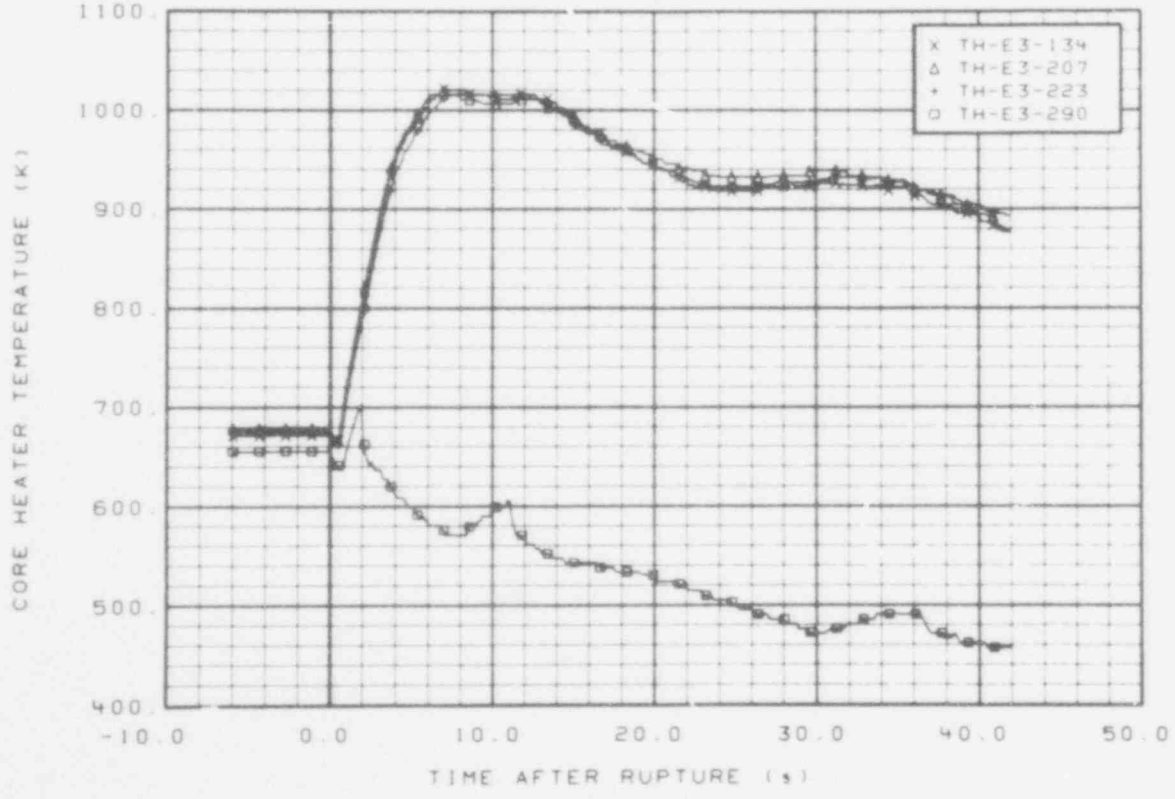

Fig. 104 Core heater temperature, Rod E-3 (TH-E3-134, TH-E3-207, TH-E3-223, and TH-E3-290), from -6 to 42 s.

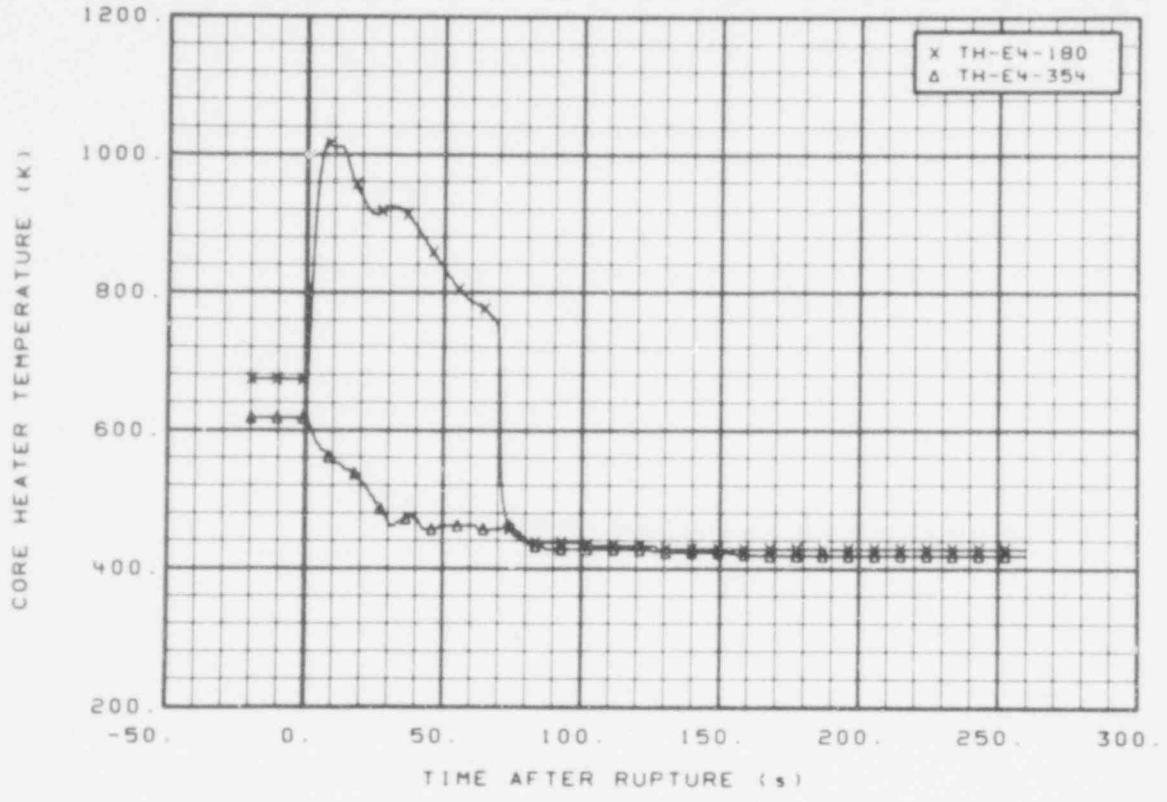

Fig. 105 Core heater temperature, Rod E-4 (TH-E4-180 and TH-E4-354), from -20 to 260 s.

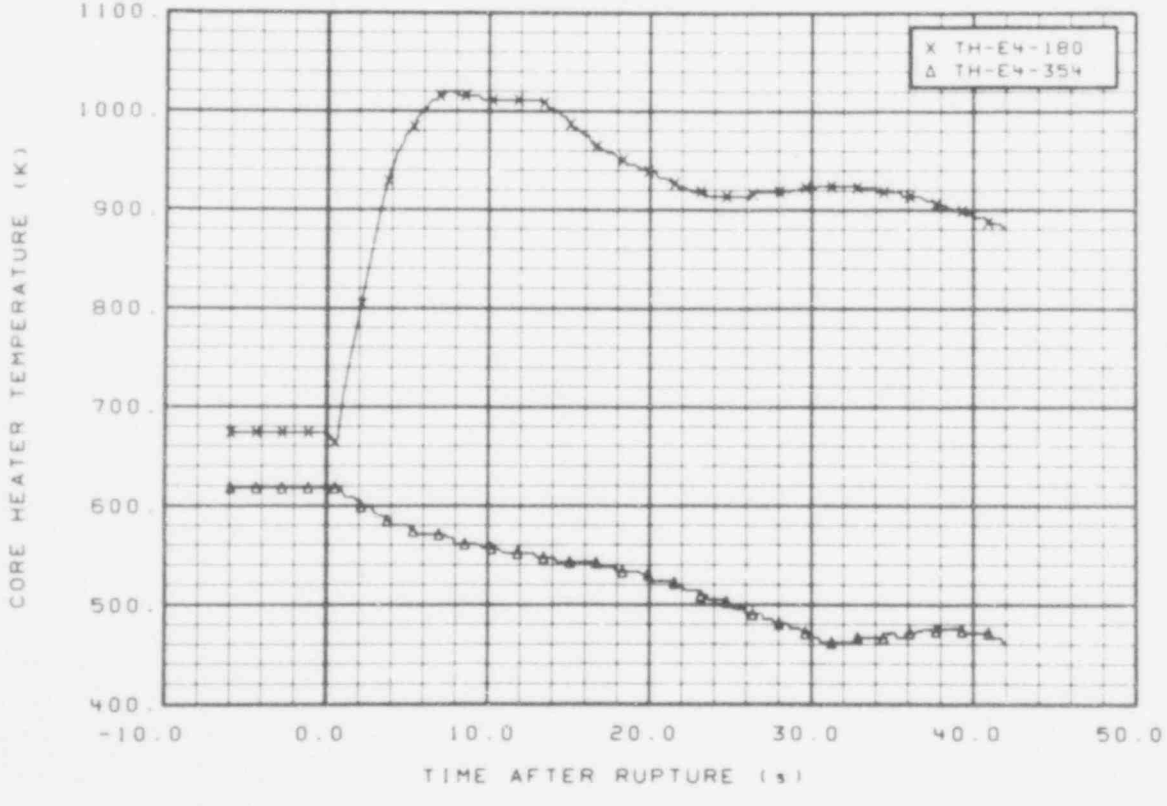

Fig. 106 Core heater temperature, Rod E-4 (TH-E4-180 and TH-E4-354), from -6 to 42 s.

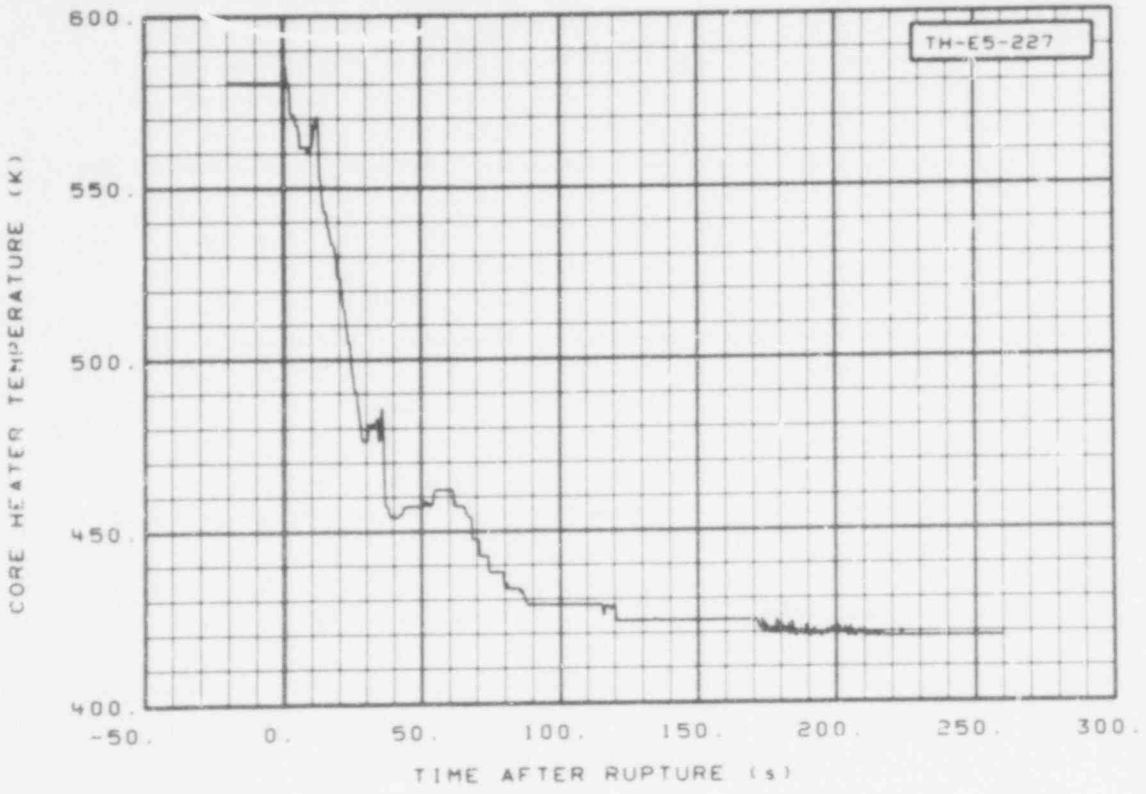

Fig. 107 Core heater temperature, Rod E-5 (TH-E5-227), from -20 to 260 s.

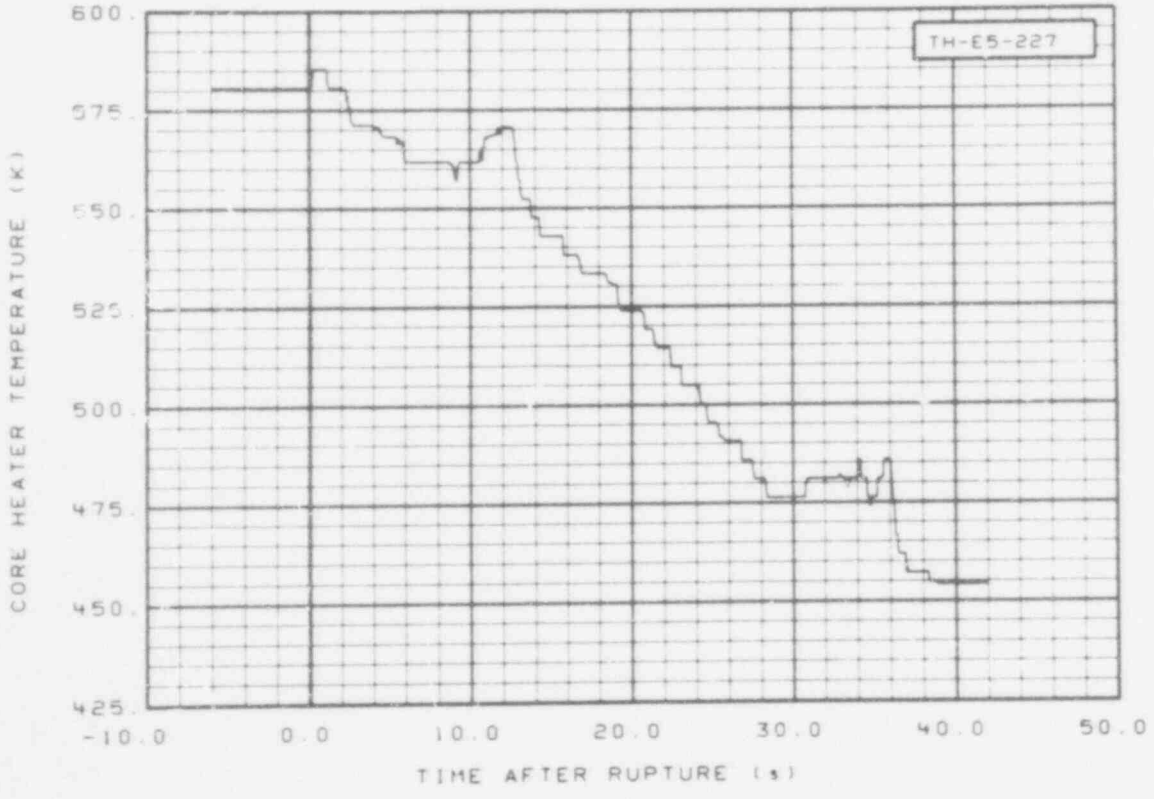

Fig. 108 Core heater temperature, Rod E-5 (TH-E5-227), from -6 to 42 s.

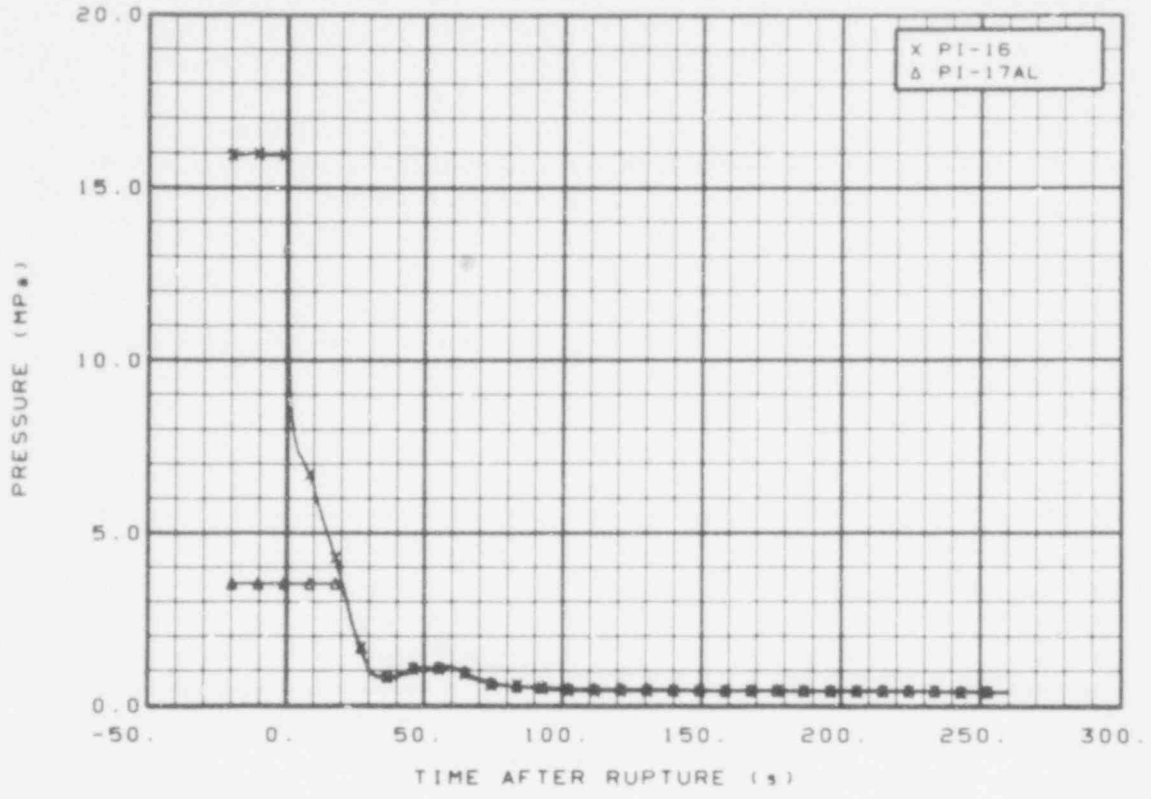

Fig. 109 Pressure in intact loop cold leg (PI-16 and PI-17AL), from -20 to 260 s.

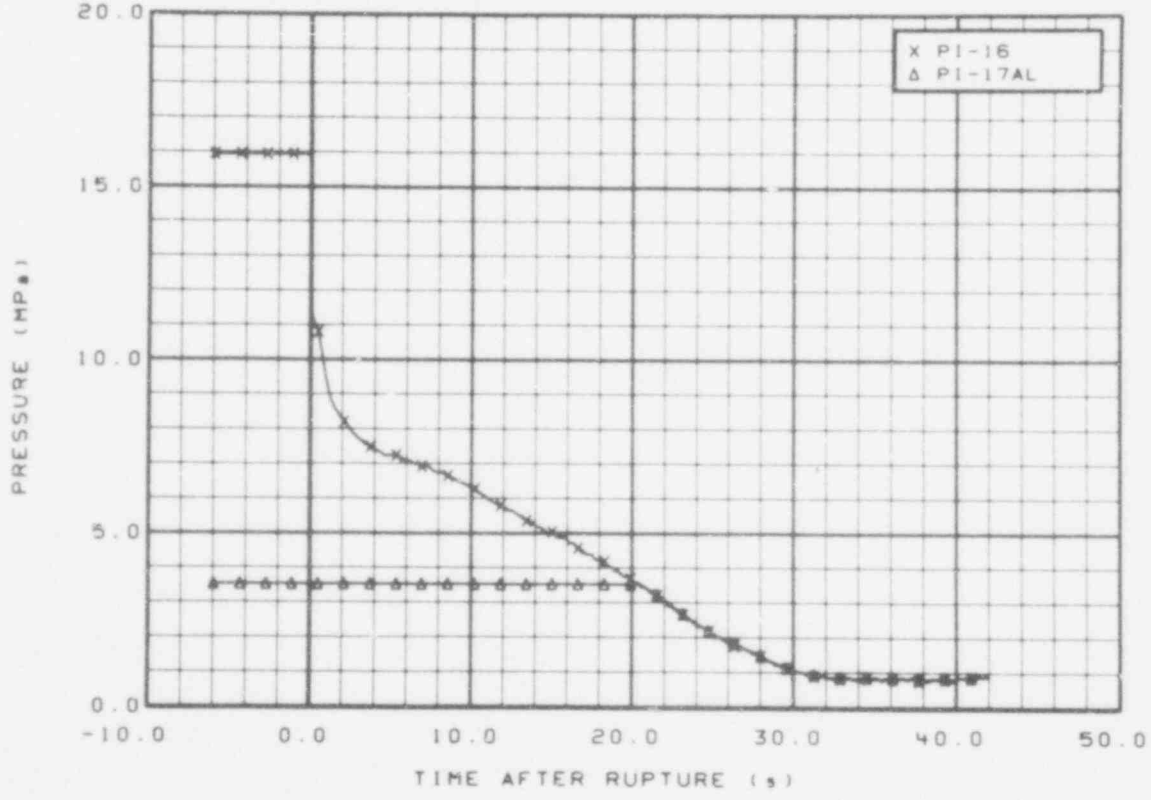

Fig. 110 Pressure in intact loop cold leg (PI-16 and PI-17AL), from -6 to 42 s.

544 098

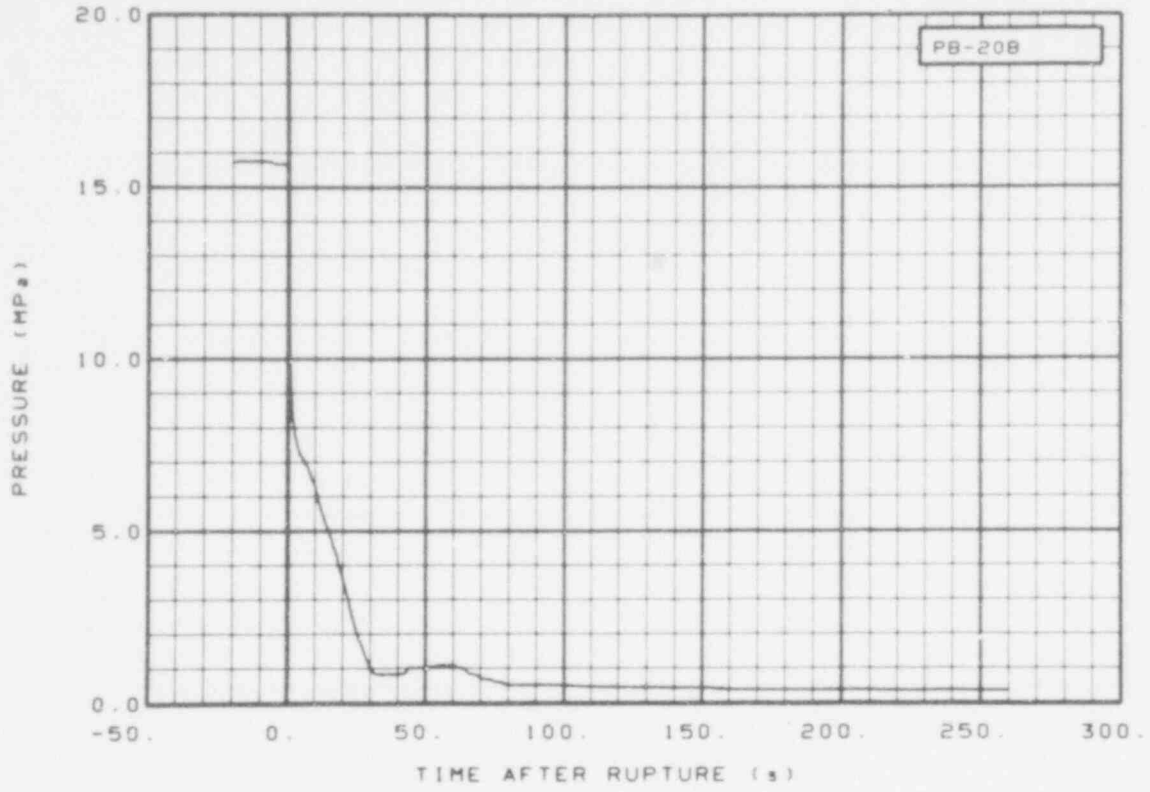

Fig. 111 Pressure in broken loop hot leg (PB-20B), from -20 to 260 s.

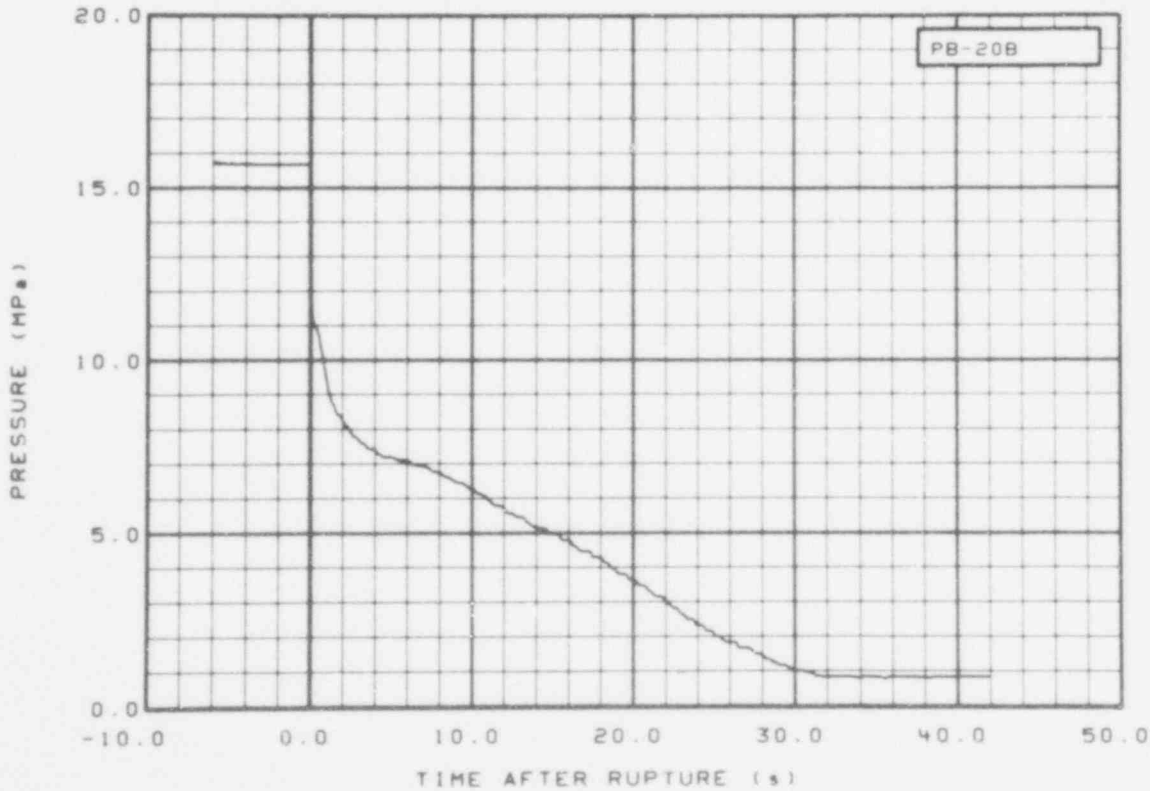

Fig. 112 Pressure in broken loop hot leg (PB-20B), from -6 to 42 s.

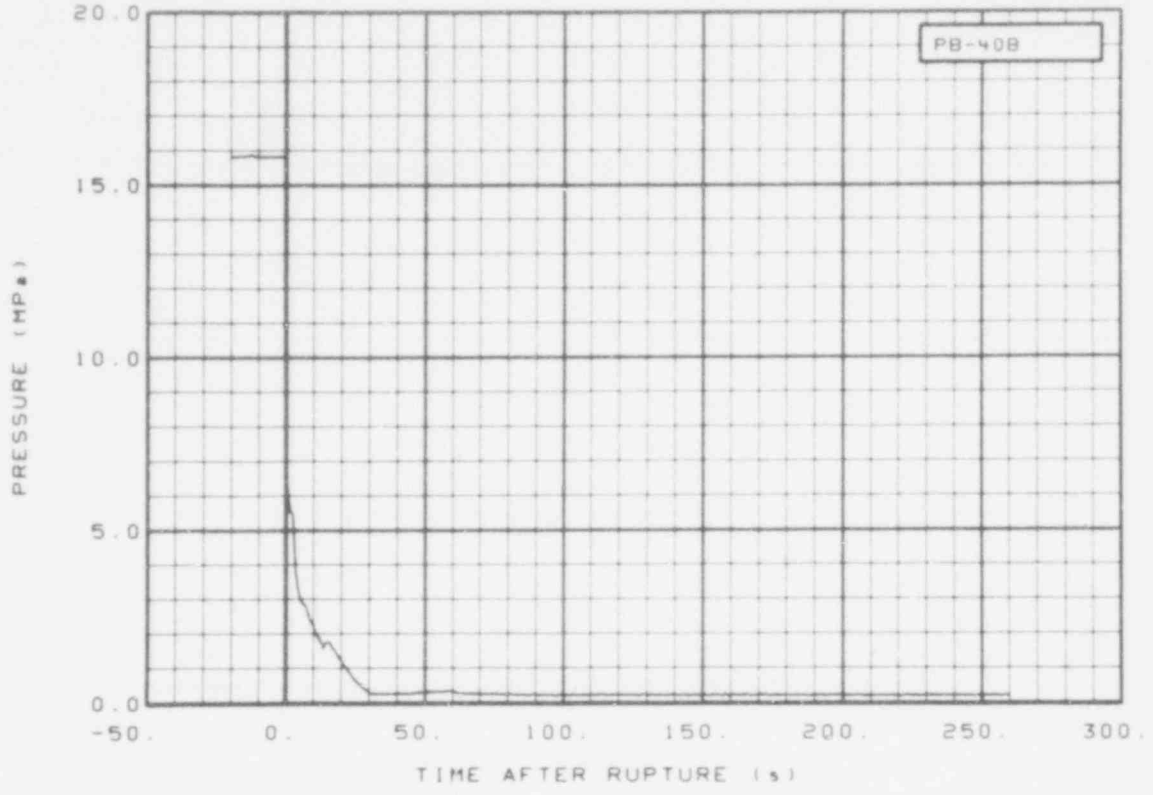

Fig. 113 Pressure in broken loop cold leg, pump side (PB-40B), from -20 to 260 s.

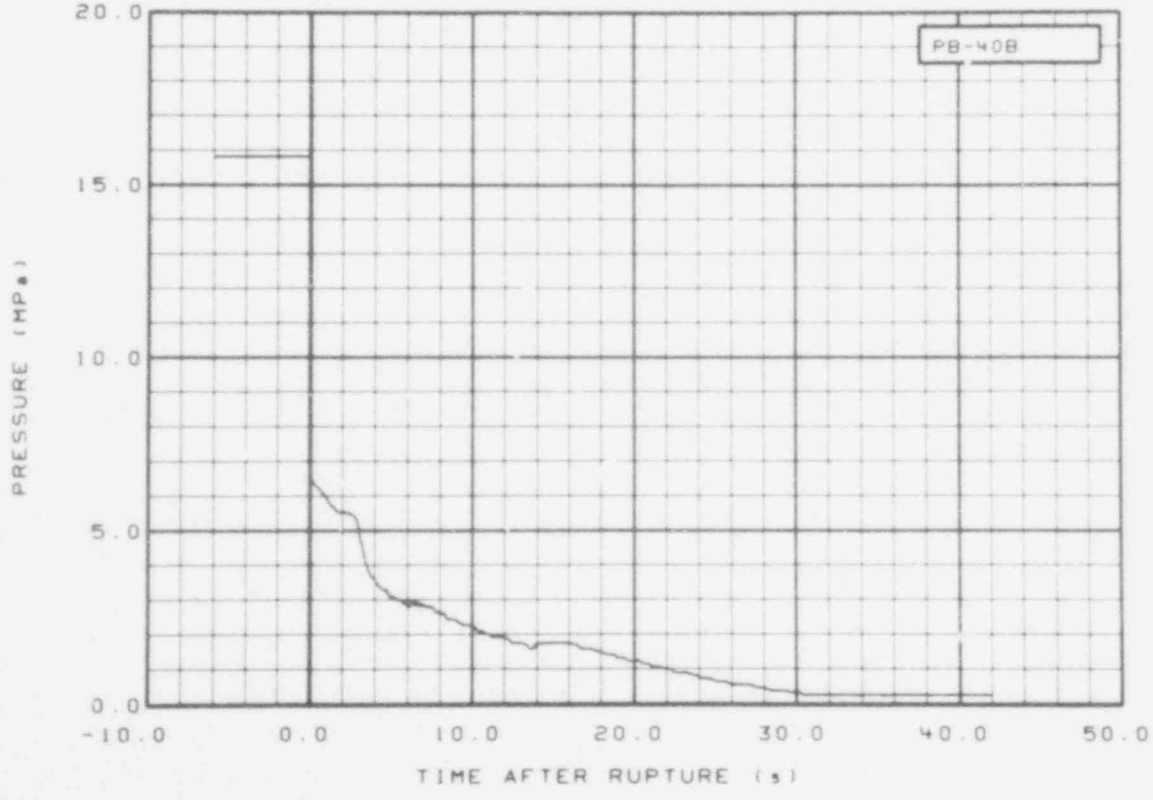

Fig. 114 Pressure in broken loop cold leg, pump side (PB-40B), from -6 to 42 s.

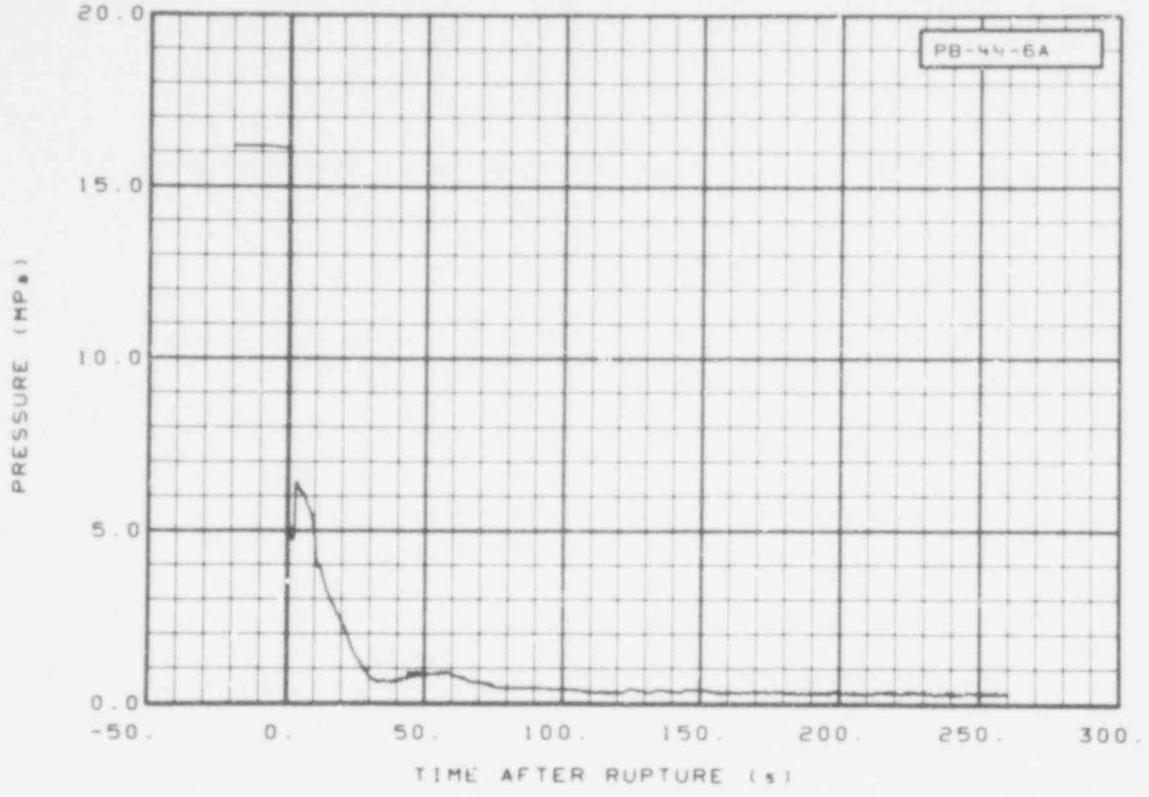

Fig. 115 Pressure in broken loop blowdown nozzle (PB-44-6A), from -20 to 260 s.

Fig. 116 Pressure in broken loop blowdown nozzle (PB-44-6A), from -6 to 42 s.

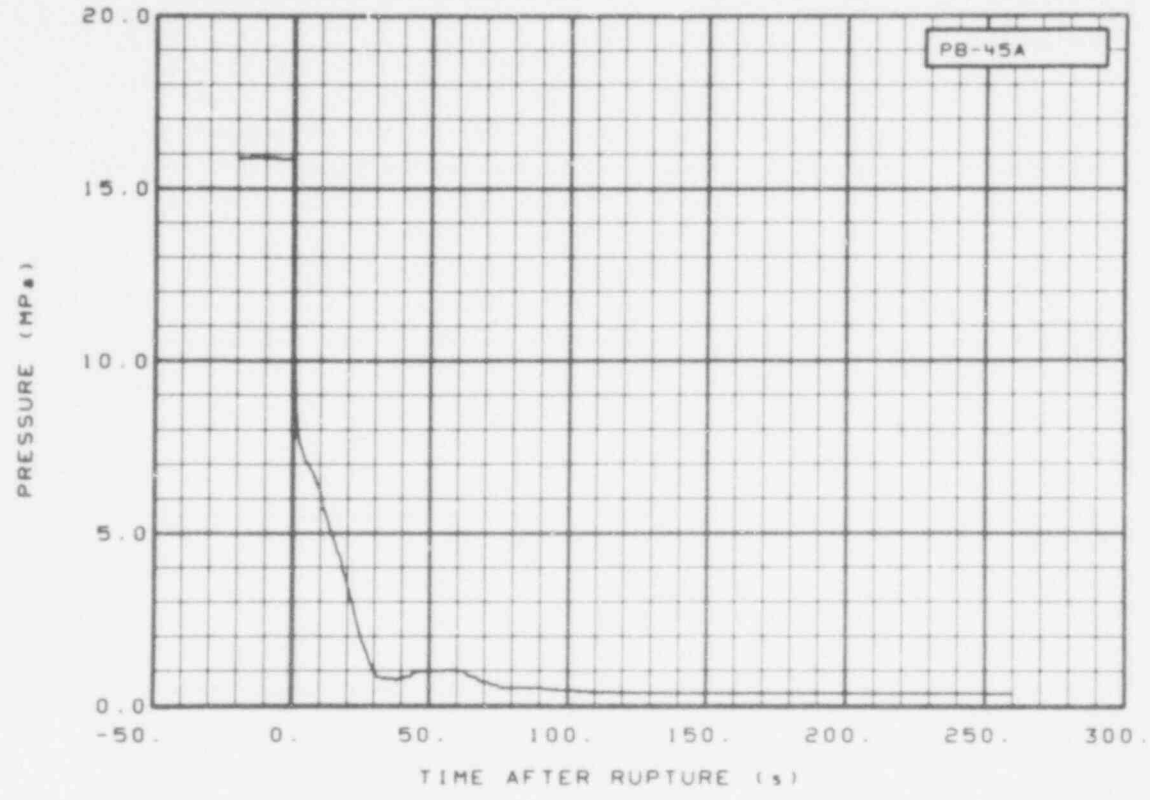

Fig. 117 Pressure in broken loop cold leg, vessel side (PB-45A), from -20 to 260 s.

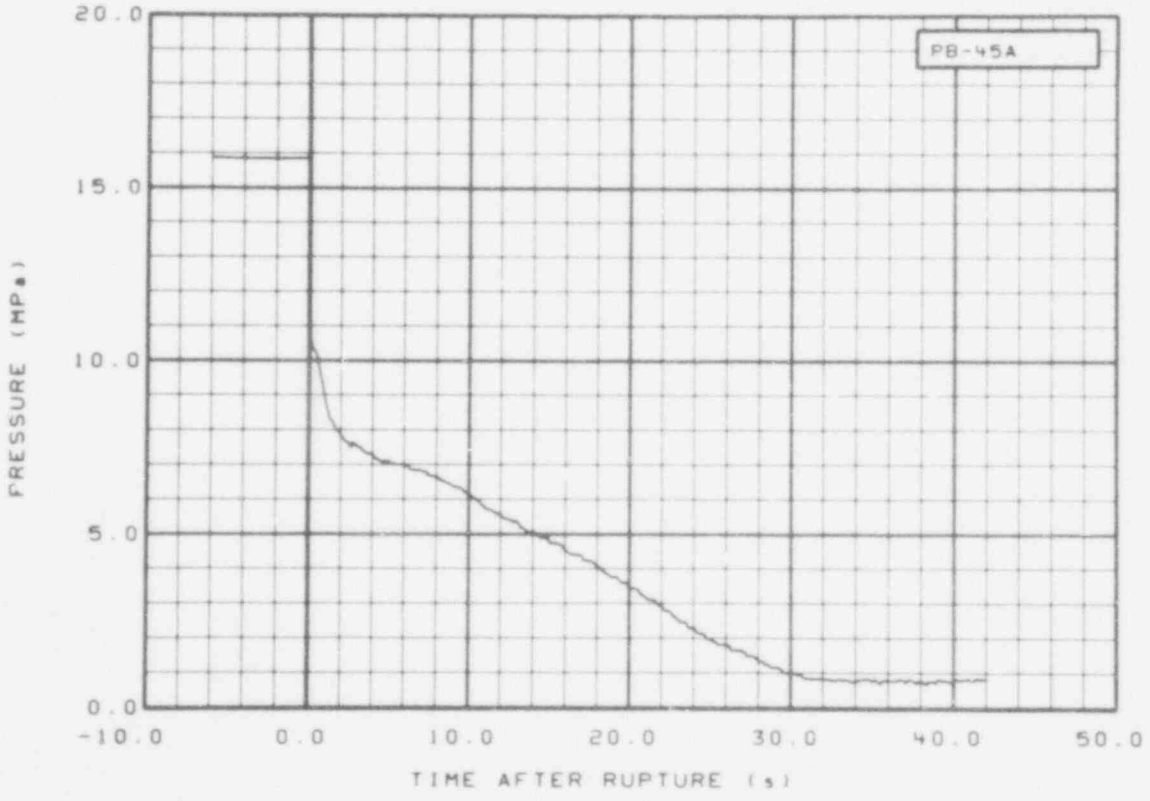

Fig. 118 Pressure in broken loop cold leg, vessel side (PB-45A), from -6 to 42 s.

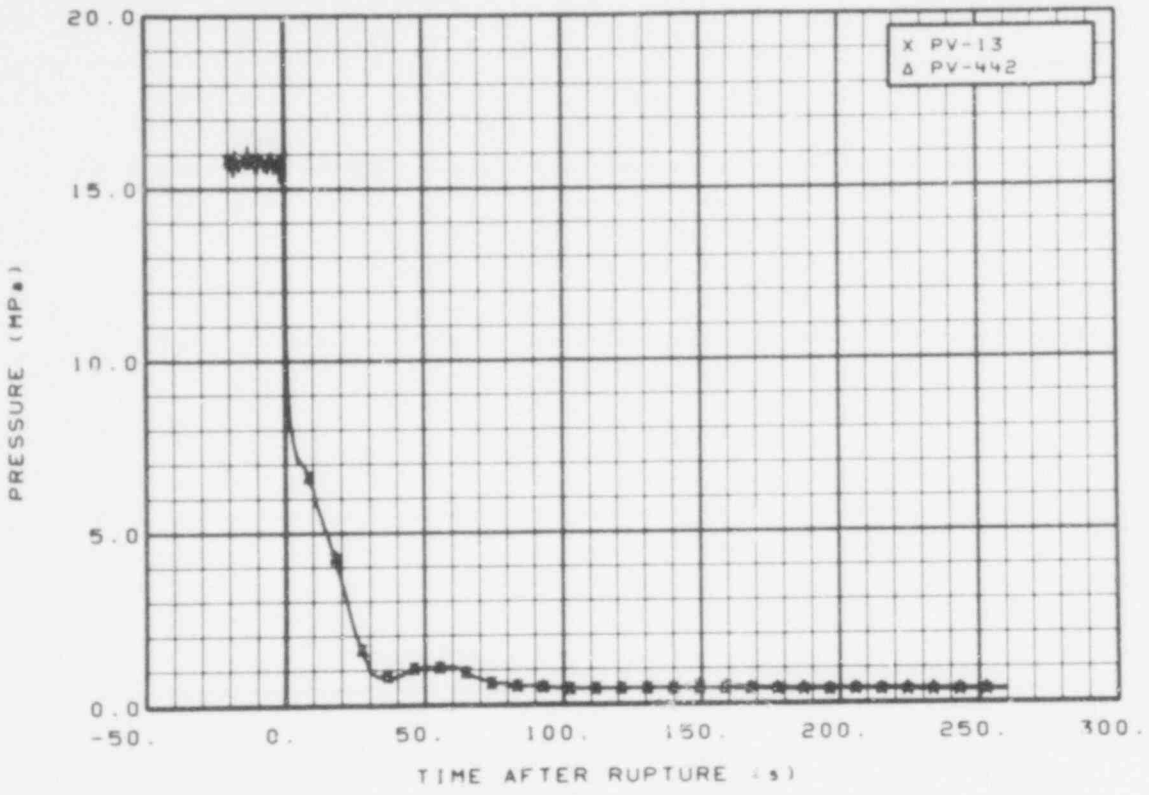

Fig. 119 Pressure in vessel upper and lower plenum (PV-13 and PV-442), from -20 to 260 s.

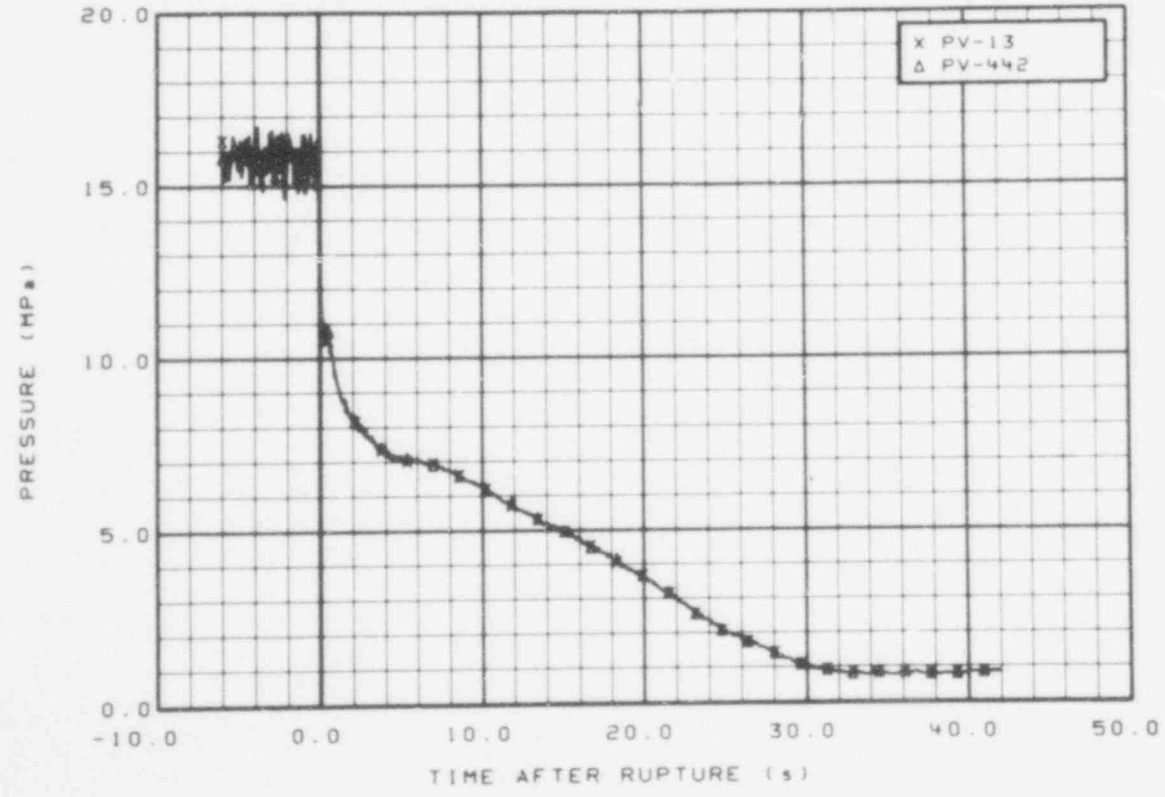

Fig. 120 Pressure in vessel upper and lower plenum (PV-13 and PV-442), from -6 to 42 s.

544 103

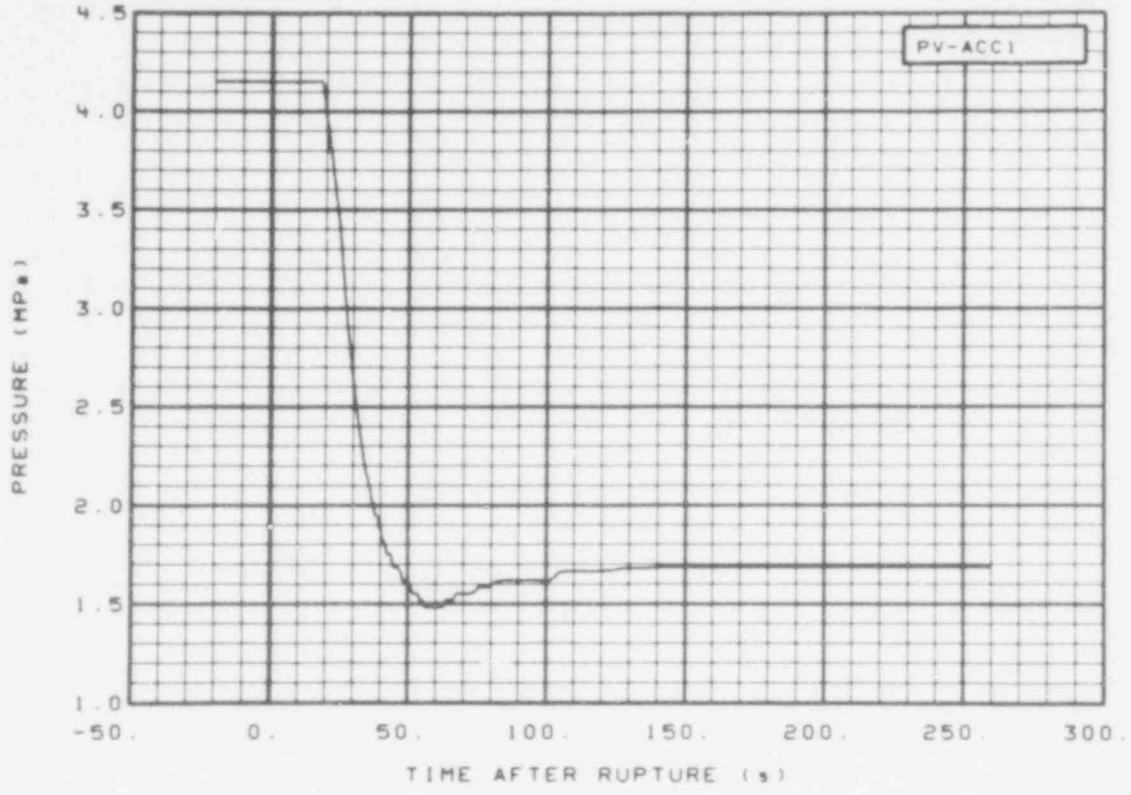

Fig. 121 Pressure in vessel ECC injection accumulator (PV-ACC1), from -20 to 260 s.

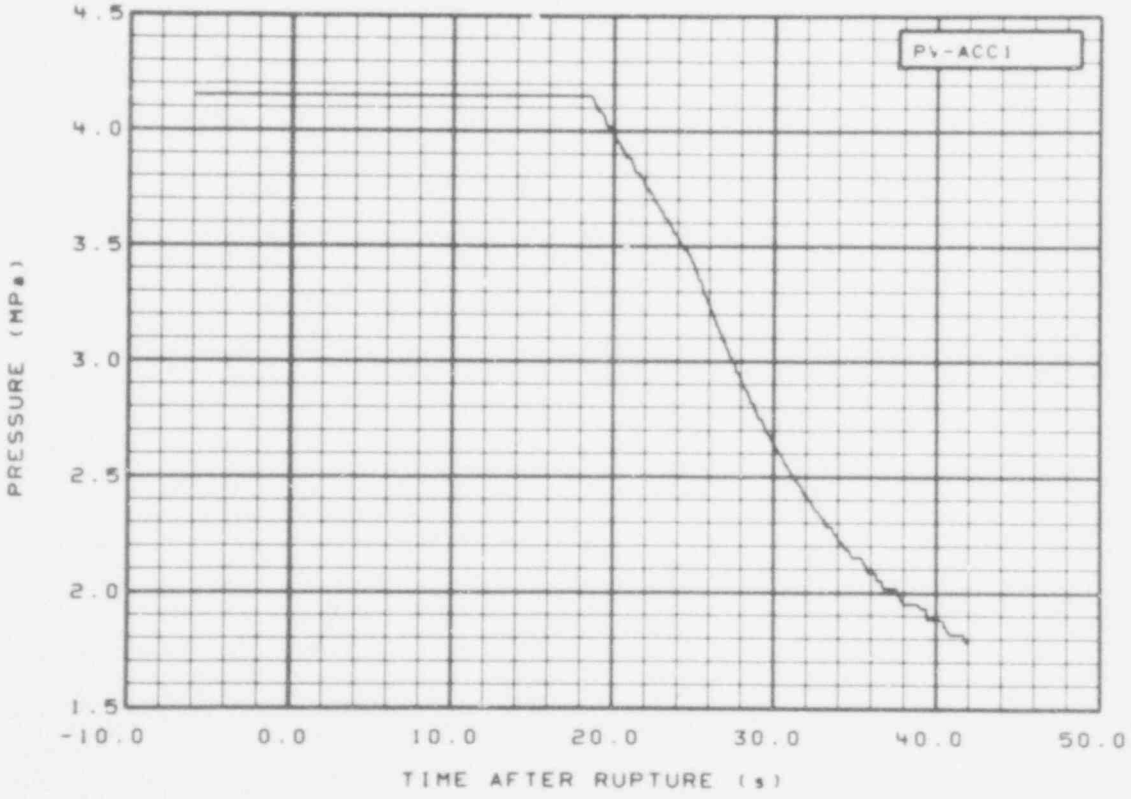

Fig. 122 Pressure in vessel ECC injection accumulator (PV-ACC1), from -6 to 42 s.

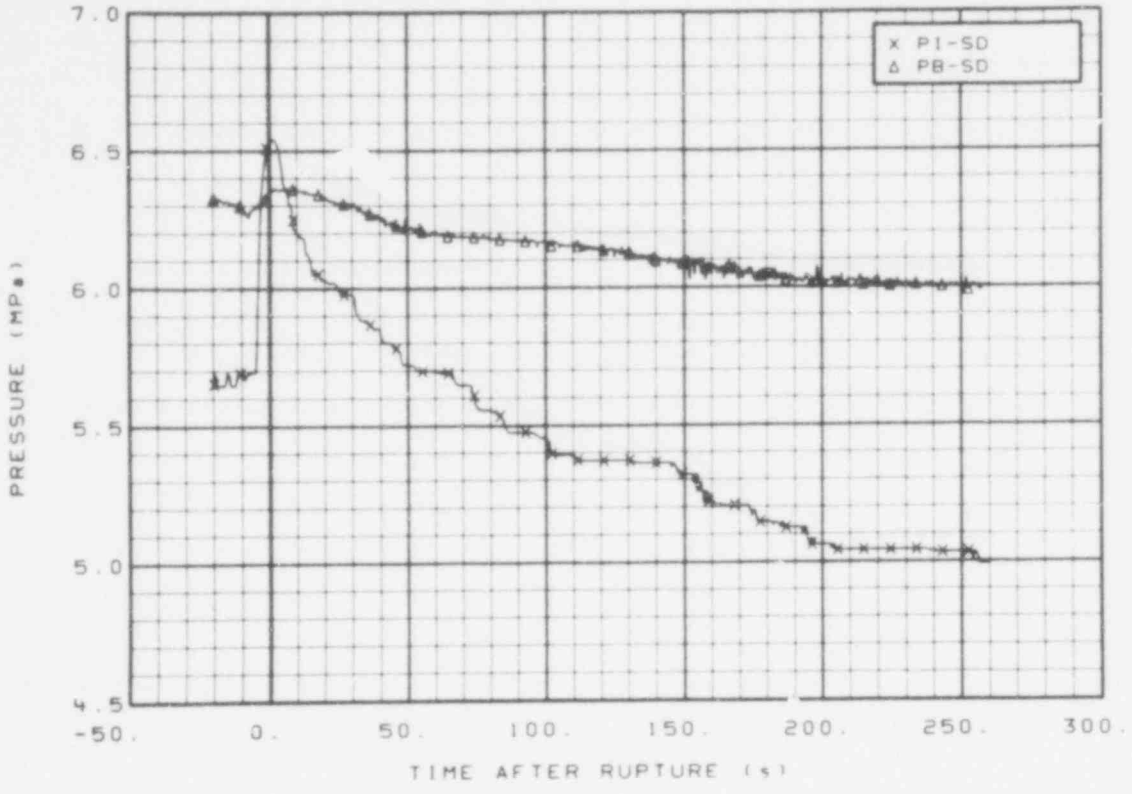

Fig. 123 Pressure in system steam generators, secondary side steam dome (PI-SD and PB-SD), from -20 to 260 s.

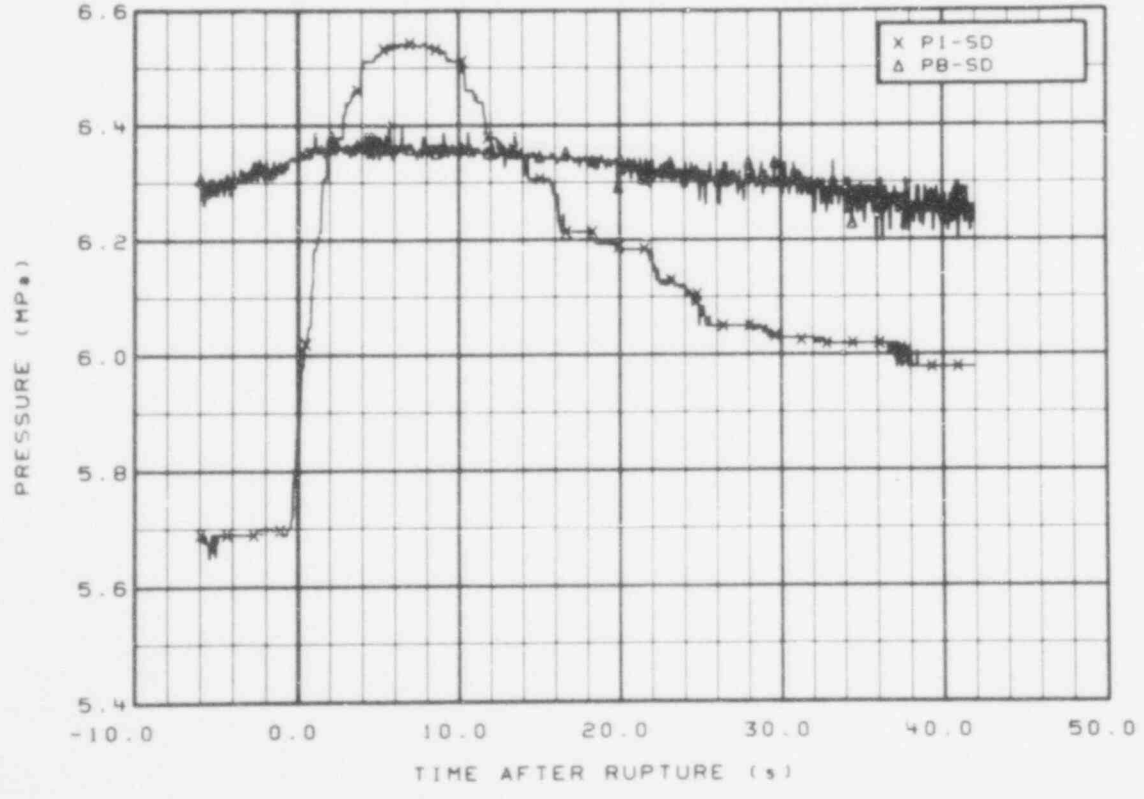

Fig. 124 Pressure in system steam generators, secondary side steam dome (PI-SD and PB-SD), from -6 to 42 s.

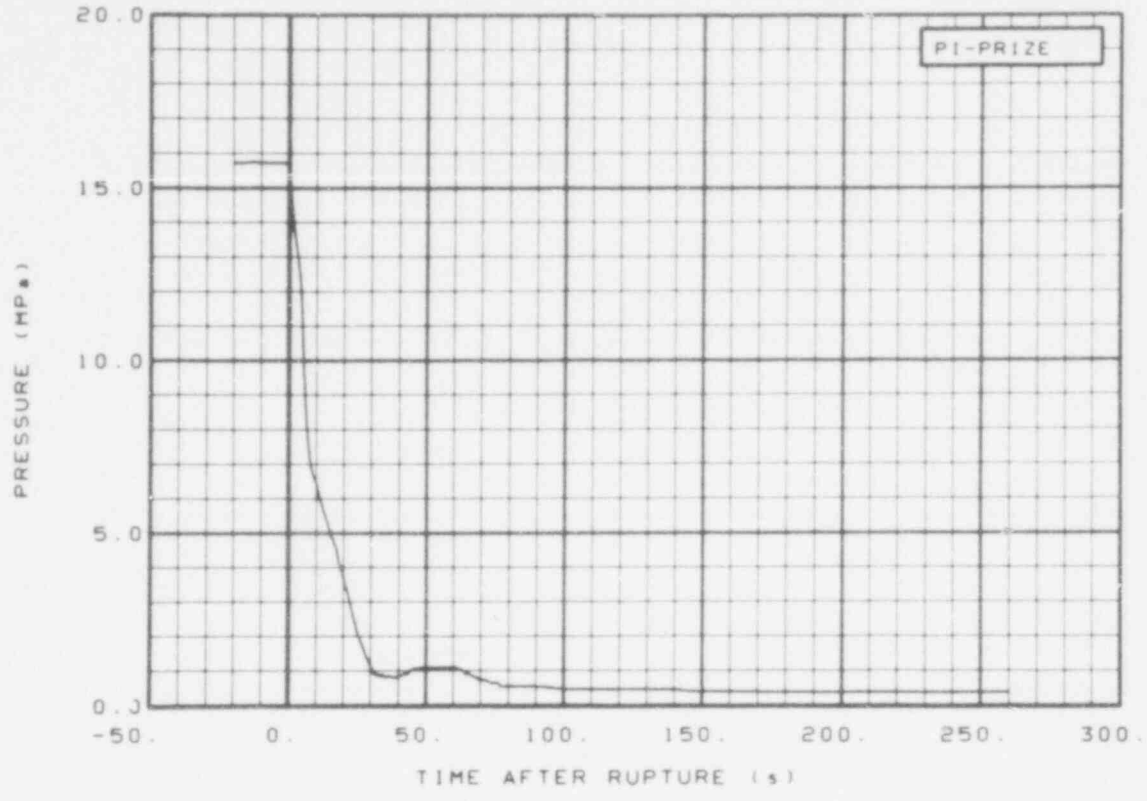

Fig. 125 Pressure in pressurizer (PI-PRIZE), from -20 to 260 s.

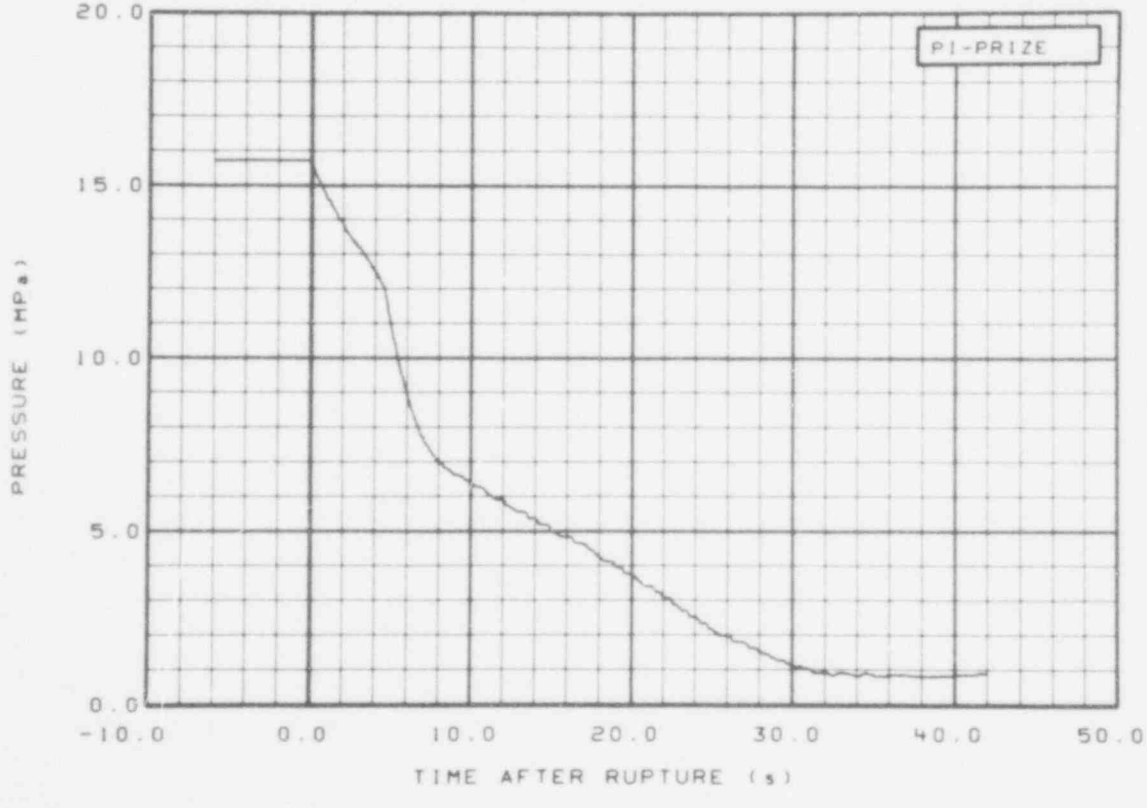

Fig. 126 Pressure in pressurizer (PI-PRIZE), from -6 to 42 s.

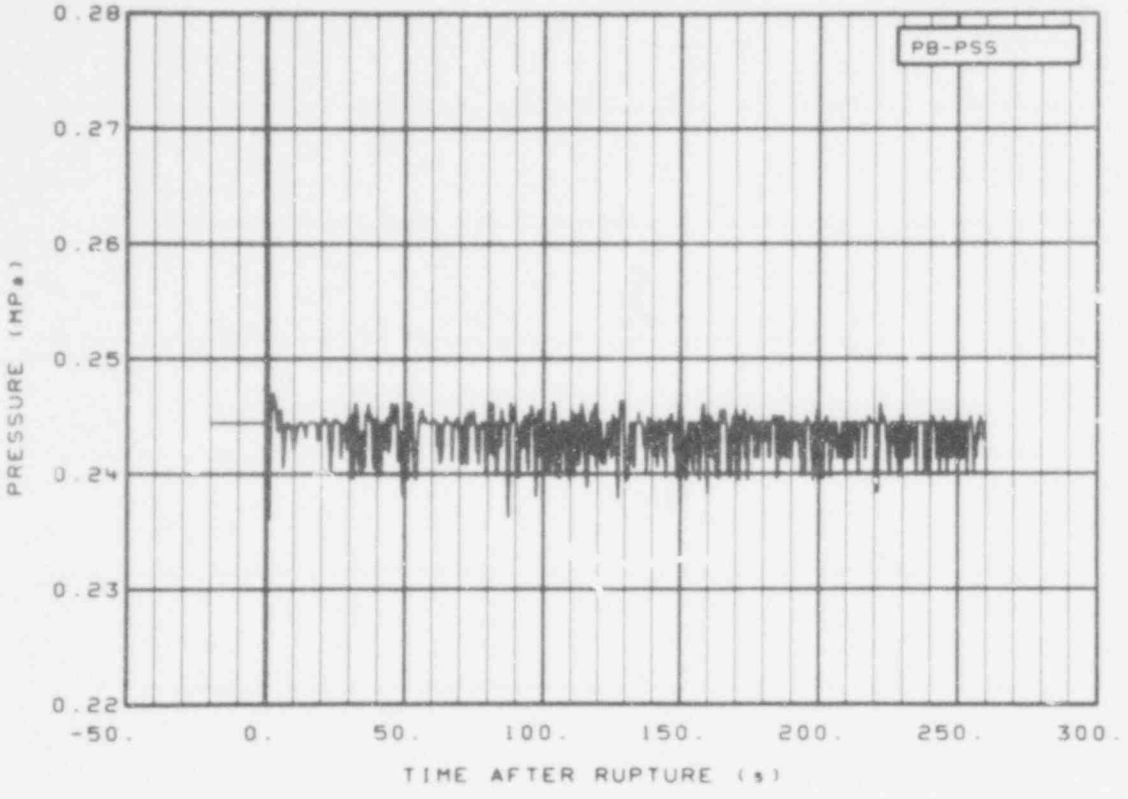

Fig. 127 Pressure in broken loop pressure suppression tank (PB-PSS), from -20 to 260 s.

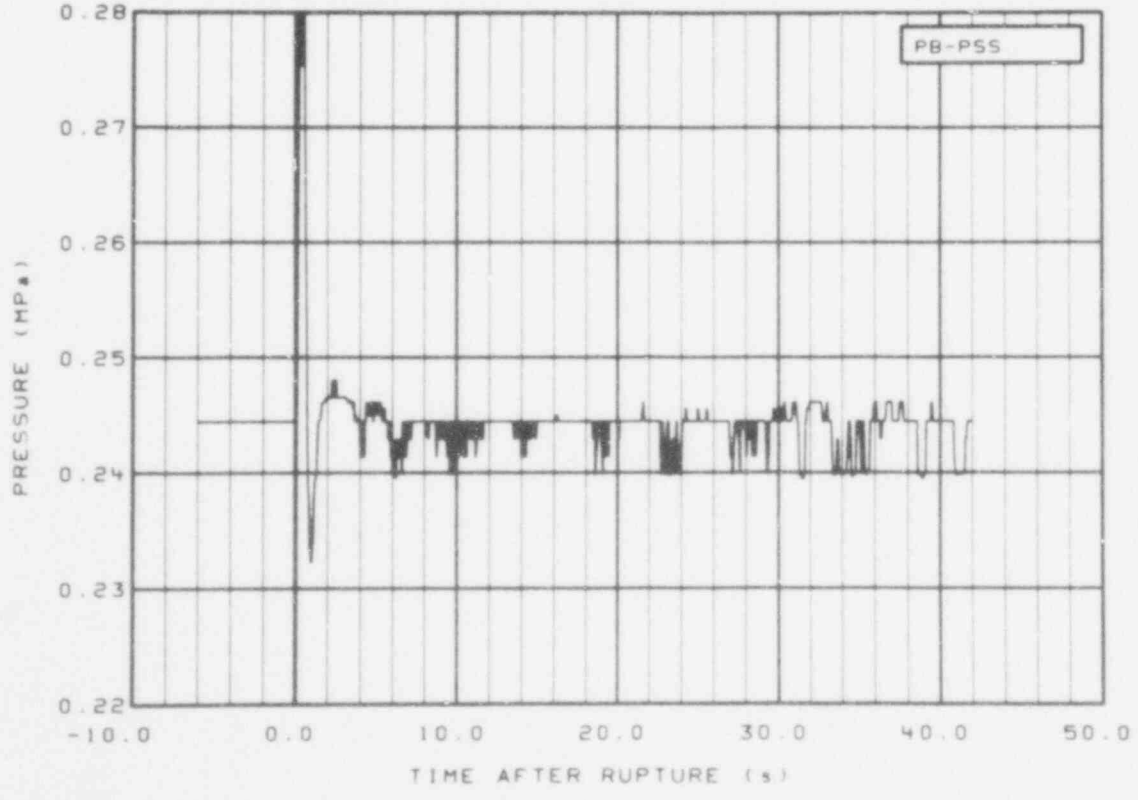

Fig. 128 Pressure in broken loop pressure suppression tank (PB-PSS), from -6 to 42 s.

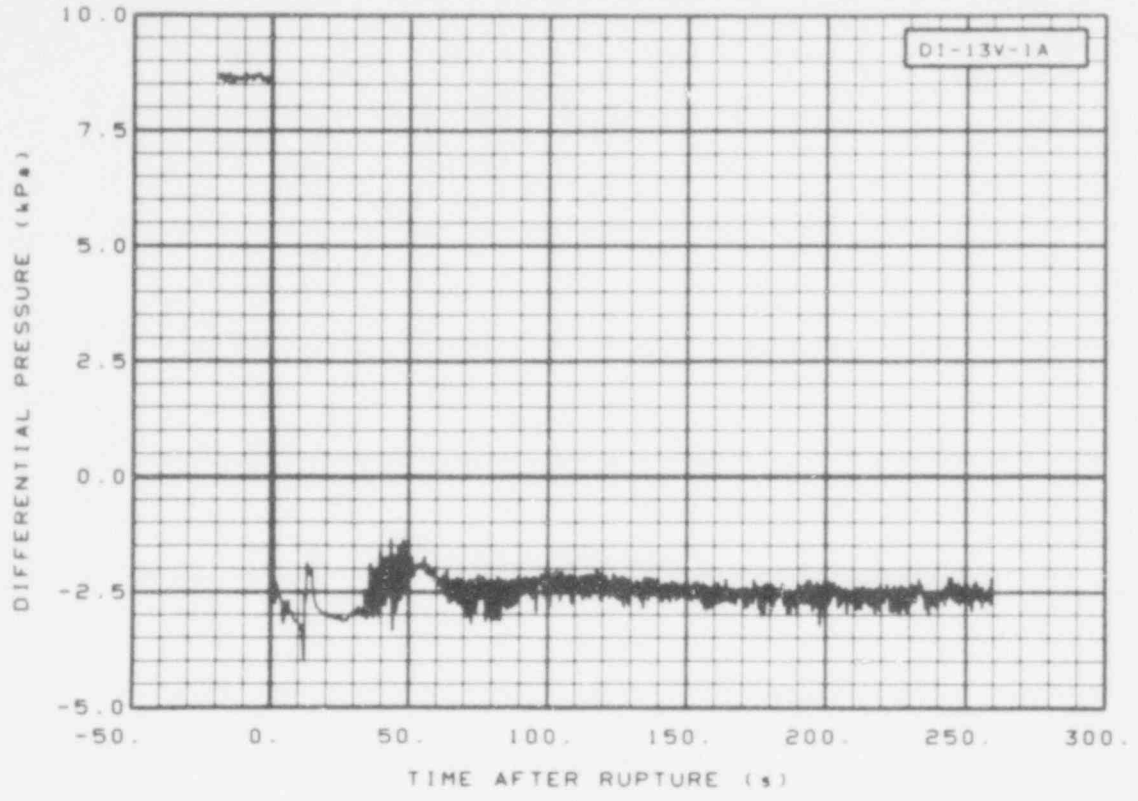

Fig. 129 Differential pressure in intact loop (DI-13V-1A), from -20 to 260 s.

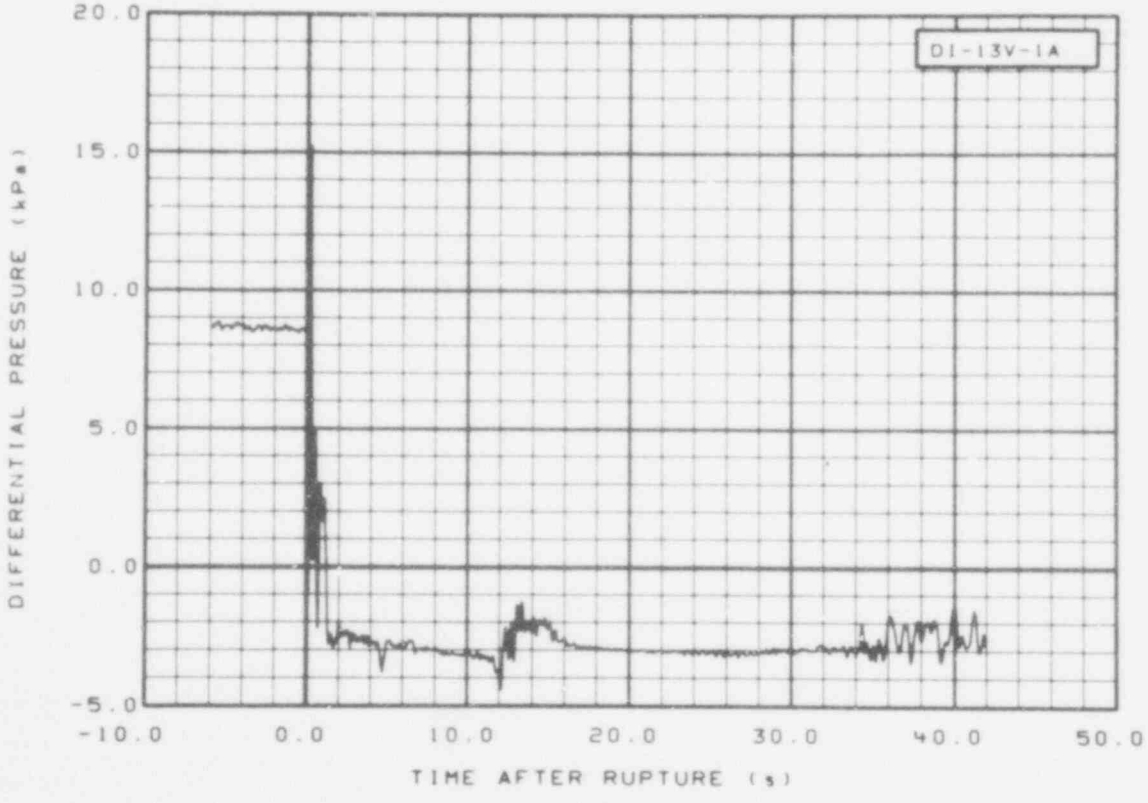

Fig. 130 Differential pressure in intact loop (DI-13V-1A), from -6 to 42 s.

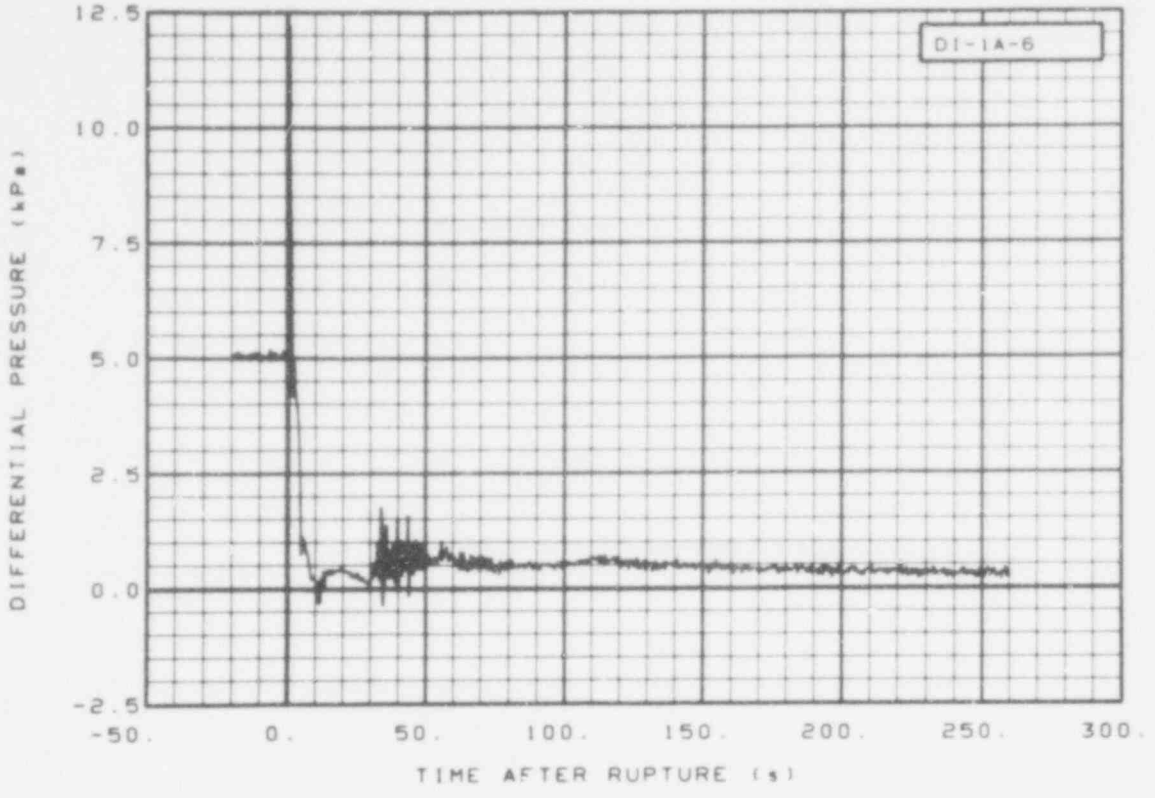

Fig. 131 Differential pressure in intact loop (DI-1A-6), from -20 to 260 s.

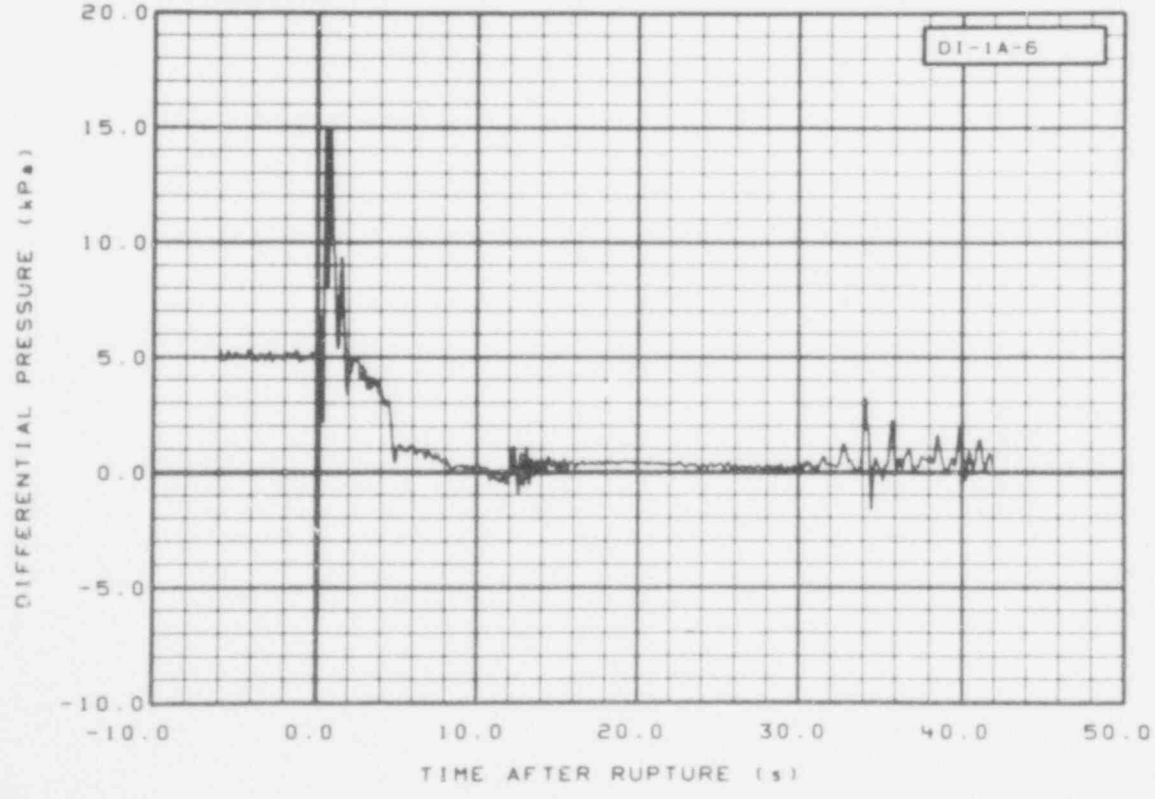

Fig. 132 Differential pressure in intact loop (DI-1A-6), from -6 to 42 s.

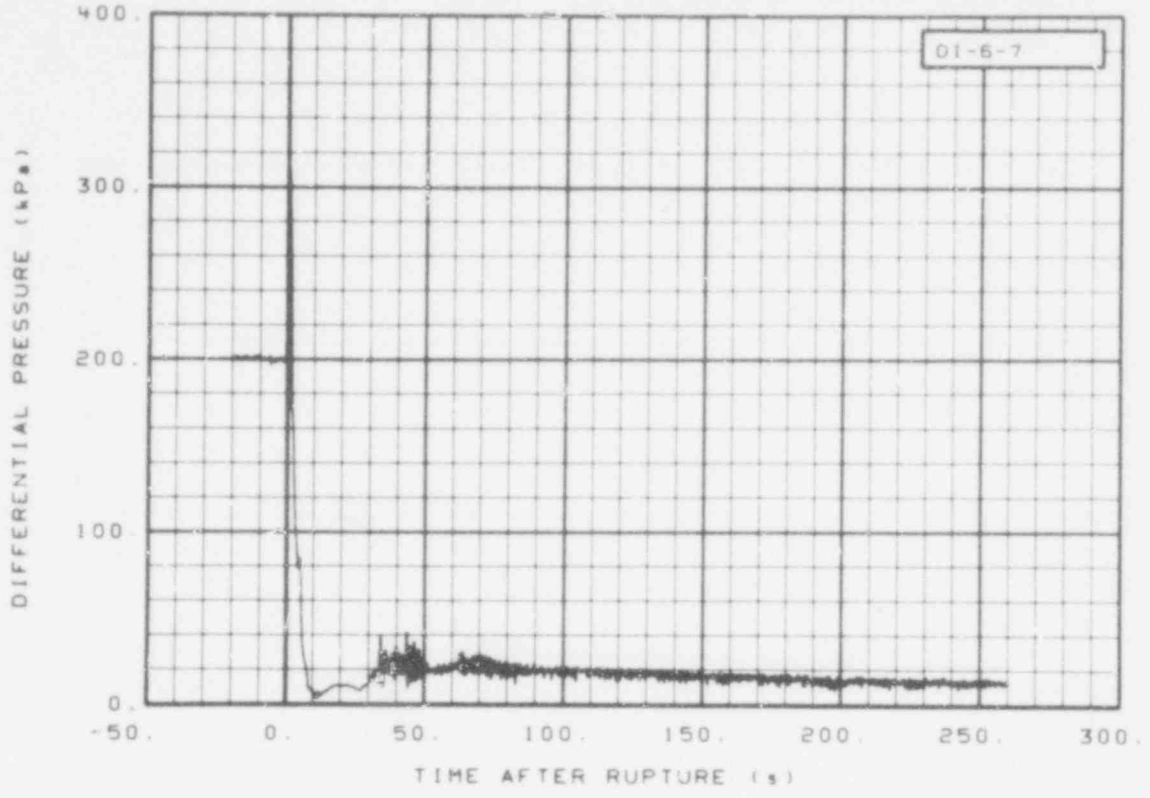

Fig. 133 Differential pressure in intact loop (DI-6-7), from -20 to 260 s.

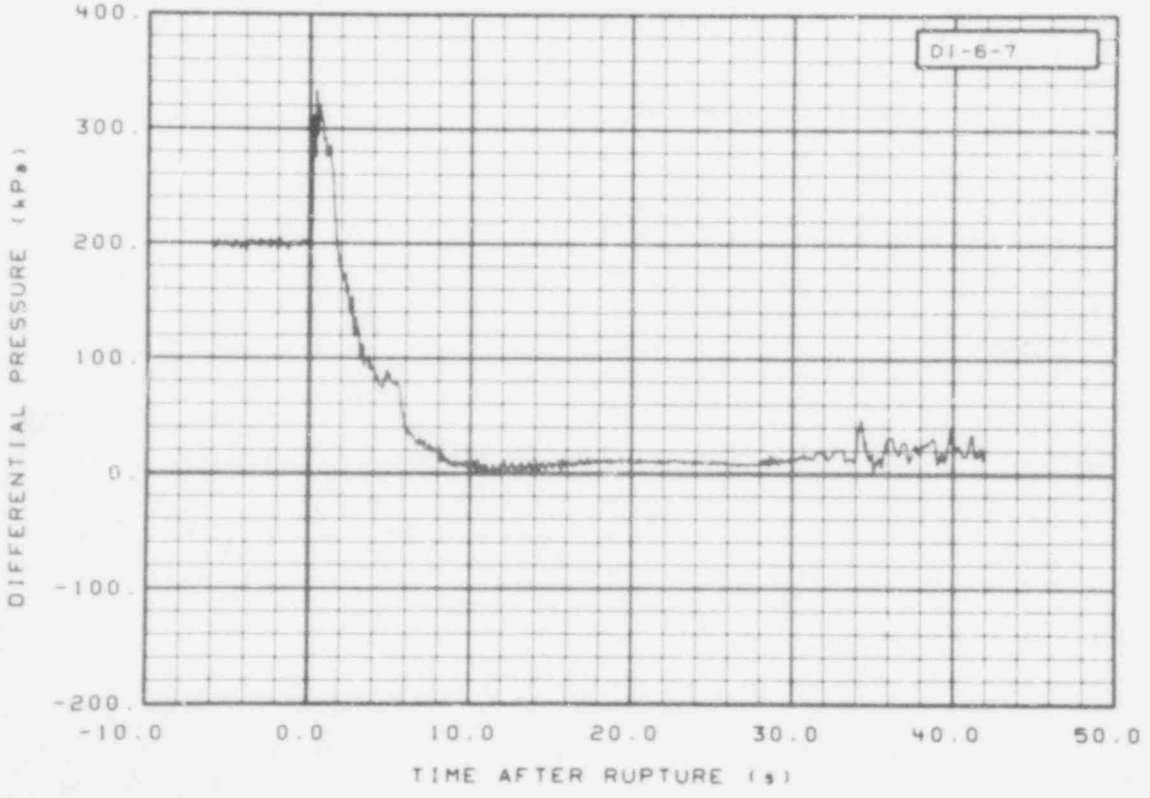

Fig. 134 Differential pressure in intact loop (DI-6-7), from -6 to 42 s.

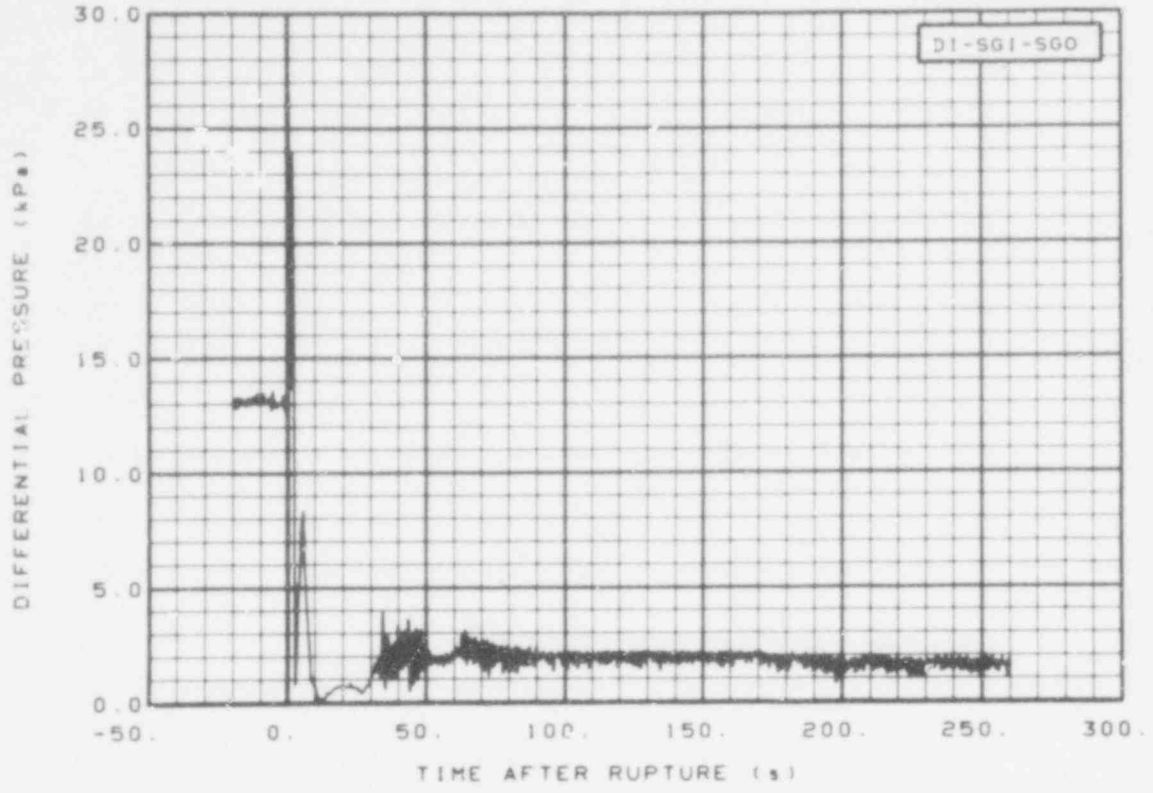

Fig. 135 Differential pressure in intact loop steam generator, inlet plenum to outlet plenum (DI-SGI-SGO), from -20 to 260 s.

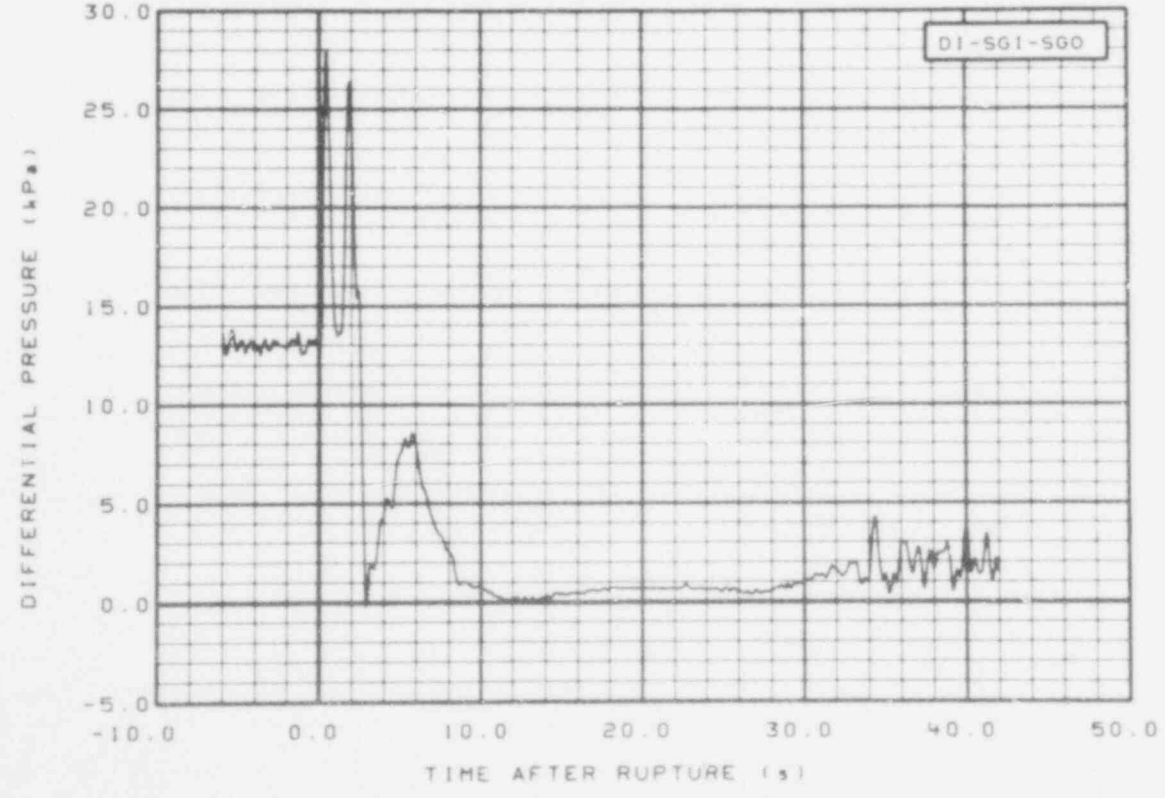

Fig. 136 Differential pressure in intact loop steam generator, inlet plenum to outlet plenum (DI-SGI-SGO), from -6 to 42 s.

5AA 111

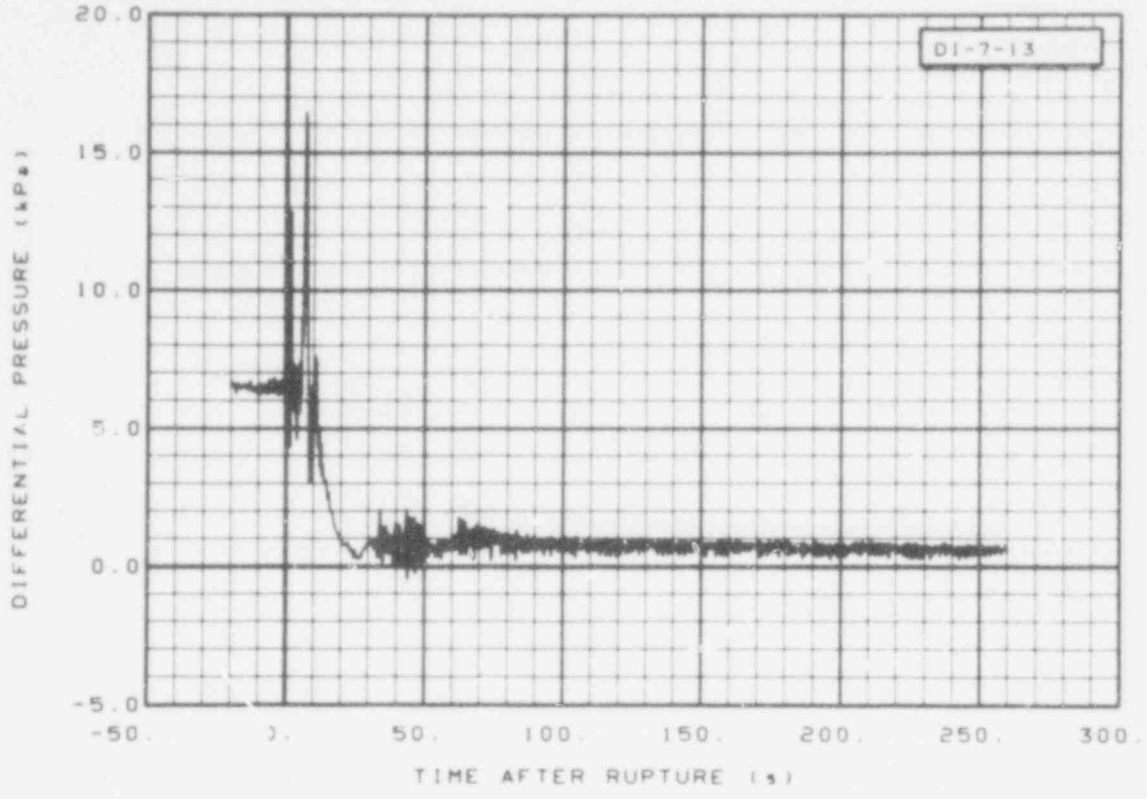

Fig. 137 Differential pressure in intact loop (DI-7-13), from -20 to 260 s.

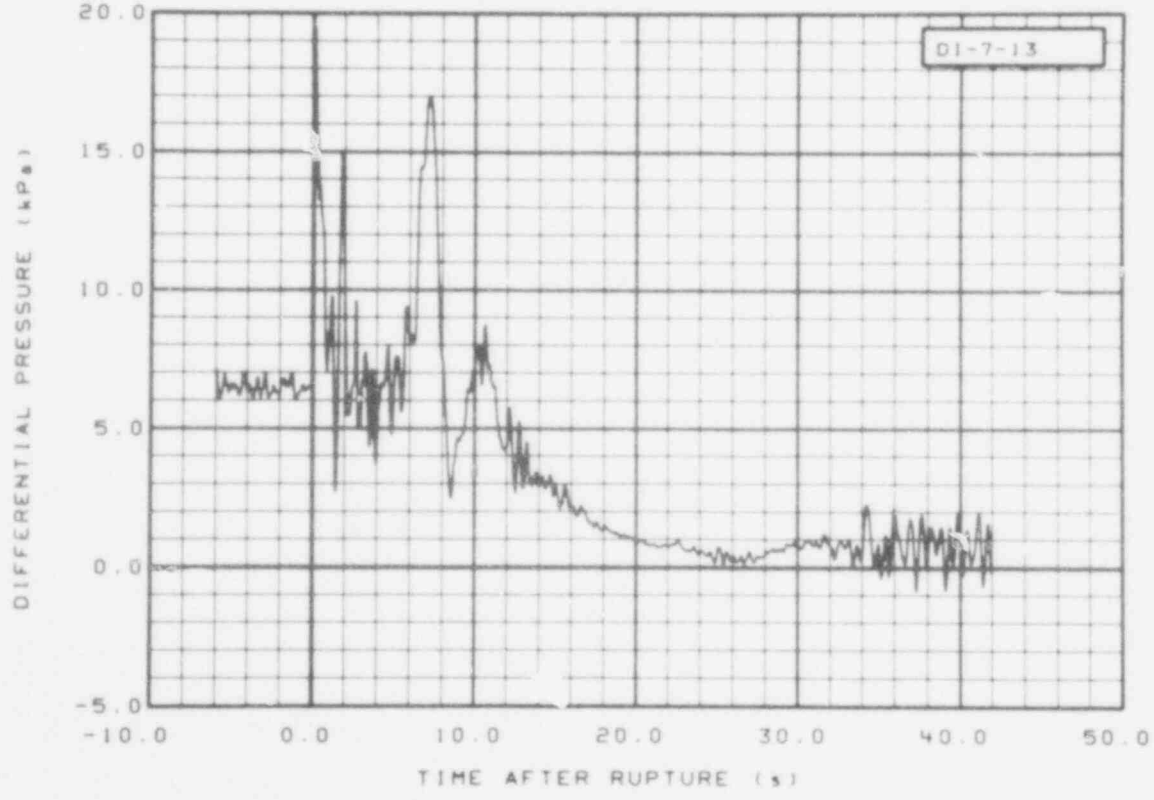

Fig. 138 Differential pressure in intact loop (DI-7-13), from -6 to 42 s.

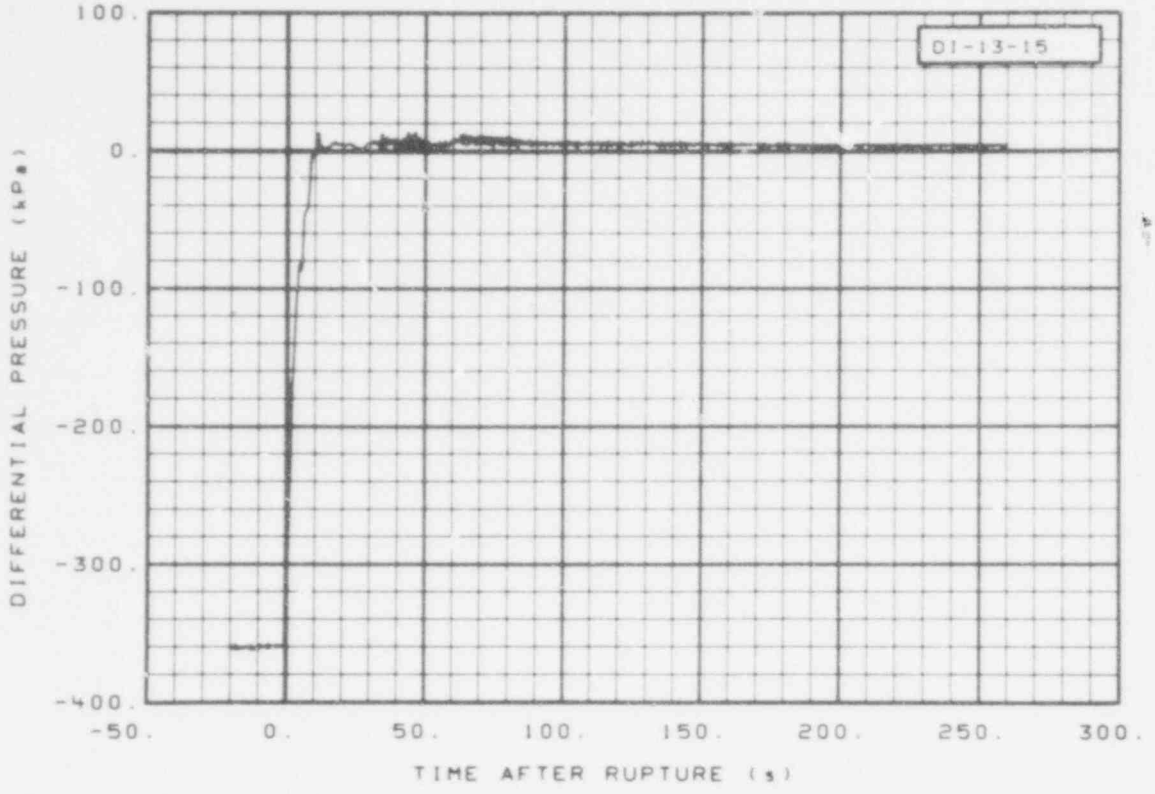

Fig. 139 Differential pressure in intact loop (DI-13-15), from -20 to 260 s.

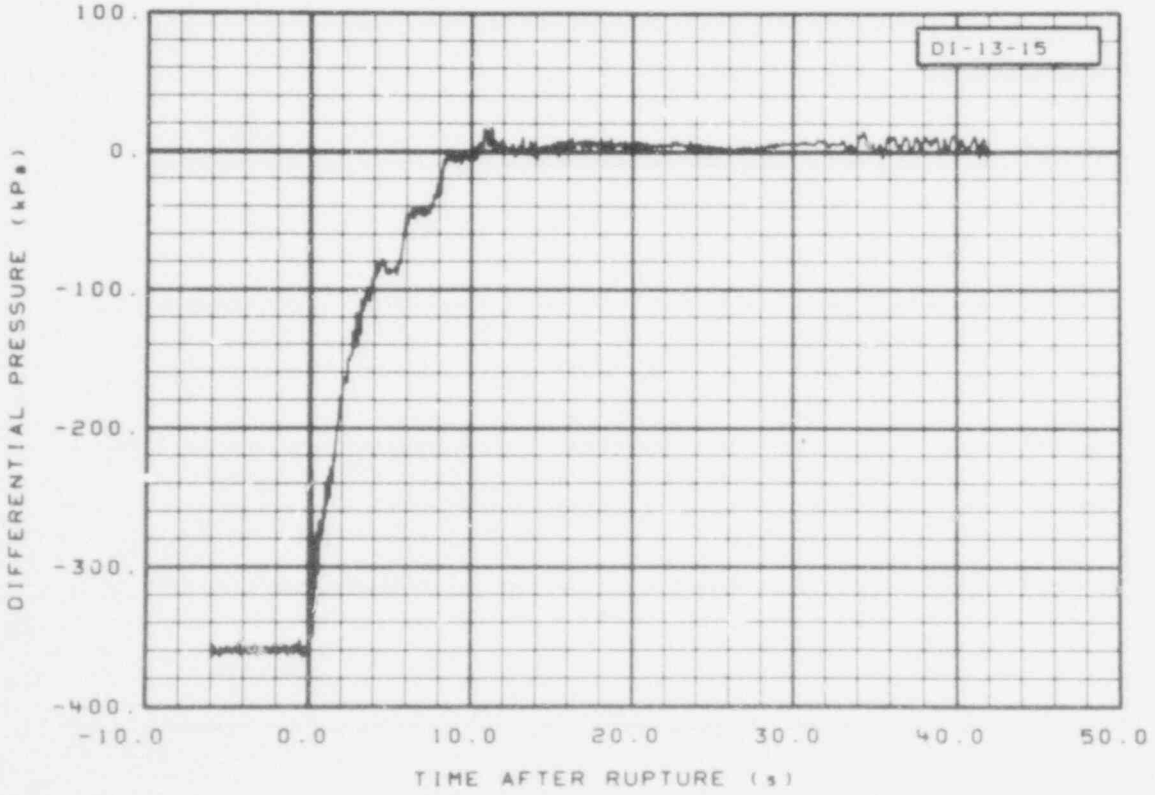

Fig. 140 Differential pressure in intact loop (DI-13-15), from -6 to 42 s.

EAA 113

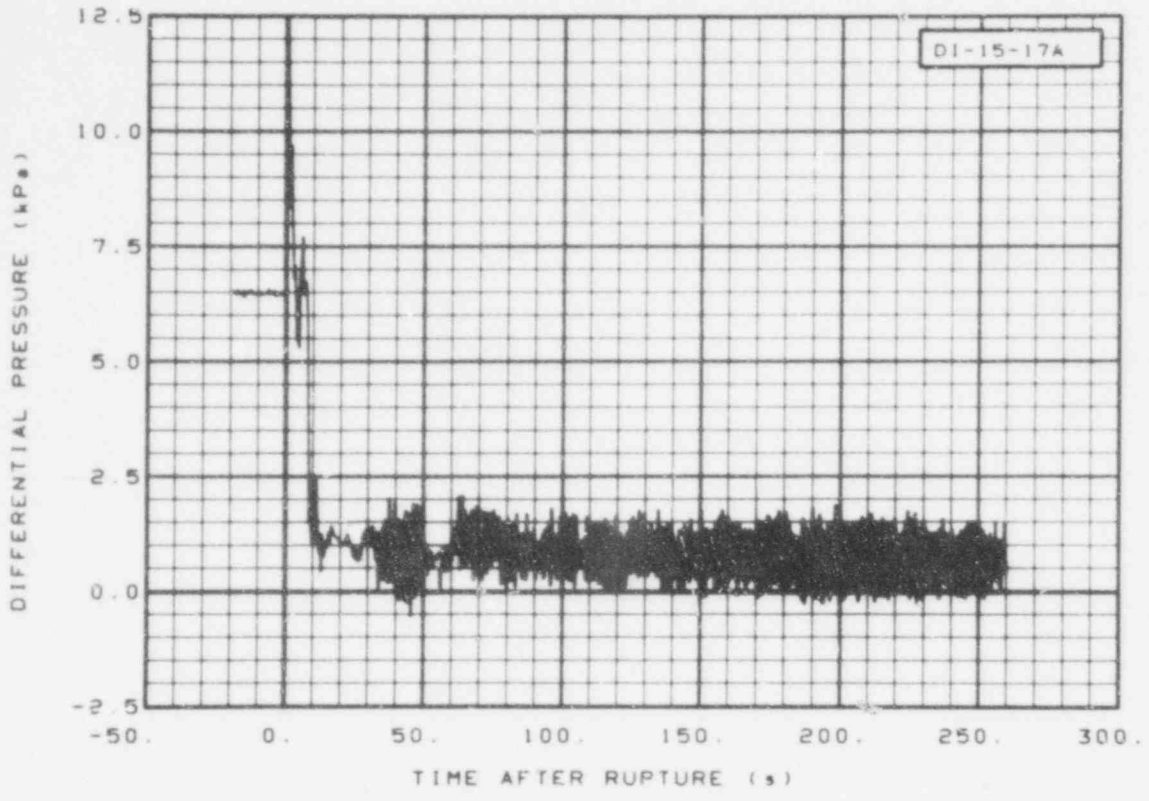

Fig. 141 Differential pressure in intact loop (DI-15-17A), from -20 to 260 s.

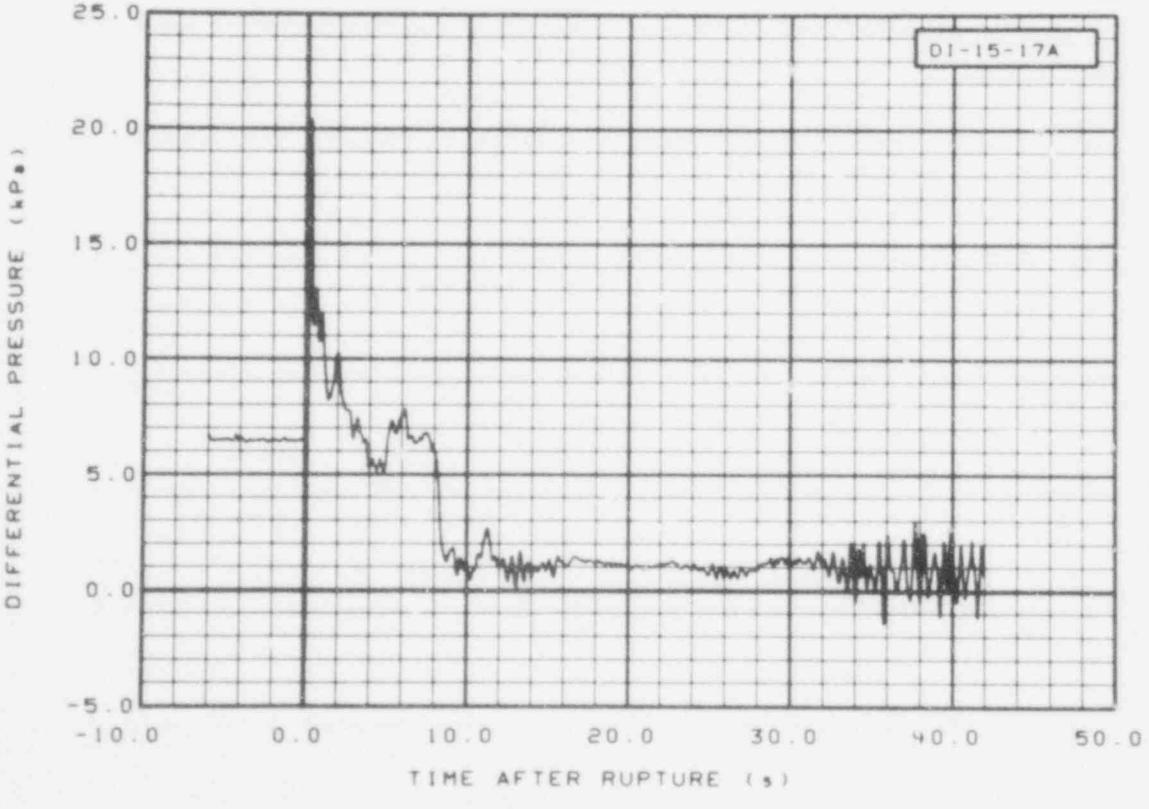

Fig. 142 Differential pressure in intact loop (DI-15-17A), from -6 to 42 s.

544 114

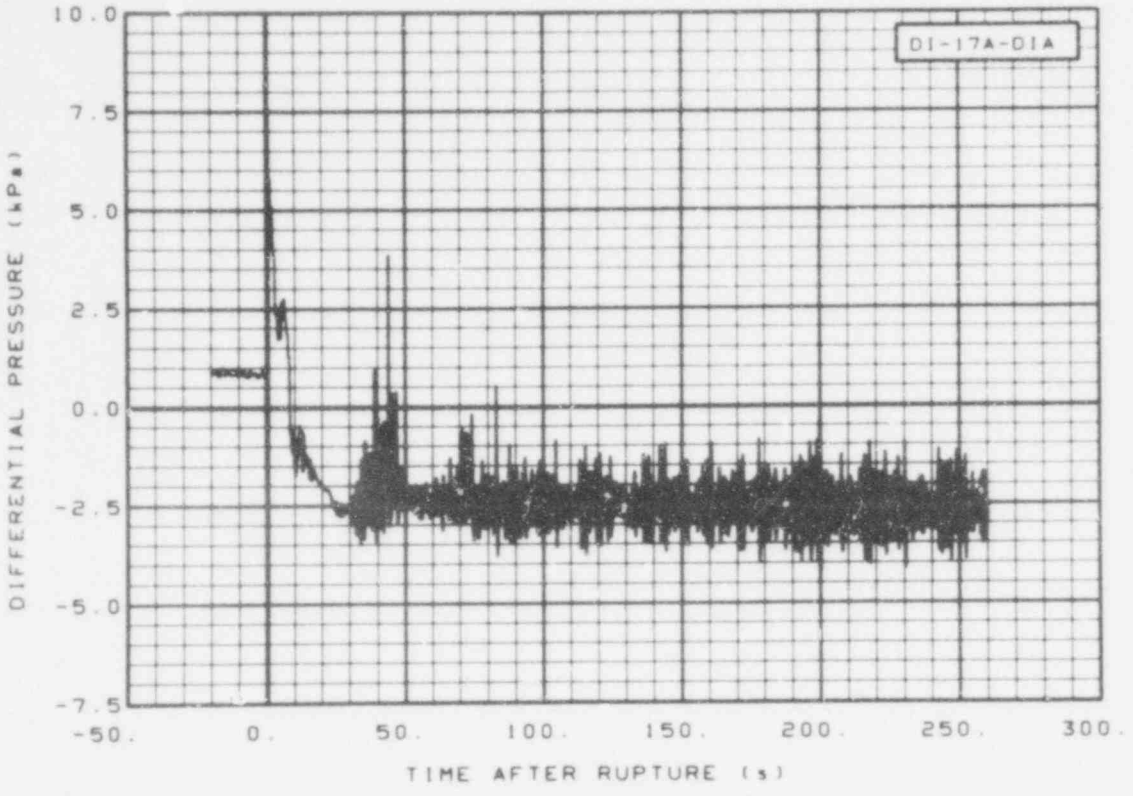

Fig. 143 Differential pressure in intact loop (DI-17A-DIA), from -20 to 260 s.

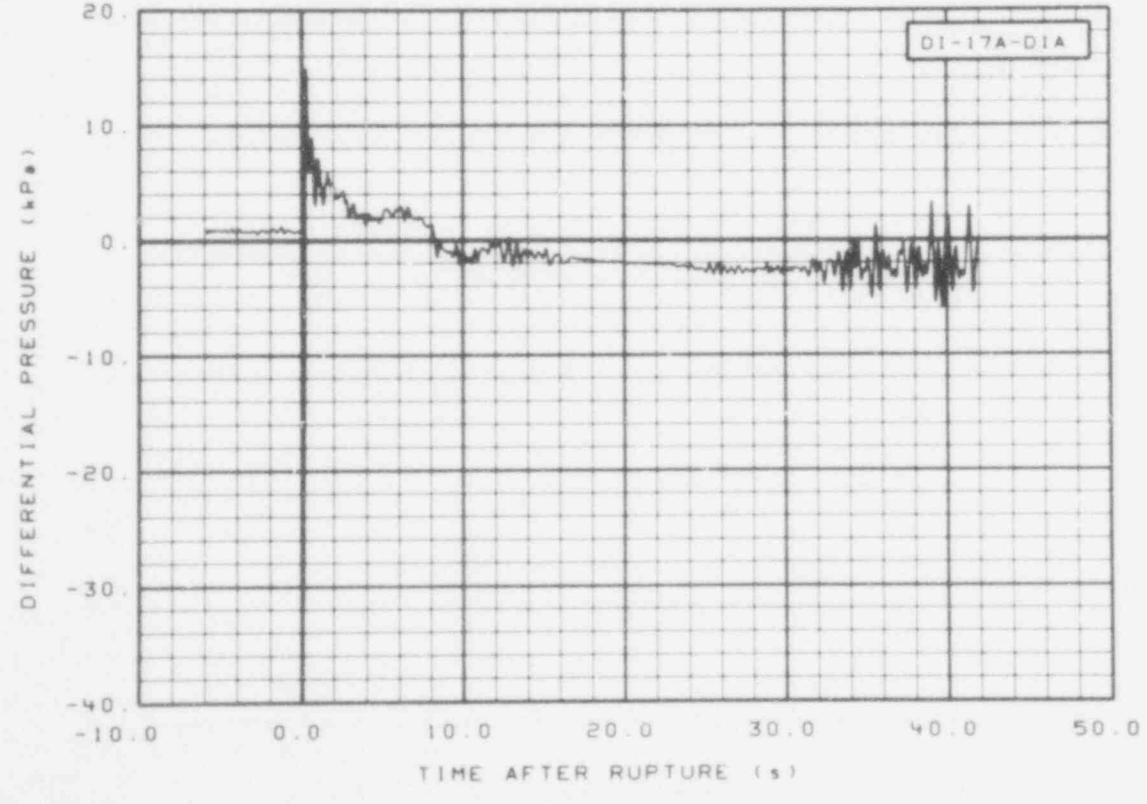

Fig. 144 Differential pressure in intact loop (DI-17A-DIA), from -6 to 42 s.

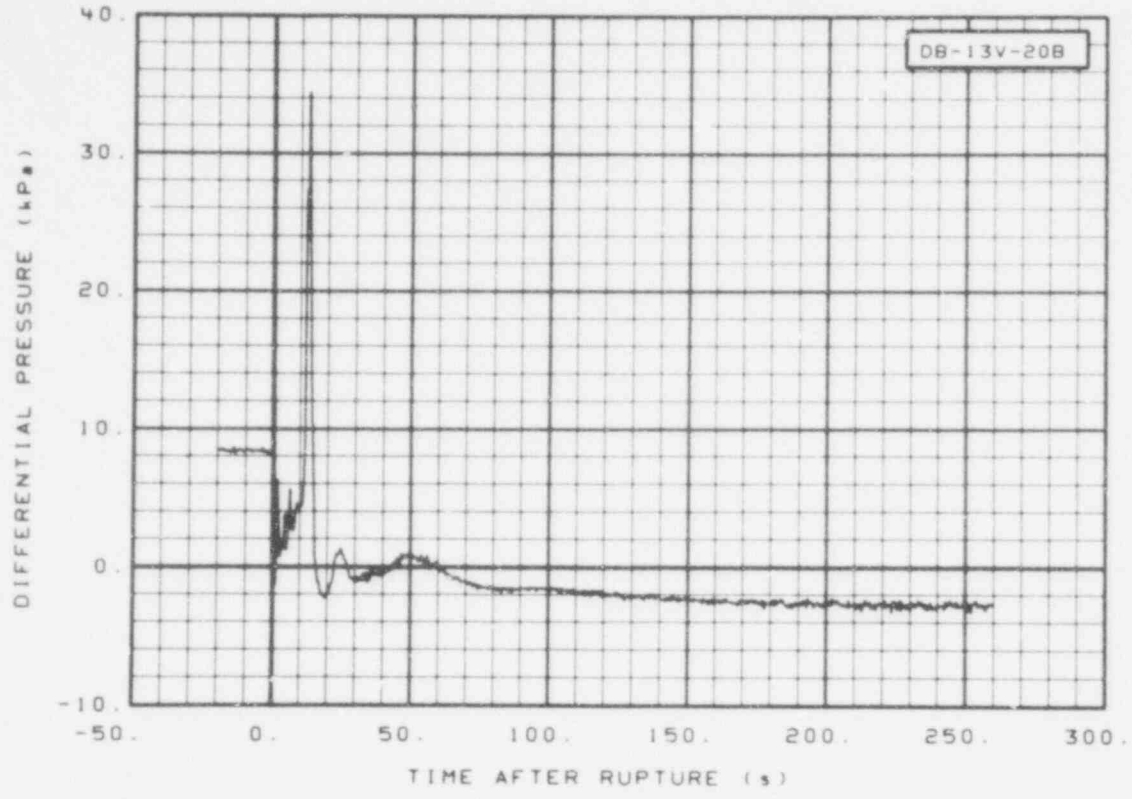

Fig. 145 Differential pressure in broken loop (DB-13V-20B), from -20 to 260 s.

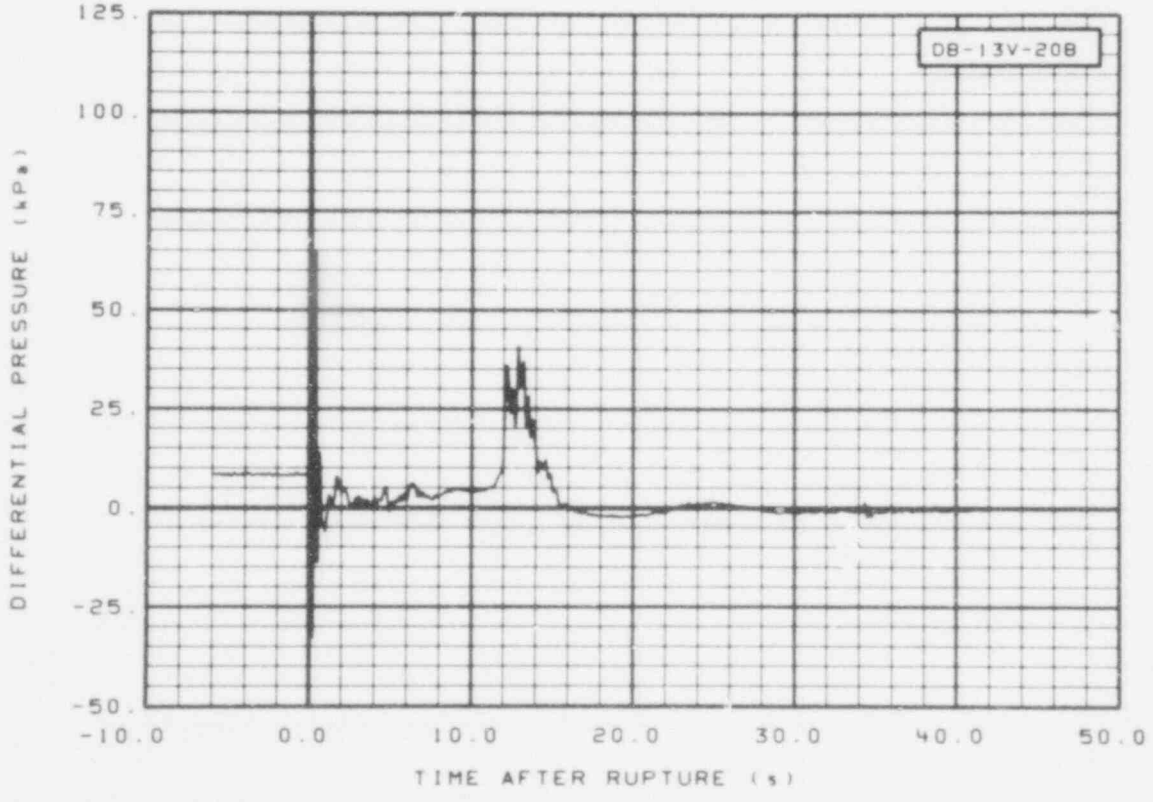

Fig. 146 Differential pressure in broken loop (DB-13V-20B), from -6 to 42 s.

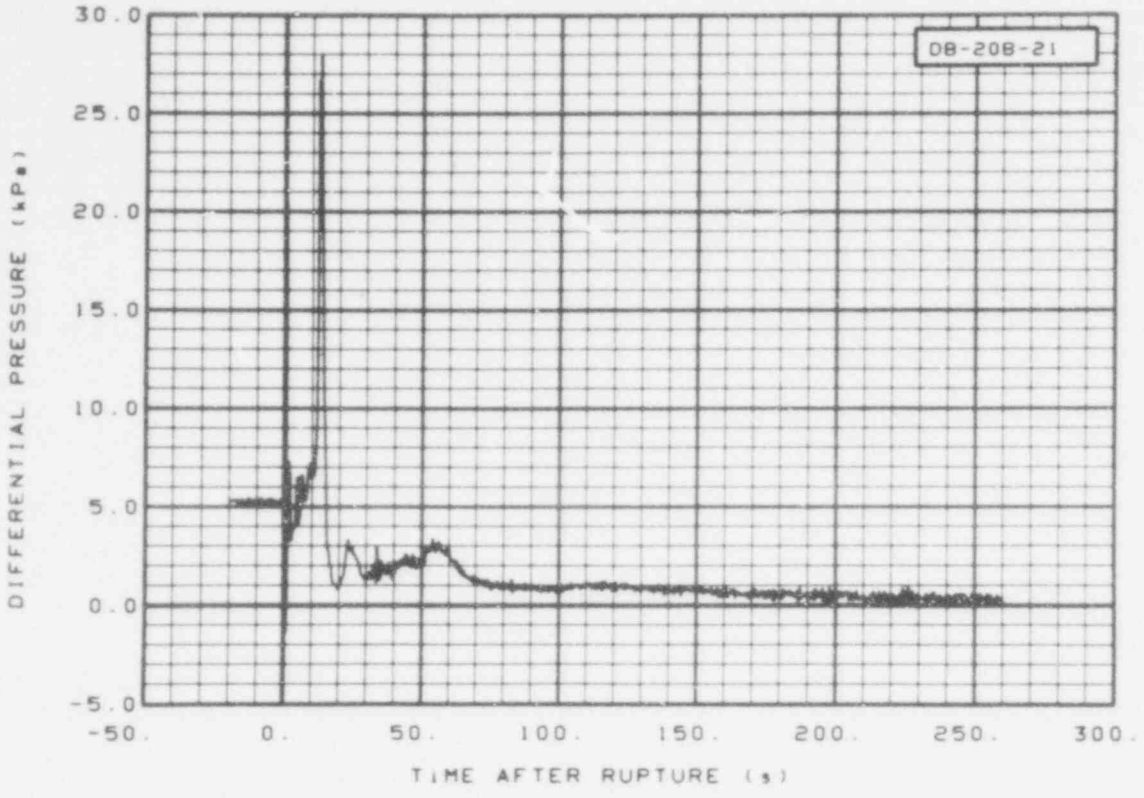

Fig. 147 Differential pressure in broken loop (DB-20B-21), from -20 to 260 s.

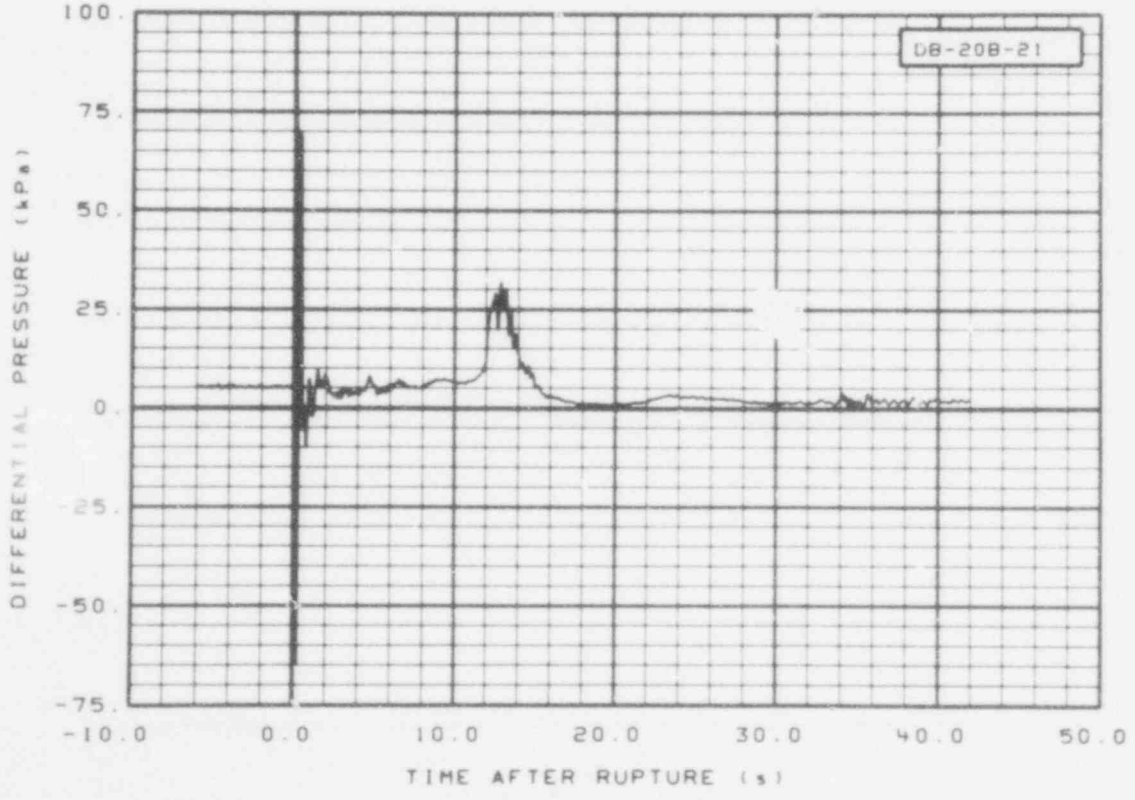

Fig. 148 Differential pressure in broken loop (DB-20B-21), from -6 to 42 s.

544 117

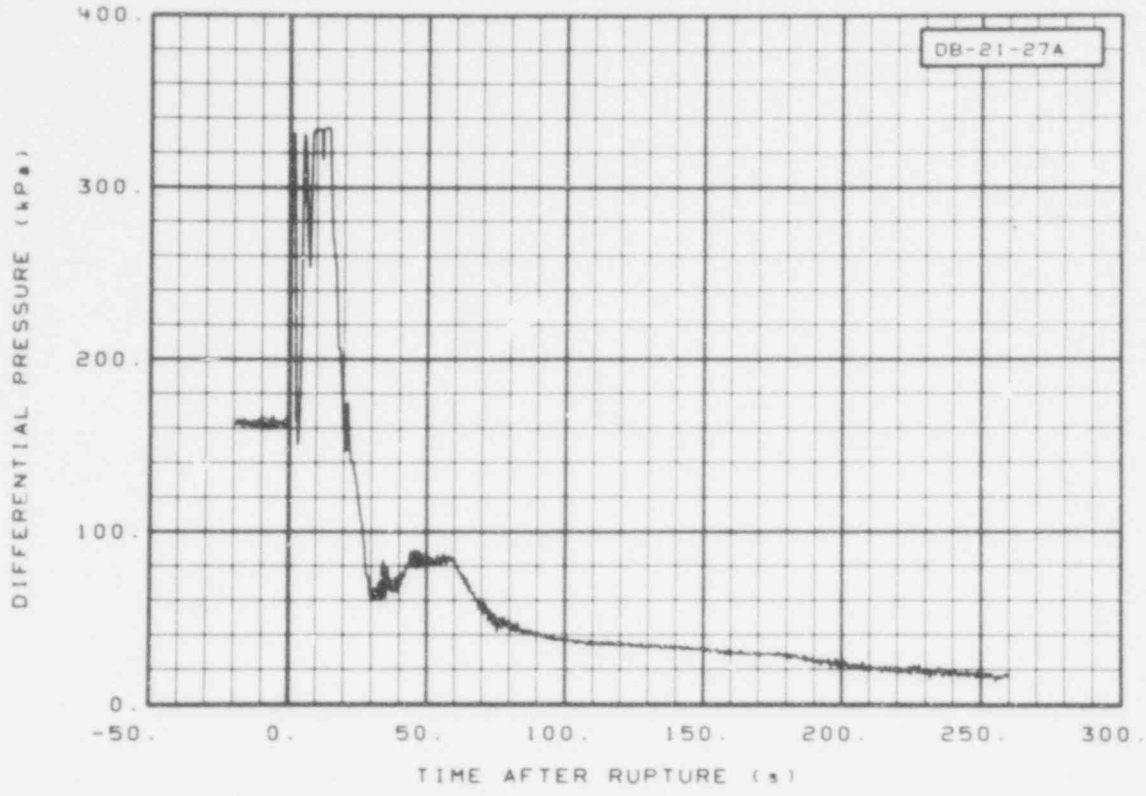

Fig. 149 Differential pressure in broken loop (DB-21-27A), from -20 to 260 s.

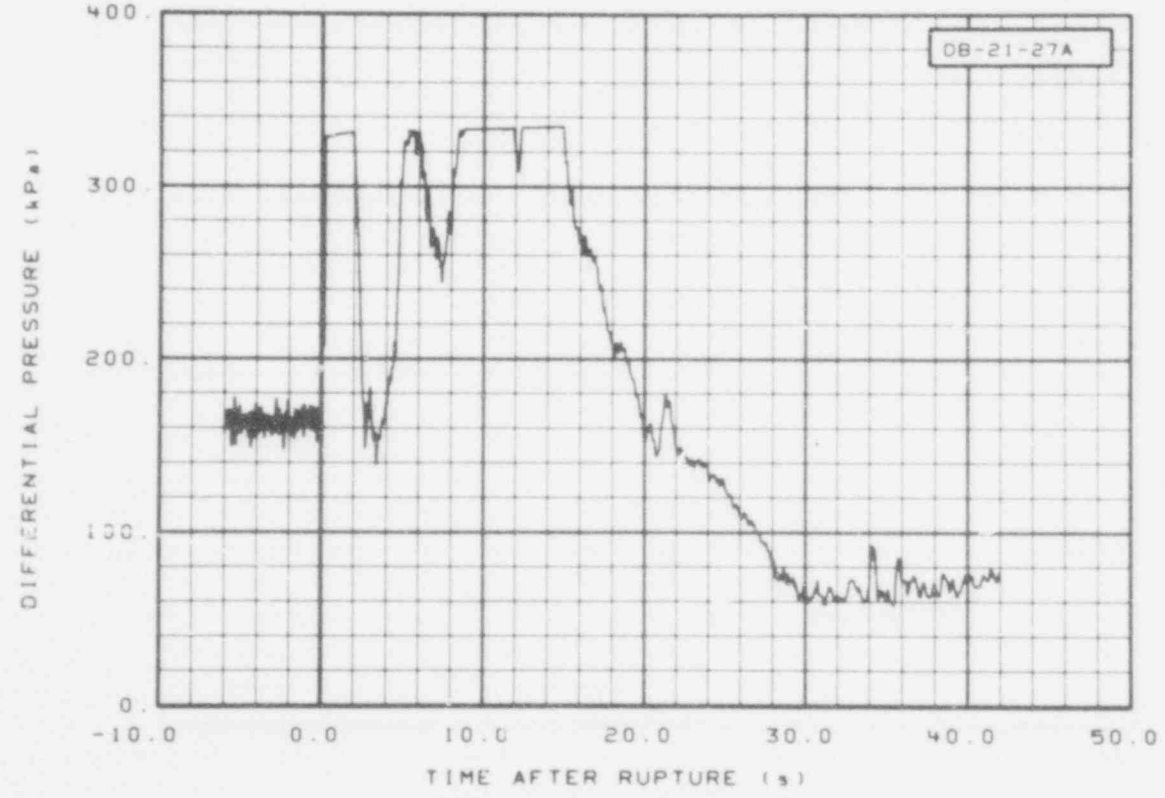

Fig. 150 Differential pressure in broken loop (DB-21-27A), from -6 to 42 s.

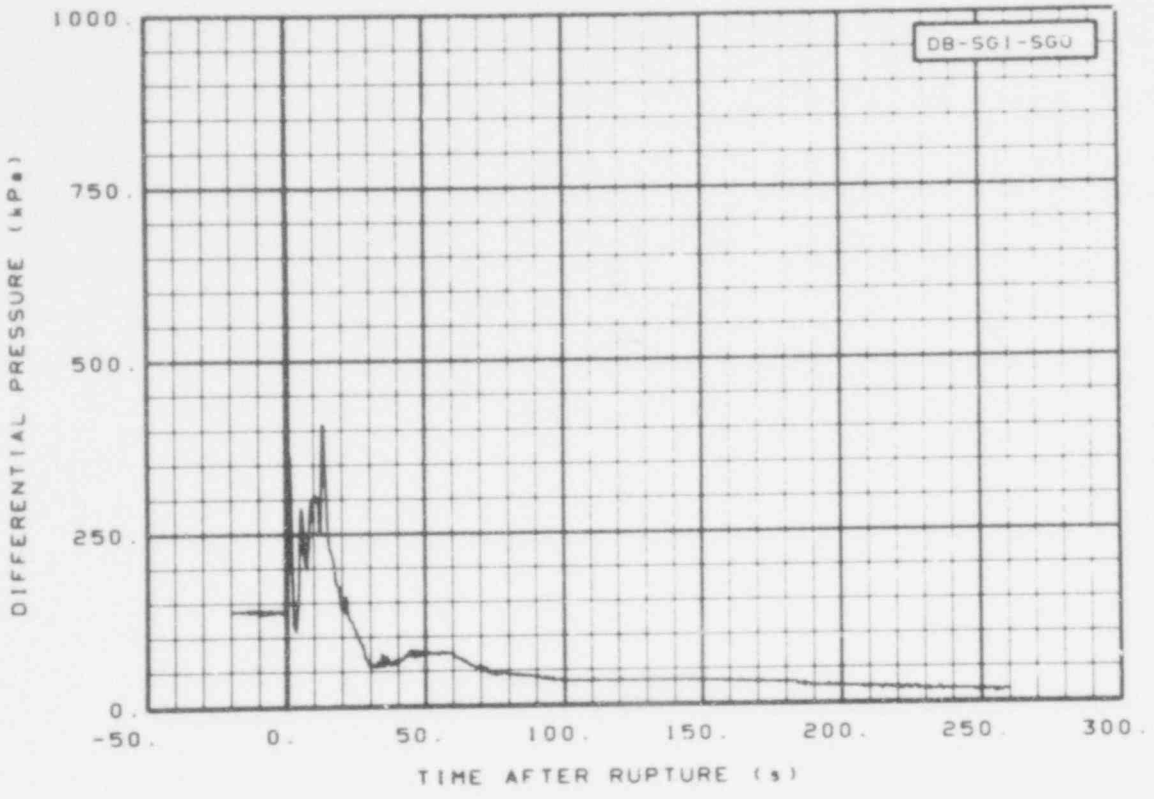

Fig. 151 Differential pressure in broken loop steam generator (DB-SGI-SGO), from -20 to 260 s.

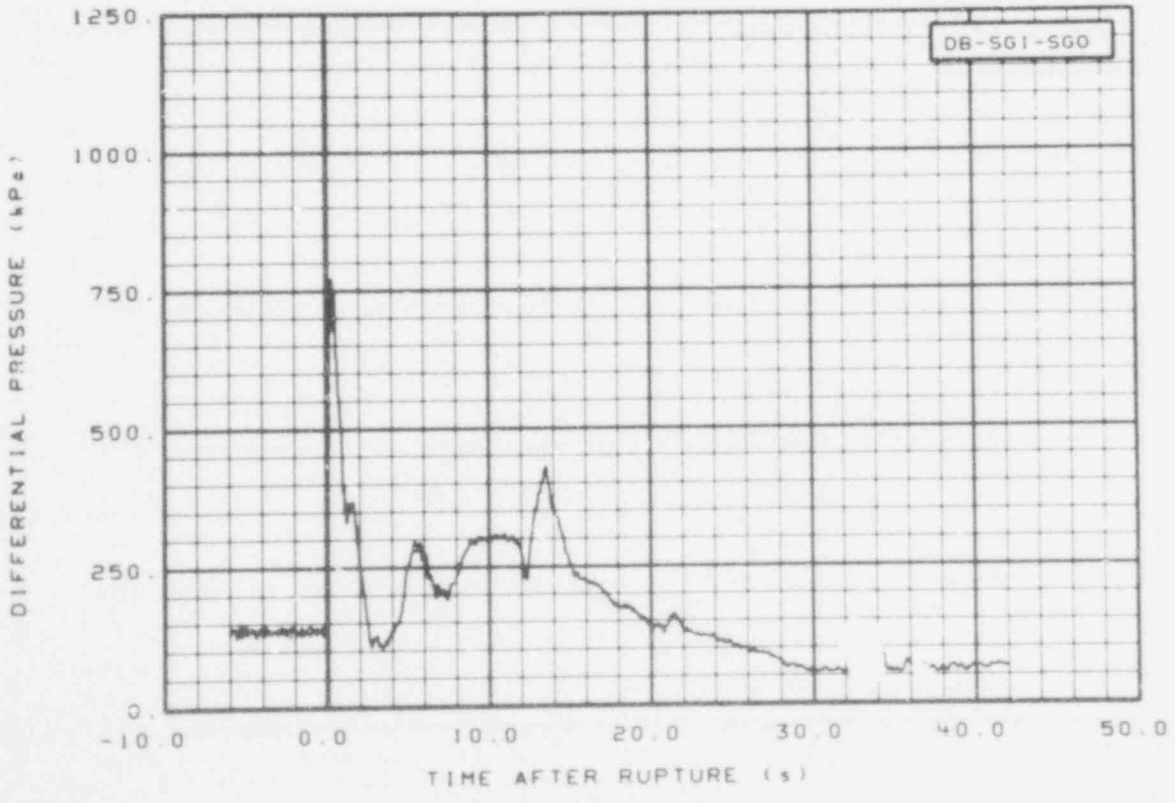

Fig. 152 Differential pressure in broken loop steam generator (DB-SGI-SGO), from -6 to 42 s.

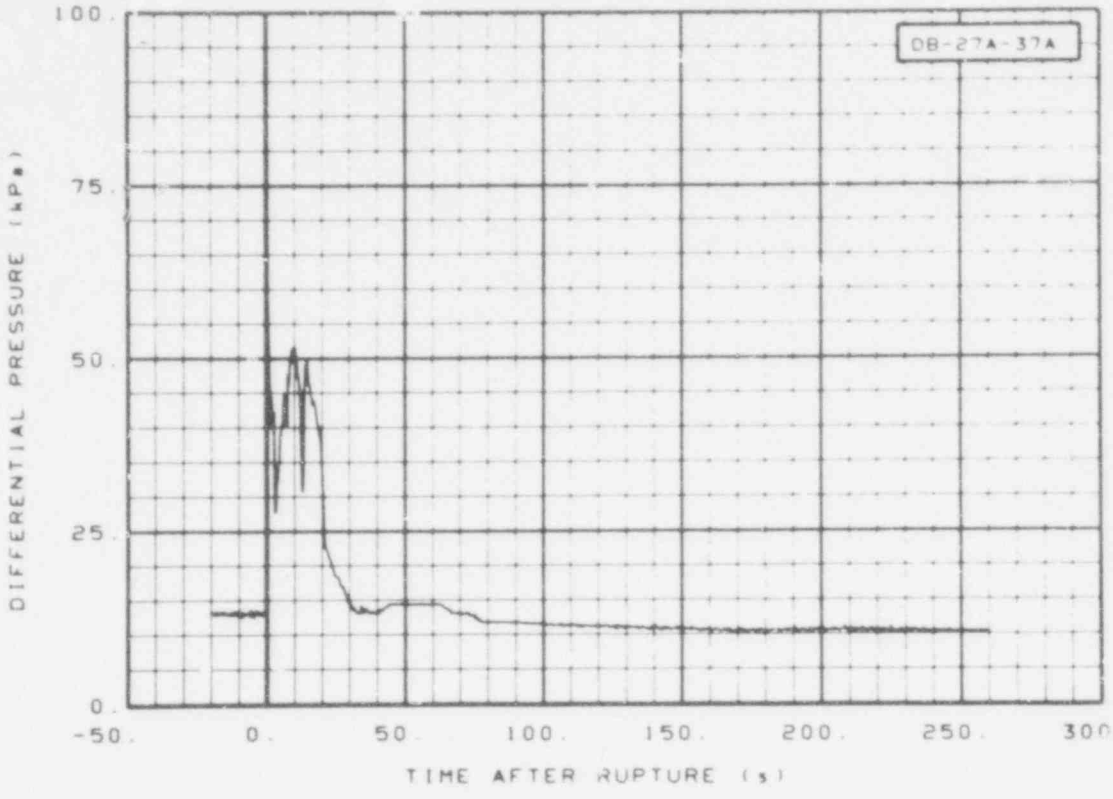

Fig. 153 Differential pressure in broken loop (DB-27A-37A), from -20 to 260 s.

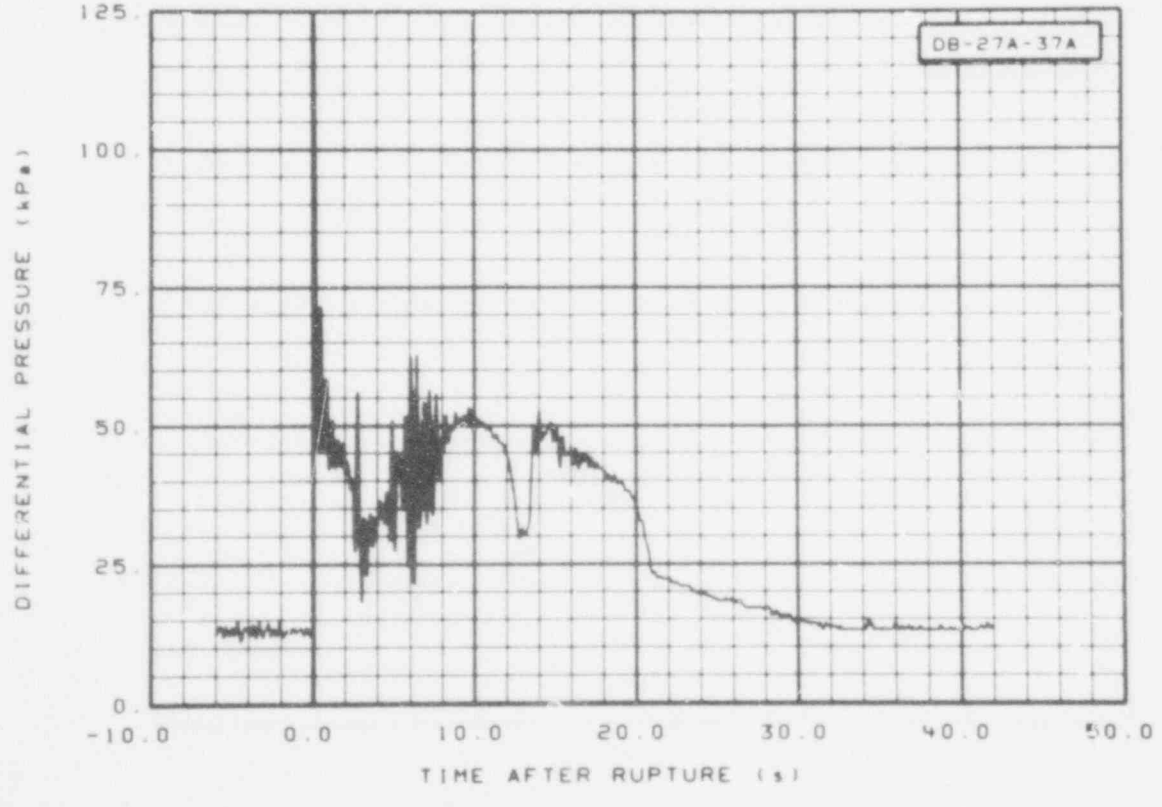

Fig. 154 Differential pressure in br··· en loop (DB-27A-37A), from -6 to 42 s.

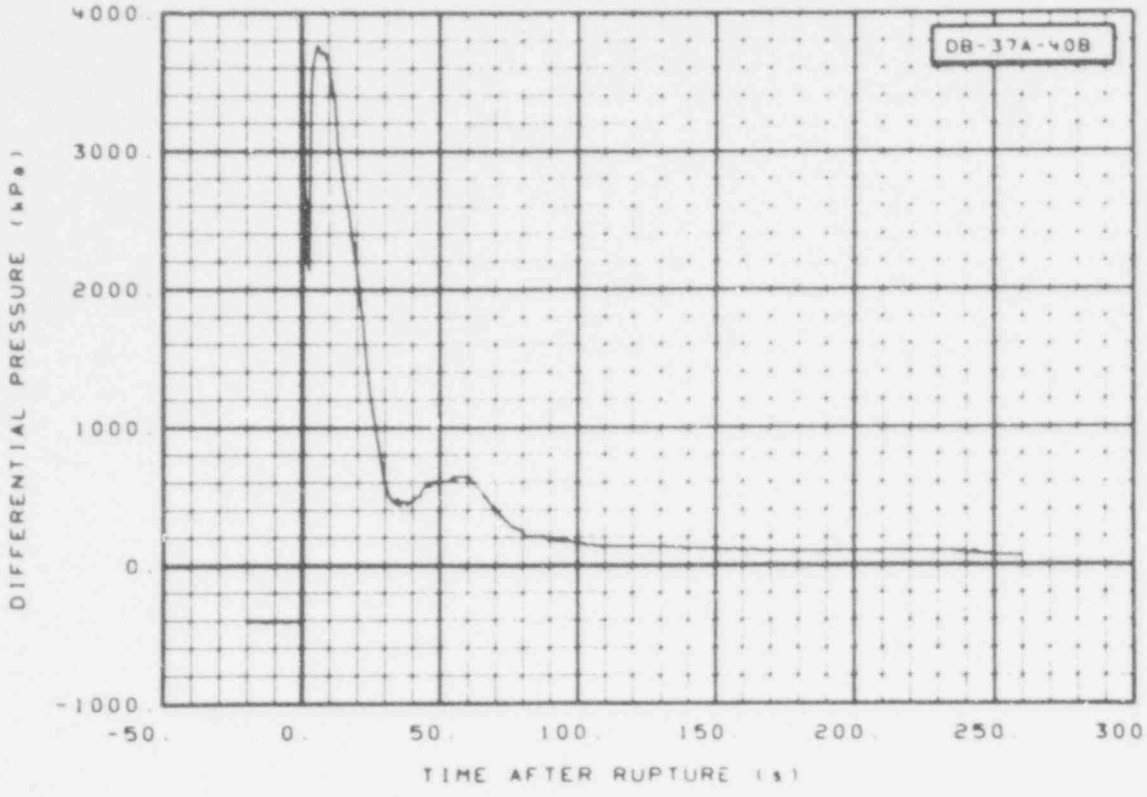

Fig. 155 Differential pressure in broken loop (DB-37A-40B), from -20 to 260 s.

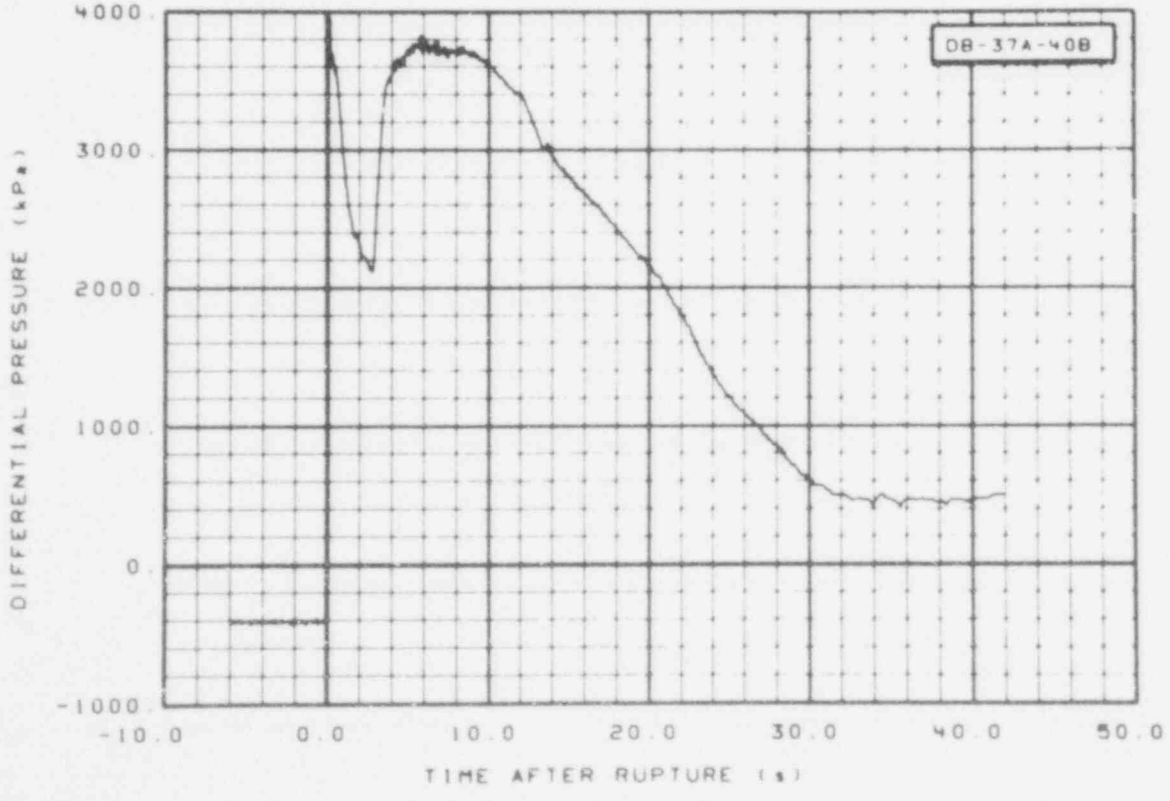

Fig. 156 Differential pressure in broken loop (DB-37A-40B), from -6 to 42 s.

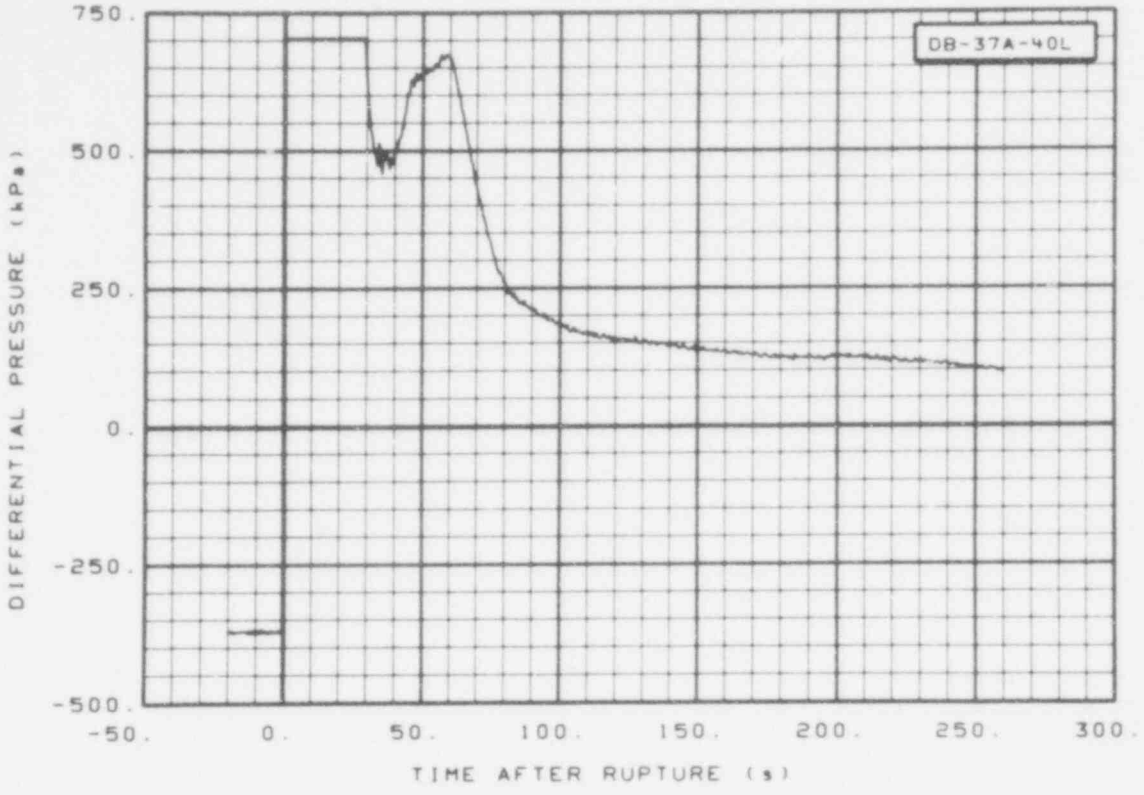

Fig. 157 Differential pressure in broken loop (DB-37A-40L), from -20 to 260 s.

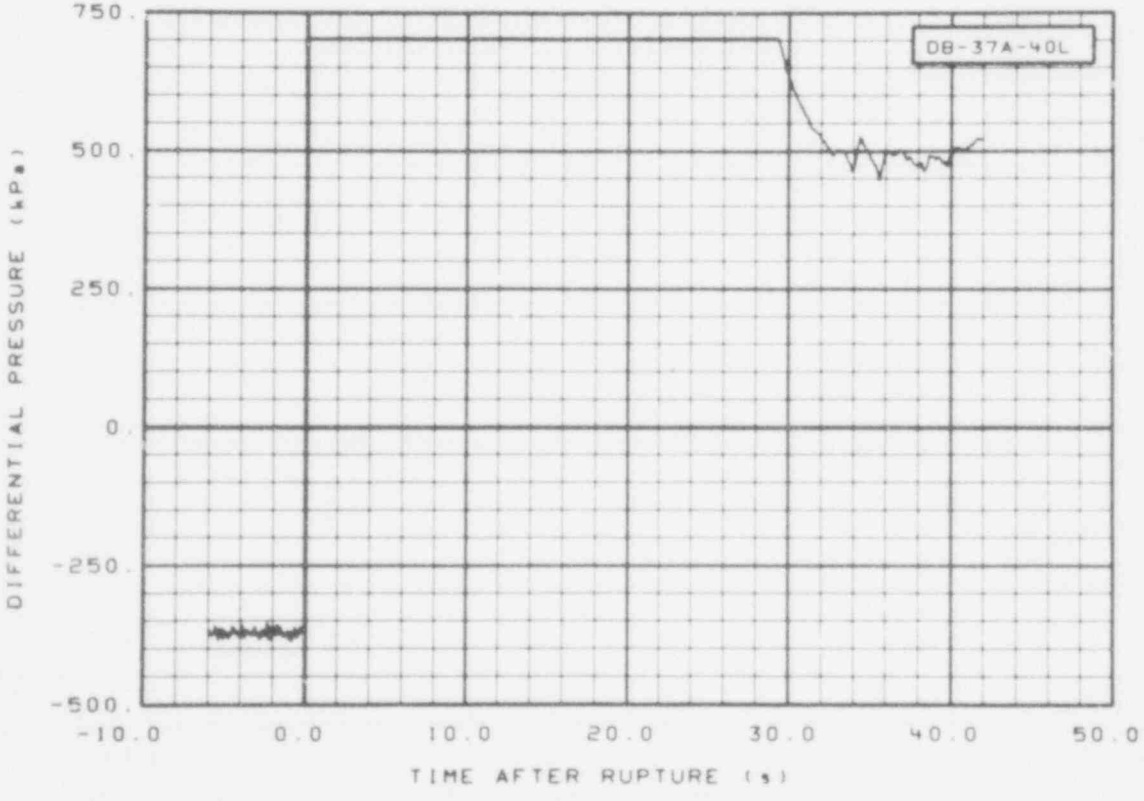

Fig. 158 Differential pressure in broken loop (DB-37A-40L), from -6 to 42 s.

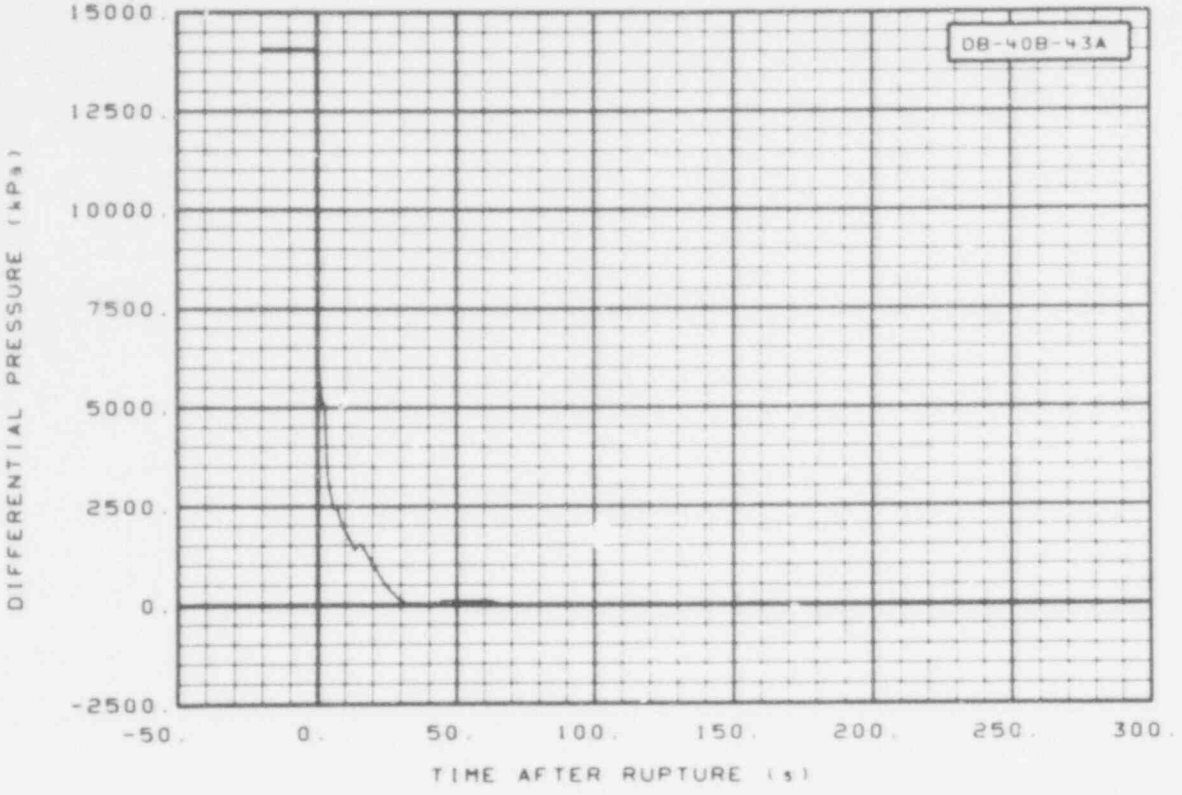

Fig. 159 Differential pressure in broken loop (DB-40B-43A), from -20 to 260 s.

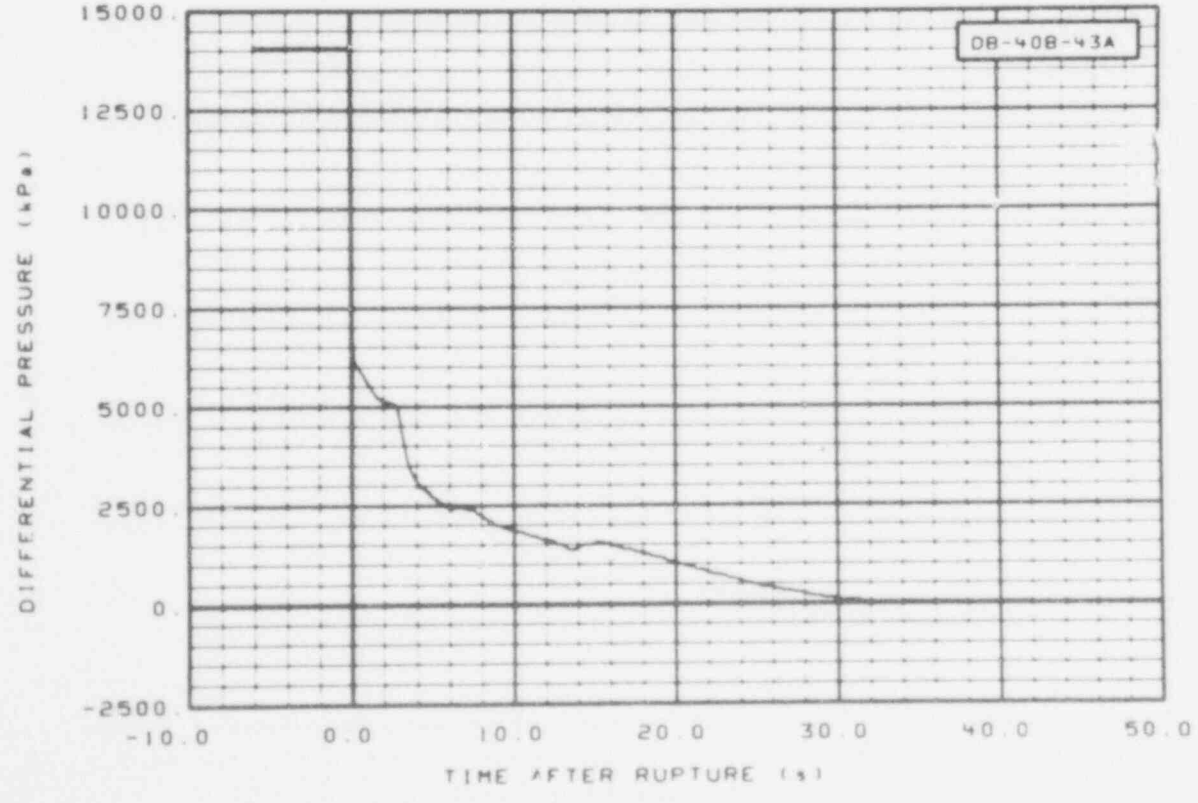

Fig. 160 Differential pressure in broken loop (DB-40B-43A), from -6 to 42 s.

514 123

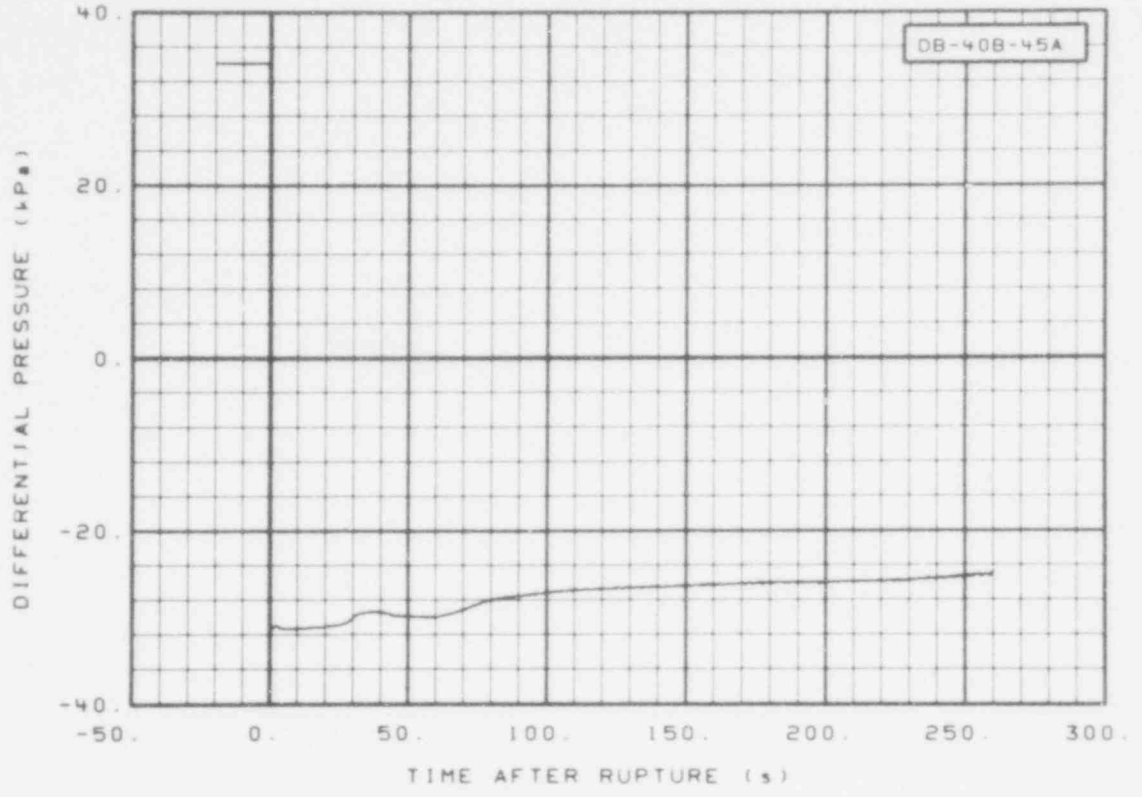

Fig. 161 Differential pressure in broken loop (DB-40B-45A), from -20 to 260 s.

Fig. 162 Differential pressure in broken loop (DB-40B-45A), from -6 to 42 s.

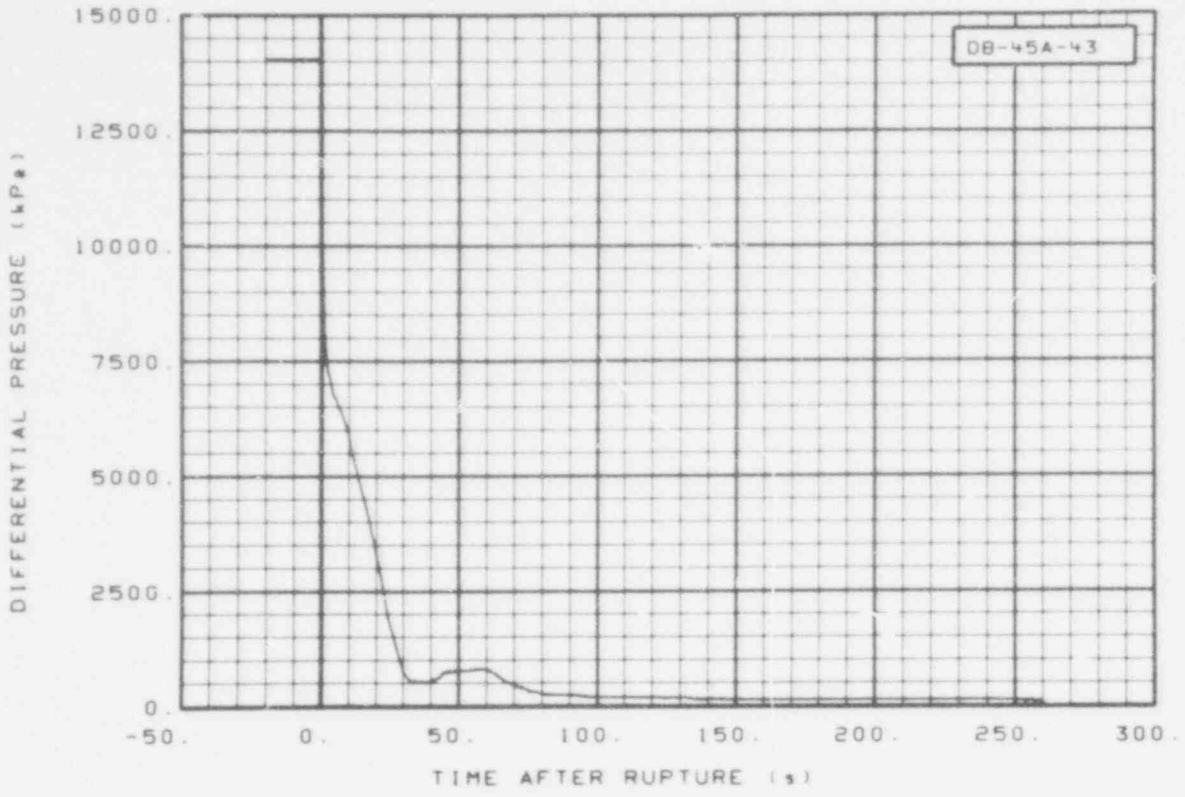

Fig. 163 Differential pressure in broken loop (DB-45A-43), from -20 to 260 s.

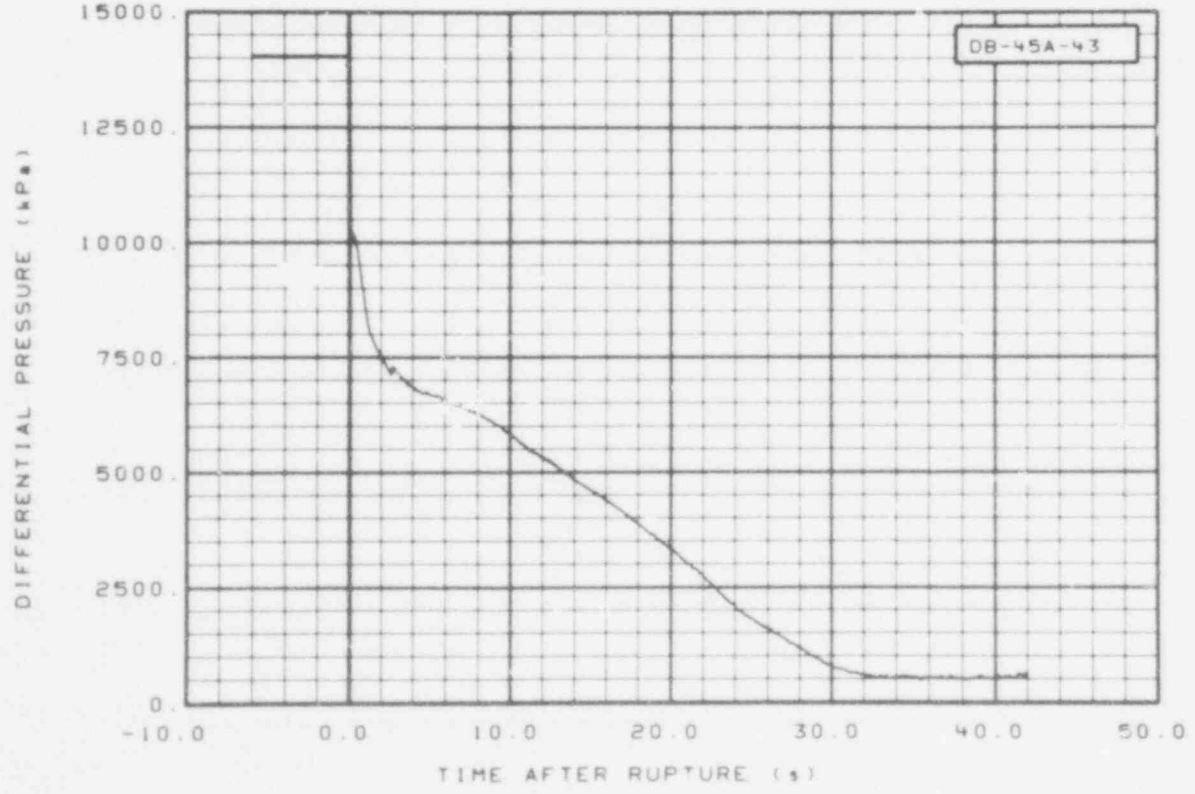

Fig. 164 Differential pressure in broken loop (DB-45A-43), from -6 to 42 s.

5AA 125

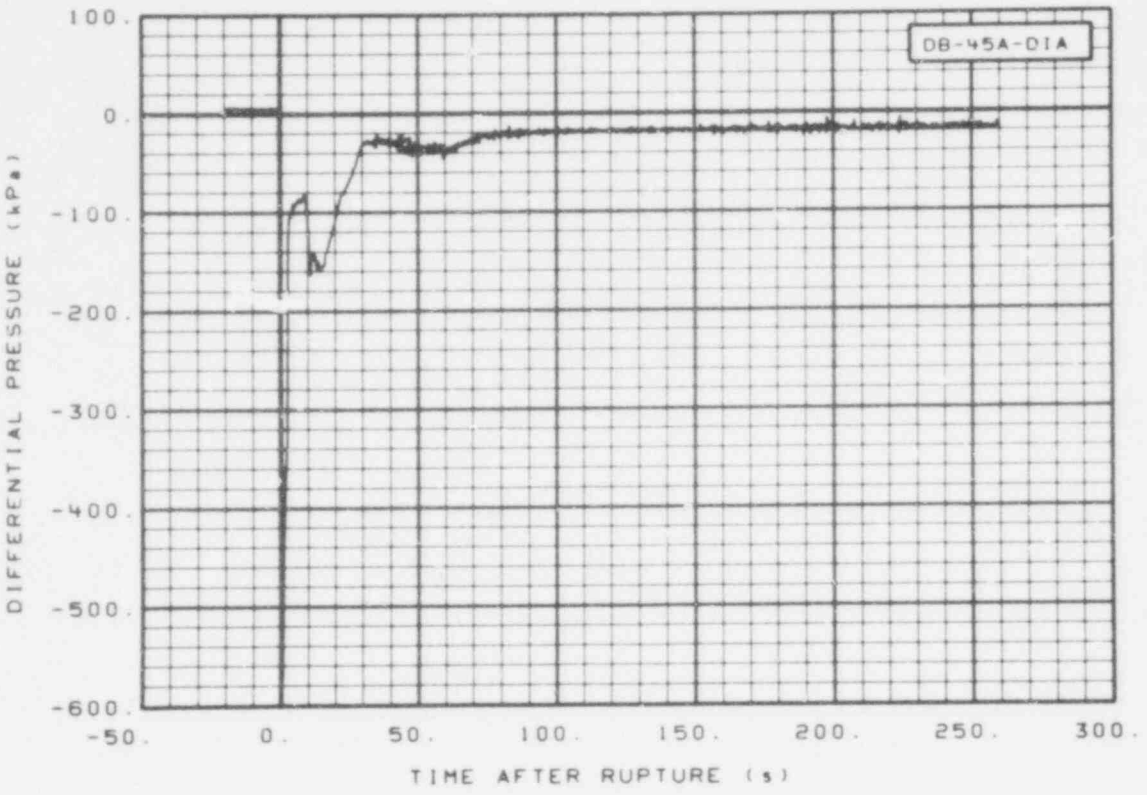

Fig. 165 Differential pressure in broken loop (DB-45A-DIA), from -20 to 260 s.

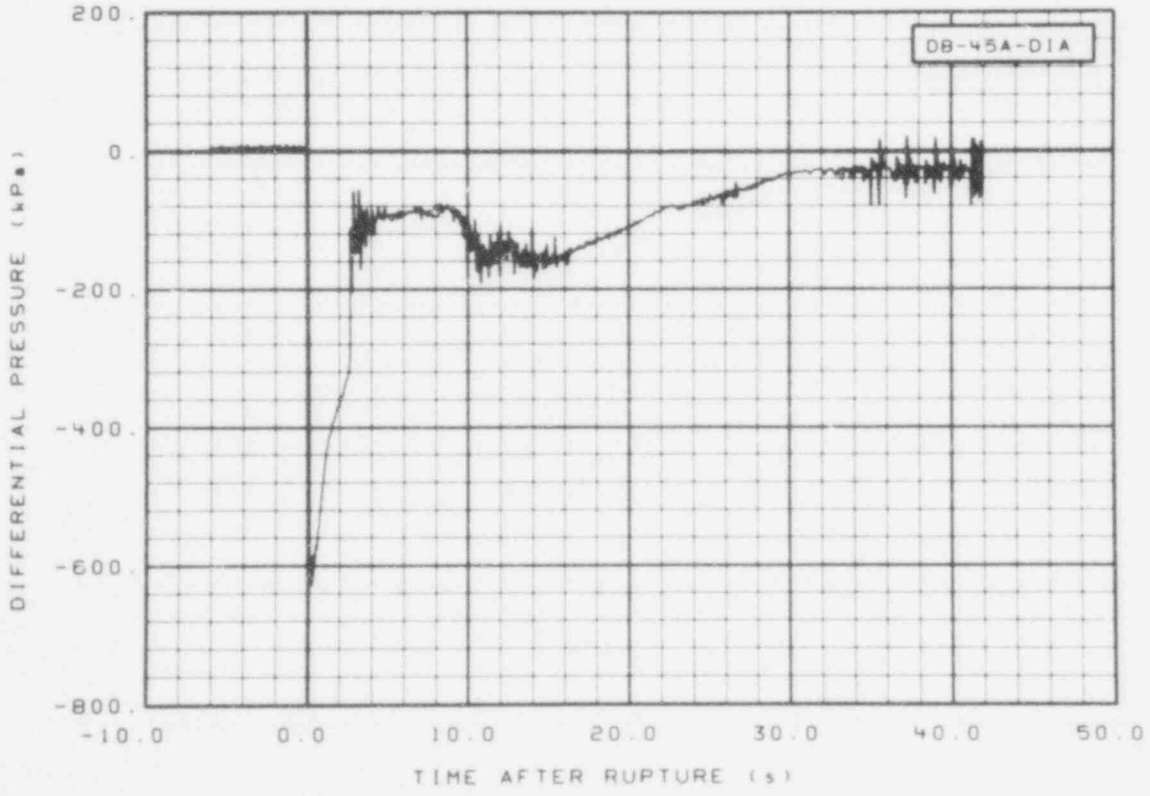

Fig. 166 Differential pressure in broken loop (DB-45A-DIA), from -6 to 42 s.

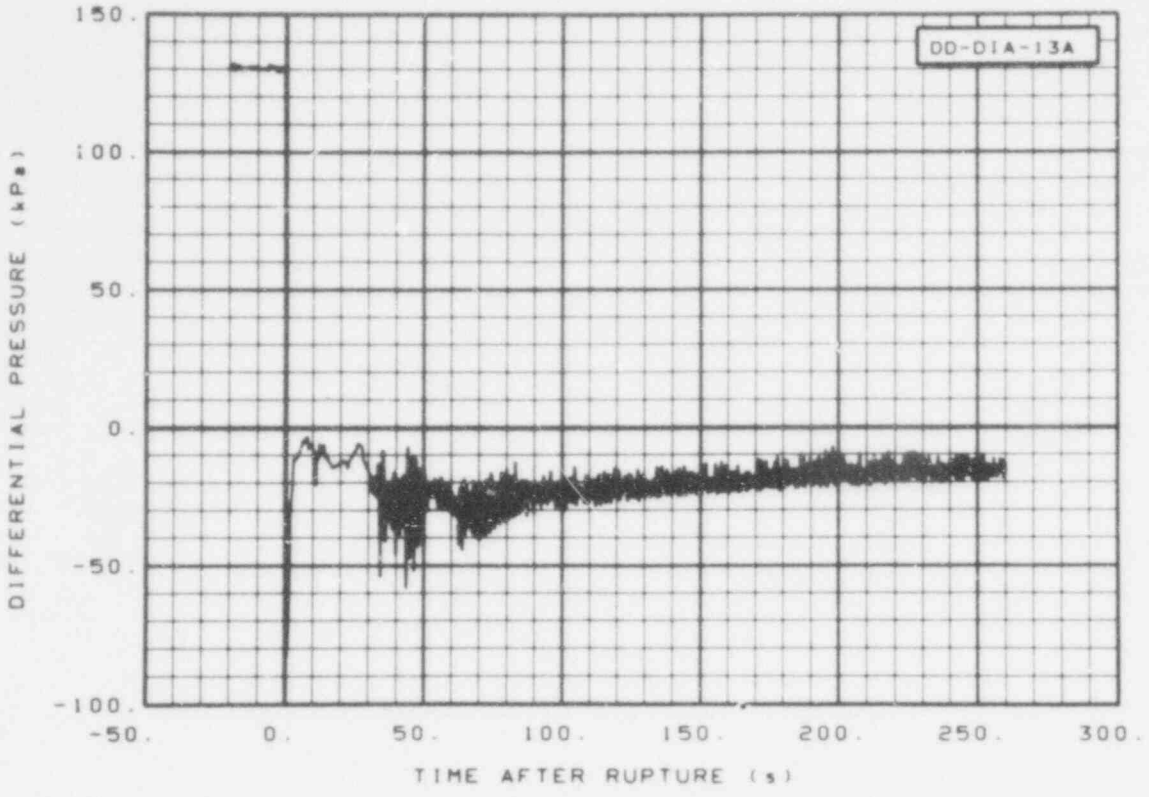

Fig. 167 Differential pressure in downcomer (DD-DIA-13V), from -20 to 260 s.

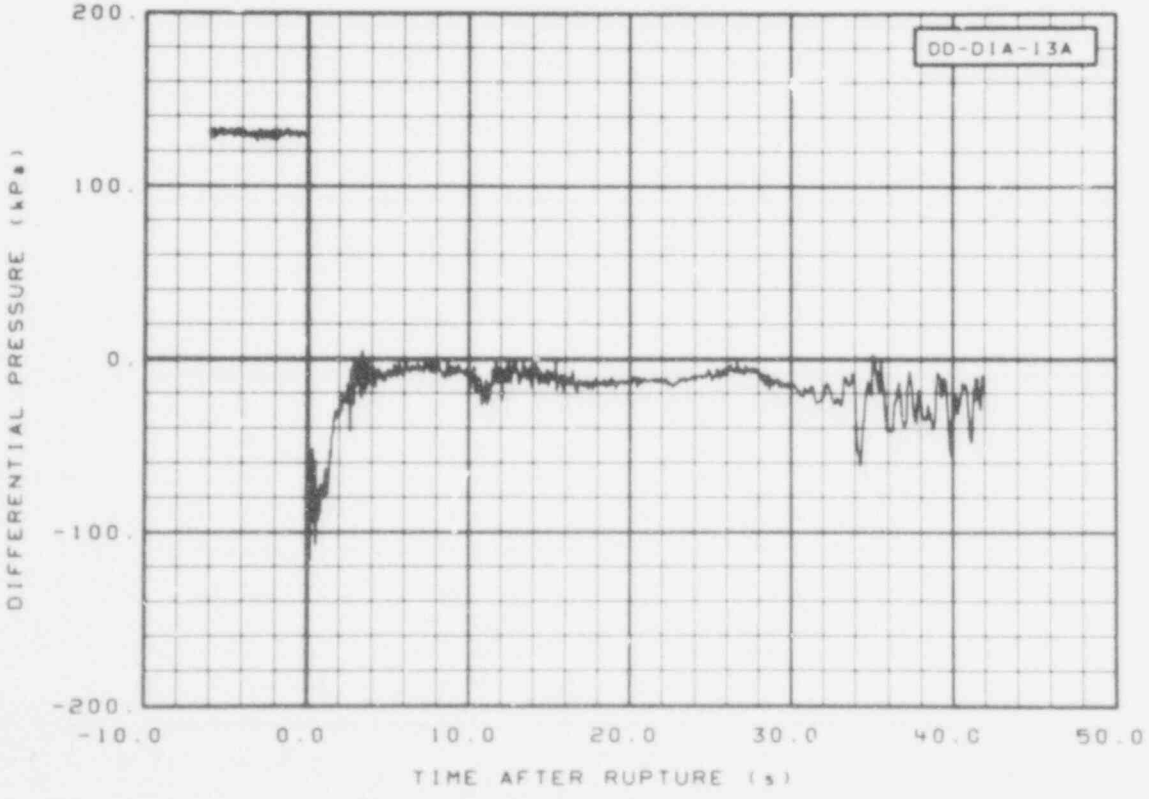

Fig. 168 Differential pressure in downcomer (DD-DIA-13V), from -6 to 42 s.

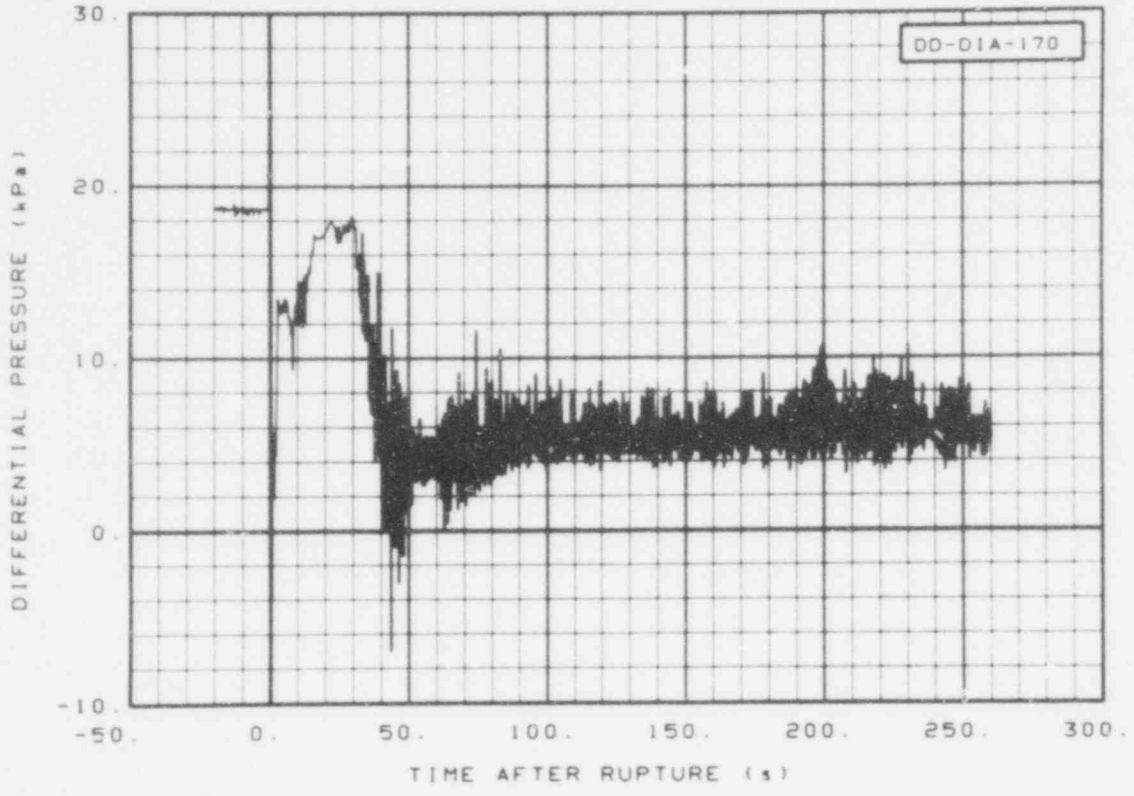

Fig. 169 Differential pressure in downcomer (DD-DIA-170), from -20 to 260 s.

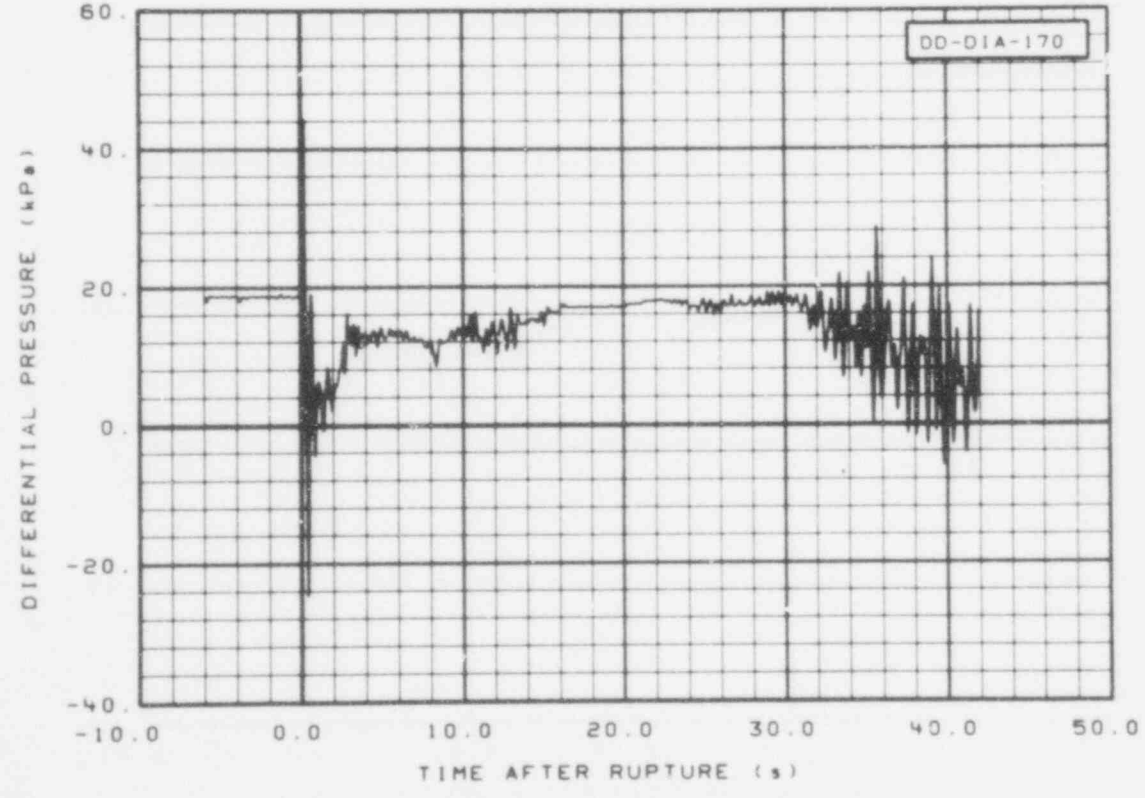

Fig. 170 Differential pressure in downcomer (DD-DIA-170), from -6 to 42 s.

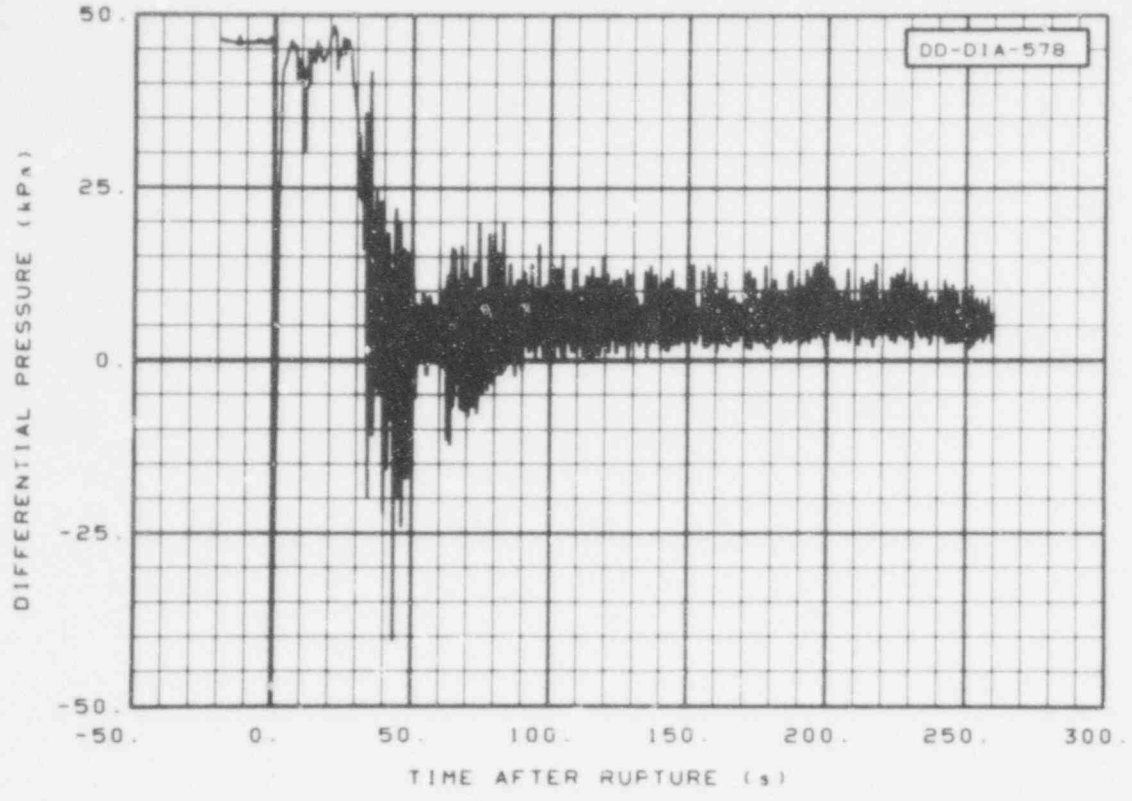

Fig. 171 Differential pressure in downcomer (DD-DIA-578), from -20 to 260 s.

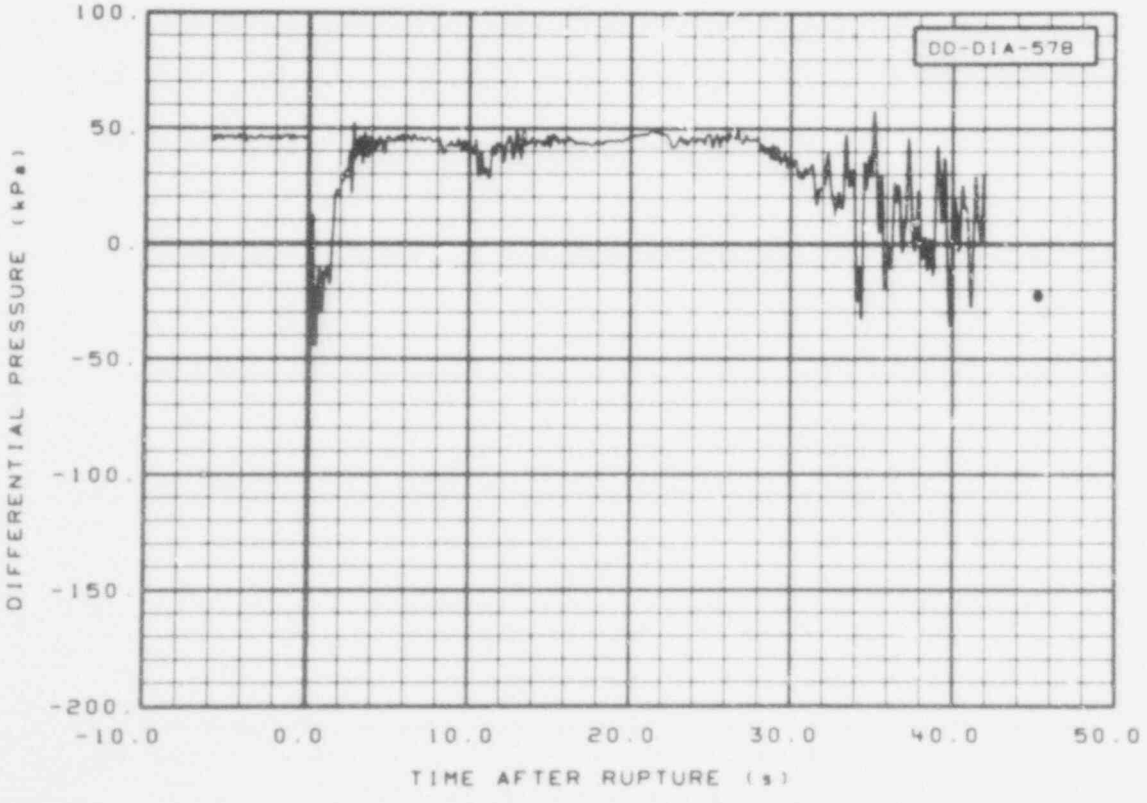

Fig. 172 Differential pressure in downcomer (DD-DIA-578), from -6 to 42 s.

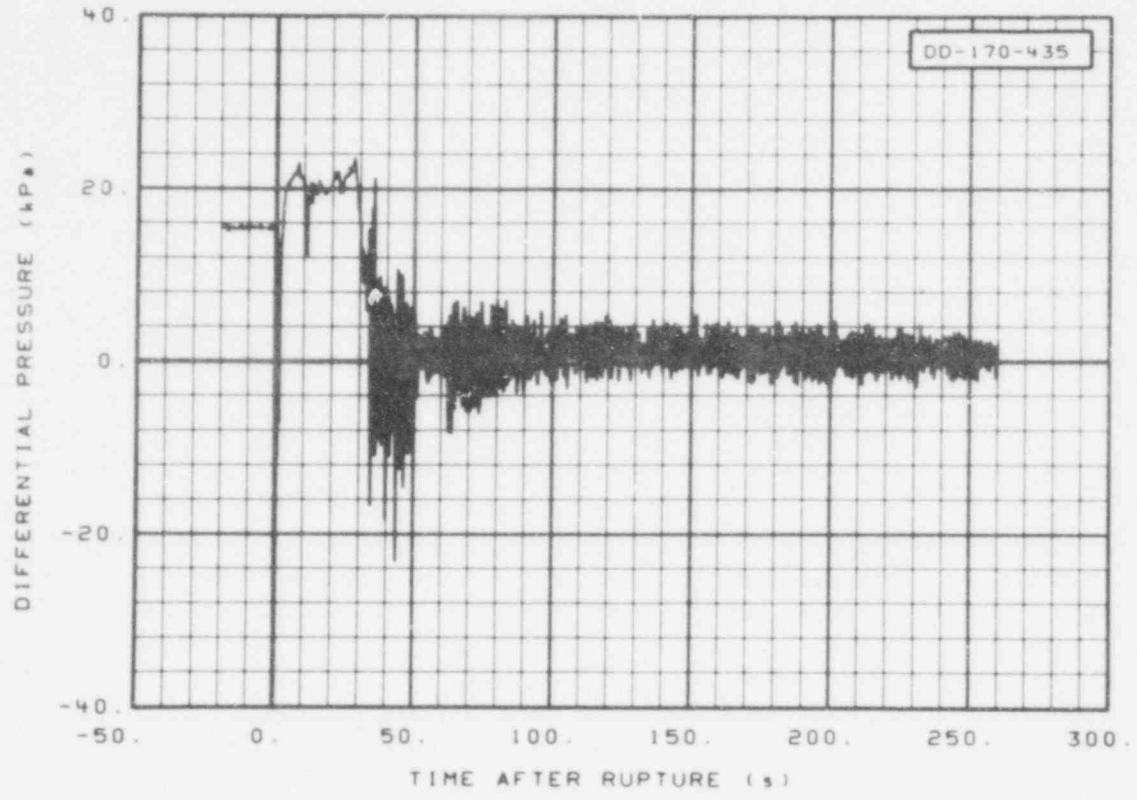

Fig. 173 Differential pressure in downcomer (DD-170-435), from -20 to 260 s.

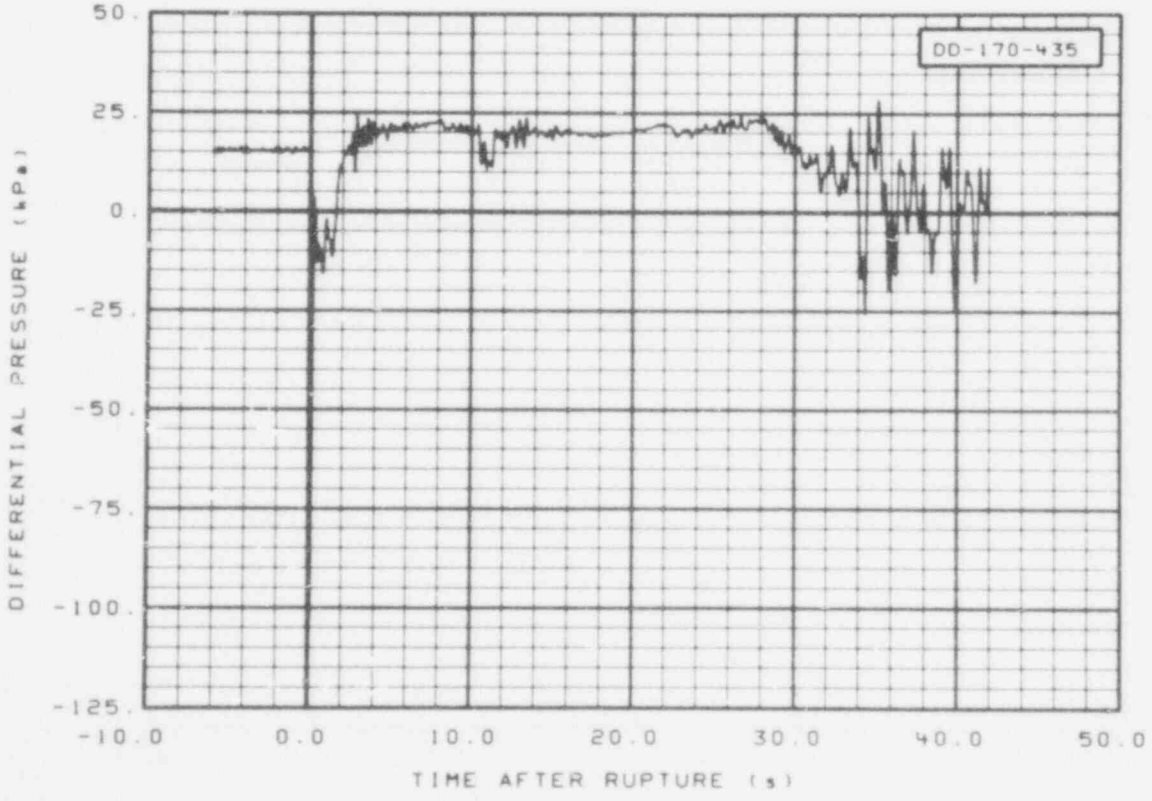

Fig. 174 Differential pressure in downcomer (DD-170-435), from -6 to 42 s.

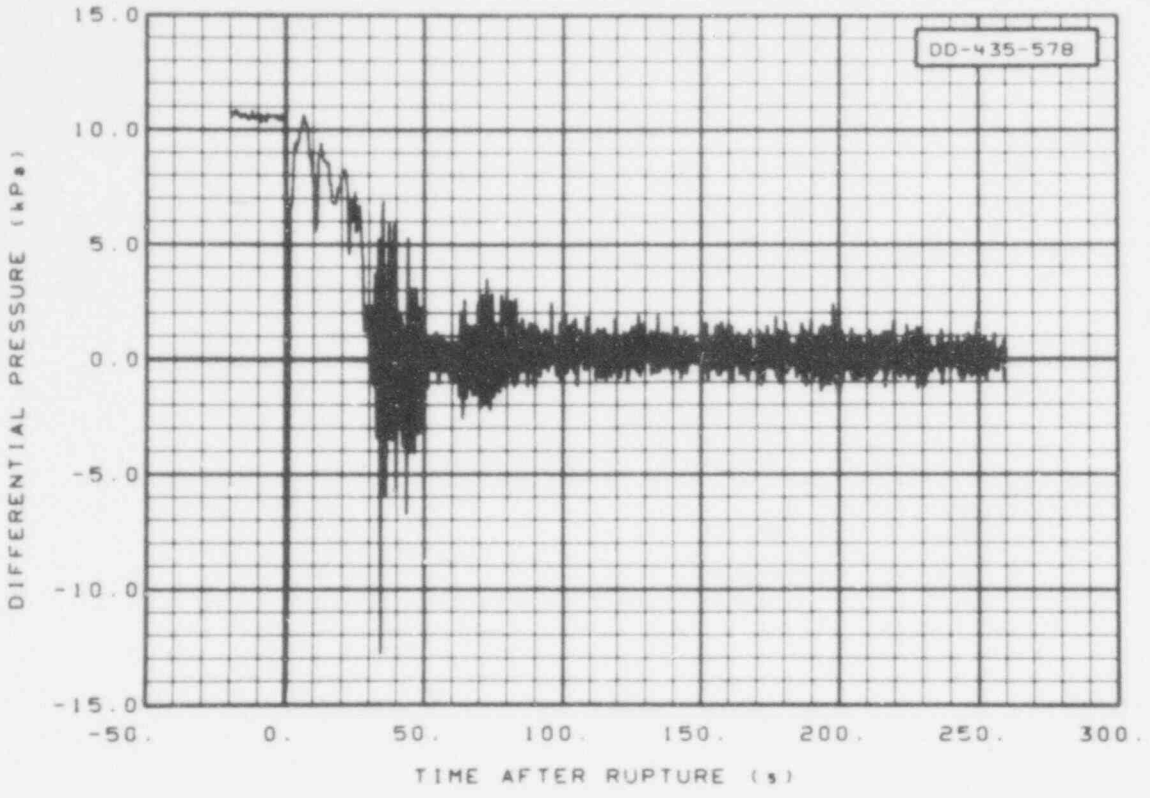

Fig. 175 Differential pressure in downcomer (DD-435-578), from -20 to 260 s.

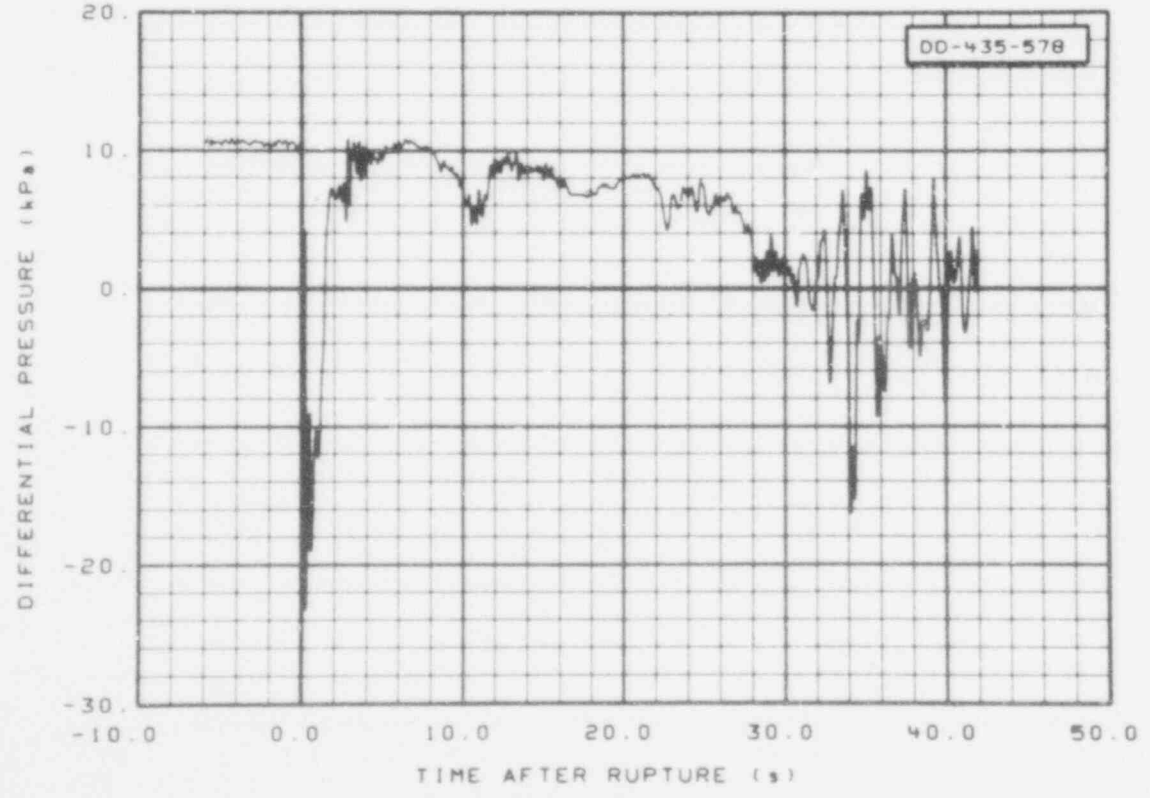

Fig. 176 Differential pressure in downcomer (DD-435-578), from -6 to 42 s.

544 131

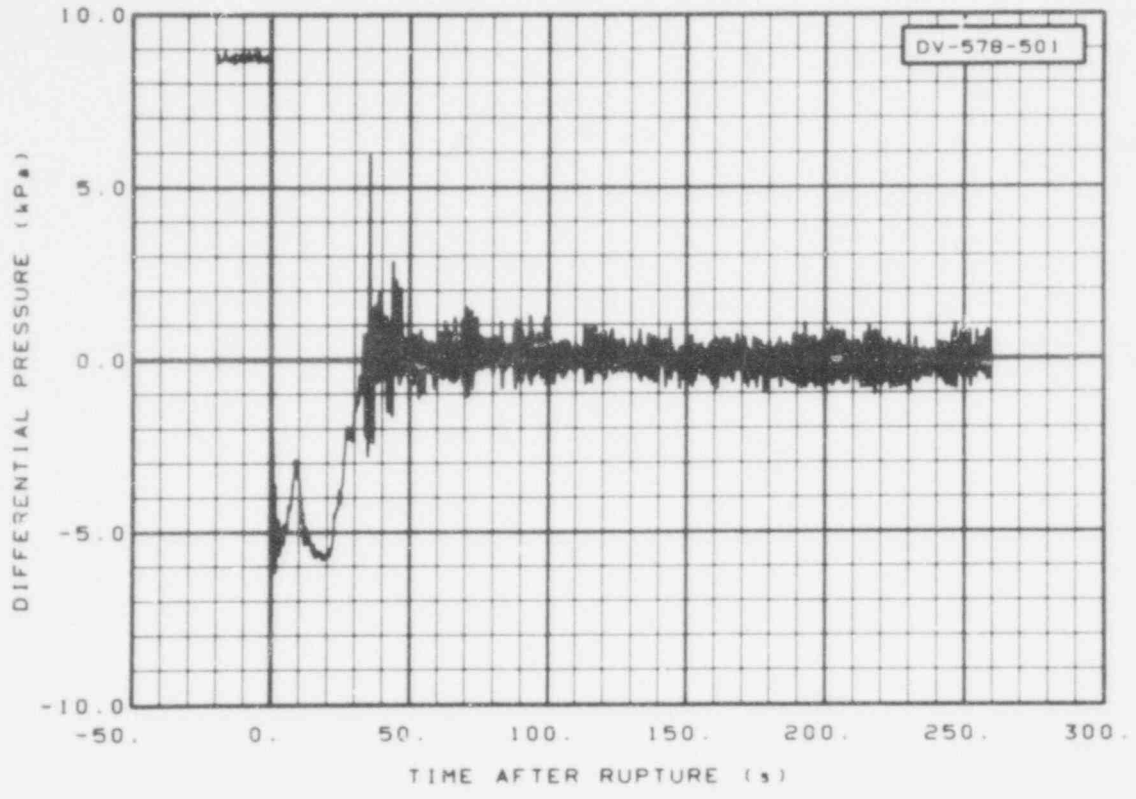

Fig. 177 Differential pressure in vessel (DV-578-501), from -20 to 260 s.

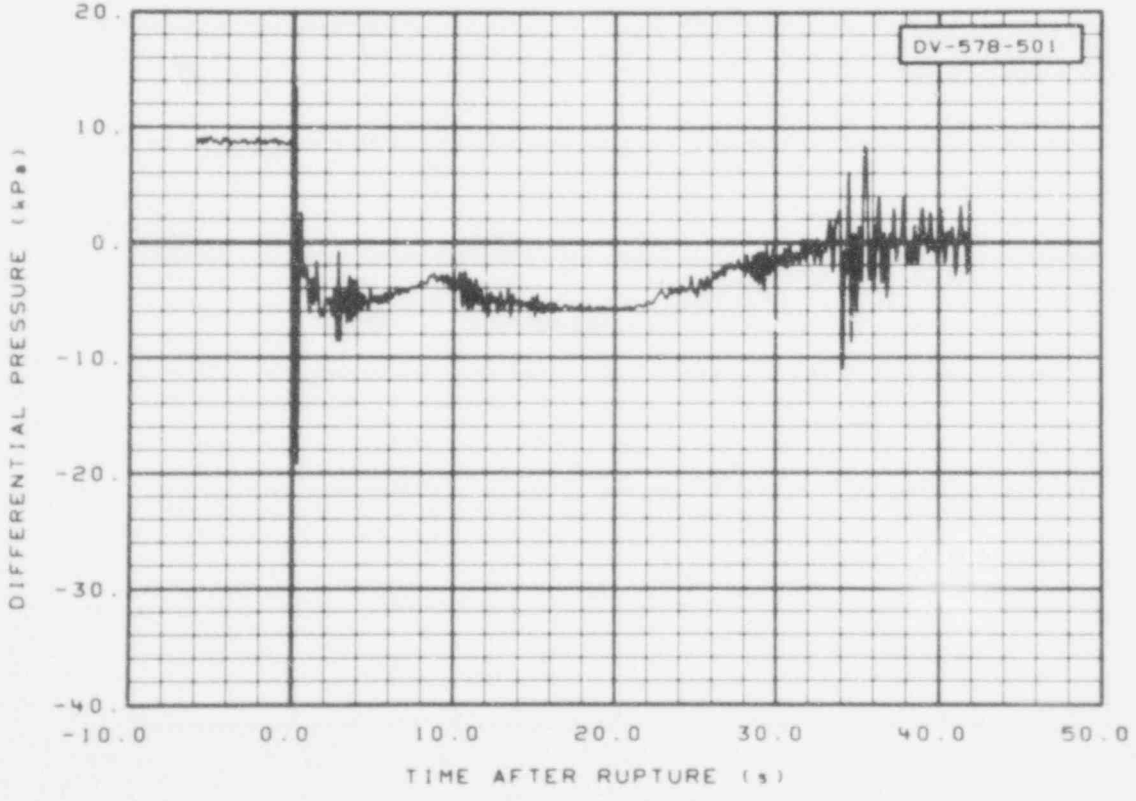

Fig. 178 Differential pressure in vessel (DV-578-501), from -6 to 42 s.

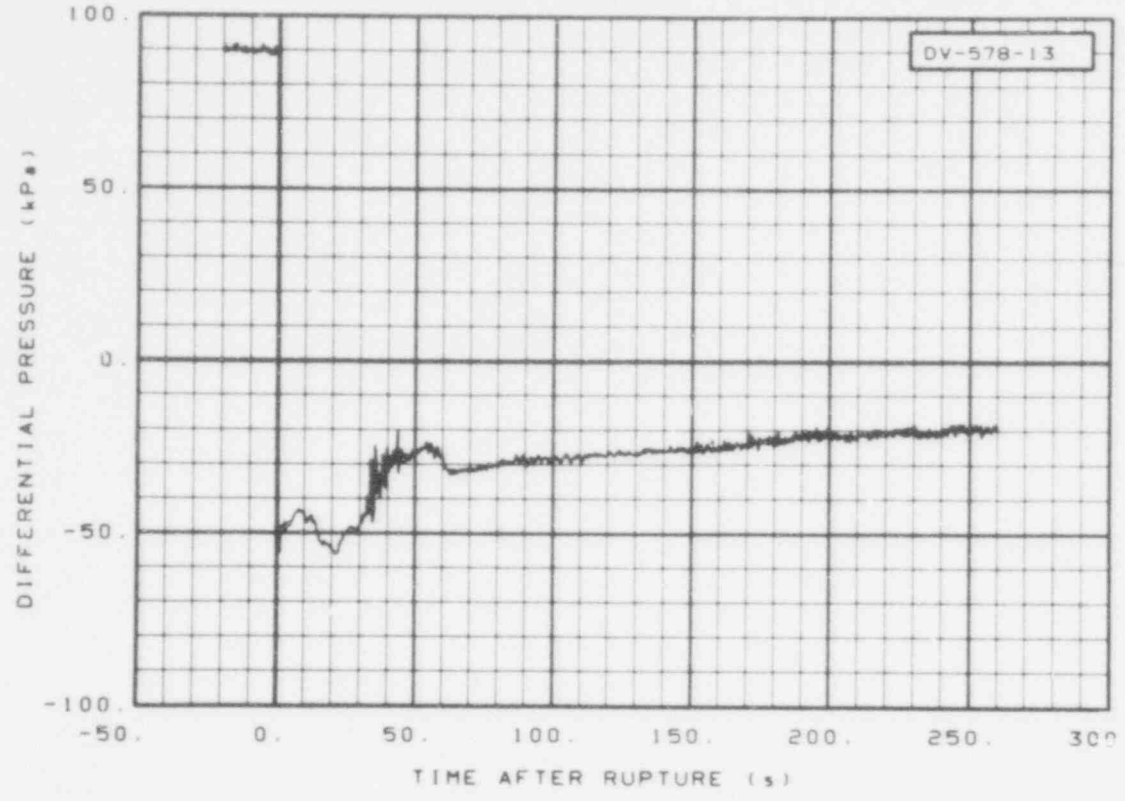

Fig. 179 Differential pressure in vessel (DV-578-13), from -20 to 260 s.

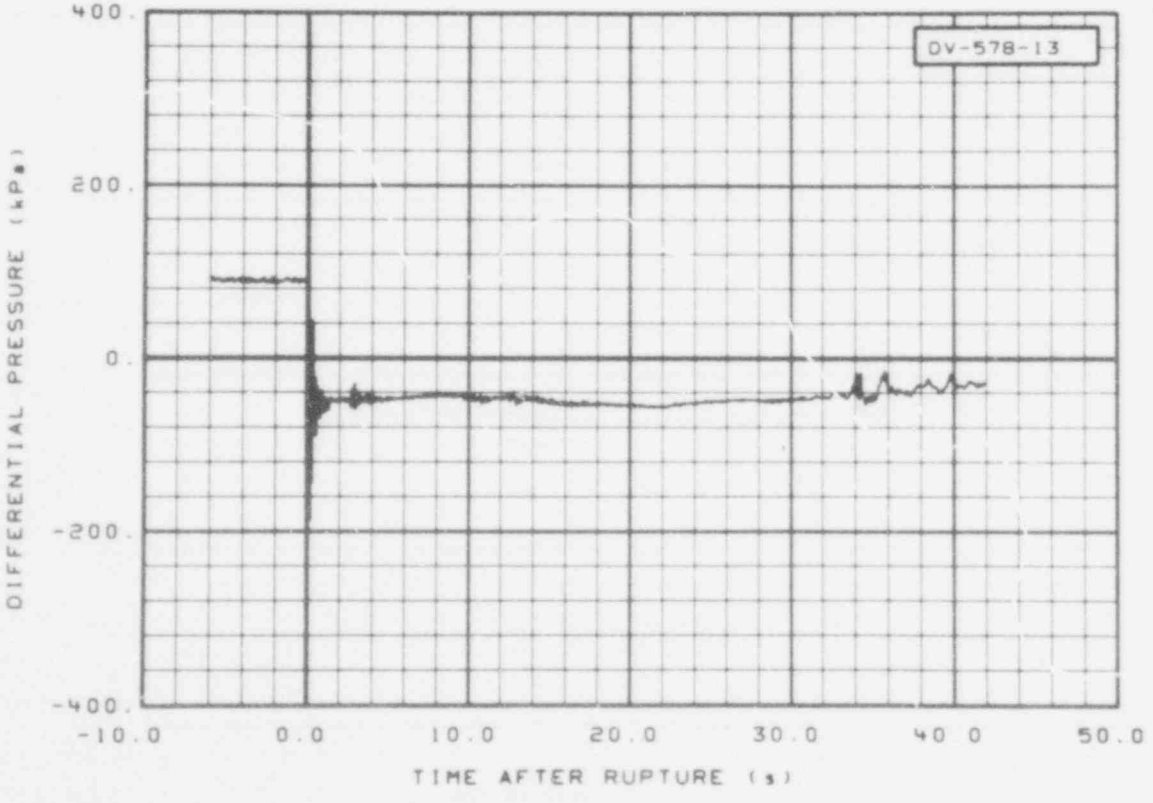

Fig. 180 Differential pressure in vessel (DV-578-13), from -6 to 42 s.

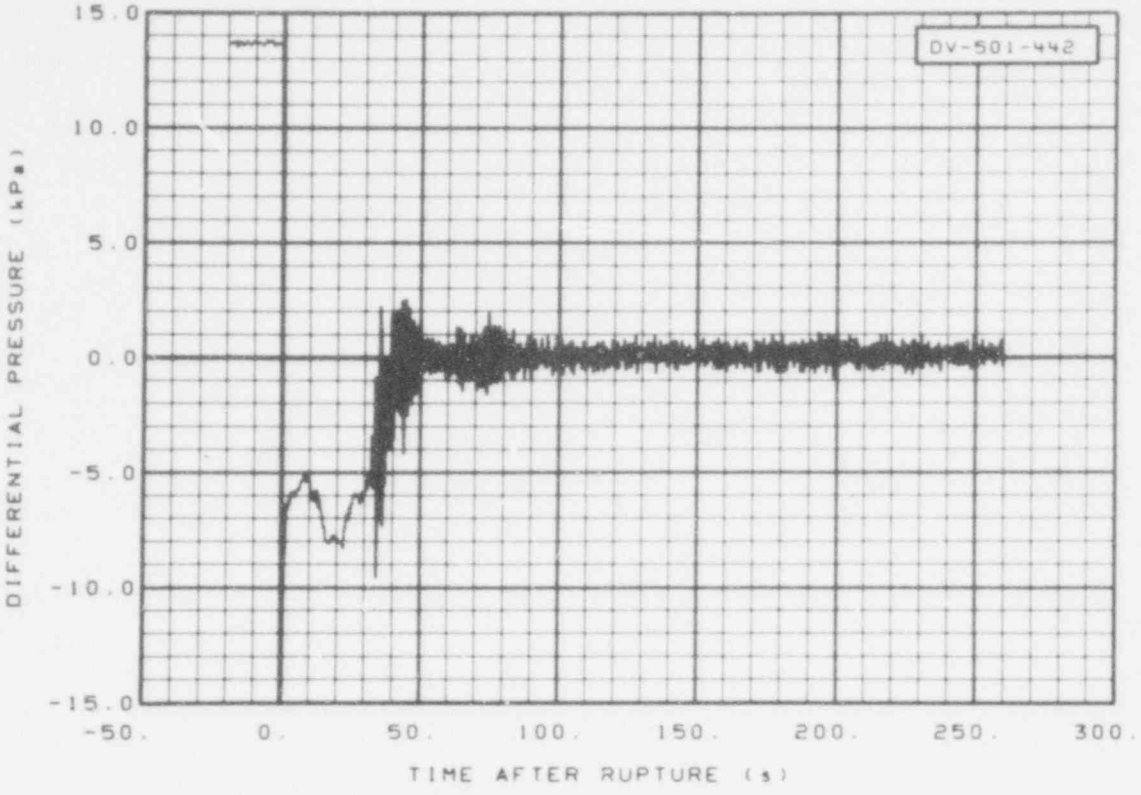

Fig. 181 Differential pressure in vessel (DV-501-442), from -20 to 260 s.

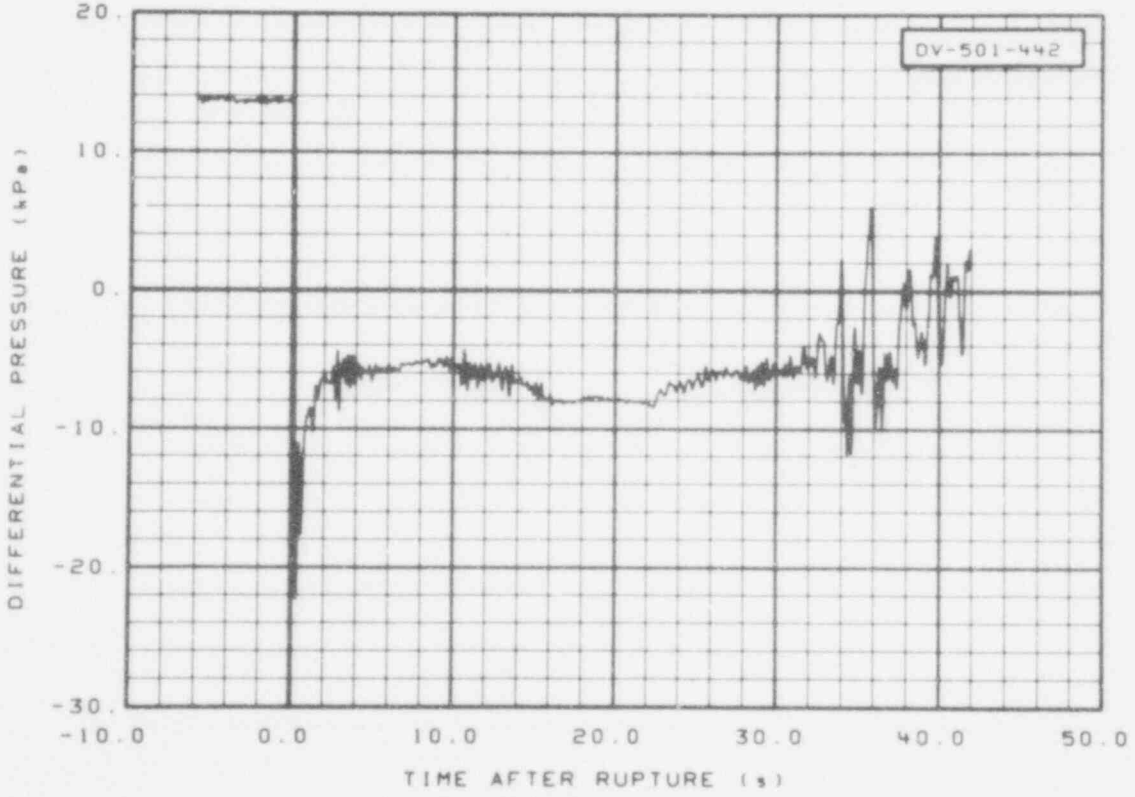

Fig. 182 Differential pressure in vessel (DV-501-442), from -6 to 42 s.

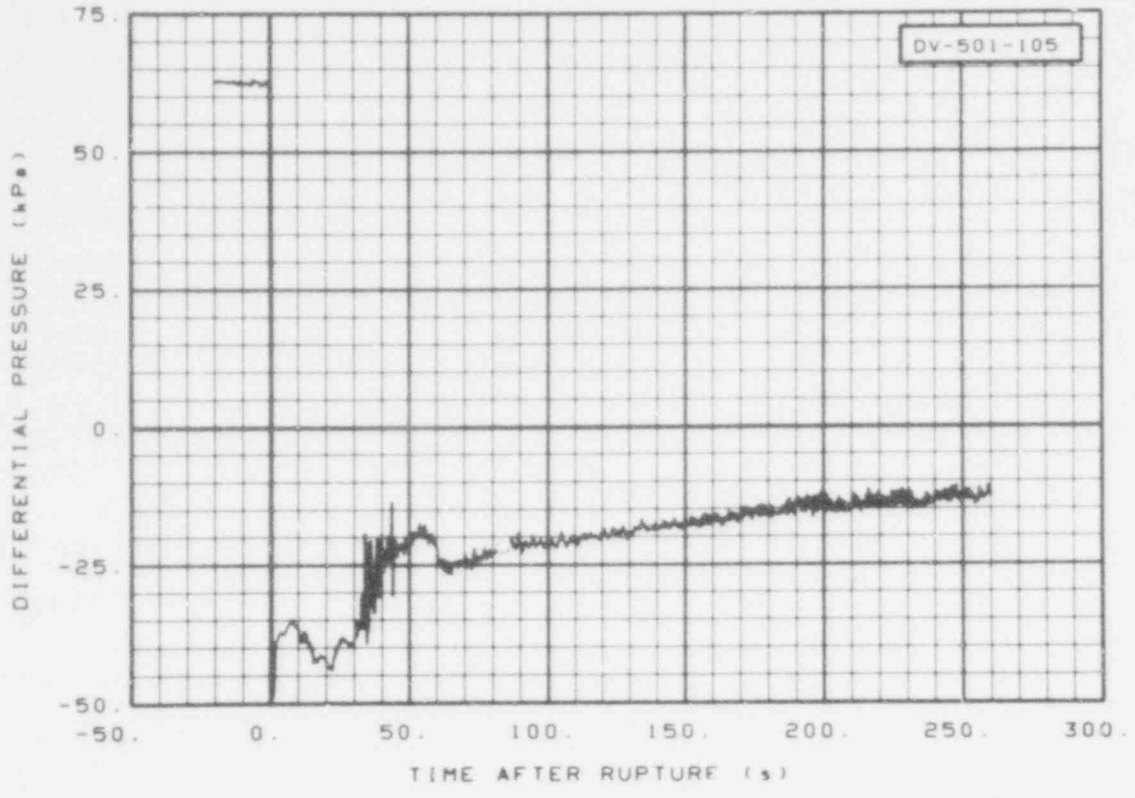

Fig. 183 Differential pressure in vessel (DV-501-105), from -20 to 260 s.

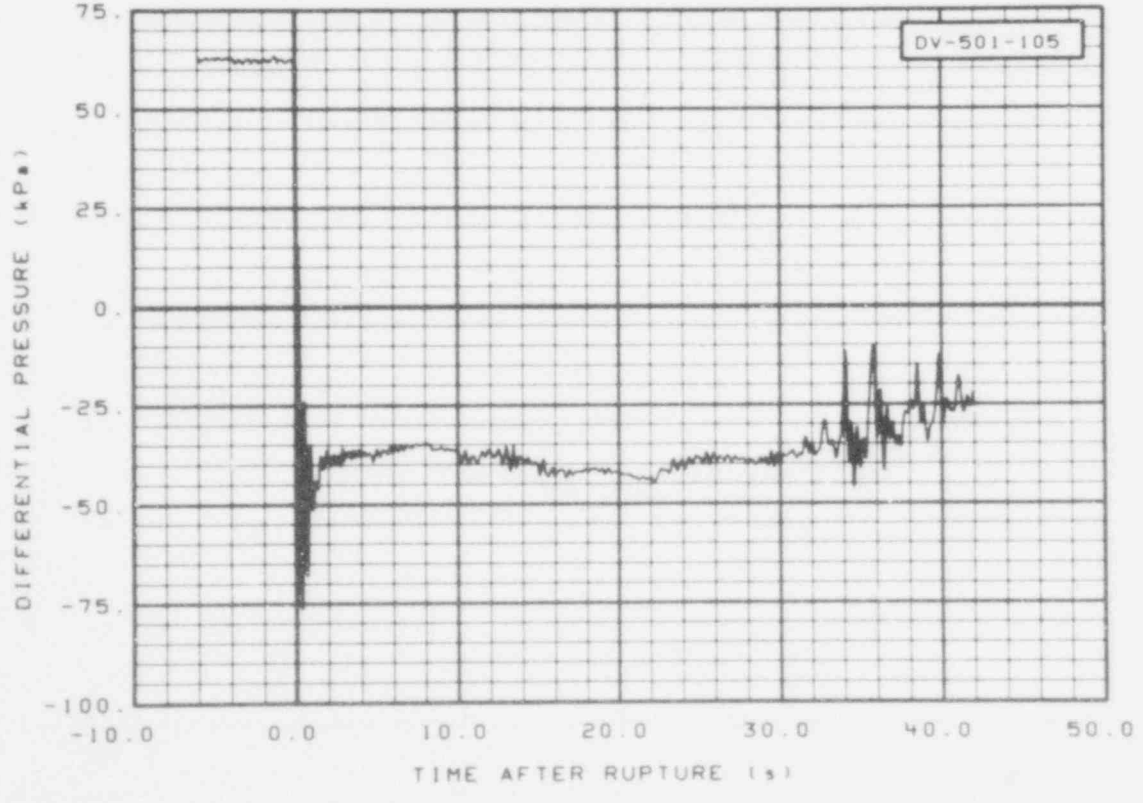

Fig. 184 Differential pressure in vessel (DV-501-105), from -6 to 42 s.

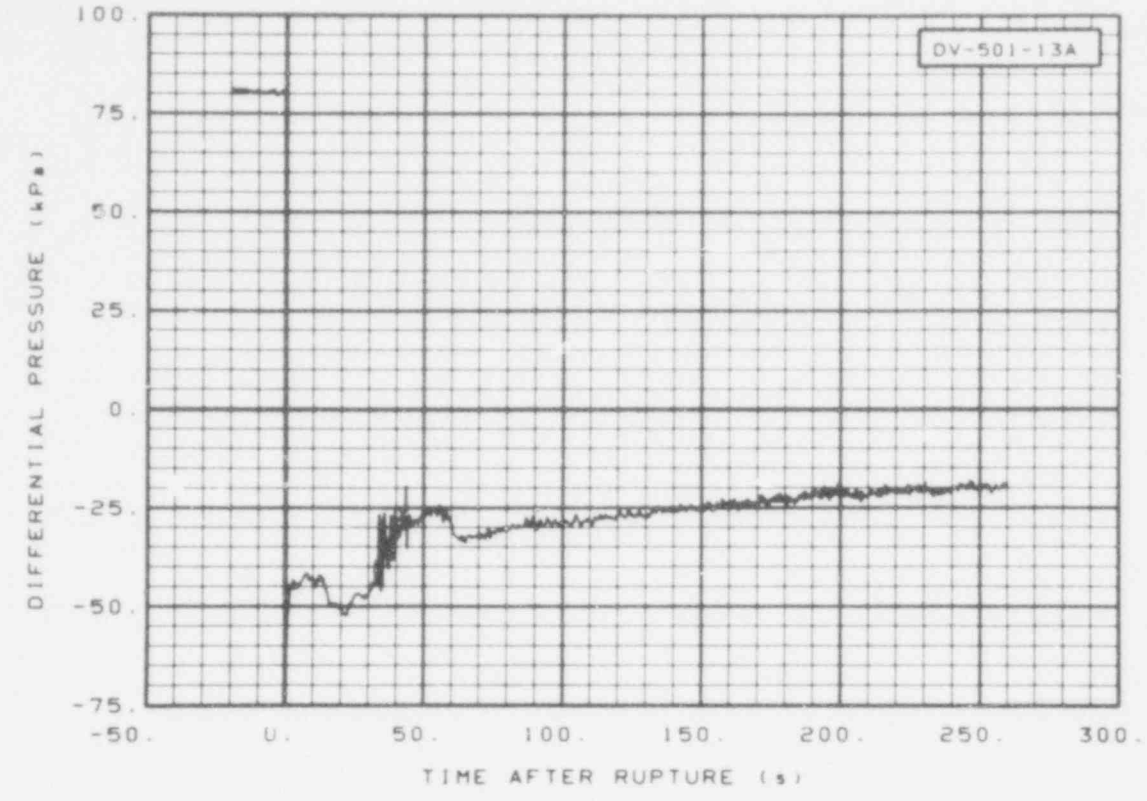

Fig. 185 Differential pressure in vessel (DV-501-13A), from -20 to 260 s.

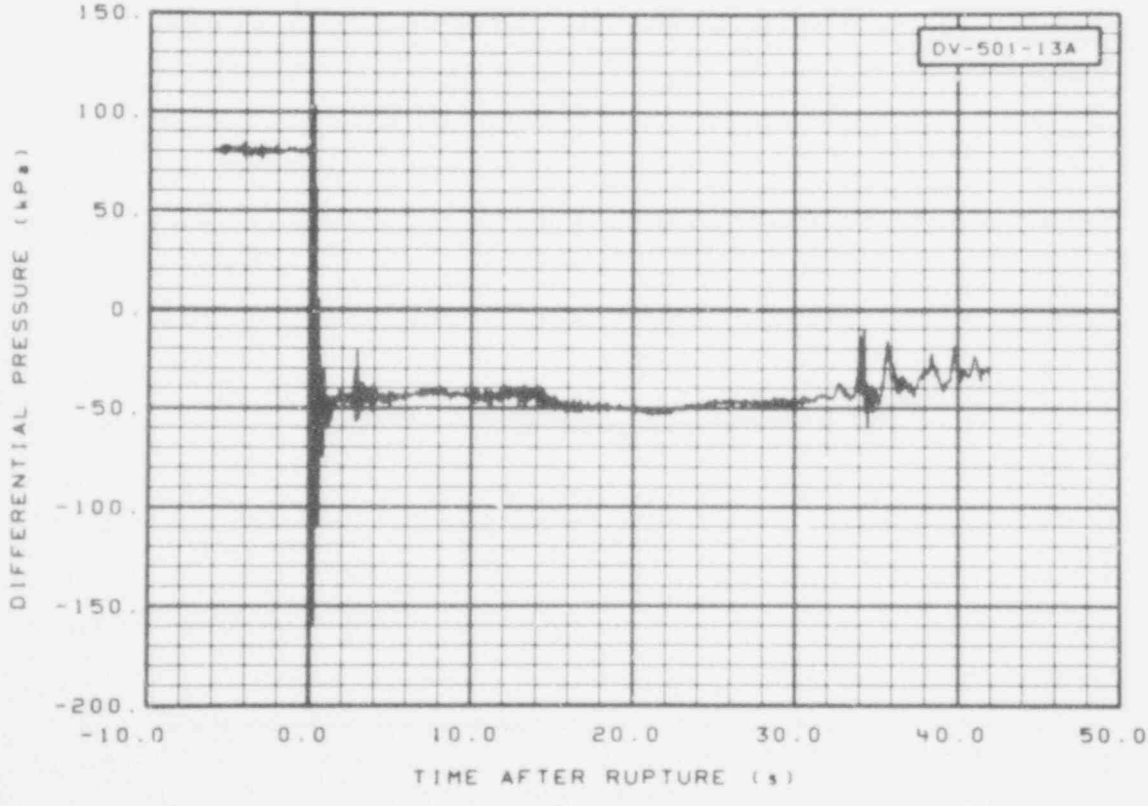

Fig. 186 Differential pressure in vessel (DV-501-13A), from -6 to 42 s.

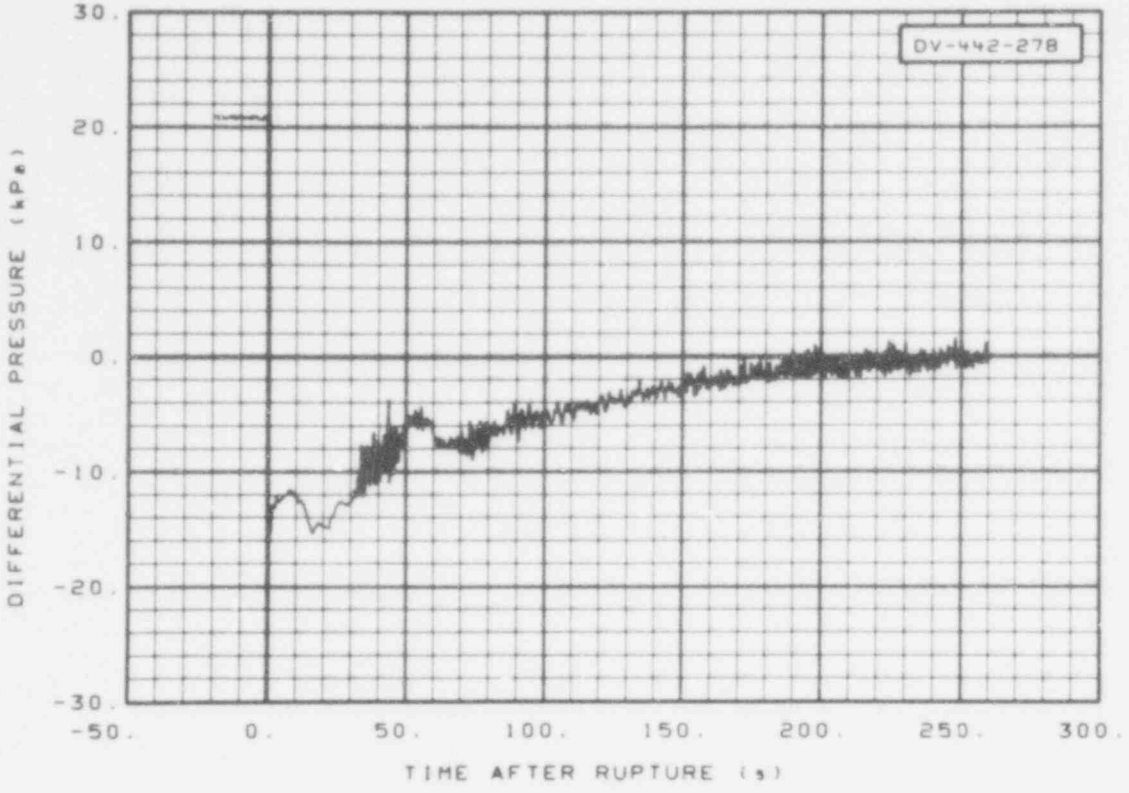

Fig. 187 Differential pressure in vessel (DV-442-278), from -20 to 260 s.

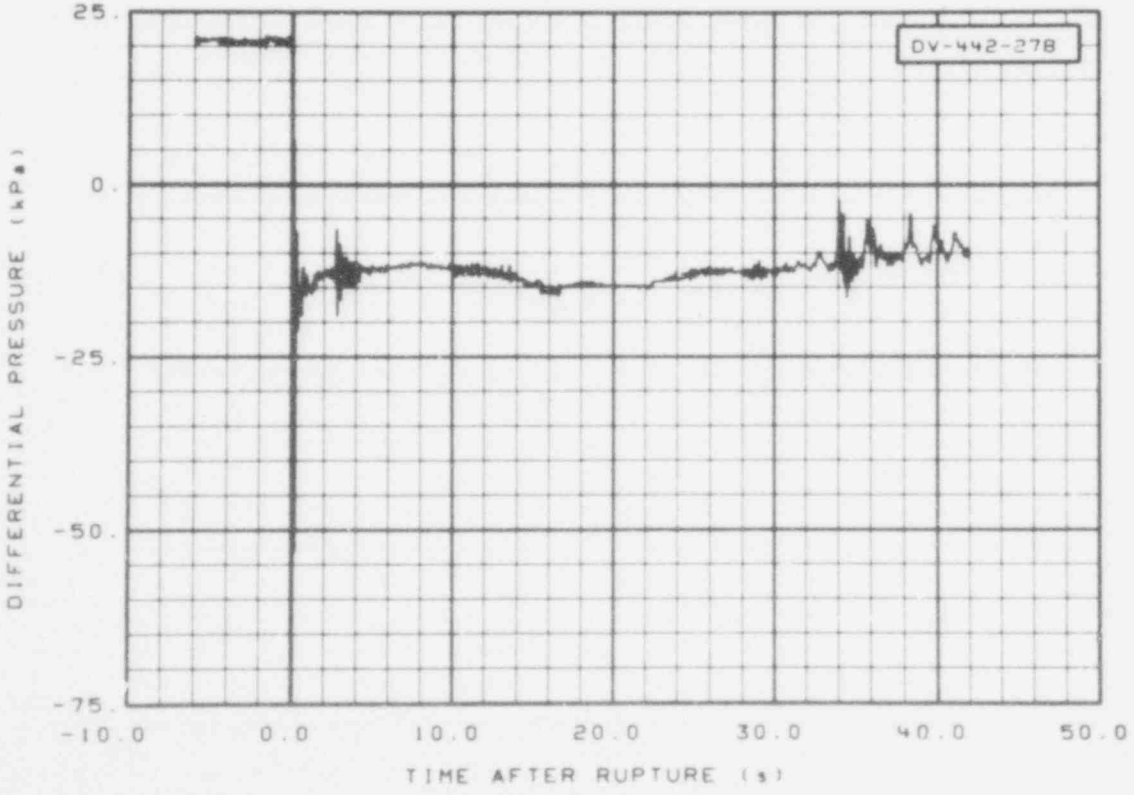

Fig. 188 Differential pressure in vessel (DV-442-278), from -6 to 42 s.

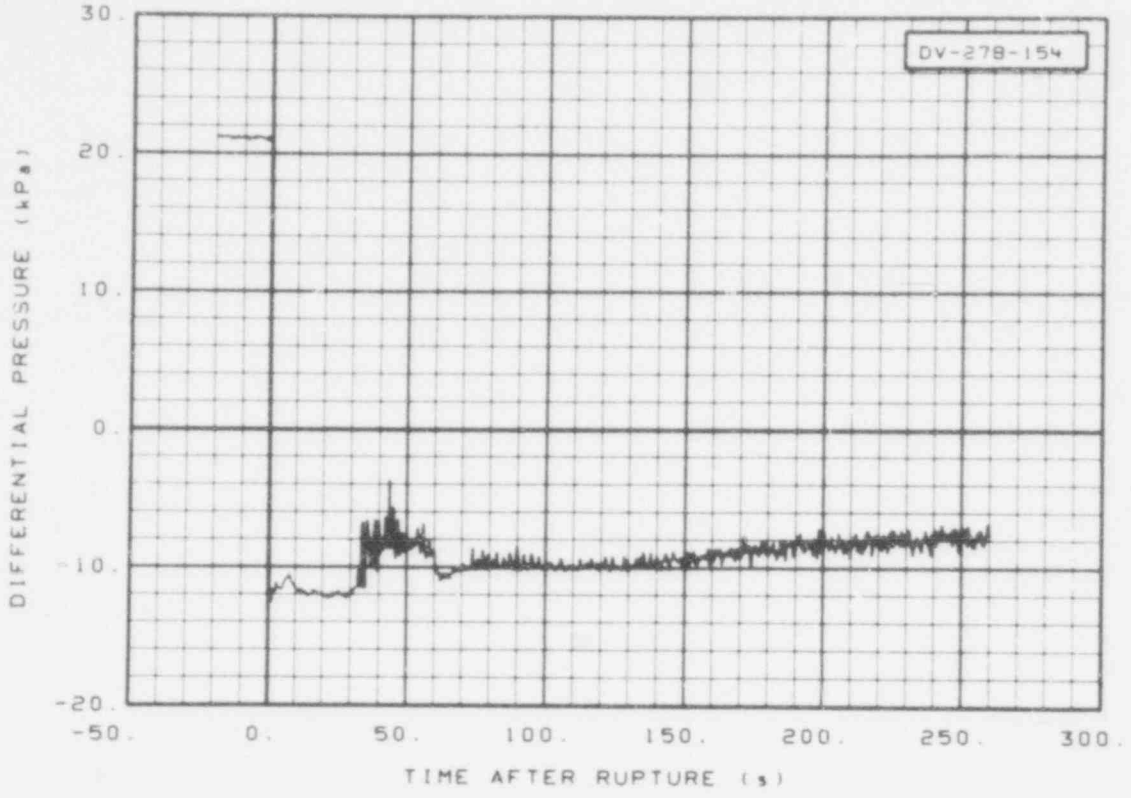

Fig. 189 Differential pressure in vessel (DV-278-154), from -20 to 260 s.

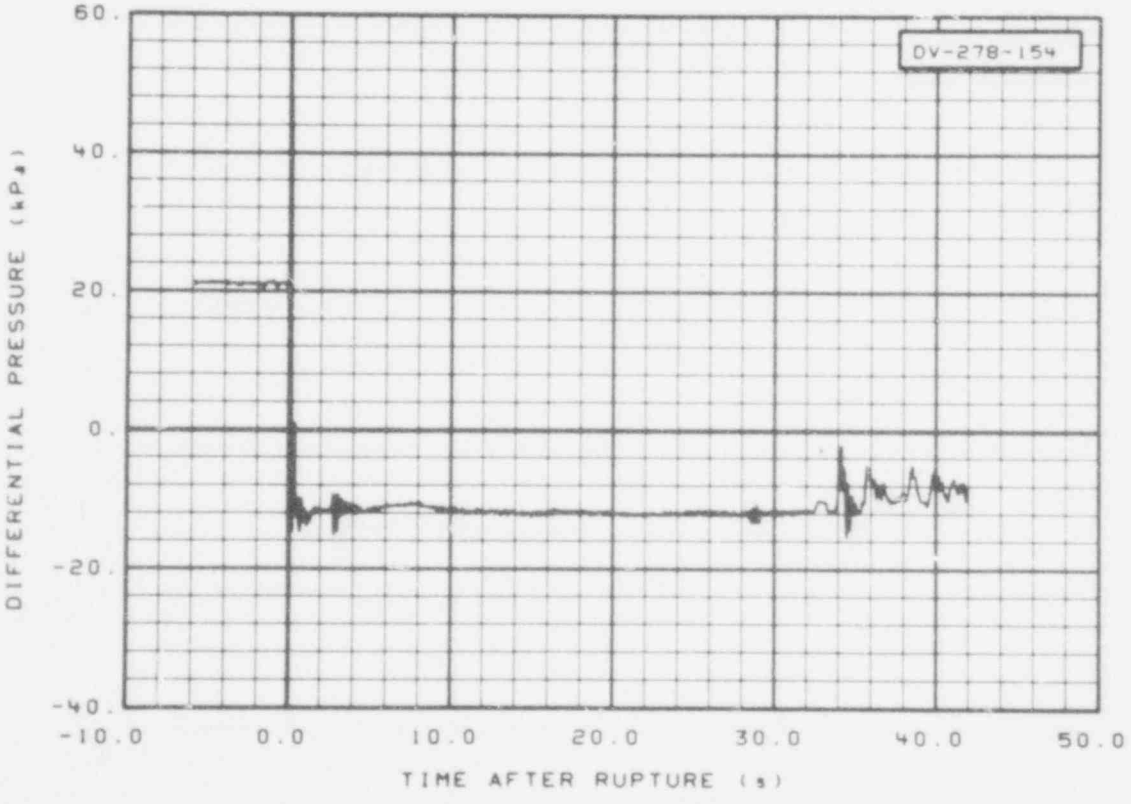

Fig. 190 Differential pressure in vessel (DV-278-154), from -6 to 42 s.

544 138

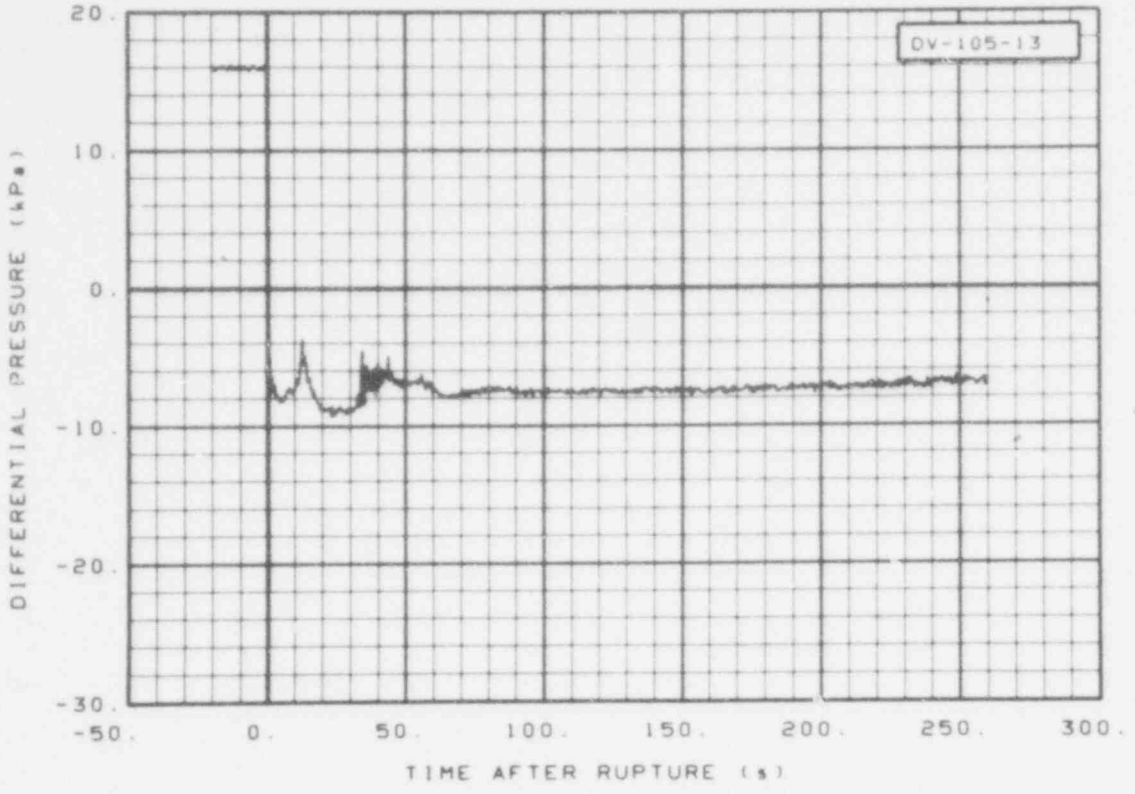

Fig. 191 Differential pressure in vessel (DV-105-13), from -20 to 260 s.

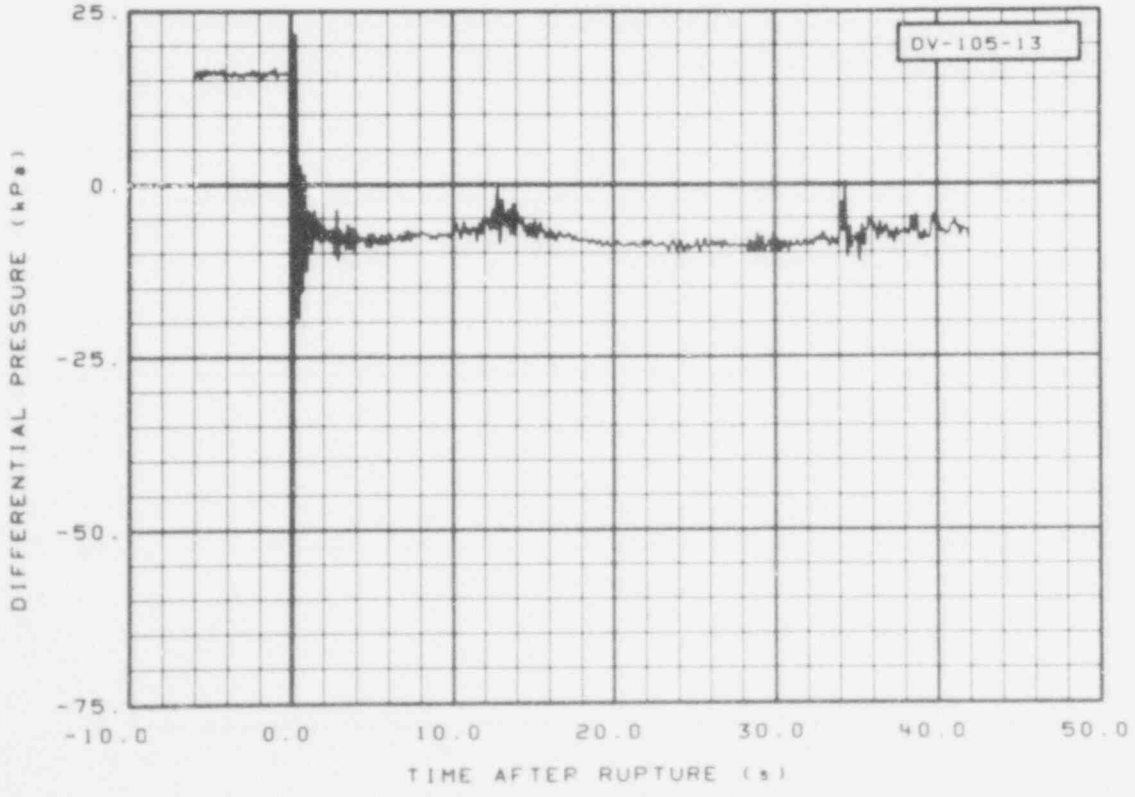

Fig. 192 Differential pressure in vessel (DV-105-13), from -6 to 42 s.

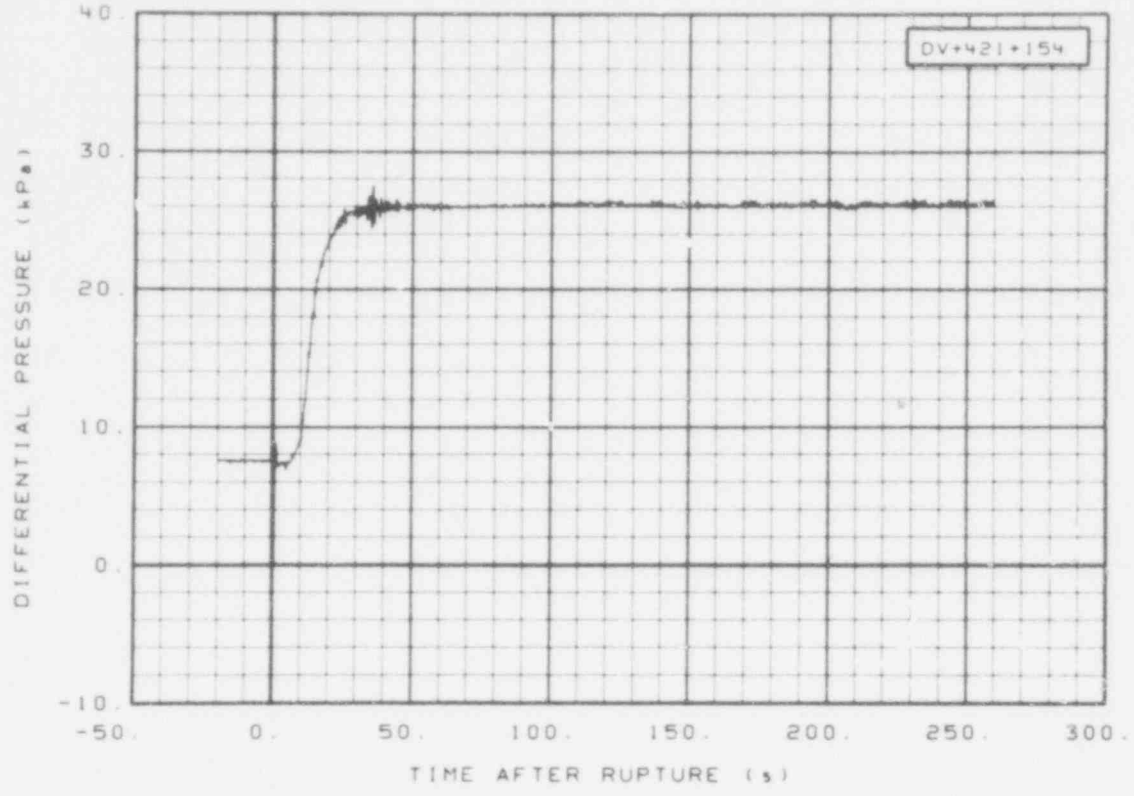

Fig. 193 Differential pressure in vessel (DV + 421 + 154), from -20 to 260 s.

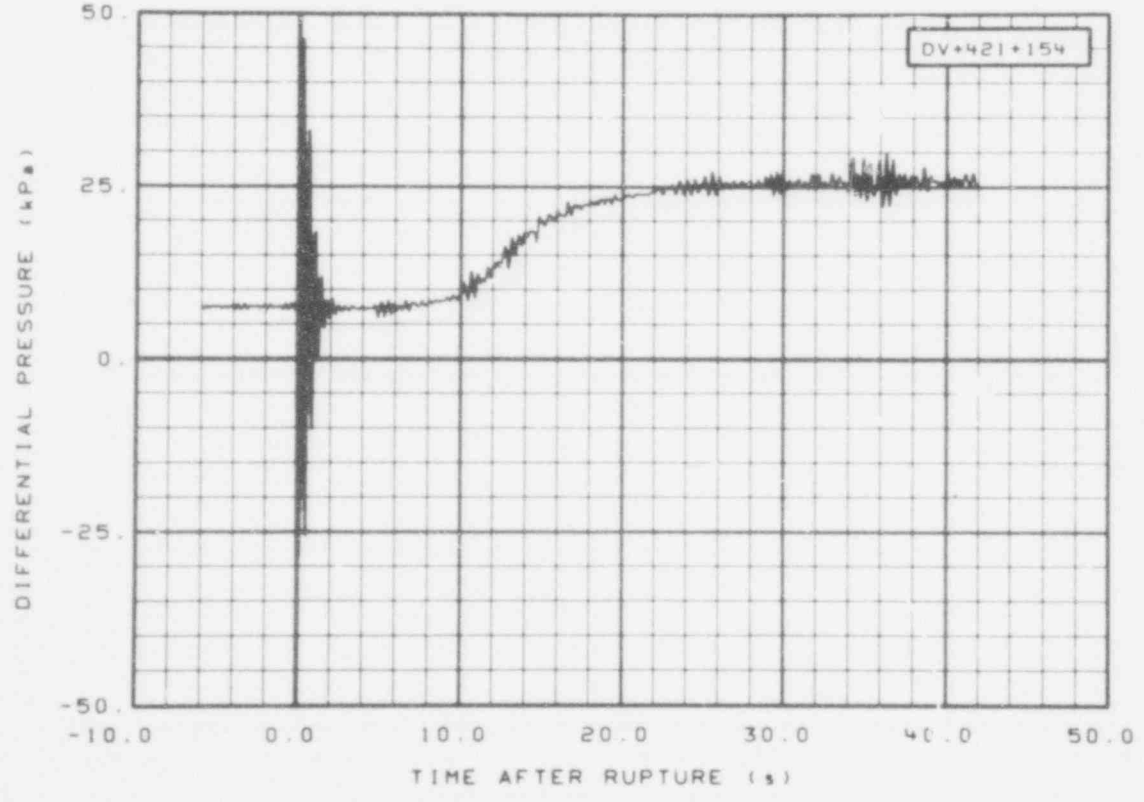

Fig. 194 Differential pressure in vessel (DV + 421 + 154), from -6 to 42 s.

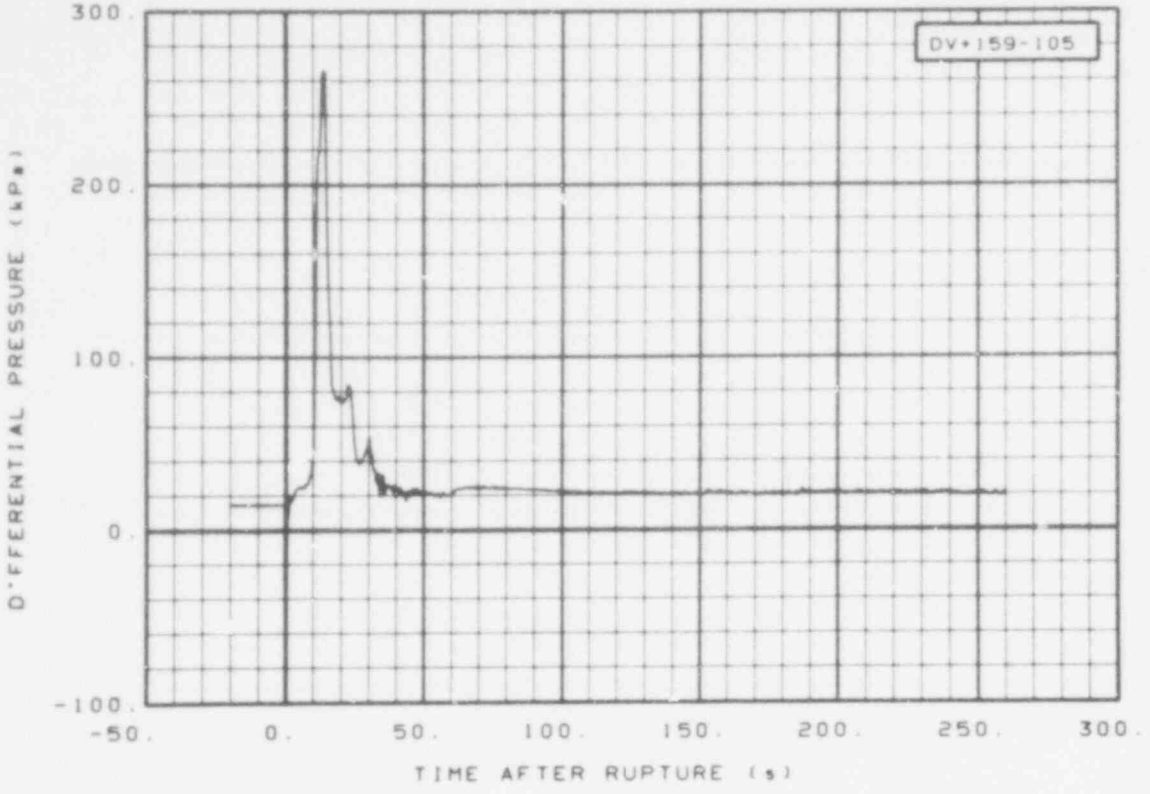

Fig. 195 Differential pressure in vessel (DV + 159-105), from -20 to 260 s.

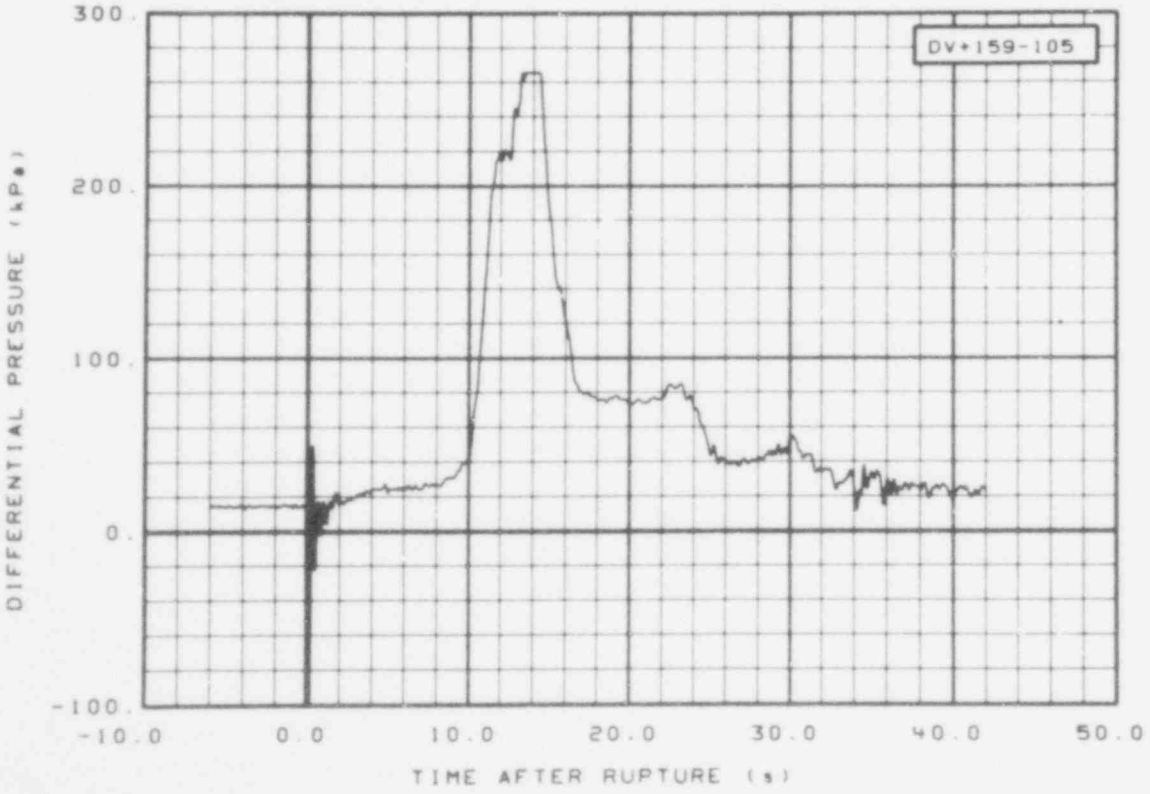

Fig. 196 Differential pressure in vessel (DV + 159-105), from -6 to 42 s.

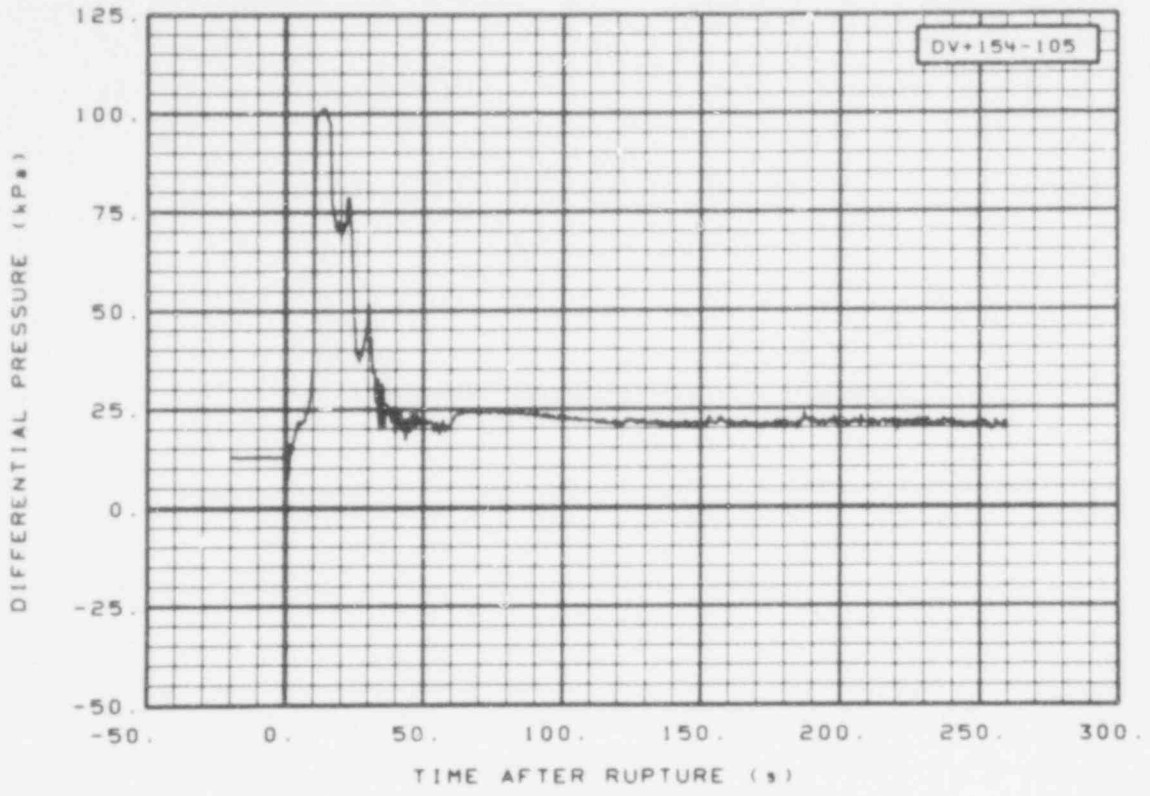

Fig. 197 Differential pressure in vessel (DV + 154-105), from -20 to 260 s.

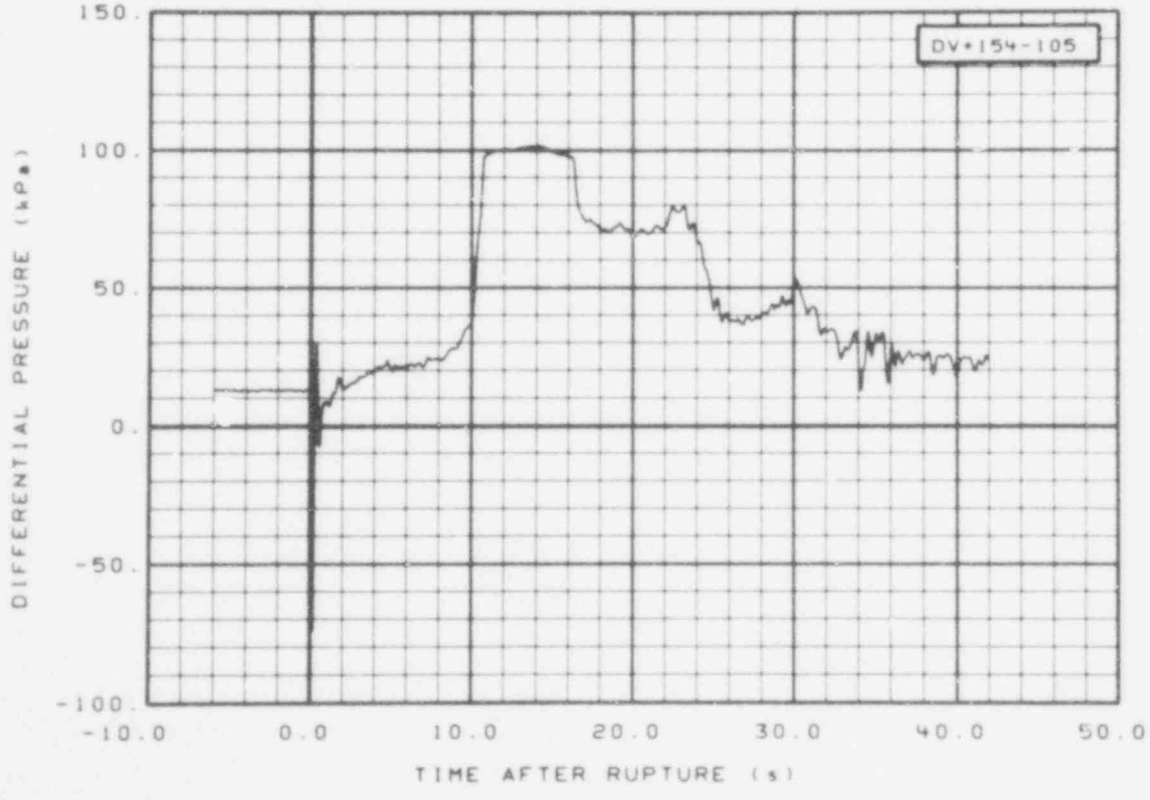

Fig. 198 Differential pressure in vessel (DV + 154-105), from -6 to 42 s.

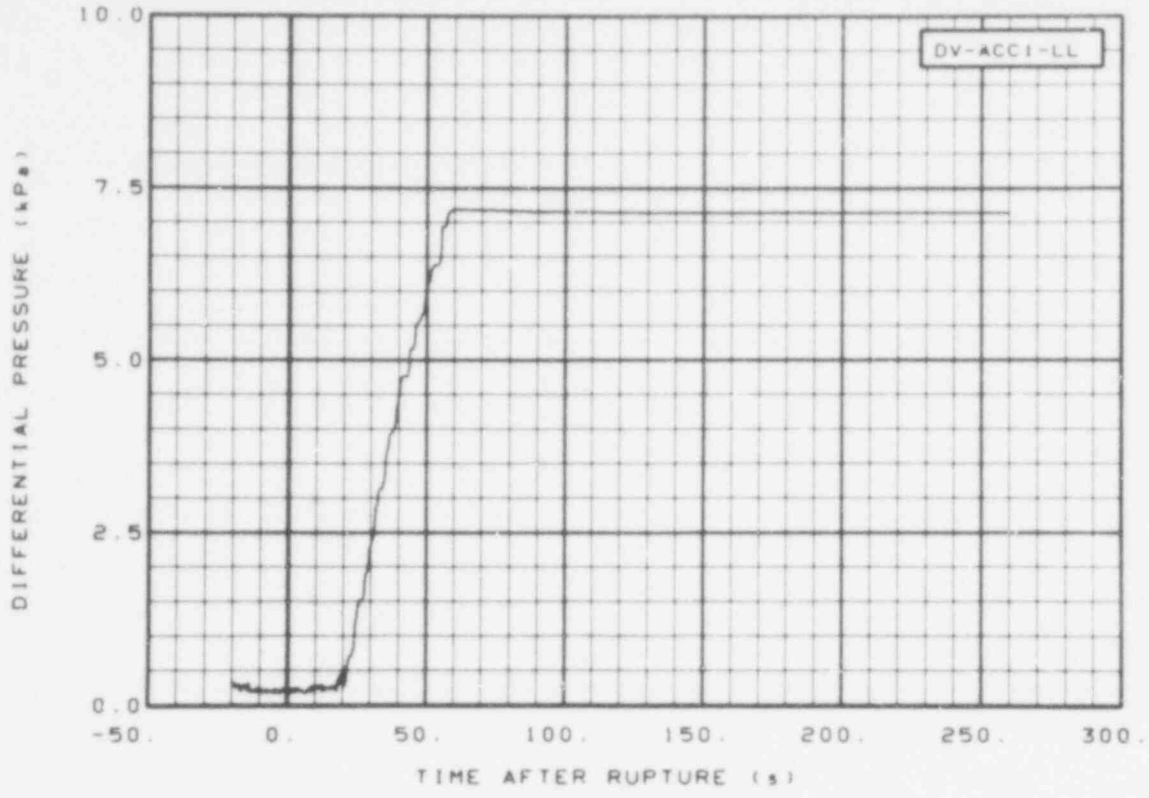

Fig. 199 Differential pressure in vessel ECC accumulator (DV-ACC1-LL), from -20 to 260 s.

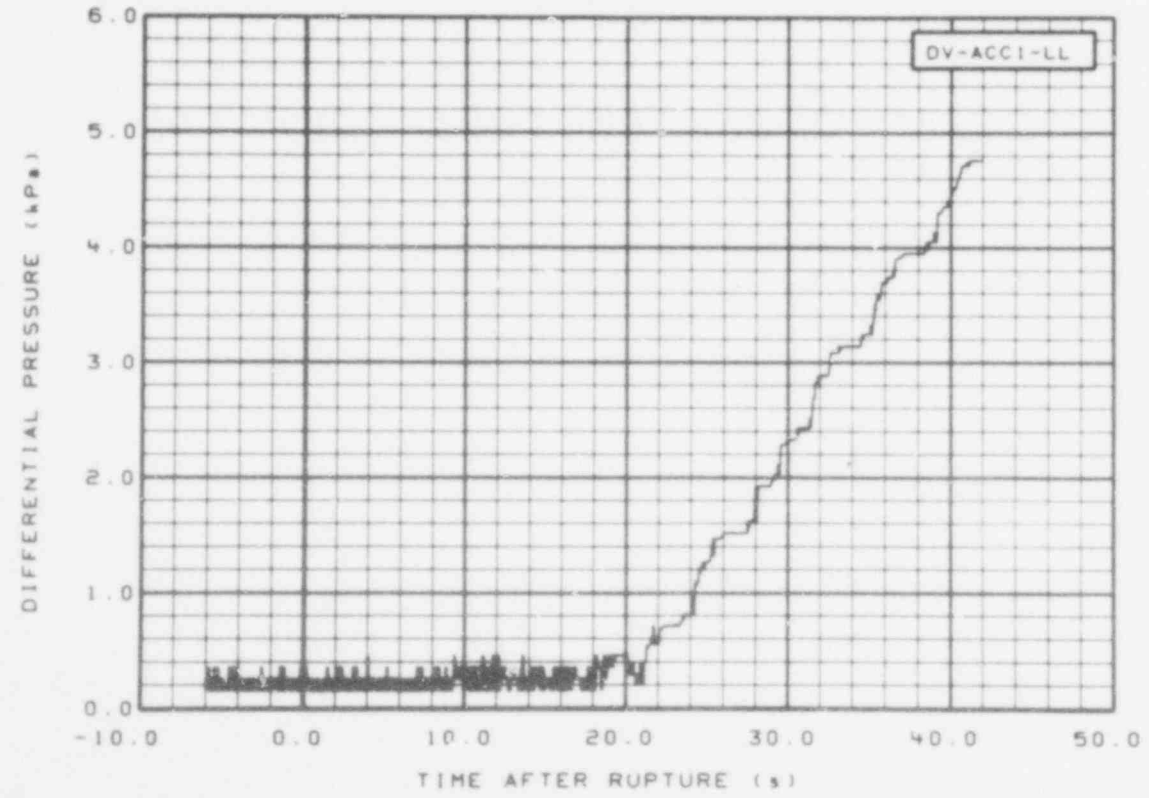

Fig. 200 Differential pressure in vessel ECC accumulator (DV-ACC1-LL), from -6 to 42 s.

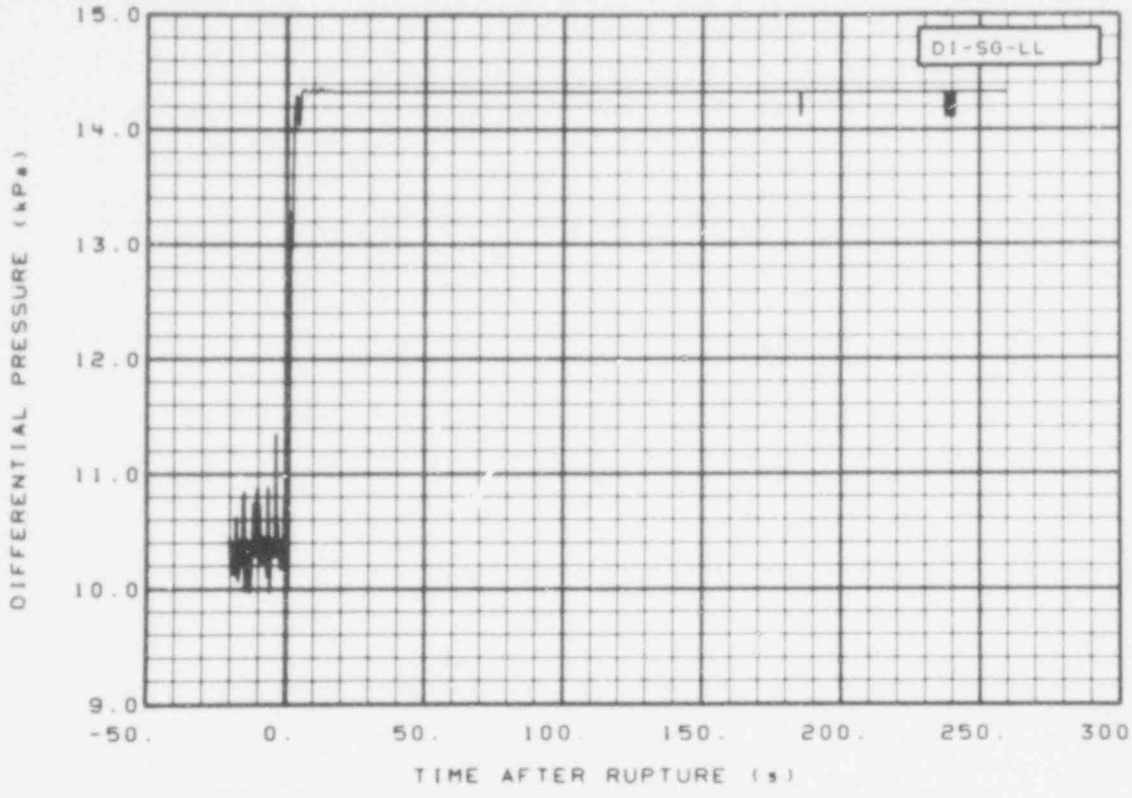

Fig. 201 Differential pressure in intact loop steam generator, secondary side liquid level (DI-SG-LL), from -20 to 260 s.

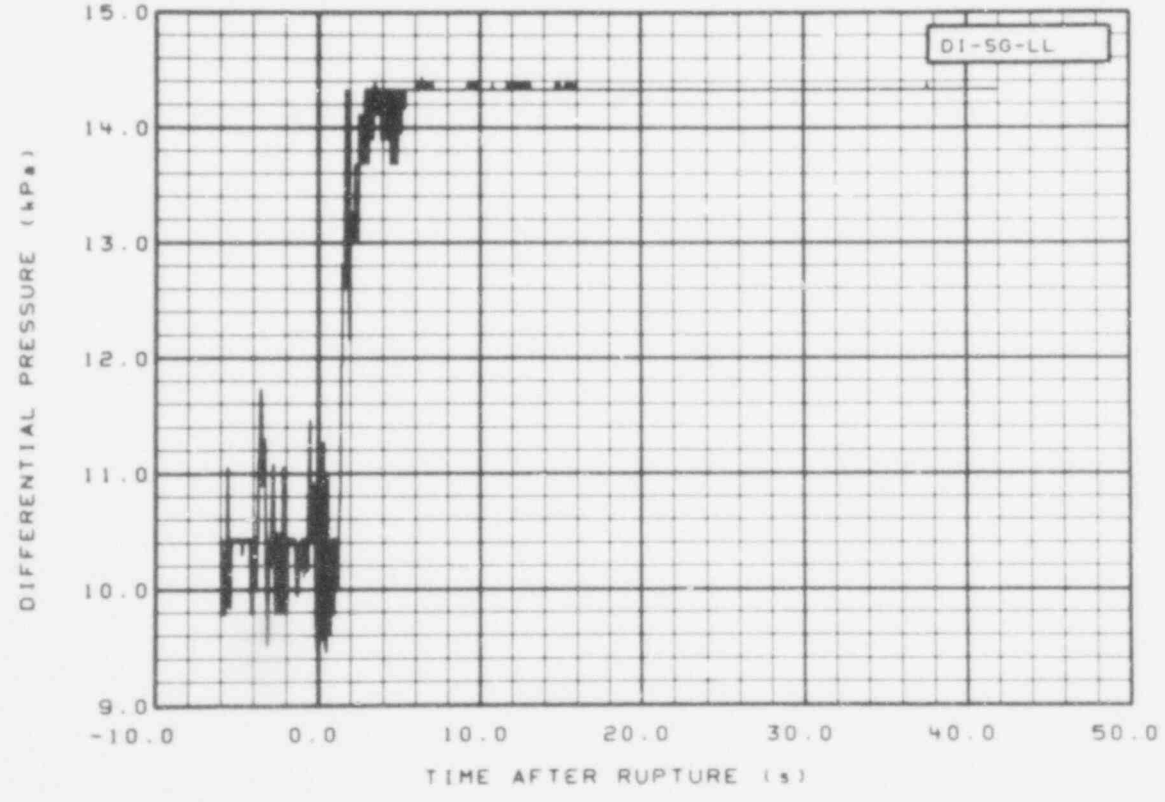

Fig. 202 Differential pressure in intact loop steam generator, secondary side liquid level (DI-SG-LL), from -6 to 42 s.

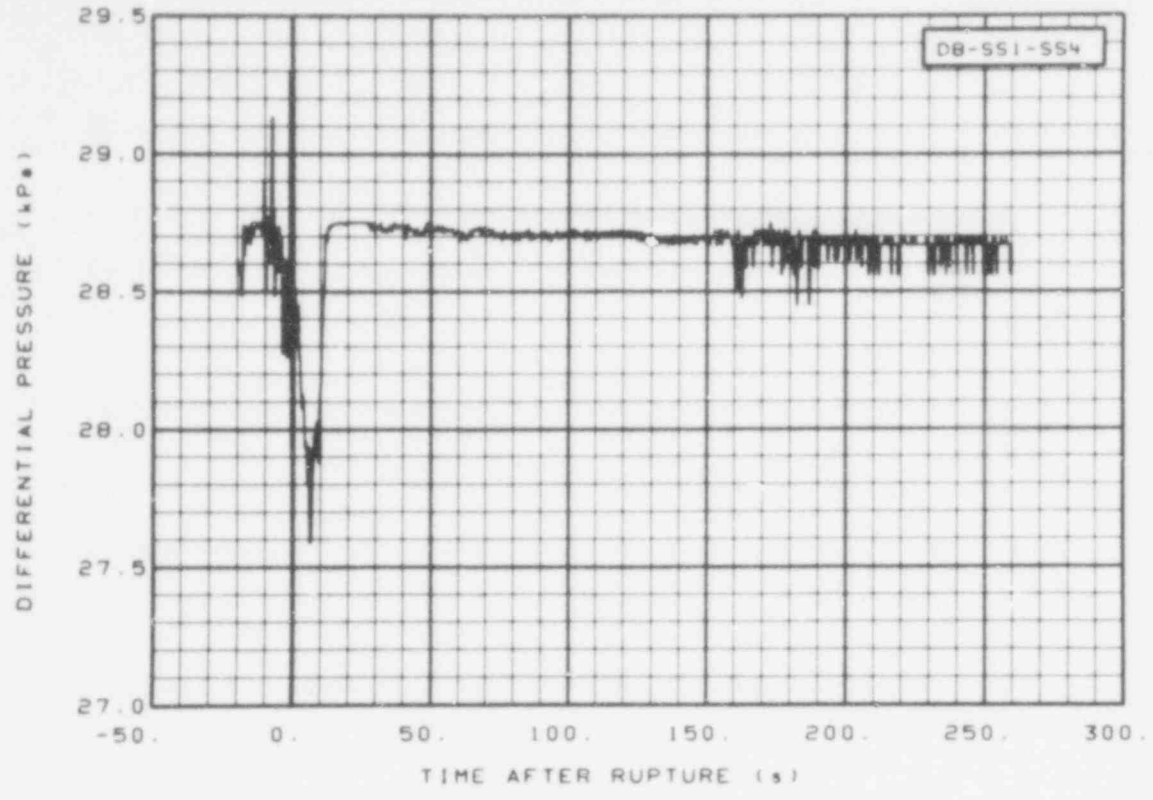

Fig. 203 Differential pressure in broken loop steam generator, secondary liquid level (DB-SS1-SS4), from -20 to 260 s.

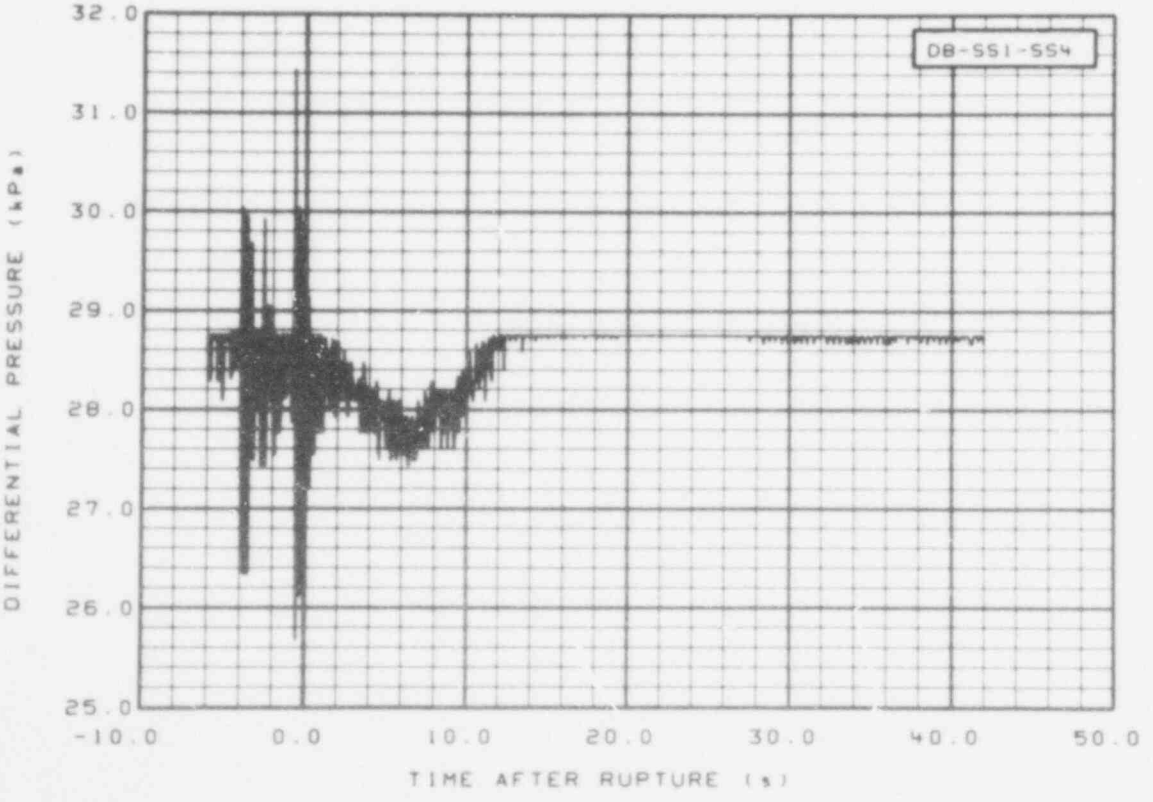

Fig. 204 Differential pressure in broken loop steam generator, secondary liquid level (DB-SS1-SS4), from -6 to 42 s.

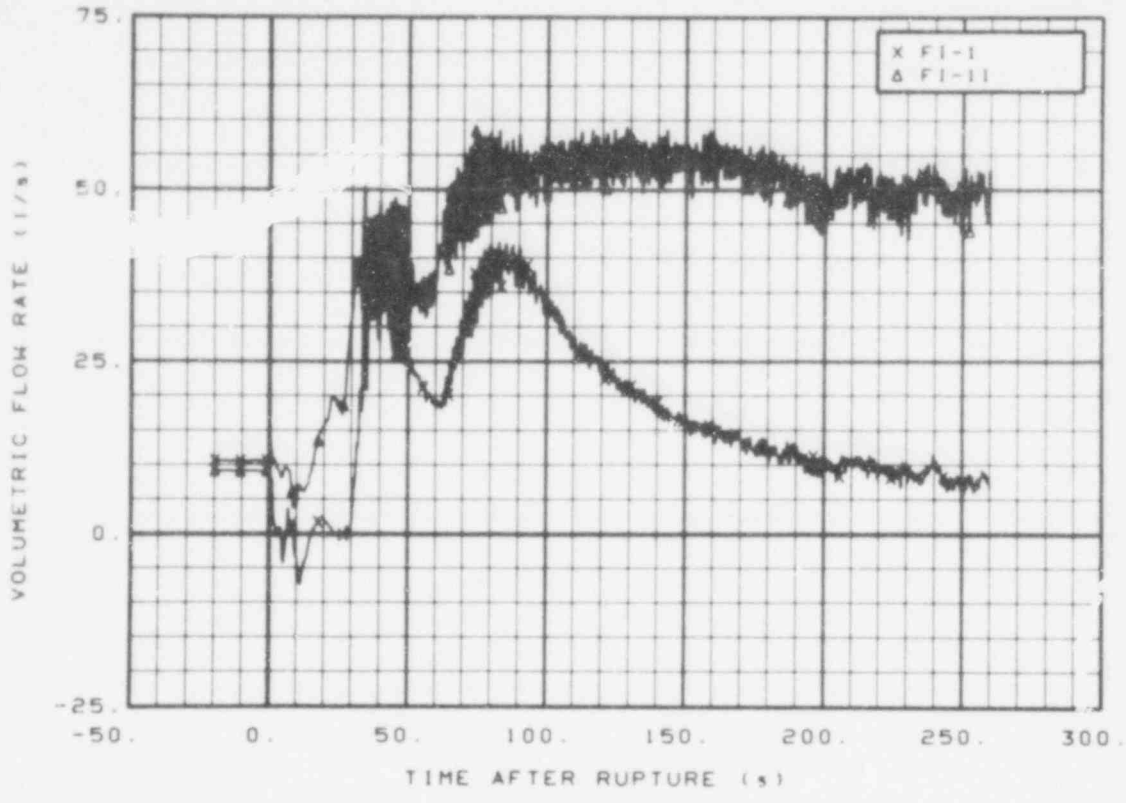

Fig. 205 Volumetric flow in intact loop (FI-1 and FI-11), from -20 to 260 s.

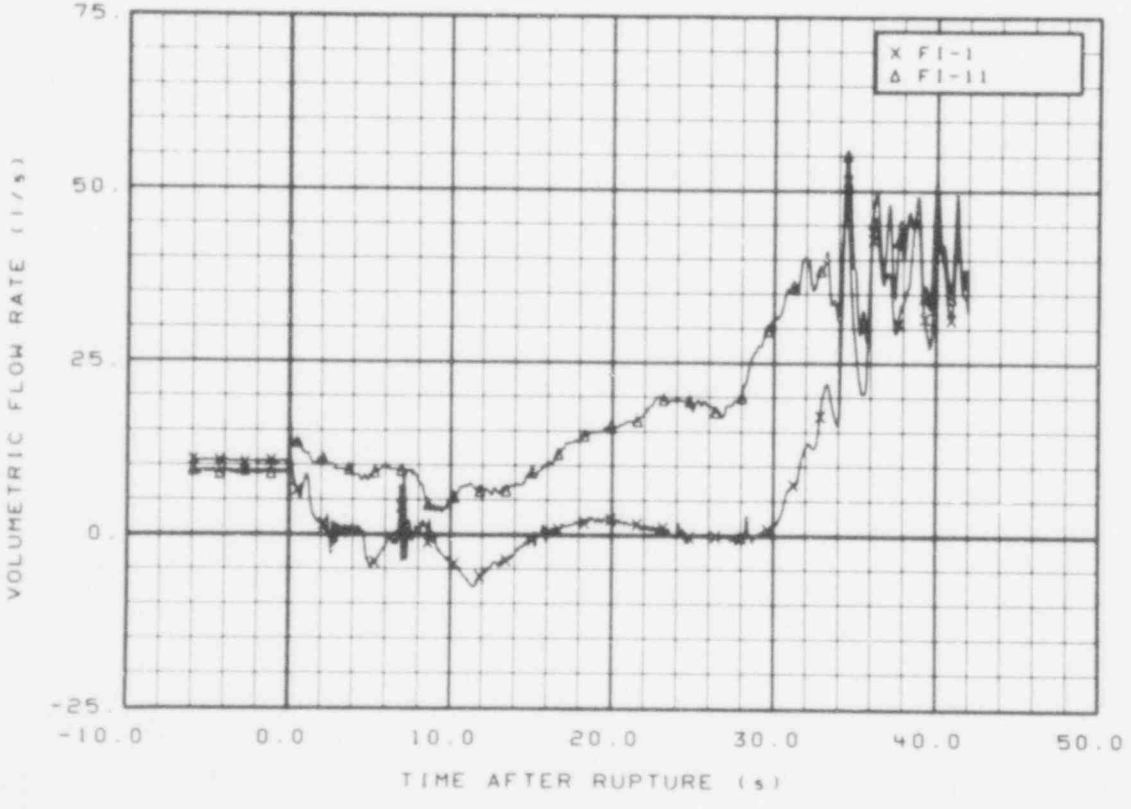

Fig. 206 Volumetric flow in intact loop (FI-1 and FI-11), from -6 to 42 s.

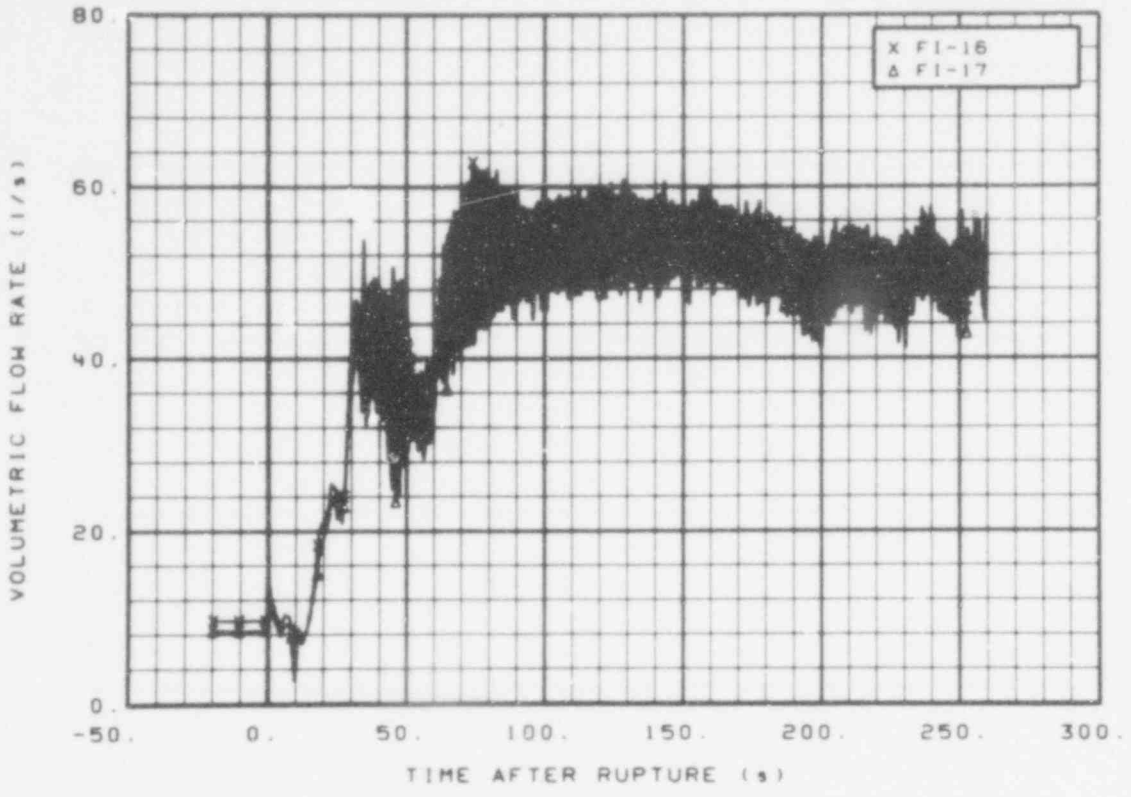

Fig. 207 Volumetric flow in intact loop (FI-16 and FI-17), from -26 to 260 s.

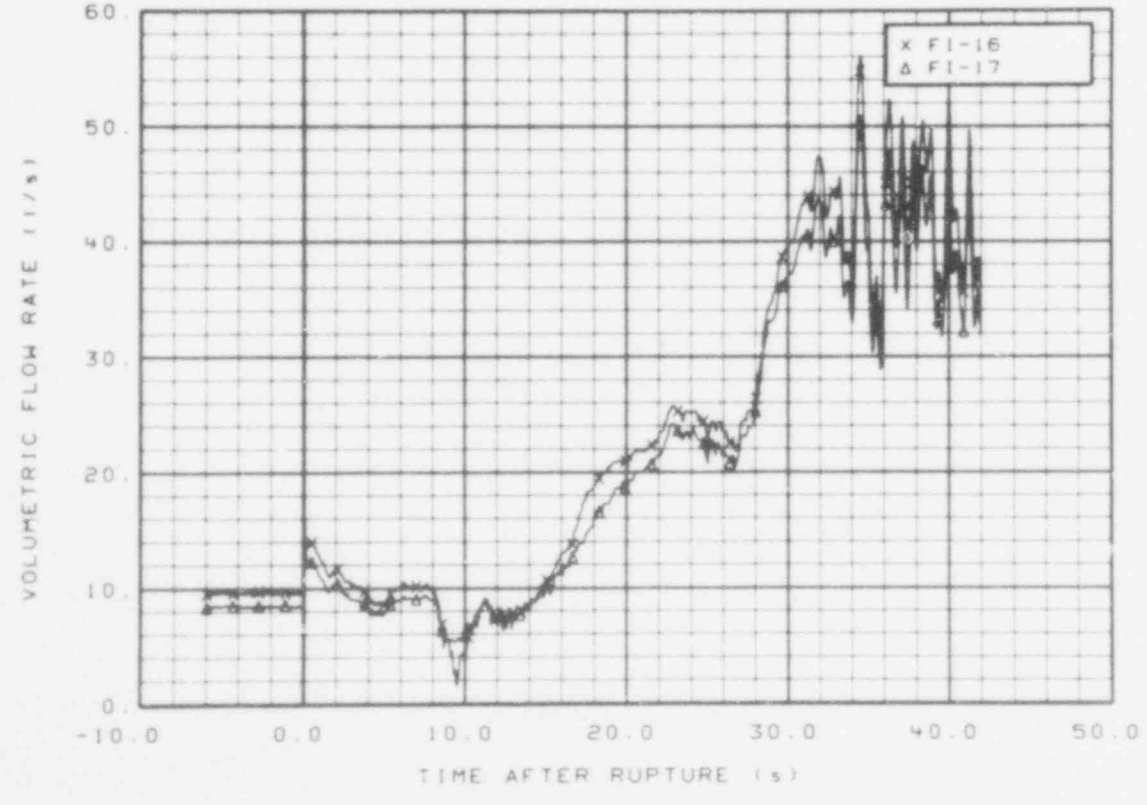

Fig. 208 Volumetric flow in intact loop (FI-16 and FI-17), from -6 to 42 s.

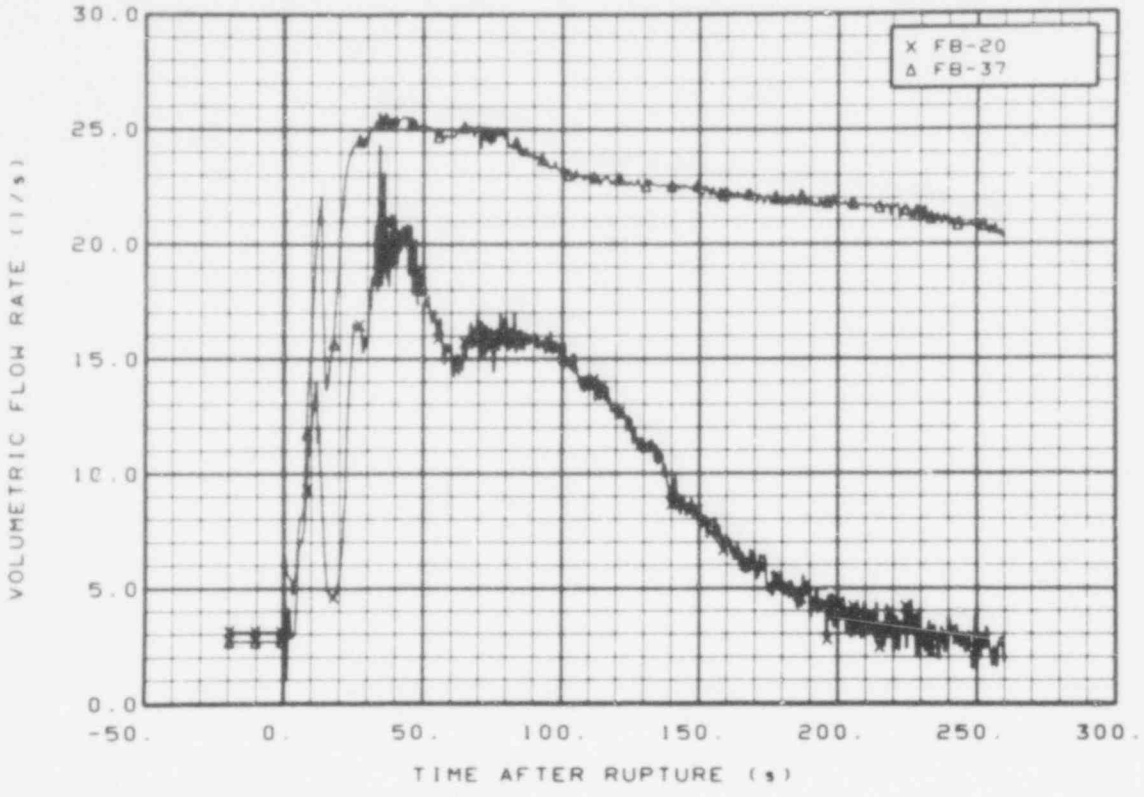

Fig. 209 Volumetric flow in broken loop (FB-20 and FB-37), from -20 to 260 s.

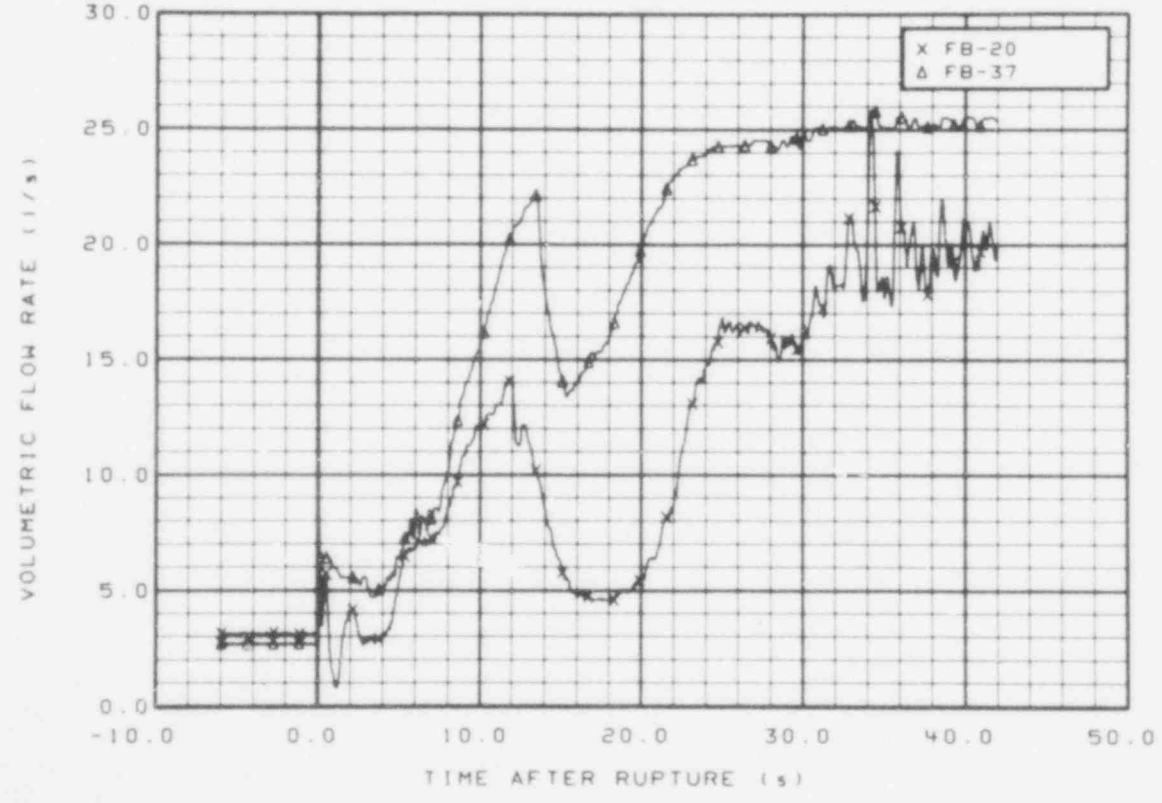

Fig. 210 Volumetric flow in broken loop (FB-20 and FB-37), from -6 to 42 s.

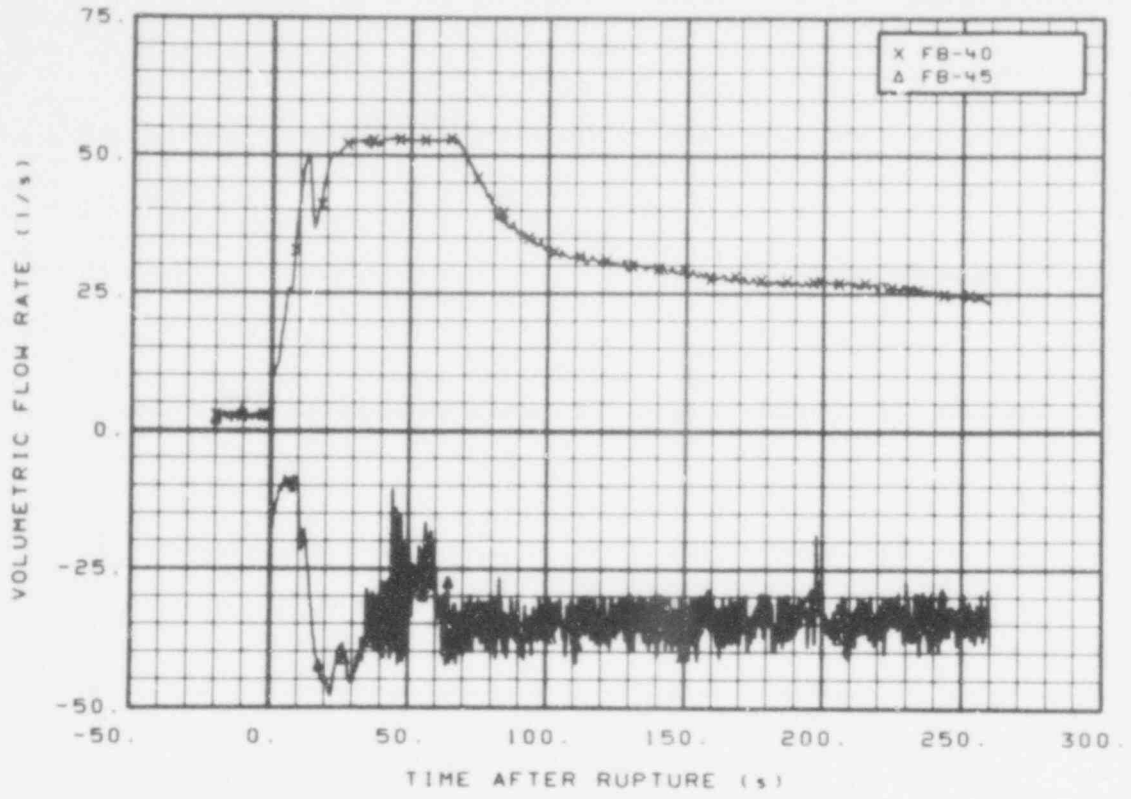

Fig. 211 Volumetric flow in broken loop (FB-40 and FB-45), from -20 to 260 s.

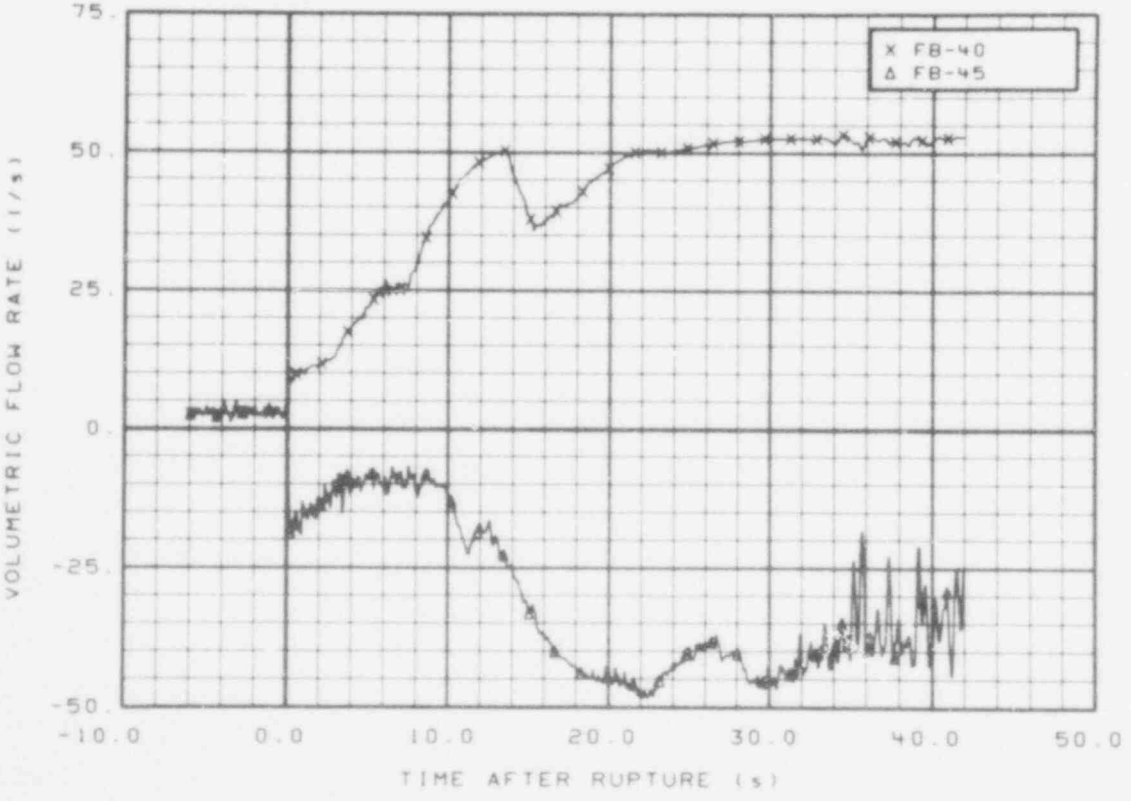

Fig. 212 Volumetric flow in broken loop (FB-40 and FB-45), from -6 to 42 s.

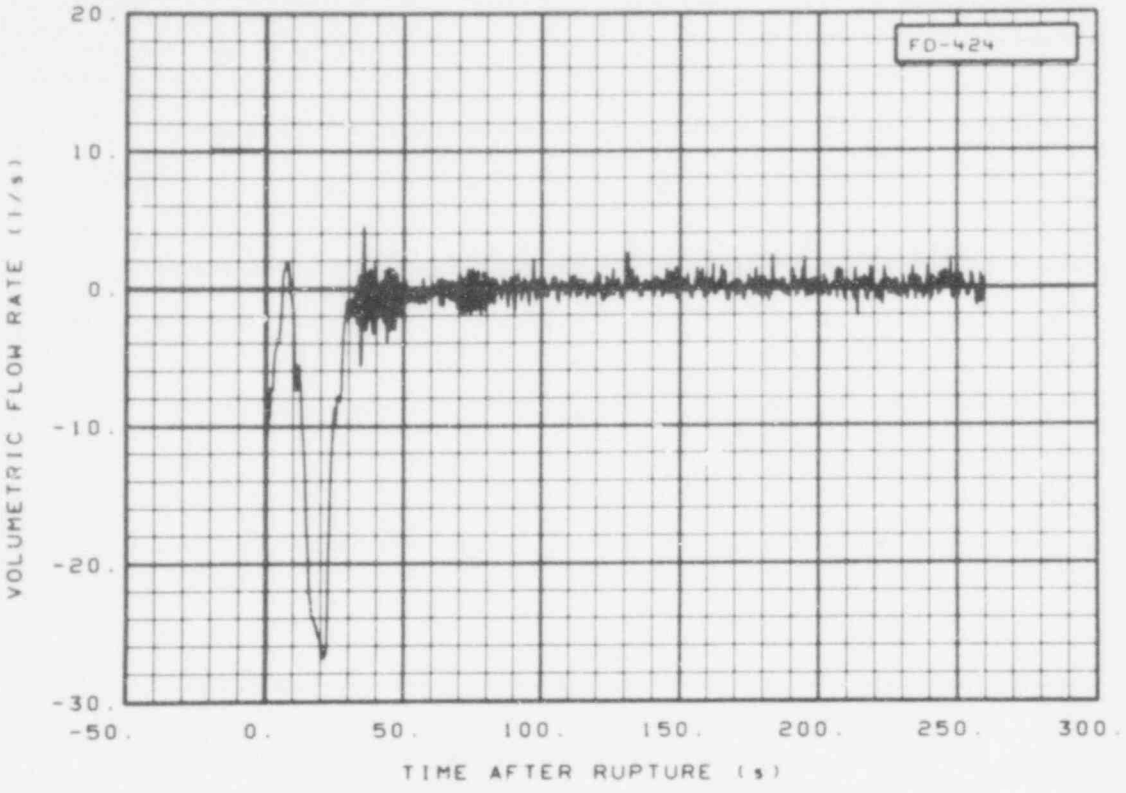

Fig. 213 Volumetric flow in downcomer (FD-424), from -20 to 260 s.

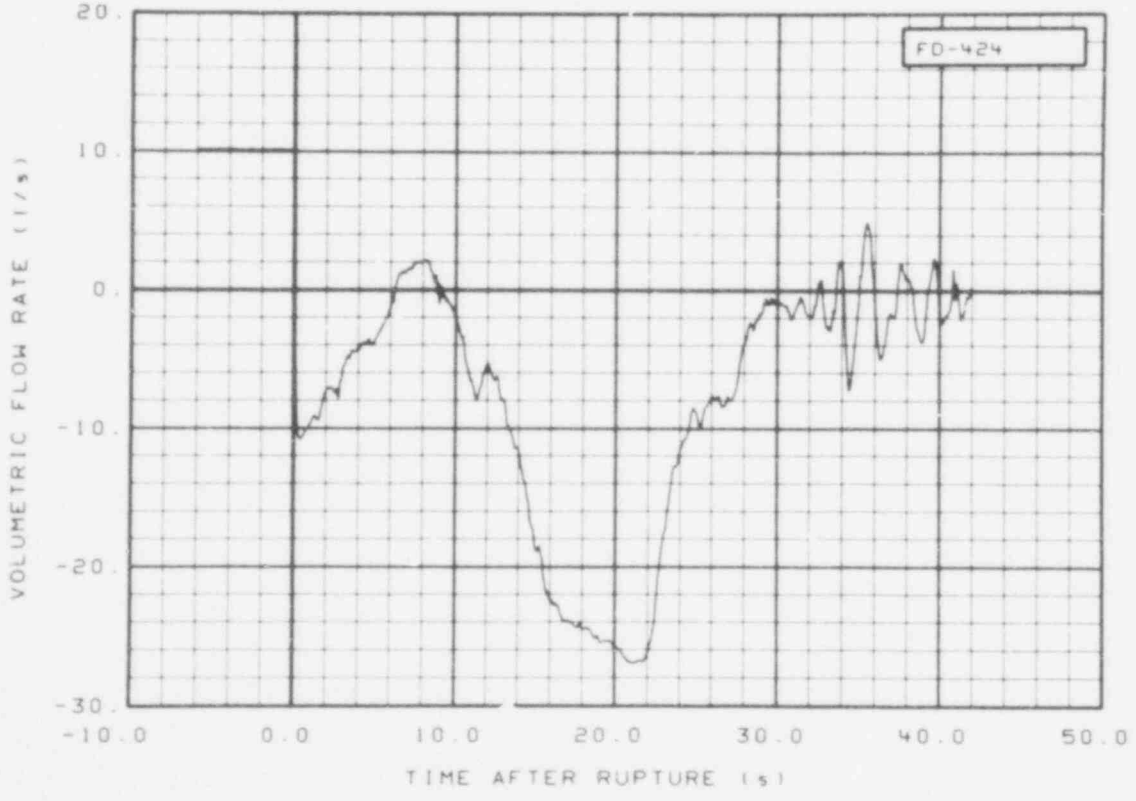

Fig. 214 Volumetric flow in downcomer (FD-424), from -6 to 42 s.

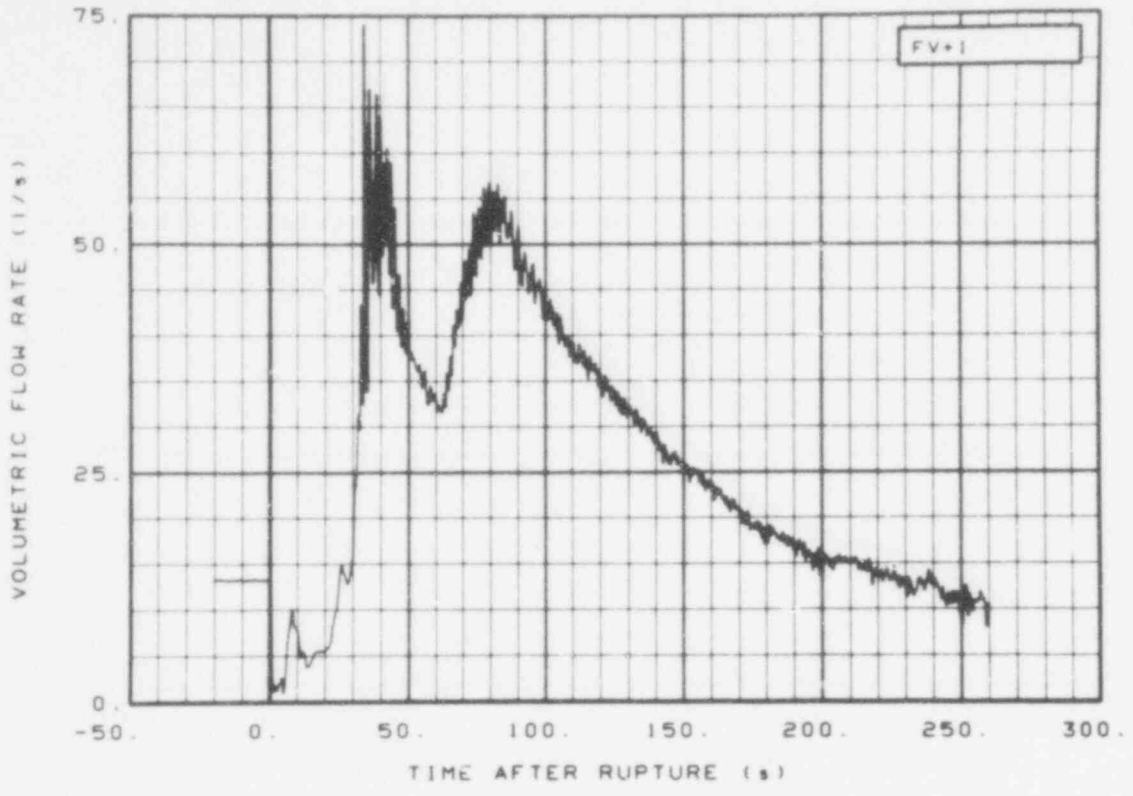

Fig. 215 Volumetric flow in vessel upper plenum (FV + 1), from -20 to 260 s.

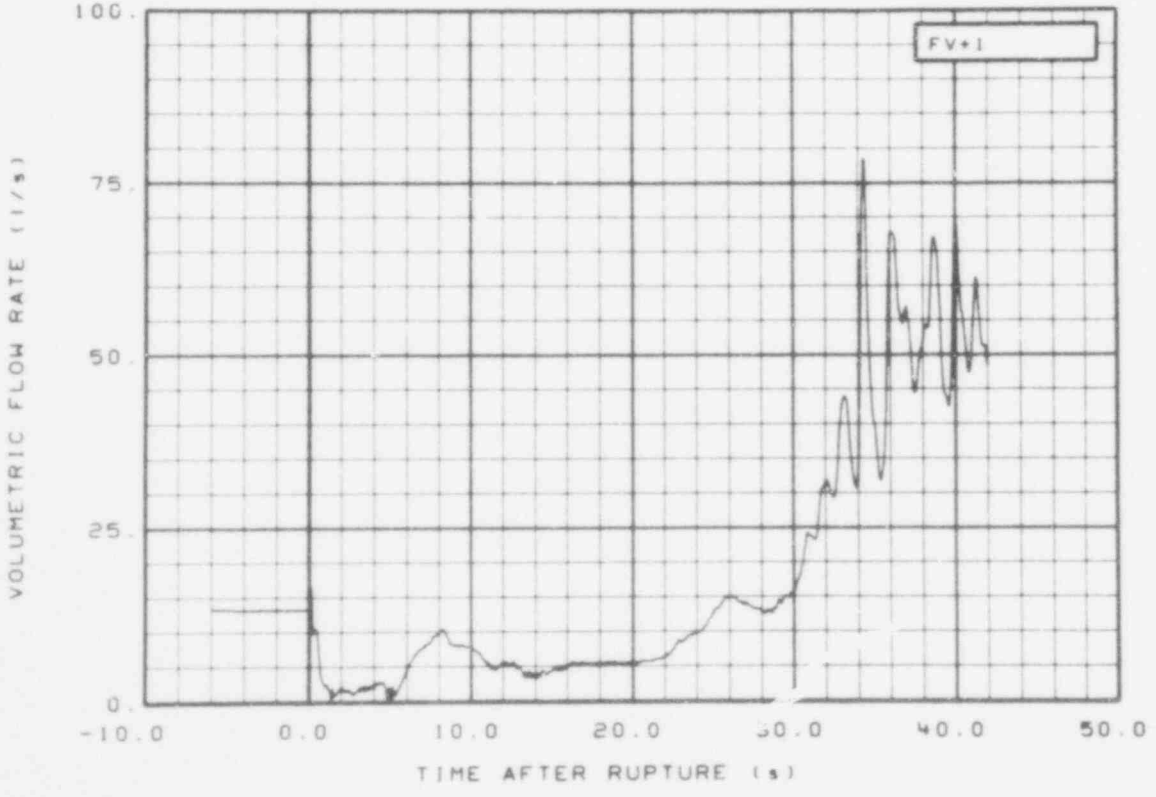

Fig. 216 Volumetric flow in vessel upper plenum (FV + 1), from -6 to 42 s.

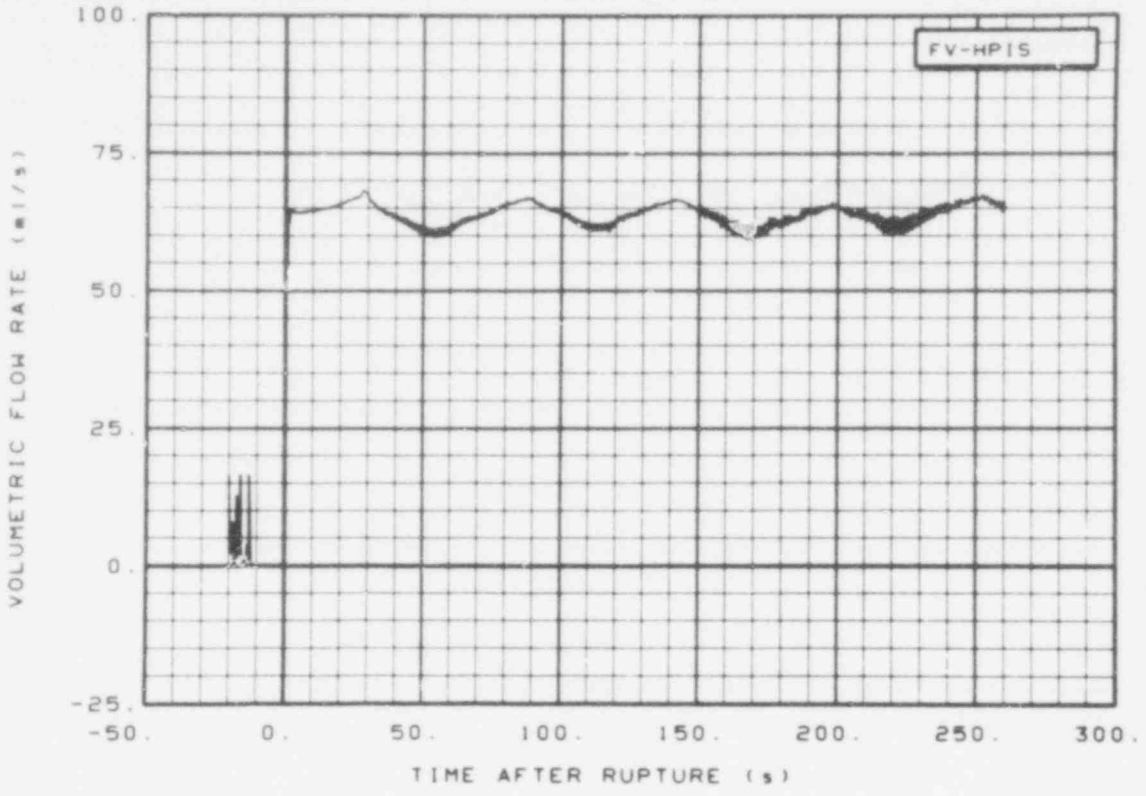

Fig. 217 Volumetric flow in vessel, high pressure injection system (FV-HPIS), from -20 to 260 s.

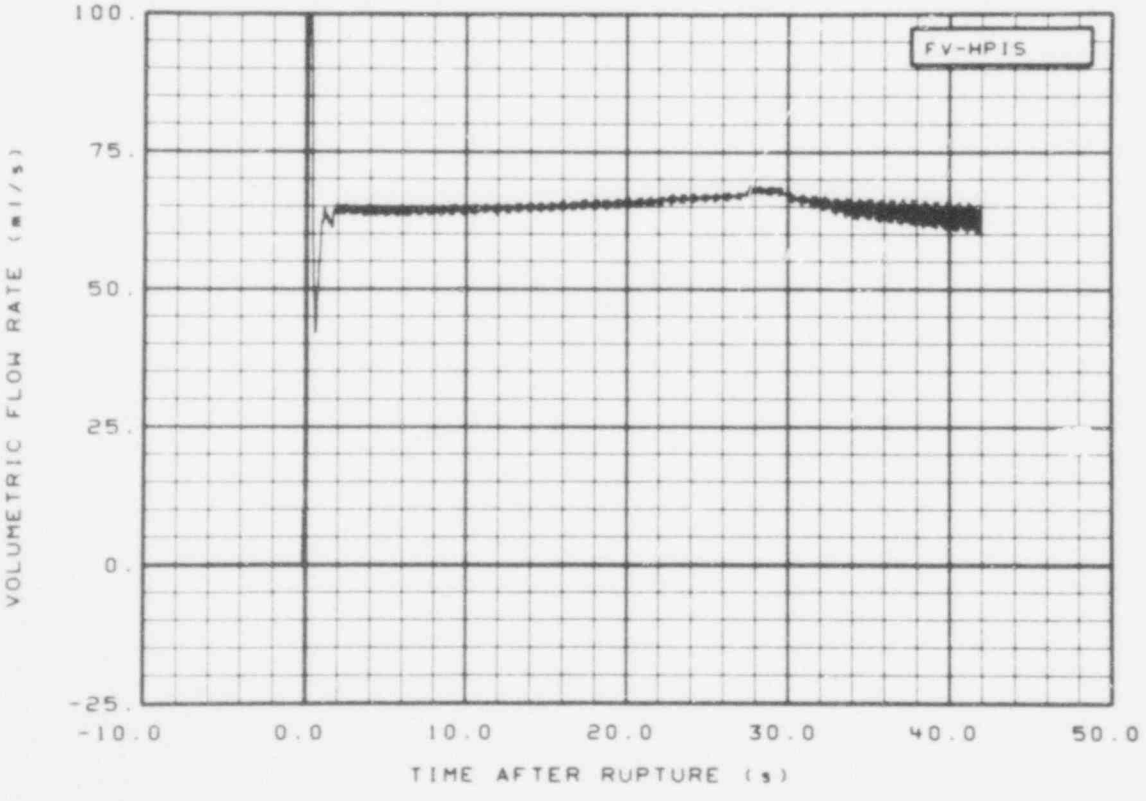

Fig. 218 Volumetric flow in vessel, high pressure injection system (FV-HPIS), from -6 to 42 s.

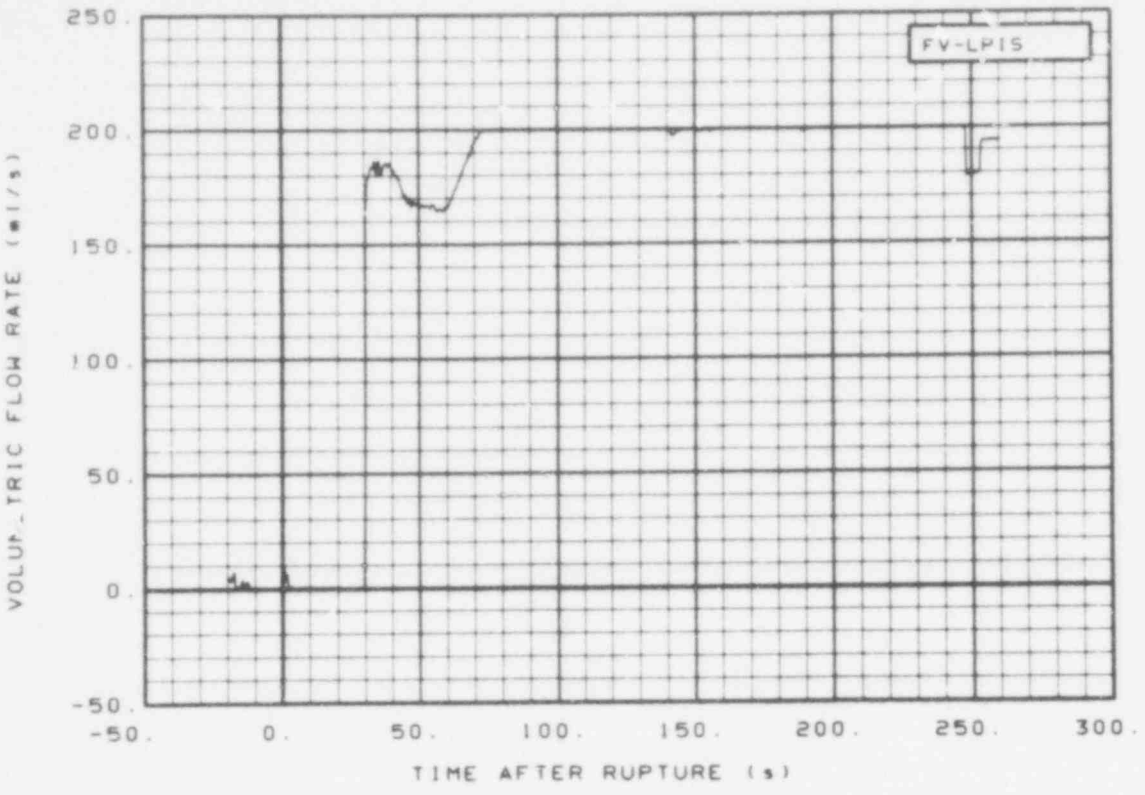

Fig. 219 Volumetric flow in vessel, low pressure injection system (FV-LPIS), from -20 to 260 s.

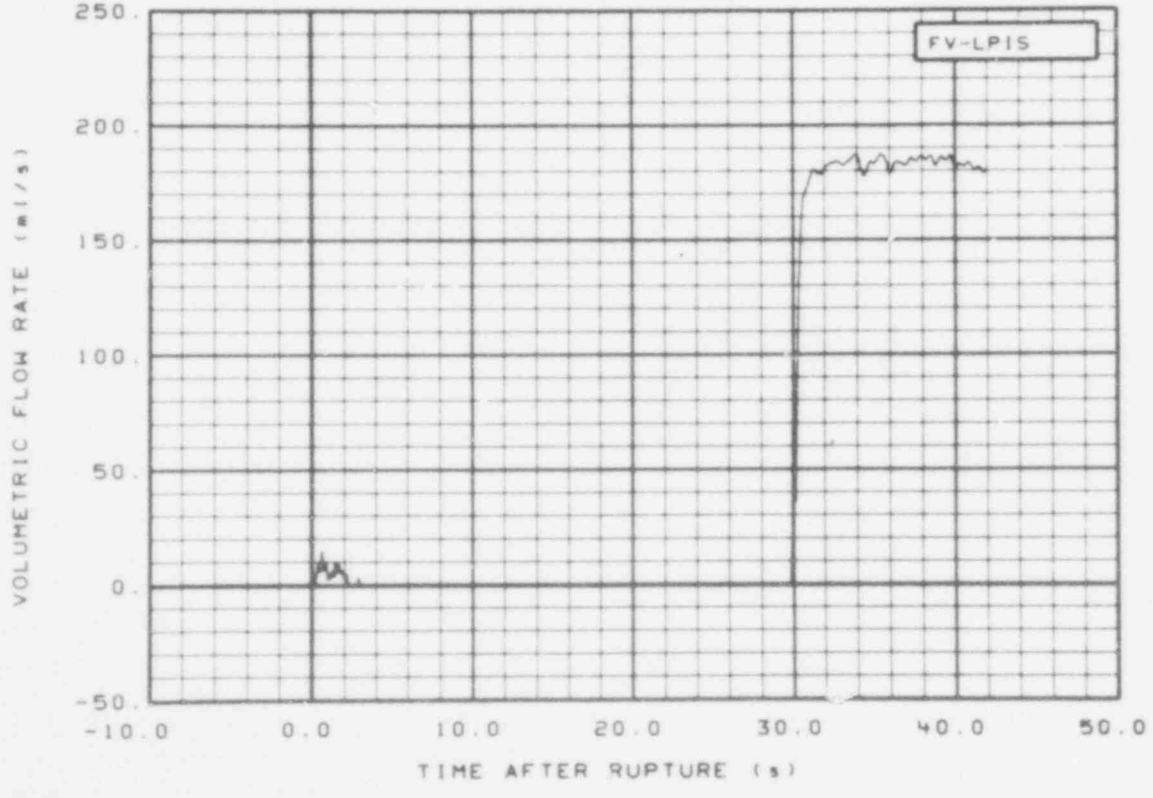

Fig. 220 Volumetric flow in vessel, low pressure injection system (FV-LPIS), from -6 to 42 s.

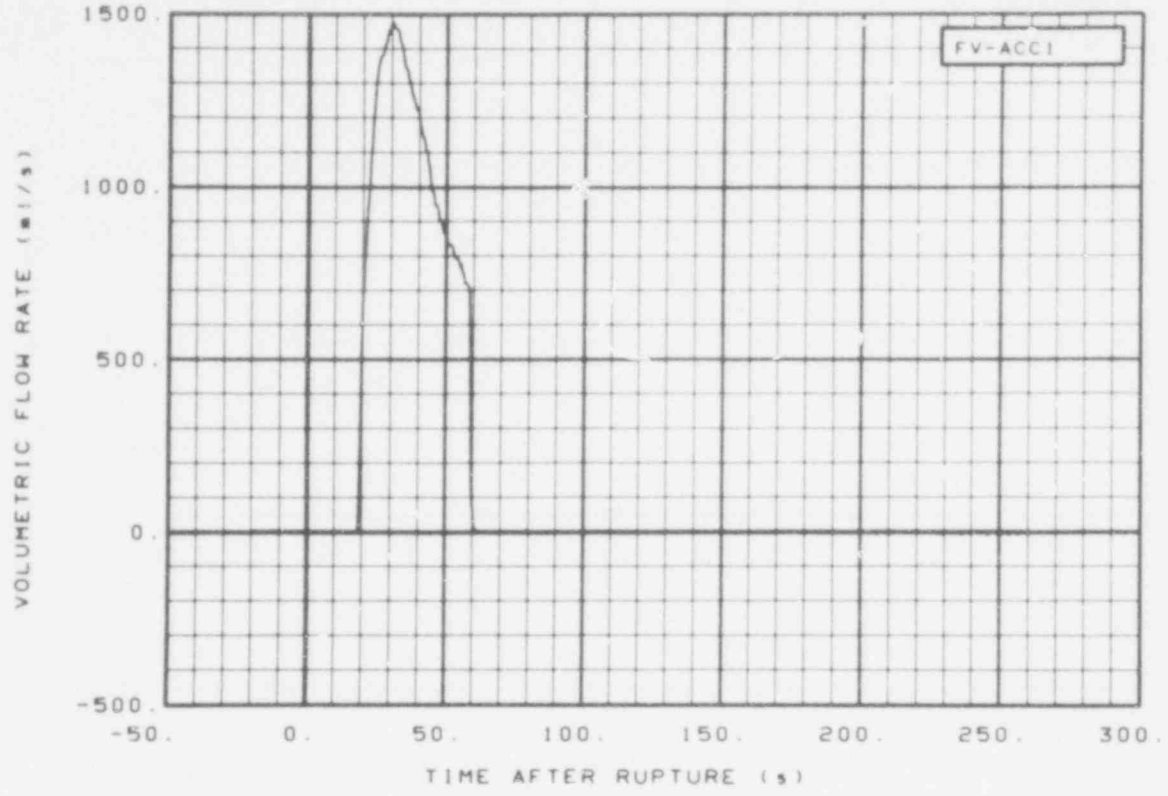

Fig. 221 Volumetric flow in vessel, ECC accumulator (FV-ACC1), from -20 to 260 s.

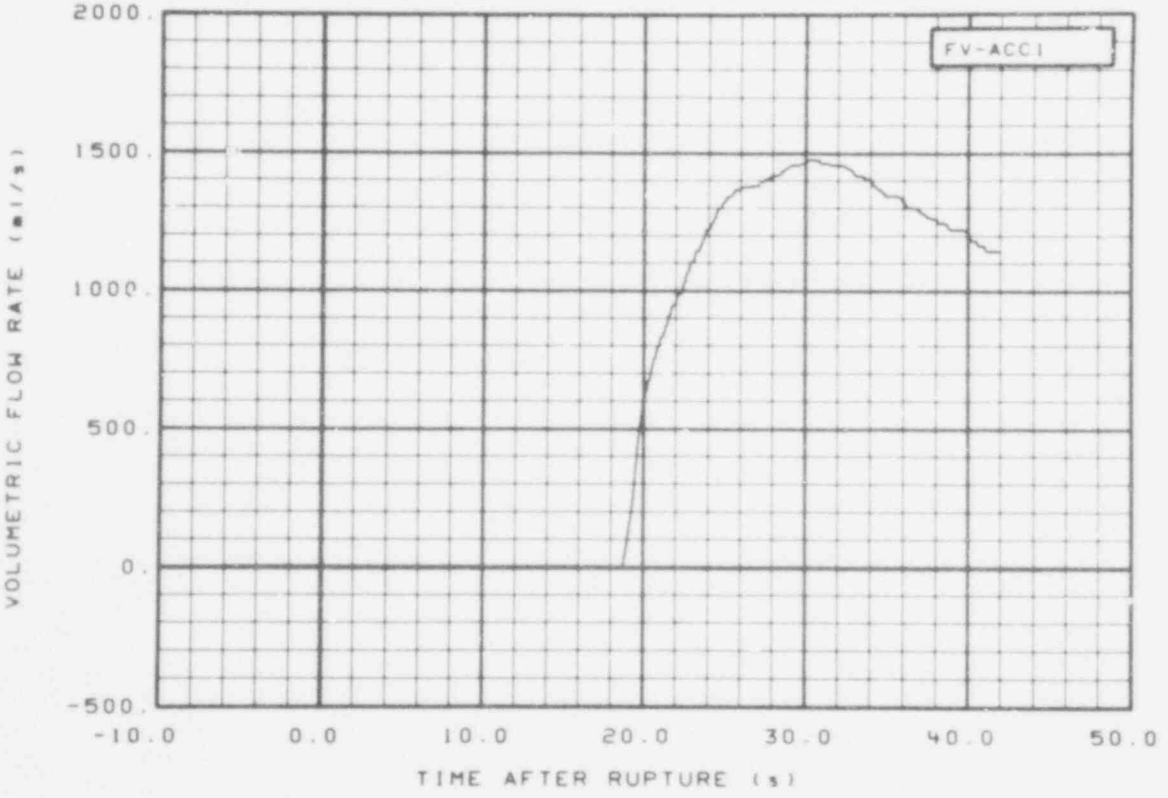

Fig. 222 Volumetric flow in vessel, ECC accumulator (FV-ACC1), from -6 to 42 s.

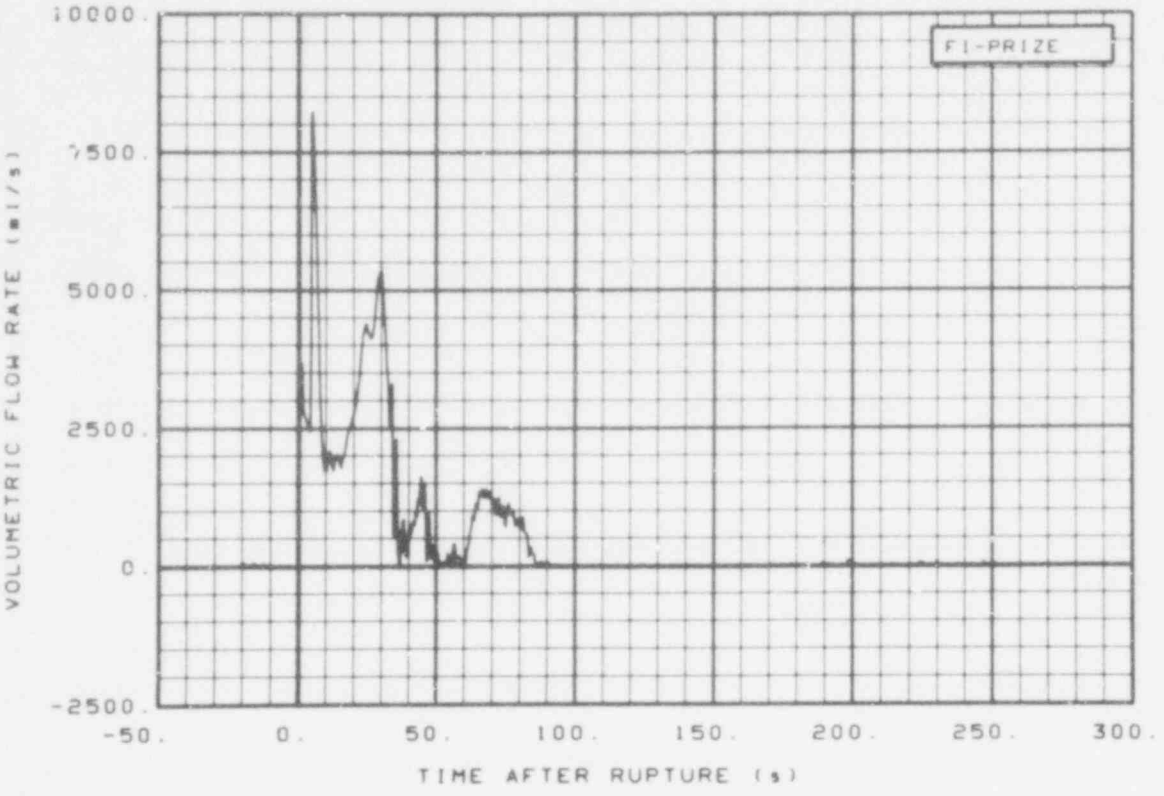

Fig. 223 Volumetric flow in intact loop, pressurizer surge line (FI-PRIZE), from -20 to 260 s.

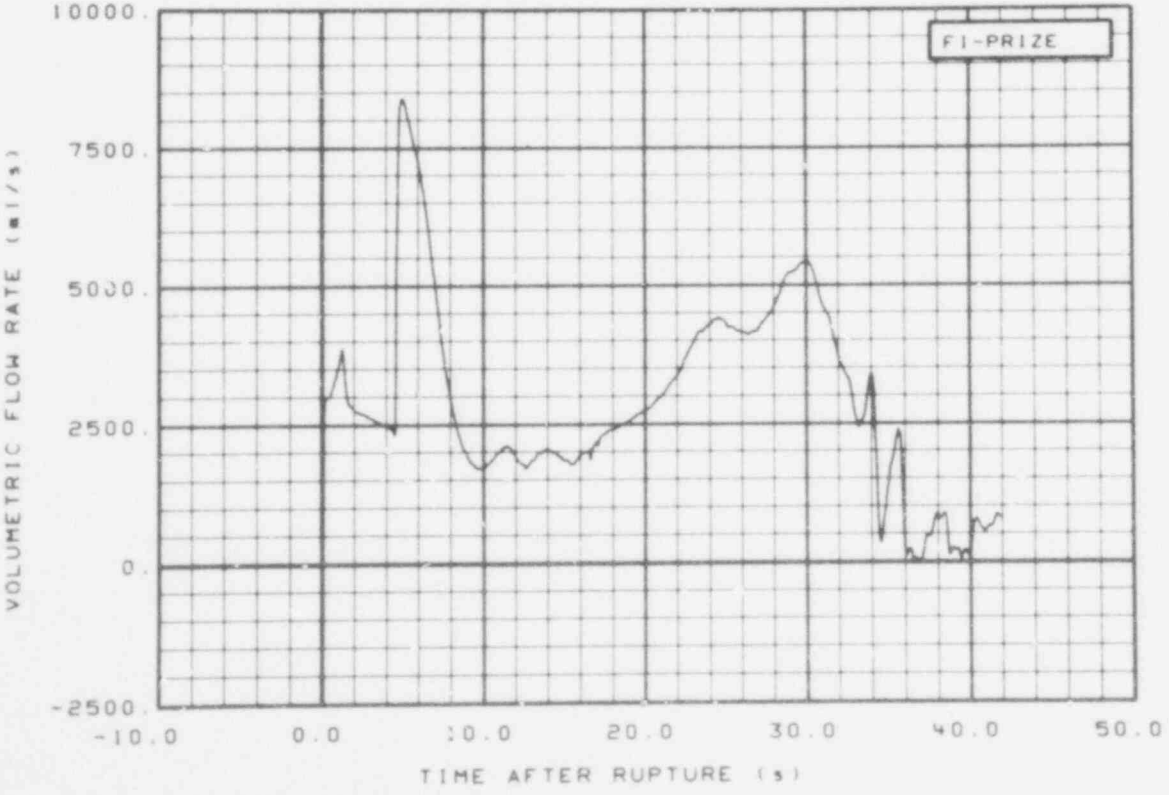

Fig. 224 Volumetric flow in intact loop, pressurizer surge line (FI-PRIZE), from -6 to 42 s.

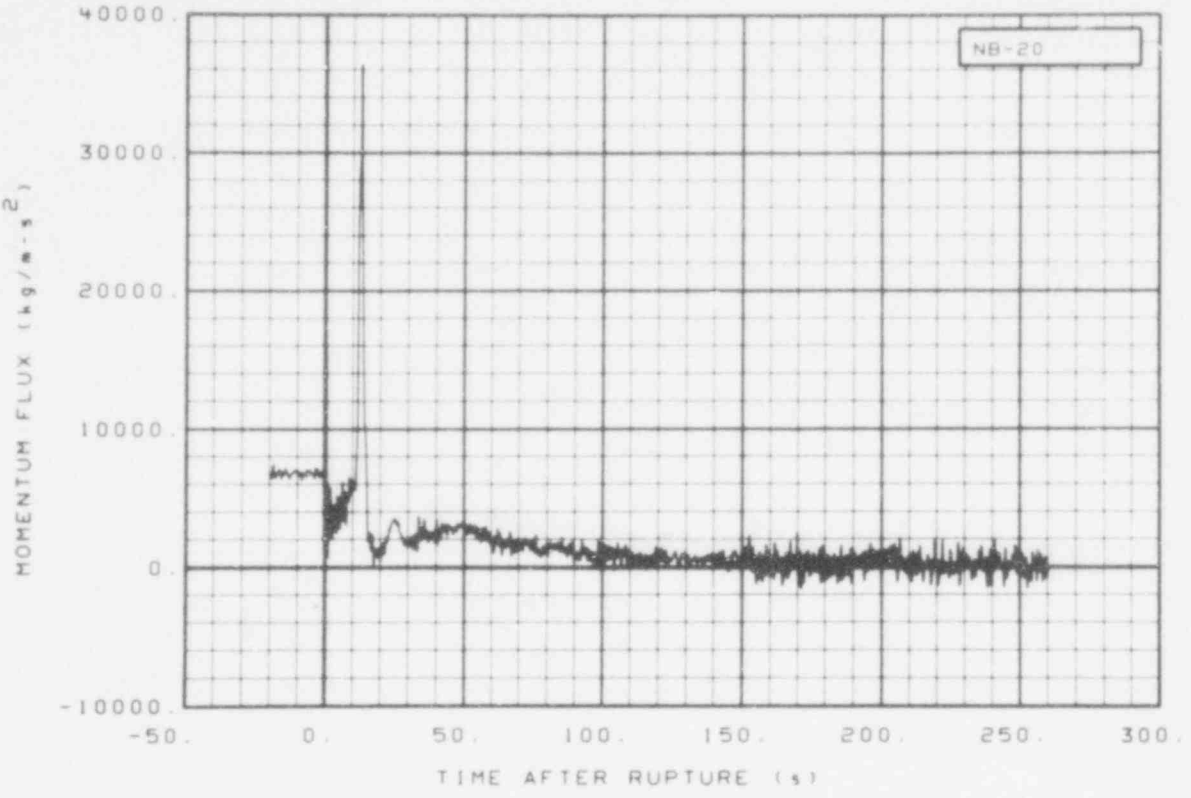

Fig. 225 Momentum flux in broken loop (NB-20), from -20 to 260 s.

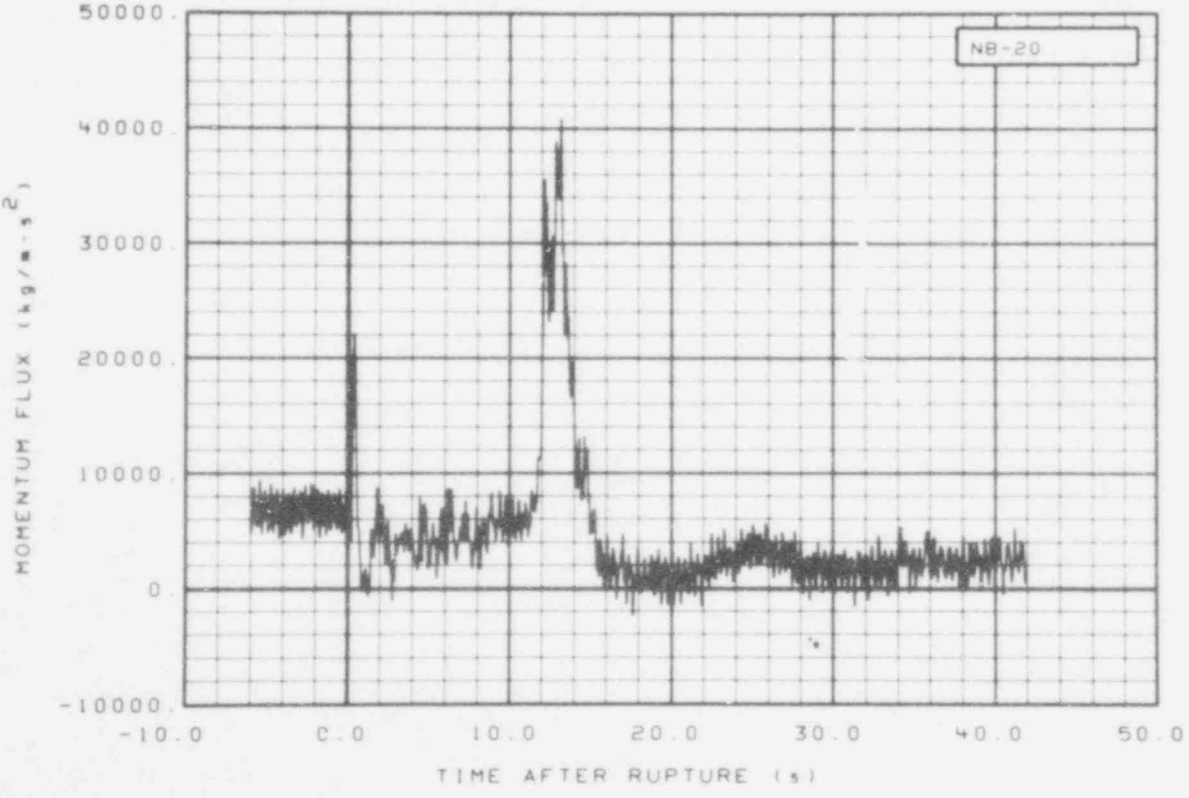

Fig. 226 Momentum flux in broken loop (NB-20), from -6 to 42 s.

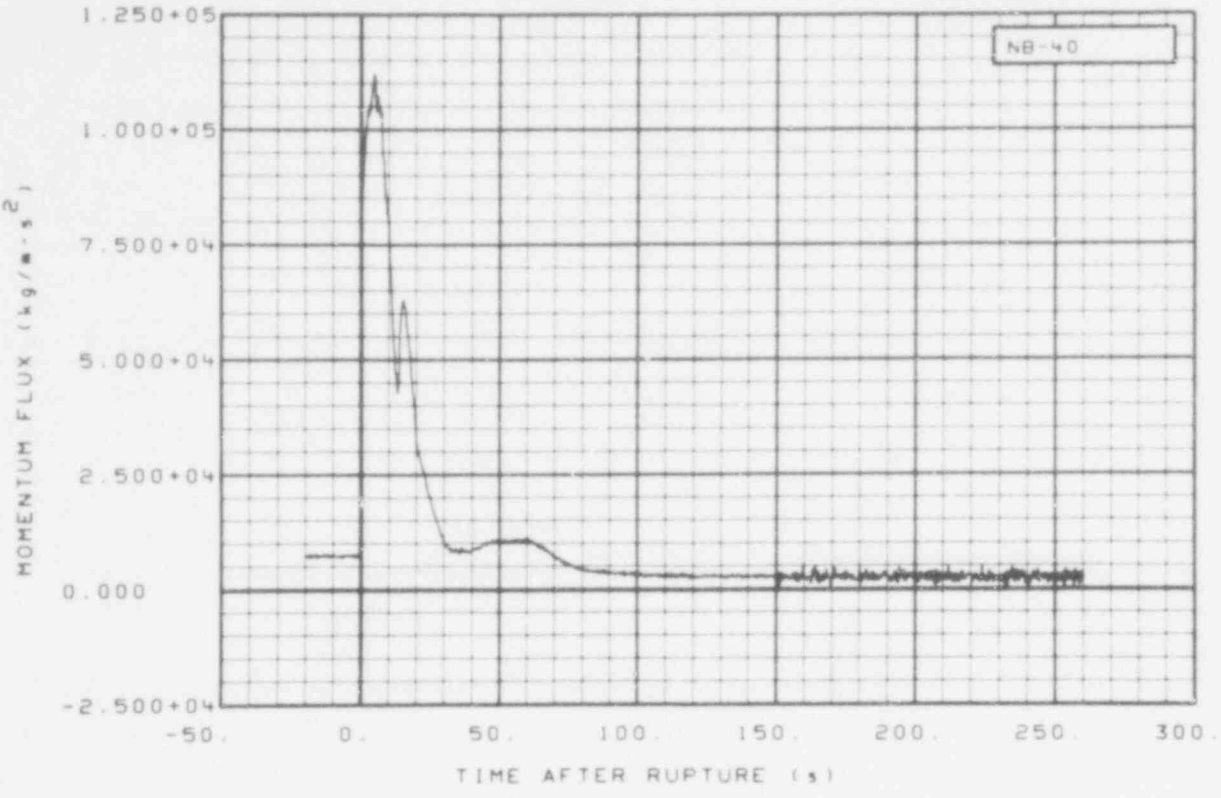

Fig. 227 Momentum flux in broken loop (NB-40), from -20 to 260 s.

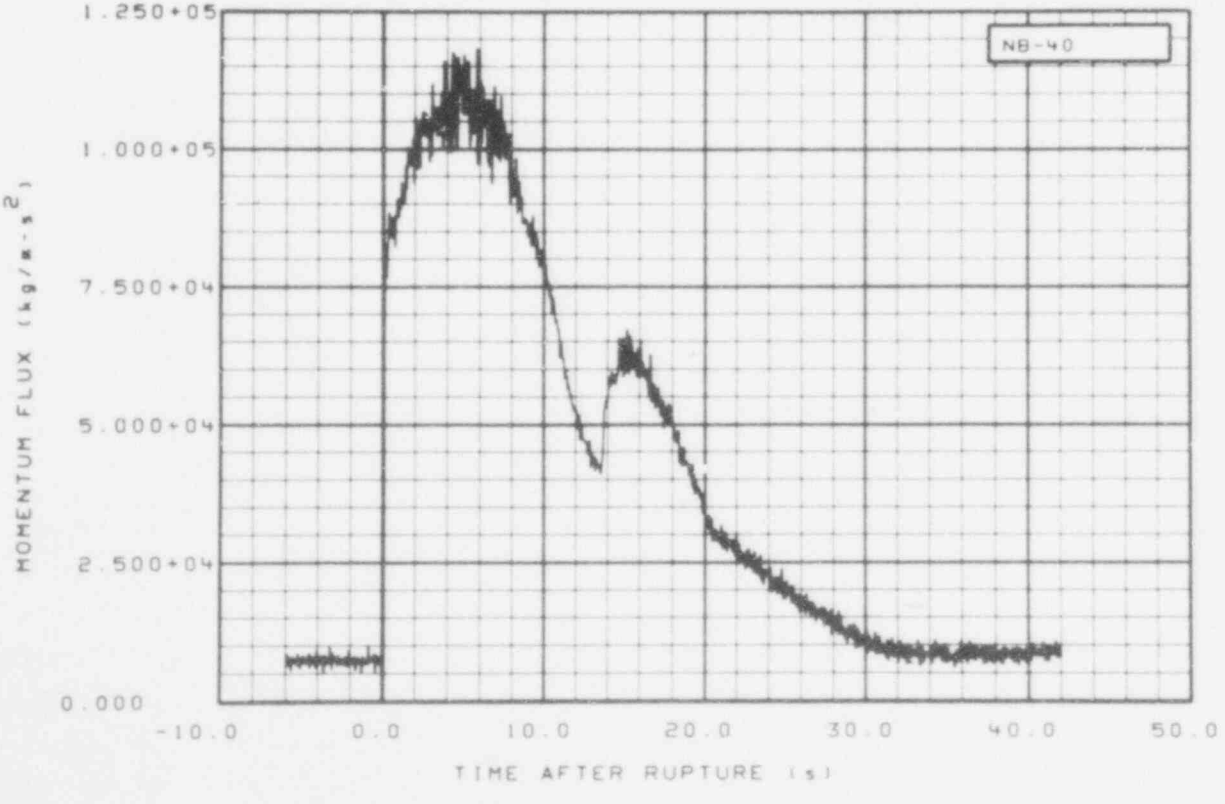

Fig. 228 Momentum flux in broken loop (NB-40), from -6 to 42 s.

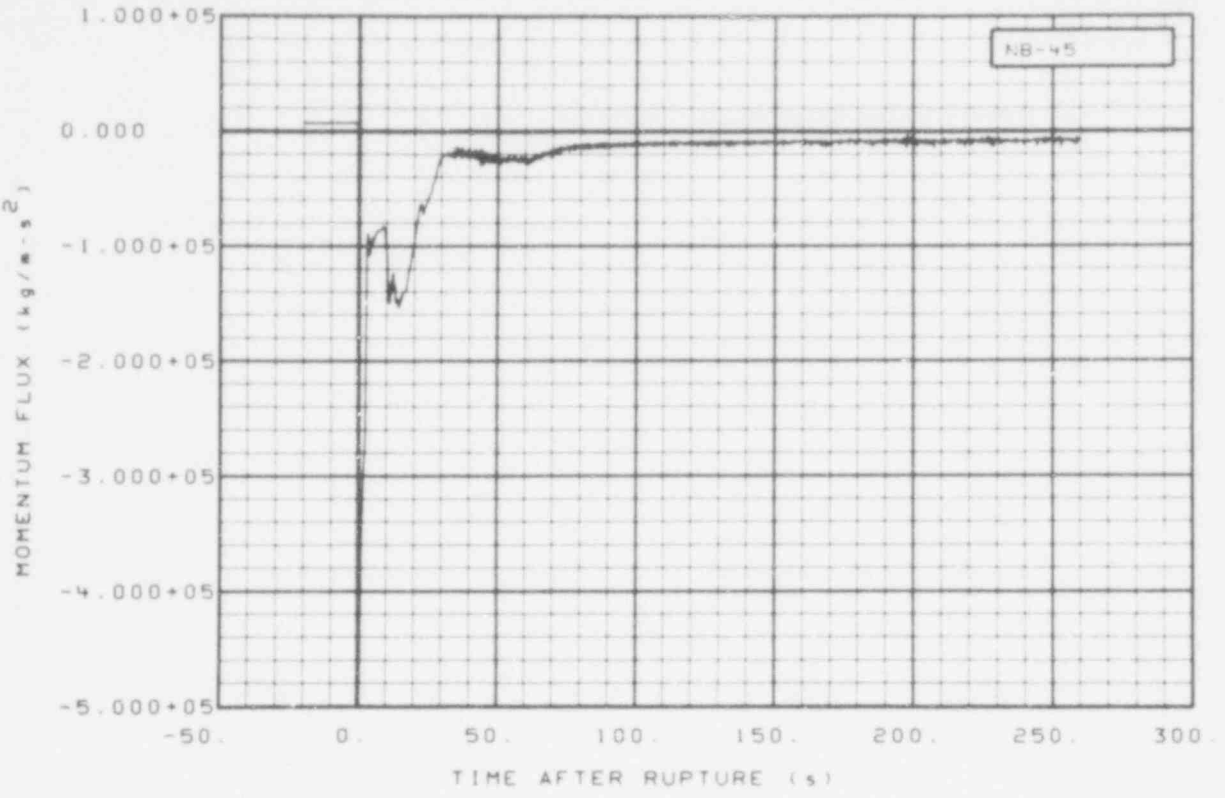

Fig. 229 Momentum flux in broken loop (NB-45), from -20 to 260 s.

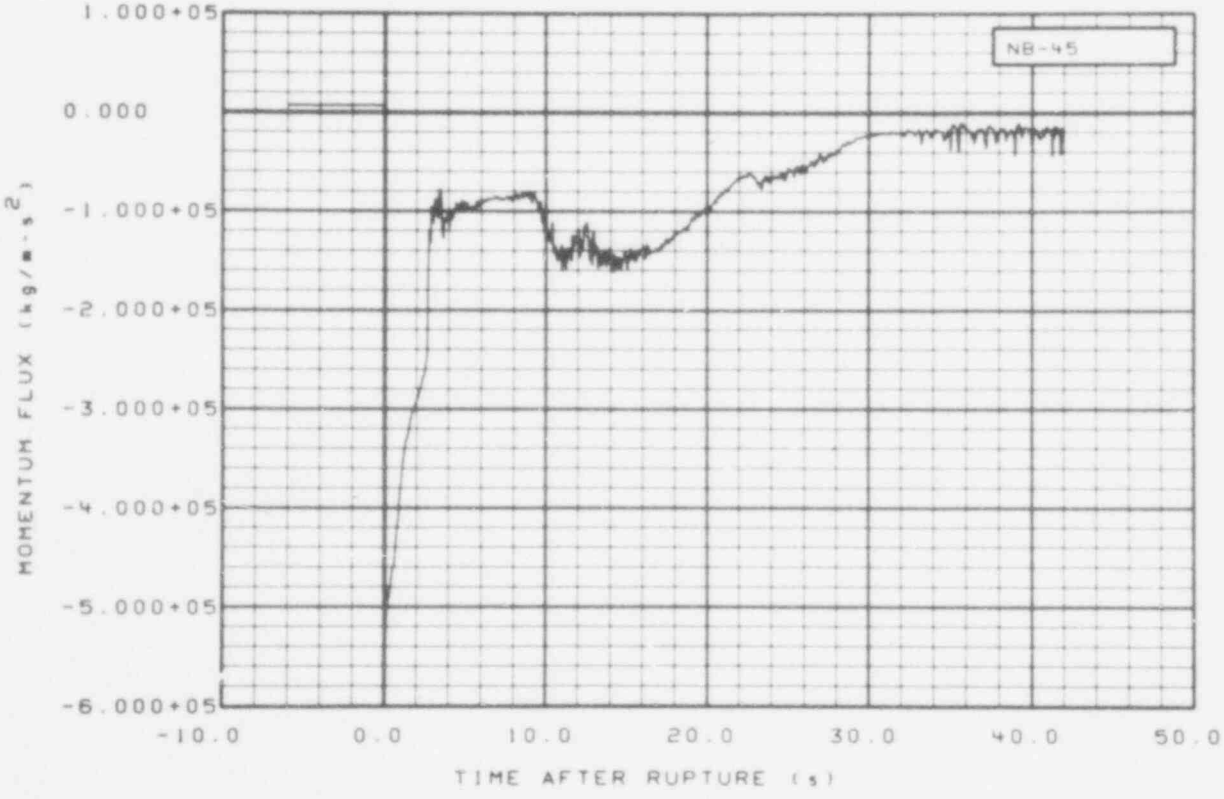

Fig. 230 Momentum flux in broken loop (NB-45), from -6 to 42 s.

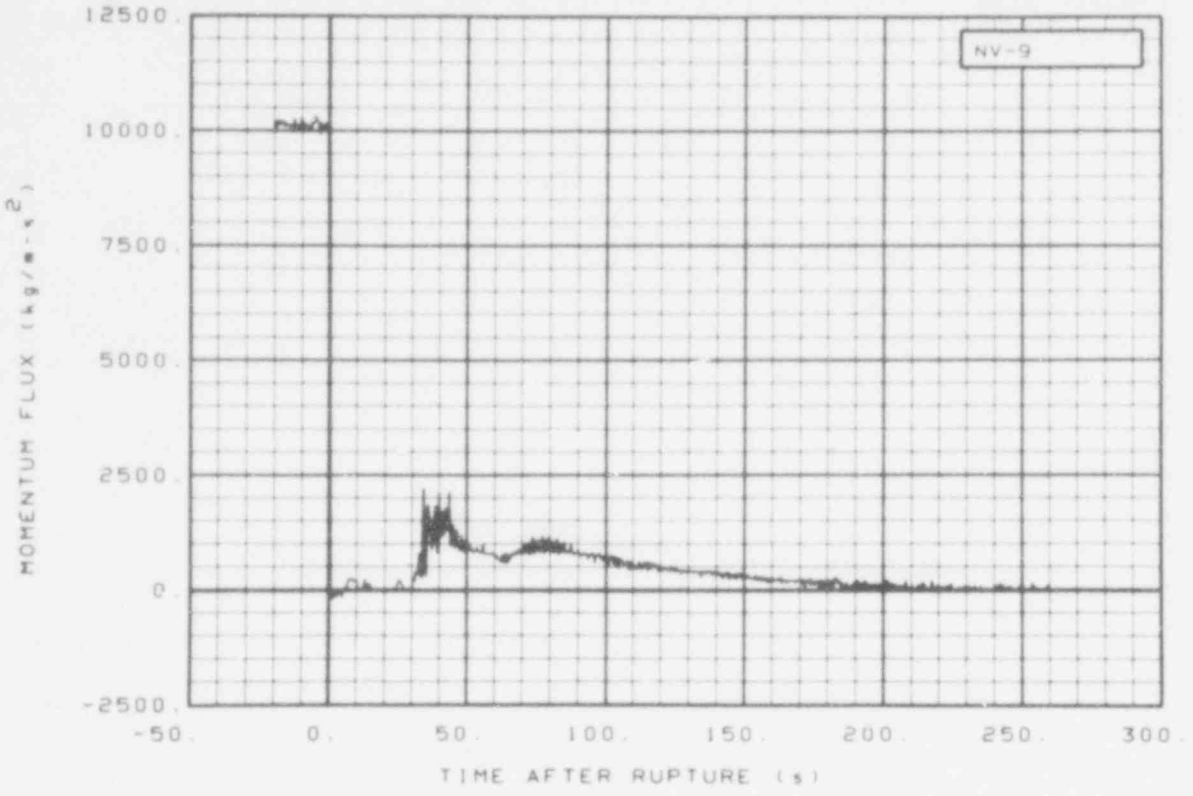

Fig. 231 Momentum flux in core inlet (NV-9), from -20 to 260 s.

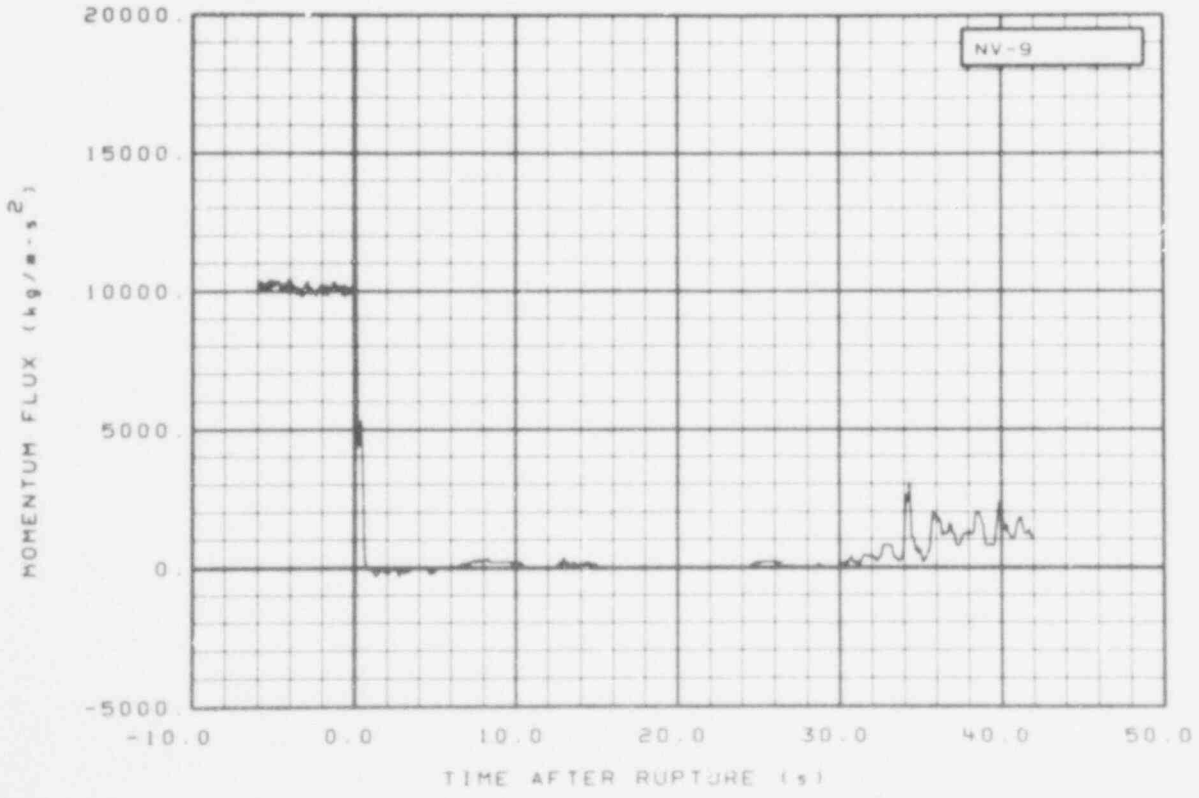

Fig. 232 Momentum flux in core inlet (NV-9), from -6 to 42 s.

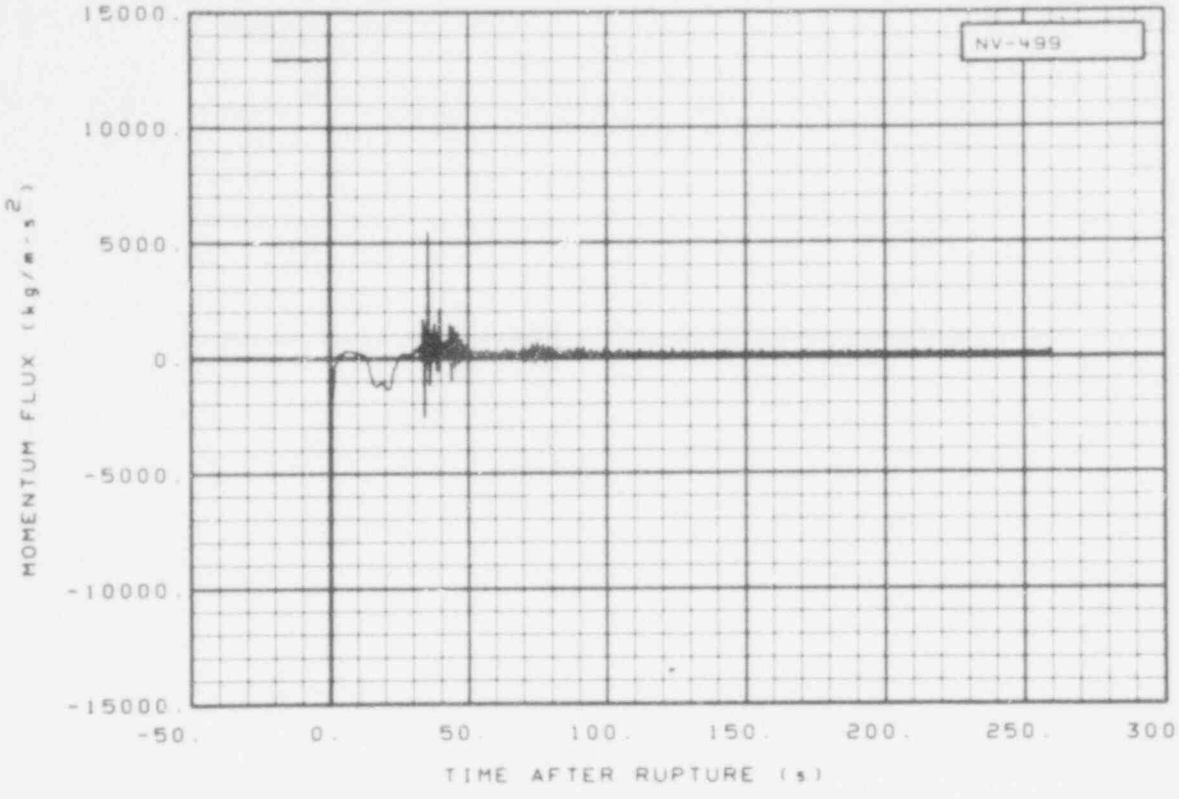

Fig. 233 Momentum flux in core inlet (NV-499), from -20 to 260 s.

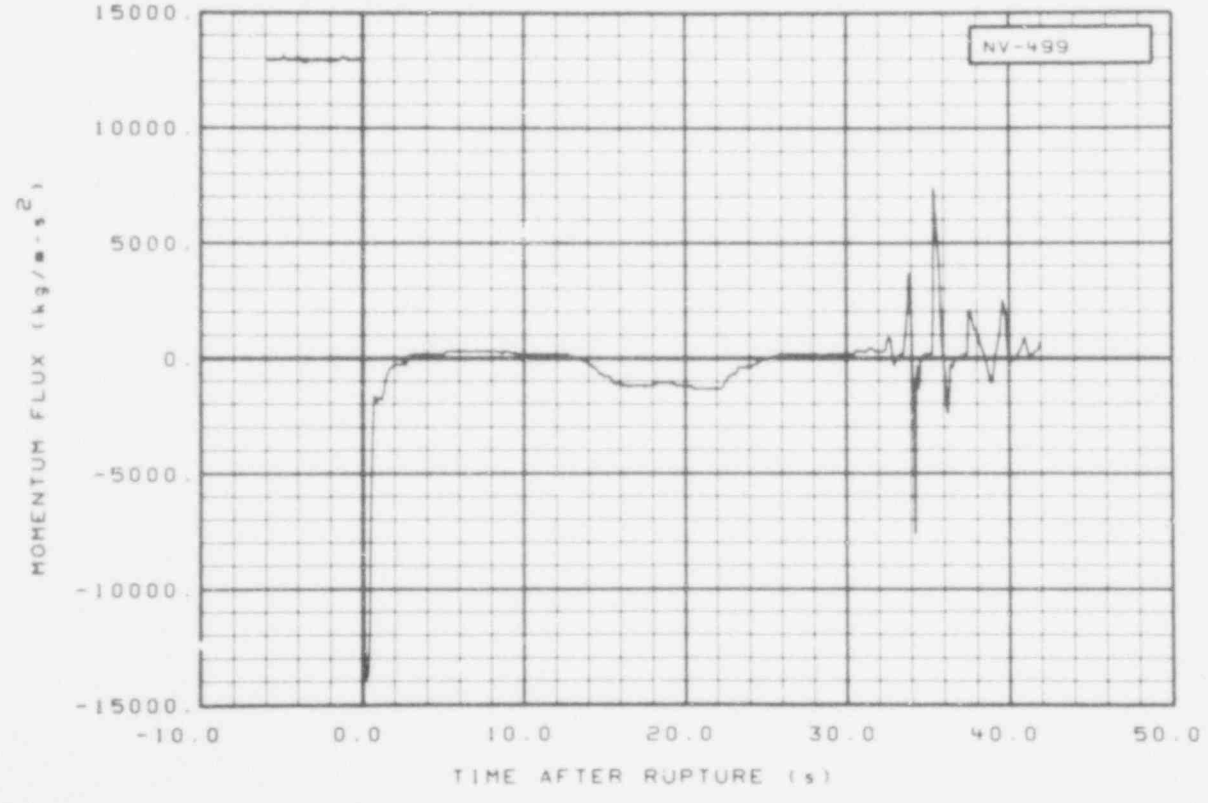

Fig. 234 Momentum flux in core inlet (NV-499), from -6 to 42 s.

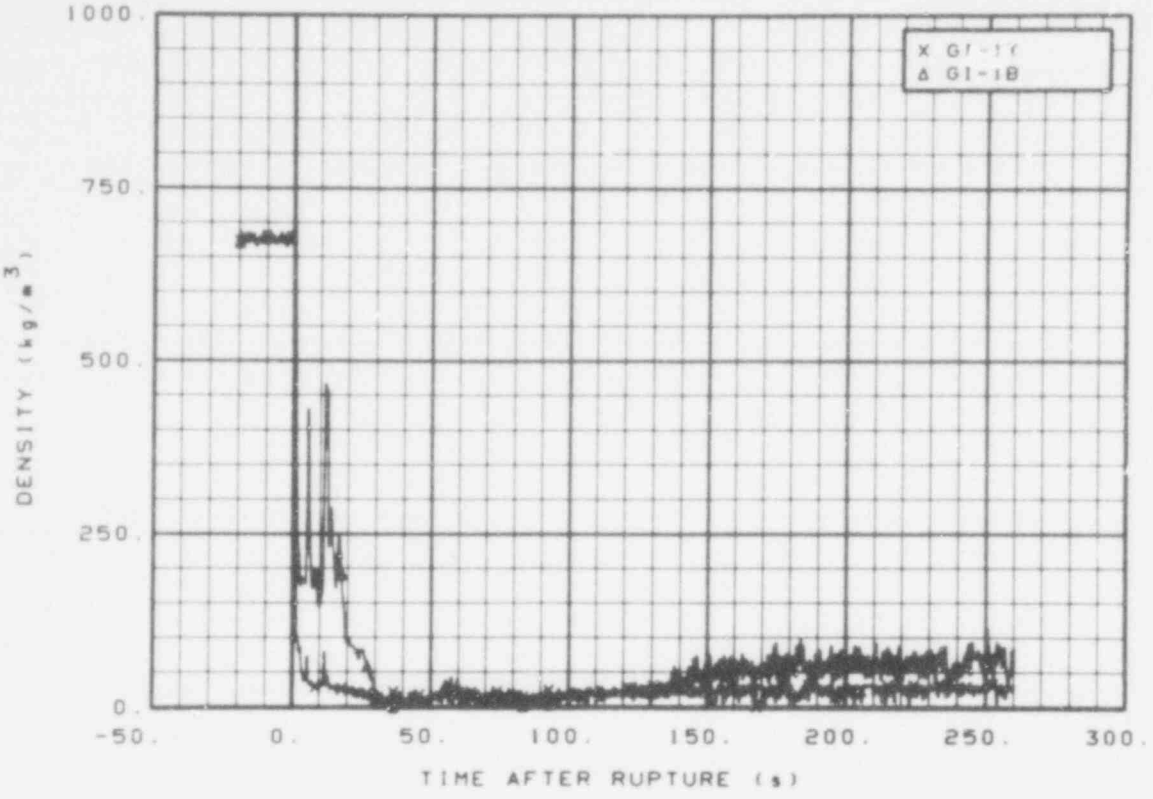

Fig. 235 Density in intact loop (GI-1T and GI-1B), from -20 to 260 s.

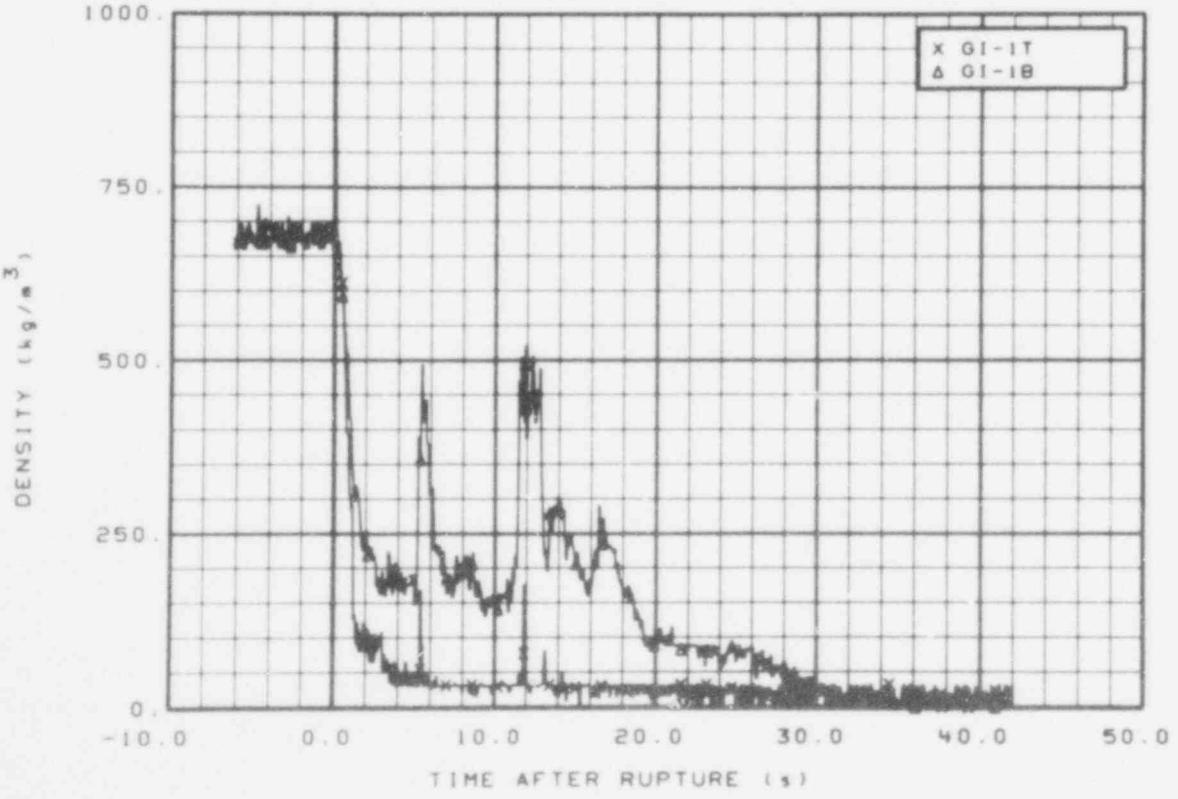

Fig. 236 Density in intact loop (GI-1T and GI-1B), from -6 to 42 s.

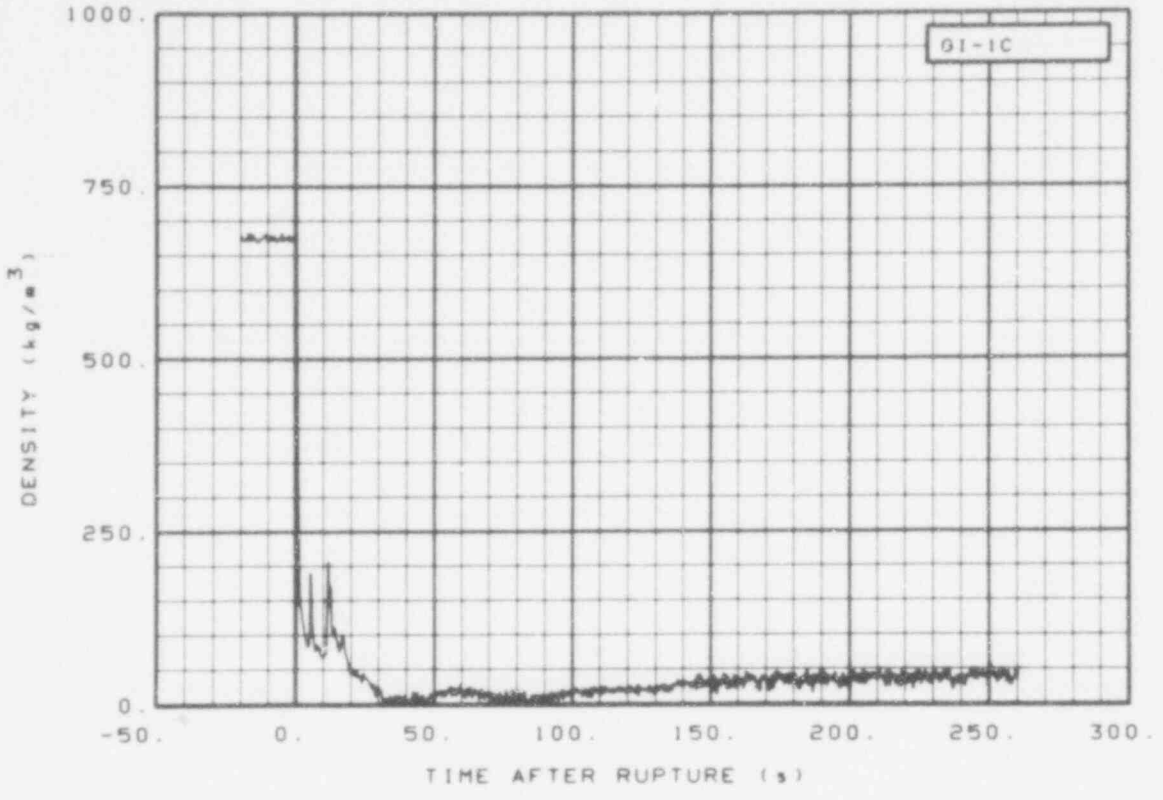

Fig. 237 Density in intact loop (GI-1C), from -20 to 260 s.

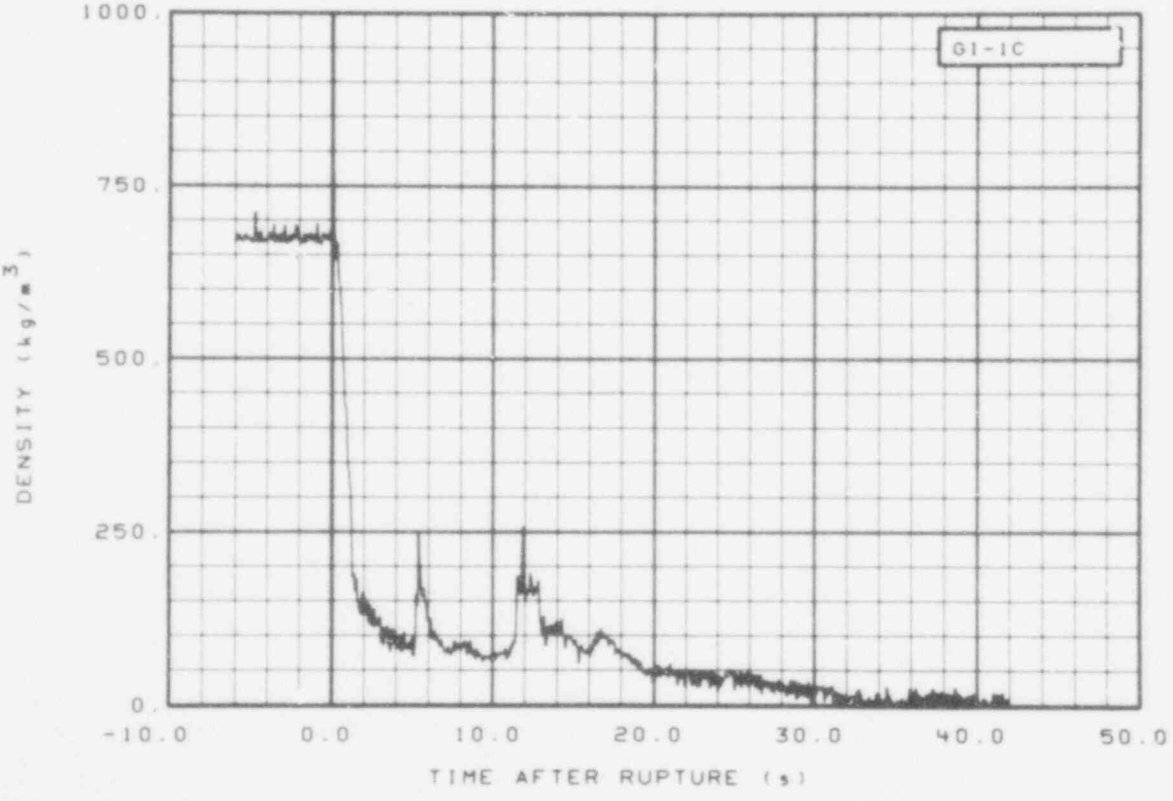

Fig. 238 Density in intact loop (GI-1C), from -6 to 42 s.

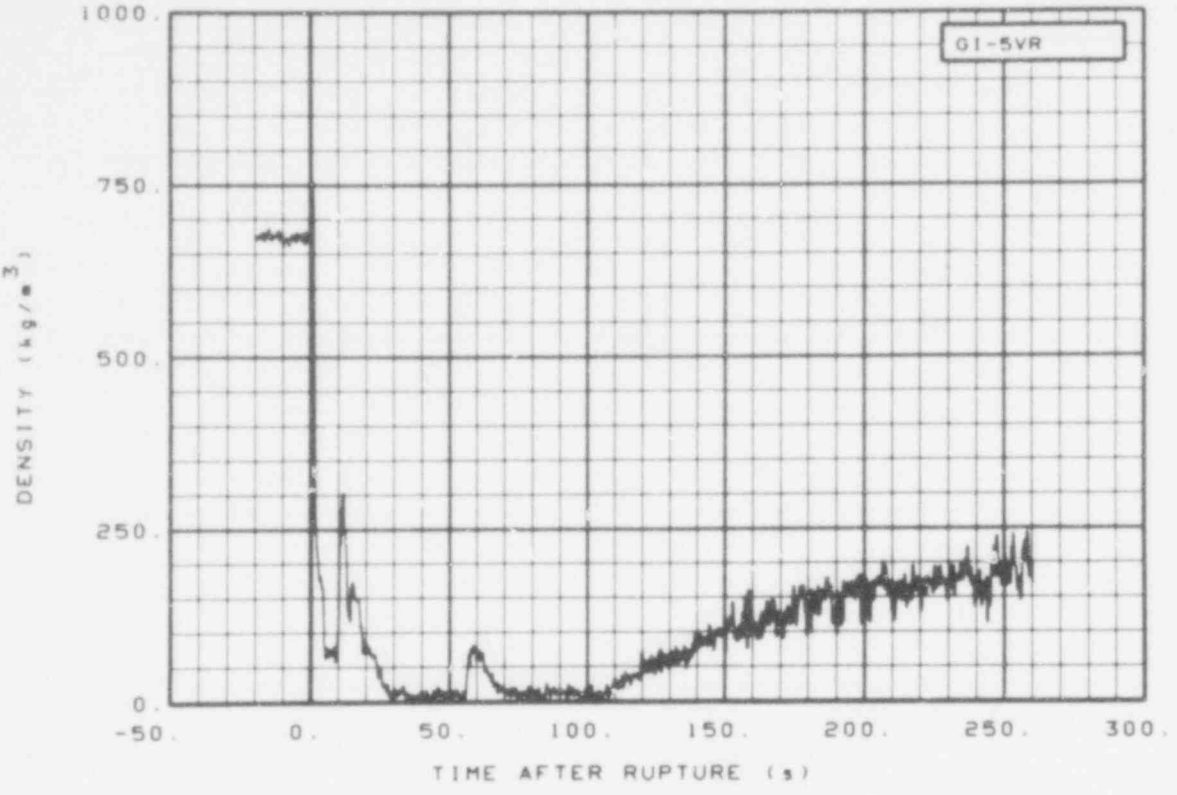

Fig. 239 Density in intact loop (GI-5VR), from -20 to 2o0 s.

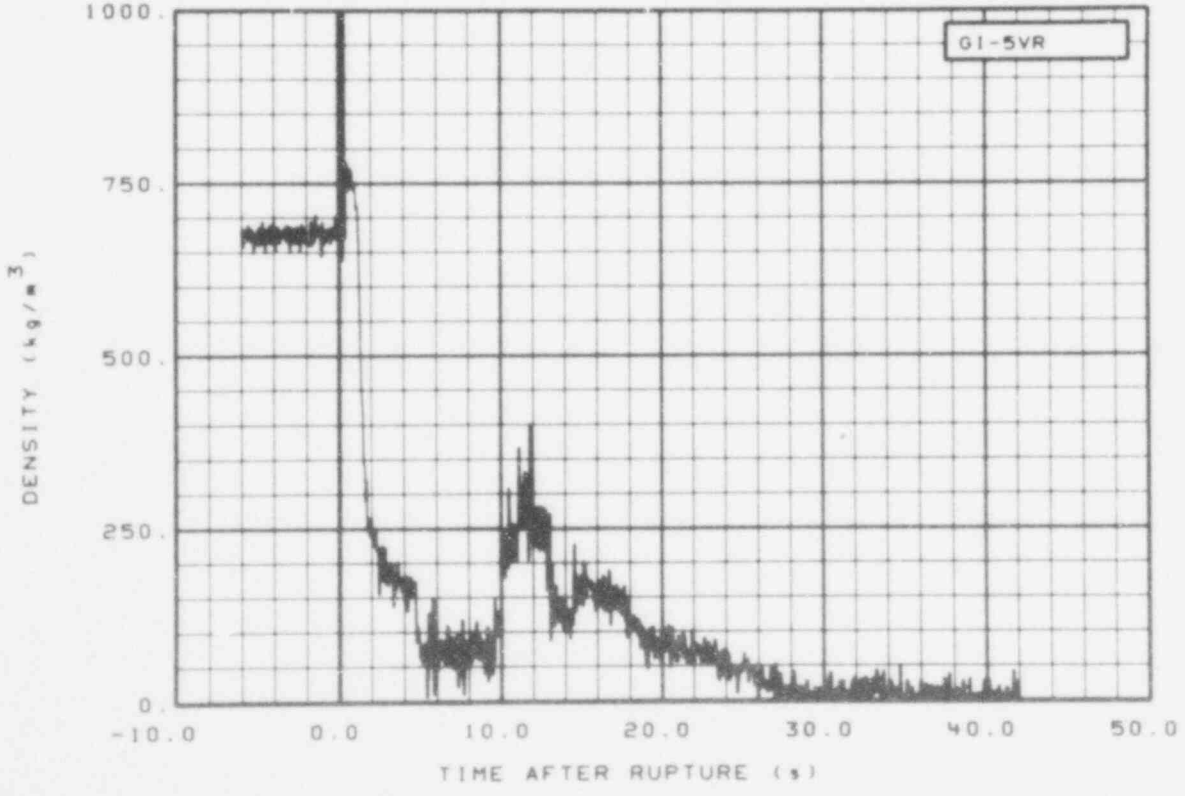

Fig. 240 Density in intact loop (GI-5VR), from -6 to 42 s.

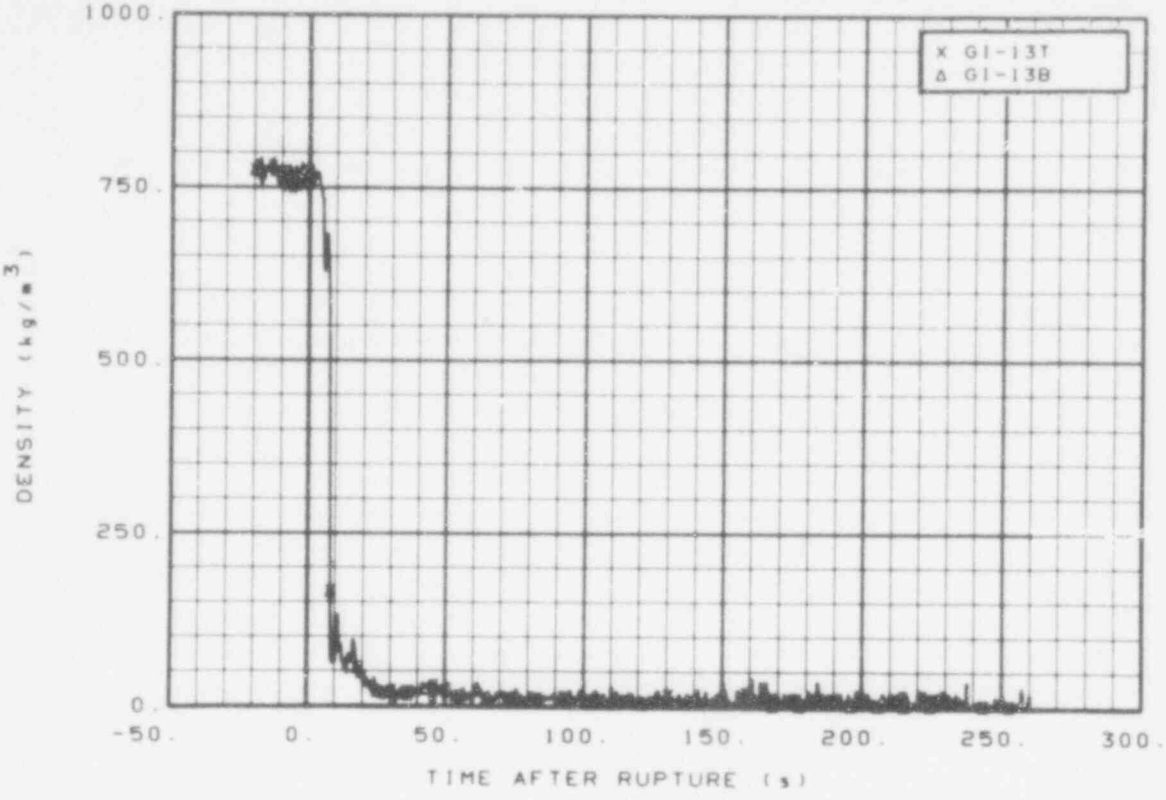

Fig. 241 Density in intact loop (GI-13T and GI-13B), from -20 to 260 s.

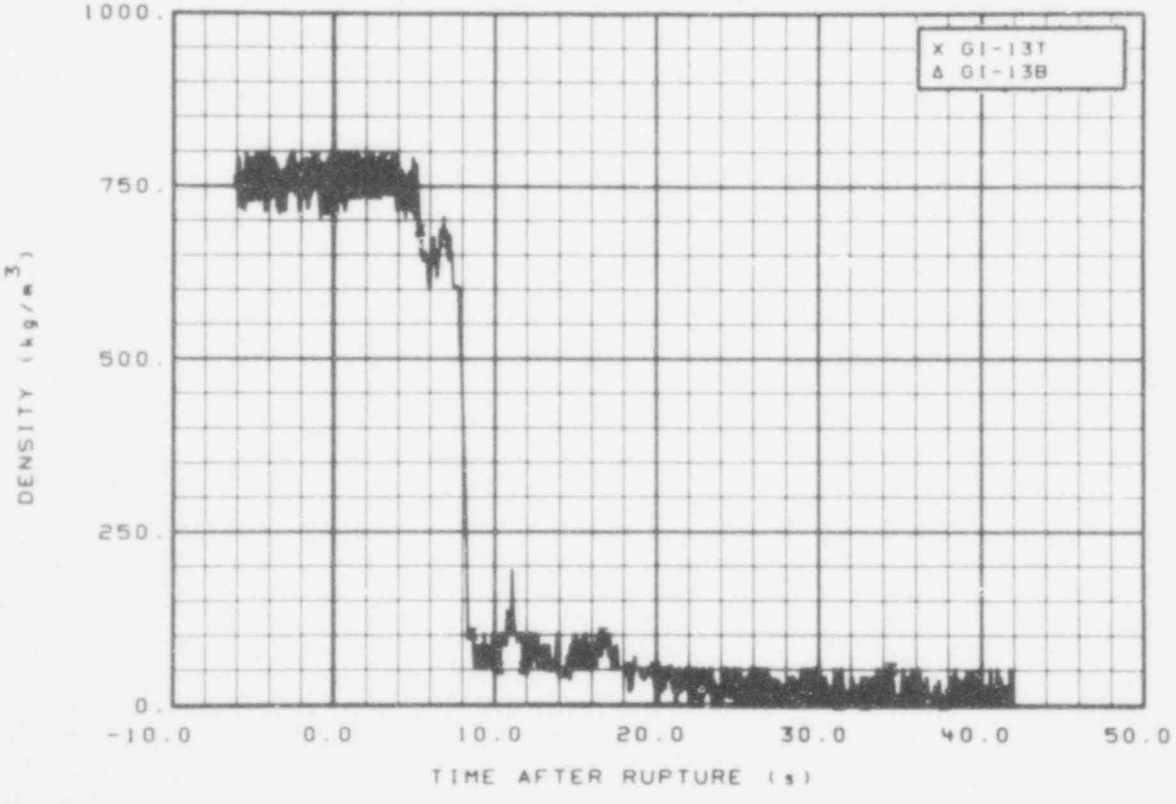

Fig. 242 Density in intact loop (GI-13T and GI-13B), from -6 to 42 s.

Fig. 243 Density in intact loop (GI-13C), from -20 to 260 s.

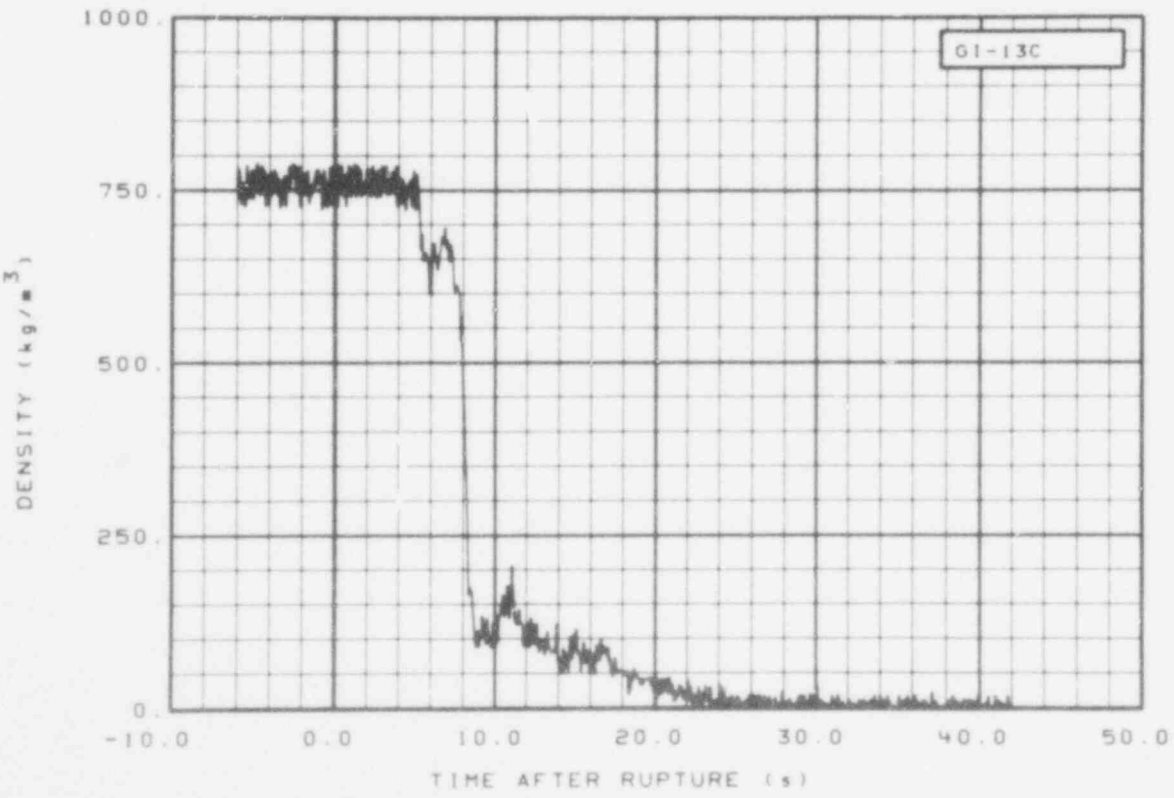

Fig. 244 Density in intact loop (GI-13C), from -6 to 42 s.

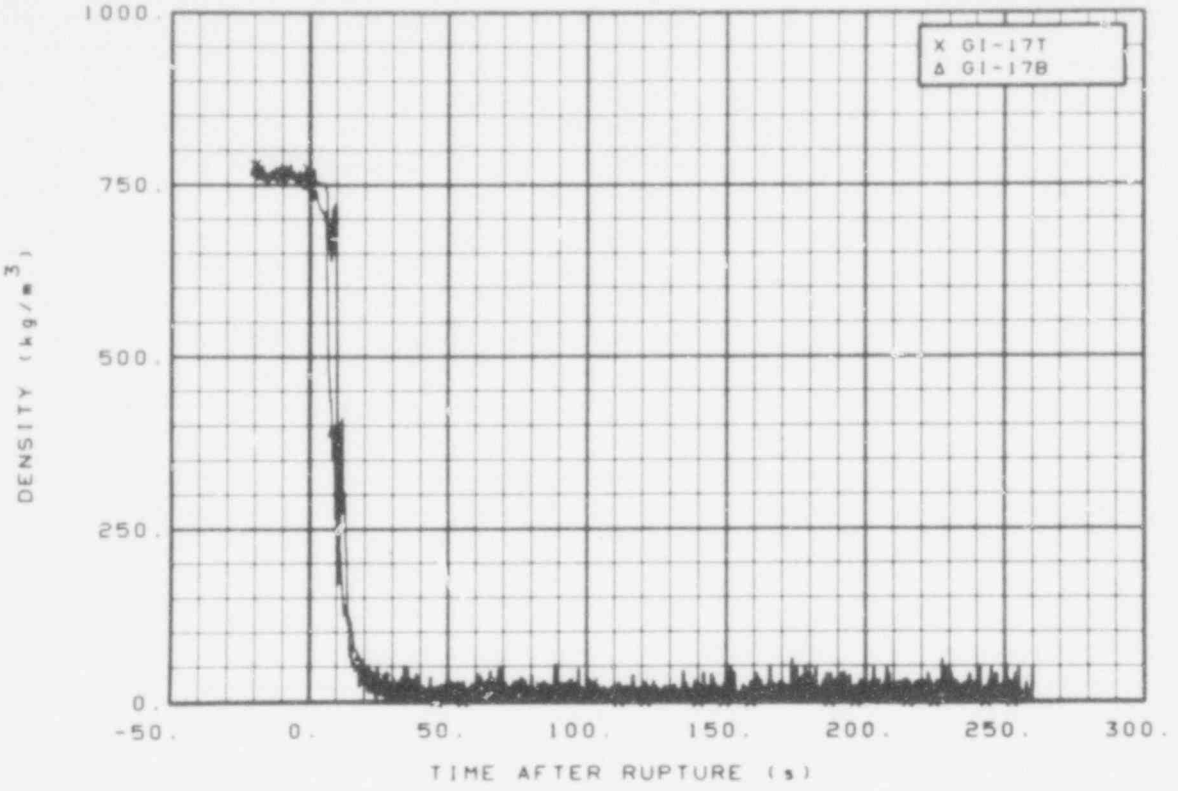

Fig. 245 Density in intact loop (GI-17T and GI-17B), from -20 to 260 s.

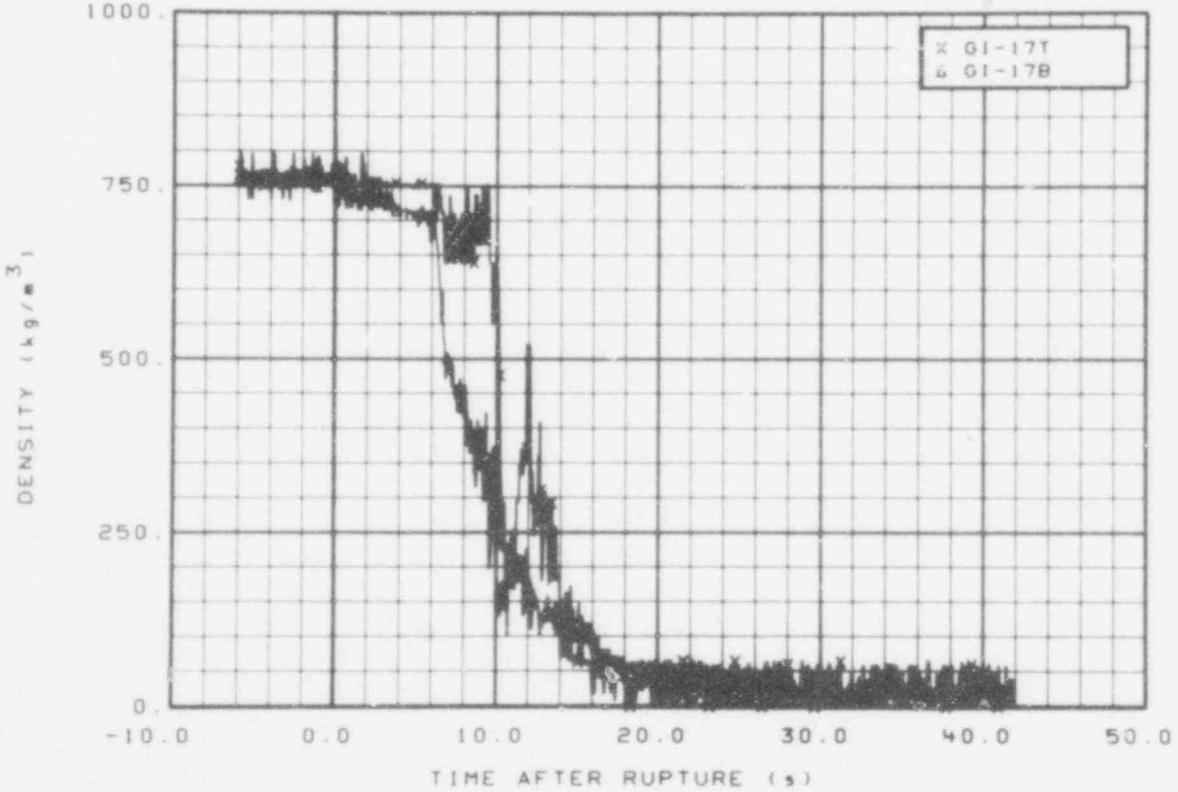

Fig. 246 Density in intact loop (GI-17T and GI-17B), from -6 to 42 s.

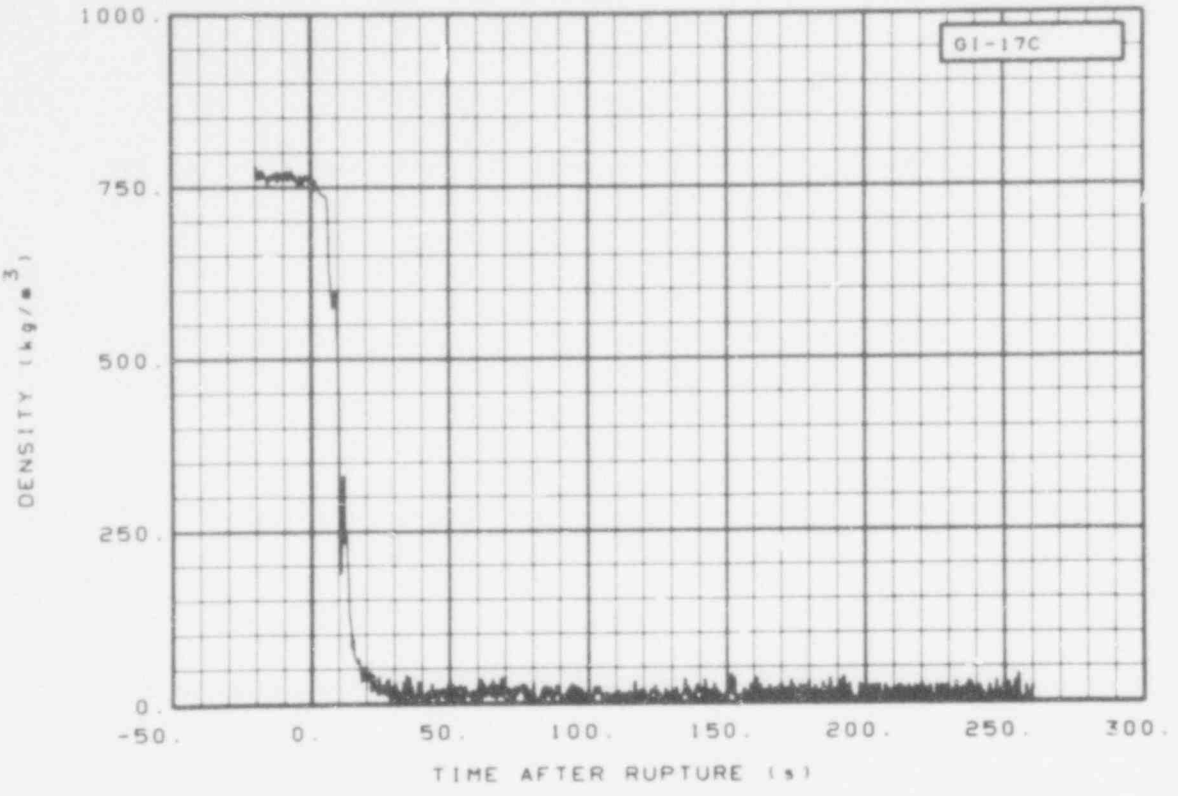

Fig. 247 Density in intact loop (GI-17C), from -20 to 260 s.

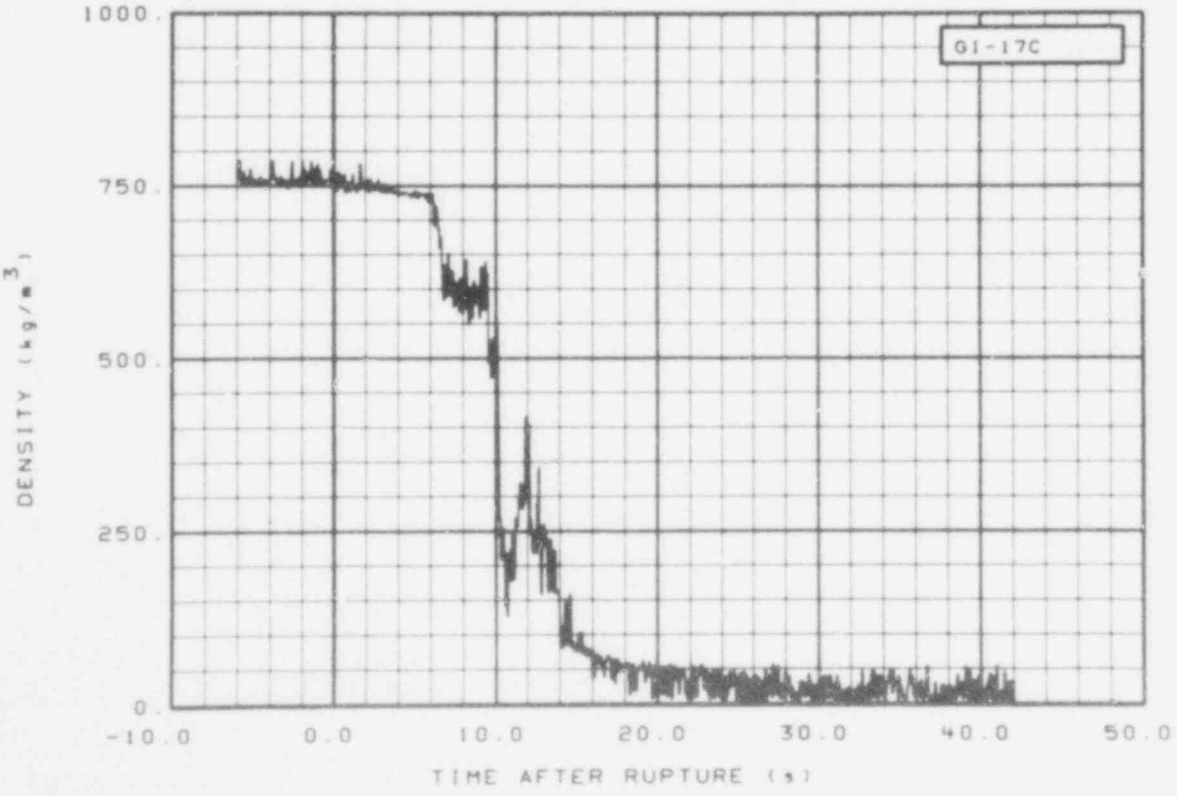

Fig. 248 Density in intact loop (GI-17C), from -6 to 42 s.

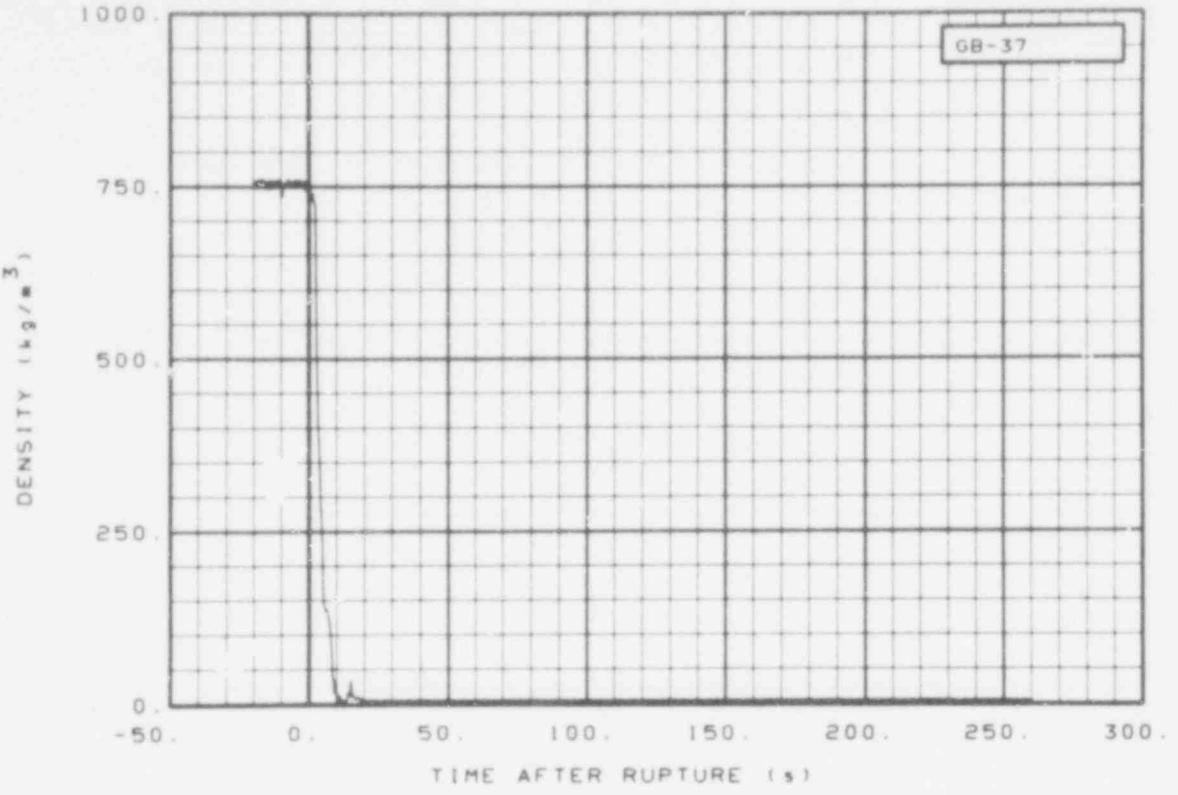

Fig. 249 Density in broker loop (GB-37), from -20 to 260 s.

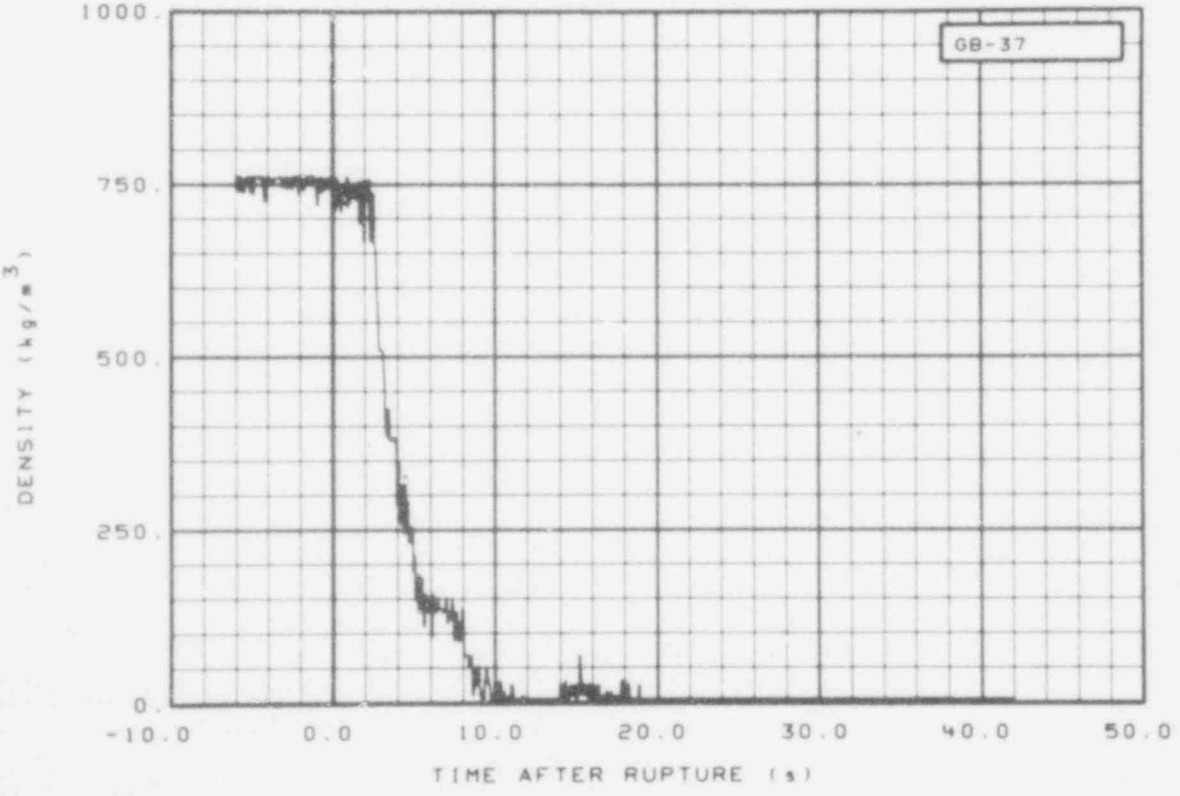

Fig. 250 Density in broken loop (GB-37), from -6 to 42 s.

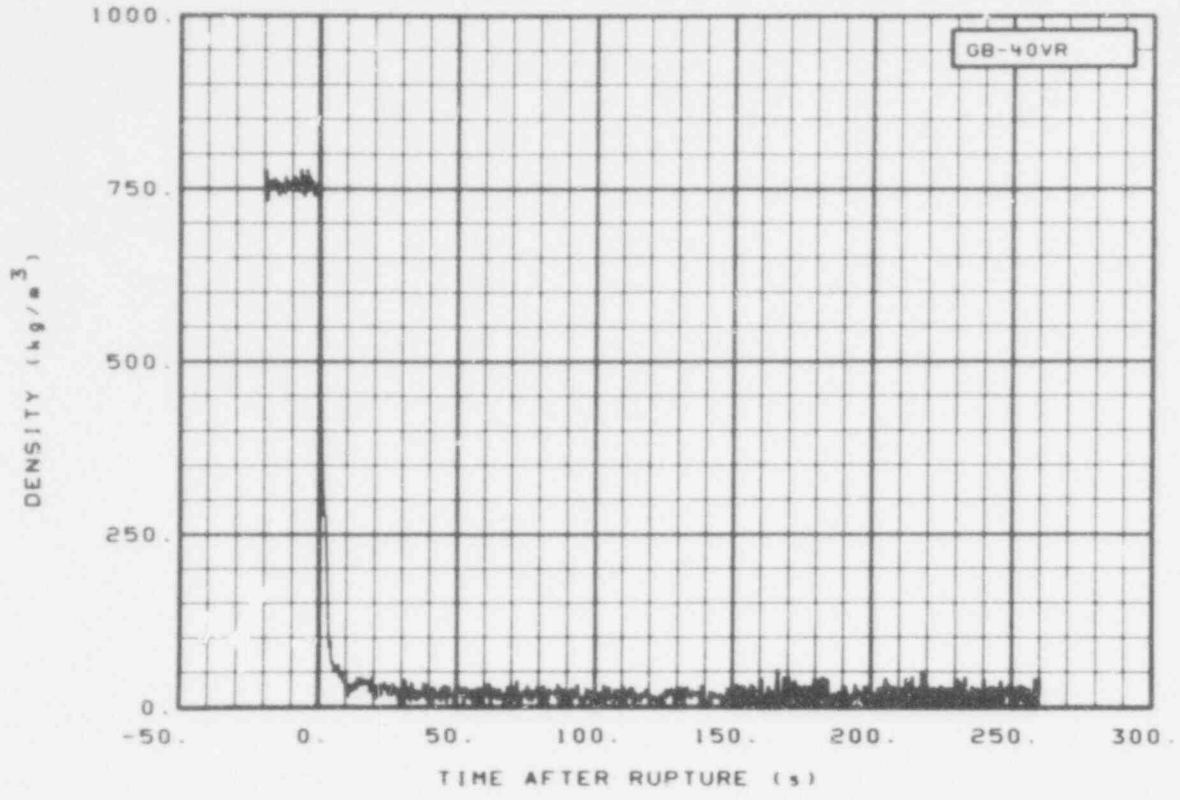

Fig. 251 Density in broken loop (GB-40VR), from -20 to 260 s.

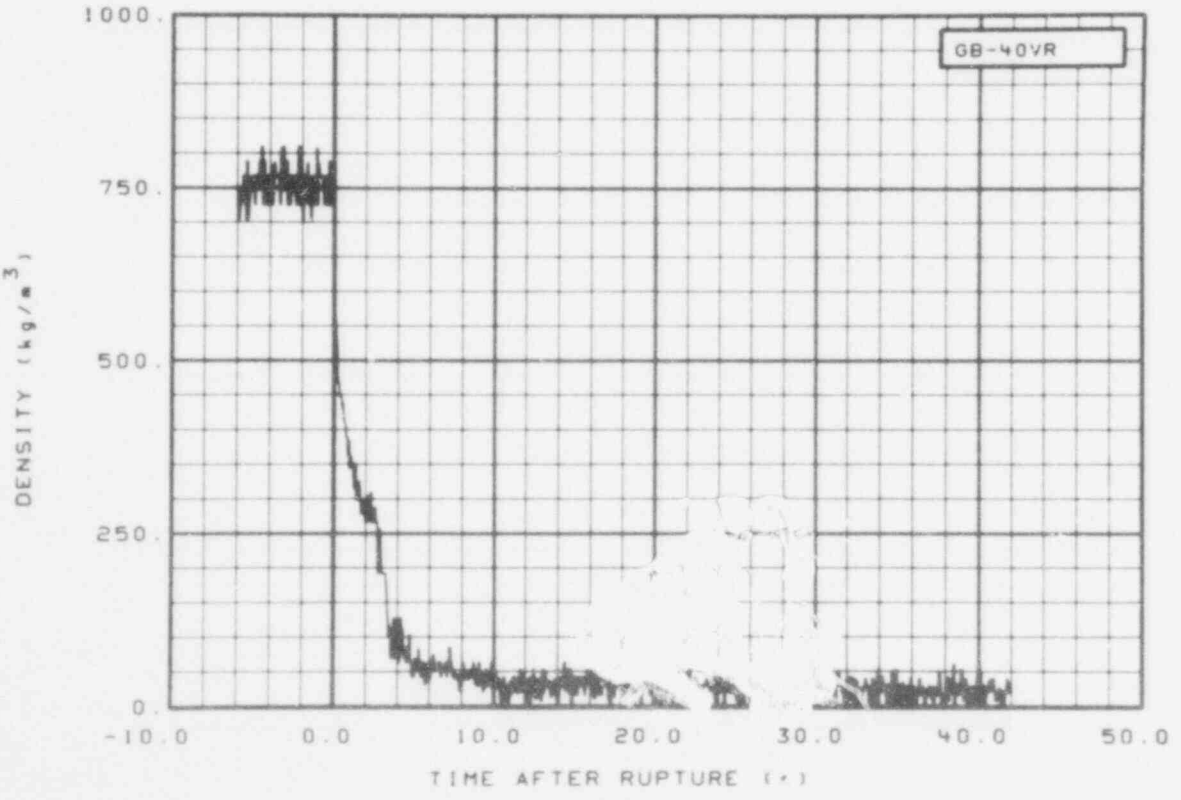

Fig. 252 Density in broken loop (GB-40VR), from -6 to 42 s.

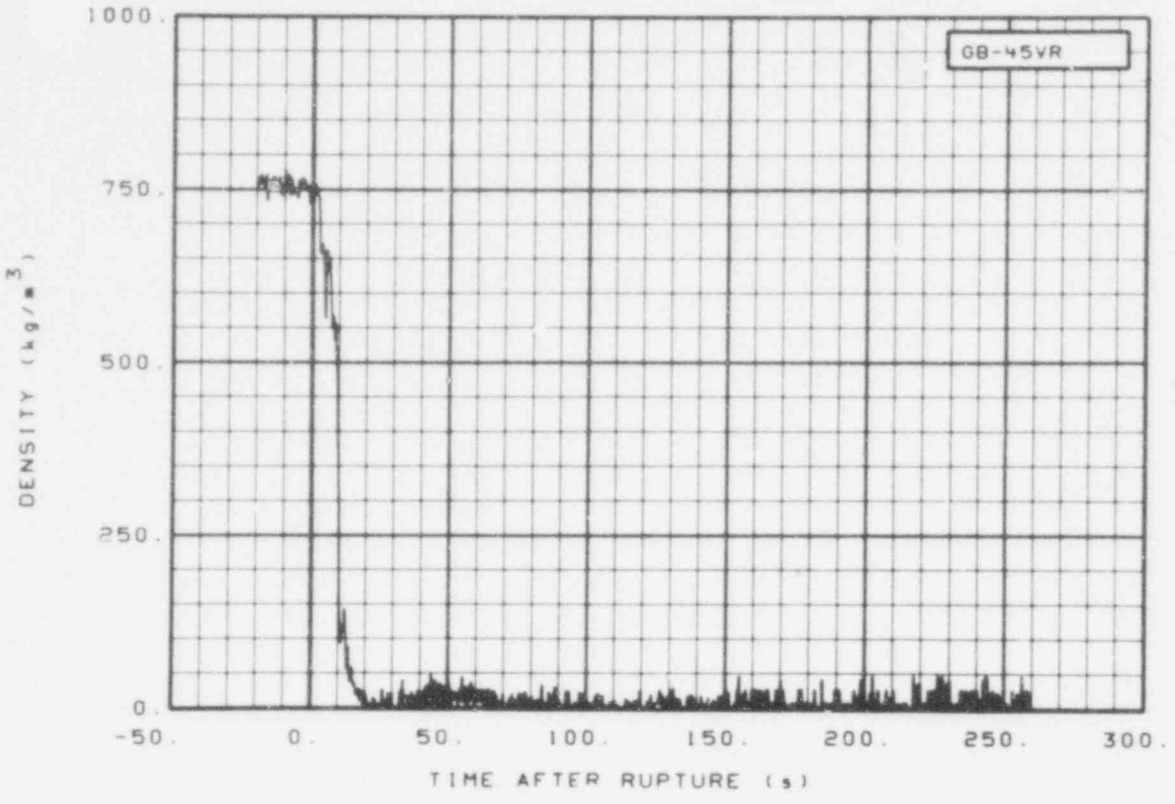

Fig. 253 Density in broken loop (GB-45VR), from -20 to 260 s.

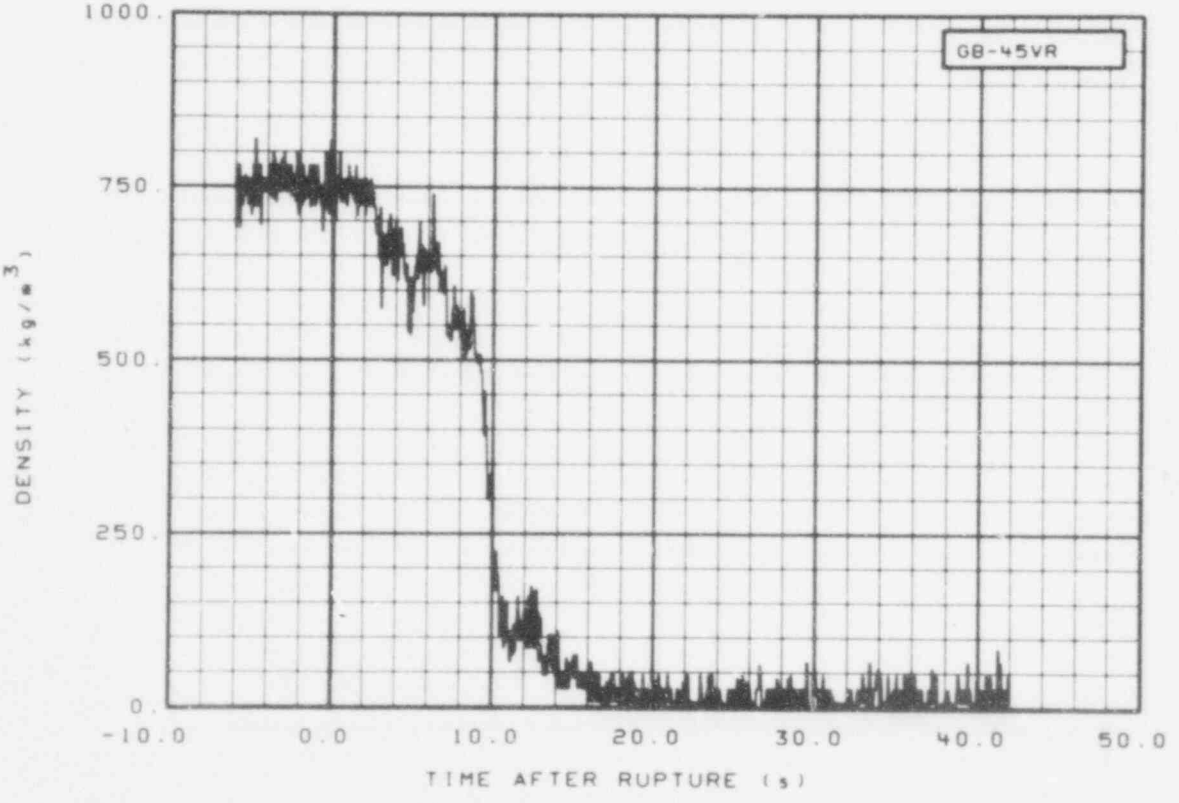

Fig. 254 Density in broken loop (GB-45VR), from -6 to 42 s.

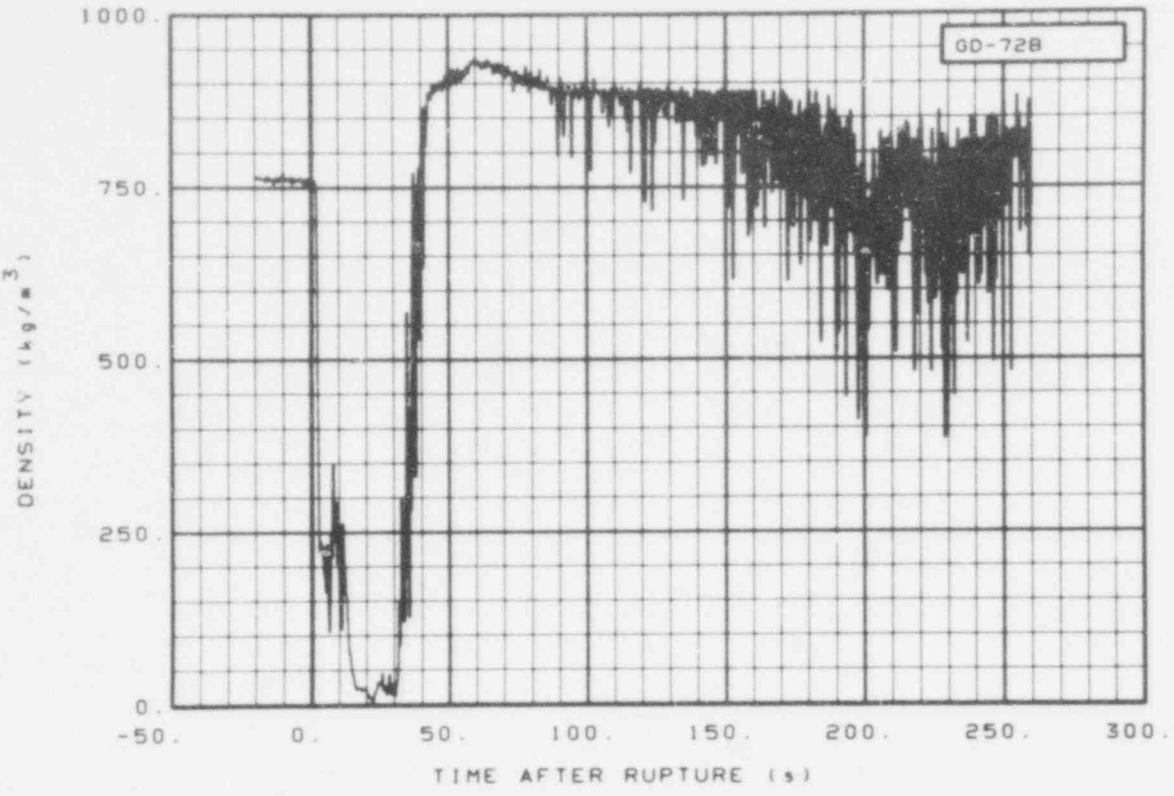

Fig. 255 Density in downcomer (GD-72B), from -20 to 260 s.

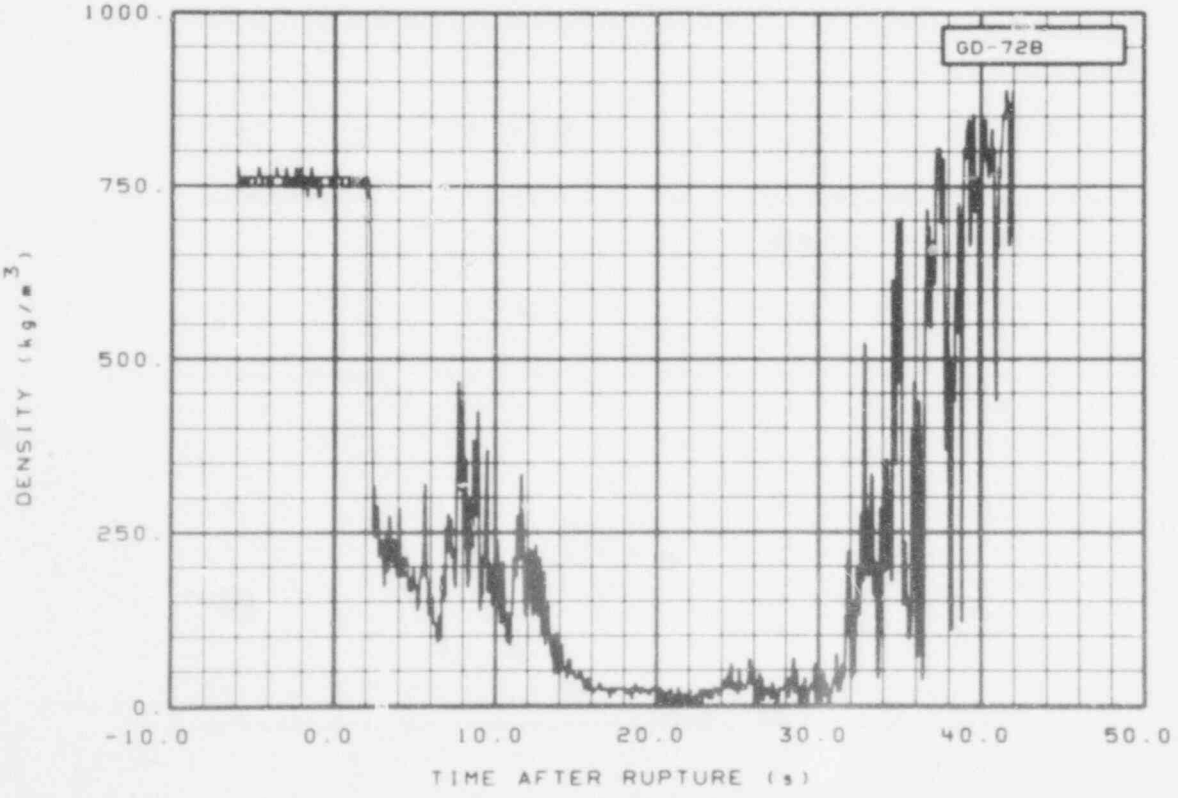

Fig. 256 Density in downcomer (GD-72B), from -6 to 42 s.

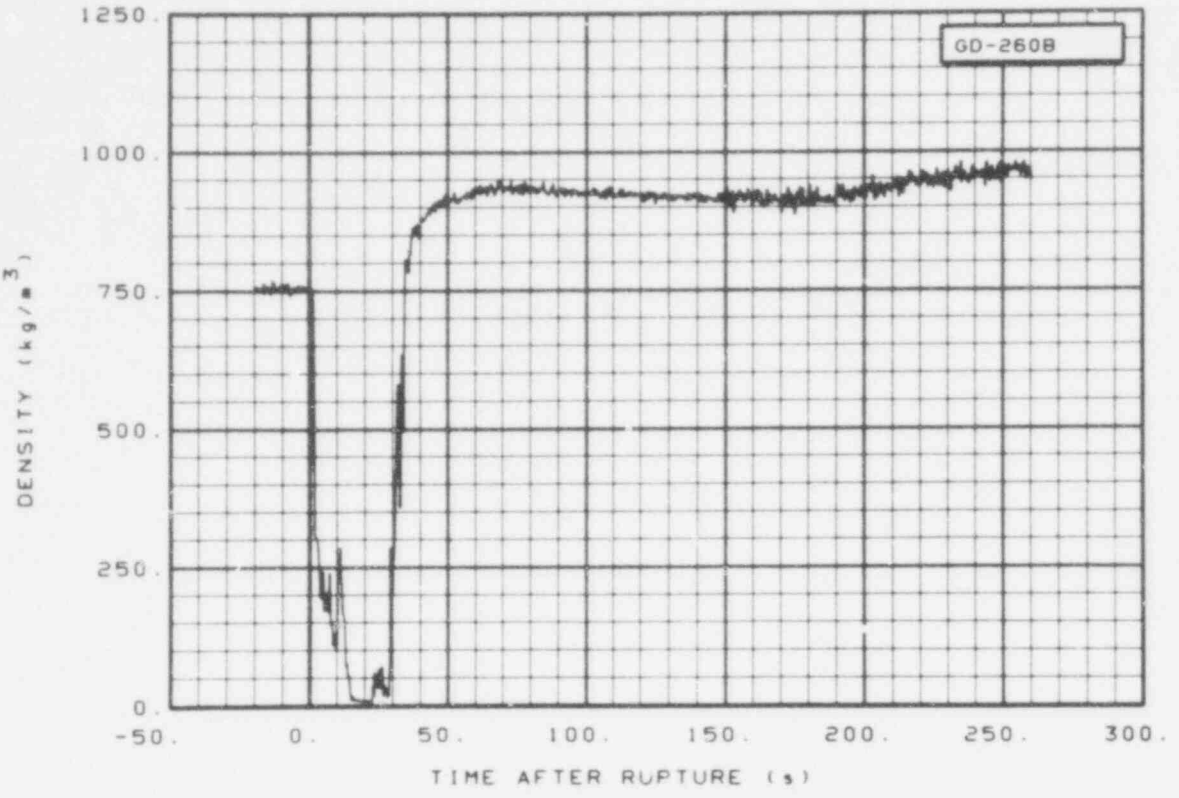

Fig. 257 Density in downcomer (GD-260B), from -20 to 260 s.

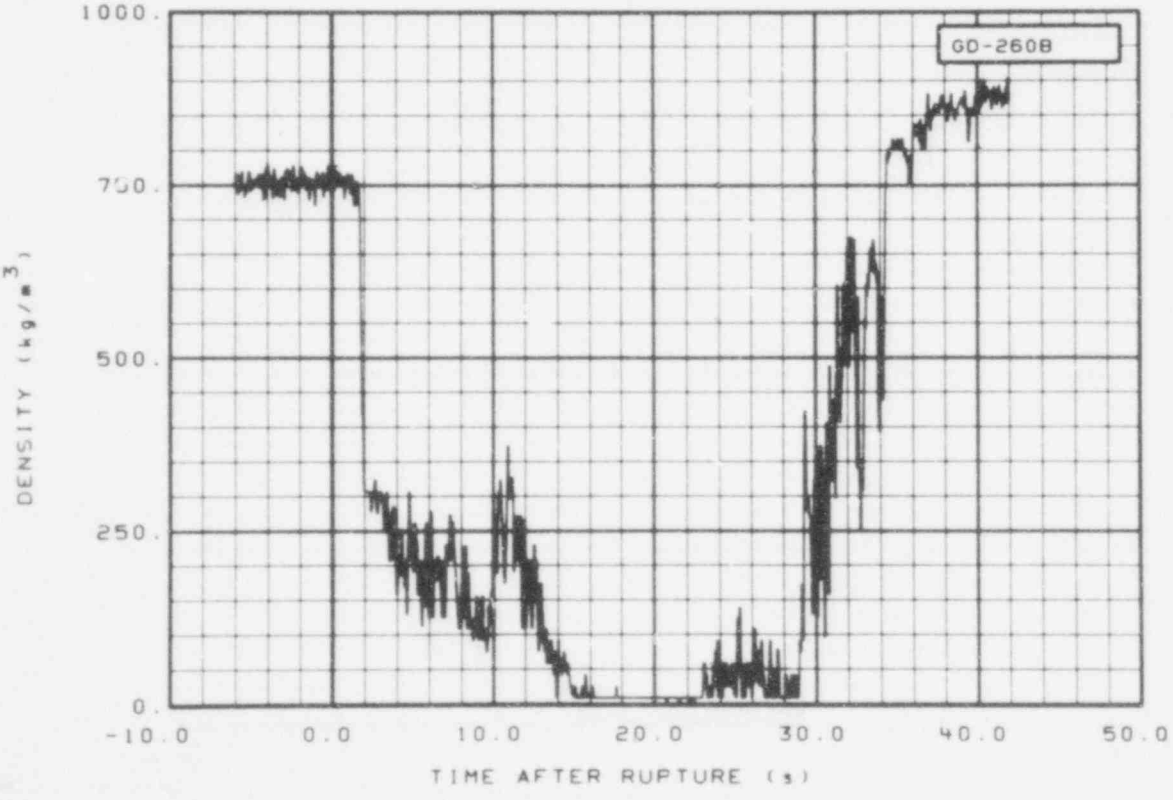

Fig. 258 Density in downcomer (GD-260B), from -6 to 42 s.

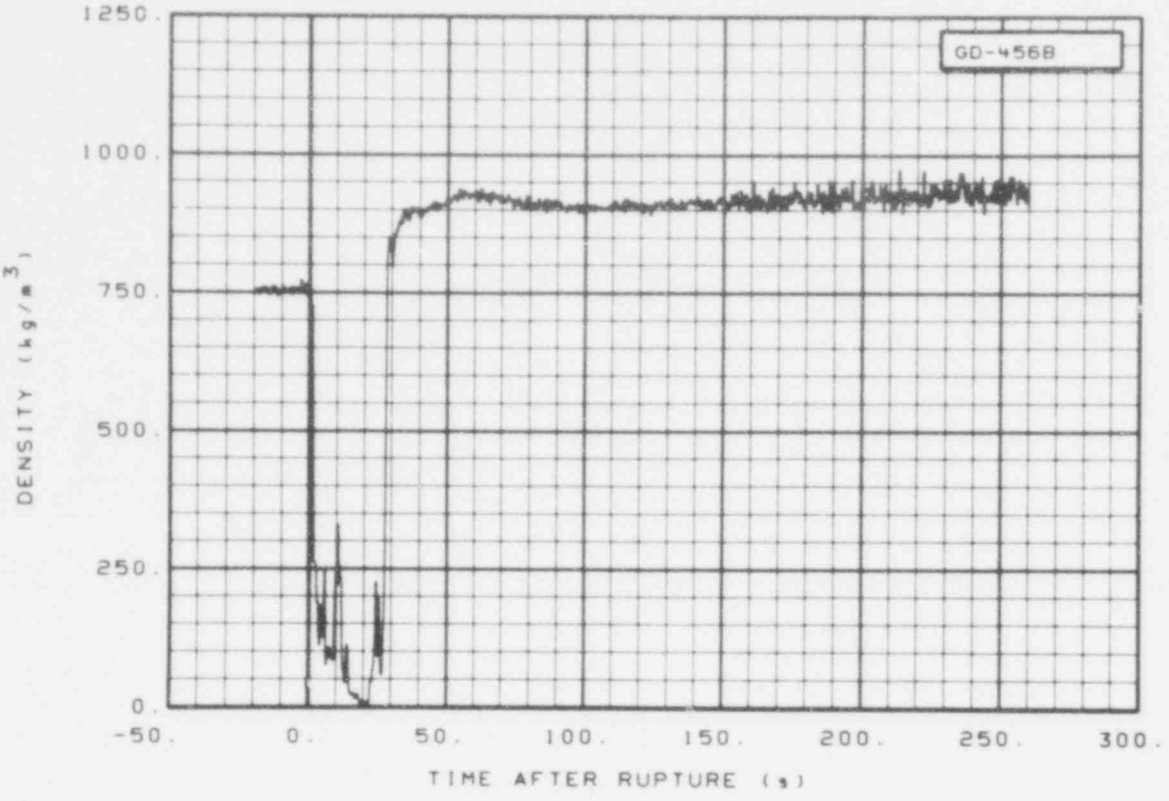

Fig. 259 Density in downcomer (GD-456B), from -20 to 260 s.

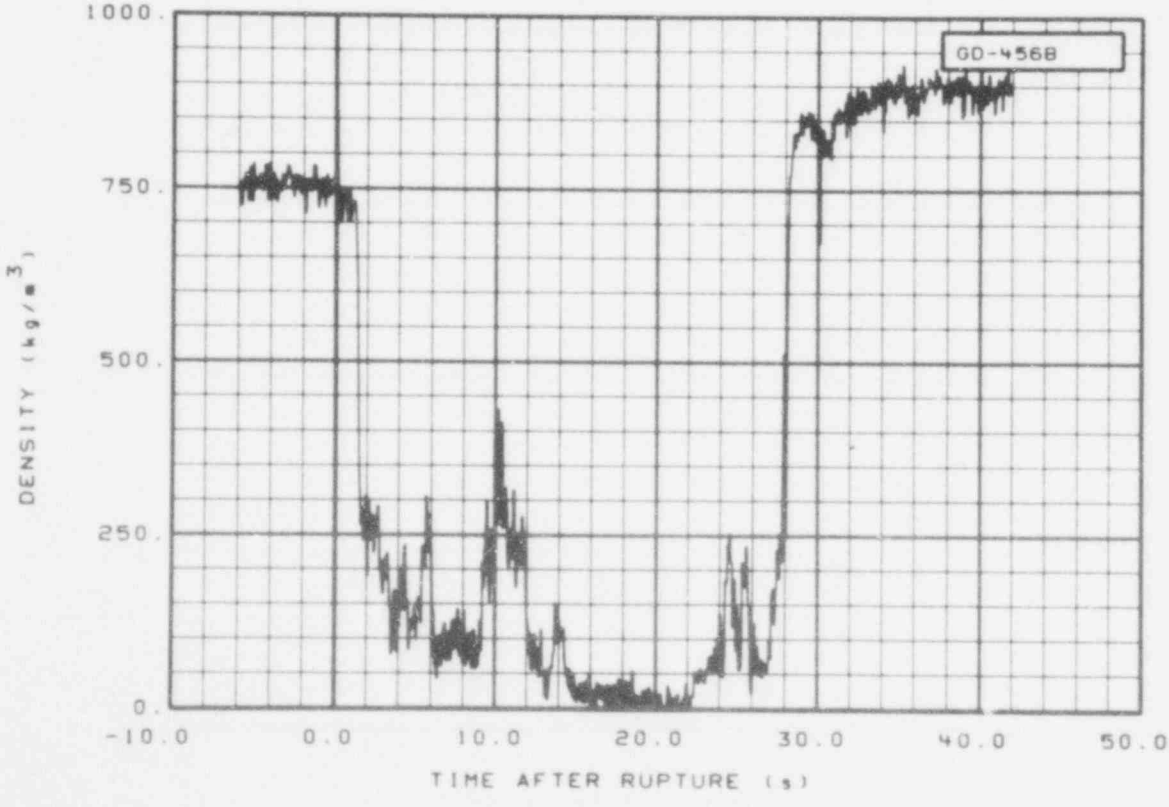

Fig. 260 Density in downcomer (GD-456B), from -6 to 42 s.

Fig. 261 Density in vessel (GV + 339), from -20 to 260 s.

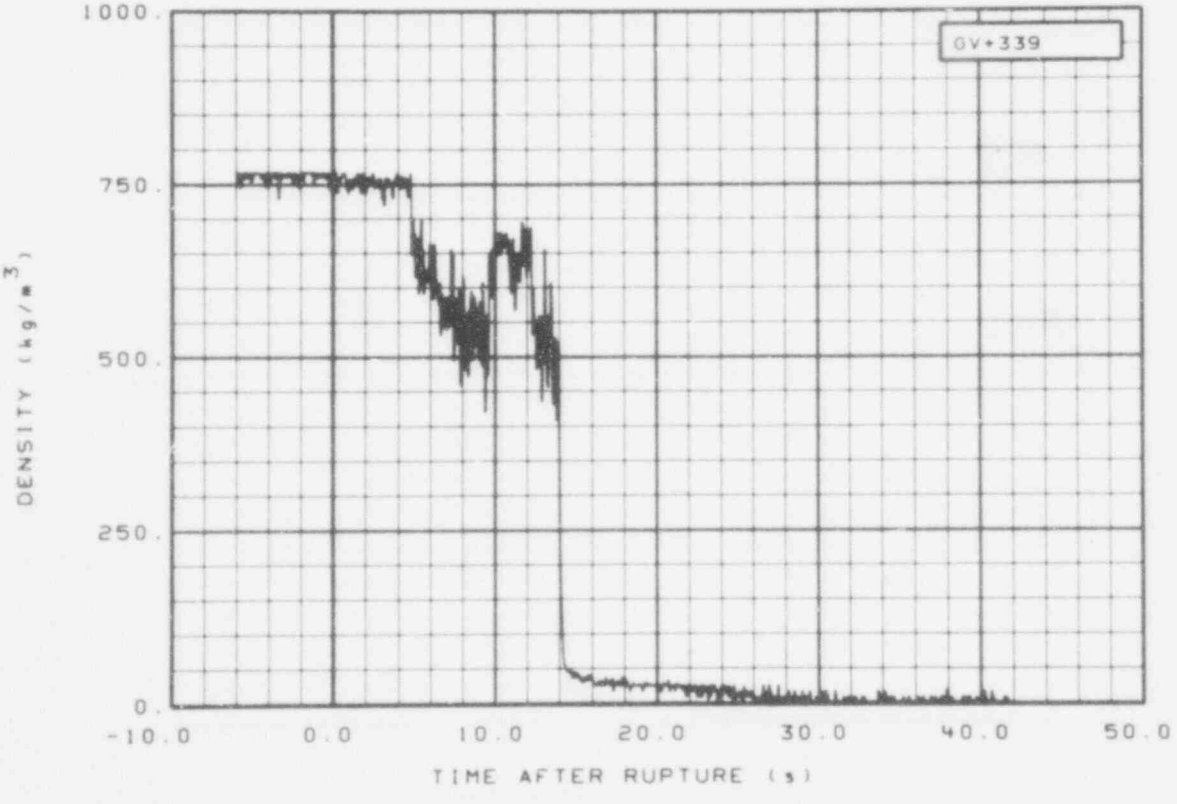

Fig. 262 Density in vessel (GV + 339), from -6 to 42 s.

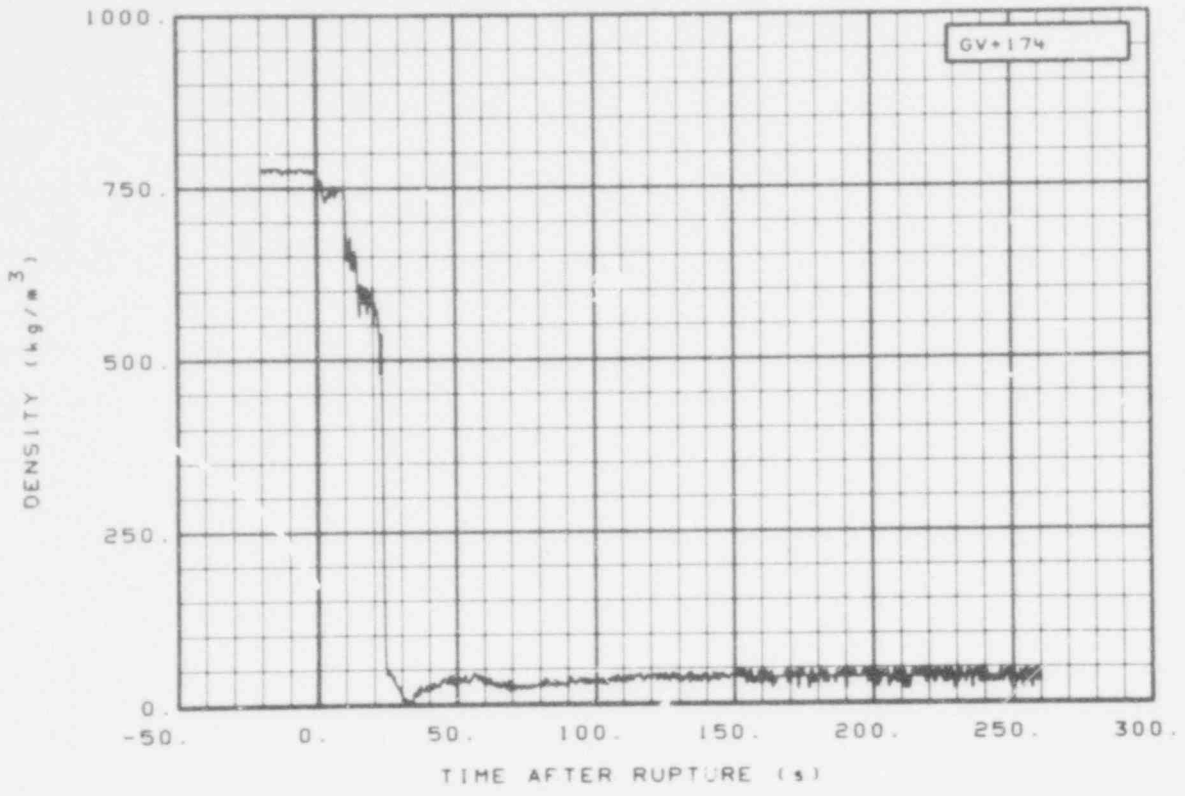

Fig. 263 Density in vessel (GV + 174), from -20 to 260 s.

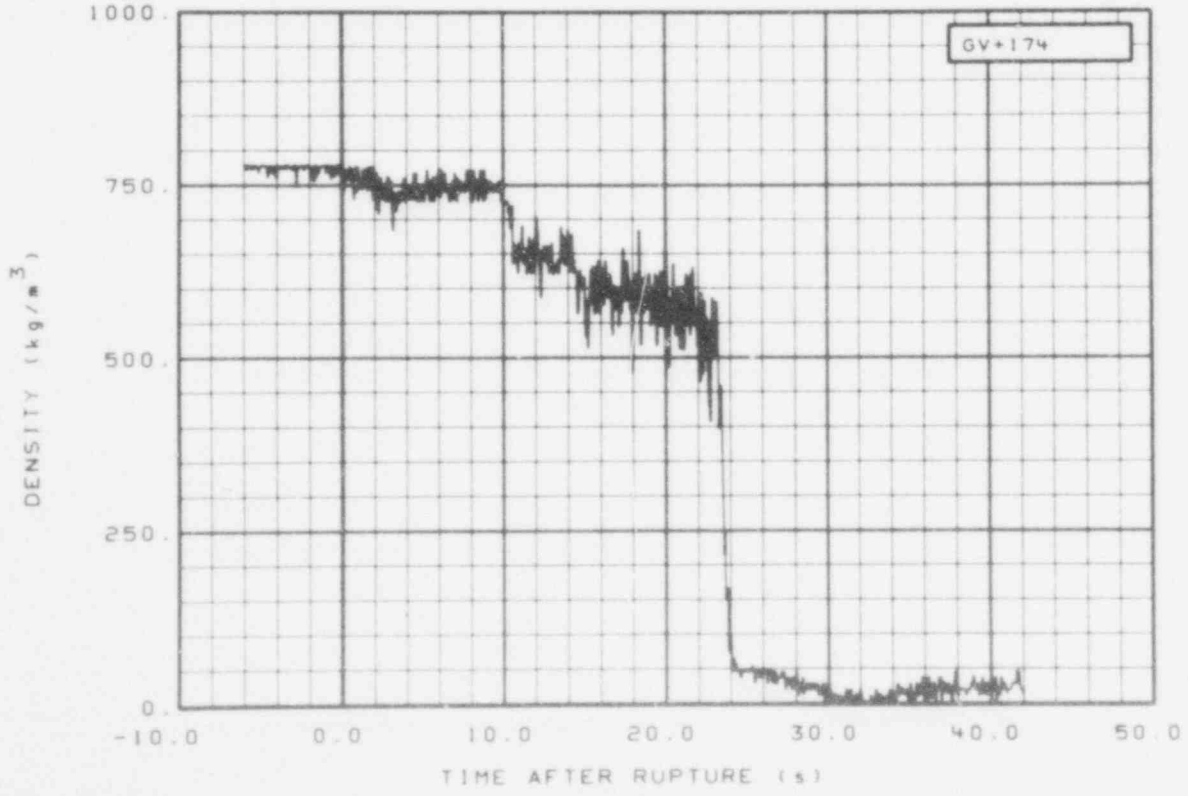

Fig. 264 Density in vessel (GV + 174), from -6 to 42 s.

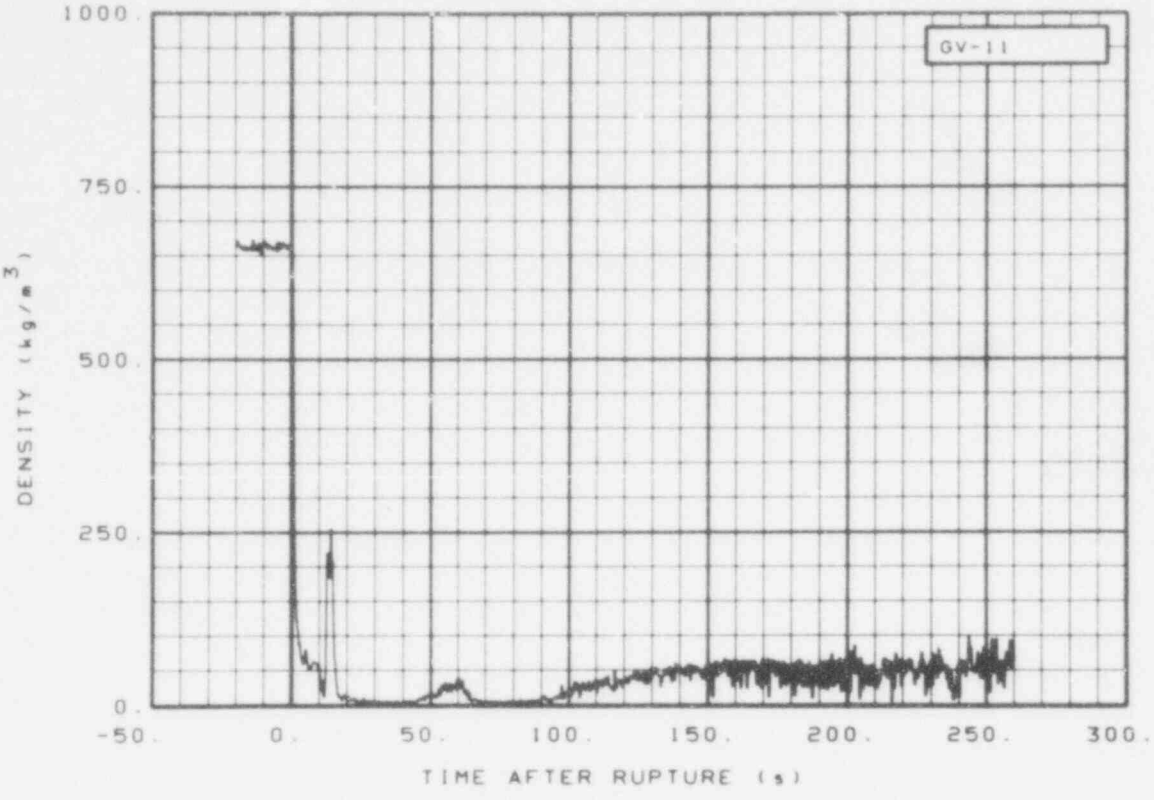

Fig. 265 Density in vessel (GV-11), from -20 to 260 s.

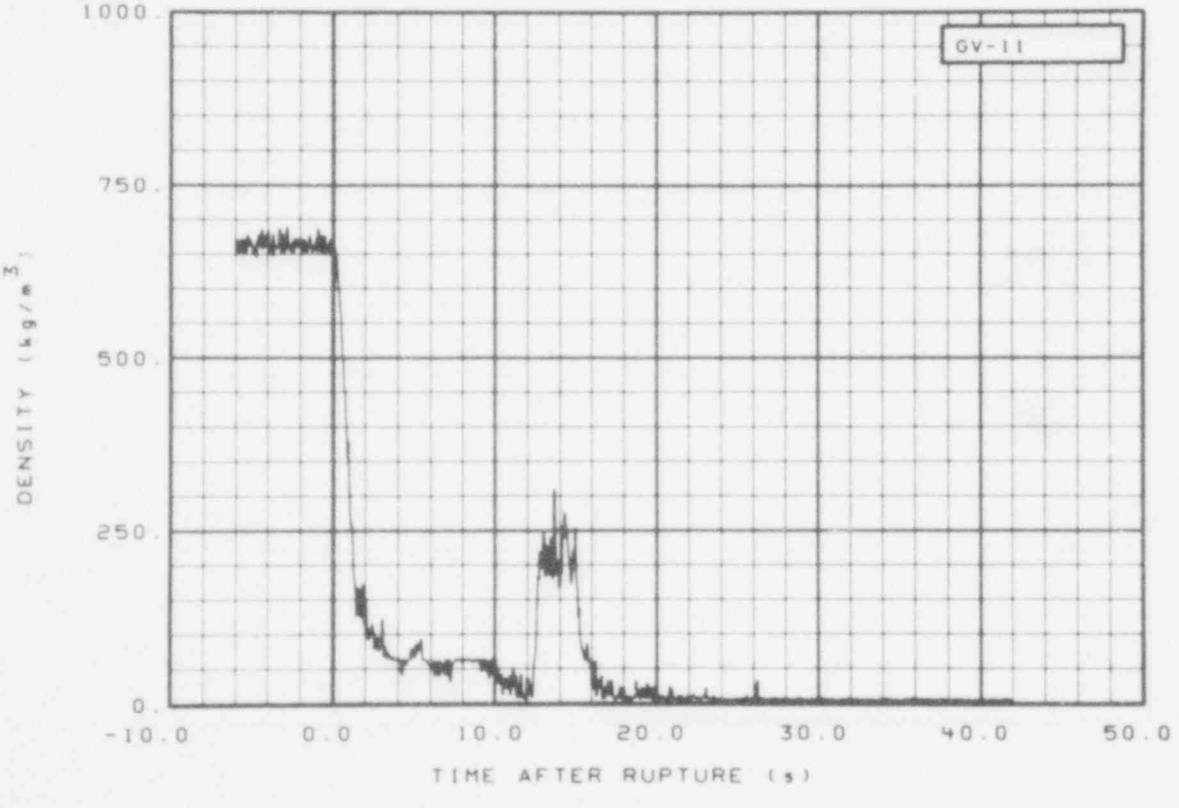

Fig. 266 Density in vessel (GV-11), from -6 to 42 s.

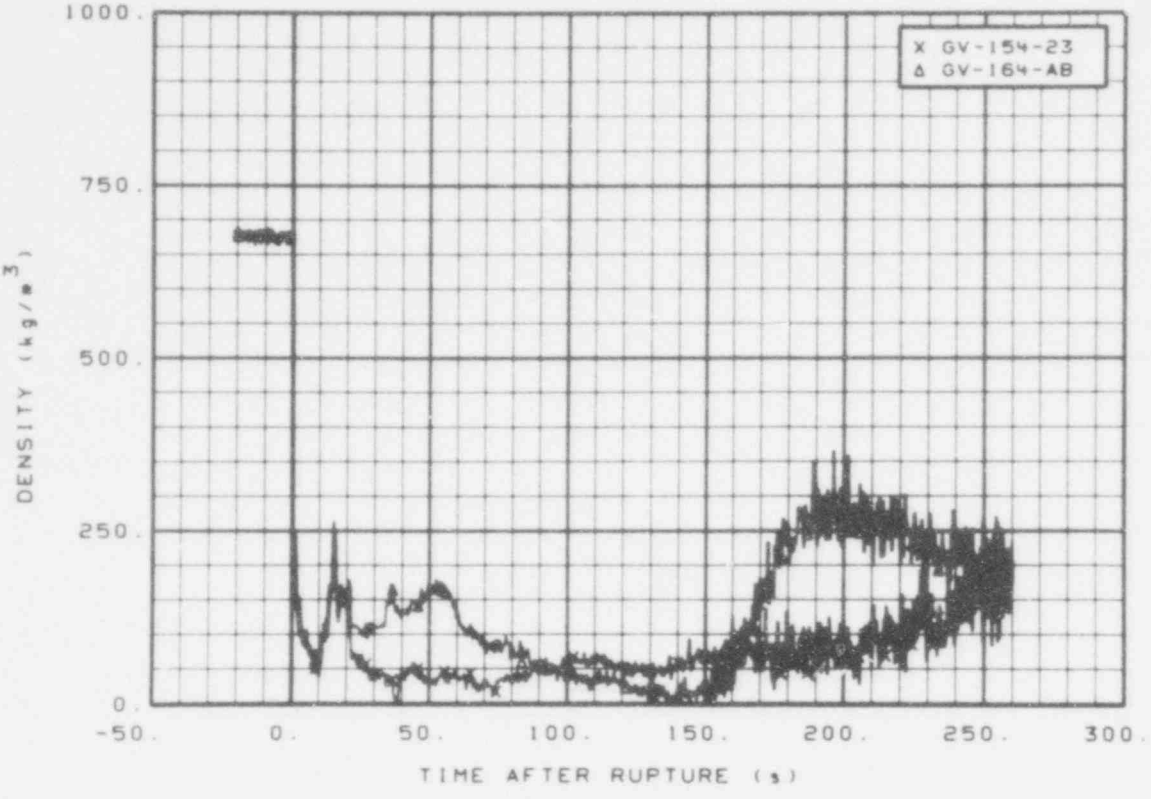

Fig. 267 Density in vessel (GV-154-23 and GV-164-AB), from -20 to 260 s.

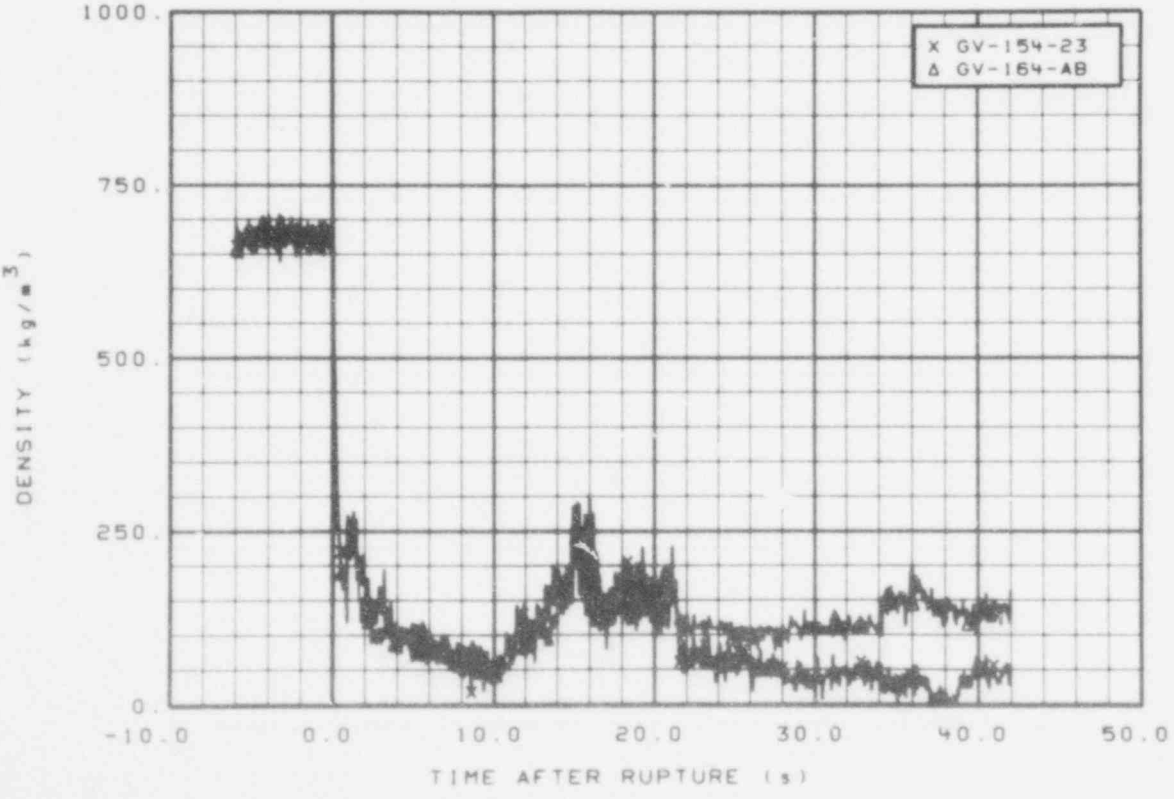

Fig. 268 Density in vessel (GV-154-23 and GV-164-AB), from -6 to 42 s.

544 177

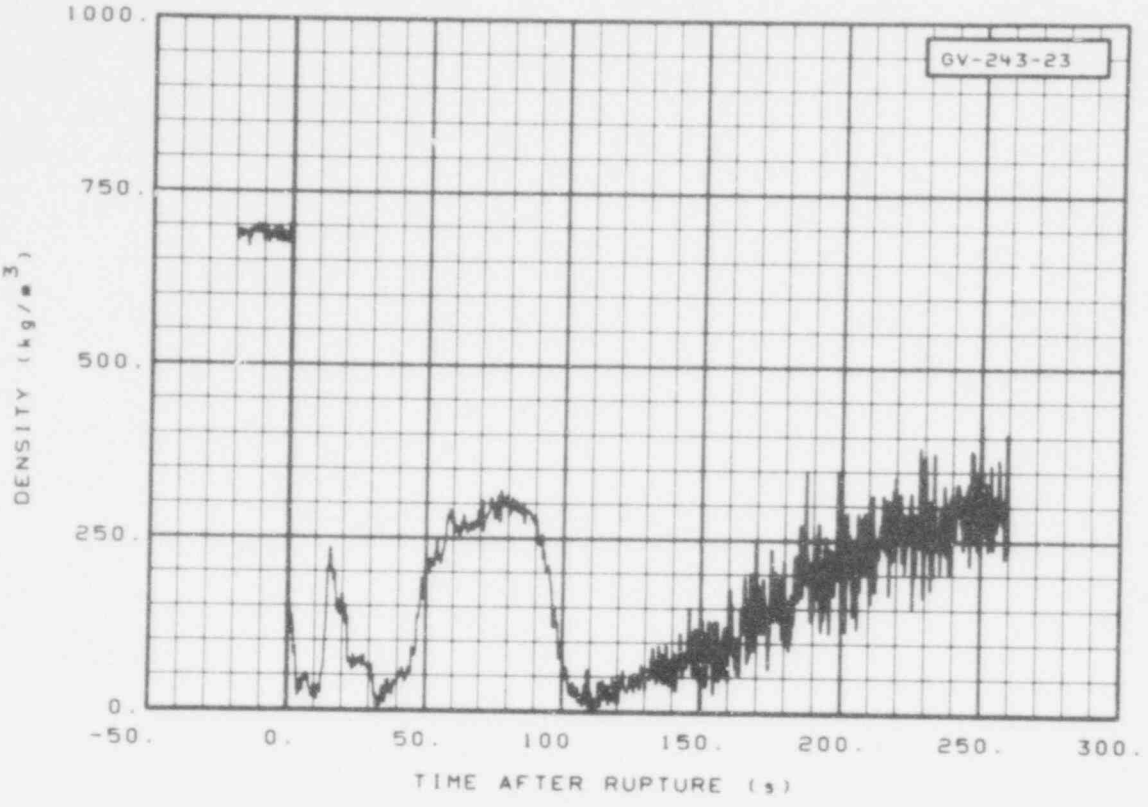

Fig. 269 Density in vessel (GV-243-23), from -20 to 260 s.

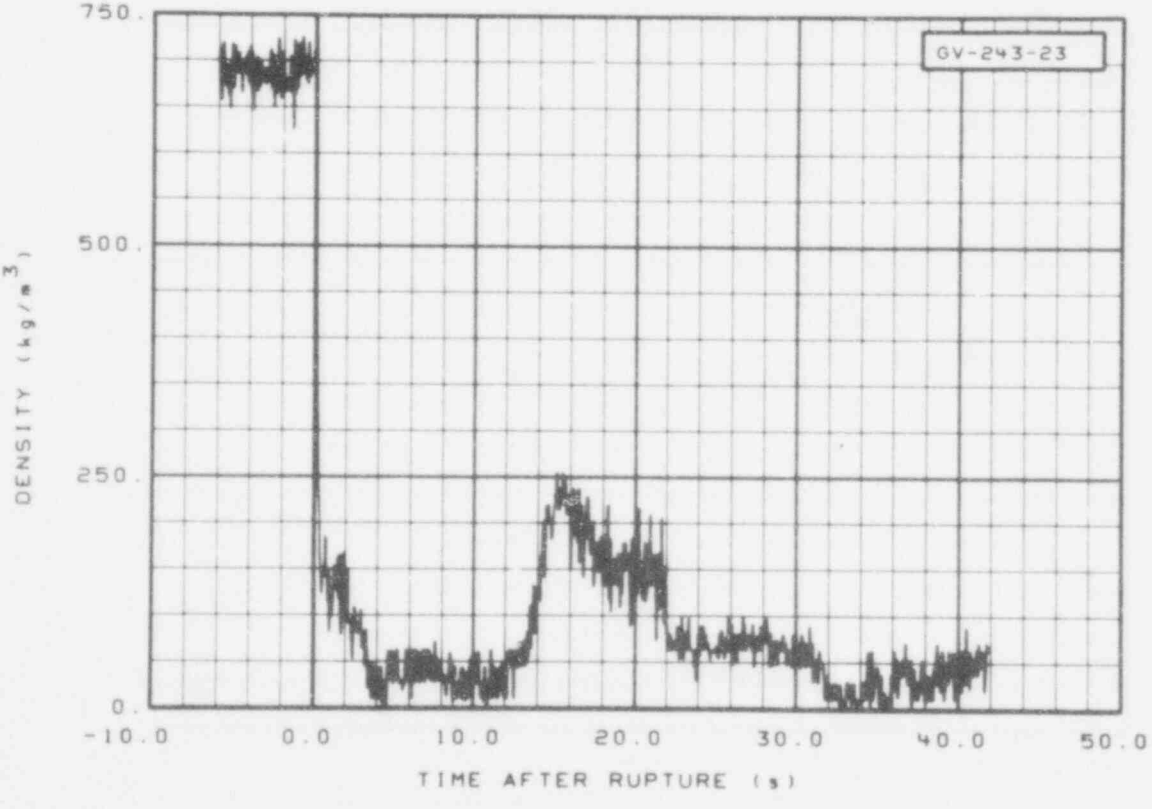

Fig. 270 Density in vessel (GV-243-23), from -6 to 42 s.

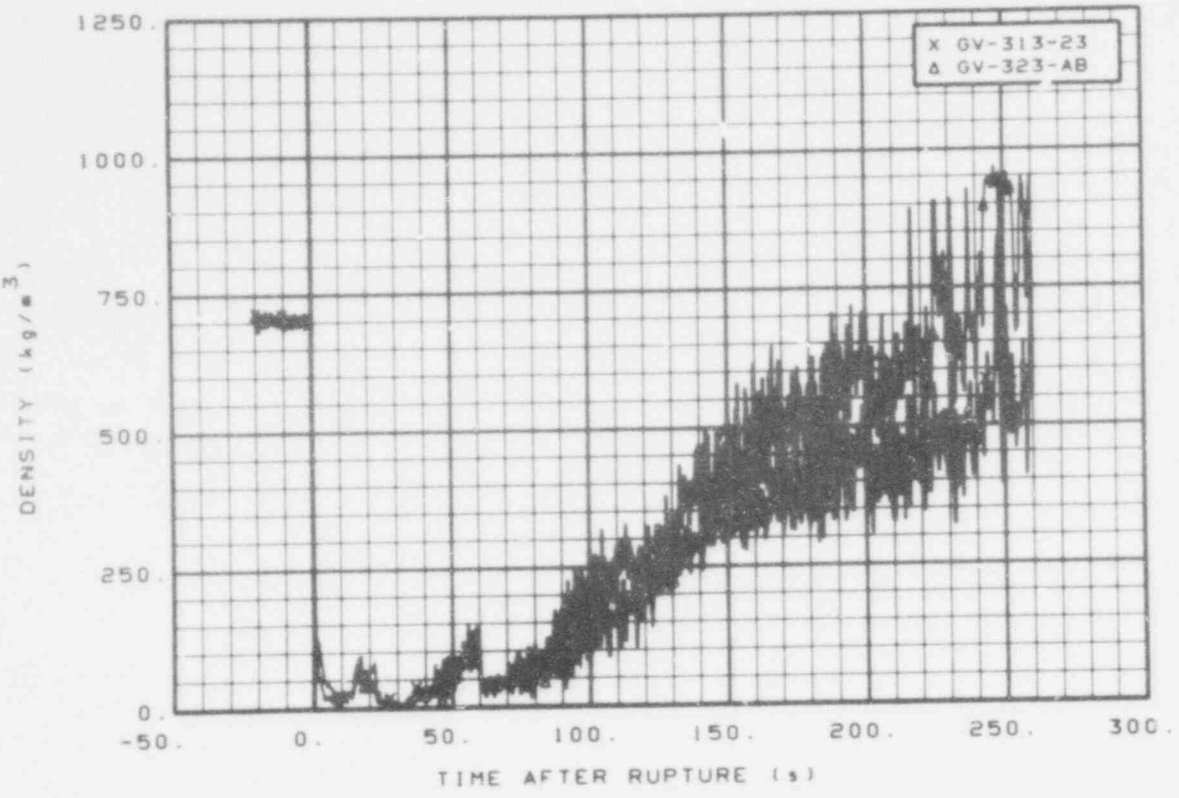

Fig. 271 Density in vessel (GV-313-23 and GV-323-AB), from -20 to 260 s.

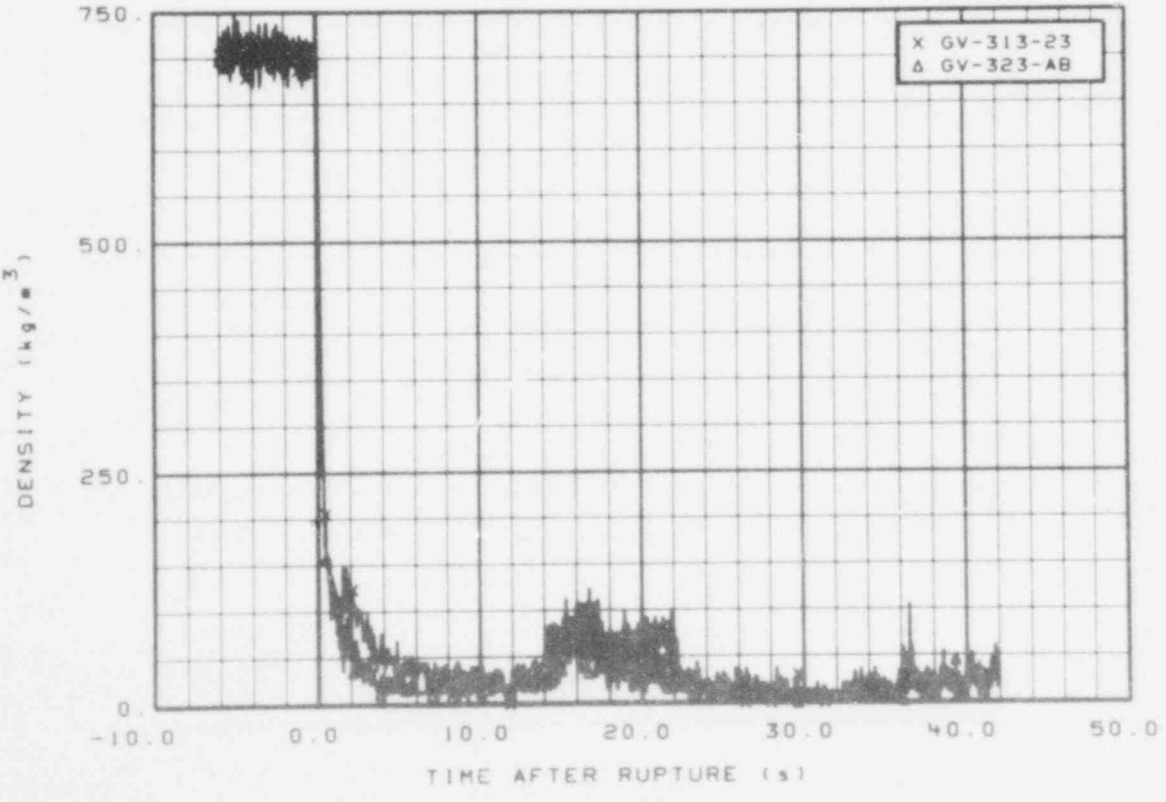

Fig. 272 Density in vessel (GV-313-23 and GV-323-AB), from -6 to 42 s.

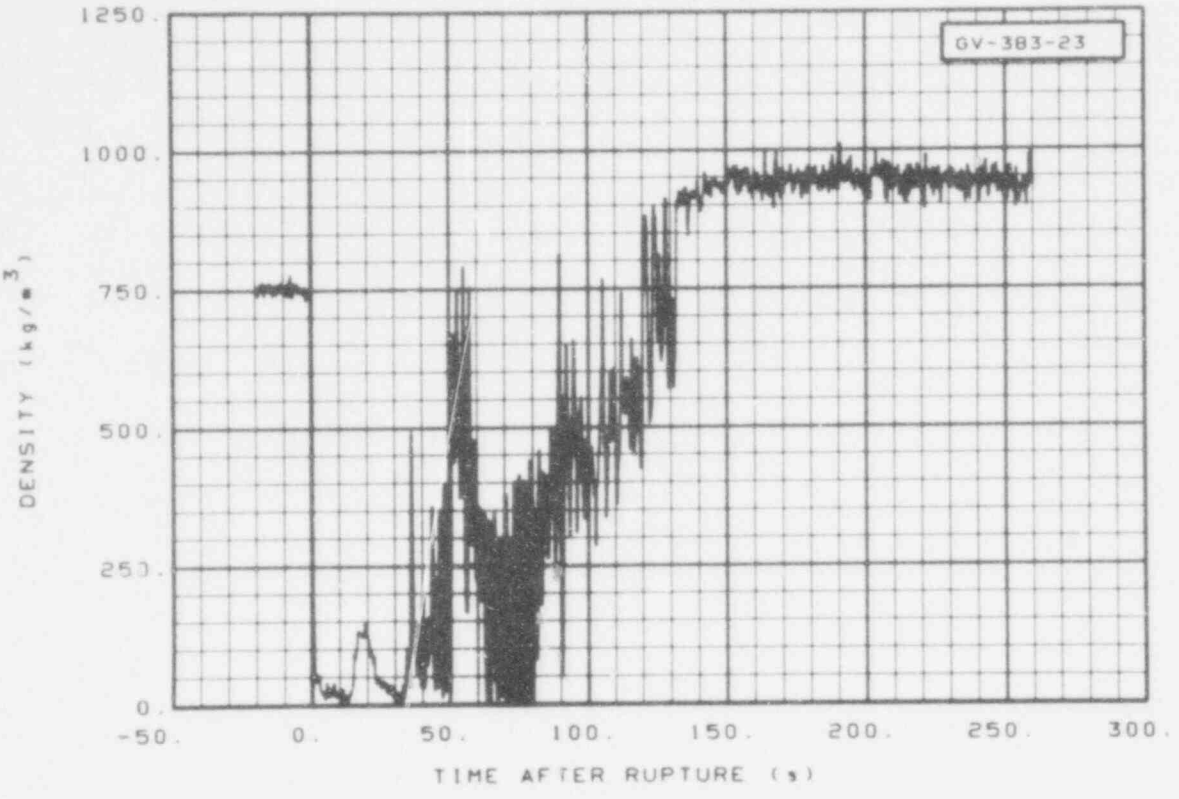

Fig. 273 Density in vessel (GV-383-23), from -20 to 260 s.

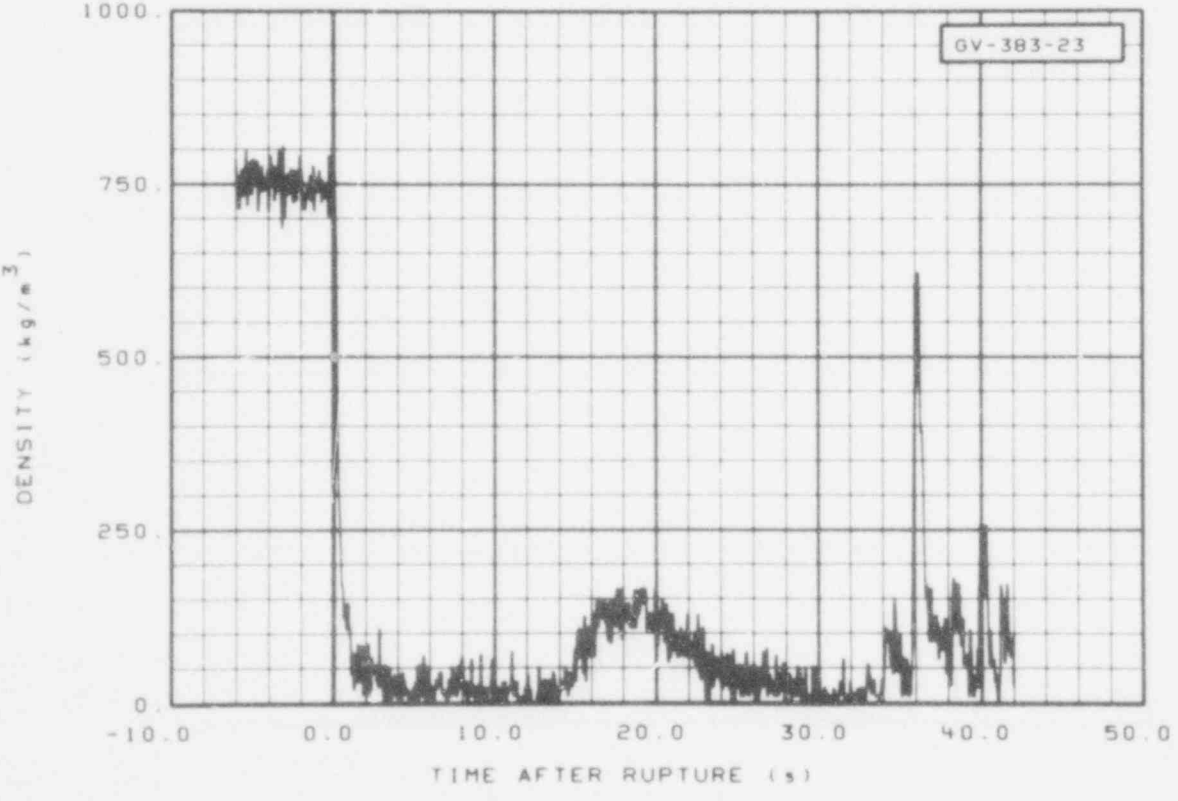

Fig. 274 Density in vessel (GV-383-23), from -6 to 42 s.

544 180

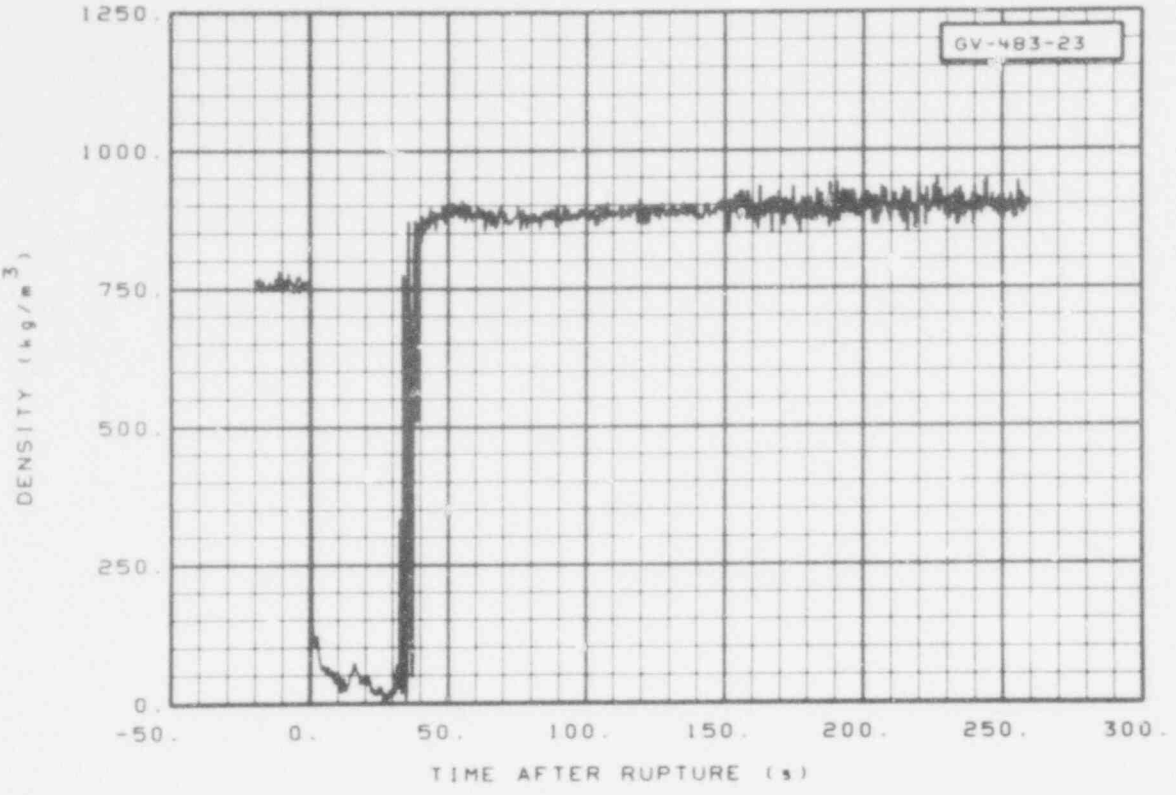

Fig. 275 Density in vessel (GV-483-23), from -20 to 260 s.

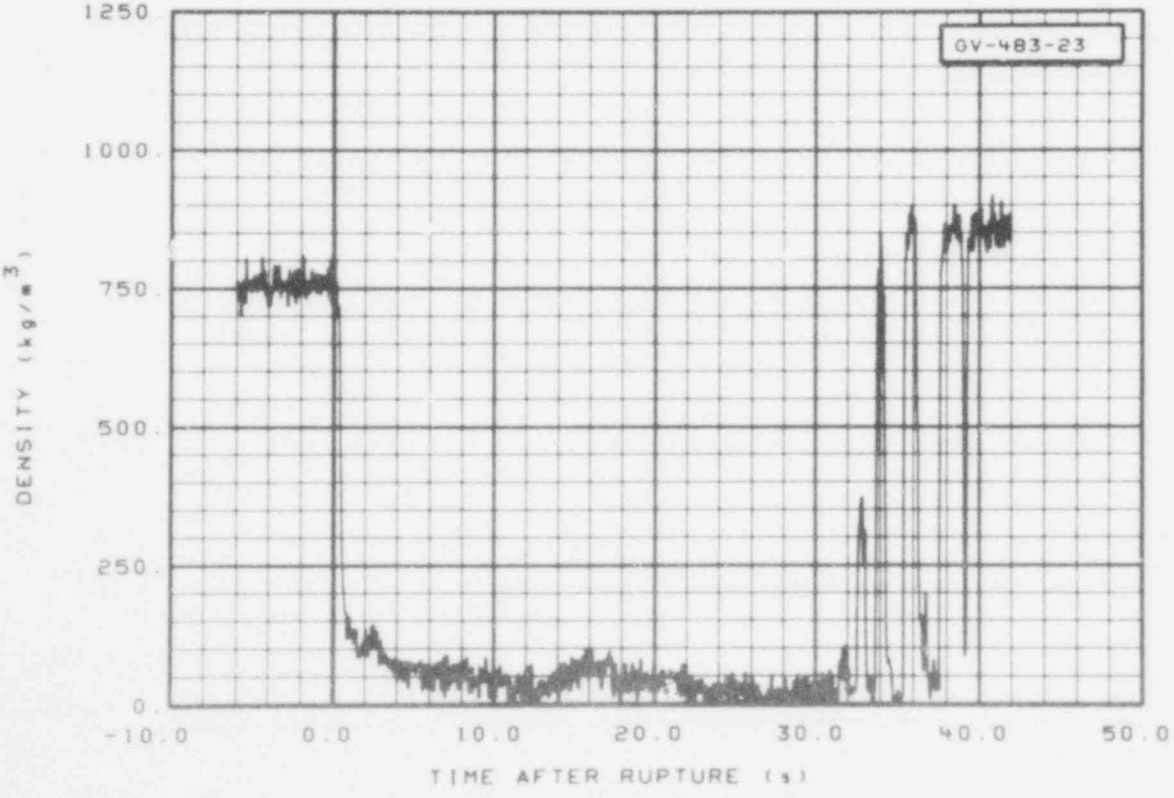

Fig. 276 Density in vessel (GV-483-23), from -6 to 42 s.

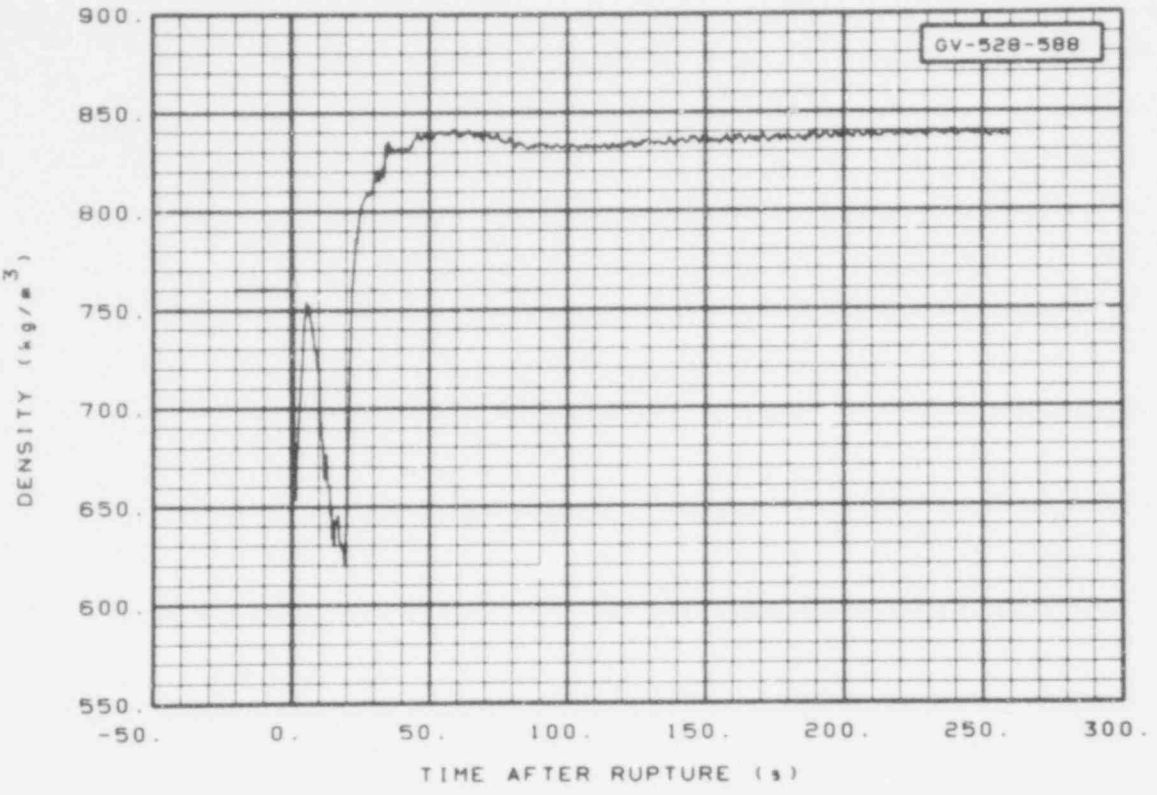

Fig. 277 Density in vessel (GV-528-588), from -20 to 260 s.

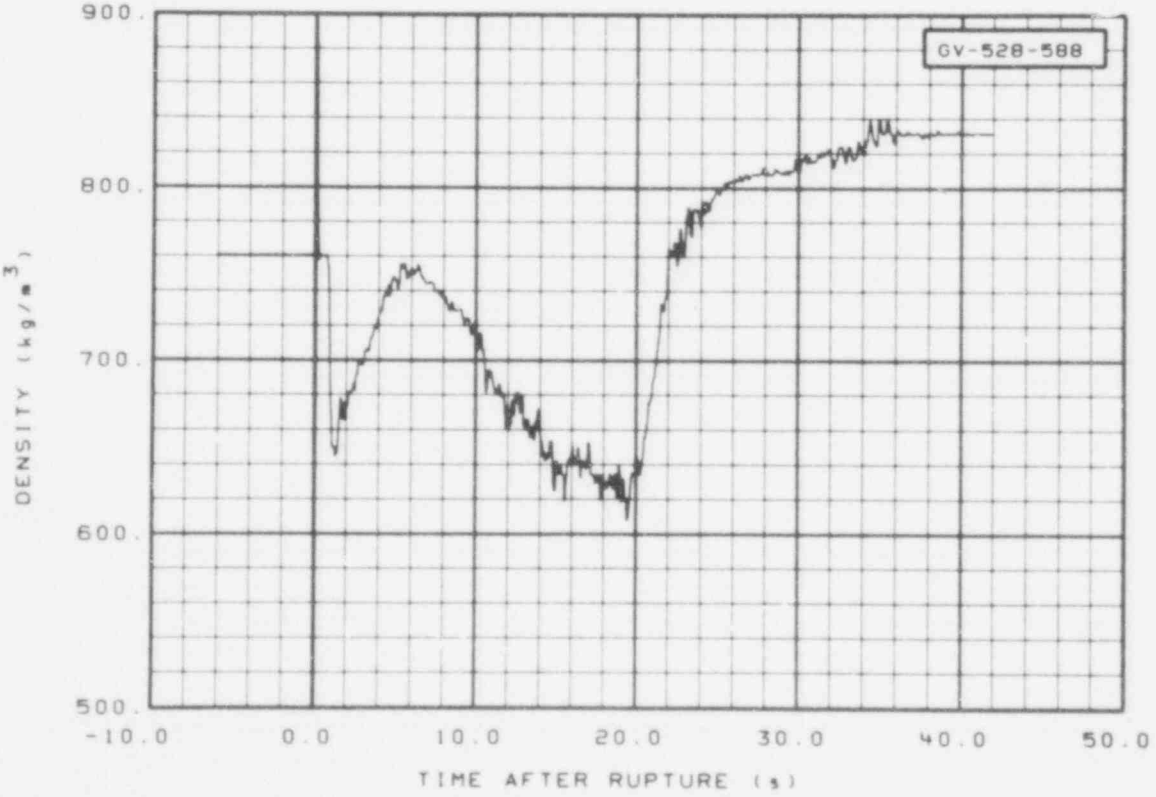

Fig. 278 Density in vessel (GV-528-588), from -6 to 42 s.

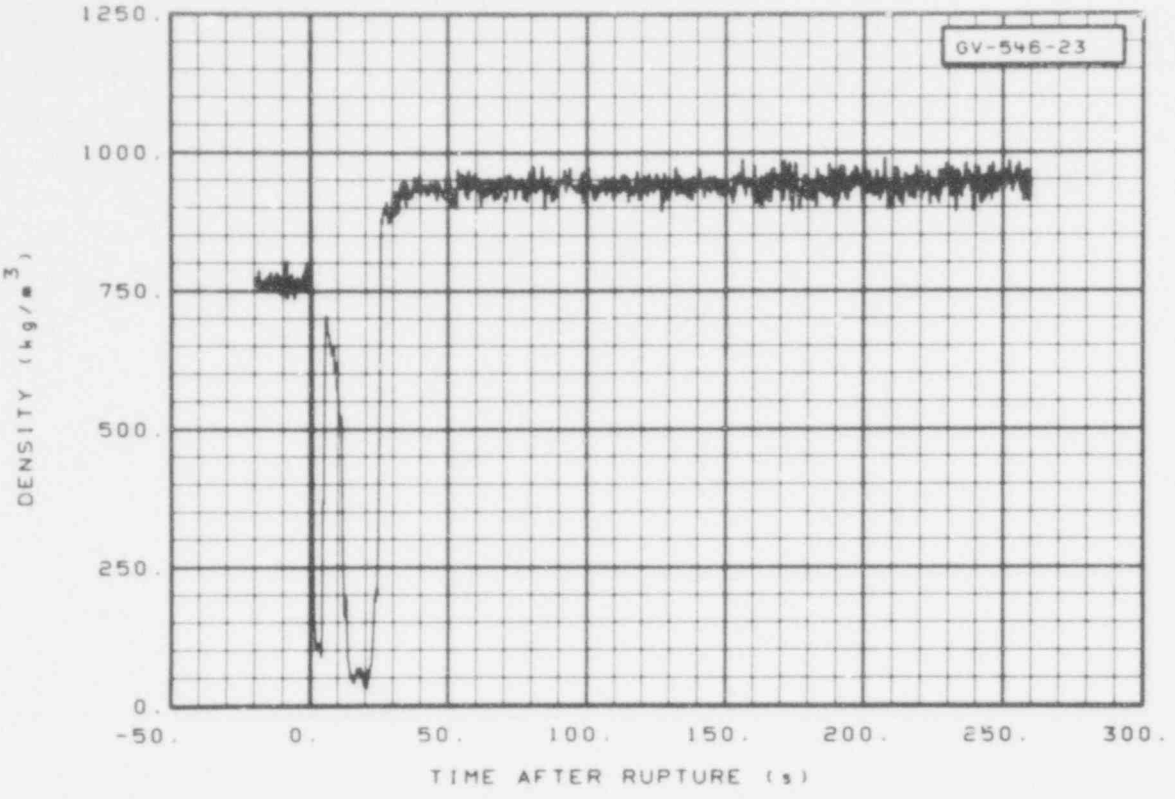

Fig. 279 Density in vessel (GV-546-23), from -20 to 260 s.

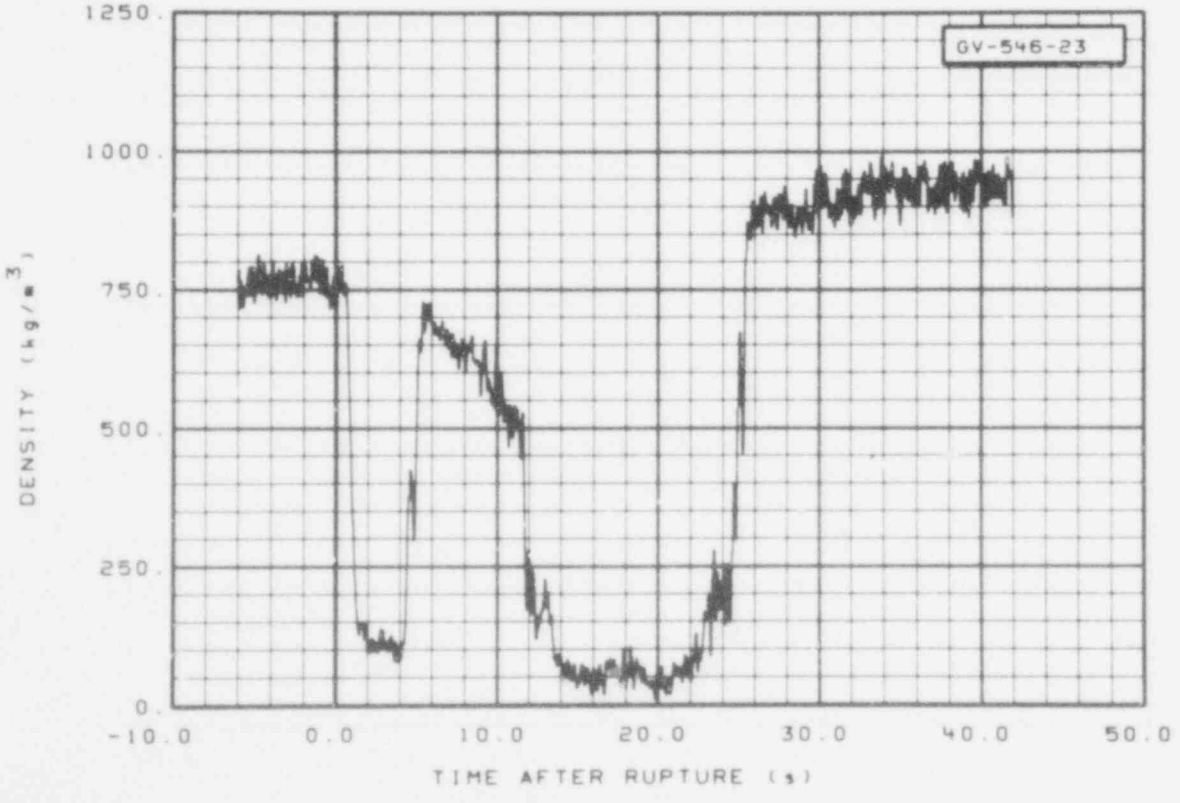

Fig. 280 Density in vessel (GV-546-23), from -6 to 42 s.

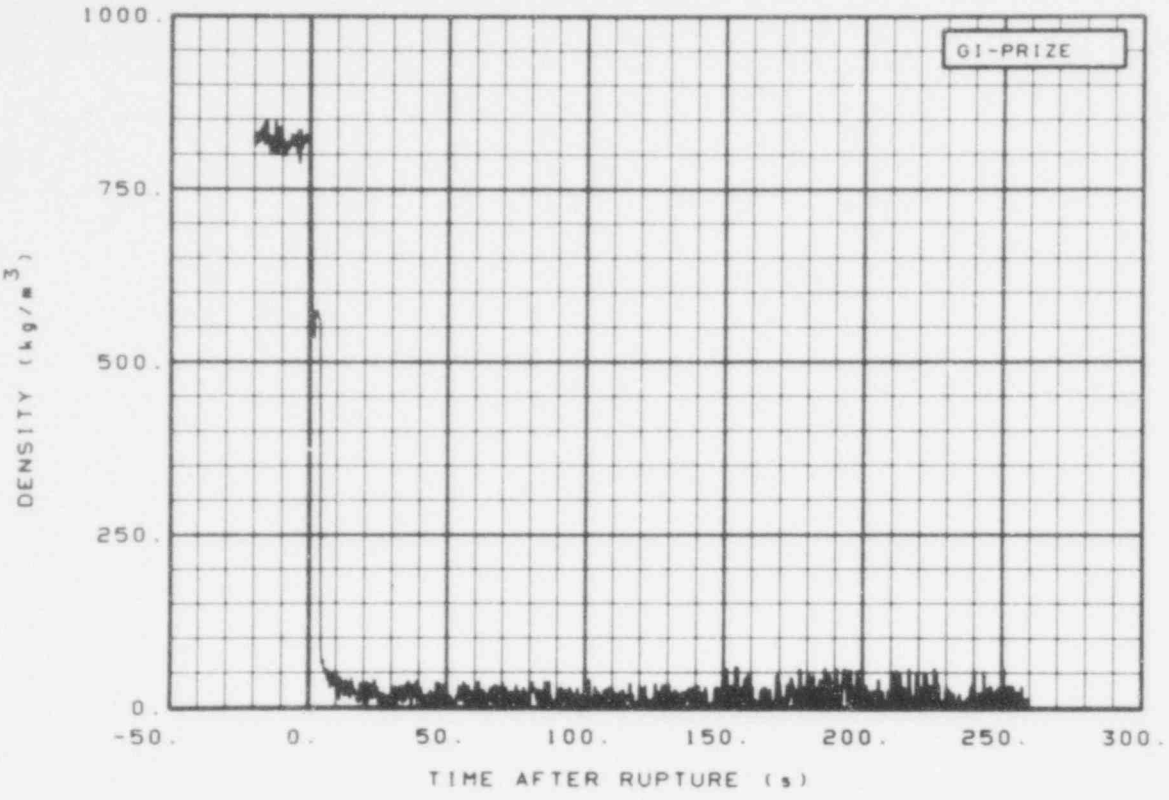

Fig. 281 Density in intact loop pressurizer (GI-PRIZE), from -20 to 260 s.

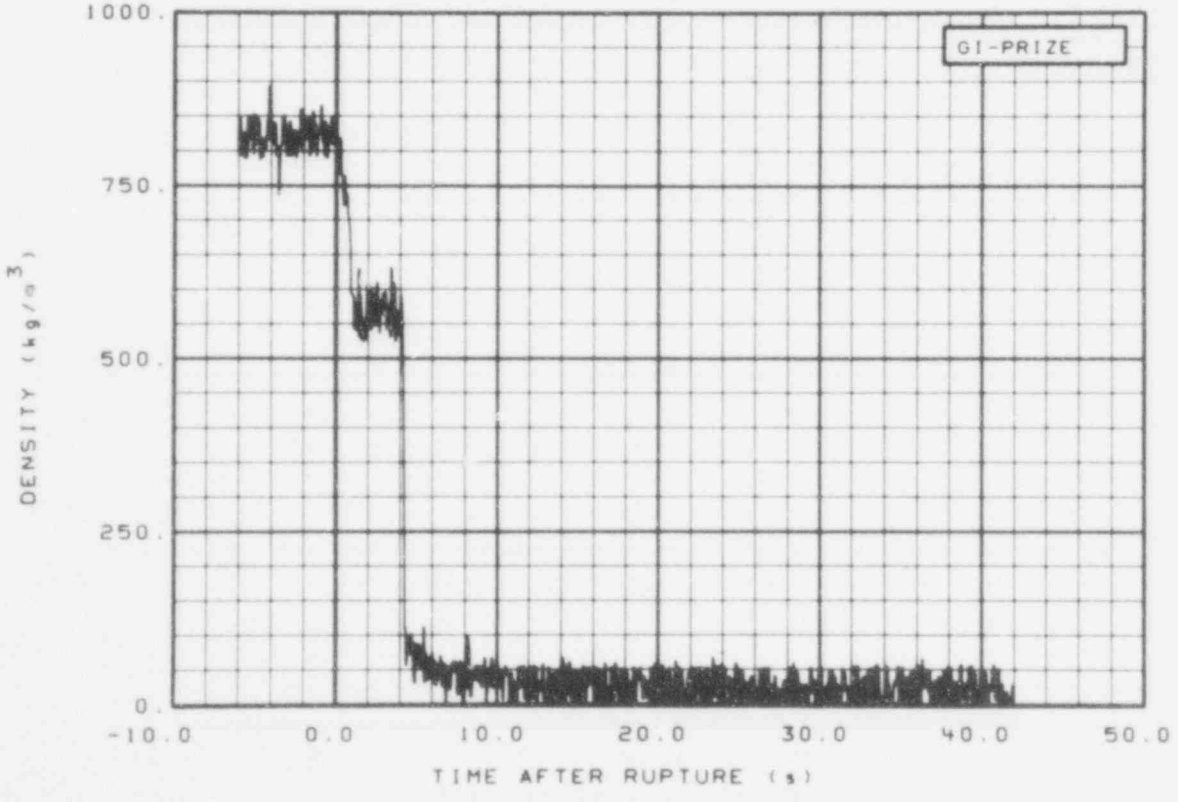

Fig. 282 Density in intact loop pressurizer (GI-PRIZE), from -6 to 42 s.

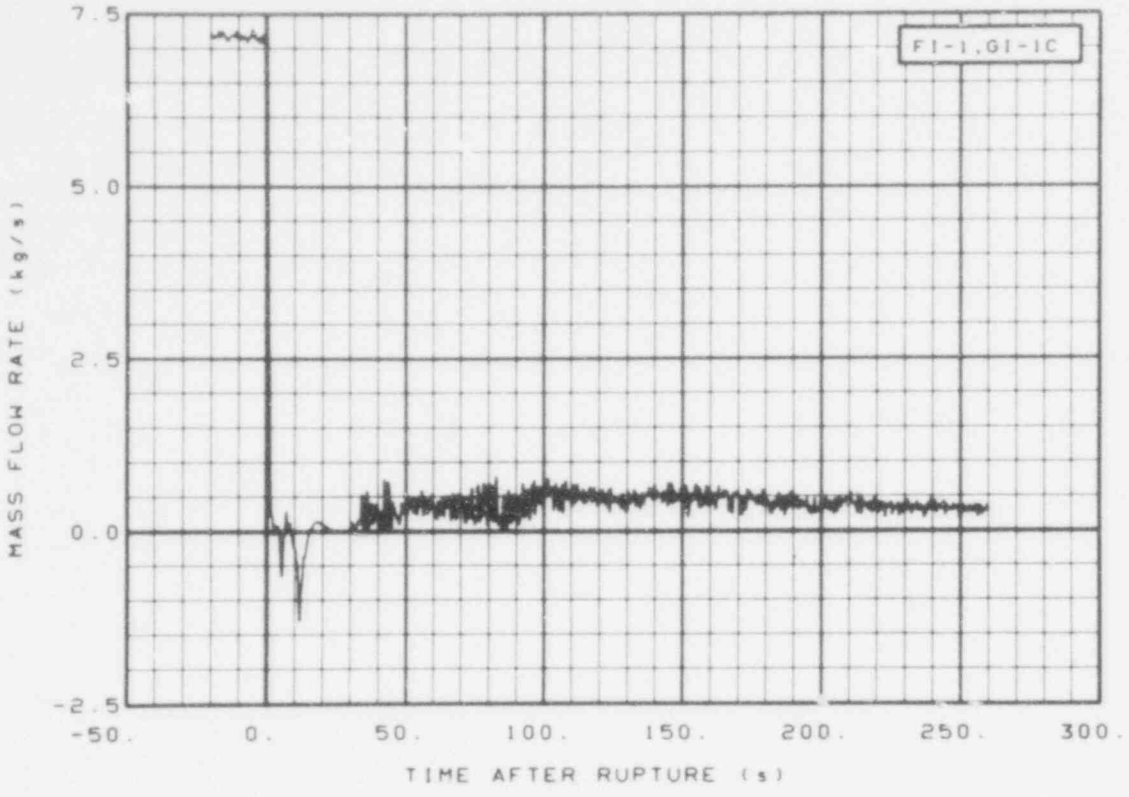

Fig. 283 Mass flow in intact loop (FI-1 and GI-1C), from -20 to 260 s.

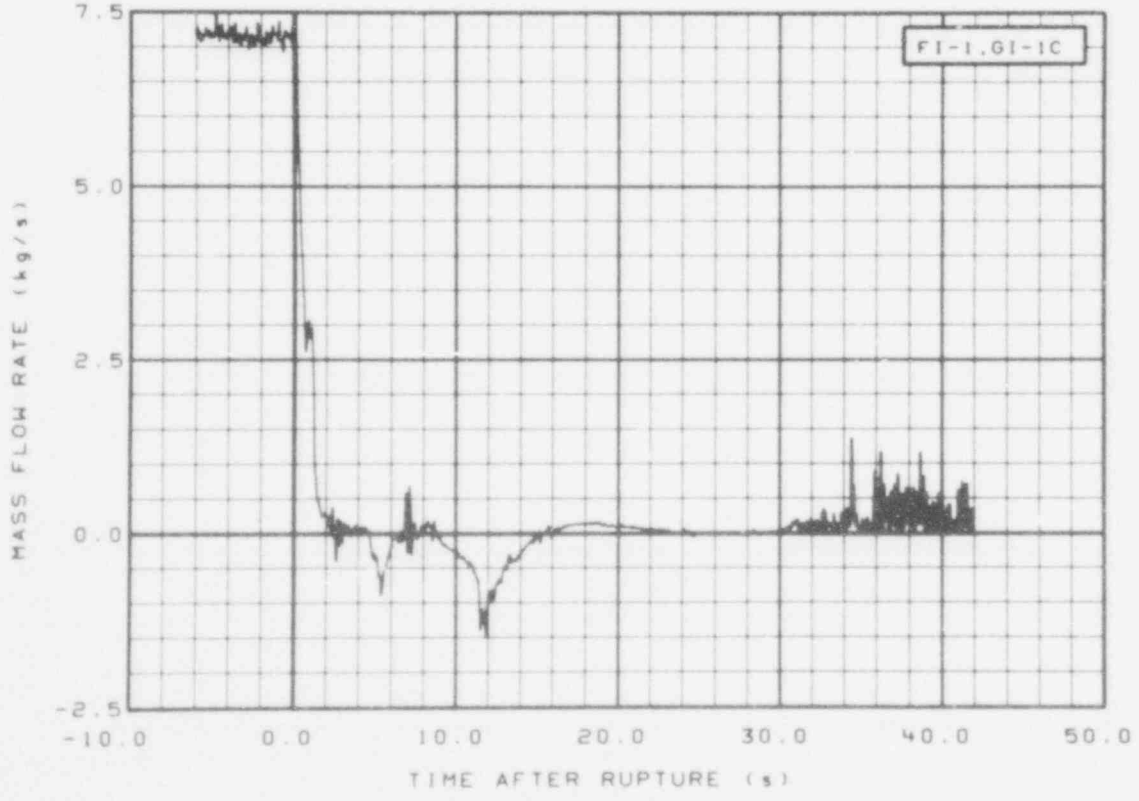

Fig. 284 Mass flow in intact loop (FI-1 and GI-1C), from -6 to 42 s.

544 185

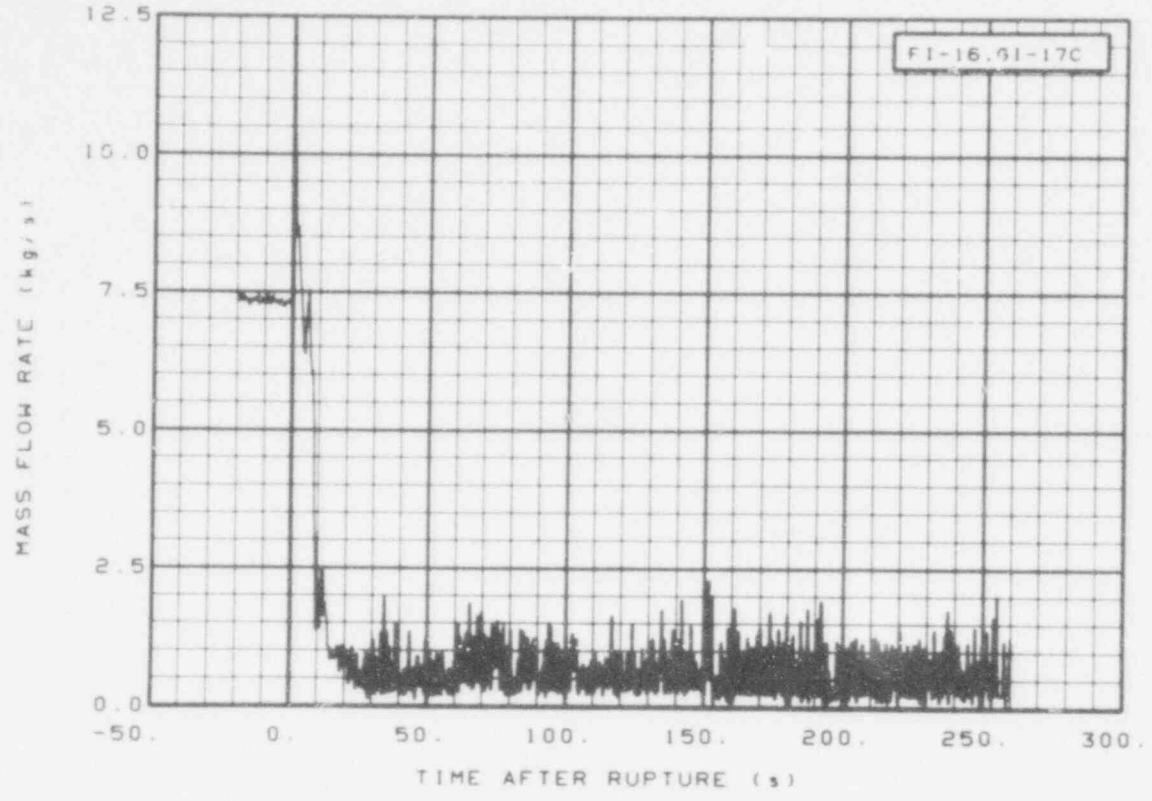

Fig. 285 Mass flow in intact loop (FI-16 and GI-17C), from -20 to 260 s.

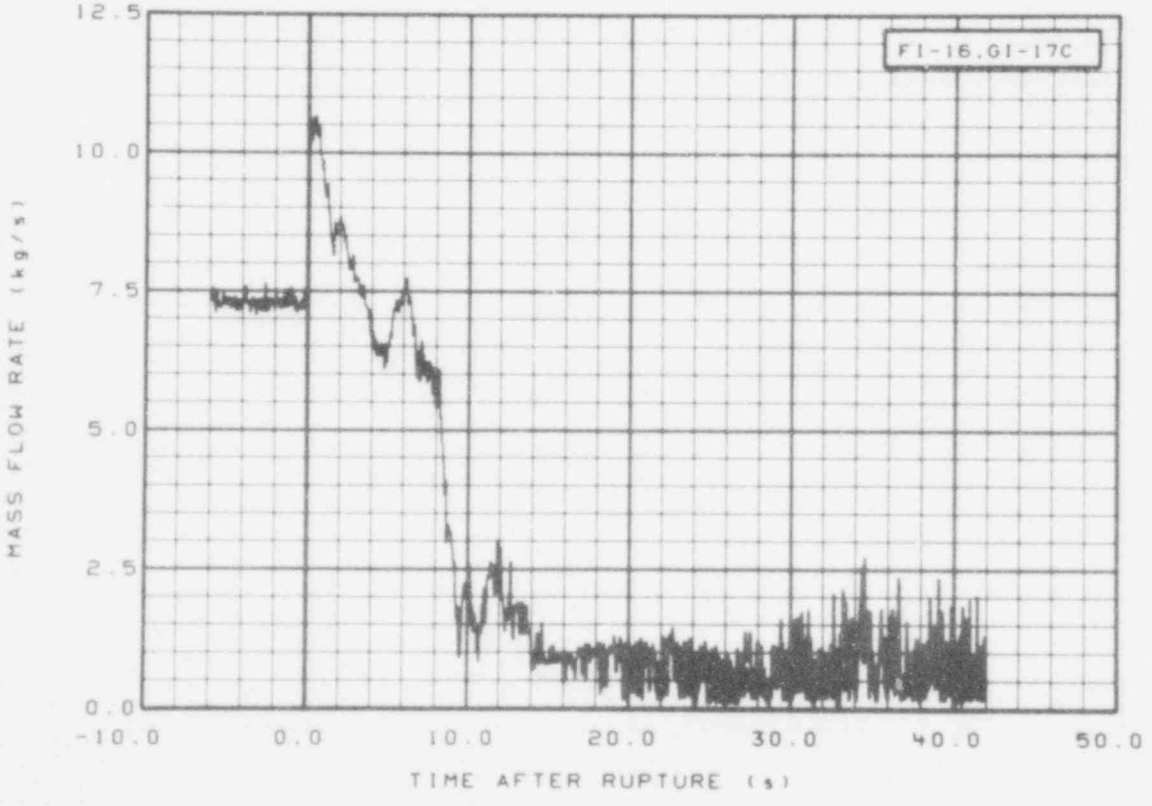

Fig. 286 Mass flow in intact loop (FI-16 and GI-17C), from -6 to 42 s.

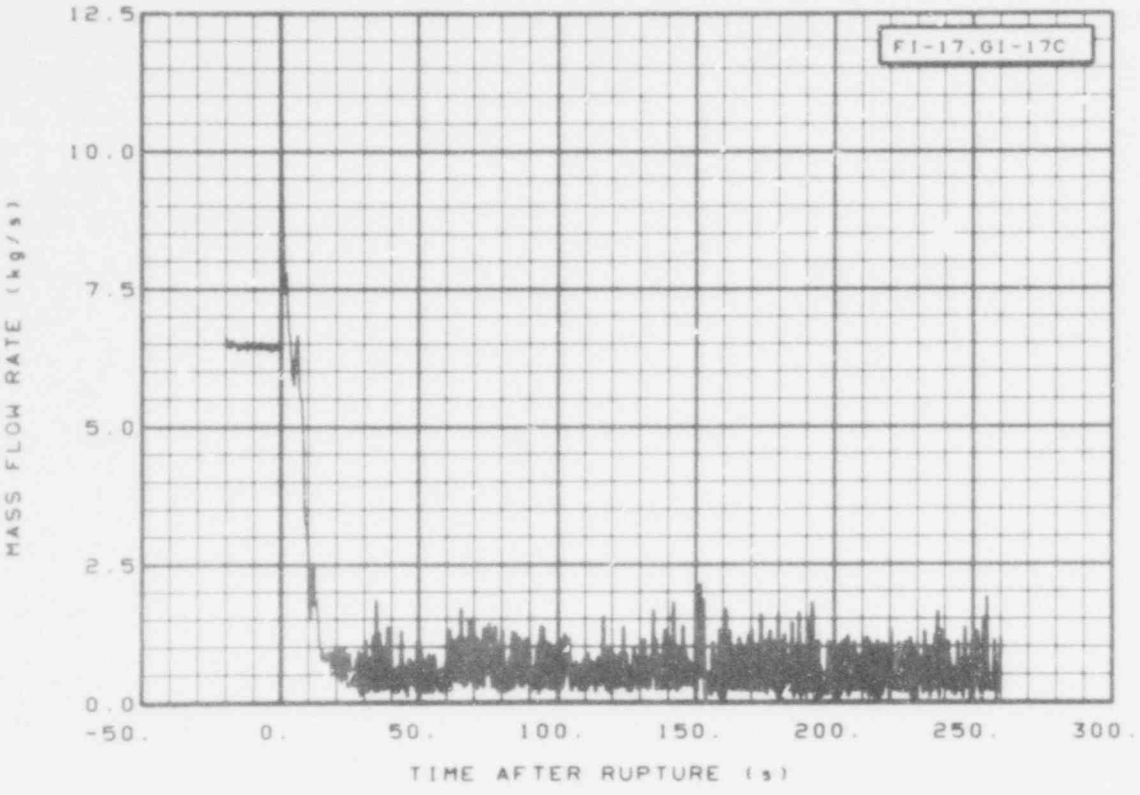

Fig. 287 Mass flow in intact loop (FI-17 and GI-17C), from -20 to 260 s.

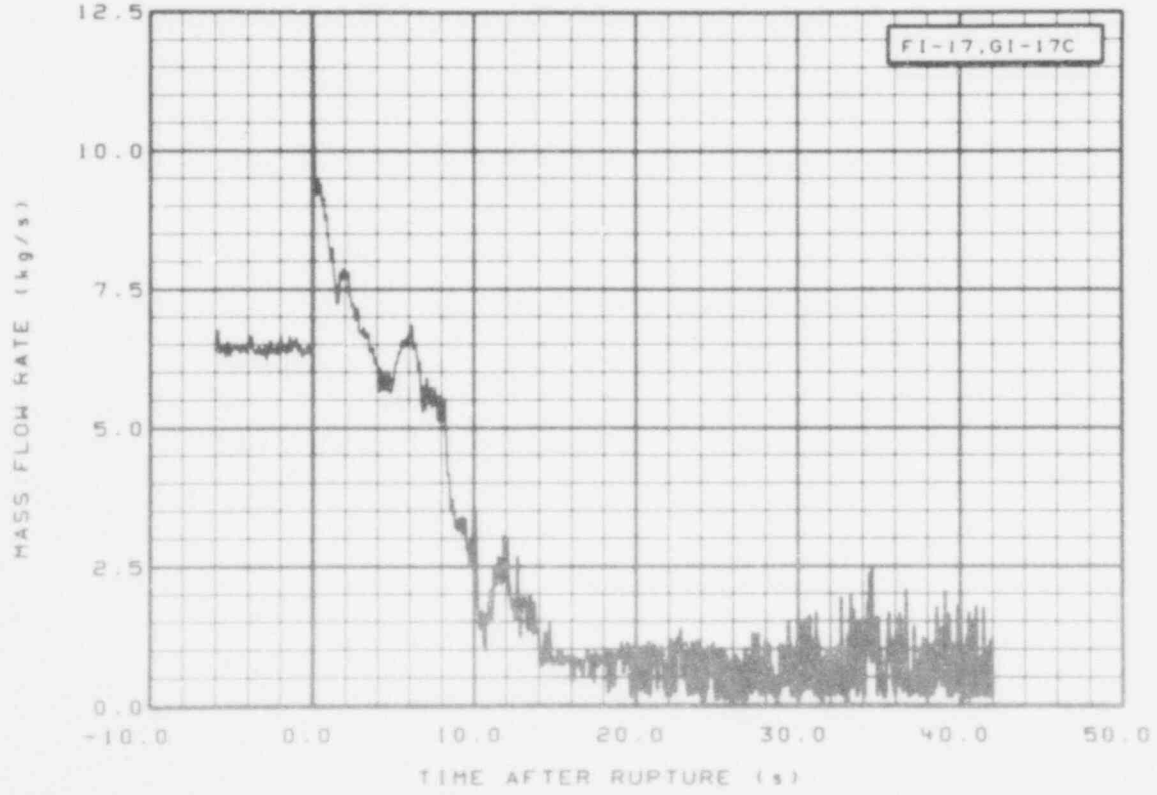

Fig. 288 Mass flow in intact loop (FI-17 and GI-17C), from -6 to 42 s.

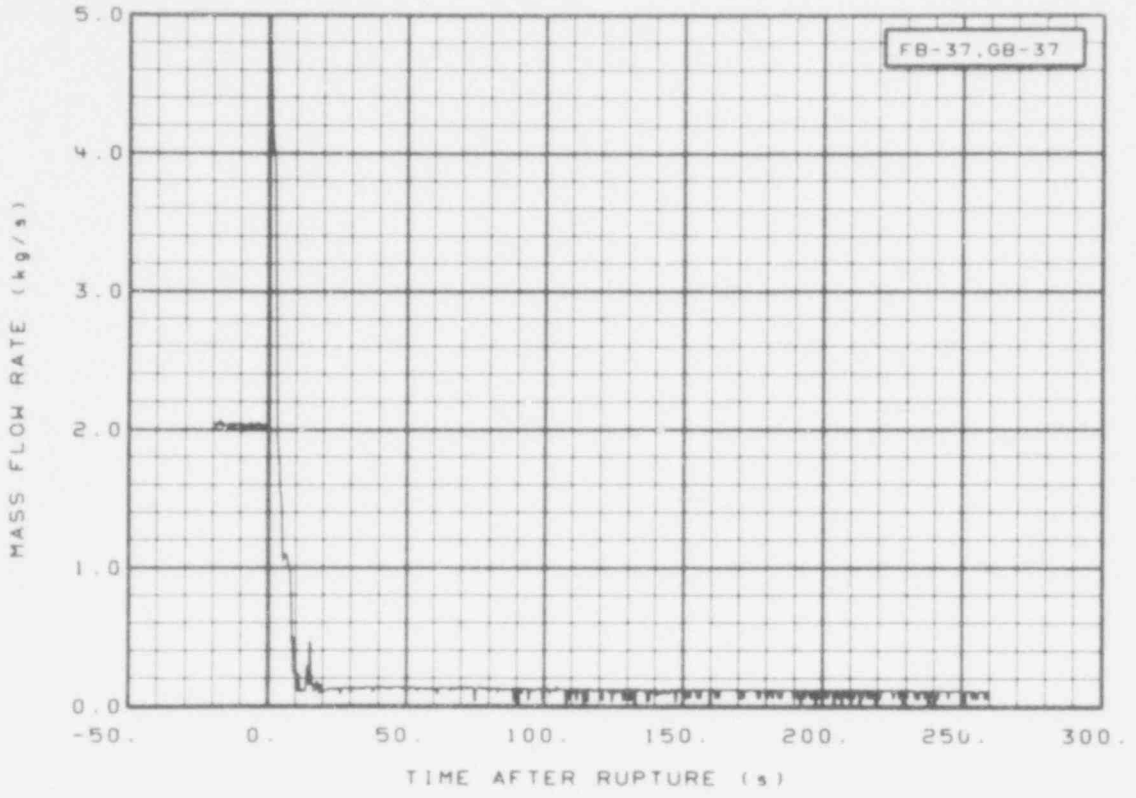

Fig. 289 Mass flow in broken loop (FB-37 and GB-37), from -20 to 260 s.

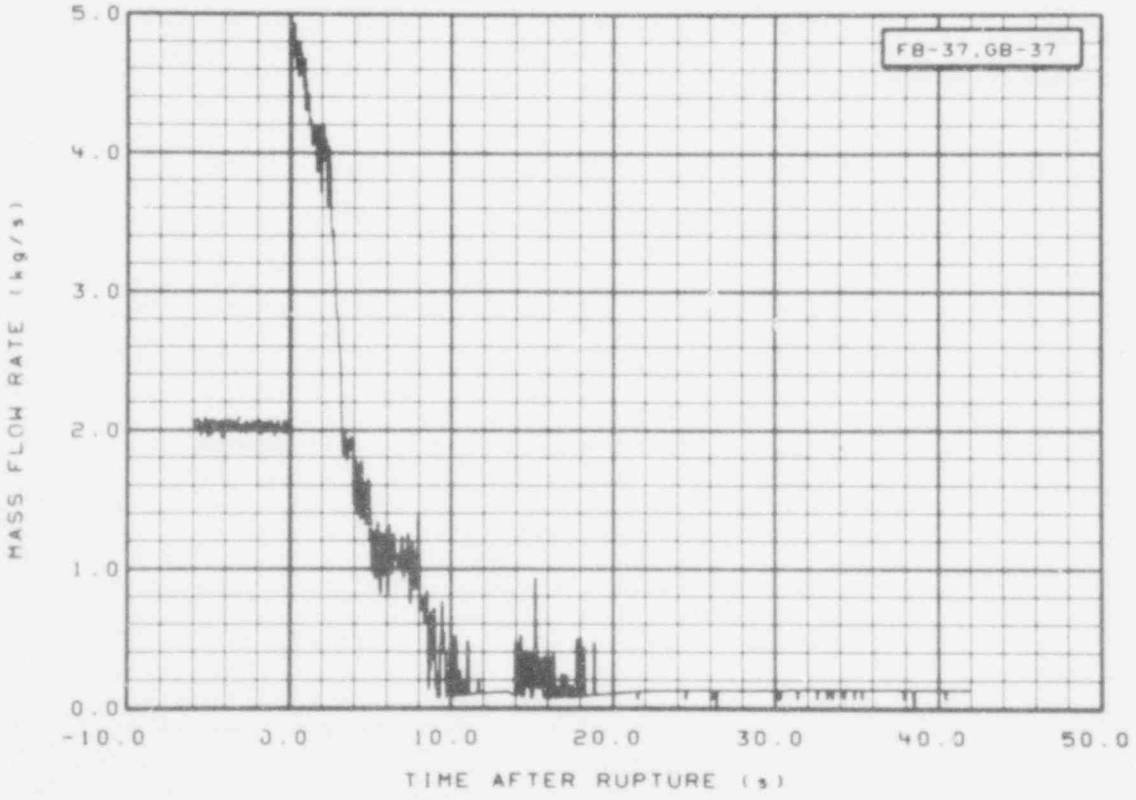

Fig. 290 Mass flow in broken loop (FB-37 and GB-37), from -6 to 42 s.

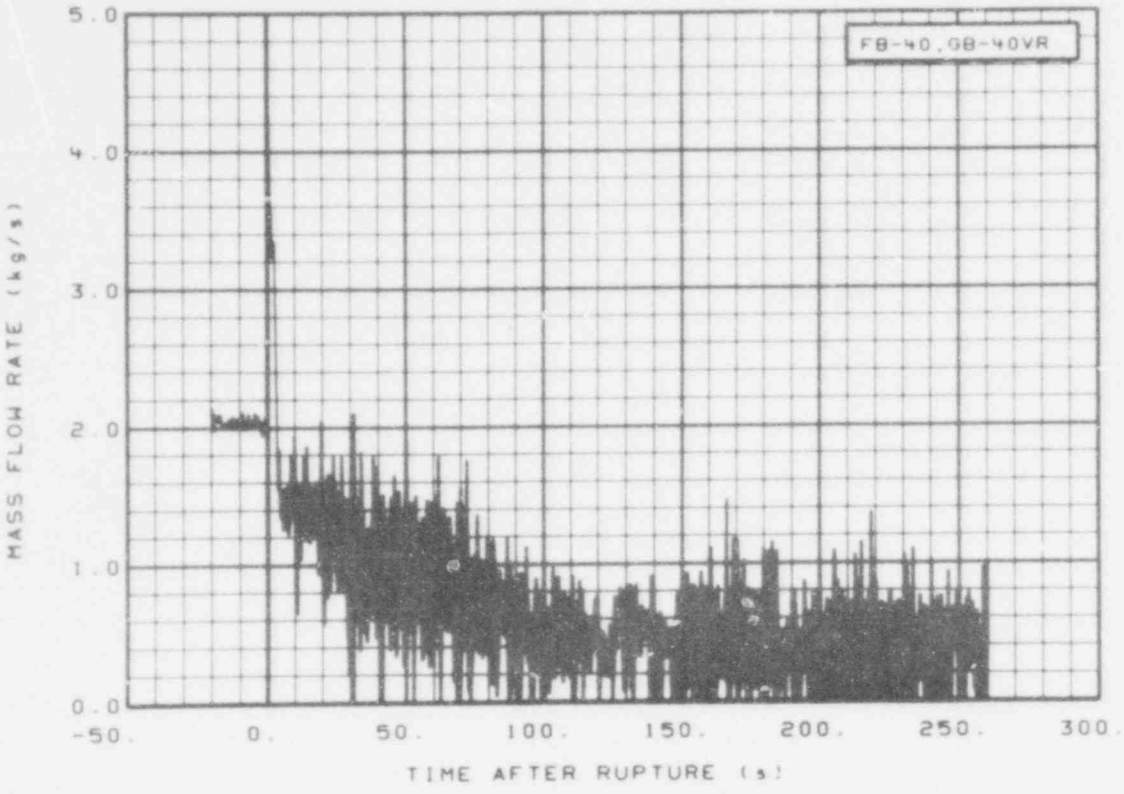

Fig. 291 Mass flow in broken loop (FB-40 and GB-40VR), from -20 to 260 s.

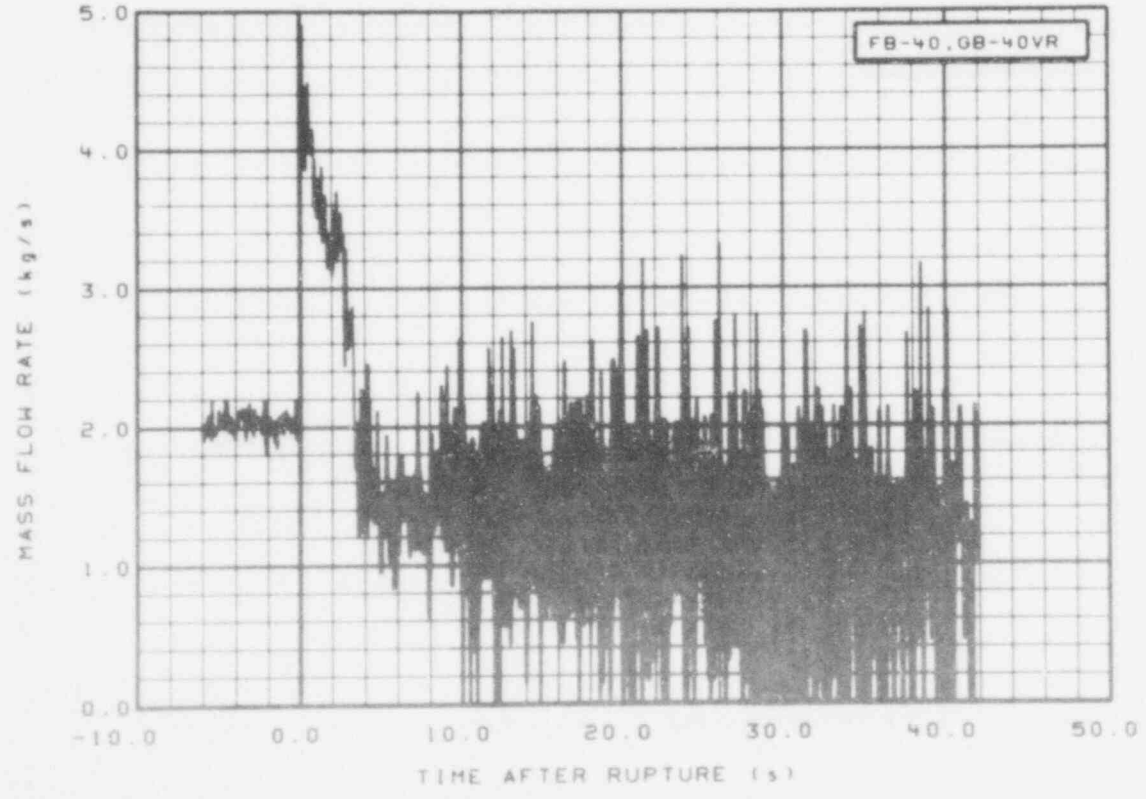

Fig. 292 Mass flow in broken loop (FB-40 and GB-40VR), from -6 to 42 s.

544 189

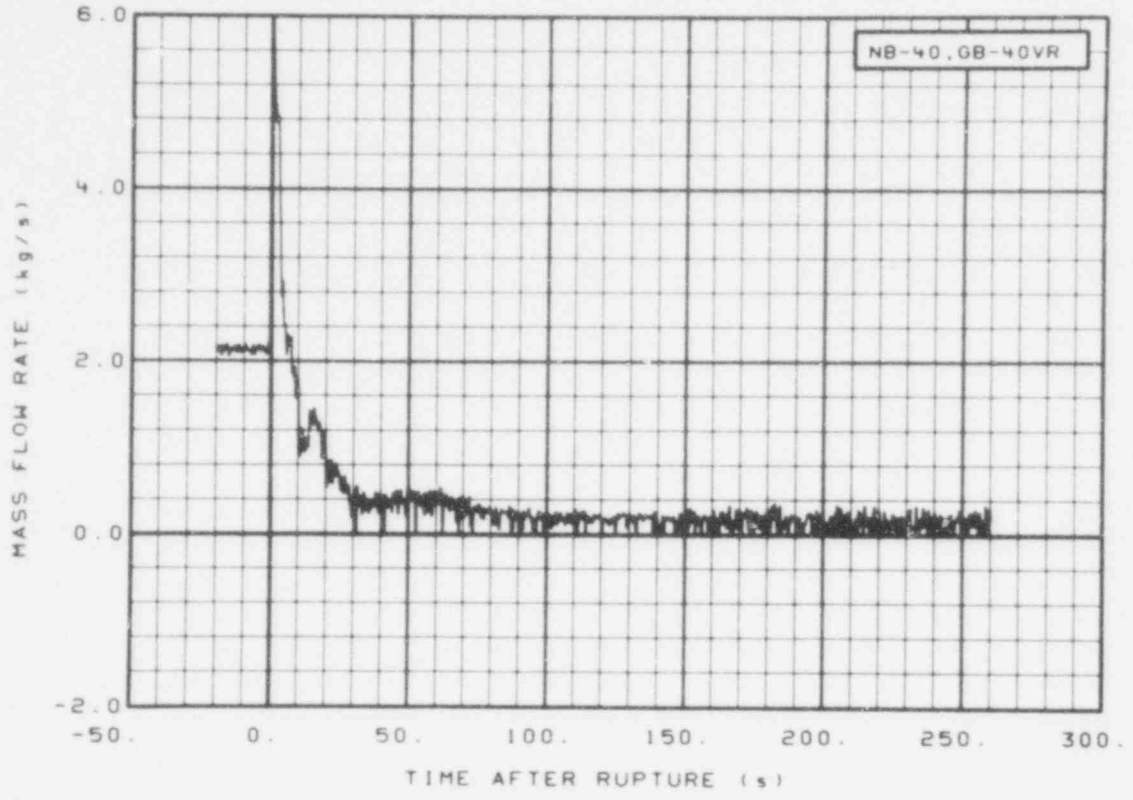

Fig. 293 Mass flow in broken loop (NB-40 and GB-40VR), from -20 to 260 s.

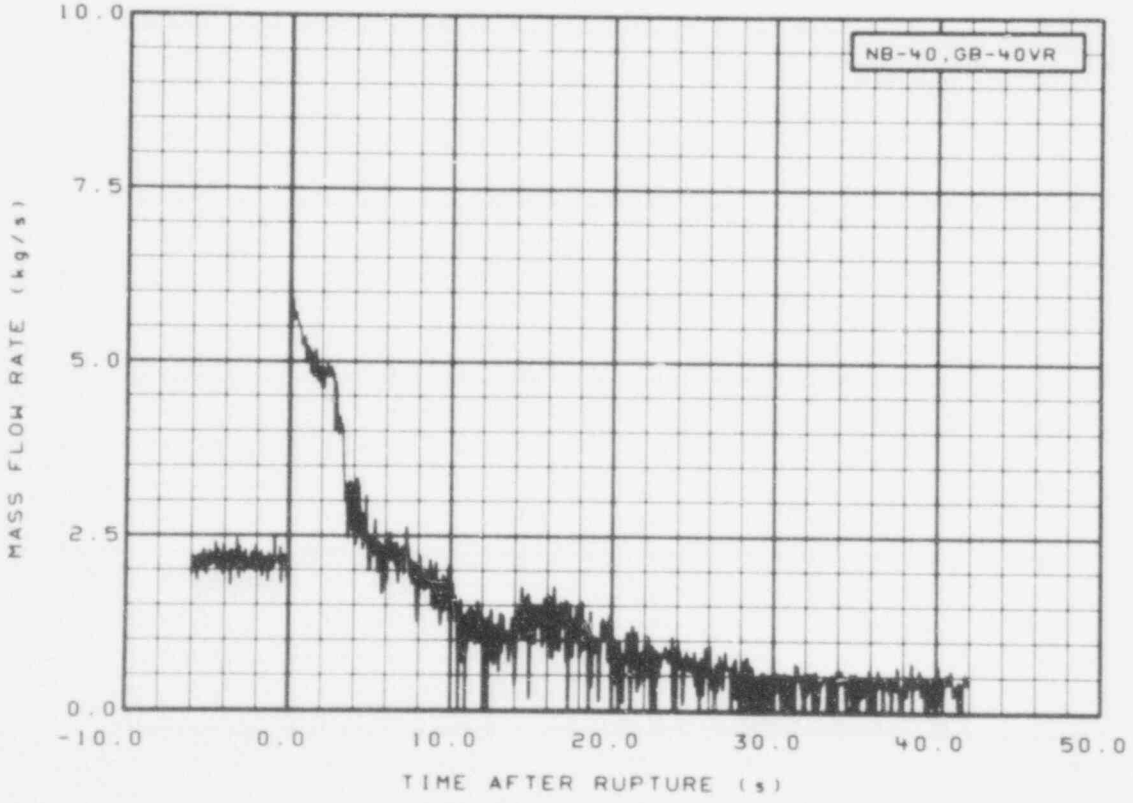

Fig. 294 Mass flow in broken loop (NB-40 and GB-40VR), from -6 to 42 s.

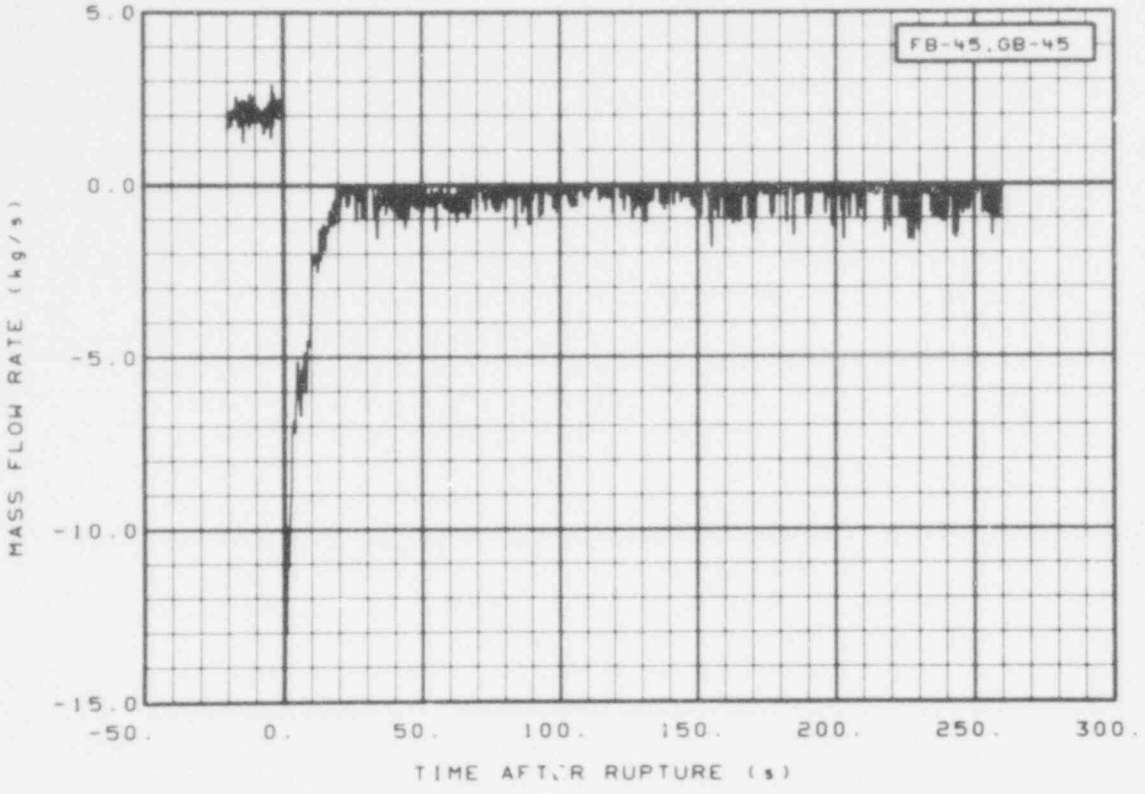

Fig. 295 Mass flow in broken loop (FB-45 and GB-45), from -20 to 260 s.

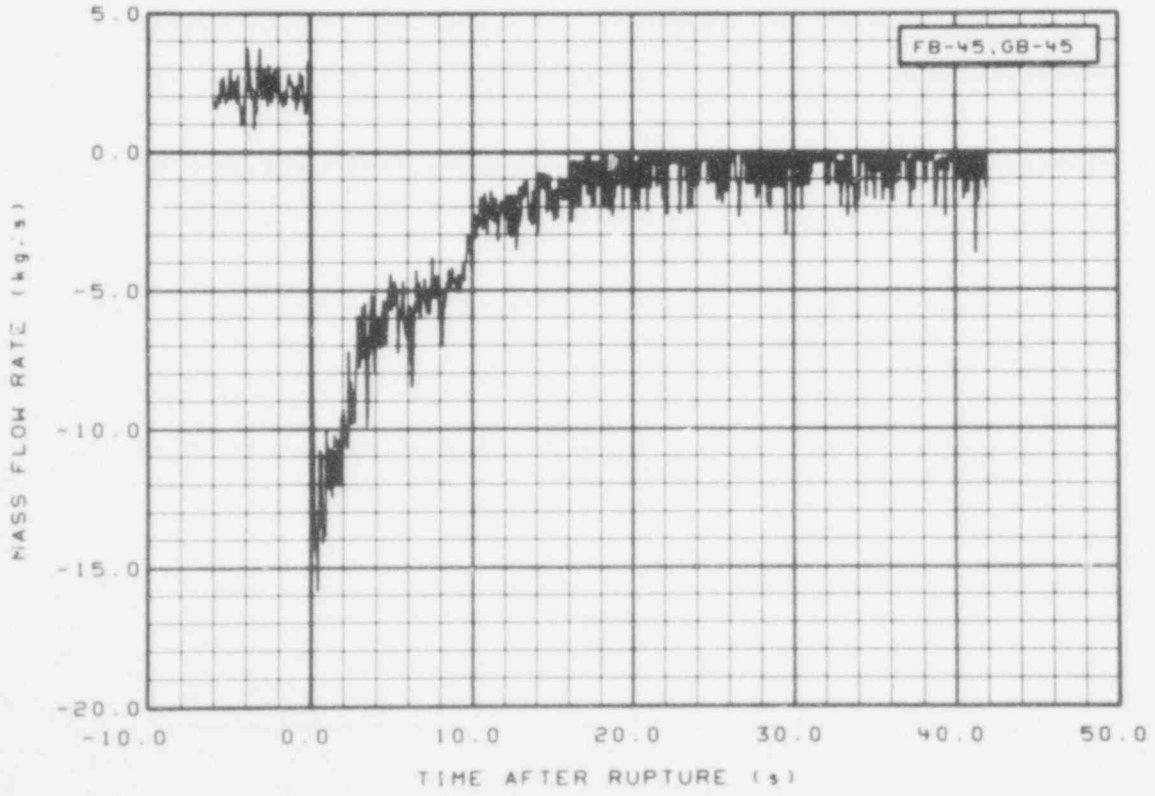

Fig. 296 Mass flow in broken loop (FB-45 and GB-45), from -6 to 42 s.

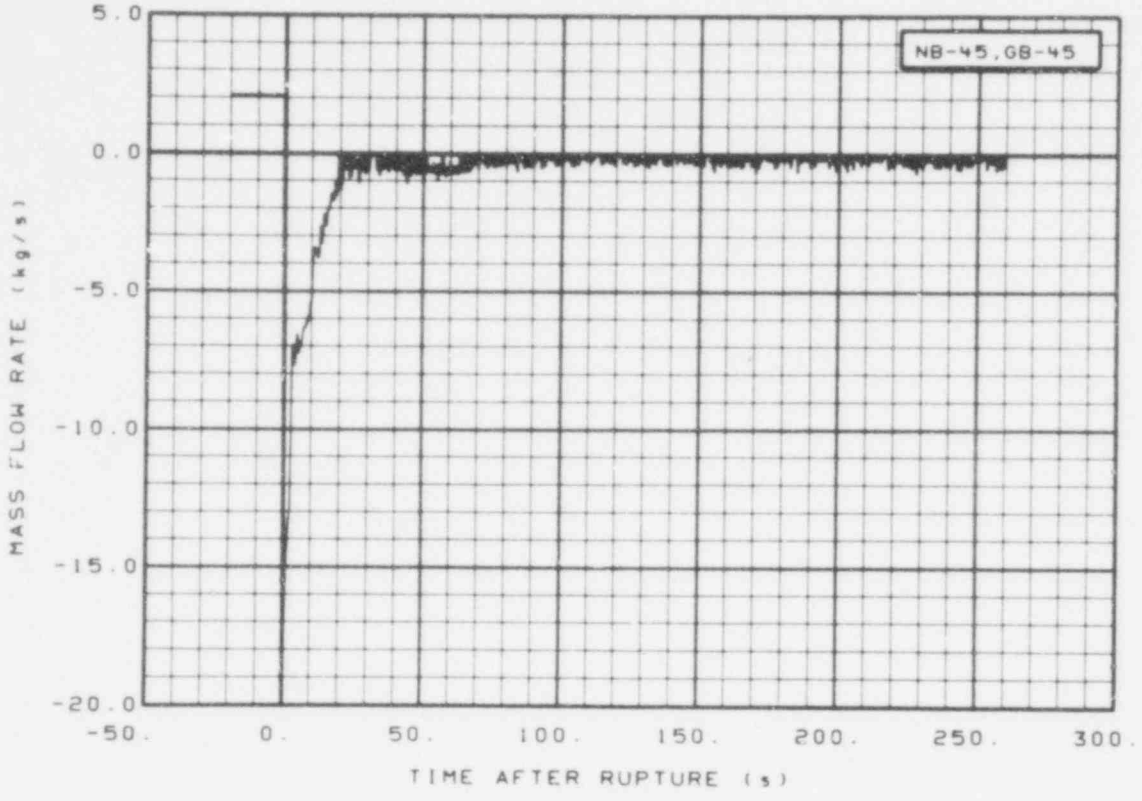

Fig. 297 Mass flow in broken loop (NB-45 and GB-45), from -20 to 260 s.

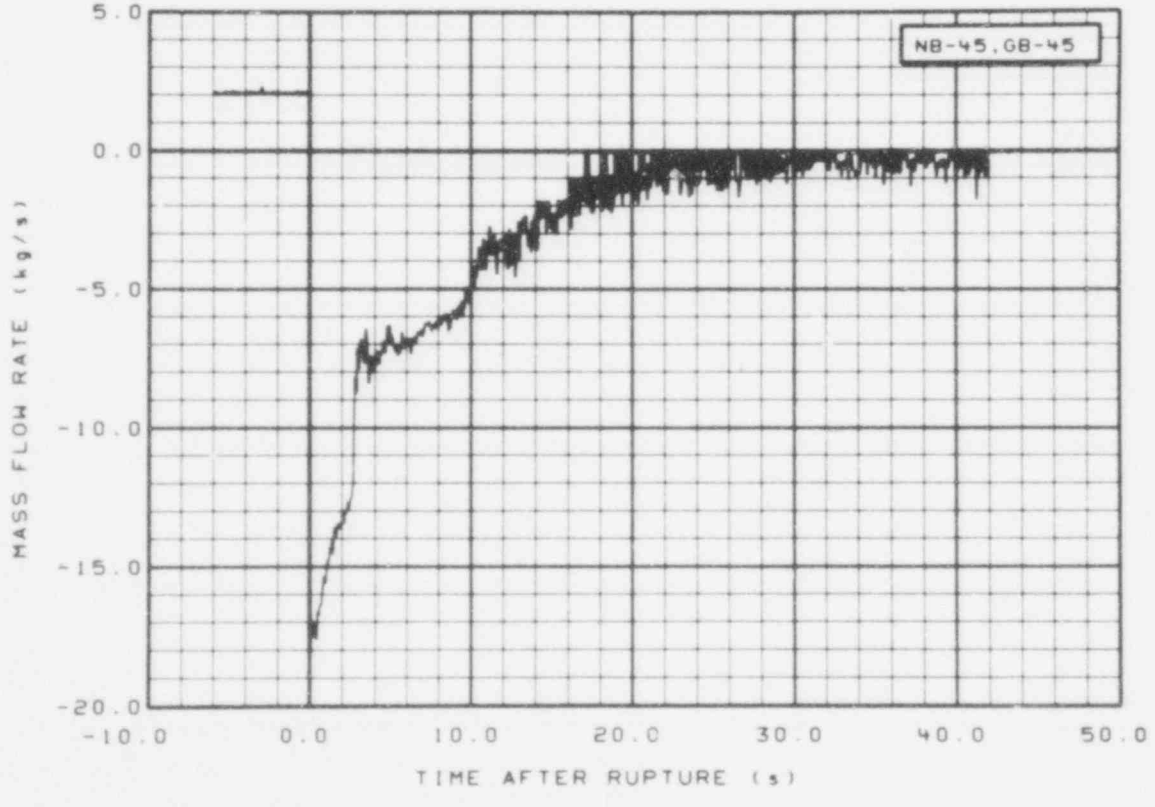

Fig. 298 Mass flow in broken loop (NB-45 and GB-45), from -6 to 42 s.

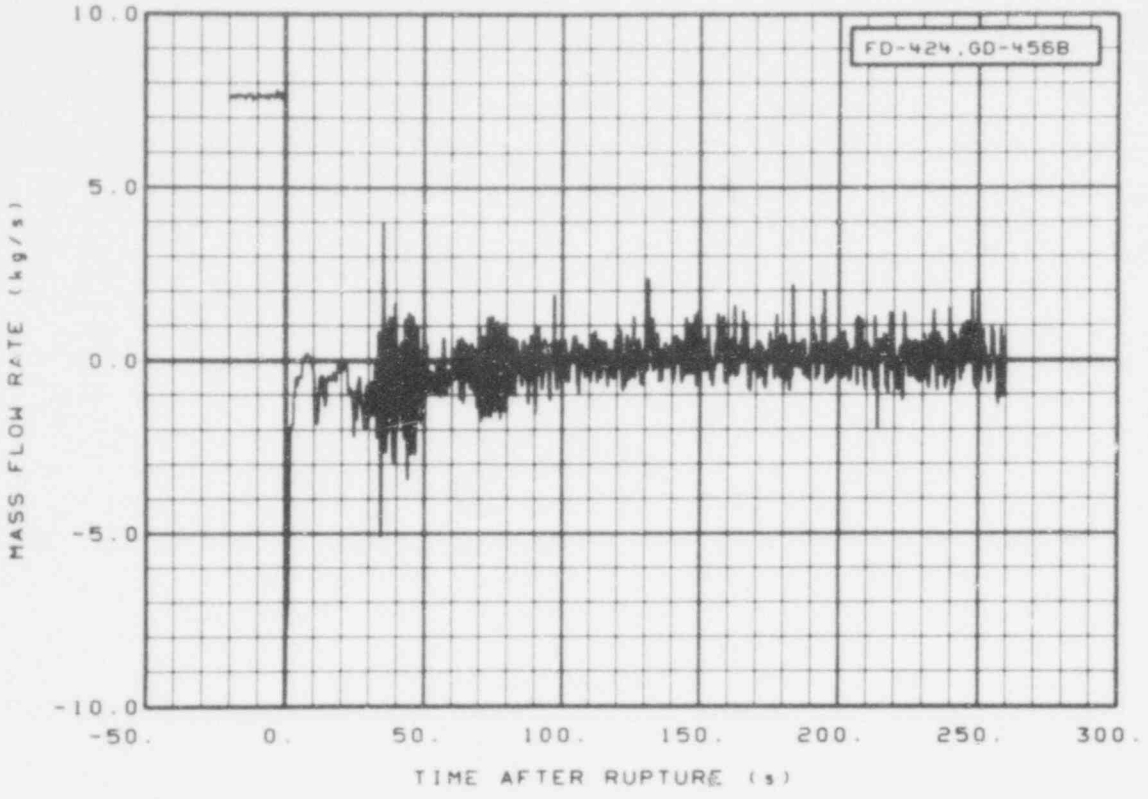

Fig. 299 Mass flow in downcomer (FD-424 and GD-456B), from -20 to 260 s.

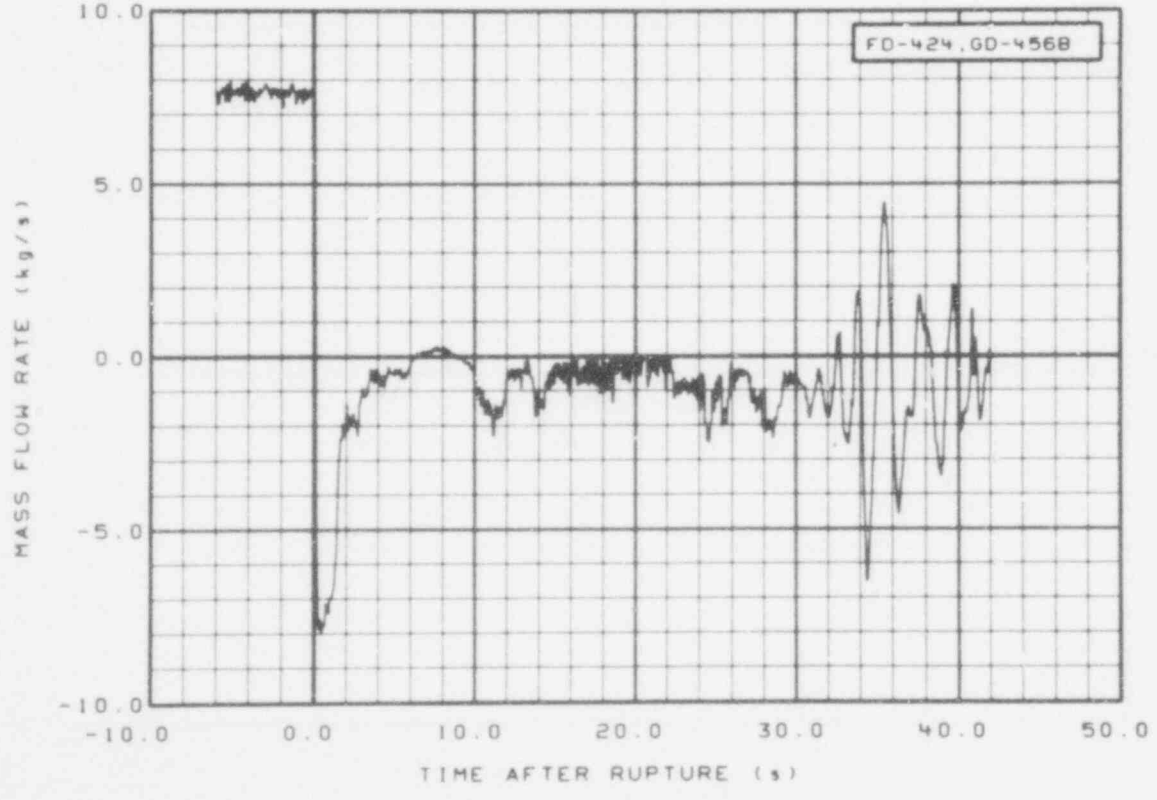

Fig. 300 Mass flow in downcomer (FD-424 and GD-456B), from -6 to 42 s.

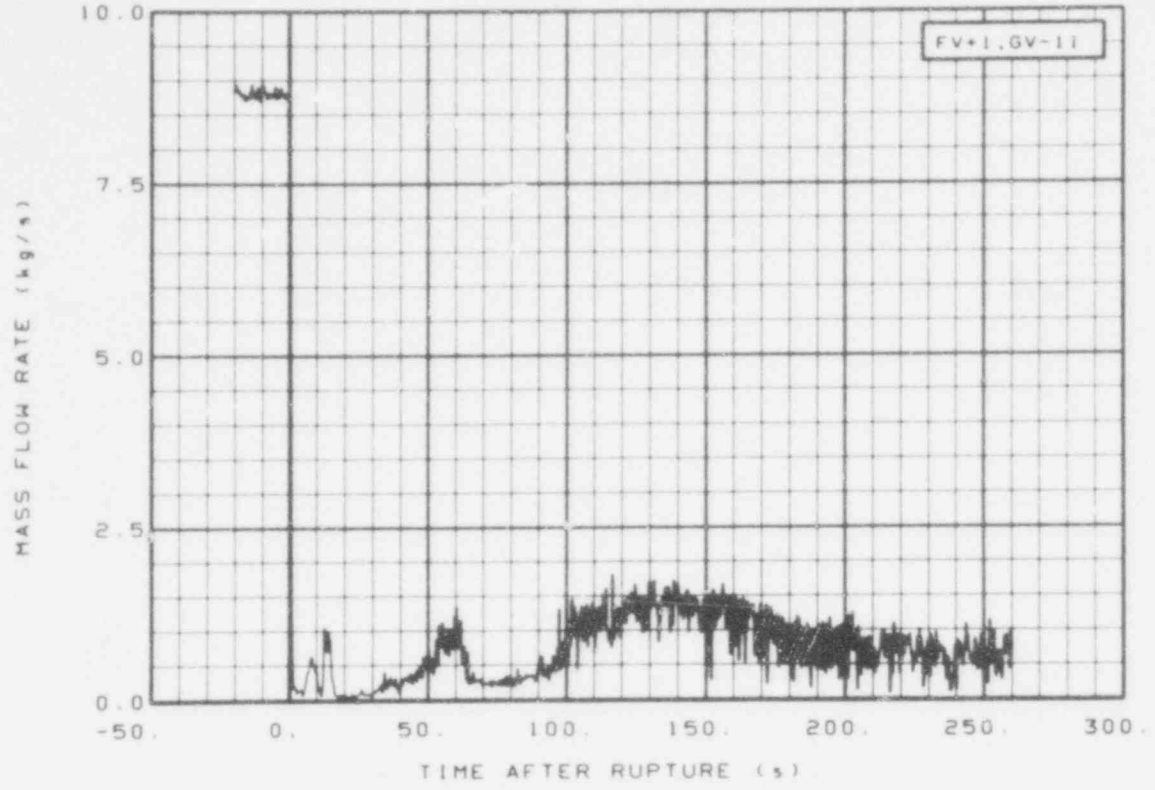

Fig. 301 Mass flow in vessel (FV + 1 and GV-11), from -20 to 260 s.

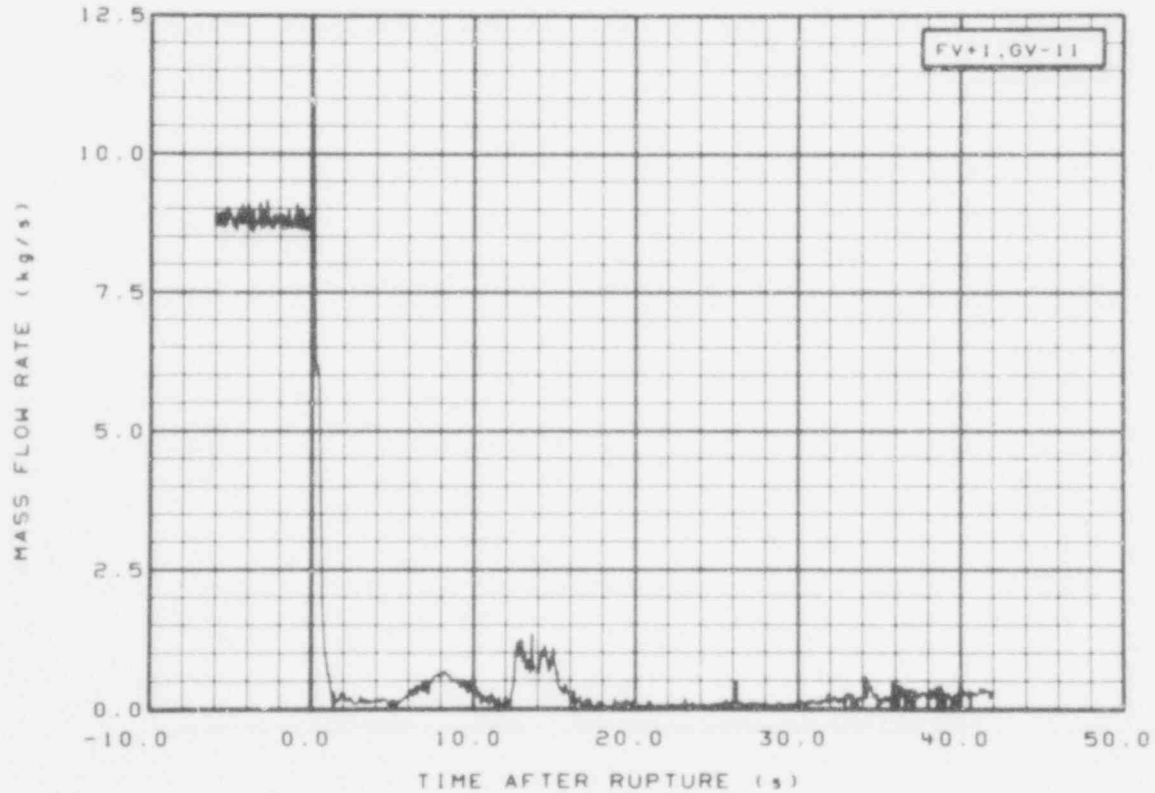

Fig. 302 Mass flow in vessel (FV + 1 and GV-11), from -6 to 42 s.

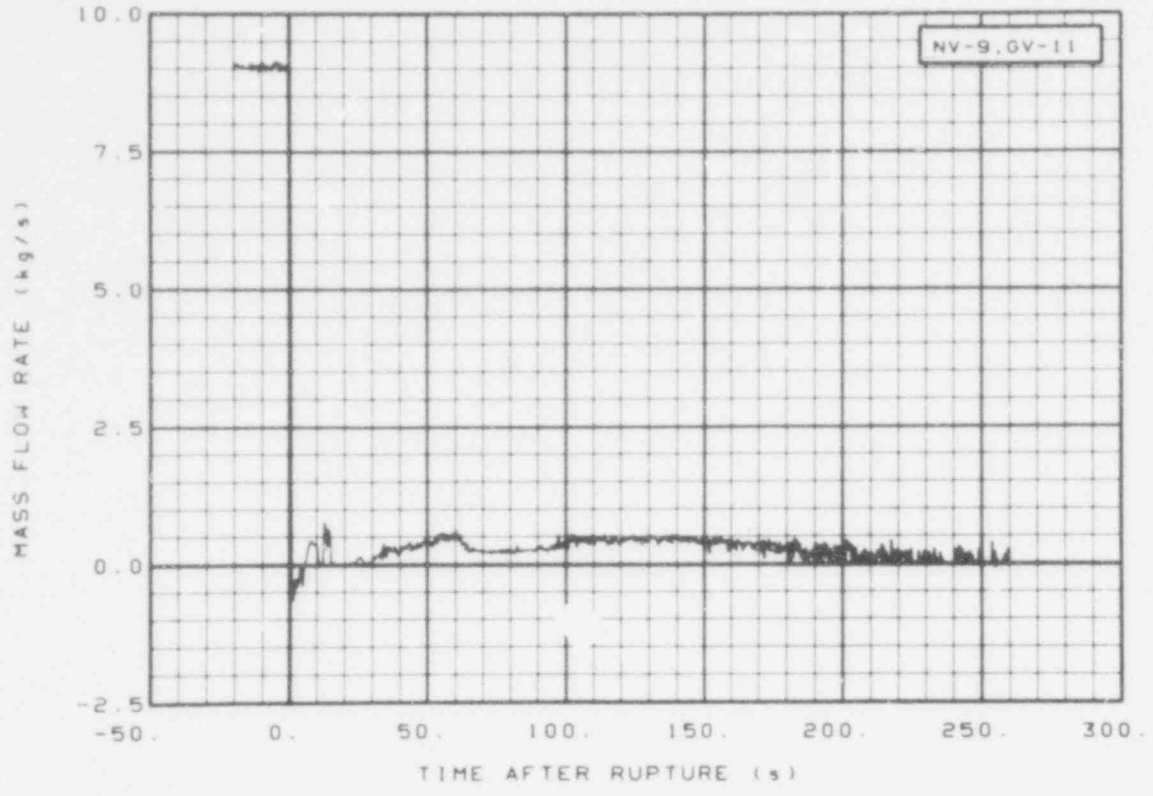

Fig. 303 Mass flow in vessel (NV-9 and GV-11), from -20 to 260 s.

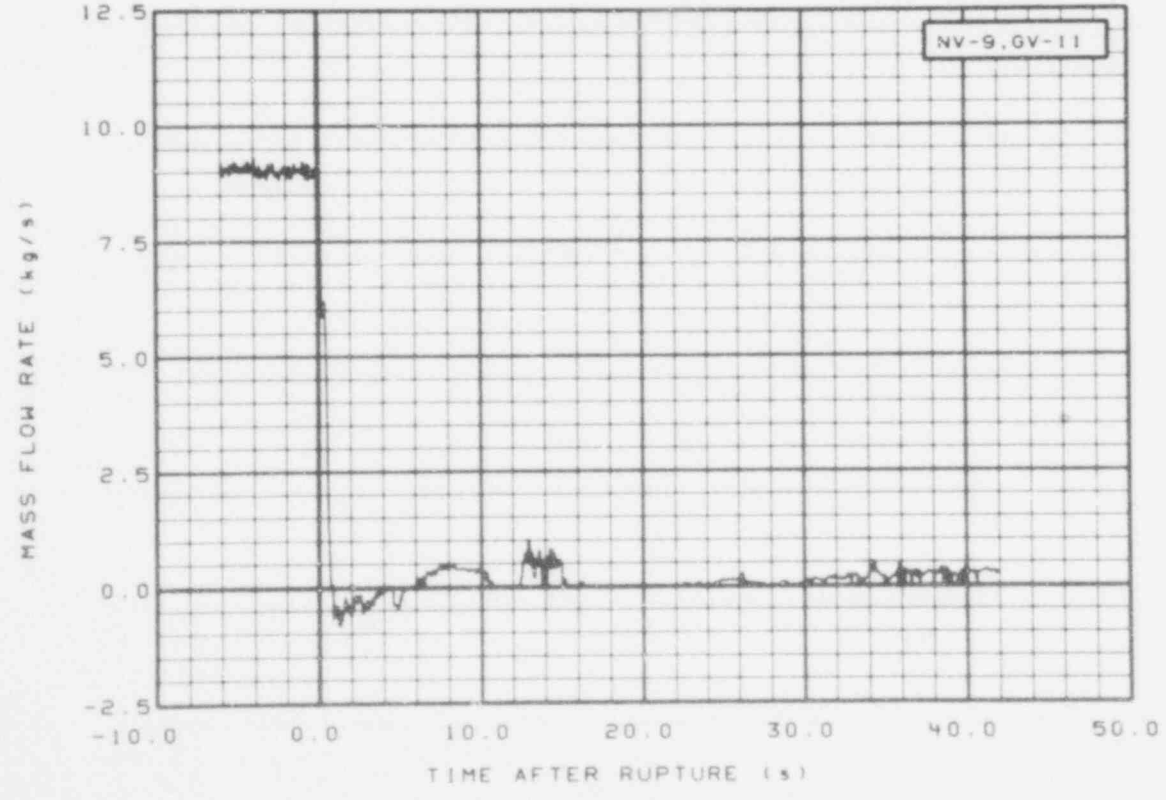

Fig. 304 Mass flow in vessel (NV-9 and GV-11), from -6 to 42 s.

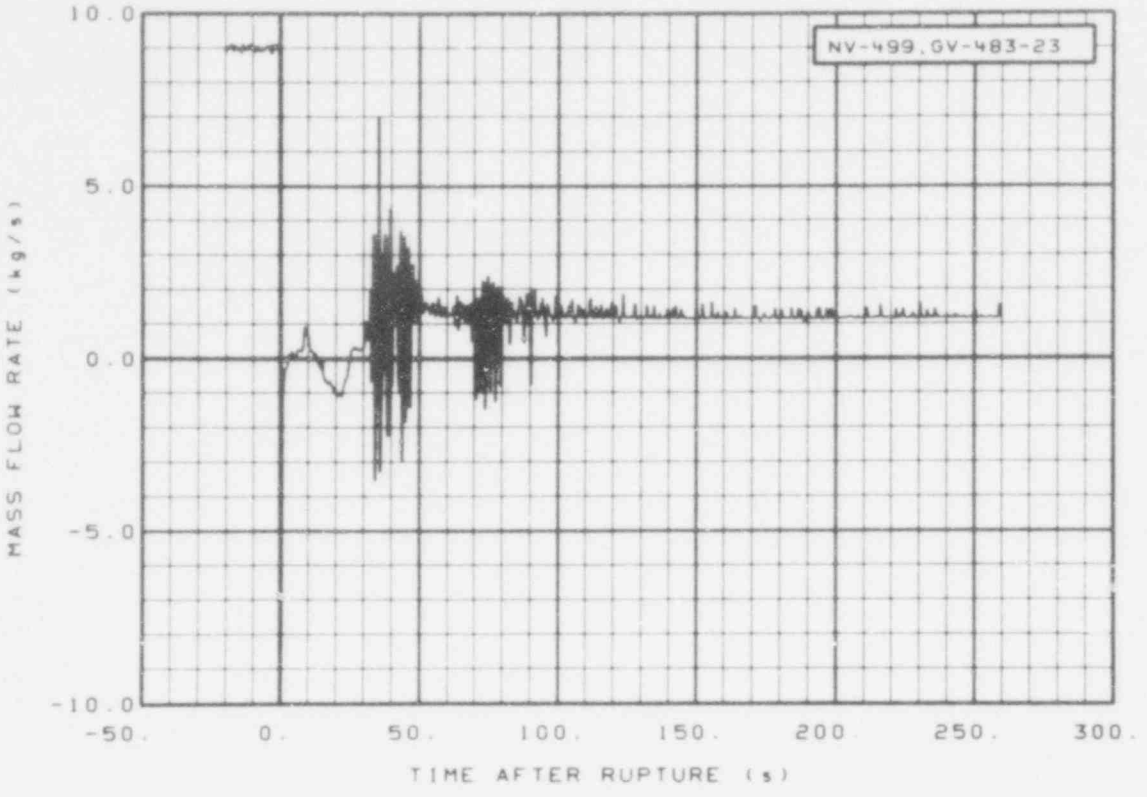

Fig. 305 Mass flow in vessel (NV-499 and GV-483-23), from -20 to 260 s.

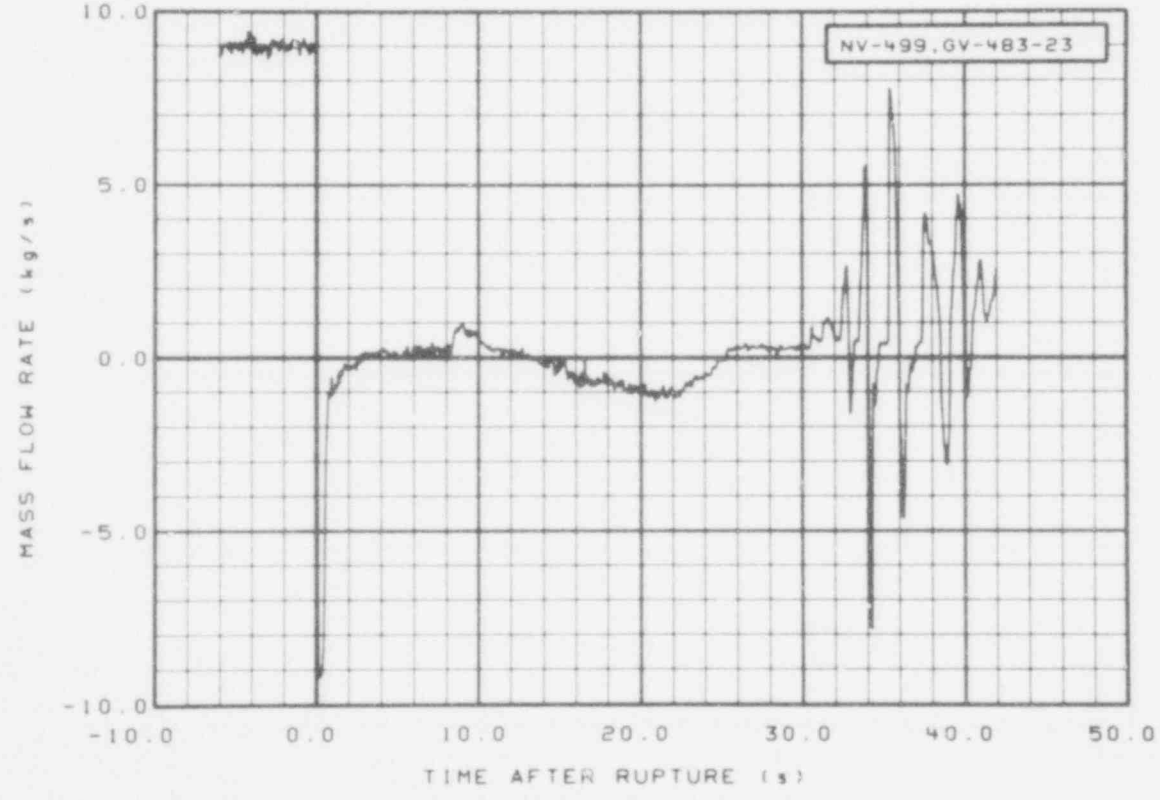

Fig. 306 Mass flow in vessel (NV-499 and GV-483-23), from -6 to 42 s.

544 196

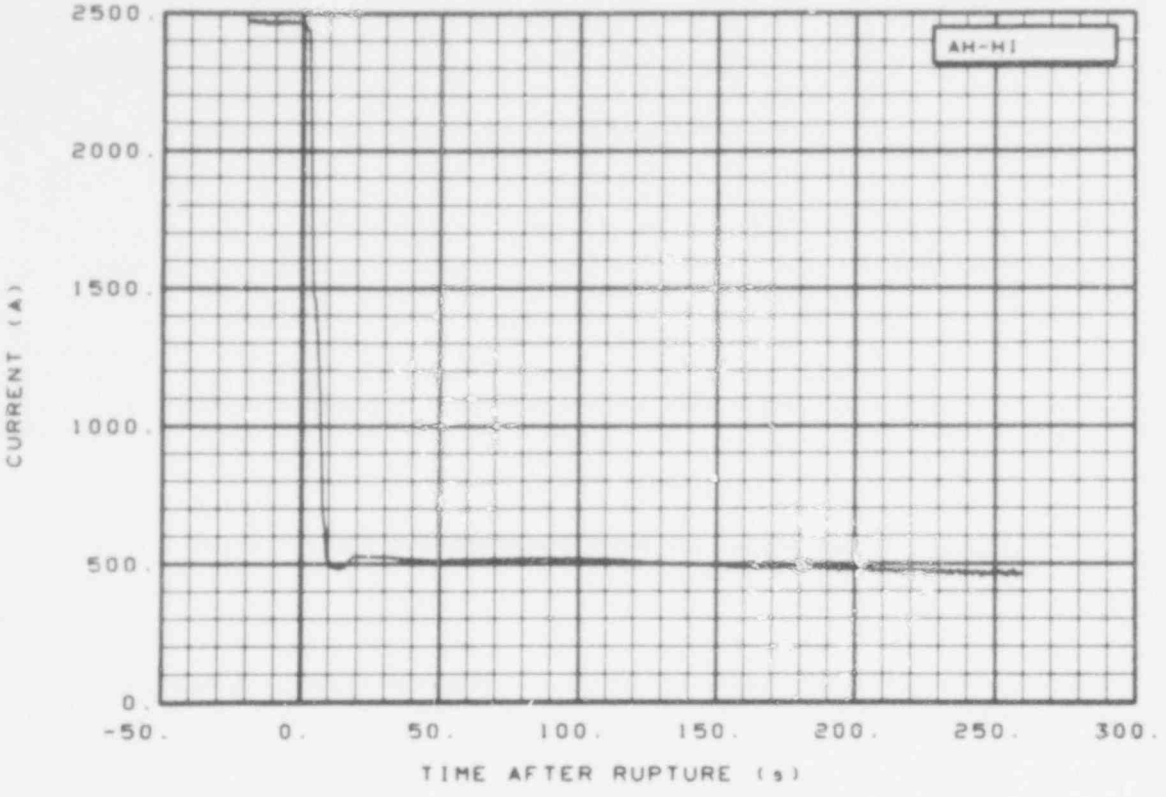

Fig. 307 Core heater high power bus amperage (AH-HI), from -20 to 260 s.

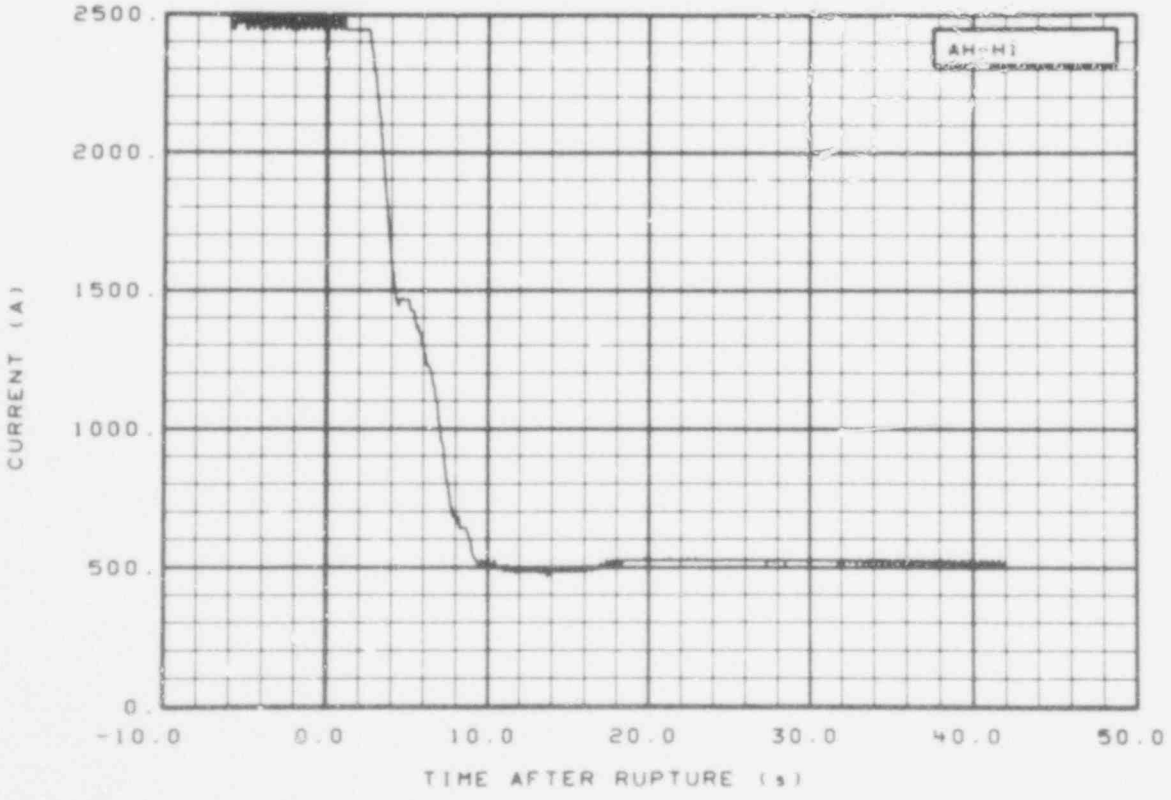

Fig. 308 Core heater high power bus amperage (AH-HI), from -6 to 42 s.

SAA 197

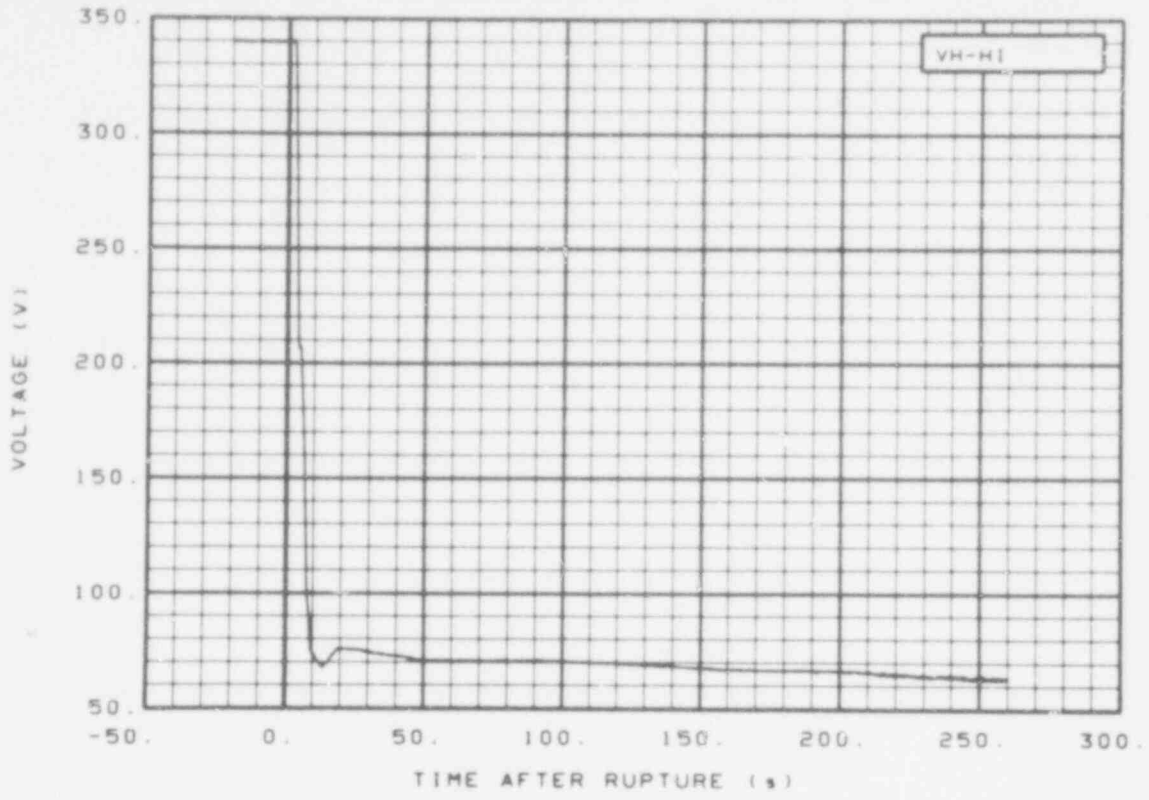

Fig. 309 Core heater high power bus voltage (VH-HI), from -20 to 260 s.

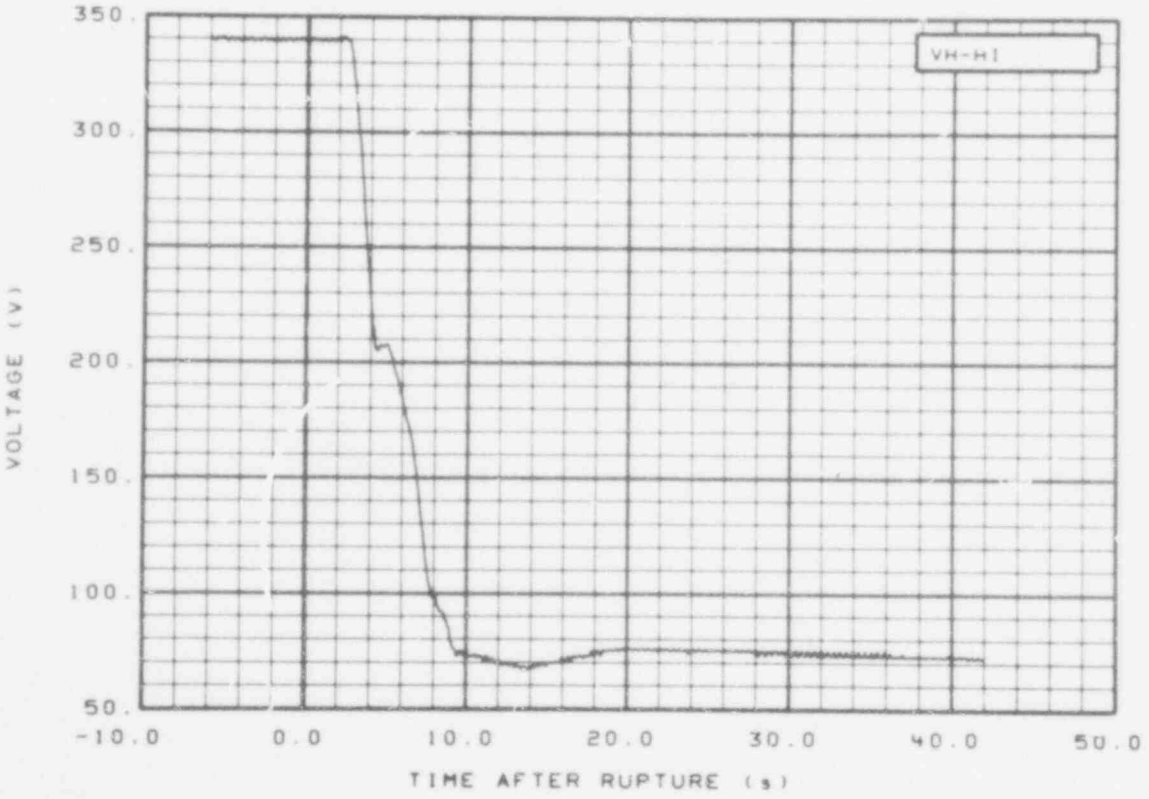

Fig. 310 Core heater high power bus voltage (VH-HI), from -6 to 42 s.

544 198

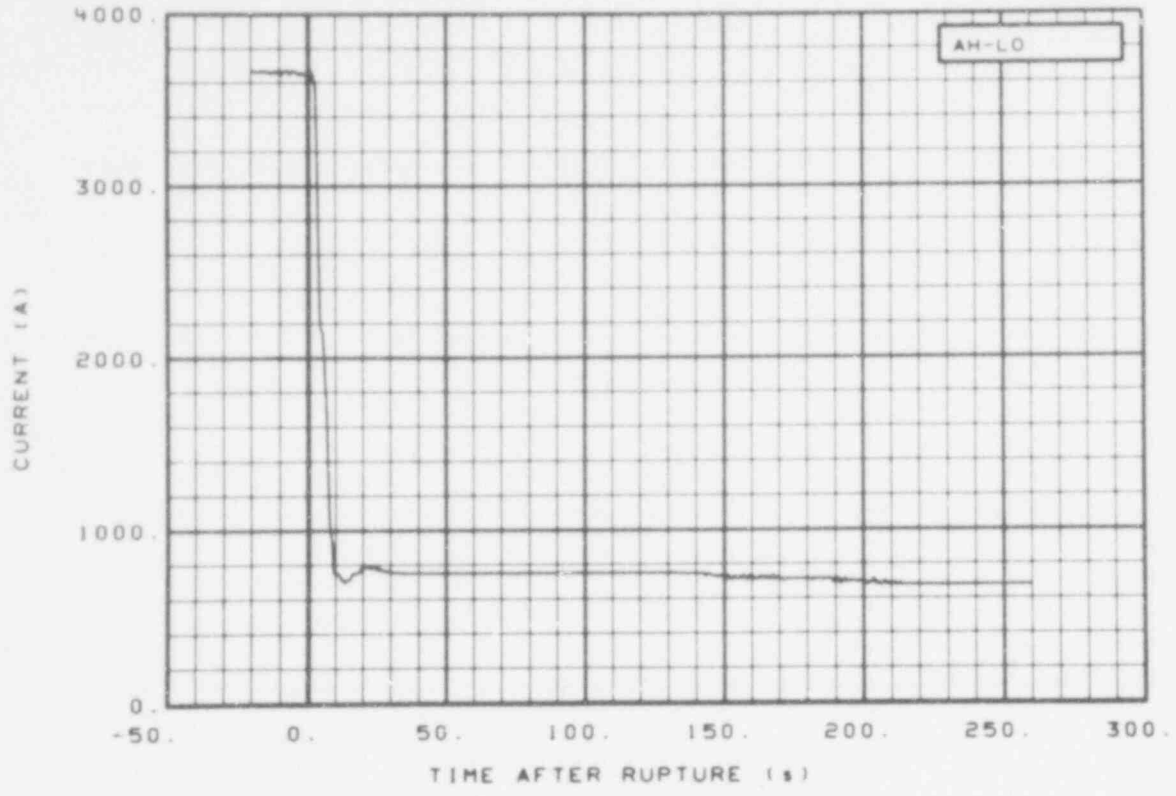

Fig. 311 Core heater low power bus amperage (AH-LO), from -20 to 260 s.

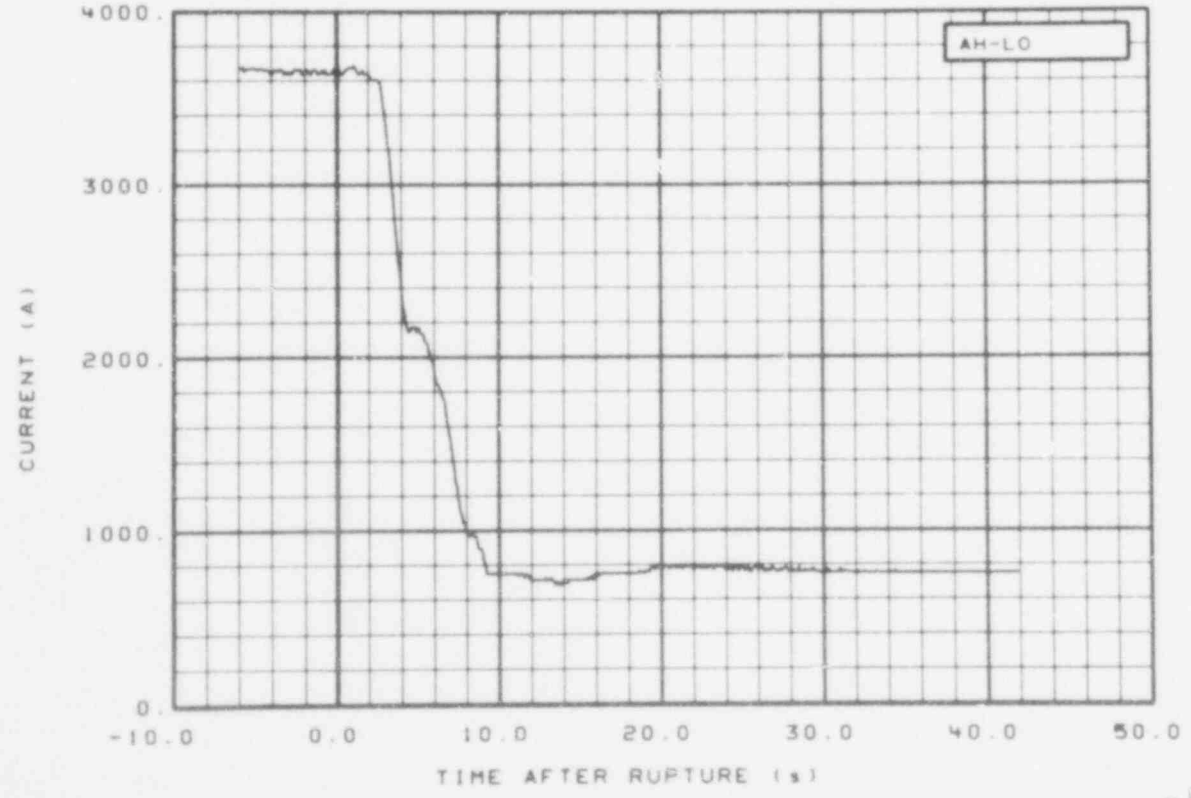

Fig. 312 Core heater low power bus amperage (AH-LO), from -6 to 42 s.

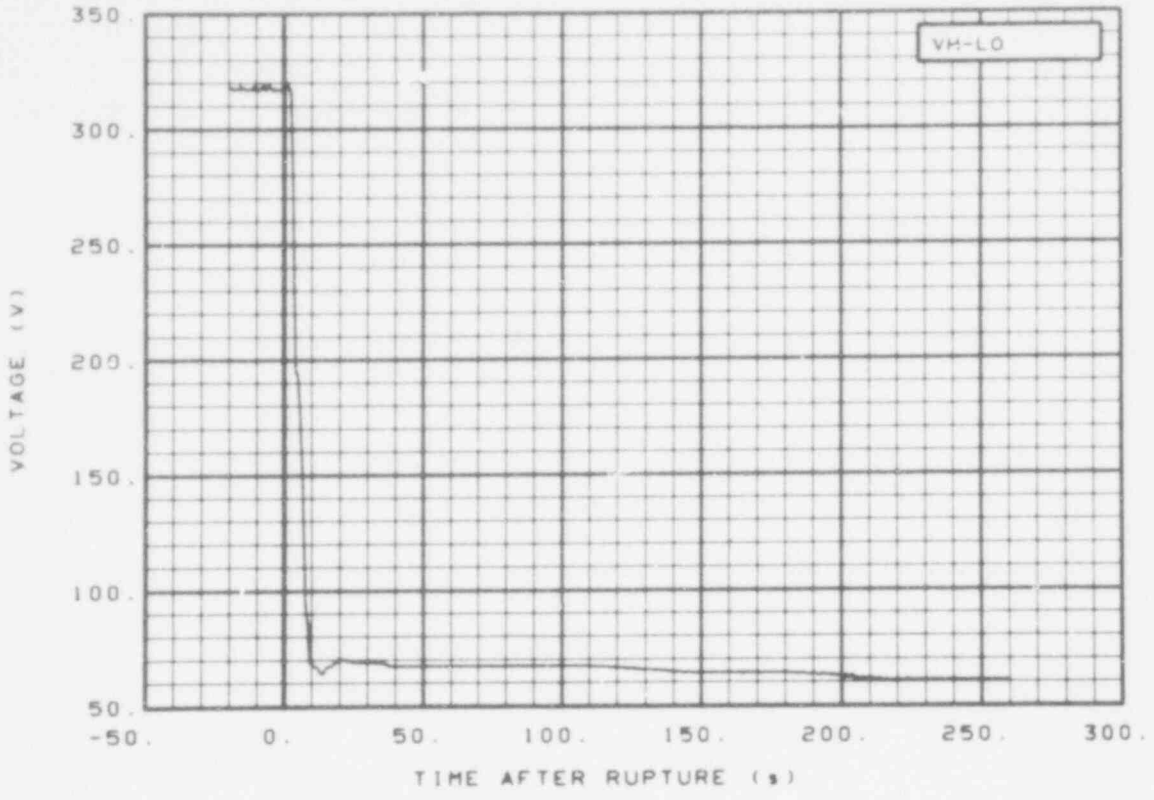

Fig. 313 Core heater low power bus voltage (VH-LO), from -20 to 260 s.

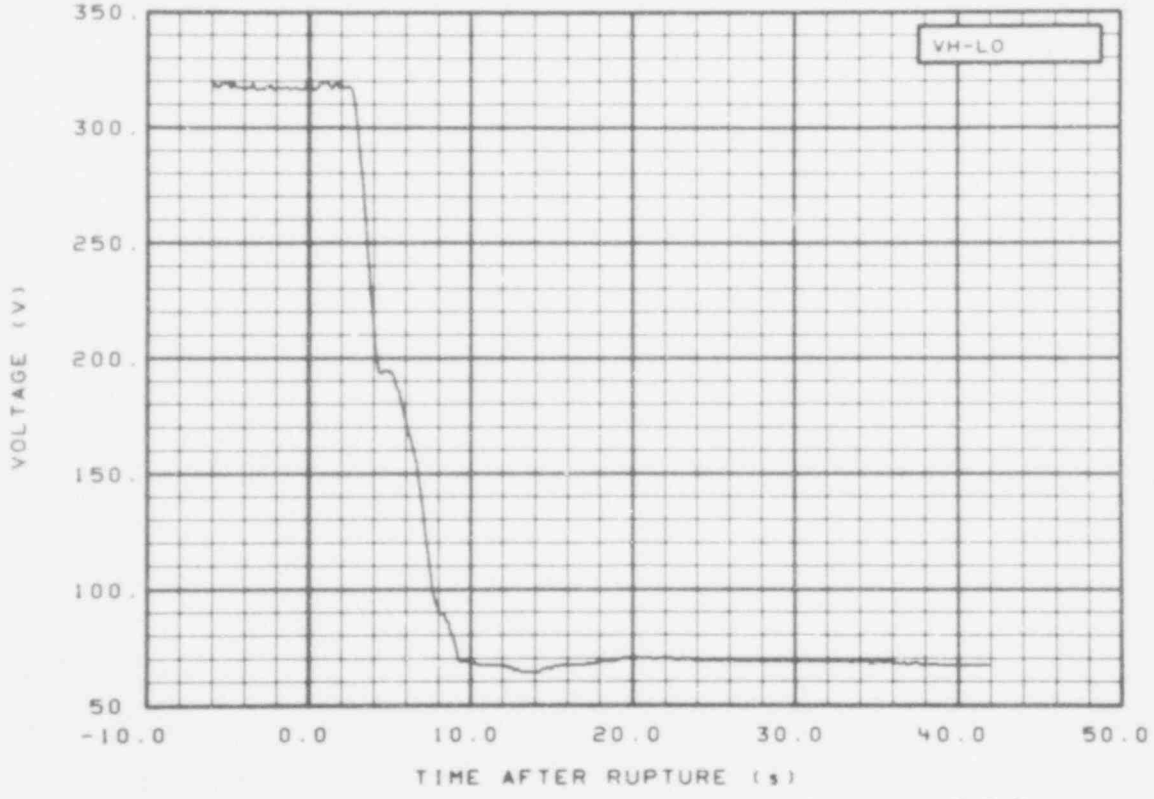

Fig. 314 Core heater low power bus voltage (VH-LO), from -6 to 42 s.

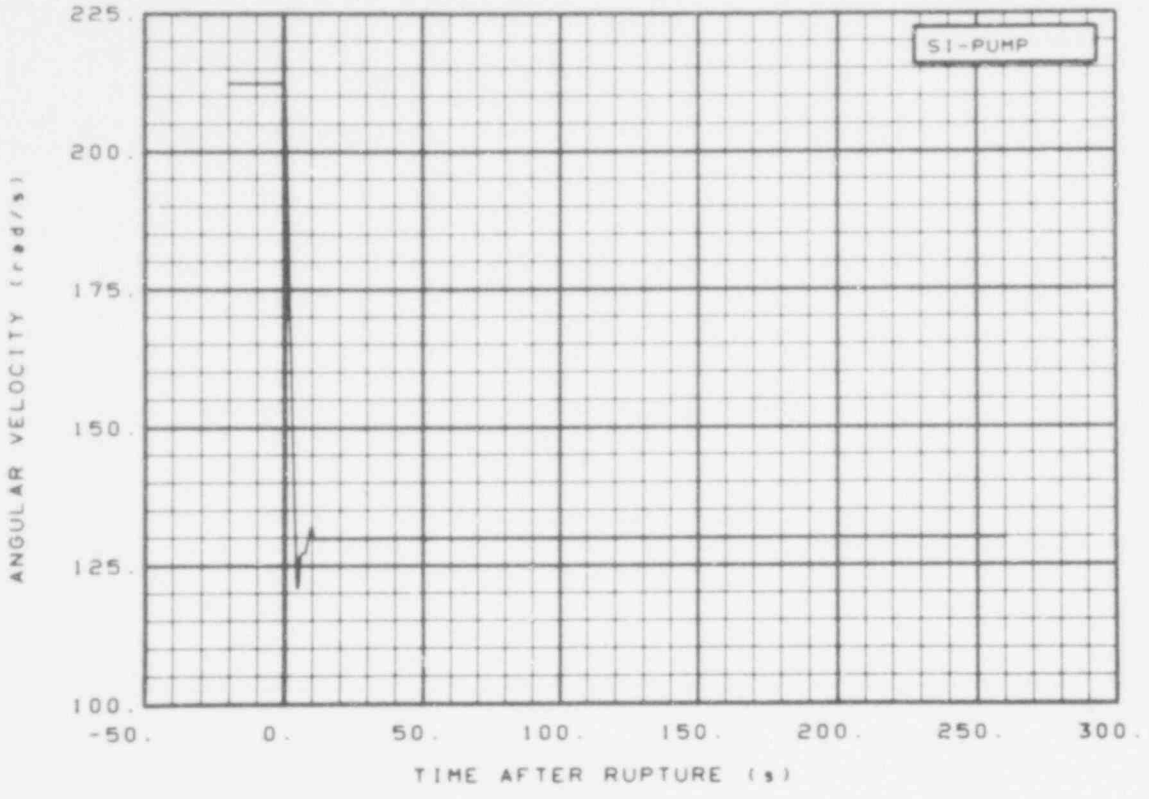

Fig. 315 Intact loop pump speed (SI-PUMP), from -20 to 260 s.

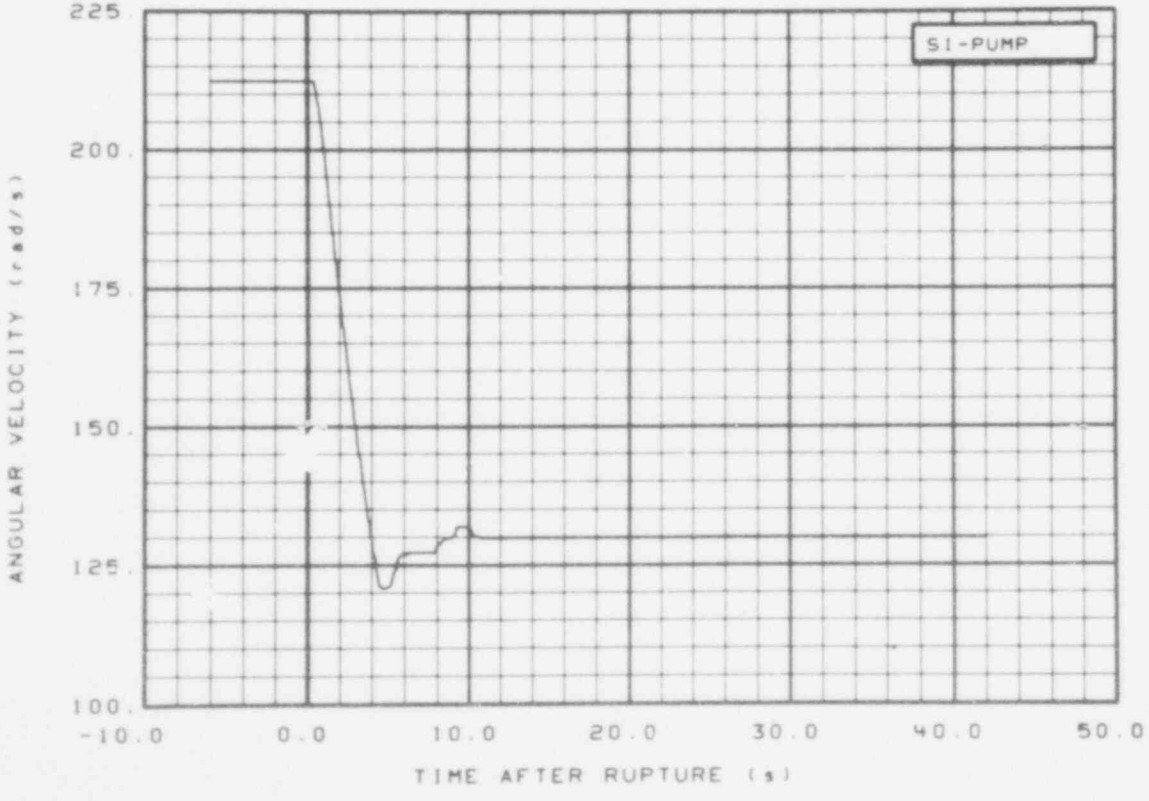

Fig. 316 Intact loop pump speed (SI-PUMP), from -6 to 42 s.

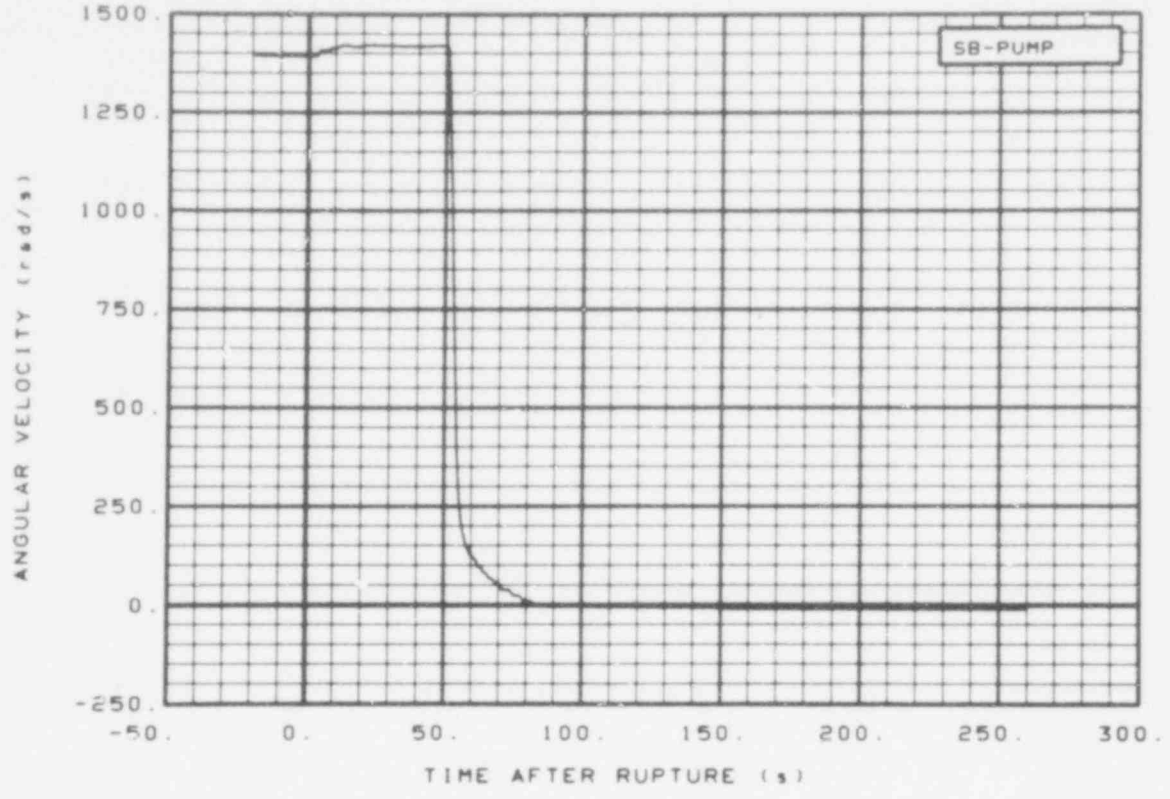

Fig. 317 Broken loop pump speed (SB-PUMP), from -20 to 260 s.

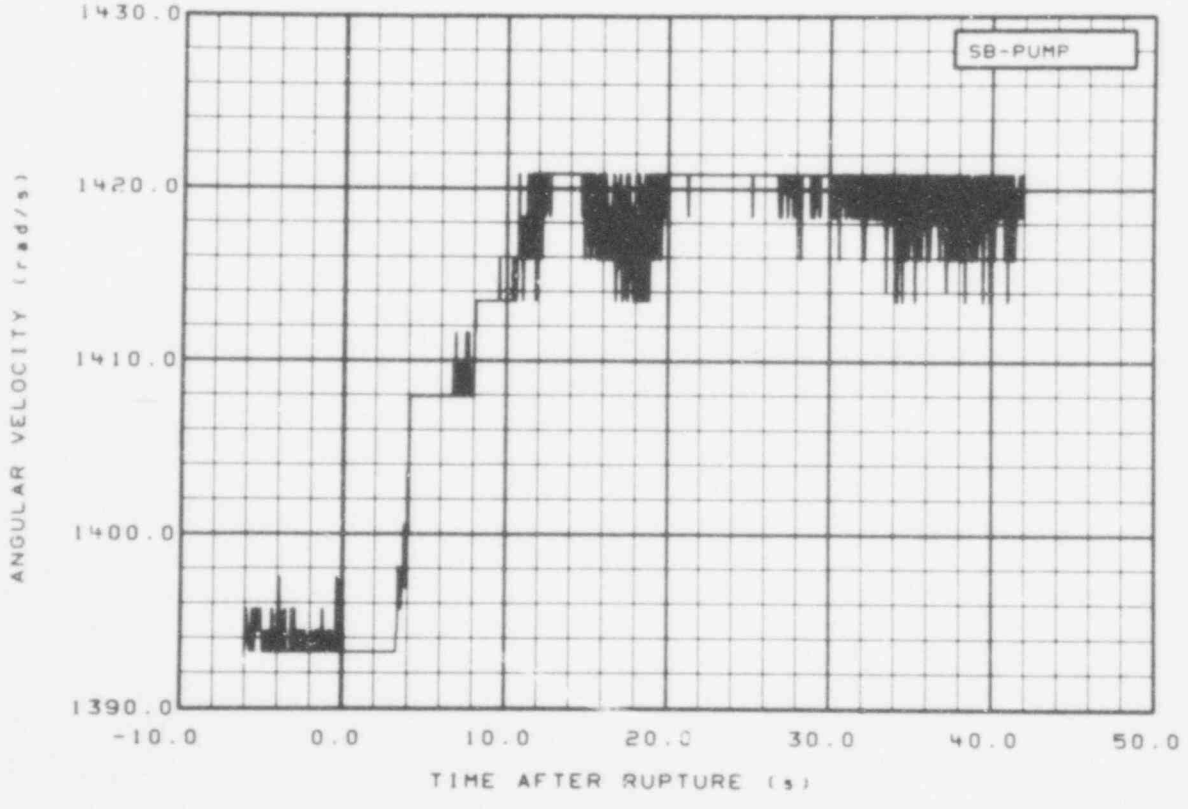

Fig. 318 Broken loop pump speed (SB-PUMP), from -6 to 42 s.

344 202

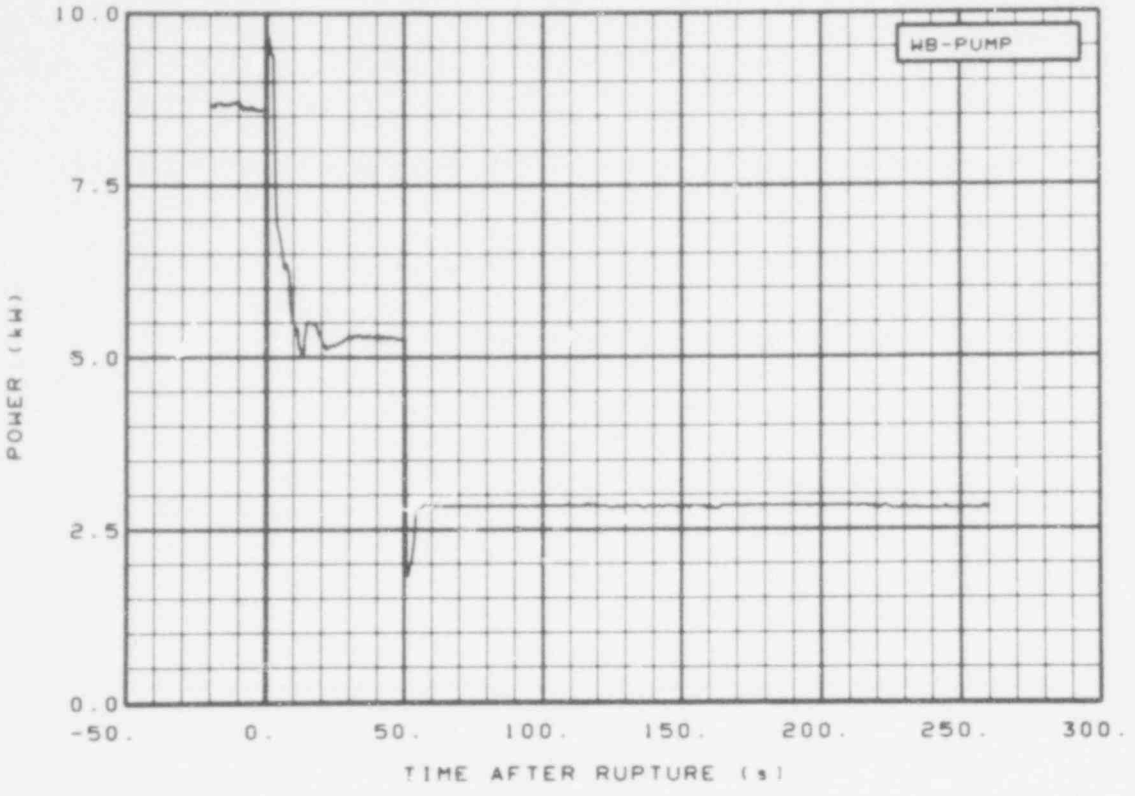

Fig. 319 Broken loop pump power (WB-PUMP), from -20 to 260 s.

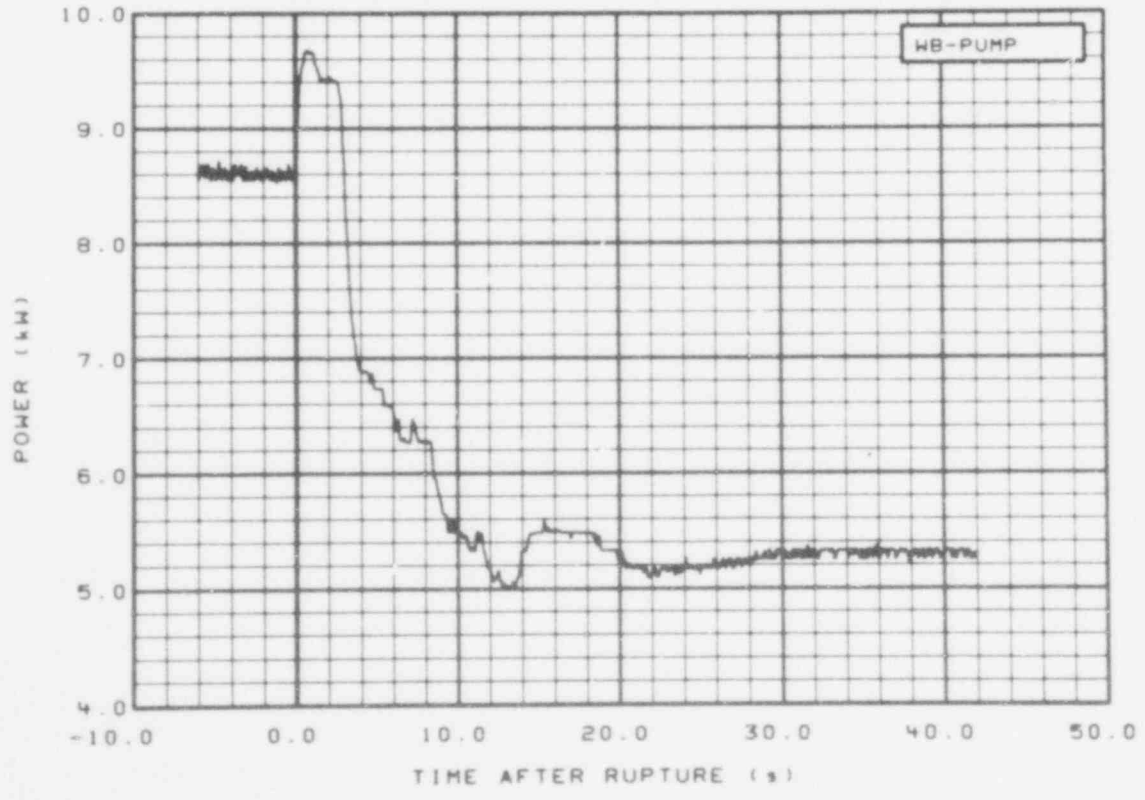

Fig. 320 Broken loop pump power (WB-PUMP), from -6 to 42 s.

544 203

IV. REFERENCES

1. L. J. Ball et al, *Semiscale Program Description*, TREE-NUREG-1210 (May 1978).

2. M. L. Patton, *Semiscale Mod-3 Test Program and System Description*, NUREG/CR-0239, TREE-NUREG-1212 (July 1978).

544 204

APPENDIX A

DATA ACQUISITION SYSTEM CAPABILITIES

APPENDIX A

DATA ACQUISITION SYSTEM CAPABILITIES

The Semiscale Mod-3 system provides for the acquisition, processing, and presentation of test data. The test data system comprises detectors, signal conditioners, signal processors, and recording and display equipment. The data obtained are principally recorded on an on-line digital system. Selected data channels are also recorded on an analog system.

The on-line digital system is called the digital data acquisition and processing system (DDAPS). The DDAPS has dual and single speed capabilities with identical storage and data output limitations. The dual speed mode is used to extend the recording time when obtaining high frequency data.

From each of up to 240 data channels, the test data system stores 20 blocks of data. Each block of data contains 920 words (each word is the abscissa and ordinate of a data point) of digital information. These 920 words represent a fixed storage display.

The maximum measured throughput rate for the system is 24 000 words per second. This throughput rate can be reduced in increments of 100 words per second. The throughput rate, the number of data channels recorded, and the fixed display of 920 points per block determine the time base for displaying the data.

After the data have been stored, data reduction can be made for presentation and analysis purposes. Because of hardware limitations and aesthetic considerations of data presentation, only certain time bases are used when the data are reduced. For data displayed from -20 to 260 s, the recorded data are made to occupy a 280-s span yielding a time base of 16 s.

Generally, 920 points from a given data channel are displayed in the nominal time base of 16 s. Integral (1 to 20) multiples of 16 s may be used as variations on the nominal time base. Because the output is fixed at 920 points, data compression is accomplished by averaging adjacent data points to give the desired compression.

APPENDIX B

POSTTEST ADJUSTMENTS TO DATA FROM SEMISCALE MOD-3 TEST S-07-8

APPENDIX B

POSTTEST ADJUSTMENTS TO DATA FROM SEMISCALE MOD-3 TEST S-07-8

Many of the transducers used in the Semiscale Mod-3 system exhibit significant sensitivity to one or more spurious inputs. Strain gage bridge circuits used in pressure transducers, differential pressure transducers, and drag discs are sensitive to changes in ambient temperature. Differential pressure cells are also sensitive to changes in system pressure. Photomultiplier tubes used as gamma ray detectors in the density transducers are sensitive to temperature changes, as well as to random variations in the locations of the radiation sources. Core power measurements depend on a calibrated resistor, whose resistance changes in values as a function of time and power level as it heats up.

Although the uncertainties introduced into the data by spurious secondary inputs generally do not exceed the specified uncertainty ranges of the transducers, significant improvement in measurement accuracy can be achieved if the secondary sensitivity can be identified and removed. Since the exact values of the spurious inputs to which different transducers might be sensitive cannot often be easily predicted and are sometimes inconvenient to measure, secondary effects have been accounted for by correcting the data after the test rather than by using elaborate real time programs in the data acquisition system computer. The methods and results of the posttest data correction analysis for Test S-07-8 are presented in the following paragraphs and tables.

1. DIFFERENTIAL PRESSURE MEASUREMENTS

Pressure sensitivity in the differential pressure cells in the main system loop is determined from the pretest system pressure check. Digital data are recorded for all measurements at ambient temperature, with no system flow, at pressures of ambient, 5313, 9010, 10 908, 12 530, and 15 172 kPa. The output of the differential pressure cells is plotted against system pressure, with the resulting plots used to describe the pressure response of the transducers.

Corrections to differential pressure data were made using the following equation:

$$F'(t) = F(t) + P_1 P(t) \qquad \text{(B-1)}$$

where

$F'(t)$ = corrected data, kPa

$F(t)$ = raw data, kPa

P_1 = pressure sensitivity, kPa/MPa

$P(t)$ = pressure data from indicated transducer used for pressure correction sensitivity, MPa.

Values of the constants are given in Table B-I.

TABLE B-I

CONSTANTS FOR DIFFERENTIAL PRESSURE MEASUREMENT CORRECTIONS
(TEST S-07-8)

Detector Identification	P_1	P(±)
DI-13V-1A	-0.024	PV-13
DI-1A-6	0	
DI-6-7	-0.053	PI-16
DI-SGI-SGO	0.027	PI-16
DI-7-13	-0.027	PI-16
DI-13-15	1.567	PI-16
DI-15-17A	0	
DI-17A-DIA	0	
DB-13V-20B	0.10	PV-13
DB-20B-21	0.09	PV-13
DB-21-27A	-1.067	PV-13
DB-SGI-SGO	2.0	PV-13
DB-27A-37A	-0.053	PV-13
DB-37A-40B	-0.90	PV-13
DB-37A-40L	-0.133	PV-13
DB-40B-43A	0	
DB-40B-45A	0.018	PB-45A
DB-45A-43	0	
DB-45A-DIA	0.467	PB-45A
DD-DIA-13V	-0.04	PI-16
DD-DIA-170	-0.057	PI-16
DD-DIA-578	-0.024	PI-16
DD-170-435	-0.055	PI-16
DD-435-578	-0.033	PI-16
DV+421+154	0.040	PV-13
DV+159-105	-0.533	PV-13
DV+154-105	0.027	PV-13
DV-579-501	-0.021	PI-16
DV-578-13A	-1.933	PI-16

TABLE B-I (continued)

Detector Identification	P_1	P(t)
DV-501-442	-0.027	PI-16
DV-501-105	0.057	PV-13
DV-501-13A	0	PI-16
DV-442-278	-0.013	PI-16
DV-278-154	-0.033	PI-16
DV-105-13A	0	
DI-SG-LL	0	
DB-SS1-SS4	0	
DV-ACC1-LL	0	

2. DENSITY MEASUREMENTS

Density calculations are based on the voltage output of the photomultiplier tubes in the gamma-attenuation densitometer assemblies. The equation used for converting voltage to density is as follows:

$$\rho = C_o + C_1 F(t) \qquad \text{(B-2)}$$

where

ρ = the density, kg/m^3

C_o = offset, kg/m^3

C_1 = conversion factor, $(kg/m^3)/v$

$F(t)$ = transducer output, v.

Constants C_o and C_1 are adjusted to match the final data to density values calculated from measured pressure and temperature values at the preblowdown and post drain conditions, effectively giving the data an in-place calibration. These calculations are made in the Mod-3 system prior to initial data release and are not considered posttest adjustments.

Some density measurements are obtained using a two-beam gamma densitometer which operates on the same basic principle of gamma attentuation as does the single-beam gamma densitometer. Each beam originates from the same gamma source and is allowed to pass through separate portions of the piping cross-sectional flow area to obtain an average density measurement in that particular region. The geometrical relationship of the gamma beam path through the piping and geometrically related variables

used for processing of data from a two-beam gamma densitometer are shown in Figure B-1. The average density measured by each individual gamma beam is obtained using the same equation as is used for the single-beam gamma densitometers.

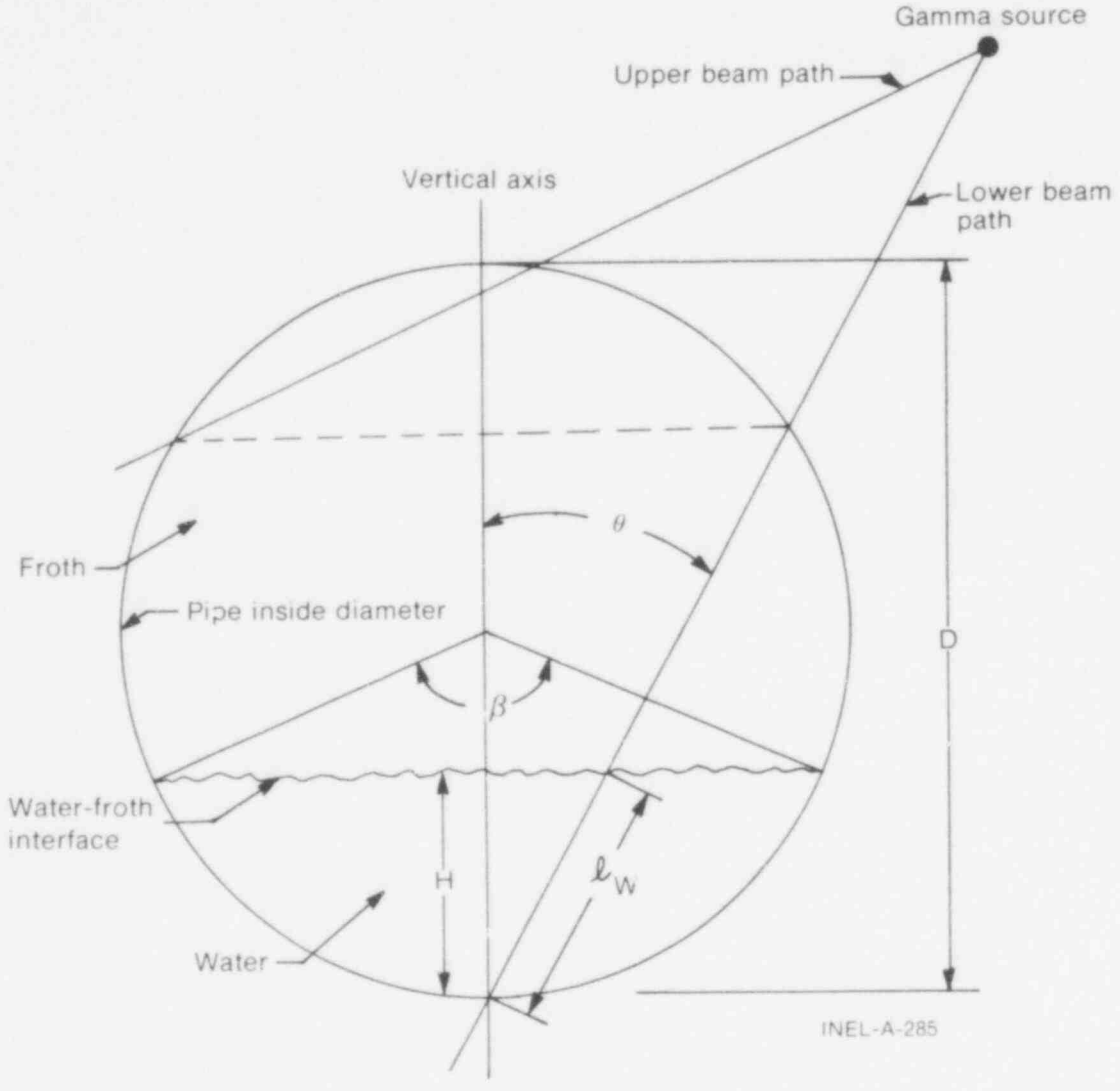

Fig. B-1 Geometry used for processing of density data obtained from two-beam gamma densitometers.

In the Semiscale Mod-3 system, two-beam gamma densitometers provide information which allows the calculation of a better average density than that obtained from a single beam in a horizontal pipe. A mathematical model is used for processing the two-beam data to obtain the improved average density information. The processing method used is based on a froth-water model coupled with information from the two individual gamma beams and related beam path and piping cross-sectional geometry. The resulting information is recorded and reported under the density measurement identification ending with a "C", for example, GI-17C.

The use of the froth-water model for obtaining average density from a two-beam gamma densitometer in a horizontal pipe is based on observations indicating that flow regimes in the Semiscale Mod-3 system can be modeled by a layer of water on the bottom of the pipe with a degree of froth on the surface. For homogeneous flow conditions such as all froth or all liquid the model remains valid. At any point in time slug flow is also modeled. The froth-water model does not model annular or inverted annular flows very

well. However, these flows are not expected to exist for significant portions of a Semiscale Mod-3 system blowdown in horizontal piping. Density gradients from the top to the bottom of the pipe may exist showing no distinct location change from water to froth. This flow is neither totally homogeneous nor stratified, but the froth-water model does provide an adequate approximation of the average density characteristic of this flow pattern.

The average density obtained by using the gamma beam geometry shown in Figure B-1 and by applying the froth-water model is given by

$$\bar{\rho} = \alpha_f \rho_1 + (1 - \alpha_f) \rho_w \text{ kg/m}^3 \quad \text{(B-3)}$$

where

$\bar{\rho}$ = average cross-sectional density

ρ_1 = average density measured by the upper beam (measures the froth density)

ρ_w = density of liquid water (at local system conditions)

α_f = $1 + (1/2\pi)(\sin\beta - \beta)$ = volumetric fraction containing froth.

The angle which β represents is shown in Figure B-1. Values for β are obtained as follows:

$$\beta = 2 \cos^{-1} (1 - 2h) \quad \text{(B-4)}$$

where

$$h = \frac{H}{D} = \cos^2\theta \left(\frac{\rho_2 - \rho_1}{\rho_w - \rho_1} \right)$$

where

H = $l_w \cos\theta$ (l_w and θ are defined in Figure B-1)

D = piping inside diameter

ρ_2 = the average density measured by the lower gamma beam.

Average density is not calculated using the two-beam froth-water model when the angle θ is not favorable due to system hardware restrictions in positioning the source. The froth-water model requires separate density sampling in both the upper and lower portions of the piping cross section.

544 212

APPENDIX C

SELECTED DATA WITH ESTIMATED TOTAL UNCERTAINTY BANDS FROM SEMISCALE MOD-3 TEST S-07-8

APPENDIX C

SELECTED DATA WITH ESTIMATED TOTAL UNCERTAINTY BANDS FROM SEMISCALE MOD-3 TEST S-07-8

Analysis has been performed on selected data from Test S-07-8 to provide a guide to the uncertainty associated with data measurements in the Semiscale Mod-3 system. The end result of the analysis is presented as uncertainty bands about the measured data which represent a 95% confidence level.

The uncertainty bands are obtained by combining uncertainties obtained from analysis of the data itself (random uncertainty) and engineering analysis of the measurement system (engineering uncertainty). The procedure by which uncertainty bands were established for the data presented in this appendix is described in the following paragraphs.

The data trace under analysis was empirically fitted with a linear difference equation, which was subject to a white noise input at each sampling time point. The objective of the empirical fitting procedure was to characterize the white noise, which was taken to represent the random uncertainty. The procedures for fitting the difference equation are discussed in depth in Reference C-1. A data trace was often segmented and different equations were fitted to each segment with statistical correlations between successive observations accounted for by the fitting procedure. The white noise input was assumed to arise from a normally distributed population. The standard deviation of the white noise, as found during the fitting procedures, was taken as an estimate of the random uncertainty standard deviation and is shown in Table C-I in appropriate engineering units. The traces of the uncertainty band analysis are shown in Figures C-1 through C-40.

Other uncertainties in the data exist because of such factors as variability in installation procedures and techniques, calibration uncertainties, variability in materials, and temperature and pressure sensitivities. These uncertainties and the procedures for estimating them are discussed in Reference C-2. They are referred to as engineering uncertainties and the estimates are largely subjective. Because of the continuing effort to improve the accuracy of the measured data, such as through the use of better transducers, better signal conditioning and processing equipment, and better calibration and installation techniques, the engineering uncertainties for data from most of the transducer systems have changed from those published in Reference C-2. Table C-II provides a summary of engineering uncertainty values obtained from current analysis techniques as applied to the data presented herein.

In addition to the normal hardware and installation related sources of engineering uncertainty, a significant measurement uncertainty results when the current transducer systems are subjected to separated two-phase flow regimes during the course of the blowdown transient. Accordingly, for those data affected (fluid density, volumetric flow, and mass flow), which are presented in this appendix, a more extensive assessment was conducted of additional engineering uncertainty due to flow regime effects. Table C-III identifies the data analyzed and the period in the blowdown process for which flow regime uncertainties were included as a part of the total engineering uncertainty. The time of occurrence of separated two-phase flow and the resulting effect on the uncertainty of the data were evaluated by considering, on an individual basis, each detector output with reference to indications by other auxiliary measurements.

The gamma densitometer density measurement data are affected by two-phase separated flow regimes. The resulting transducer output is a measurement of the average attenuation of the gamma beam through the measured medium. The beam attenuation, in turn, is interpreted through physical relationship to be a measure of the average density along the beam path. When stratified type flow was considered present, the gamma beam attenuation was considered to be a result of a liquid layer and steam at system conditions. With this assumption and the system geometry, a void fraction was calculated and a new "effective" average density was calculated. The difference between the average density based on the assumption of homogeneous conditions and the average density for stratified conditions was considered to be the uncertainty.

544 214

The flow regime uncertainties of the turbine flowmeter were estimated by calculating a void fraction and the cross-sectional liquid and steam flow area for stratified flow. This calculation was accomplished using methods similar to those used to calculate the average density for stratified flows. A simple model was used to equate the forces on the turbine with the assumption of a known void fraction, stratified flow, known component densities, and slip ratio greater than unity. This process provided phase velocities. With the phase densities, velocities, and void fraction, a volumetric flow rate could be calculated. The difference between this value and the measured value was considered to be the uncertainty.

The overall standard deviation of a data point is taken as the root of the sum of the random uncertainty variance and the total engineering uncertainty variance; that is:

$$\sigma_o = \sqrt{\sigma_R^2 + \sigma_E^2} \qquad \text{(C-1)}$$

where

σ_o = overall standard deviation of a data point

σ_R^2 = random uncertainty variance

σ_E^2 = engineering uncertainty variance.

The uncertainty bands for the data are computed about the value given by the fitted difference equation y_i at time point i; that is:

$$\text{uncertainty band} = y_i \pm 1.96\,\sigma_o \,. \qquad \text{(C-2)}$$

With due regard to the fact that σ_E has been estimated subjectively, the uncertainty band may be interpreted as an approximate 95% confidence interval within which any true value of the measured variable is consistent with the data.

On certain occasions, the symmetrical uncertainty band given by Equation (C-2) is not appropriate. On those occasions, asymmetrical uncertainty bands were computed; that is, with the width being greater on one side of y_i than on the other.

Finally, the original data trace, along with its uncertainty band from Equation (C-2), was input to a computer plot package. The resulting plot contained the actual data trace surrounded by an uncertainty band derived both from random uncertainty and engineering uncertainty considerations. The indicated uncertainty bands after thermocouple dryout occurred for the fluid temperature measurements should be ignored. Uncertainty bands for these segments of the data were not obtained and bands only appear because of limitations in the plotting package.

REFERENCES

C-1. G. E. P. Box and B. M. Jenkins, *Time Series Analysis — Forecasting and Control*, San Francisco: Holden-Day, 1970.

C-2. E. M. Feldman and S. A. Naff, *Error Analysis for 1-1/2-Loop Semiscale System Isothermal Test Data*, ANCR-1188 (May 1975).

TABLE C-I

RANDOM UNCERTAINTY STANDARD DEVIATION
(TEST S-07-8)

Measurement	Random Uncertainty Standard Deviation σ_R	Period of Application (s)	Figure
TFI-1	0.009	-20 to -0.278	C-1
	1.2	-0.278 to 3.48	
	0.533	3.48 to 31	
	1.357	31 to 59	
	0.334	59 to 268	
TFB-20	0.209	-20 to -0.278	C-2
	1.527	-0.278 to 3.48	
	0.819	3.48 to 28	
	1.933	28 to 45	
	0.643	45 to 108	
	0.212	108 to 268	
TFD-294	0.128	-20 to 1.3	C-3
	2.150	1.3 to 4.7	
	2.833	4.7 to 36	
	3.814	36 to 61	
	0.973	61 to 268	
TFV-578A	0.011	-20 to 0.348	C-4
	1.445	0.348 to 4.42	
	1.567	4.42 to 60	
	0.522	60 to 268	
TIFV+79D	0.731	-20 to 0.661	C-5
	0.702	0.661 to 4.73	
	0.427	4.73 to 30	
	0.228	30 to 42	
	0.743	42 to 46	
	0.087	46 to 208	
	0.407	208 to 240	
	0.069	240 to 268	
TFG-5AB-45	0.0	-20 to -0.3	C-6
	16.96	-0.3 to 5.4	
	7.54	5.4 to 12	
	31.05	12 to 17	
	1.56	17 to 23	
	17.80	23 to 30	
	15.90	30 to 36	
	40.67	36 to 40	
	1.34	40 to 268	

TABLE C-I (continued)

Measurement	Random Uncertainty Standard Deviation σ_R	Period of Application (s)	Figure
TMI-1T16	0.003	-20 to 0.974	C-7
	0.381	0.974 to 4.42	
	0.424	4.42 to 60	
	0.294	60 to 268	
TMB-20B16	0.086	-20 to 1.29	C-8
	0.620	1.29 to 4.73	
	0.575	4.73 to 26	
	0.450	26 to 67	
	0.183	67 to 104	
	0.283	104 to 268	
TMD-364	0.072	-20 to 12	C-9
	0.236	12 to 120	
	0.360	120 to 268	
TMV+79D	0.541	-20 to -0.278	C-10
	0.647	-0.278 to 3.80	
	0.387	3.80 to 27	
	0.030	27 to 198	
	0.234	198 to 228	
	0.106	228 to 268	
TH-C2-8	0.072	-20 to -0.278	C-11
	2.37	-0.278 to 3.17	
	5.40	3.17 to 23	
	4.20	23 to 80	
	0.728	80 to 268	
TH-C2-180	1.71	-20 to 0.348	C-12
	8.21	0.348 to 5.0	
	4.95	5.0 to 127	
	4.59	127 to 268	
PI-16	0.006	-20 to -0.278	C-13
	0.986	-0.278 to 3.17	
	0.025	3.17 to 268	
PB-45A	0.003	-20 to -0.278	C-14
	1.05	-0.278 to 3.48	
	0.046	3.48 to 80	
	0.006	80 to 268	
PV-ACC1	0.0001	-20 to 18	C-15
	0.012	18 to 22	
	0.005	22 to 268	

5A4 217

TABLE C-I (continued)

Measurement	Random Uncertainty Standard Deviation σ_R	Period of Application (s)	Figure
PB-SD	0.006	-20 to 0.974	C-16
	0.007	0.974 to 150	
	0.012	150 to 268	
DI-6-7	1.565	-20 to 0.035	C-17
	29.24	0.035 to 4.42	
	3.27	4.42 to 30	
	5.74	30 to 50	
	2.27	50 to 268	
DI-7-13	0.149	-20 to -0.591	C-18
	2.72	-0.591 to 7.86	
	0.518	7.86 to 30	
	0.438	30 to 50	
	0.185	50 to 268	
DB-37A-40L	1.847	-20 to -0.591	C-19
	215.3	-0.591 to 2.852	
	0.238	2.852 to 29	
	6.223	29 to 33	
	8.889	33 to 59	
	2.806	59 to 268	
DD-DIA-578	0.253	-20 to -0.591	C-20
	17.0	-0.591 to 4.42	
	1.974	4.42 to 30	
	11.35	30 to 50	
	4.576	50 to 90	
	2.890	90 to 268	
DV-501-105	0.257	-20 to -0.591	C-21
	19.690	-0.591 to 2.852	
	0.953	2.852 to 30	
	3.970	30 to 50	
	0.854	50 to 268	
DI-SG-LL	0.252	-20 to 0.974	C-22
	0.509	0.974 to 5.043	
	0.032	5.043 to 268	
FI-1	0.032	-20 to -0.278	C-23
	1.355	-0.278 to 3.478	
	0.856	3.478 to 30	
	1.648	30 to 33	
	5.257	33 to 50	
	1.083	50 to 268	

TABLE C-I (continued)

Measurement	Random Uncertainty Standard Deviation σ_R	Period of Application (s)	Figure
FI-17	0.028	-20 to -0.278	C-24
	1.054	-0.278 to 3.165	
	0.685	3.165 to 32	
	3.813	32 to 61	
	2.690	61 to 268	
FB-45	0.409	-20 to -0.278	C-25
	3.447	-0.278 to 5.043	
	1.693	5.043 to 36	
	4.621	36 to 59	
	3.183	59 to 268	
FD-424	0.004	-20 to -0.278	C-26
	3.582	-0.278 to 4.417	
	0.684	4.417 to 29	
	1.245	29 to 50	
	0.647	50 to 268	
FV+1	0.019	-20 to -0.278	C-27
	1.243	-0.278 to 4.730	
	0.673	4.730 to 32	
	7.215	32 to 50	
	0.999	50 to 268	
FV-LPIS	0.984	-20 to 29	C-28
	15.360	29 to 34	
	1.255	34 to 68	
	0.231	68 to 247	
	2.944	247 to 251	
	1.380	251 to 268	
GI-1T	3.845	-20 to -0.278	C-29
	42.30	-0.278 to 4.10	
	12.73	4.10 to 14	
	7.032	14 to 268	
GI-1B	5.111	-20 to -0.278	C-30
	27.14	-0.278 to 3.48	
	47.44	3.48 to 19	
	5.388	19 to 137	
	14.675	137 to 268	
GI-1C	3.140	-20 to -0.278	C-31
	31.25	-0.278 to 4.73	
	16.75	4.73 to 30	
	5.96	30 to 268	

TABLE C-I (continued)

Measurement	Random Uncertainty Standard Deviation σ_R	Period of Application (s)	Figure
GI-17T	6.670	-20 to 6.3	C-32
	65.950	6.3 to 11	
	68.354	11 to 17	
	20.612	17 to 268	
GI-17B	5.77	-20 to 5	C-33
	33.70	5 to 11	
	7.69	11 to 268	
GI-17C	5.78	-20 to 1.9	C-34
	14.58	1.9 to 8	
	42.95	8 to 20	
	7.78	20 to 268	
GB-45VR	13.48	-20 to 4.4	C-35
	38.87	4.4 to 11	
	19.23	11 to 150	
	20.07	150 to 268	
GV-11	4.504	-20 to -0.278	C-36
	24.96	-0.278 to 5.4	
	9.18	5.4 to 12	
	39.64	12 to 18	
	5.738	18 to 150	
	16.32	150 to 268	
FI-1, GI-1C	0.037	-20 to -0.28	C-37
	0.601	-0.28 to 5	
	0.112	5 to 35	
	0.110	35 to 268	
FI-17, GI-17C	0.047	-20 to -0.28	C-38
	0.607	-0.28 to 5	
	0.302	5 to 19	
	0.358	19 to 268	
FB-45, GB-45VR	0.310	-20 to -0.28	C-39
	2.622	-0.28 to 5	
	0.516	5 to 20	
	0.363	20 to 268	
FV-1, GV-11	0.063	-20 to 0.035	C-40
	0.749	0.035 to 5	
	0.124	5 to 95	
	0.249	95 to 268	

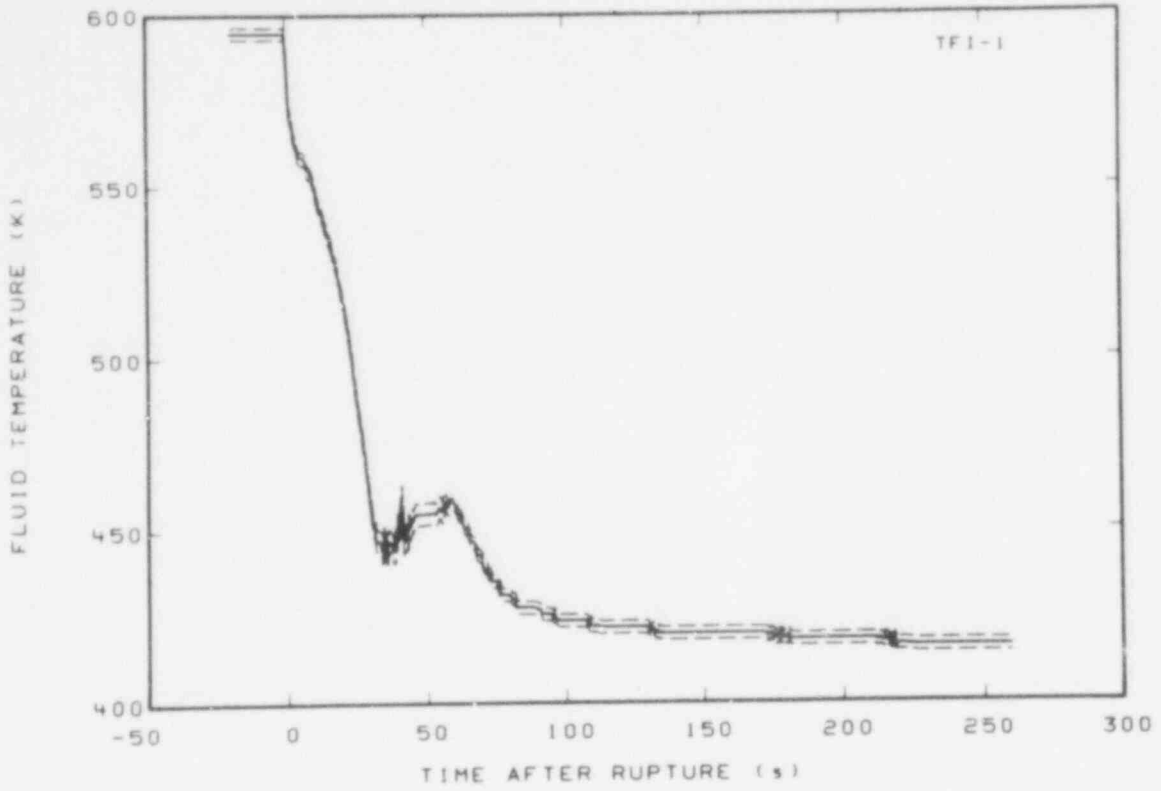

Fig. C-1 Fluid temperature in intact loop(TFI-1).

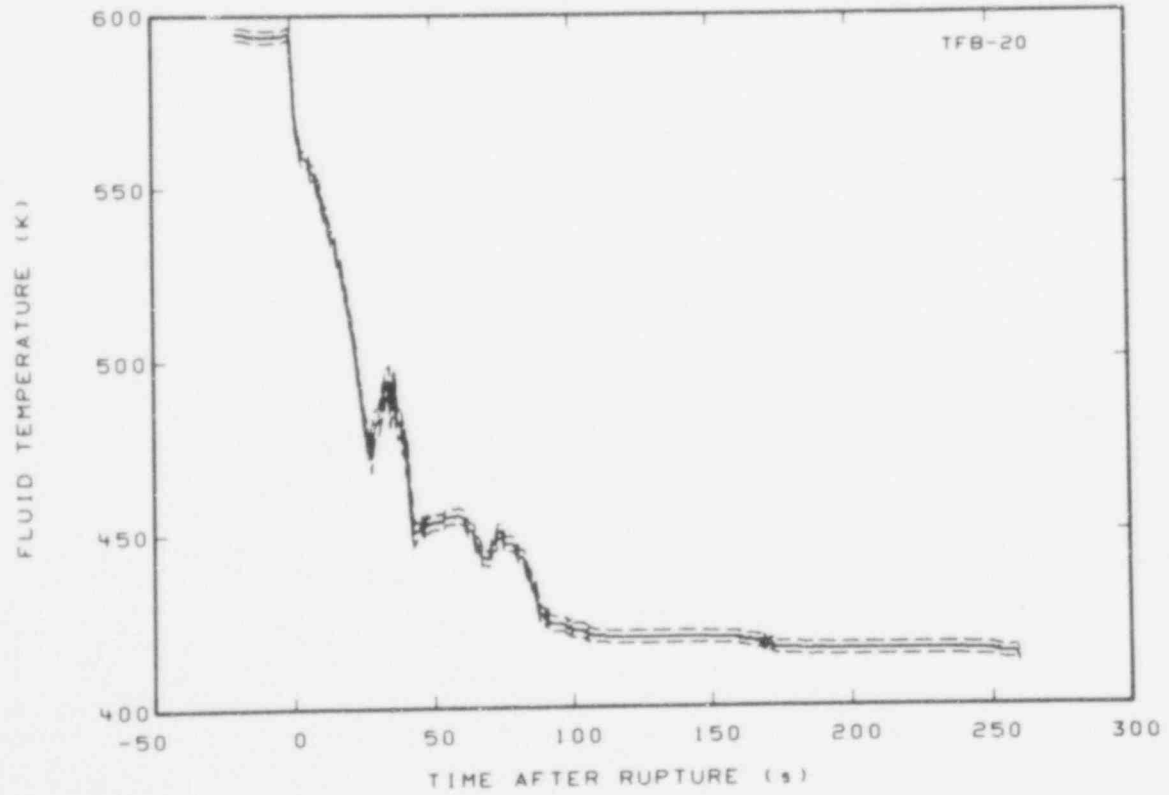

Fig. C-2 Fluid temperature in broken loop (TFB-20).

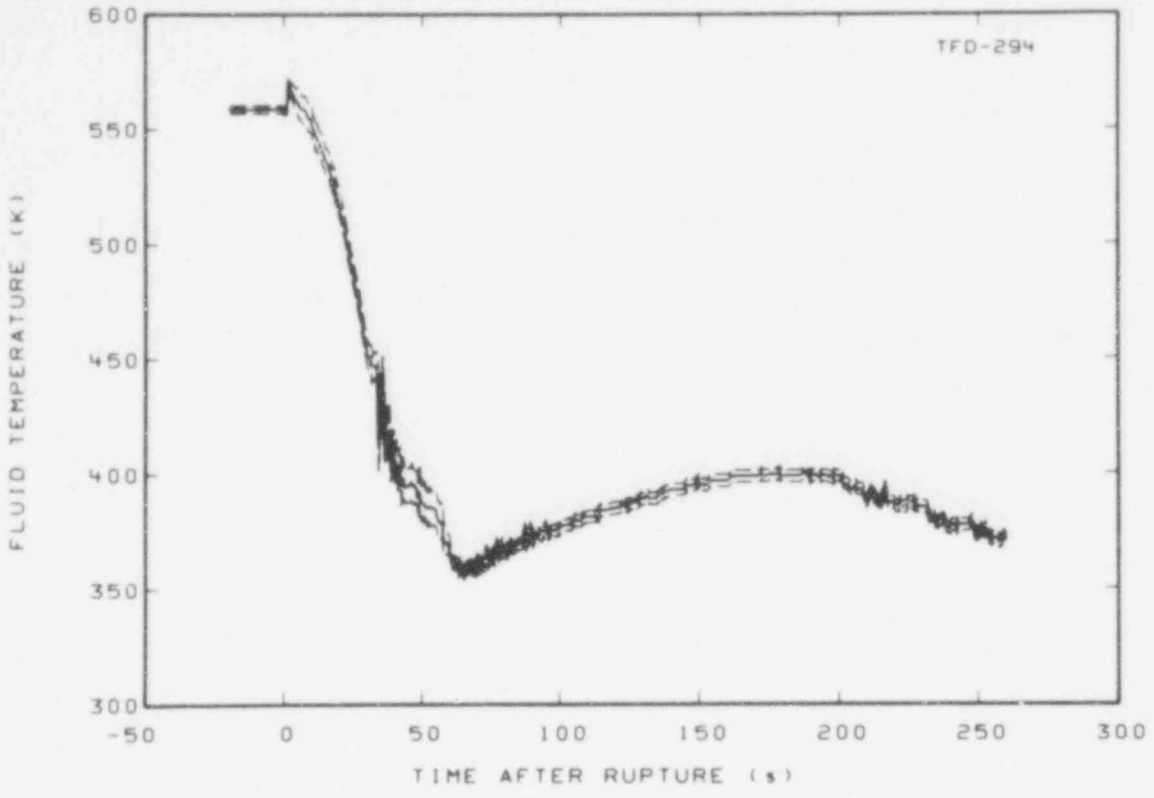

Fig. C-3 Fluid temperature in downcomer (TFD-294).

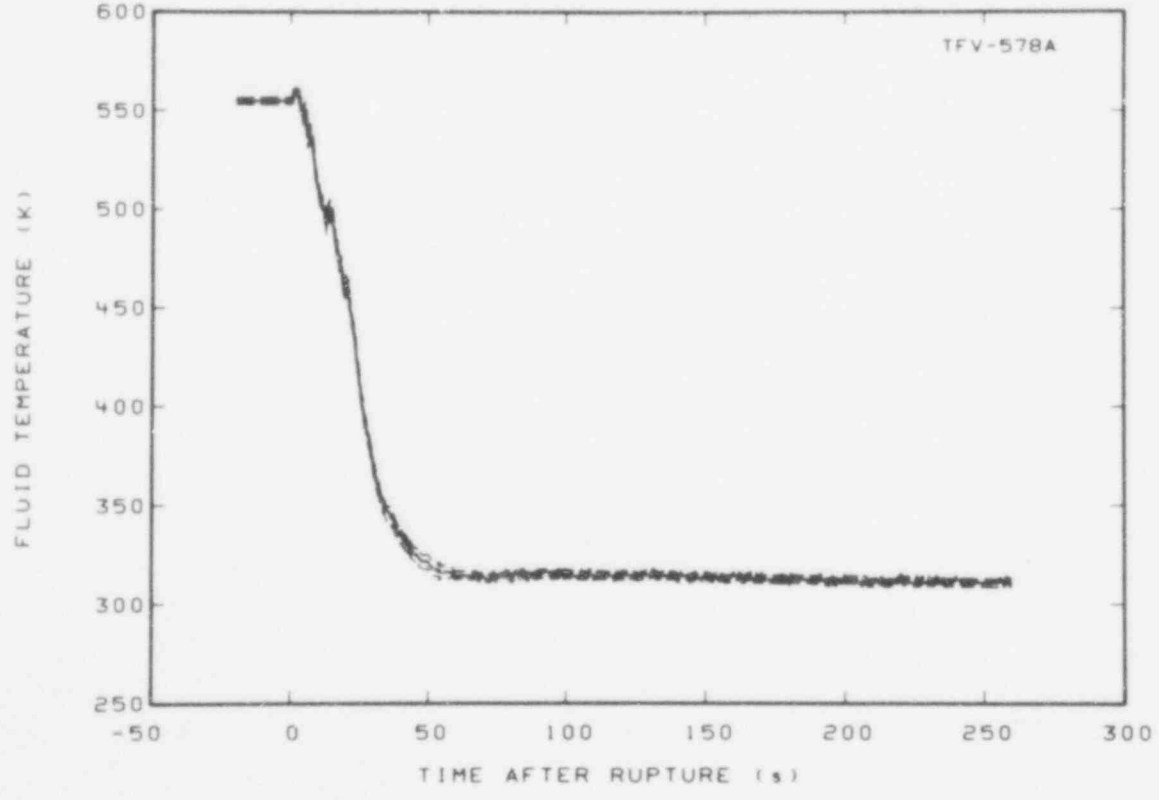

Fig. C-4 Fluid temperature in vessel (TFV-578A).

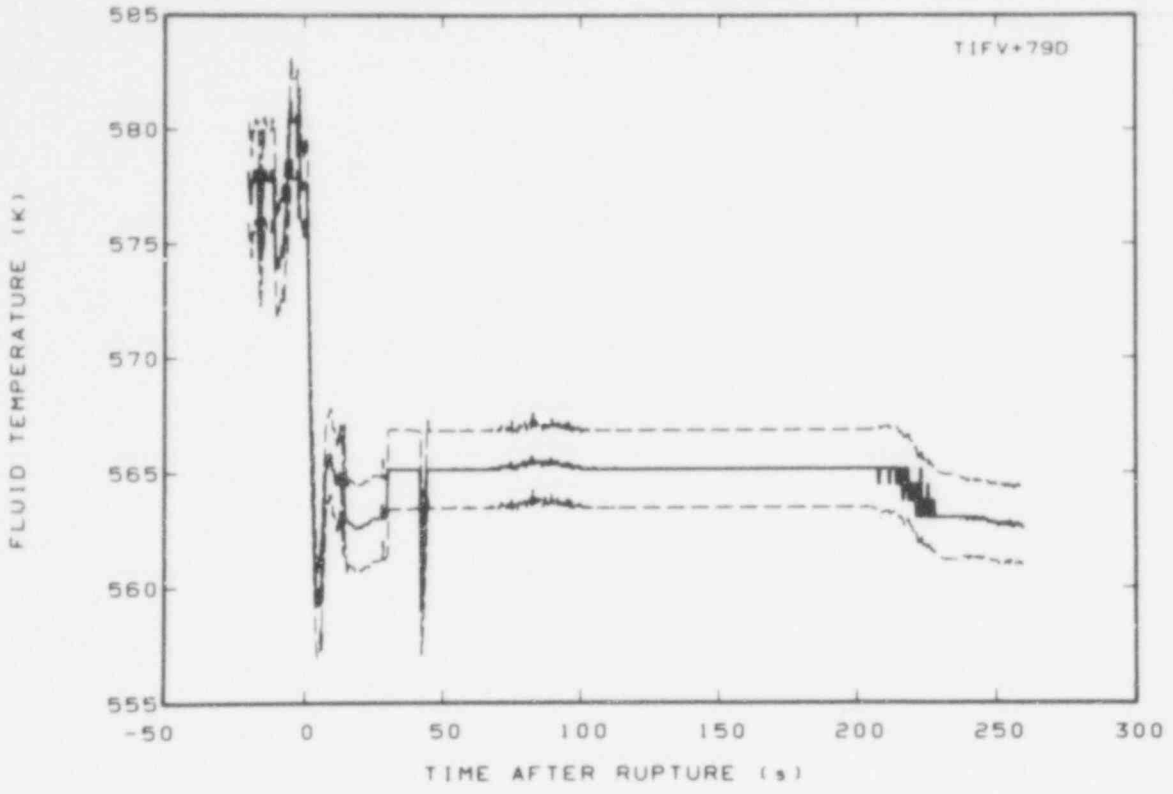

Fig. C-5 Fluid temperature in vessel (TIFV + 79D).

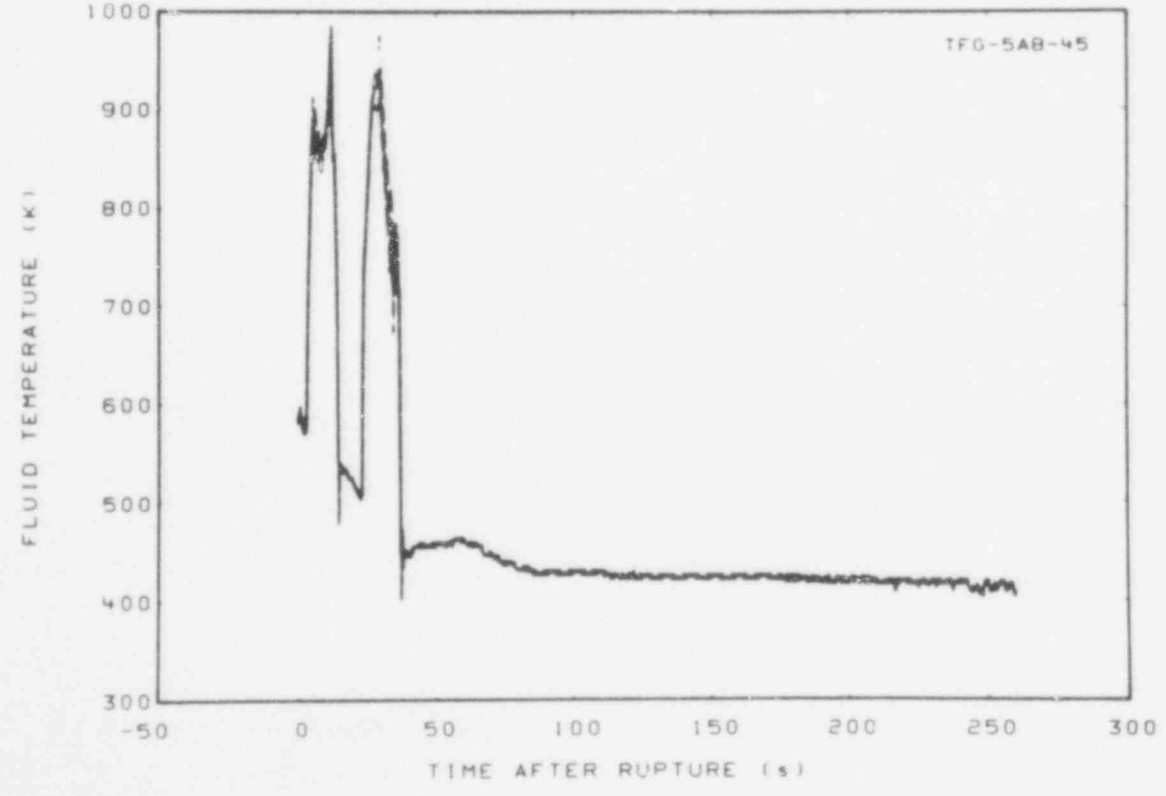

Fig. C-6 Fluid temperature in core, Grid Spacer 5 (TFG-5AB-45).

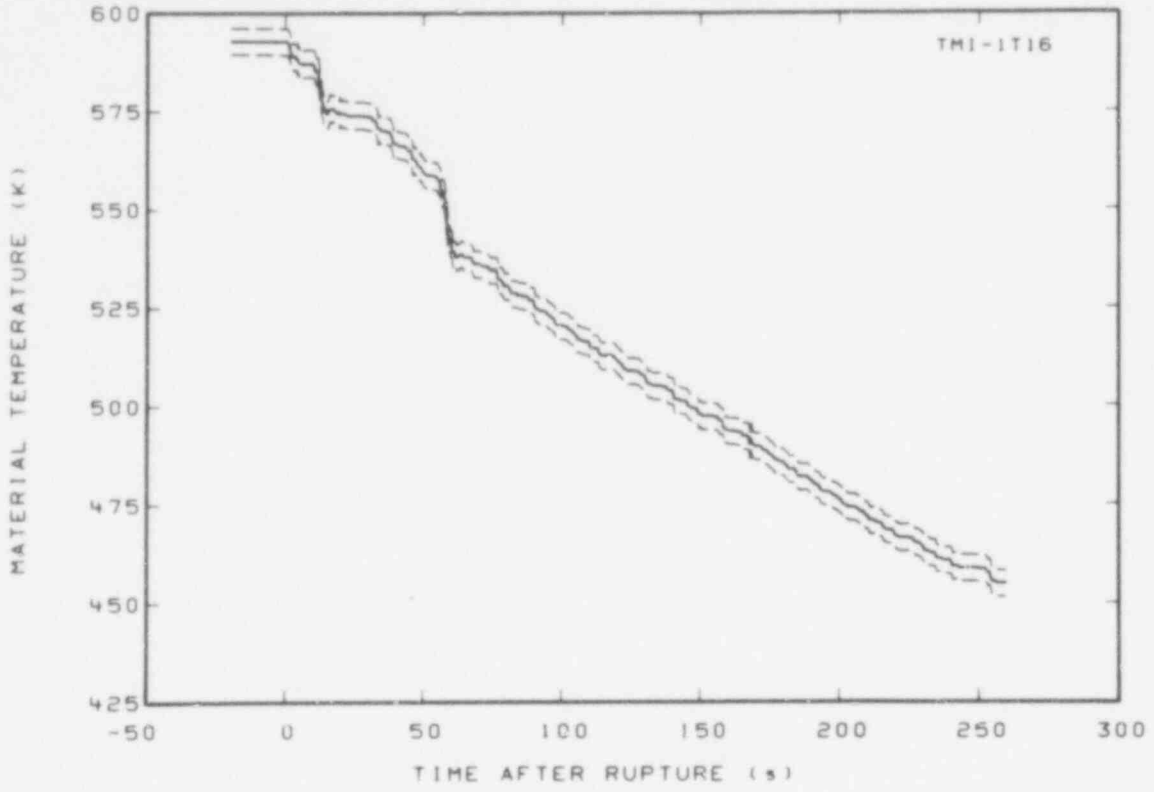

Fig. C-7 Material temperature in intact loop hot leg (TMI-1T16).

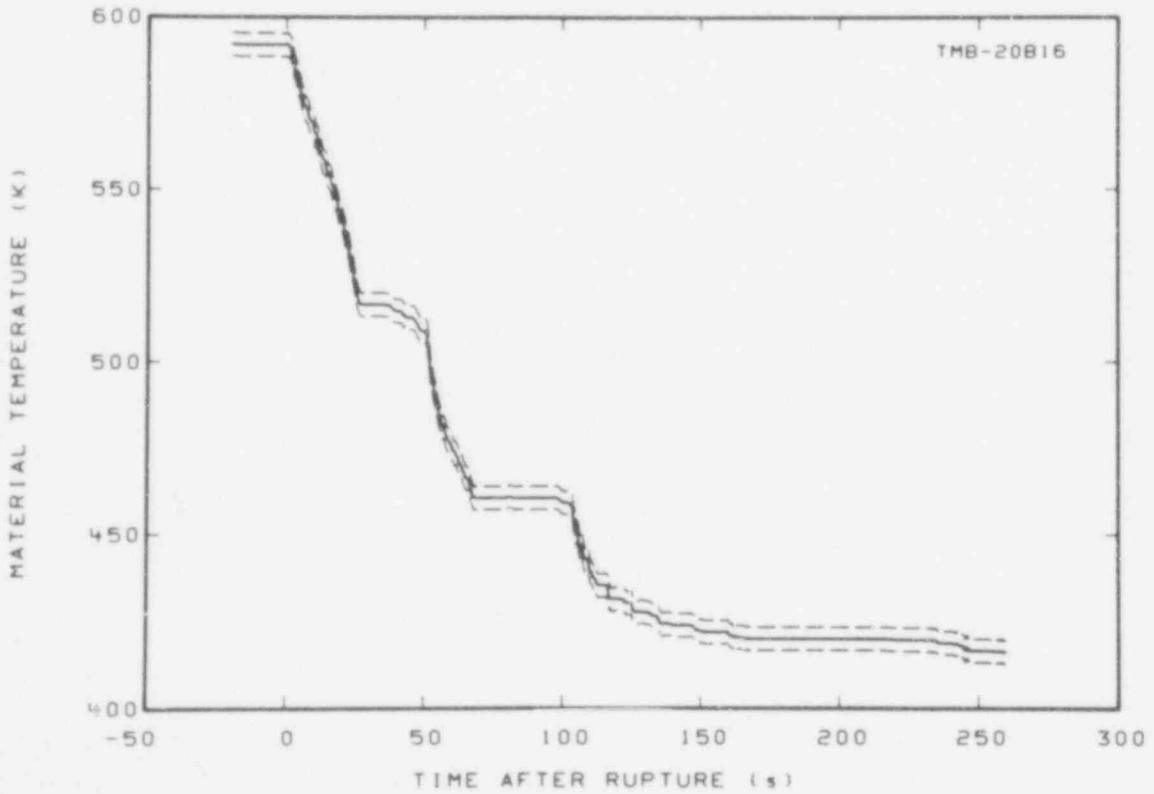

Fig. C-8 Material temperature in broken loop hot leg (TMB-20B16).

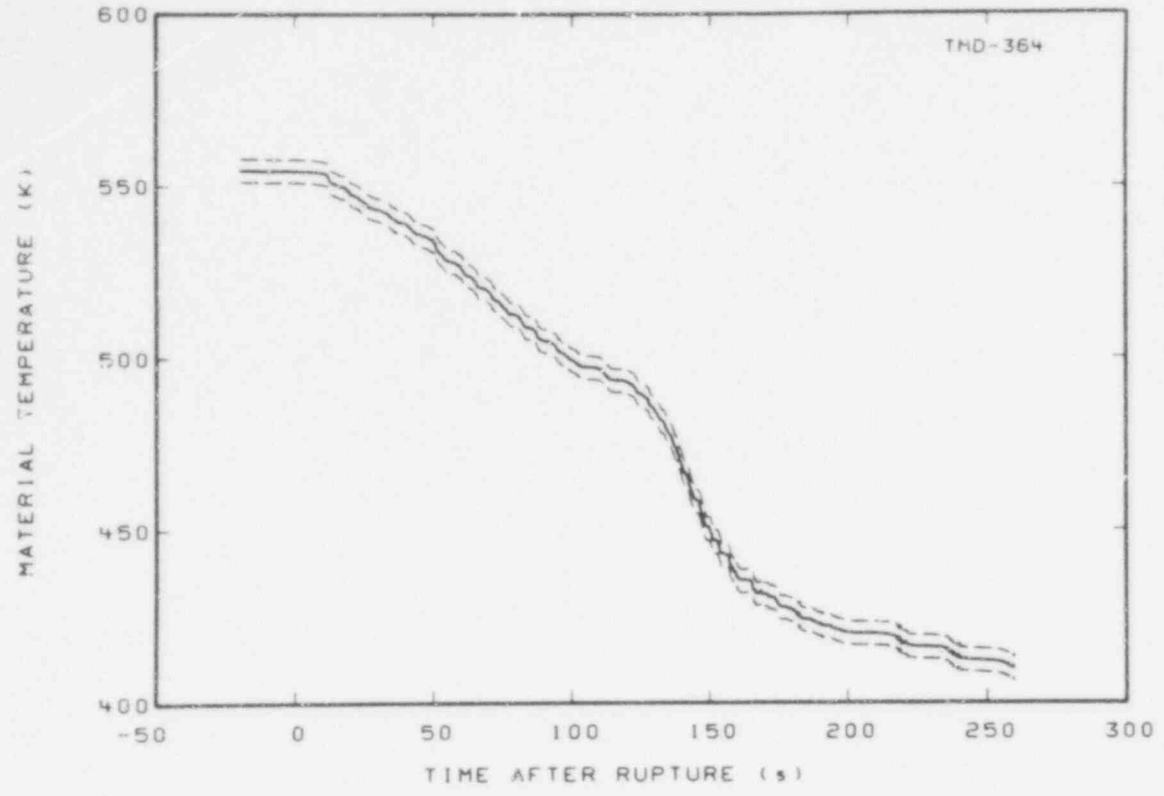

Fig. C-9 Material temperature in downcomer (TMD-364).

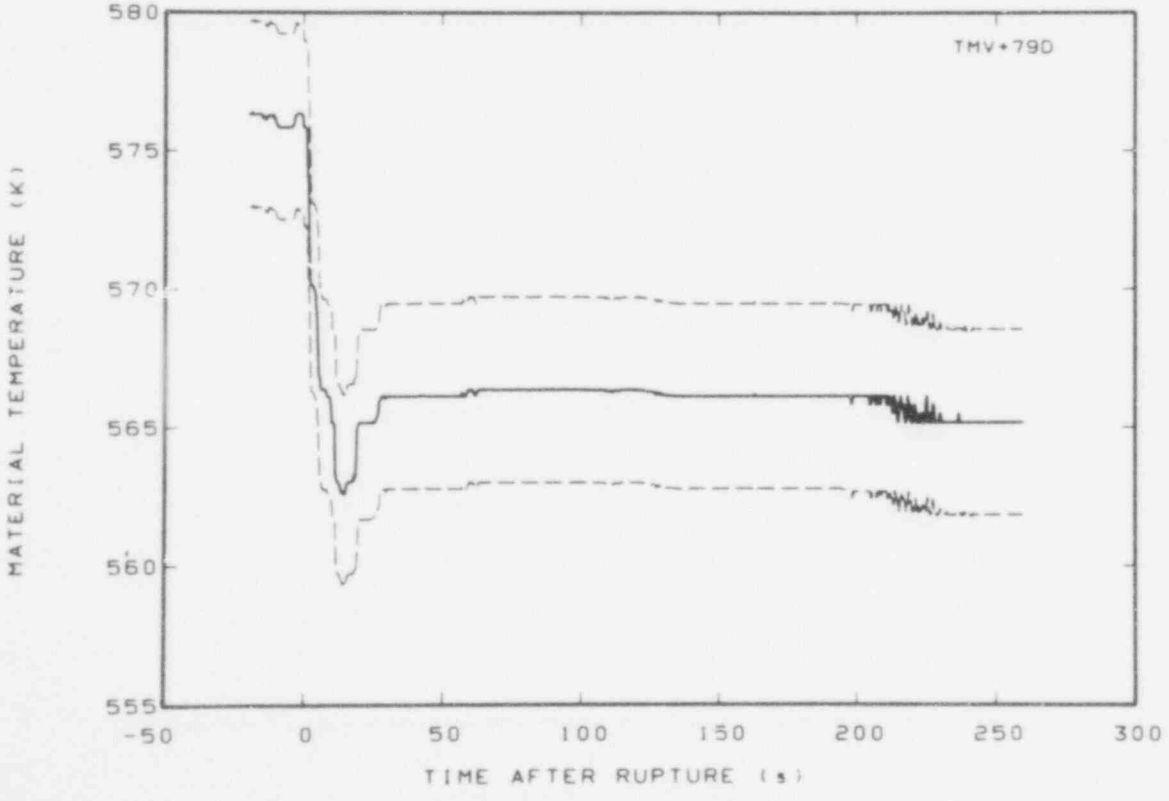

Fig. C-10 Material temperature in vessel (TMV + 79D).

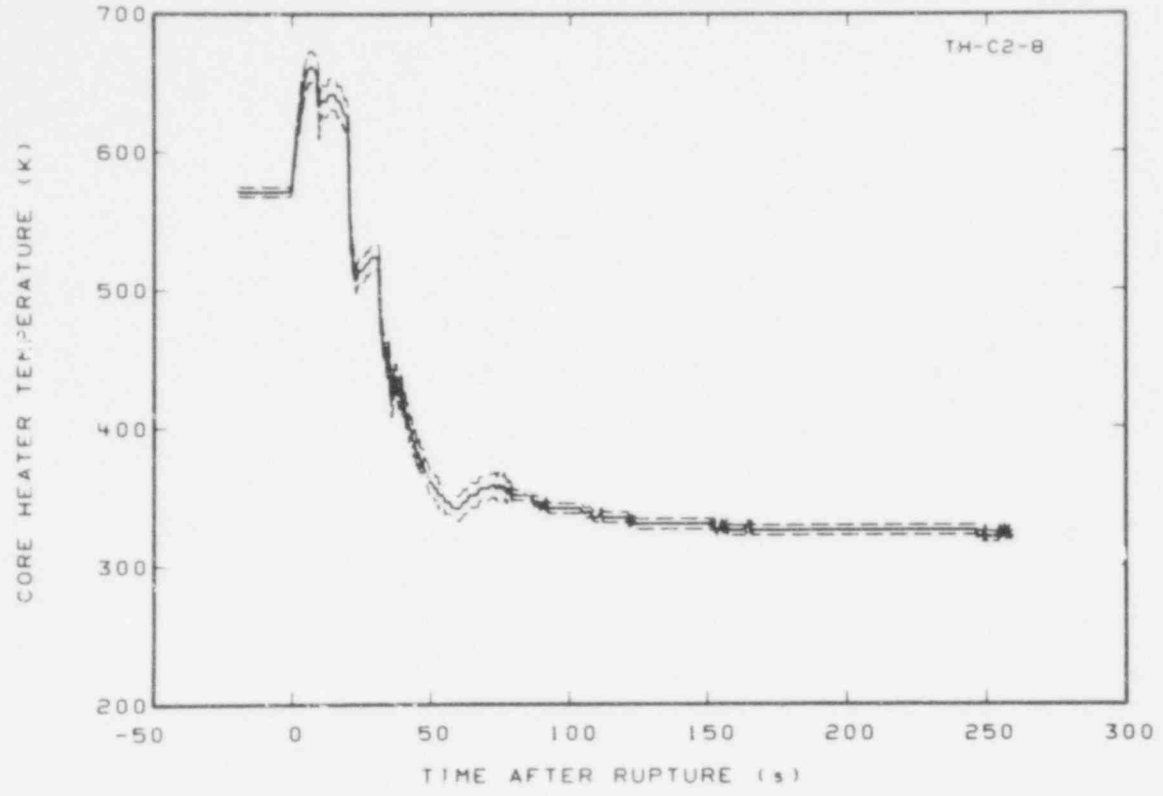

Fig. C-11 Core heater temperature, Rod C-2 (TH-C2-8).

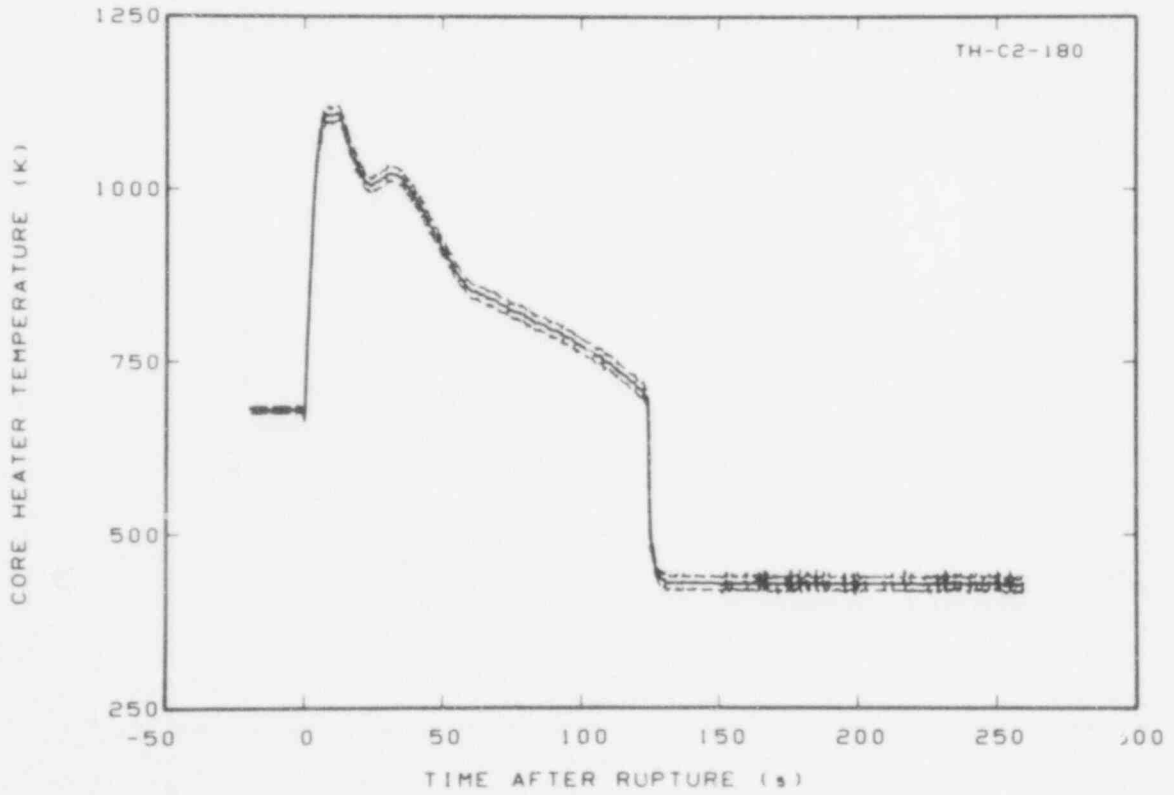

Fig. C-12 Core heater temperature, Rod C-2 (TH-C2-180).

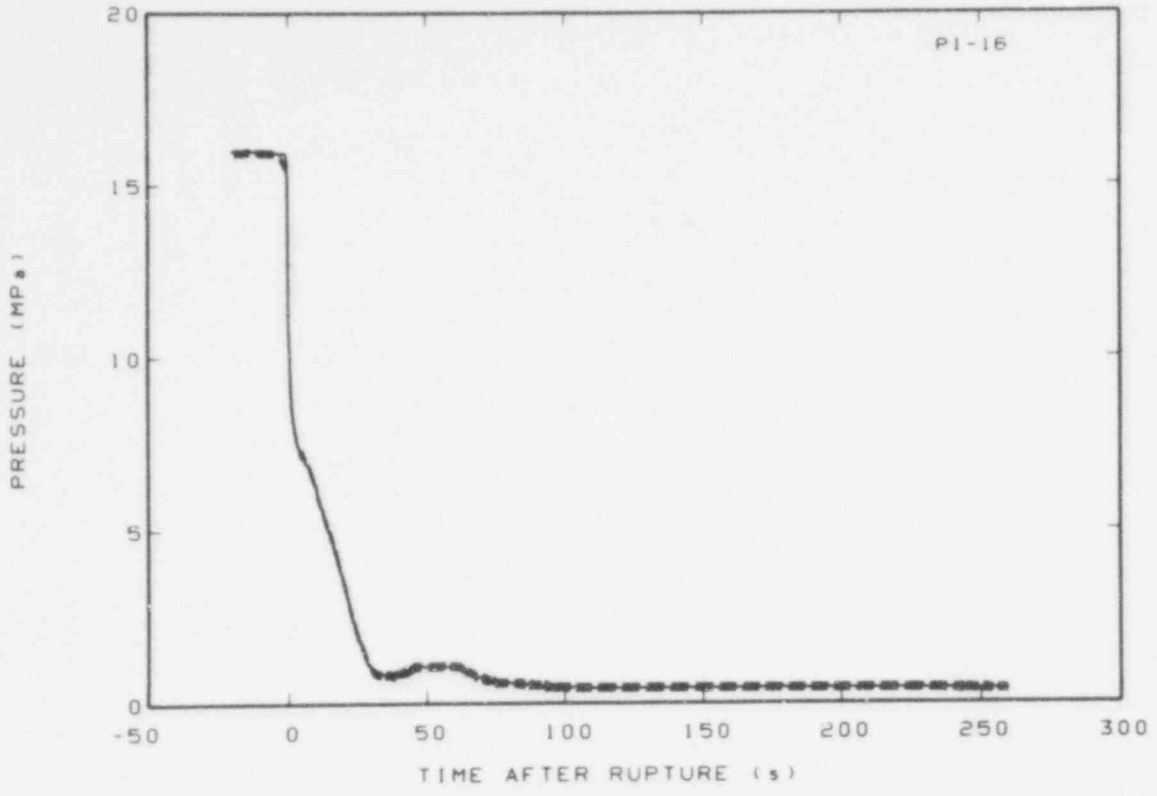

Fig. C-13 Pressure in intact loop cold leg (PI-16).

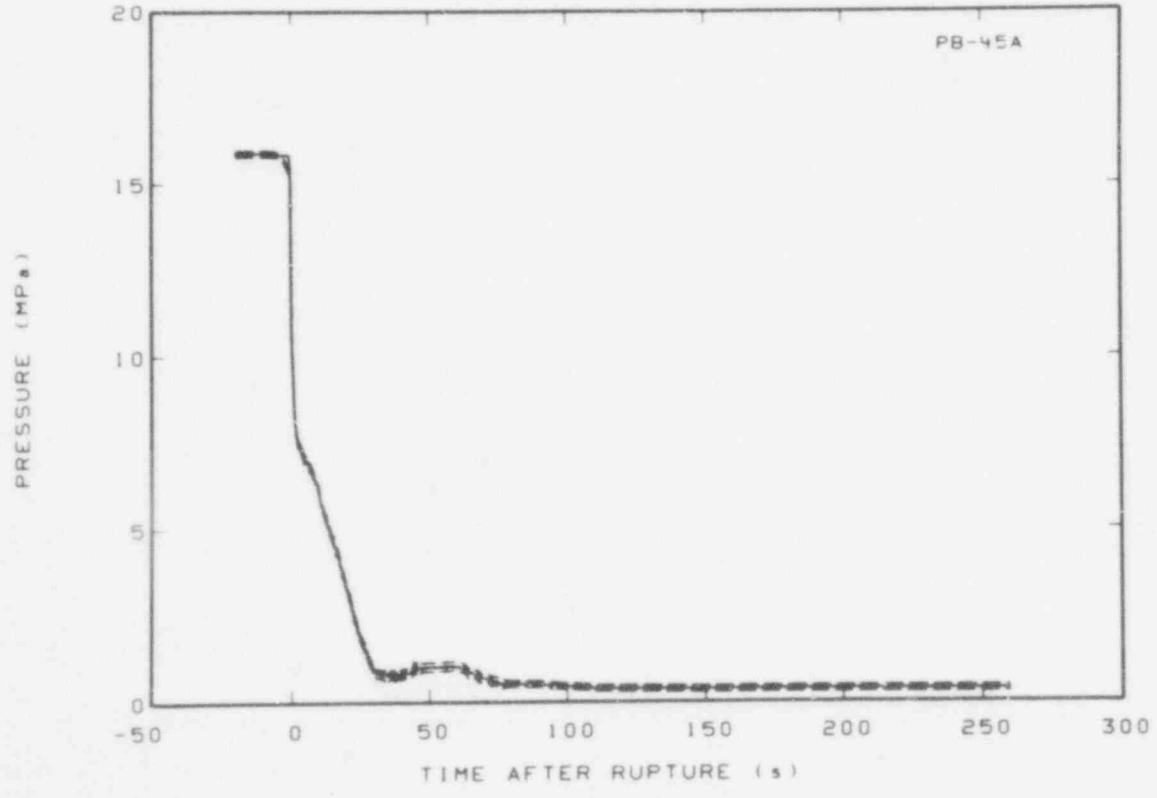

Fig. C-14 Pressure in broken loop cold leg (PB-45A).

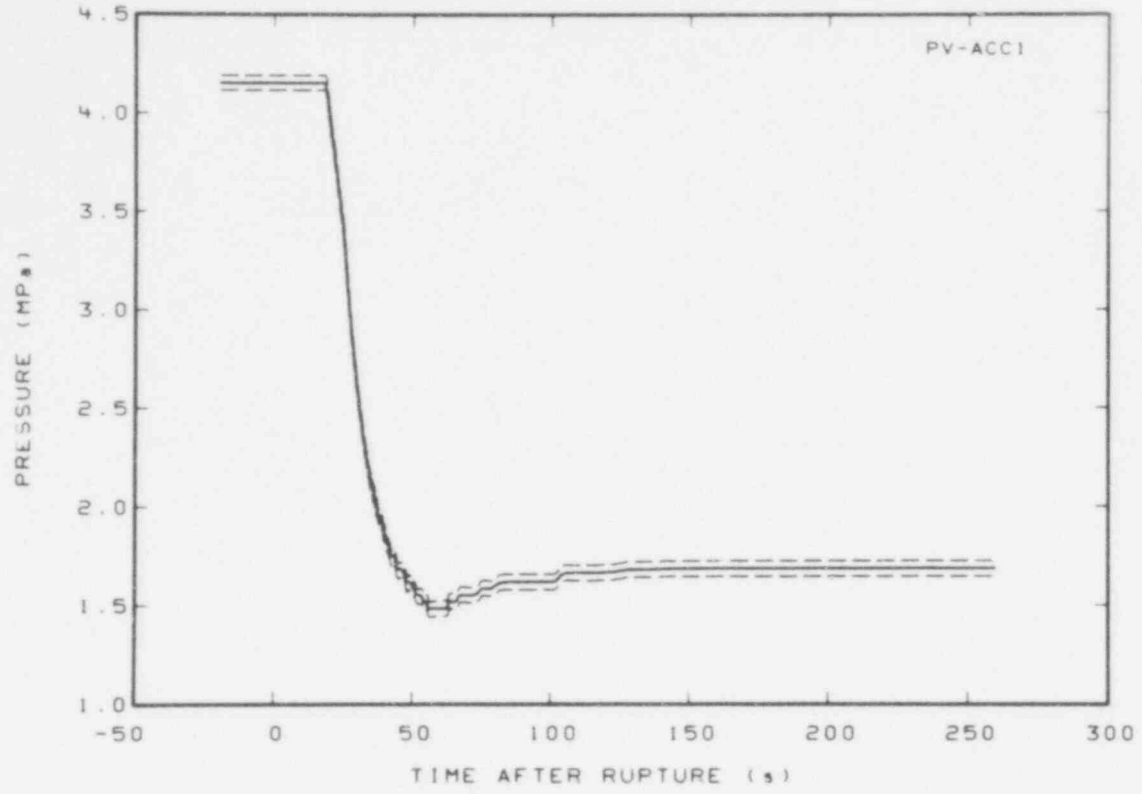

Fig. C-15 Pressure in vessel accumulator (PV-ACC1).

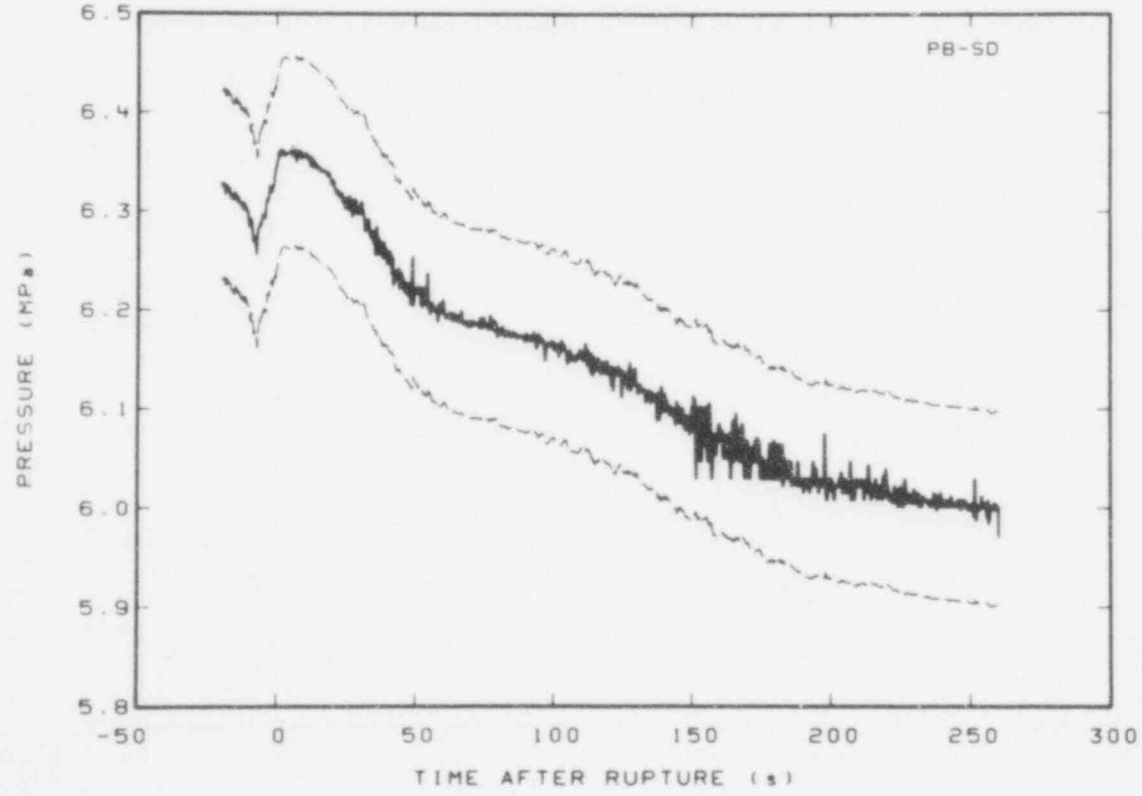

Fig. C-16 Pressure in broken loop steam generator, secondary side steam dome (PB-SD).

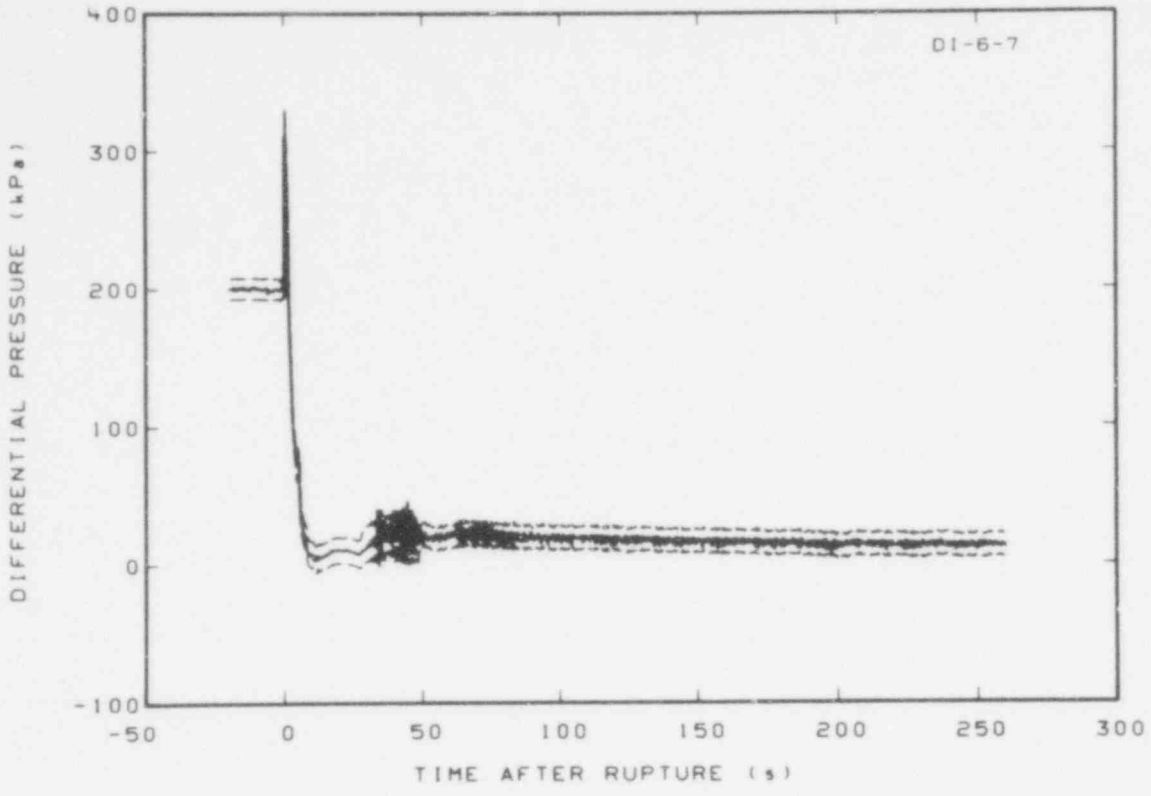

Fig. C-17 Differential pressure in intact loop (DI-6-7).

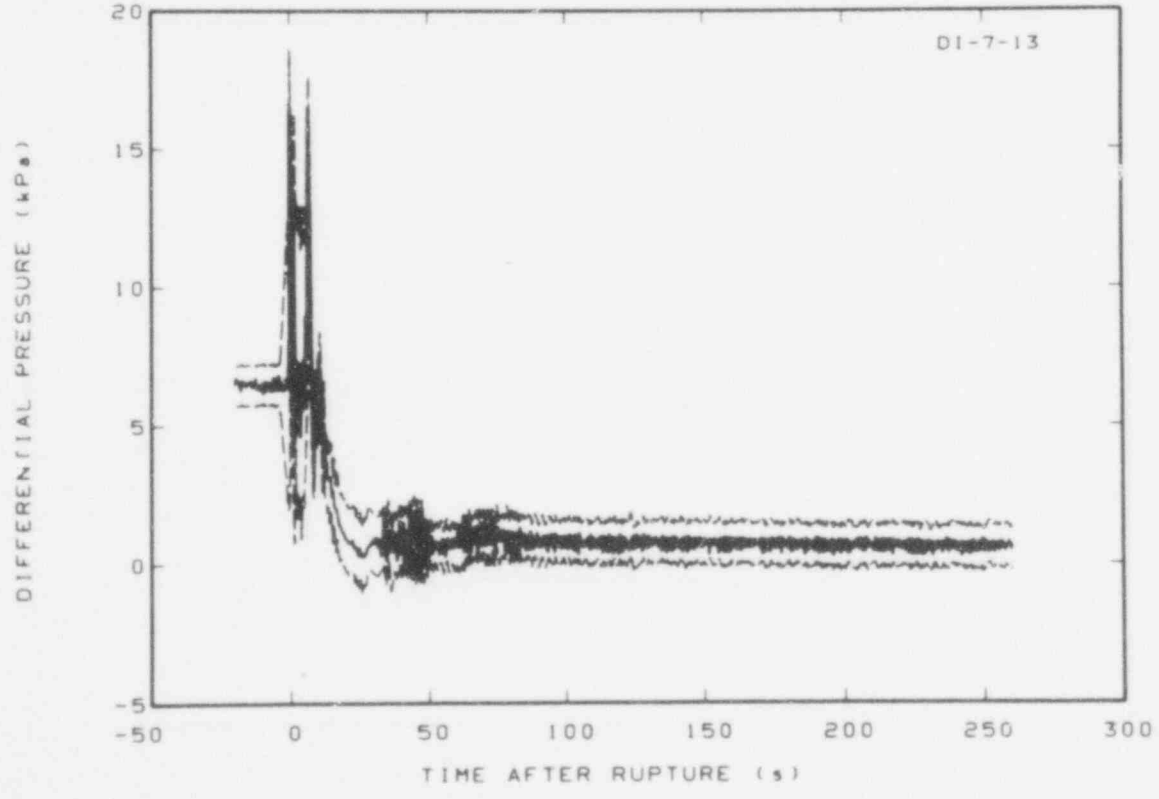

Fig. C-18 Differential pressure in intact loop (DI-7-13).

514 229

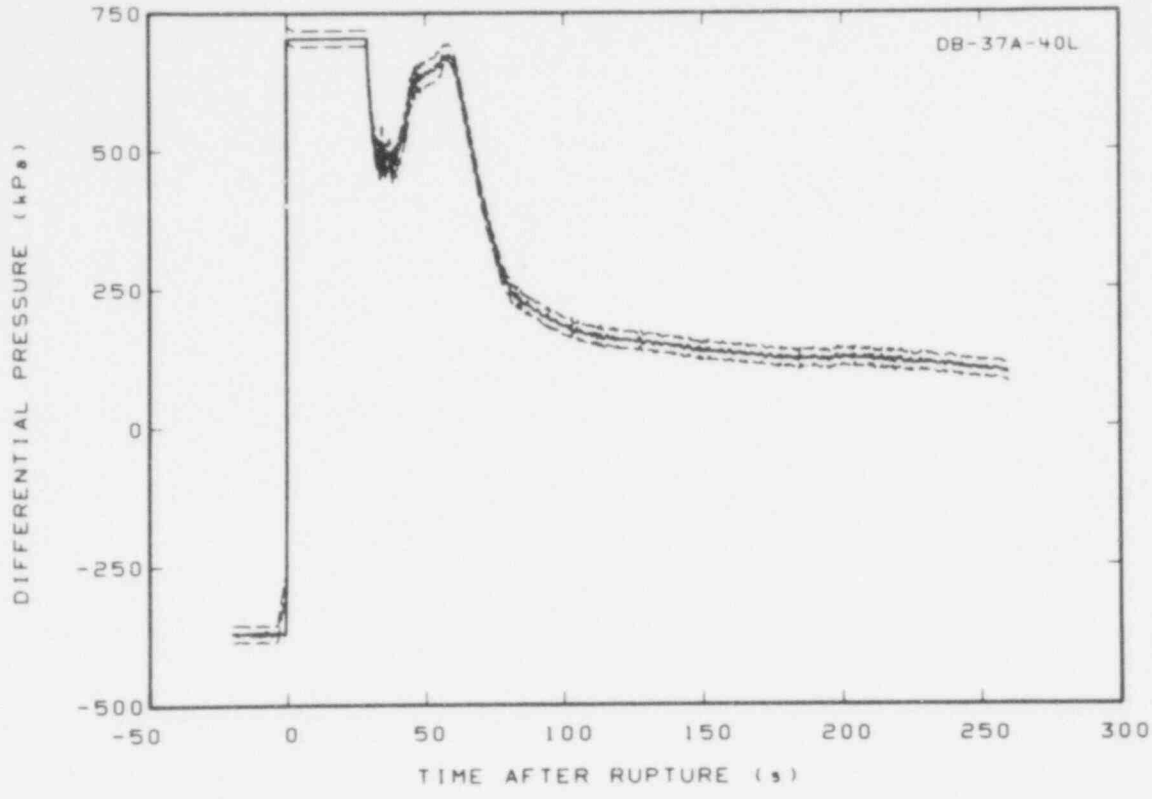

Fig. C-19 Differential pressure in broken loop (DB-37A-40L).

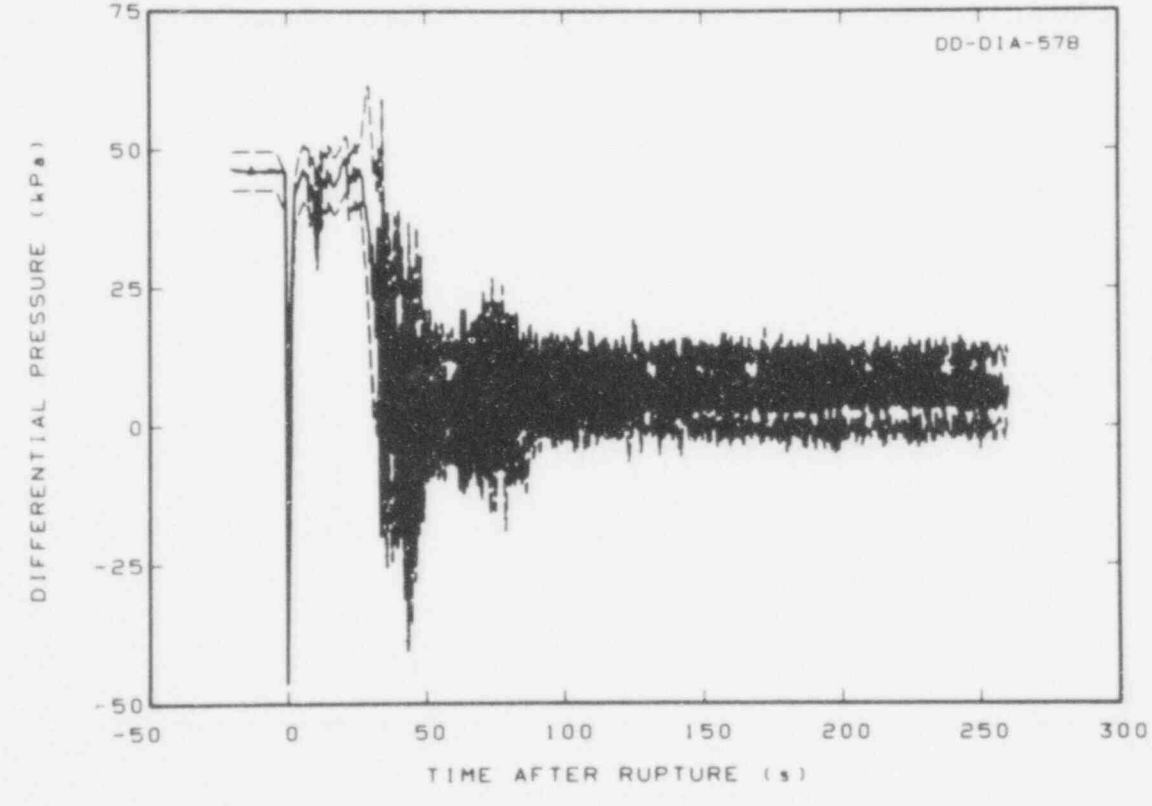

Fig. C-20 Differential pressure in downcomer (DD-DIA-578).

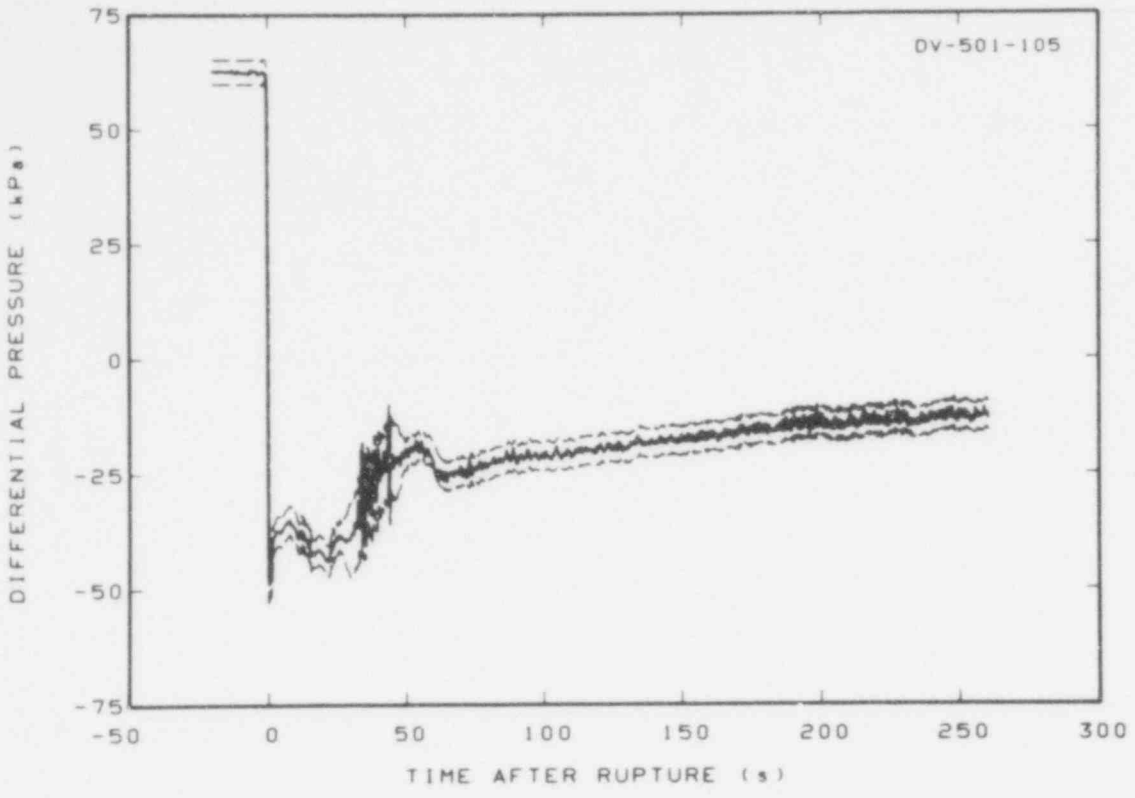

Fig. C-21 Differential pressure in vessel (DV-501-105).

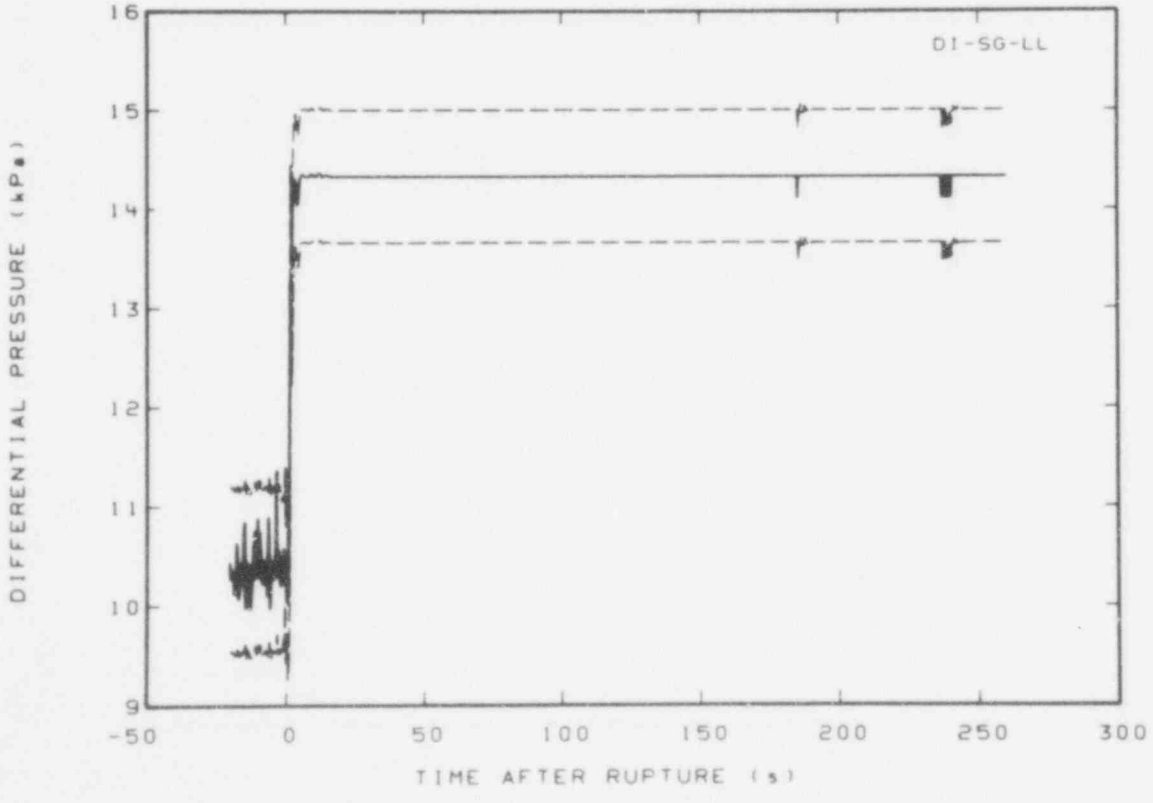

Fig. C-22 Differential pressure in intact loop steam generator, secondary side liquid level (DI-SG-LL).

544 231

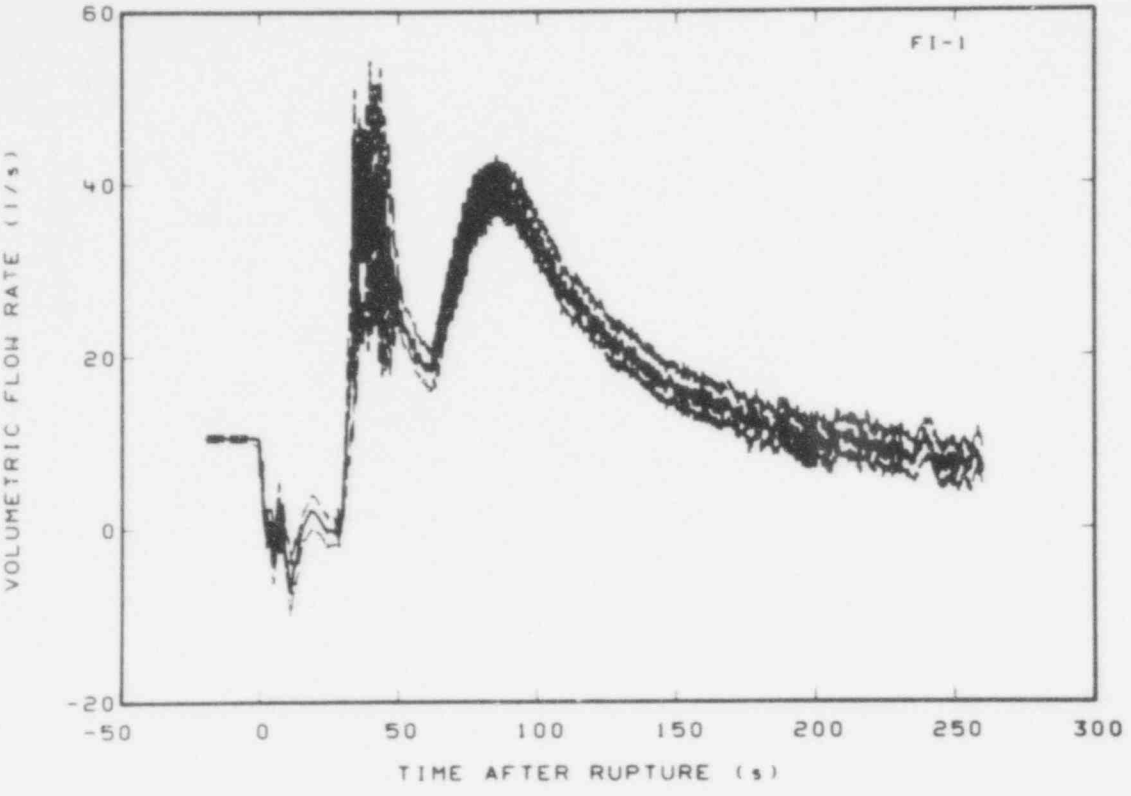

Fig. C-23 Volumetric flow in intact loop (FI-1).

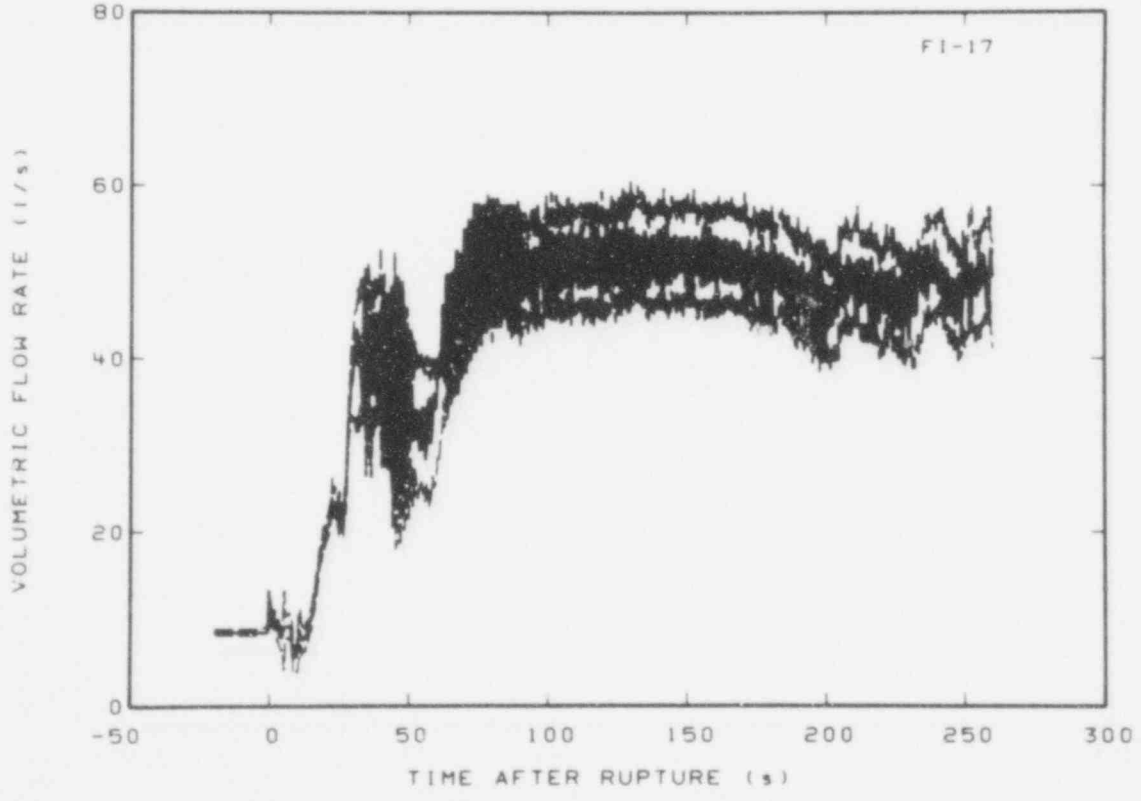

Fig. C-24 Volumetric flow in intact loop (FI-17).

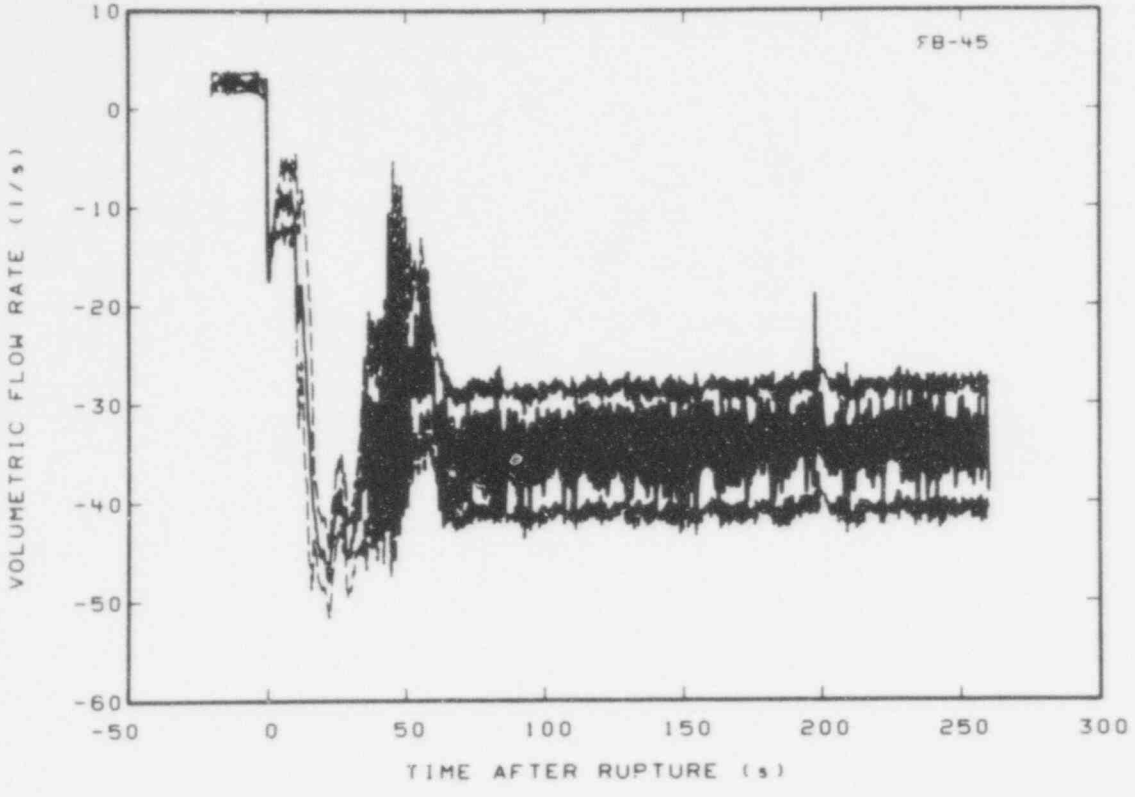

Fig. C-25 Volumetric flow in broken loop (FB-45).

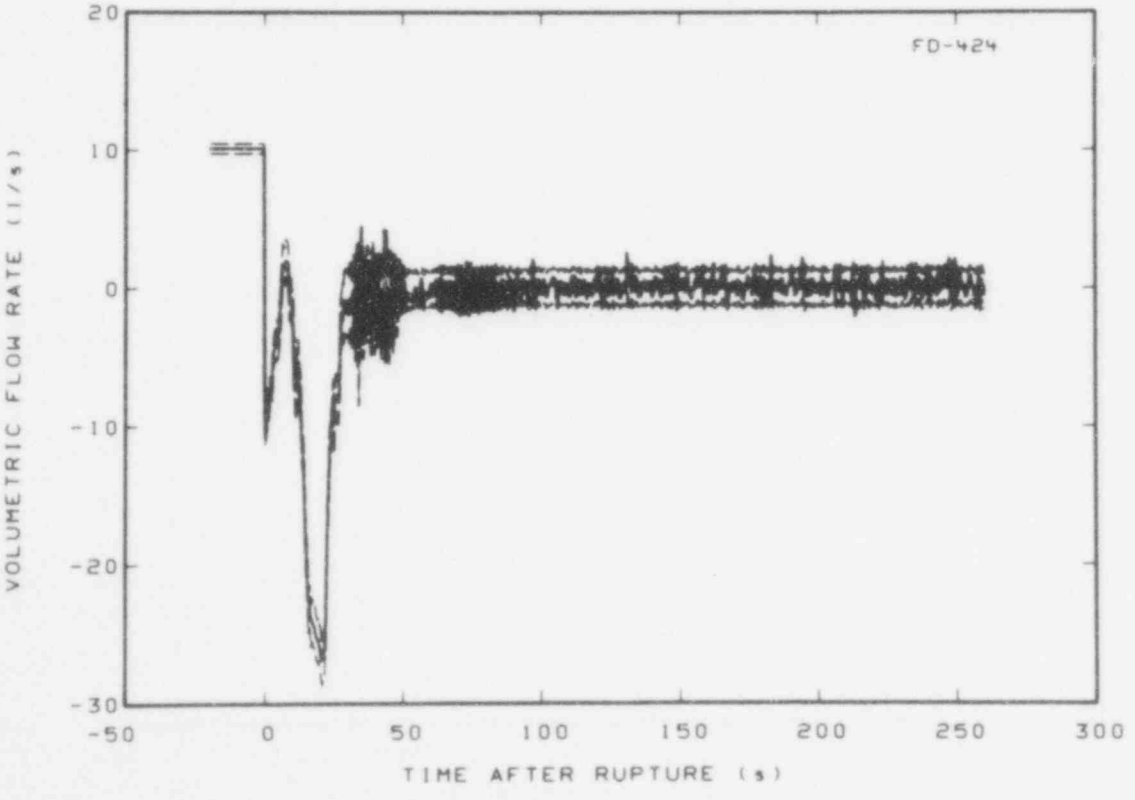

Fig. C-26 Volumetric flow in downcomer (FD-424).

SAA 233

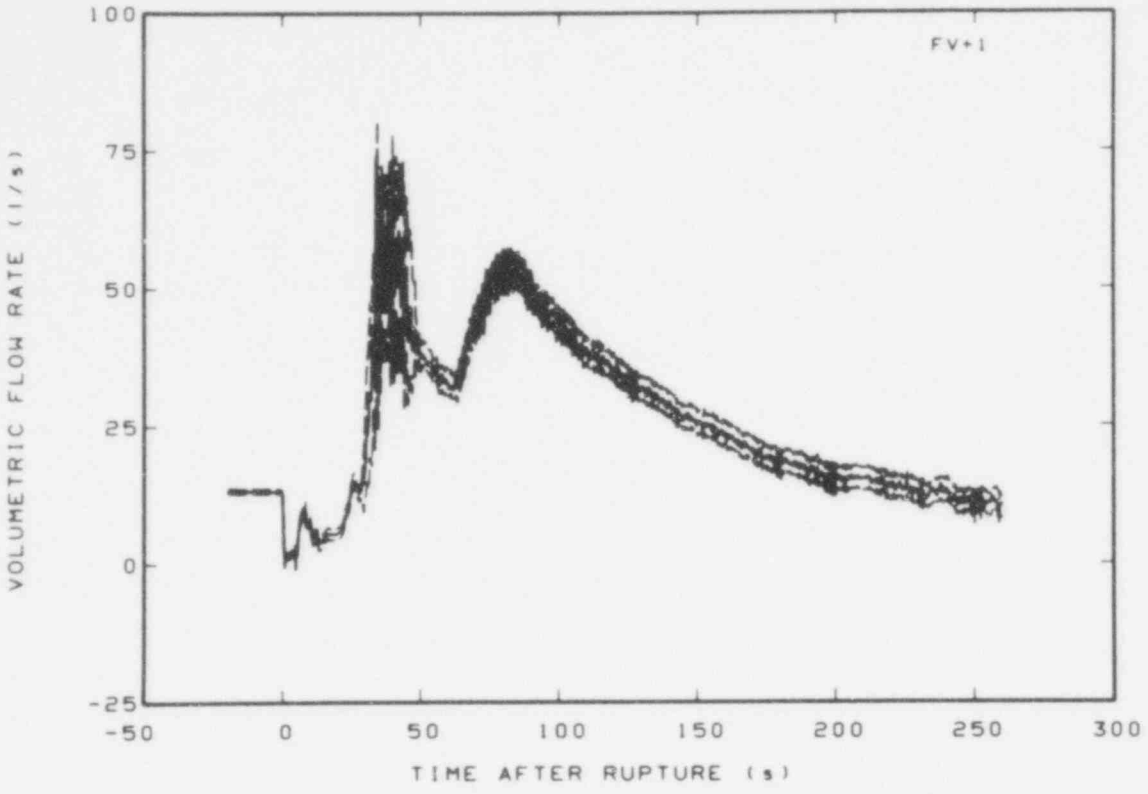

Fig. C-27 Volumetric flow in vessel upper plenum (FV + 1).

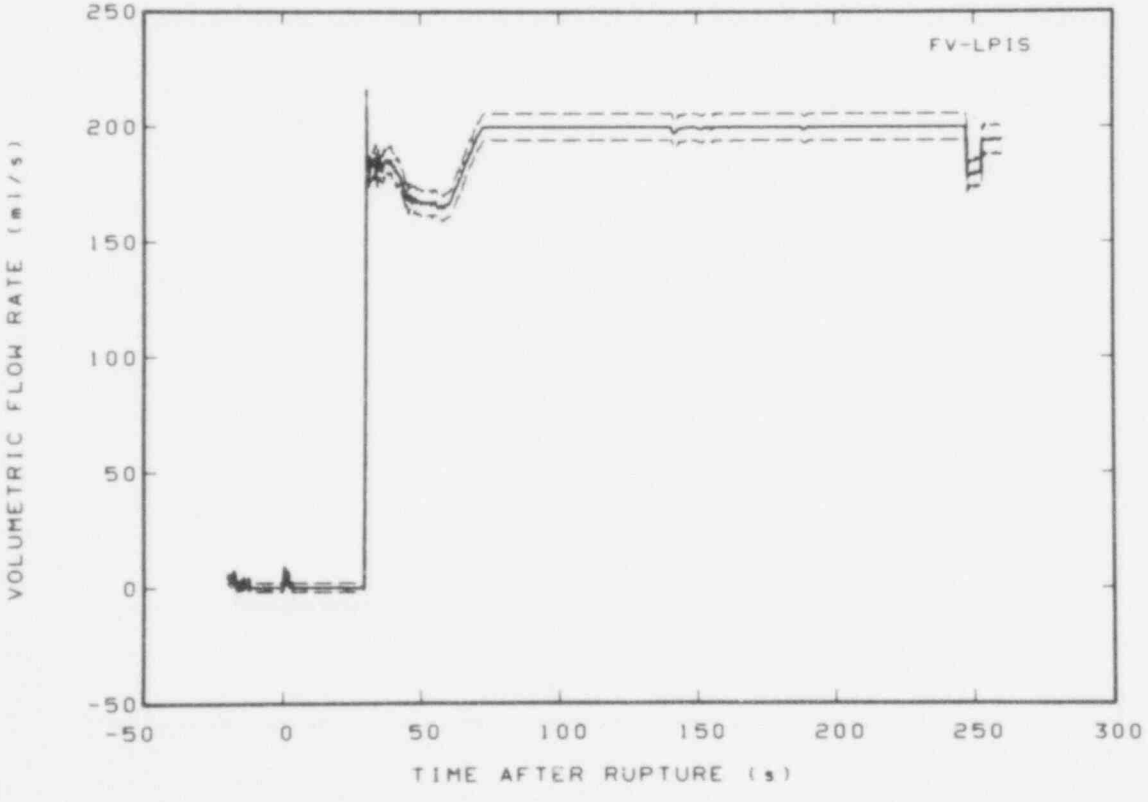

Fig. C-28 Volumetric flow in vessel lower plenum, low pressure injection system (FV-LPIS).

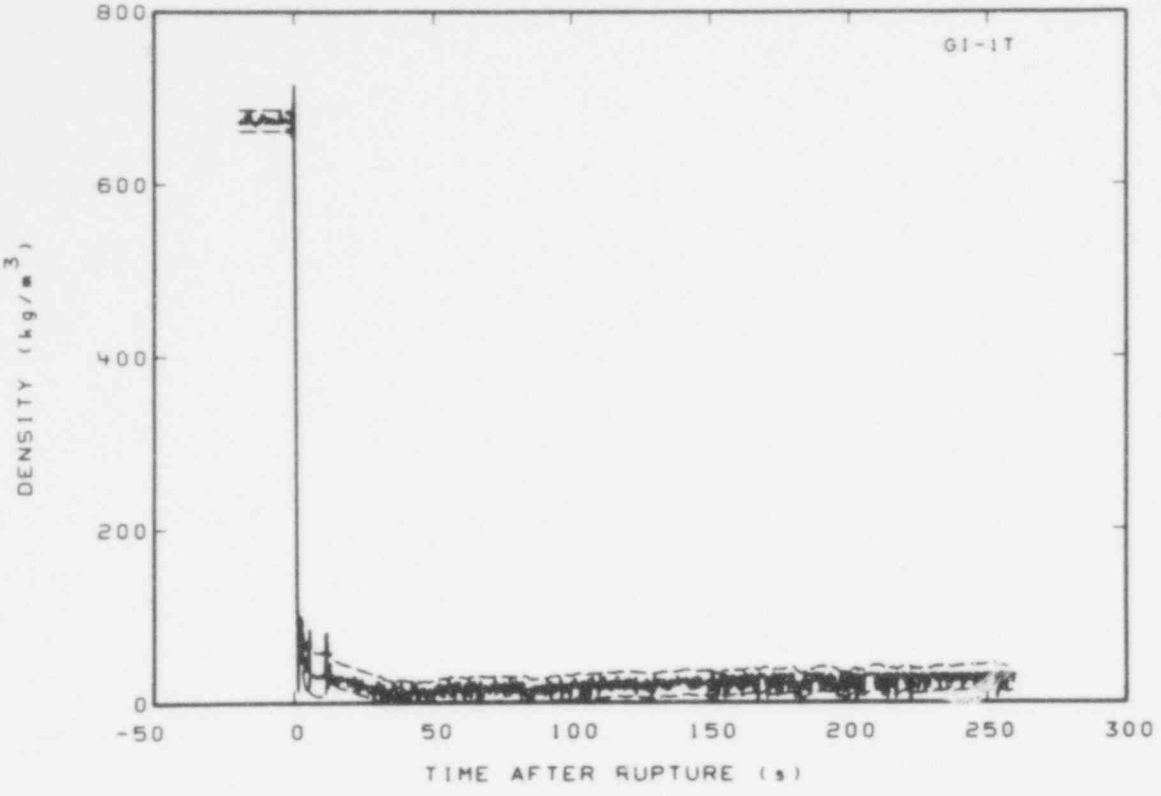

Fig. C-29 Density in intact loop (GI-1T).

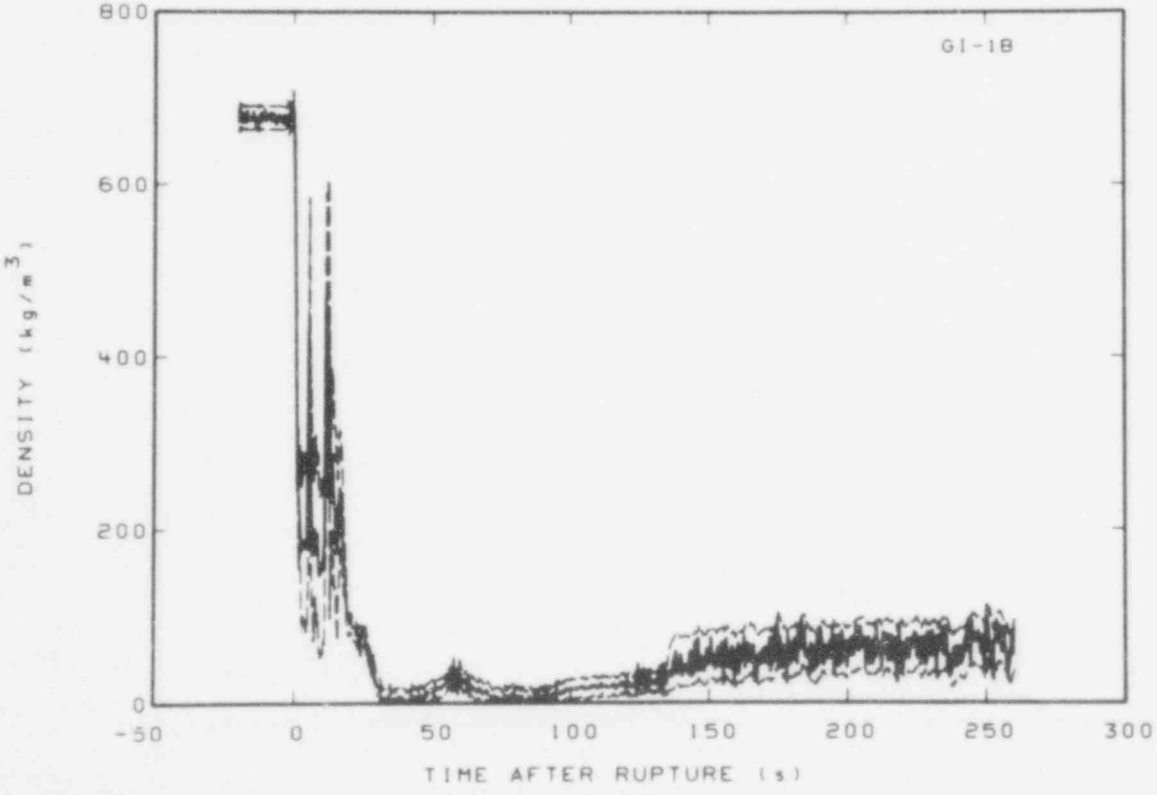

Fig. C-30 Density in intact loop (GI-1B).

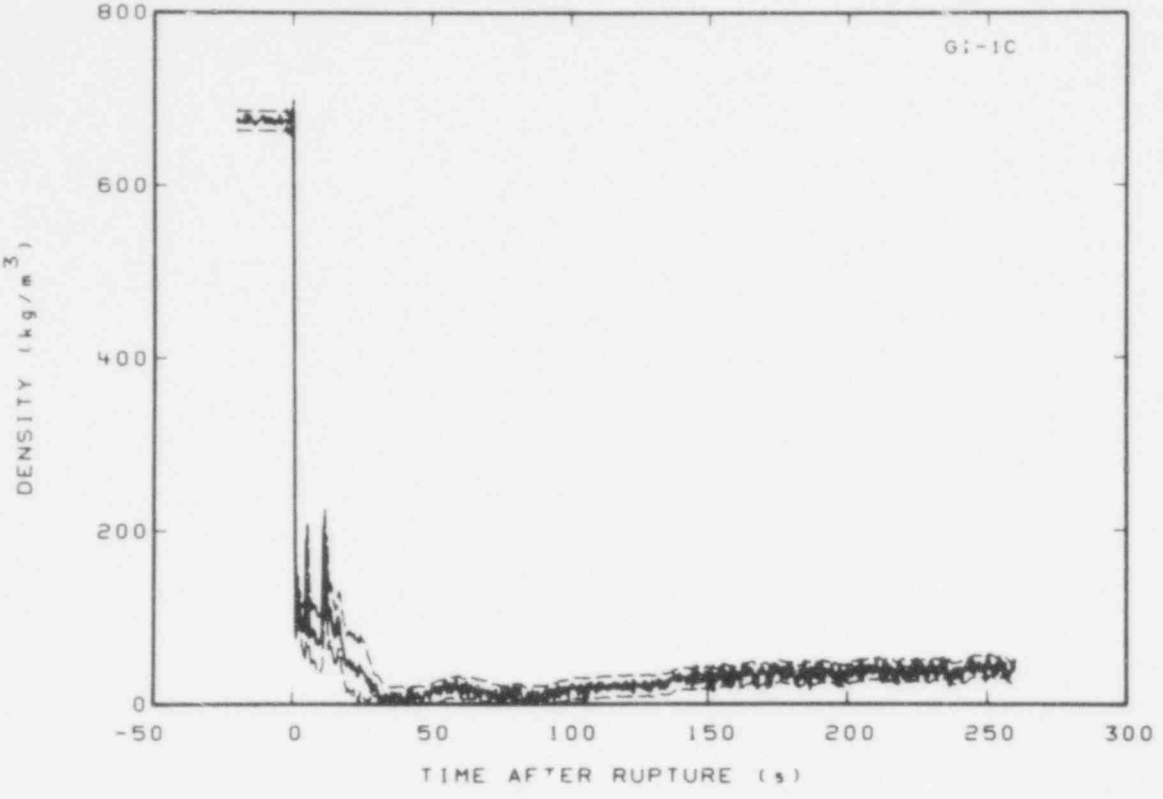

Fig. C-31 Density in intact loop (GI-1C).

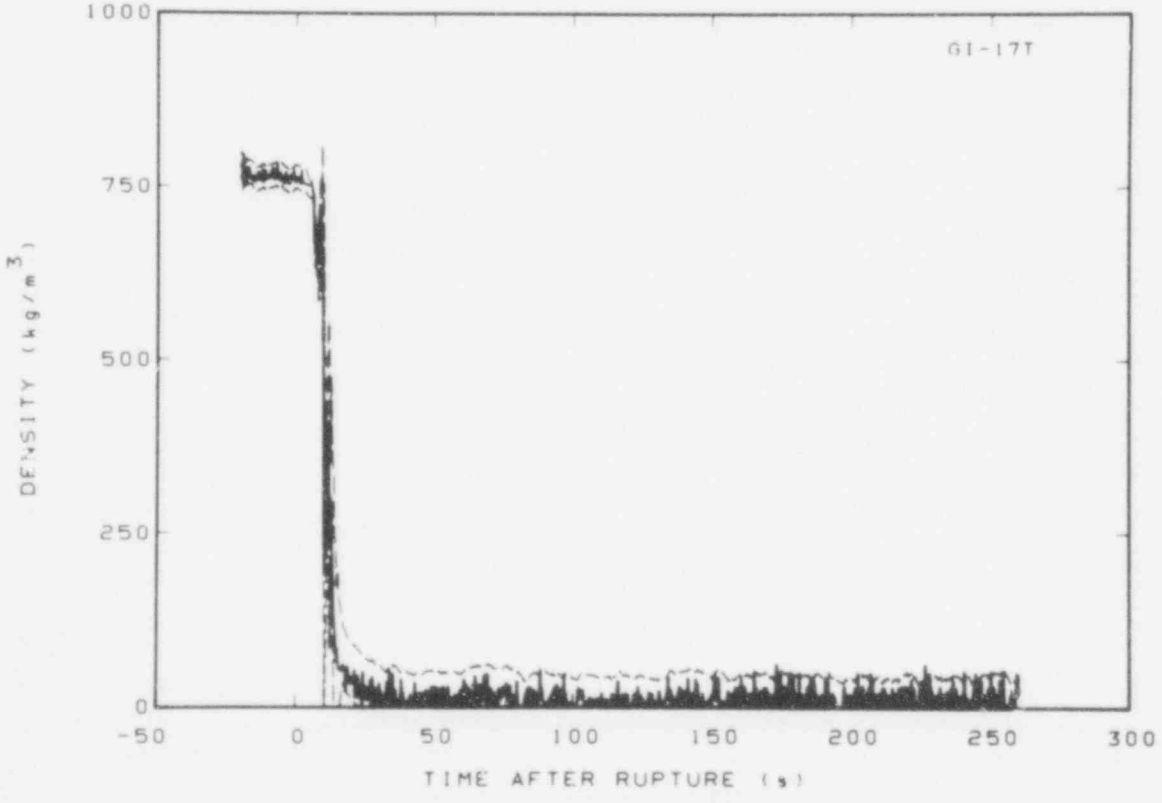

Fig. C-32 Density in intact loop (GI-17T).

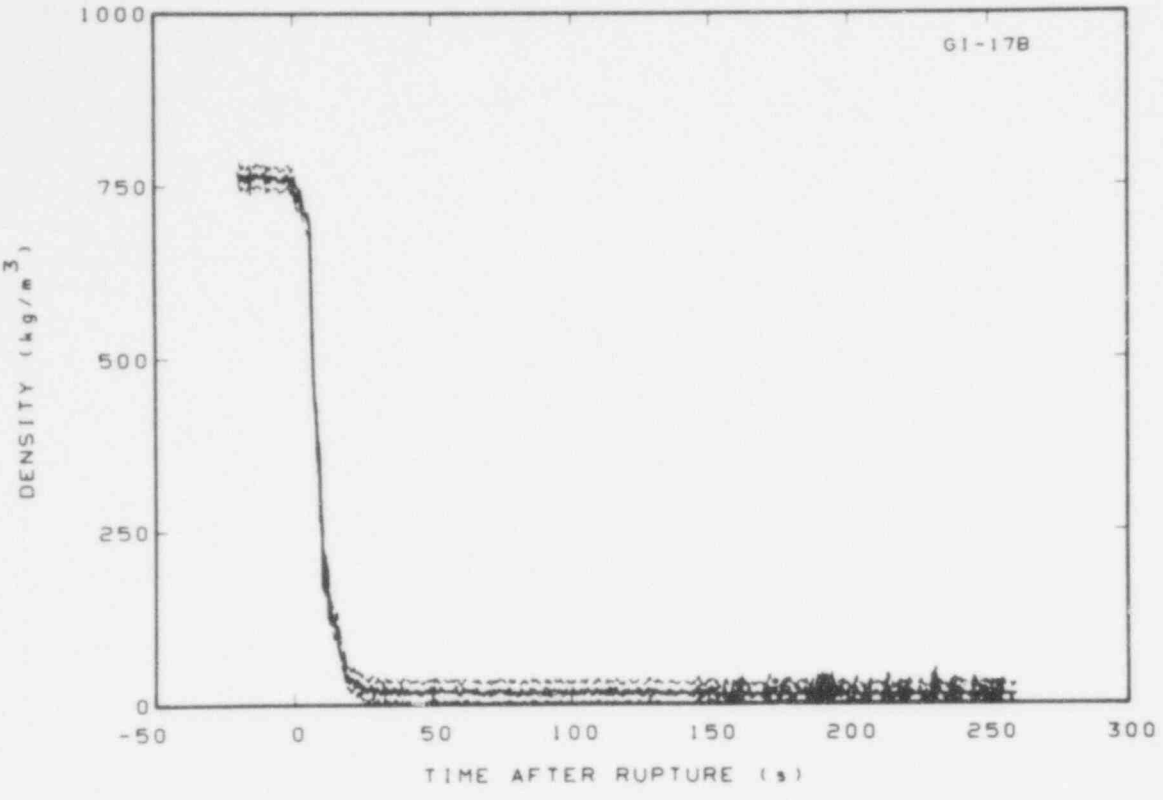

Fig. C-33 Density in intact loop (GI-17B).

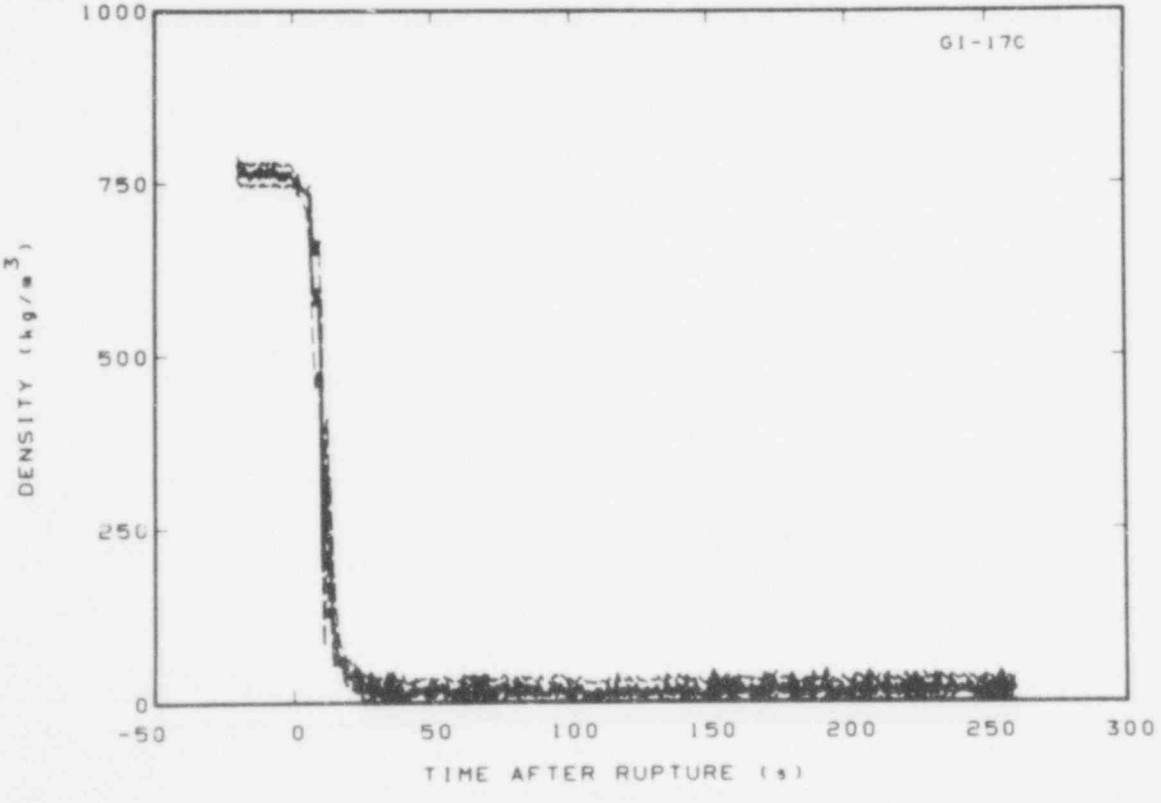

Fig. C-34 Density in intact loop (GI-17C).

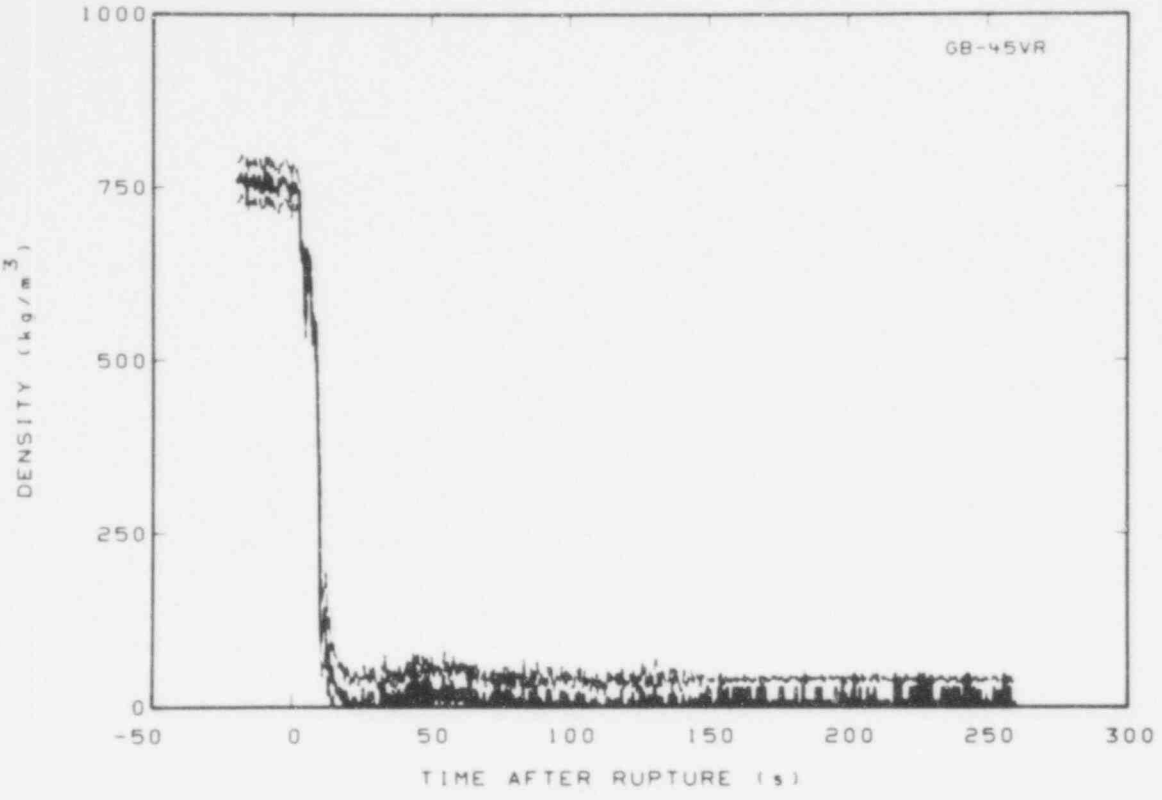

Fig. C-35 Density in broken loop (GB-45VR).

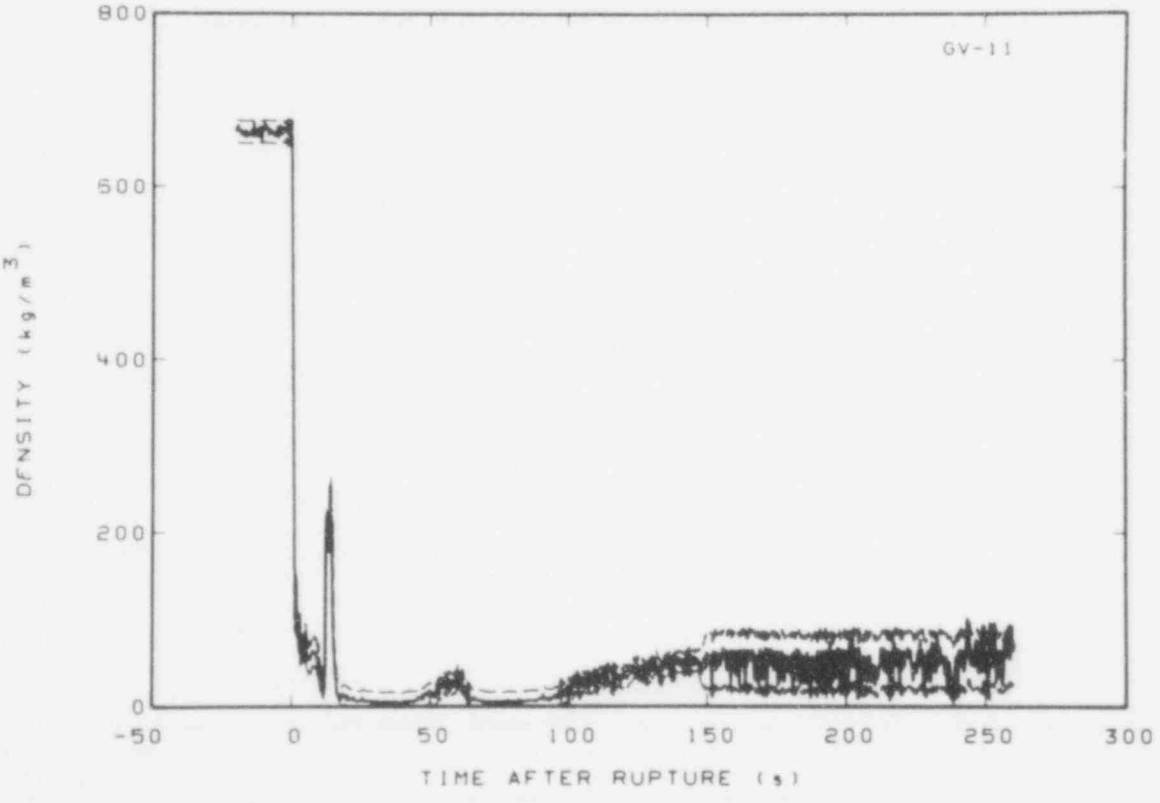

Fig. C-36 Density in vessel (GV-11).

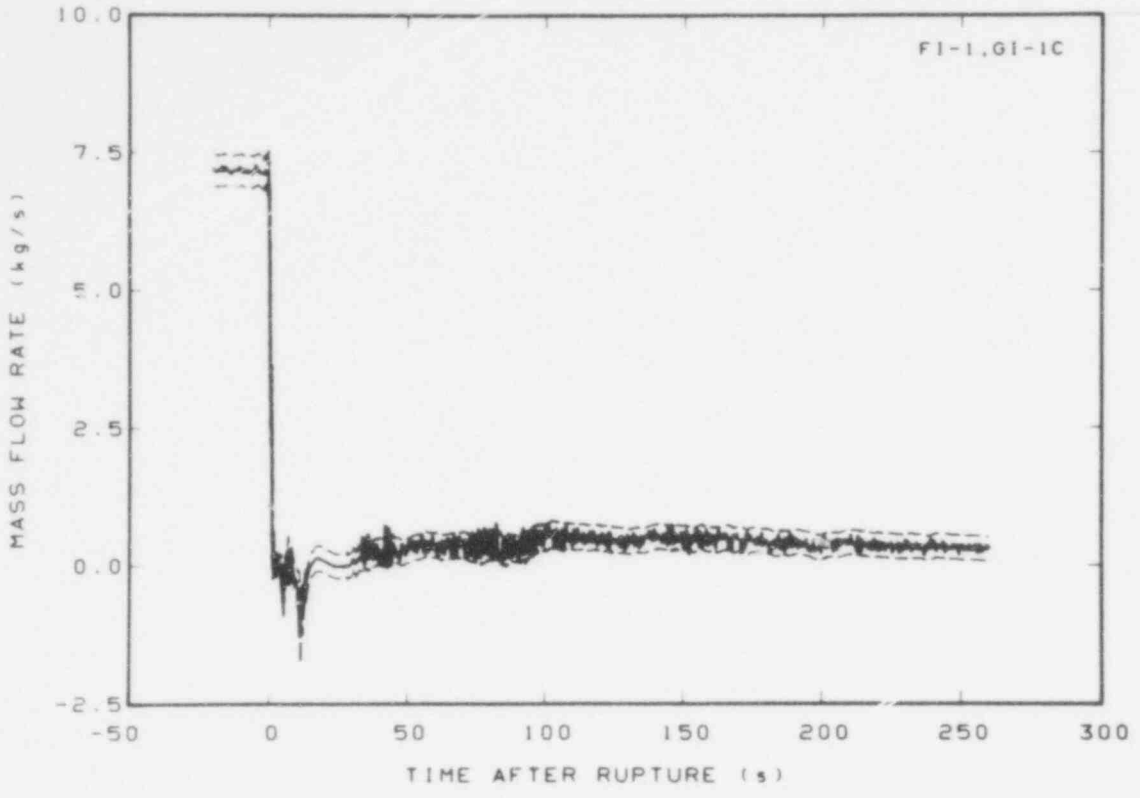

Fig. C-37 Mass flow in intact loop (FI-1 and GI-1C).

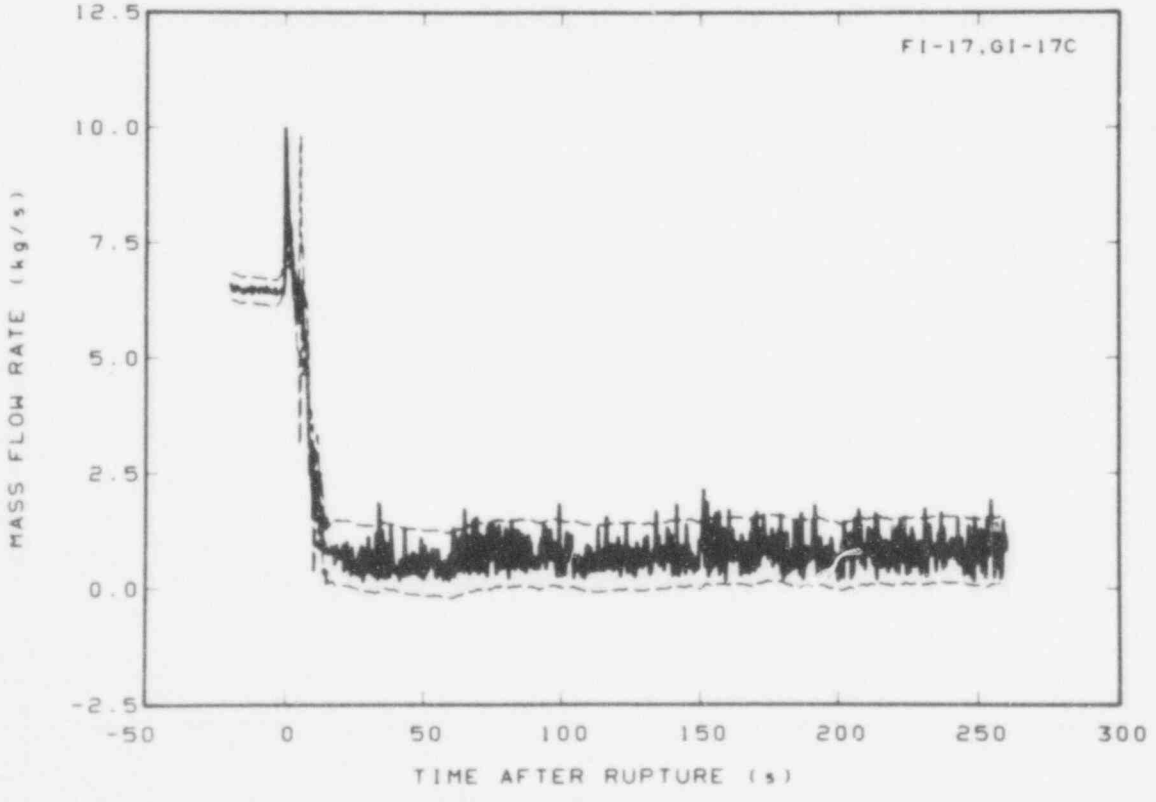

Fig. C-38 Mass flow in intact loop (FI-17 and GI-17C).

544 239

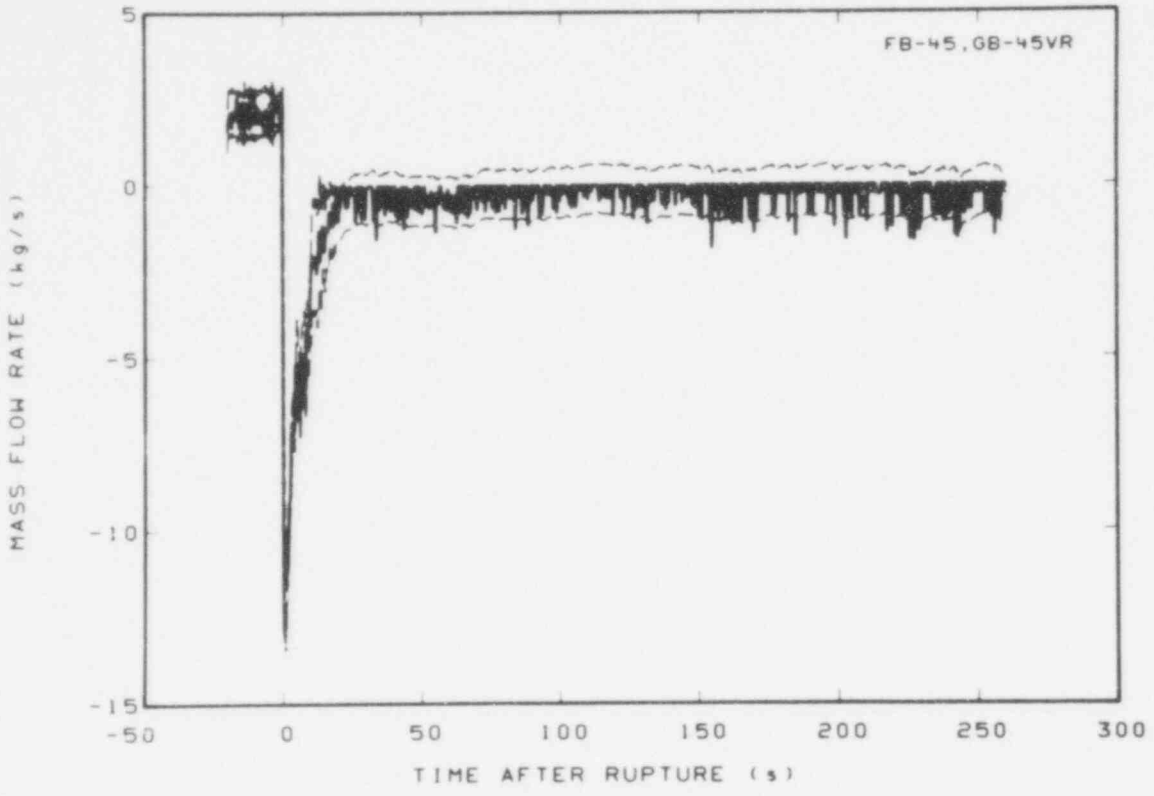

Fig. C-39 Mass flow in broken loop (FB-45 and GB-45VR).

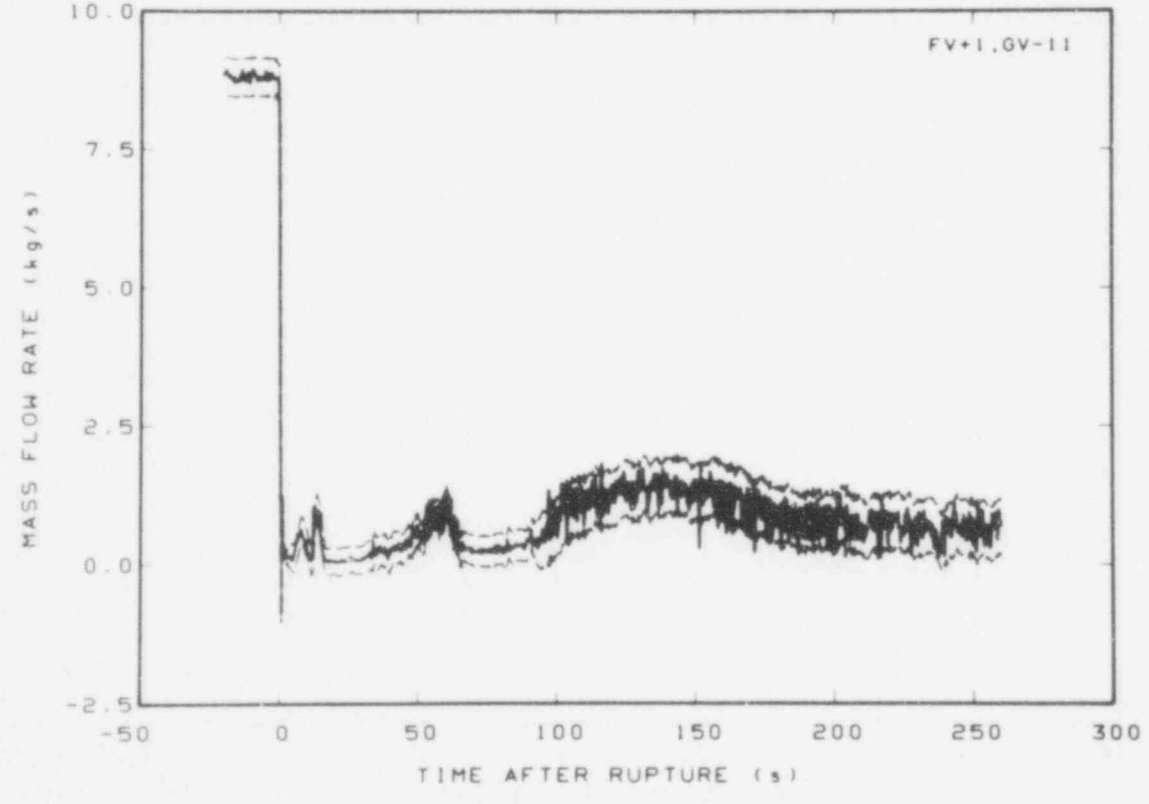

Fig. C-40 Mass flow in vessel (FV + 1 and GV-11).

TABLE C-II

GENERAL MEASUREMENT ENGINEERING UNCERTAINTY SOURCES AND UNCERTAINTY VALUES
(TEST S-07-8)

Measurement Category	Uncertainty Sources	Uncertainty Value	Expected Uncertainty Values
Fluid Temperature	Changes in homogeneity of the thermocouple wire due to cold working	$\pm$1.11 K	$\pm$1.66 K, R $\leq$ 550 K[a]
	Data interpretation from standard reference tables	$\pm$1.11 K, to 550 K $\pm$0.0021 R, R > 550 K	$\pm[1.42 + (0.0021\ R)^2]^{1/2}$, R > 550 K[a]
	General data acquisition processing	$\pm$0.42 K	where R = transducer reading (K)
	Thermal aging of the thermocouples	$\pm$0.28 K	
Material Temperature	Changes in homogeneity of the thermocouple wire due to cold working	$\pm$1.11 K	
	Thermocouple radial position	$\pm$2.78 K	$\pm$3.33 K, R $\leq$ 550 K
	Data interpretation from standard reference tables	$\pm$1.11 K, to 550 K $\pm$0.0021 R, R > 550 K	$\pm[9.75 + (0.0021\ R)^2]^{1/2}$, R > 550 K

TABLE C-II (continued)

Measurement Category	Uncertainty Sources	Uncertainty Value	Expected Uncertainty Values
Material Temperature (continued)	General data acquisition and processing	+0.42 K	where R = transducer reading (K)
	Thermal aging of the thermocouples	±0.28 K	
Pressure	Entrance effects	±0.3% of transducer full scale	±0.44% of transducer full scale
	Calibration	±0.26% of transducer full scale	
	Temperature sensitivity	±0.13% of transducer full scale	
	General data acquisition and processing	±0.15% of system full scale	
Differential Pressure	Installation	±0.3% of transducer full scale	

TABLE C-II (continued)

Measurement Category	Uncertainty Sources	Uncertainty Value	Expected Uncertainty Values
Differential Pressure (continued)	Calibration Transducer ranges +4.96 through ±199.26 kPa	$\pm[(0.05) + (0.5\ R/FS)^2]^{1/2}$ % of transducer full scale	±2% of transducer full scale[b] where R = transducer reading (kPa) FS = transducer range full scale (kPa)
	Transducer ranges ±3.44.74, ±689.47, ±3447 kPa	$\pm[(0.03) + (0.5\ R/FS)^2]^{1/2}$% of full scale	
	Transducer ranges ±6894, ±10 342 kPa	$\pm[(0.02) + (0.5\ R/FS)^2]^{1/2}$% of full scale	
	Temperature sensitivity	±0.5% of transducer full scale	
	General data acquisition and processing	±0.15% of system full scale	
	Air entrapment	±0.069 kPa	
Density	Calibration	±1.0% of reading (kg/m^3)	c
	Detector system Uncertainty	±2.1 kg/m^3	
	General data acquisition and processing	±0.15% of system full scale (kg/m^3)	

TABLE C-II (continued)

Measurement Category	Uncertainty Sources	Uncertainty Value	Expected Uncertainty Values
Density (continued)	Flow regime	Gr[c] where Gr = flow regime uncertainty (kg/m^3)	
Volumetric Flow (turbine flowmeter)	Calibration instrument reading	±0.25% of transducer full scale	
	Calibration standards	±19.56 x 10^{-2} 1/s	
	Velocity profile	±2.9% of reading	
	Frequency-to-voltage conversion	±0.25% of transducer full scale	c
	General data acquisition and processing	±0.15% of system full scale	
	Dead bands	±5% of transducer full scale	
	Flow regimes	c	

TABLE C-II (continued)

Measurement Category	Uncertainty Sources	Uncertainty Value	Expected Uncertainty Values
Mass Flow Rate (from volumetric flow and density data)	Combined results from individual uncertainty sources for volumetric flow and density data[d]	c	c

a. This value is no longer valid after thermocouple dryout occurs.

b. Value is based on observed system performance. It is more conservative than that obtained from the statistical summation of the identified engineering uncertainties.

c. Uncertainty value is time and flow regime dependent.

d. The general method for combining volumetric flow or momentum flux with density data to obtain mass flowrate and the resulting uncertainties in the data are explained in Reference C-2.

TABLE C-III

TIME PERIODS WHEN FLOW REGIME UNCERTAINTIES WERE APPLIED
(TEST S-07-8)

Detector Identification	Time During Which Flow Regime Uncertainties Were Applied (s)	Figure
FI-1	1 to 21; 98 to 268	C-23
FI-17	1 to 12	C-24
FB-45	10 to 17	C-25
GI-1C	1 to 21; 98 to 268	C-31
GI-17C	1 to 12	C-34
GB-45VR	10 to 17	C-35
FI-1, GI-1C	1 to 21; 98 to 268	C-37
FI-17, GI-17C	1 to 12	C-38
FB-45, GB-45VR	10 to 17	C-39

DISTRIBUTION RECORD FOR NUREG/CR-0814
(TREE-1228)

Internal Distribution

1 - R. J. Beers, ID

2 - P. E. Litteneker, ID

3-5 - INEL Technical Library

6-10 - Authors

11-41 - Special Internal

External Distribution

42-50 - Special External

51-52 - Saul Levine, Director
Office of Nuclear Regulatory Research, NRC
Washington, D.C. 20555

53-341 - Distribution under R2, Water Reactor Safety Research - Systems Engineering